GEOCHEMICAL ENGINEERING REFERENCE MANUAL

Contract #DE-AC03-81SF11520

Submitted to:

Mr. Tony Adduci
DOE-SNF-FGS
1333 Broadway
Oakland, California 94612

TR84-64
January 1984

TerraTek

UNIVERSITY RESEARCH PARK · 420 WAKARA WAY · SALT LAKE CITY, UTAH 84108 · (801) 582-2220

GEOCHEMICAL ENGINEERING REFERENCE MANUAL

Prepared by:

Dr. Lawrence B. Owen
Terra Tek, Inc.
420 Wakara Way
Salt Lake City, Utah 84108

and

Dr. Donald E. Michels
Republic Geothermal, Inc.
11823 East Slauson Avenue
Santa Fe Springs, California 90670

Submitted to:

Department of Energy
San Francisco Operations Office
1333 Broadway
Oakland, California 94612

Attn: Mr. Tony Adduci

Submitted by:

Terra Tek, Inc.
University Research Park
420 Wakara Way
Salt Lake City, Utah 84108

TR 84-64
January, 1984

TABLE OF CONTENTS

Table of Contents (continued) Page

Table of Contents (continued) Page

Table of Contents (continued) Page

Table of Contents (continued) Page

Table of Contents (continued) Page

Table of Contents (continued) Page

LIST OF FIGURES

List of Figures (continued)

List of Figures (continued)

List of Figures (continued)

List of Figures (continued)

List of Figures (continued)

List of Figures (continued)

List of Figures (continued)

LIST OF TABLES

List of Tables (continued)

Chapter I

INTRODUCTION

I. INTRODUCTION

I-1. Introduction

The discipline of Geochemical Engineering as defined by the U.S. DOE involves those field and laboratory activities that pertain to the determination of geothermal liquid and gas compositions, reservoir liquid and gas compositions and the methods utilized in obtaining and analyzing representative samples. The discipline also concerns itself with the general problem of scale deposition and methods of preventing and removing scale accumulations that might interfere with operation of a geothermal facility. An extremely important facet of the Geochemical Engineering discipline concerns itself with the treatment of spent geothermal liquids to render them suitable for subsurface disposal via injection wells. The discipline is also concerned with the possible extraction of valuable minerals from geothermal brine either by self-sufficient independent operations or as the result of secondary processes operated in conjunction with a hydrogen sulfide (H_2S) control process or as part of a scale and solids control program. Control of H_2S emissions is considered within the discipline, however, whether or not attempts are made to recover valuable by-products such as sulfur.

Geochemical support is usually required early in any geothermal development program. Initially, geochemists assist with the exploration effort that has as its primary goals the discovery of new resources and compilation of preliminary estimates of resource size and production potential. In the absence of production wells which penetrate into the geothermal reservoir, indirect indicators of hot fluids at depth, such as application of chemical geothermometers, measurement of gas emanations and completion of quantitative petrographic analysis of available core from the subsurface as well as samples

of surface outcrops, can be utilized. These data are critically appraised along with available geologic and geophysical data in arriving at a siting decision for the first deep exploration wells.

The determination of the true reservoir brine and gas composition is usually a primary goal along with delineation of reservoir productivity and size during the early stages of resource production. Knowledge of reservoir fluid composition is useful in delineating production zones and in establishing normal or typical production characteristics of wells. If, at a later date, a significant change in production fluid composition is noted, reasons for the change in production characteristics can be evaluated with attention directed at the possibility of casing breaks which allow overlying reservoirs to contribute to total production. Changes in reservoir production may suggest that step-out wells be completed in a somewhat different manner than the initial exploration wells. Informed decisions in these matters requires that an adequate geochemical baseline data set has been compiled against which subsequently obtained data might be compared.

A compelling reason for obtaining high quality geochemical data from a new production well is to permit a rapid assessment of the potential for scale deposition and brine treatment requirements if spent brine is to be reinjected. This type of data is essential in the planning and construction of larger production and energy conversion facilities. The accurate determination of total noncondensable gas in the production fluids is also an important requirement if a flash steam energy conversion cycle is to be installed.

Injection and scaling problems dominate the area of operational difficulties associated with the exploitation of high temperature geothermal resources for power production. The most extensive hydrothermal resources in the U.S. suitable for power production are located in the Imperial Valley of southeast-

ern California. Attempts to harness this huge resource dating back to the early 1960's and continuing to the present have been severely hampered by the magnitude of scale deposition in wells and surface facilities and injectability problems that have resulted from attempts to reinject chemically unstable brines. However, in the last several years, significant progress has been made in understanding the mechanisms of scale deposition and the requirements for proper pretreatment of spent brine prior to reinjection. Methods developed for handling hypersaline Imperial Valley brines can also be used to advantage in the development of lower salinity geothermal resources. Proper application of the new technologies can be considered an important area of involvement for geochemical engineers.

There is no formal academic discipline devoted to the development of geochemical engineers. Trained personnel with experience in the various technologies are most usually chemists, geochemists or chemical engineers with practical experience in the development and operation of geothermal facilities. However, an extensive technical literature has developed over the last 20 years, so that it is possible to develop an understanding of specific problems, such as scale deposition, and suggested remedial procedures by reference to the appropriate technical papers. Much of the material reviewed in this report was compiled on the basis of review of technical papers discovered after completing an extensive computer-aided search. A number of databases are available which can provide rapid insight into specific problem areas that may be encountered in hydrothermal developments. Utilization of computer search services, offered by many Universities and public libraries, provides an economical and convenient means of rapidly researching particular areas of interest. It is also now feasible for individuals to conduct their own computer-aided literature reviews by accessing various on-line database services.

A comprehensive directory of available databases is provided in Ref. 1. The user must be equipped with an appropriate video terminal and a modem which links the users terminal with the database via the telephone lines.

I-2. Sources of Information

The principle sources of information used in compiling this report included the following:

1. The COMPENDEX on-line database service provided by:

   Engineering Information, Inc.
   345 East 47th Street
   New York, New York 10017
   (212) 644-7635
   (800) 221-1044

2. A tabulation of USGS Geothermal Research Program publications available from the U.S. Geological Survey, Menlo Park, California 94025. The U.S. Geological Survey also maintains a database service called GEOTHERM. Information regarding use of this service can be obtained from:

   The Data Base Manager and Operations Officer
   U.S. Geological Survey
   345 Middlefield Road, MS-84
   Menlo Park, California 94025
   (415) 323-8111, ext. 2906

3. The Lawrence Berkeley National Laboratory, Berkeley, California, established an on-line remote access database called GRAD which is described in Refs. 2-3. This database contains information on geothermal energy resources for selected areas, covering development from initial exploratory surveys to plant construction and operation.

4. The Geothermal Resources Council (GRC), Davis, California 95617 publishes transactions of technical papers presented at the annual meeting of the GRC. The transactions were manually searched for relevant papers.

5. The relevant geothermal files of the DOE/SAN Office, Oakland, California were reviewed during the initial stages of this project.

6. Annual bibliographies summarizing technical work sponsored by the Electric Power Research Institute (EPRI) were reviewed. Copies of bibliographies, technical reports and proceedings of the annual EPRI Geothermal Program Review can be obtained from:

   EPRI
   3412 Hillview Avenue
   Palo Alto, California 94304

I-3. Commercial Geothermal Services

A current listing of active geothermal operators-developers and architectural and engineering firms is available upon request from the Geothermal Resources Council, Davis, California. Additional information concerning specialty consulting services in such areas as geochemistry, exploration geophysics, reservoir engineering, etc. can be obtained from the U.S. Geological Survey, the Electric Power Research Institute and the Gas Research Institute (located in Chicago, Illinois). These organizations provided funding for special research programs which are intended to promote the development of geothermal resources. They make extensive use of contractors and consultants with expertise in various technical disciplines of importance in the development of geothermal resources.

I-4. Acknowledgements

The authors would like to thank Dr. Jonathan Hanson of Terra Tek Research for his contribution of technical details regarding the calculation of subsurface temperature distributions about an injection well and the HP-67 calculator code for computing the temperature distribution. The authors would also like to note that the introductory comments in Chapter IV regarding injection well performance and design were originally written by Mr. M. D. Campbell of Keplinger and Associates for inclusion in Ref. 4. These comments are pertinent and appropriate for consideration in the early planning stages of any geothermal operation that will involve subsurface injection. Finally, the assistance and support of Mr. Tony Adduci of DOE/SAN is greatly appreciated.

I-5. References

1. Edelhart, M. and Davies, O., 1983, OMNI Online Database Directory: MacMillan Publishing Co., New York.

2. Lawrence, J.D., Leung, K. and Yen, W., 1981, A User's Guide to the Geothermal Resource Areas Database: Univ. of Calif., Lawrence Berkeley National Laboratory Report LBL-11492.

3. Lawrence, J.D. Lepman, S.R., Leung, K. and Phillips, S.L., 1981, A Geothermal Resource Database for Monitoring the Progress of Development in the United States: Univ. of Calif., Lawrence Berkeley National Laboratory Report LBL-10418.

4. Owen, L.B. and Quong, R., Editors, Improving the Performance of Brine Wells at Gulf Coast Strategic Petroleum Reserve Sites: Univ. of Calif., Lawrence Livermore National Laboratory Report UCRL-52829.

Chapter II

PHYSICAL AND CHEMICAL PROPERTIES OF GEOTHERMAL BRINE AND STEAM

II. PHYSICAL AND CHEMICAL PROPERTIES OF GEOTHERMAL BRINE AND STEAM

II-1. Chapter Summary

This chapter describes methods used to generate data on the physical and chemical properties of geothermal brine, steam and condensate. Quality assurance methods are summarized. Liquid and gas sampling techniques and supported on-site analytical facilities are also described. A useful field chemistry program is one with the capability of providing rapid generation of physical and chemical parameters needed to understand overall systems performance. For example, chloride concentration, total dissolved solids concentration and density data are important considerations in the evaluation of production fluid enthalphy. Spent brine turbidity data are useful in assessing brine processing equipment performance and probable injection well response. Quantitative chemistry data on liquid and gas streams are best generated using field preserved samples subsequently analyzed in conventional analytical chemistry laboratories. These laboratories need not be located in close proximity to field sites for reasons other than convenience. This approach eliminates the expense and problems associated with operation and maintenance of sophisticated analytical equipment in a field environment.

II-2. Introduction

Geothermal fluids present a broad range of circumstances that require several different approaches in order to obtain samples that, collectively, can represent the fluid in useful ways. The objectives for sampling also vary such that results which are useful for one purpose are not applicable to other purposes and could even be misleading. Furthermore, the compositions of geothermal fluids are broadly variable and sampling approaches that are practical in one geothermal field are impractical in another. Significantly,

geothermal fluids, especially flashing liquids, are chemically different at different points in the flow stream. Sampling at one point in the flow stream in effect captures a snapshot of a moving target. In order for the snapshot to be useful (interpretable) one needs to know in a chemical way, how the point of sampling is related to the rest of the fluid's flow path.

In the hardware to which these sampling methods apply the temperature and pressure may appear stable at the point of sampling, but the fluid passing that point may be experiencing changes in temperature and pressure at rates of tens of units per minute. Laboratory concepts of chemical equilibrium do not apply well to fluids in a context so dynamic as geothermal production. A host of chemical reactions are initiated when a geothermal liquid begins to flash (yield vapors of water and dissolved gases), but the pace of the reactions cannot always keep up with the buildup of the thermodynamic drive for the reactions. Consequently, some components are present in multiple chemical forms, but the proportions are not the same from one sampling point to another nor are the proportions reliably the same as at long-time equilibrium at the same temperature(s). When vapor develops in a flashing system, components become partitioned between vapor and liquid according to how their own chemical properties interact with the changing chemical and physical environment of the system.

The goal of completely characterizing the fluid(s) from a geothermal well cannot often be gained by a single visit. Partly this is because the fluids are seldom fully accessible, especially for a new well that is just being brought into condition to produce fluids. Also, the finer details of sample capture and preservation are developed in an iterative way, adapting the methods to fit the specific chemical natures of the fluids, the hardware actually installed to handle the fluid, and the purposes that data is to serve.

Even with good and thorough sampling, characterizing fluid from a geothermal well can only be completed in a relative way. A well taps a resource which may be non-uniform for geological and hydrological reasons. Some wells tap multiple prductive zones so that the fluid which issues from the wellhead is a blend. The multiple zones do not always contribute the same proportions of flow to the total fluid, hence real compositional variations can occur at the wellhead. Even a single producing zone may involve compositional differences across its volume and those differences can be detected in wellhead samples as longer term trends that represent bulk movement of fluid in the reservoir.

Reservoirs come in multiple physical types that require different approaches to sampling. Some wells tap single-phase liquid that is superheated and over-pressured in the sense that during flow, at the place where well meets production zone the actual pressure exceeds the vapor pressure of the liquid, including the vapor pressure due to dissolved gases. If such a well is pumped so that the liquid still is overpressured, hence single-phase liquid when it reaches surface equipment, then a unique set of circumstances are available for sampling.

More often, wells are not pumped and flashing begins while the fluid still is in the well -- the single-phase liquid is basically inaccessible there and sampling efforts are aimed at the liquid and vapor components after they have been physically separated in specialized surface equipment. Notably, some components of the pre-flash liquid may remain in the wellbore as post-flash scale and remain inaccessible to sampling efforts. This is particularly unfortunate because the availability of scale components in the pre-flash liquid is an important chemical characteristic of the resource. Such downhole losses deserve to be estimated and wellhead sampling provides one kind of data for the attempt.

In some cases, a reservoir that is basically a one-phase liquid can be tapped so that flashing occurs before the liquid enters the wellbore. Whether this is desirable depends on several factors outside the scope of this description. The apparent composition of fluids in the surface equipment reflect this mode of production and may require an adjustment in the sampling motive and methods.

Some wells tap reservoirs that deliver a fluid that is essentially steam, uncomplicated by flashing. However, the steam carries a host of condensable and non-condensable gases. Sampling is complicated by heat losses through surface equipment and this results in a film of liquid water on the piping that interacts strongly with the gas components and also with methods for tapping the lines to obtain samples.

Because the contexts of geothermal fluids are diverse and dynamic, obtaining representative samples requires careful consideration. Only rarely is one's interest in the fluid limited to the point where samples are collected. More often, the intent of sampling is to characterize the fluid at some place up the flow direction which was inaccessible or inappropriate for sampling. Sometimes the intent concerns places down the flow direction where sampling is awkward or unrepresentative.

Sampling an operating geothermal electric plant presents a different set of circumstances than sampling discovery/development wells that are expected to eventually feed an electric plant. In an active plant, conformance to criteria can be measured directly, at least in principle. Before a plant is built, the design engineer is interested in the same criteria and components, but uses data from short-term tests of wells to engineer specific functions and responses into the plant. It is intended that when operations begin they will be in conformance with design criteria, but demonstration of success in this matter cannot occur until the plant has operated for a time.

The raw analytical data seldom is useful in the form it was obtained. Most often, it is adjusted, expanded, or reduced in conformance with one's judgement about how the point of sampling fits into the overall flow schematic relative to where one's interest is actually focused. Whether the adjustments to data are appropriate and accurately done depends jointly on how accurately one's concepts of the overall process fit the facts (which may be directly measureable only with poor precision) and how the context of sampling and analysis has yielded a datum that fits into a model in the intended way.

Only a few contexts of sampling have the desirable property of allowing the data to be extended up or down the flow path in a logically defendable way. Even for these, the extent to which extrapolation is valid may be limited. Namely, these are samplings of vapor-free liquid and liquid-free vapor. They are present and accessible at only a small number of locations (in flow streams) and it is these places alone that can yield usefully coherent samples.

Because the context of sampling is important to the useability/extendability of the data, non-chemical data is required to accurately describe the context of the sampling. This includes the extent of flashing, usually expressed as percent of the produced fluid which has vaporized. Temperature data are valuable for subsequent calculations about places in the flow path beyond the points of sampling. Pressures also are valuable data since their divergence from the pressure-temperature curve for pure boiling water shows the net effects of dissolved salts and gases. Rates of fluid production by wells at the time of sampling are important because some components appear to vary with production rate.

Production history for the well/facility being sampled is useful in describing the context of sampling and how it extends in a historical sense. This is especially important in assessing short-term flow tests of new wells

which may yield samples contaminated with drilling and completion fluids. In all circumstances, limited information is gained from a single context of sampling; several contexts will eventually be used. The results sought should be mutually supportive in describing the composition, its dynamic changes within equipment, and trends over time.

Sampling geothermal fluids must also conform to requirements of safety for personnel and for equipment. The potential for bursting vessels or tubing connections or wrongly opening valves is real and could lead to serious scalding or flying projectiles. Discovery wells and new field developments are generally noisy places that involve much vigorous activity by many people not involved with the sampling. Nonroutine operations are the rule and safety requires much alertness in addition to care, planning, and coordination.

Complete chemical characterization of a geothermal resource usually requires a complicated strategy for sampling and analysis. Mainly this is because in the early stages of discovery/development a simple sample of liquid is not obtainable. Most commonly, the fluid issuing from a discovery/development well has been partly flashed to steam and some scale components are lost to inaccessible places in the well.

The geochemists role at this point is to obtain samples of the many components that exist in the separated steam and liquid portions. Some are incompletely separated, hence sampling and interpretation must account for this. The scale-prone materials must be sampled in special ways or some means found to estimate their pre-flash concentrations.

From the several kinds of samples and data, the geochemist describes a pre-flash liquid which represents the resource. Reconstruction of these pre-flash liquid characteristics must recognize all the chemical reactions that are initiated during the flashing that preceded sampling. This recon-

struction is as complicated as the chemical behavior of the liquid and is necessary because the conditions of sampling are not the same as conditions of plant operation.

It is the characteristics of the reconstructed fluid that are needed by the design engineer. When the reconstruction is accurately done, the design engineer can propose alternative hardware designs and evaluate the chemical consequences. This kind of evaluation, iterated over a range of plant designs, will yield the design best suited for the individual resource a geothermal field provides.

A single characterization effort involves 3 to 10 samples in a suite. The exact number depends on the stage of development of a well and the kinds of complications entailed in the sampling and analysis. Each sampling is generally tailored for a specific fluid and context of sampling/analysis/interpretation. Repeat sampling will be done partly to resolve questions raised by earlier results and partly to begin defining how the chemical properties of a well's output will change as the resource is exploited. Forecasts of changes in the fluid are important inputs to the design engineers. Each well in the field must be characterized in order to find the range of chemical behaviors the entire field presents.

The perils due to misunderstood chemical behavior can be serious and costly. Proper execution and iteration of the sampling/analysis/interpretation sequence requires a thorough understanding of processes that occur in wellbores, geochemistry, analytical chemistry, and field operations. Furthermore, translating that information into a form usable by design engineers demands that the chemist know much about the engineer's needs and the functions of process equipment. A broad range of expertise is required to erect a geothermal plant that runs smoothly. Chemical aspects cannot be treated lightly.

II-3. Field Chemistry Program

Kindle and Woodruff[1] have developed a flowchart (Figure II-1) illustrating analytical requirements for characterizing a typical geothermal process stream. The geothermal flow to be sampled could be either liquid or steam. Special techniques for sampling two phase liquid-gas flow streams are described in Section IV. The factors which influence accuracy of geothermal analytical determinations include:

1. Process stream compositional variations
   a. with time
   b. with flow rate
   c. with sampling point location (e.g. single phase vs. two phase; percent steam flashing, etc.).
2. Sampling techniques
3. Pre-analysis sample deterioration
4. Analytical methods
5. Skill of the analyst.

An understanding of these factors and the realities of typical hydrothermal field development projects is essential in designing and implementing a chemistry assessment program that yields accurate results.

The first steps in design of a field chemistry program should be to define the program objectives and to evaluate the nature and characteristics of the well test surface facility. Questions such as the availability of a full-scale steam separator, capable of yielding a single phase process stream for characterization, and the ability of the developer or site operator to measure and quantify production well flow characteristics, especially accurate measurement of percent steam flash, are extremely important. In the absence of surface steam separation equipment, the chemical monitoring program will have to provide a small separator if meaningful chemical data are to be obtained.

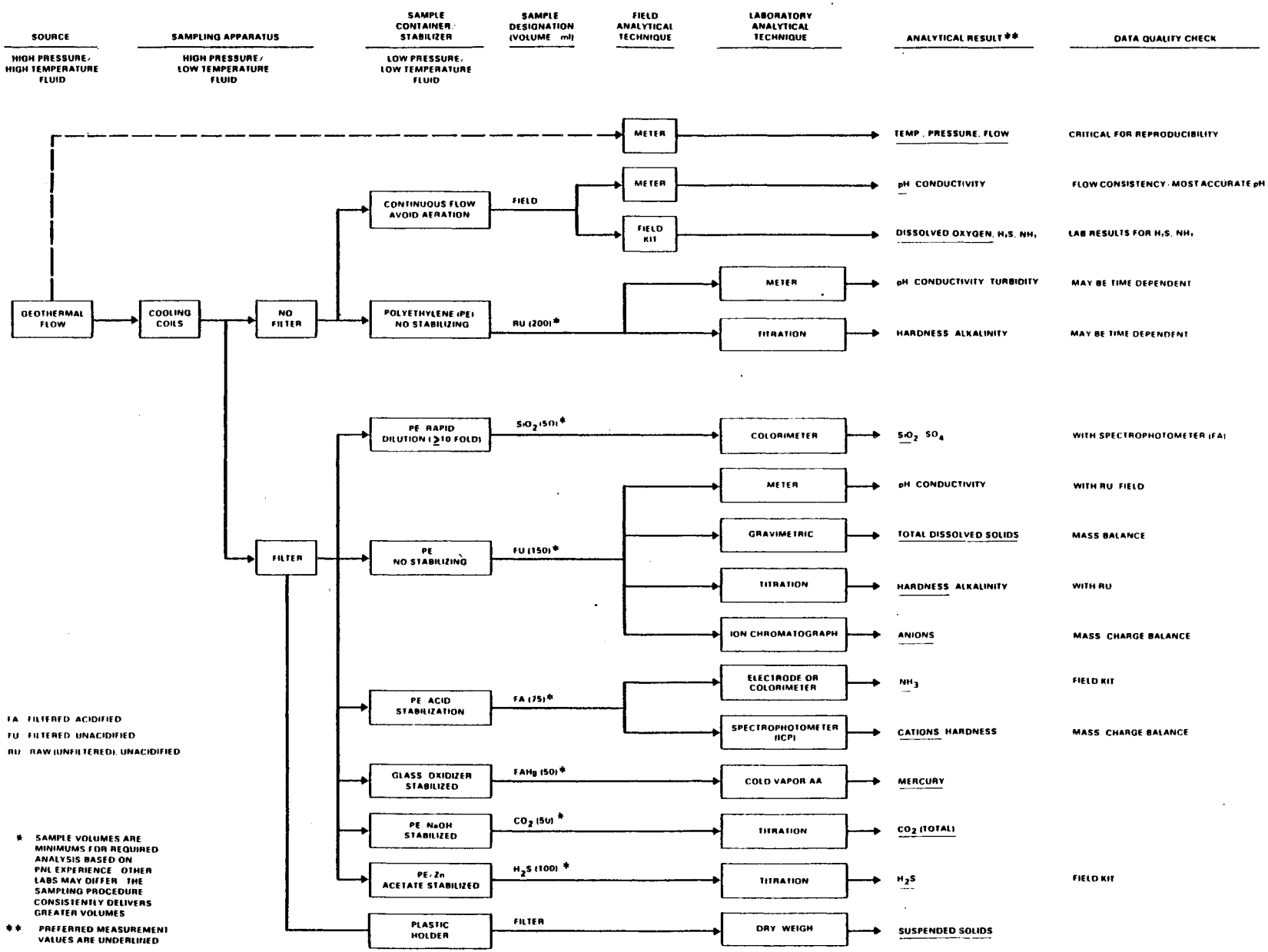

Figure II-1. Flowchart for Sampling Analysis. (From Ref. 1)

The alternative of using traversing probes to obtain liquid samples from two-phase lines, seldom yields unequivocal results except when collecting fully flashed liquids (residual liquids that have reached atmospheric pressure by adiabatic boiling).

A problem with all sampling techniques is to insure that a representative sample is obtained for analysis. The best situation is one in which a large steam separator is available to process the total flow from a geothermal well. This type of operation insures that liquid samples are not diluted with condensed steam and provides a reference for non-condensable gas calculations. Since any sampling operation pulls only a relatively small side stream (1 to 10 gpm) from the main flow (300 to 2000 gpm), the sampled stream must be made representative. Use of a small side stream separator of the Webre type[2] requires a relatively low throughput. If the sampling port is a two phase flowline, non-representative samples could be obtained. The sampling port should be equipped with a traversing probe or a fixed probe located near the bottom of the flow line with an internal extension into the flow stream. Sampling two-phase flows from a vertical pipe, for example the wellhead casing, is preferable to sampling along a horizontal pipe. Some recommended sampling procedures for various process streams are described more fully in a subsequent section.

Useful on-site analytical capabilities are listed below. Asterisks indicate tests best done in the field. More field capability is appropriate for extended well tests:

1. Physical Parameters

   *a. liquid density
   *b. suspended solids concentration
    c. turbidity

2. Chemical Parameters

a. total dissolved solids concentration
*b. chloride concentration
*c. pH
*d. alkalinity
*e. dissolved ammonia concentration
f. dissolved oxygen concentration
g. sulfate concentration
*h. dissolved sulfide concentration
*i. miscellaneous tests as necessary for specific field sites or R&D programs
*j. capability to collect and preserve samples for subsequent laboratory analysis

A practical on-site analytical laboratory is schematically illustrated in Figure II-2. An analytical equipment list is provided in Table II-1. Some specific items of equipment, such as analytical balances, have been referenced in Table II-1. These references are provided as examples only. Similar equipment supplied by other manufacturers with equivalent capabilities would be satisfactory. In most cases, it may be necessary to purchase a trailer to house the chemistry laboratory because extensive renovation needed to facilitate analytical work may negate conventional leasing terms.

Depending upon the scope of a particular project, construction and outfitting of a fully equipped field chemistry facility may not be warranted. The duration of a particular project and the overall objectives of the project will usually dictate whether comprehensive field capabilities should be provided. The minimum analytical requirements or some subset of them can provide an adequate level of support for short duration testing programs. If a project is beyond the exploration stage such that energy conversion system design and geothermal water handling facilities are being evaluated, an on-site well-equipped chemistry facility becomes very important.

The field chemistry laboratory should be equipped with adequate storage and shelf space for the various items of glassware and supplies. Kitchen-type

FIGURE II-2. FLOOR PLAN - FIELD CHEMISTRY LABORATORY

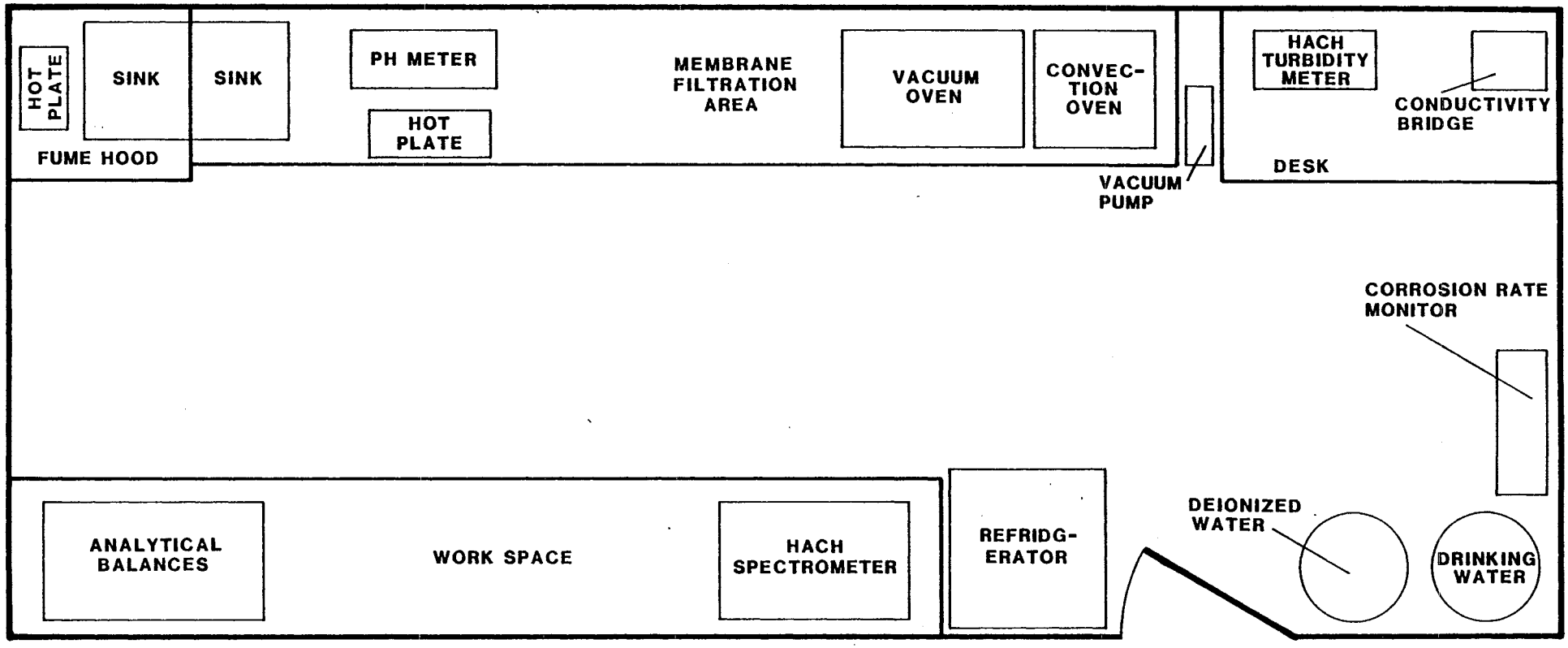

Table II-1

Suggested Field Chemistry Laboratory Equipment List

Quantity	Description
	Analytical Equipment
1	Metler AK-160 Analytical Balance (Resolution to 0.1 mg)
1	Sartorious 1364 MP Top Loading Balance (Optional - Resolution to 0.01 gm)
1	HACH Model 16800 Portable Turbidimeter (Optional)
1	HACH Ratio Turbidimeter - Model 18900 (Optional)
1	HACH Direct Reading Engineer's Laboratory DR-EL 14
1	Bausch & Lomb Model 88 Spectrophotometer (Optional)
1	Orion Model 701A Digital pH/mV meter
2	Orion Model 070110 ATC Electrode
2	Ross Combination pH Electrode
1	Orion Model 95-10 Ammonia Electrode
1	Orion Model 95-02 Carbon Dioxide Electrode
1	Portable Digital Multimeter
2	Portable Digital Thermometer
2	CHEMetrics Dissolved Oxygen Kit (0-12 ppm)
2	CHEMetrics Dissolved Oxygen Kit (0-1 ppm)
1	GAST Vacuum Pump/Compressor Model 70-300
1	LABCONCO Model 28 Fume Hood
1	Fisher Model 215F Convection Oven
1	Fisher Model 281 Vacuum Oven
2	Stirring Hot Plate
1-2	Desiccator
1	Energetics Science 2000 Series H_2S Analyzer (Optional)
2	L/I Lab Industries Repipet Dispenser
1	Oxford Macro-Set Pipett (1-5 ml)
1 ea	Eppendorf Digital Pipett (10 µl, 100 µl, 1000 µl)
1	Refrigerator
	Glassware:
5	10 ml Volumetric Flask
5	50 ml Volumetric Flask
5	100 ml Volumetric Flask
3	200 ml Volumetric Flask
3	500 ml Volumetric Flask
2	1000 ml Volumetric Flask
6	25 ml Graduated Cylinder
5	Graduated Cylinders - 250 ml, 10 ml
2	1 Liter Graduated Cylinder
2	2 liter Plastic Graduated Cylinders
20	125 ml Erlenmeyer Flask
2 each	Long Stem Funnel Pipets: 1 ml, 2 ml, 5 ml, 10 ml, 25 ml

Table II-1 (continued)

Field Chemistry Laboratory Equipment List

Quantity	Description
	Bottles
4	500 ml Squirt Bottles
6	125 ml Polyethylene Wash Bottles
	Assorted Polyethylene Sample Bags (Fisher Scientific)
4	2 ml Beaker
5	30 ml Beaker
20	100 ml Polyethylene Beaker
24	100 ml Polyethylene Beaker (Fisher Scientific)
20	500 ml Polyethylene Beaker
8	600 ml Polyethylene Beaker
6	1000 ml Polyethylene Beaker
25	100 ml Nalgene Bottles
12	50 ml Polyethylene Bottles
72	100 ml Polyethylene Bottles
6	500 ml Polyethylene Bottles
6	500 ml Polyethylene Bottles
	Filtration Equipment
4	Nucleopore Membrane Filters
1	Flecker Membrane Filtration Set (Fisher Scientific)
5 ea	Millipore Type HA 45 mm diameter, 0.45 μm and 10 μm membrane filters
5-10	Nucleopore 42 mm diameter membrane filter pads
1	Box Millipore Swinnex® Disc Filter Holders and 10 ml capacity plastic syringes
	Miscellaneous Laboratory Supplies
1	Tool Kit
1	First Aid Kit
3	Bottle Absorbant
1	Fire Extinguisher
	Magnetic Stir Bars - Various Sizes
	Plastic Throw-Away Gloves
	High Temperature Gloves
	Kimwipes®
	Dessicator
500	Oxford Pipett Tips
1	Box, Tygon® Tubing
1	Hand Operated Vacuum Pump
1	Motor Driven Vacuum Pump

cabinets and work surfaces of Formica® are relatively inexpensive, available in most areas of the U.S. and ideally suited to the needs of a field laboratory. The refrigerator is useful for preserving chemical reagents especially in western U.S. areas where ambient temperatures can be quite high. An adequate air-conditioning system and AC power service is essential for convenient and trouble free operation. The power load should be carefully analyzed as the current drain due to the operation of ovens, hotplates, a refrigerator, analytical equipment, ventilation equipment, air-conditioning and lighting can be surprisingly high. Proper and trouble free operation of the laboratory demands that the power source be dependable.

The most difficult piece of conventional laboratory equipment to operate in the field environment is the analytical balance. A modern digital balance with resolution to 0.1 mg or better is extremely sensitive to mechanical vibrations or other disturbances. Proper performance of the balance can only be achieved by isolating the unit from sources of vibration. Achievement of an adequate level of vibration isolation in a small trailor may be difficult to realize even when substantial shock mountings are employed. The problem is due to the fact that most small trailers will shift position slightly under the influence of personnel moving about inside of the trailer. Geothermal sites are by nature noisy. Large machinery may be moving nearby and vibrations set-up by compressor units can cause significant problems. The analytical balance is one of the most important pieces of equipment in the laboratory so steps should be taken to preclude difficulties.

A simple but completely effective way to isolate sensitive analytical balances from mechanical disturbances is to provide a mounting platform for the balance that is totally decoupled from the trailer. This can be accomplished by installing a rigid steel pipe in concrete directly beneath the position where the balance is to be used. Appropriate holes are drilled through the laboratory bench and cabinets to pass the pipe. The pipe is

secured in concrete either by digging a hole and directly cementing the pipe in place or by centering the pipe inside of a large tractor or truck tire and then filling the tire with concrete. The ground mount for the pipe should be set-up so that a telescoping pipe section can be inserted into the mount from inside of the trailer after the ground mount is installed. A cement filled tire is convenient because it can be positioned easily using a forklift. The opposite end of the support pipe is welded to a flat steel plate upon which the analytical balance is placed. If care is taken to level the mounting pipe and support plate, the leveling controls of the analytical balance will work as intended. Care should also be taken to insure that no objects come in contact with the mounting pipe especially if it passes through a storage cabinet. The size of the mounting plate should be large enough to support both the analytical balance and a two place resolution top loading balance, if one is to be used in the field.

The time and effort required to install an adequate balance support will be well rewarded in terms of absolutely trouble free operation. It is quite impressive to demonstrate the mount to a visitor by vigorously stamping your foot on the floor next to the balance without causing any perceptible disturbance.

An important aspect concerned with the operation of a field laboratory is the quality or purity of water used to mix reagents and, most importantly, used as a diluent for the preserving of liquid samples that will eventually be submitted for quantitative analysis. In many areas of the U.S., water service companies can provide triple distilled water in five gallon plastic or glass bottles. The bottles are placed on top of a conventional water cooler. These units are quite satisfactory for routine work. However, one should periodically submit samples of the distilled water for analysis to determine the level

of background or blank corrections. The water should be qualified by chemical analysis before accepting it for use in the laboratory. A conventional water cooler should also be provided as a source of wash and drinking water.

As an alternative, one can use commercially available deionizing columns or stills specifically designed for laboratory use to supply pure water. The scientific supply catalogs (e.g. Fisher Scientific, VWR, etc.) describe such equipment. It is also possible to consider use of a deionization column in conjunction with the use of high purity bottled water. All water, regardless of its source, should be prefiltered using a 0.45 micron membrane filter prior to use. This is especially important for accurate determination of suspended solids and total dissolved solids. Quantities of prefiltered water can be stored in large polyethylene bottles equipped with a bottom spigot.

Large amounts of water are usually needed to clean glassware and equipment. The most convenient set-up is to provide a sink in the labratory that is equipped with an external drain and a large supply of potable water in an outside tank. Most local water supply companies can install the storage tank and stand. A tank with a 100 to 200 gallon capacity or greater would be appropriate. The sink should be drained into a 50 gallon drum which can be drained as necessary to a brine pit. Access to the drum by a forklift will greatly simplify the process of draining the drum. The drain line from the sink to the drum should be equipped with an air bleed port. Conventional sink fixtures can be used in the laboratory.

In those circumstances when field work coincides with periods of below freezing weather, arrangements would have to be made for the installation of heated external water tanks, if available. Electrically heated tanks would be most convenient, but the added electrical load imposed by the heaters would have to be accommodated. If external water tanks are not available, the

laboratory would have to function without auxillary water supplies. The external drain can be maintained, however, by charging the drum with a quantity of antifreeze or salt. The use of small containers placed immediately under the sink in the laboratory can also be considered.

The ultimate size of the laboratory facility will depend on its intended function and the funds available for installation. In general, the largest possible work space should be provided. Minimum dimensions for the type of facility illustrated in Figure II-2 is about 20 feet long by 8 feet wide. The width of the space between the parallel benches should be at least three feet. This type of facility will support two personnel fairly comfortably. The facility is, however, not large enough to afford reasonable working space for more than two people. The inclusion of the desk is necessary to facilitate book work, calculations, record keeping and other similar activities. Shelving placed in the appropriate locations can be used to store equipment such as a continuous recording electrochemical corrosion monitor which does not require any more than occasional attention.

II-4. Documentation

A typical field program that has been organized to evaluate resource productivity and to characterize the properties of the reservoir liquids and gases can ultimately result in the collection of literally hundreds of samples. The samples could represent produced water or brine, noncondensable gases, solid scale and suspended solids samples as well as samples of process water that might be used to purge instruments, pit brines and so forth. Accurate record keeping is essential to all projects. The maintenance of records is also important because a single sample, say of scale, might be subdivided and subjected to a variety of analytical procedures. A primary responsibility of the chief chemist or geochemist is to insure that all collected samples are

properly labelled and recorded. On large field projects, good planning is required prior to the arrival of personnel in the field. The U.S. EPA refers to the documentation of a sample as the sample's Chain of Custody[2].

The elements which comprise the Chain of Custody that are relavant to geothermal operations are:

1. Sample labels
2. A field log book
3. A chain-of-custody record
4. Sample analysis worksheets

II-4-1. Sample Identification

Sample labels must be attached to sample bottles or bags (in the case of solids) in such a way that insures that the label will not become detached from the sample container. Gummed paper labels or tags can be used, but it is important to insure that indelible ink is used in recording the information. A simple measure that can be taken with almost any system used to record data on a sample container is to place strips of transparent cellophane tape over the written data. This measure will eliminate concerns about water or moisture contact reducing or eliminating legibility of recorded information. One can also write information directly on a sample container and protect the legend using cellophane tape.

The minimum level of information required on a sample container should include:

1. Sample number
2. Date and time of collection
3. Place of collection
4. Name of collector

Preprinted gummed labels can be used to simplify the sample collection procedure. The size of the labels should be appropriate for the size of the sample container. An example of a useful sample label is provided in Figure II-3.

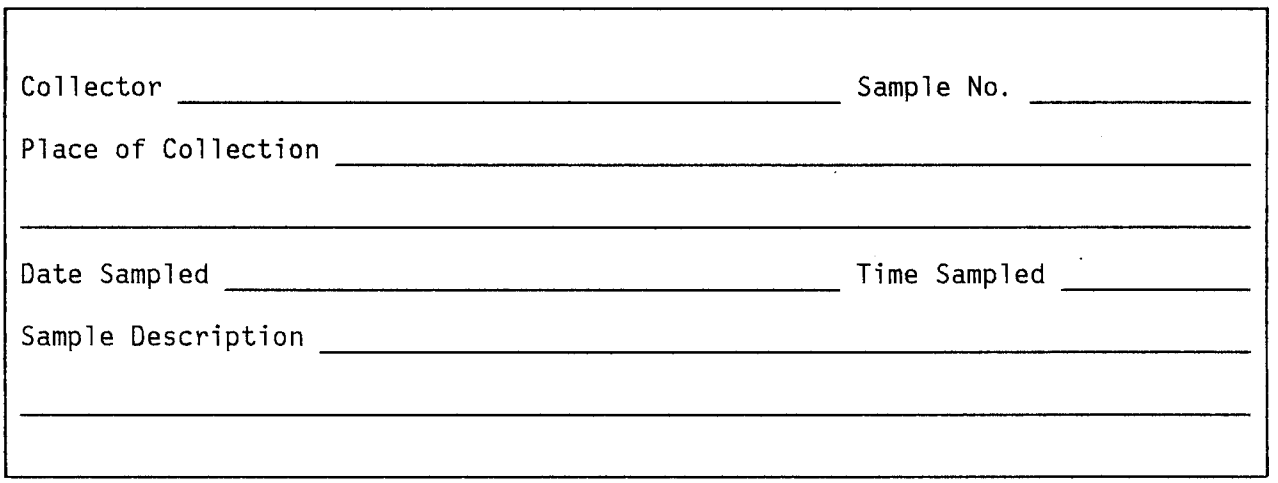

Figure II-3. Suggested Format for a Sample Container Label (Modified After Ref. 2).

II-4-2. Logging of Samples

A bound sample log book must be employed to record all pertinent information about collected samples. The degree of detail included in the log should be sufficient to permit one not acquainted with a specific project to be able to read and understand where particular samples were collected, their identity, and the kinds of characterization studies that were anticipated to be performed. This sample log should be maintained as a distinct entity. A separate log book should be used for recording labortory notes and results.

The sample log must be maintained in a bound notebook ideally with numbered pages. Log books are available from University Book Stores and the scientific supply houses that are designed for this purpose. Sequential sample numbers should be used to identify all collected samples. Suffix designations can be attached to the basic sample number to identify sample splits submitted for various types of analytical studies. An example of a typical sample log is provided in Figure II-4. The first page of the log or the inside of the front cover should contain a legend with the following information:

1. Title of the log and a brief description of the contents.
2. Name and address of the collector's organization.
3. Name and phone number of the chief chemist or project leader.
4. A note which guarantees return postage in the event the log is lost.

II-4-3. The Laboratory Notebook

A separate bound hardcover log book should be used as a laboratory notebook. The volume should be identified as to purpose and ownership as described previously for the sample log. The purpose of the laboratory log is to record all data and notes in conjunction with the characterization of samples, preparation of reagents, modification of procedures and any other activities performed in the laboratory. Laboratory determinations of, for

Figure II-4. A Typical Sample Logbook Format.

Sample Number	Date/Time of Collection	Project Identification	Description of Sampling Point and Sampling Methodology	Sample Volume/Size	Purpose of Sampling	Signature

example, brine density or chloride concentration would be described including all data such as volumes of samples, weights and calculated final results. The laboratory notebook is the only official record of field activities that can adequately describe the field analytical work. Therefore, it should be maintained with care and some diligence should be exercised to insure that all necessary information is recorded. Disclosures of new processes or inventions that may arise as a result of the field activities can also be recorded in the laboratory notebook. Such entries should be witnessed by having the appropriate personnel sign the dated entry.

II-4-4. Transporting Samples

Periodic shipment of samples from field sites to analytical facilities may be necessary during the course of an extended field program. It may also be necessary to ship samples in bulk at the conclusion of a field program. The use of any mode of commercial transportation for shipment of samples requires compliance with hazardous waste regulations. Normally, geothermal solid scale samples or sludge samples can be assumed not to be hazardous. Problems could be encountered, however, in the transport of large volume liquid samples. Air transport of such samples, especially acid solutions must comply with hazardous materials regulations (U.S. DOT Hazardous Material Table 49 CFR 172.101). In most instances, small volume liquid and solid samples, if properly packaged and nonflammable, will represent no hazard.

A convenient and highly reliable mode of shipping involves use of interstate bus services such as provided by Greyhound and Trailways. These companies maintain freight handling services which have proven to be very reliable. An advantage is that bus service may be available in areas where air transportation is not. Regardless of the mode of transport, care should be exercised to insure that samples are properly sealed and packaged. Liquid samples are

usually placed in glass or polyethylene bottles equipped with screw caps. The caps should be tightly wrapped with electrical tape to preclude leakage due to loosening or loss of bottle caps. An air space representing approximately 10 percent by volume of the bottle capacity should be maintained to allow for sample expansion due to temperature or barometric pressure changes[2]. Placing sample bottles in a sealed polyethylene bag is a further safeguard against leakage of liquids.

When shipped samples arrive at their destination they should be checked for integrity and immediately logged in. Before any further disposition of the samples can be considered, proper verification and logging of the samples by a designated individual is essential. It is helpful whenever possible to include a copy of the field sample description or field sample log entry to help insure that no confusion arises about the identity or disposition of samples.

Analysis of Samples - The final disposition of field samples must be handled in a manner that eliminates any possibility for confusion regarding the types of needed analyses or the identity of a particular sample. Often, it will be necessary to subdivide samples for different kinds of analysis. The accurate tracking of all splits of the same sample is very important. Utilization of Sample Analysis Request forms is one good way of tracing samples. This is especially important if samples are sent to outside laboratories for analysis. Figure II-5 illustrates one example of a useful Sample Analysis Request Form.

II-4-5. Quality Assurance

To avoid confusion in the expression of analytical results, the general guideline for significant figures and rounding off provided in Standard Methods[3] should be followed. When reporting analytical results for a liquid

Figure II-5. Sample Analysis Request Form.

Name of Company or Organization _____

Name of Submitter _____

Address and Phone Number of Company or Organization _____

Date of Submittal _____

Name of Laboratory to Receive Sample _____

Address and Phone Number of Laboratory _____

Name of Contact at Laboratory _____

Data Analytical Results Received _____

Requested Services:

Collector's Sample Number	Laboratory's Sample Number	Type of Sample (Solid, Liquid, Gas)	Requested Analyses	Comments

sample, units of mg/l (ppm by volume) should be used. Concentrations less than 0.1 mg/l should be expressed as µg/l. Concentrations of 10,000 mg/l or greater should be expressed as weight percent:

$$\% \text{ by Weight} = (\text{mg/l})/(10{,}000 \times \text{Specific Gravity})$$

Analytical data for solids are expressed in ppm by weight or µg/g. The conversion of liquid phase constituent concentration from a ppm volume basis to a ppm weight basis is accomplished by dividing mg/l by the specific gravity of the liquid.

II-4-6. Validity of Analytical Data

The validity of a chemical analysis is controlled by the precision and accuracy of the analytical techniques employed in the characterization of a sample. Accuracy refers to the statistical deviations between the measured amounts of a component in samples and the actual amount of that component in the sample[3]. Precision is the reproducibility of an analytical result performed repeatedly on a homogeneous sample without reference to the agreement of the average result with the true value of the observed value[3]. The analyst should be aware of methods for evaluating precision and accuracy as well as the factors that can influence the reliability of a result. In geothermal operations, sampling deficiencies can be a common source of apparently divergent analytical results. It is important, therefore, to insure that analytical techniques are not deficient so that sources of divergent results can be properly evaluated.

The basic technique for establishing accuracy and precision of an analytical technique is to perform repetitive analysis of standard solutions of known composition. The statistical methodology for evaluating analytical precision and accuracy are described in detail in Refs. 2-6. The more elabor-

ate statistical methods, such as the method of standard additions, are needed for complex brines that have strong interactions among components. The charge and mass balance should always be computed for a quantitative analysis of a liquid sample. The charge balance indicates the agreement between total anions and total cations in a sample. The mass balance indicates the agreement between total dissolved solids based on the sum of measured anions and cations and the measured value of the total dissolved solids.

II-4-7. Charge Balance

Theoretically, the difference between the sum of anions and the sum of cations, expressed in units of meq/l must be equal to zero. Deviations from the theoretical balance occur because of analytical variations. Obviously, accurate assignment of electrical charge must be made to the dissolved species in the sample. The analysis must also be complete so that no major species are ignored in the calculation of charge balance. The charge balance does not include dissolved silica or any other components present in solution as neutral species. Uncharged species, however, are included in the calculation of the mass balance. The decision as to what constitutes an acceptable analysis is based on repetitive analysis of standard solutions and application of basic statistical procedures. If one assumes a normal distribution for a sequence of repetitive analyses, the deviation from the mean can be evaluated by the calculation of standard deviation:

In a normal distribution, 99.70% of the measurements will lie within three standard devitions (3σ) of the mean (Figure II-6). The 3σ criteria can then be used as an indicator of goodness of an analytical result. In similar fashion the 95% confidence interval can be used as the acceptance criteria:

$$\bar{x} \pm t\sigma\sqrt{n} \qquad \text{(II-2)}$$

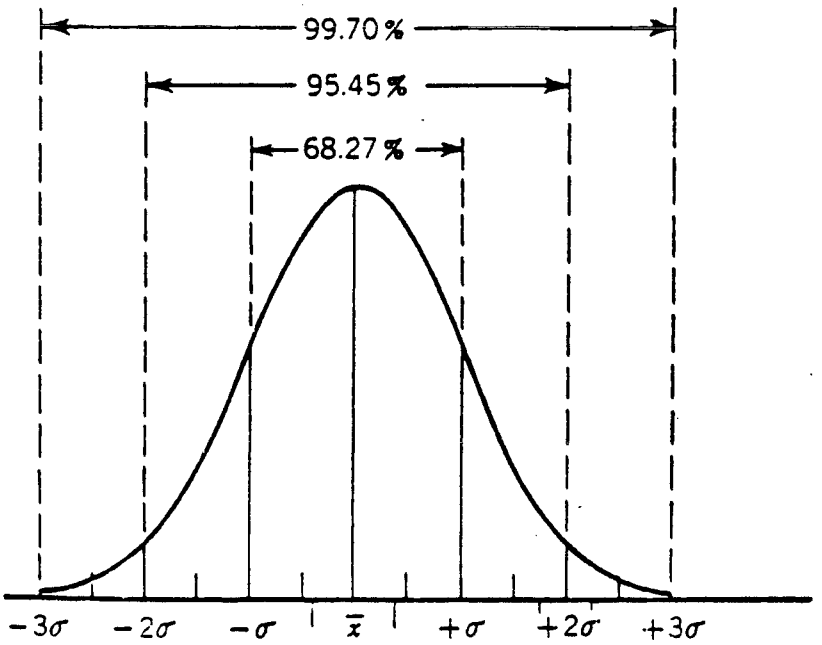

Figure II-6. Gaussian or normal curve of frequencies. (From Ref. 3).

n	*t*
2	12.71
3	4.30
4	3.18
5	2.78
10	2.26
∞	1.96

Table II-2. The use of compensates for the tendency of small numbers of samples to underestimate the variability. (From Ref. 3).

where values of t are summarized in Table II-2. An application of statistical procedures to charge balance data is useful. For general assessment of the reliability of a series of analytical results. This type of assessment presupposes that the analytical uncertainties associated with the determination of each dissolved species present in a sample are known. If one is evaluating a brine solution containing many dissolved constituents, then the suitability of the analytical techniques employed for characterization of samples should have been established based on repetitive analyses of standard brine solutions. The calculated statistical criteria are then based directly on the uncertainties of the analytical techniques that will subsequently be used to characterize field samples.

To facilitate comparisons of a large number of analyses, the charge balance can be defined as the ratio of the sums of the anions and cations as follows[1]:

$$\text{Charge Balance} = \frac{\varepsilon \text{ anion concentrations (meq/l)}}{\varepsilon \text{ cation concentrations (meg/l)}} \qquad \text{(II-3)}$$

A perfect charge balance would be indicated by a value of 1.00.

II-4-8. Mass Balance

The mass balance is, by definition, the difference between the value of measured total dissolved solids and the sum of the measured dissolved species in an analyzed sample. For convenience, the mass balance can be expressed as a ratio[1]:

$$\text{Mass Balance} = \frac{\text{measured total dissolved solids (mg/l)}}{\text{total dissolved species (mg/l)}} \qquad \text{(II-4)}$$

All dissolved species, including silica, are considered in the calculation of the sum of measured dissolved species. Samples which contain large fractions of volatile components, such as bicarbonate or ammonia that may be lost during analysis can cause the calculated value of the mass balance to be less than 1.00. When evaluating the cause of deviations the presence and effect of volatiles should always be considered. For example, volitization of NH_4 (ammonium) may result in the loss of an equivalent amount of bicarbonate. Silica (SiO_2) will retain two molecules of water after dehydration of the sample. An important source of error in the derivation of a mass balance is also due to inaccurate measurement of total carbonate. The inaccuracy in measurement may stem from delay in analysis from the time the sample was first collected. For these reasons, the mass balance is best considered as an index of sample complexity and the analytical reproducibility.

II-4-9. Data Reporting Formats

Modern analytical instrumentation for the quantitative analysis of samples such as the Inductively Coupled Plasma Spectrometer (ICP) can rapidly generate prodigious amounts of data. On a long duration field project the amount of analytical data for liquid and solid samples can rapidly grow to the point where real problems can arise in summarizing the data in a format that best illustrates important relationships. An analyst has three primary options in considering the manner in which data will be presented:

II-4-9a. Variation Diagrams can be develped which illustrate the changes in dissolved species concentration as a function of time (Figure II-7). This type of data presentation might be used to show fluctuations that could be a result of changes in facility operating parameters or actual fluctuations in reservoir fluid composition. The utility of a time variation data display will depend to a large extent on the amount and frequency of sample collection in

comparison to the duration of the field program. For example, a sampling interval of once per day may be perfectly satisfactory for a continuous three month field test, but totally unsatisfactory for a field test of three days duration. A disadvantage of the time variation diagram data display is that it is difficult to evaluate the quality of a given analysis since several diagrams would be needed to display all of the analytical data for a given sample. It would also be difficult for anyone desiring to know actual absolute values for dissolved species concentrations to obtain this information since these values would have to be interpolated from the time variation plots. The time variation plot is an excellent vehicle for illustrating selected time dependent changes in a few dissolved species, but a more thorough method of reporting analytical data should have a higher priority.

II-4-9b. Data Reports - The most obvious way to present analytical data is in the form of separate tables which summarize analytical values for each sample that was analyzed. The major difficulties with this method of data presentation are: 1) the bulk of material that might have to be included in a report, and 2) the difficulty of intersample comparisons. The data reports document the collection phase of the data interpretation program, but the interpretation requires test data be assembled in a more orderly and concise way.

II-4-9c. Integrated Data Tables - A complete tabulation of analytical data for up to 35 samples can be incorporated into a single presentation as illustrated in Figure II-8. This matrix format provides comprehensive data on important chemical and physical properties of liquid samples. Charge balance data is incorporated into the table. Mass balance data could also be included in the format. The obvious advantages of this format for the presentation of

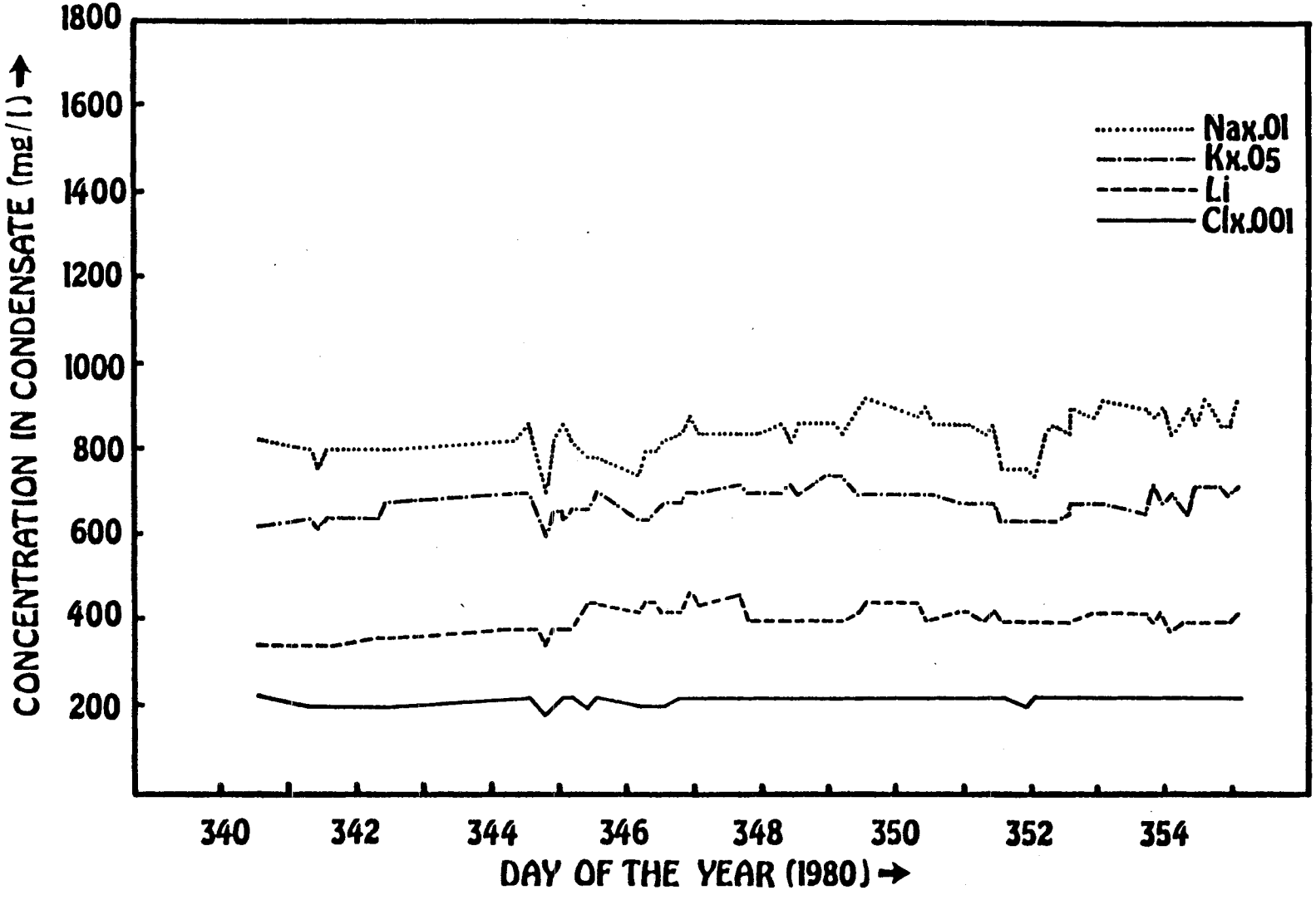

Figure II-7. Variation diagram illustrating fluctuations of four dissolved species in a hypersaline geothermal brine during a 15.5 day operating period (From Ref. 7).

Figure II-8. An Integrated Analytical Data
All values are in units of mg/

Quantitative Chem. Sample Number	1001	1002	1003	1006	1012	1013	1029	1031	1032	1034	1038	1108	1113	11178	1119	1121	1123
Date (1982)																	
Time																	
pH																	
Total Dissolved Solids ($x10^5$ µg/g)																	
Suspended Solids																	
Density (g/cc)																	
Temperature (°C)																	
Total Bicarbonate Alkalinity (as $CaCO_3$) To pH 5.1																	
To pH 4.8																	
To pH 4.5																	
To pH 3.7																	
Cl^- ($x10^5$)																	
PO_4																	
Na																	
K																	
Ca																	
Mg																	
Fe																	
Al																	
SiO_2																	
B																	
Li																	
Sr																	
Zn																	
Ag																	
As																	
Au																	
Ba																	
Be																	
Bi																	
Cd																	
Ce																	
Co																	
Cr																	
Cu																	
La																	
Mn																	
Mo																	
Ni																	
Pb																	
Sn																	
Sb																	
Te																	
Th																	
Ti																	
U																	
V																	
W																	
Zr																	
Total Cations (meq/L)																	
Total Anions (meq/L)																	
Percent Deviation																	

a) Species not detected are indicated by ND

Species not analyzed are indicated by --

l Data Table Format.
of mg/l unless otherwise indicated.[a]

1123	1125	1127	1129	1142	1150	1153	1155	1159	1164	1173	1181	1182	--	1185	1190	1205

large amounts of analytical data are: 1) interrelationships between a large suite of samples is easily accomplished, 2) the quality of the analyses can be determined in terms of the mass and charge balances, 3) anomalies in certain dissolved species can readily be detected, 4) the space in a report required for the analytical data is greatly minimized, and 5) the progression from left-to-right across the matrix is time-related.

Preparation of an integrated data matrix is somewhat more involved than the simple tabulation of sample data in separate tables. This data presentation format was used extensively in the reporting of analytical data obtained in conjunction with a one month continuous flow test at the South Brawley Geothermal Field in Southern California[8]. The tables were first prepared using large sheets of graph paper (22 inches x 16 inches). Data entries were made by hand with a pencil. Anomalies in the data were evaluated and in some cases analytical difficulties were discovered. Where necessary, samples were reanalyzed. The rough draft of the table was then re-typed in four parts. Each portion of the table after proofing was photographically reproduced and the four sections of the tables were then cut out and pasted up as a single large sheet. The final copy of the table was prepared by a commercial offset printing service using paper stock with dimensions of 11 inches x 17 inches.

Subsequent data evaluation and interpretation may require consideration of ratio of selected dissolved species, calculated chemical geothermometer data, etc. These activities may benefit from development of secondary data matrices that have the same ordering of columns as the primary data matrix (Figure II-8).

II-5. Sampling Methods

Excellent summaries of liquid sampling techniques are provided in Refs. 1 and 3. A similar discussion for solid samples or sludge samples is provided in Ref. 2. This material should be carefully reviewed before designing a field program if the personnel in charge of the chemical monitoring effort are not experienced or otherwise familiar with geothermal operations. The critical aspects of collection of geothermal samples involves knowledge of the precollection history of the sample. That is to say, that knowledge about the total steam flash upstream of the sampling point is essential if the significance of the analytical data is to be fully recognized. Major objectives of geothermal sampling programs are the definition of reservoir fluid composition and discovery of time-dependent changes in reservoir fluid composition that might occur during a prolonged well test. Neither of these objectives can be realized if the thermodynamic state at the sampling point is unknown.

Sample preservation is also critical to the overall goals of an analytical program. Hydrolytic reactions involving primarily dissolved iron can cause precipitate formation in samples within hours of collection. Failure to dilute samples while they are being collected can result in the precipitation of dissolved silica. The analyst should also be aware that certain types of analyses must be performed soon after collection of samples to avoid loss of volatile or reactive species. Special techniques are also required to adequately collect and subsequently analyze gases.

II-5-1. Sample Collection

The collection of high pressure/temperature samples for analysis requires special techniques to insure the integrity of the sample and the safety of personnel. The basic methodology for obtaining liquid or gas samples is illustrated in Figure II-9[1]. A high pressure/temperature sidestream is ob-

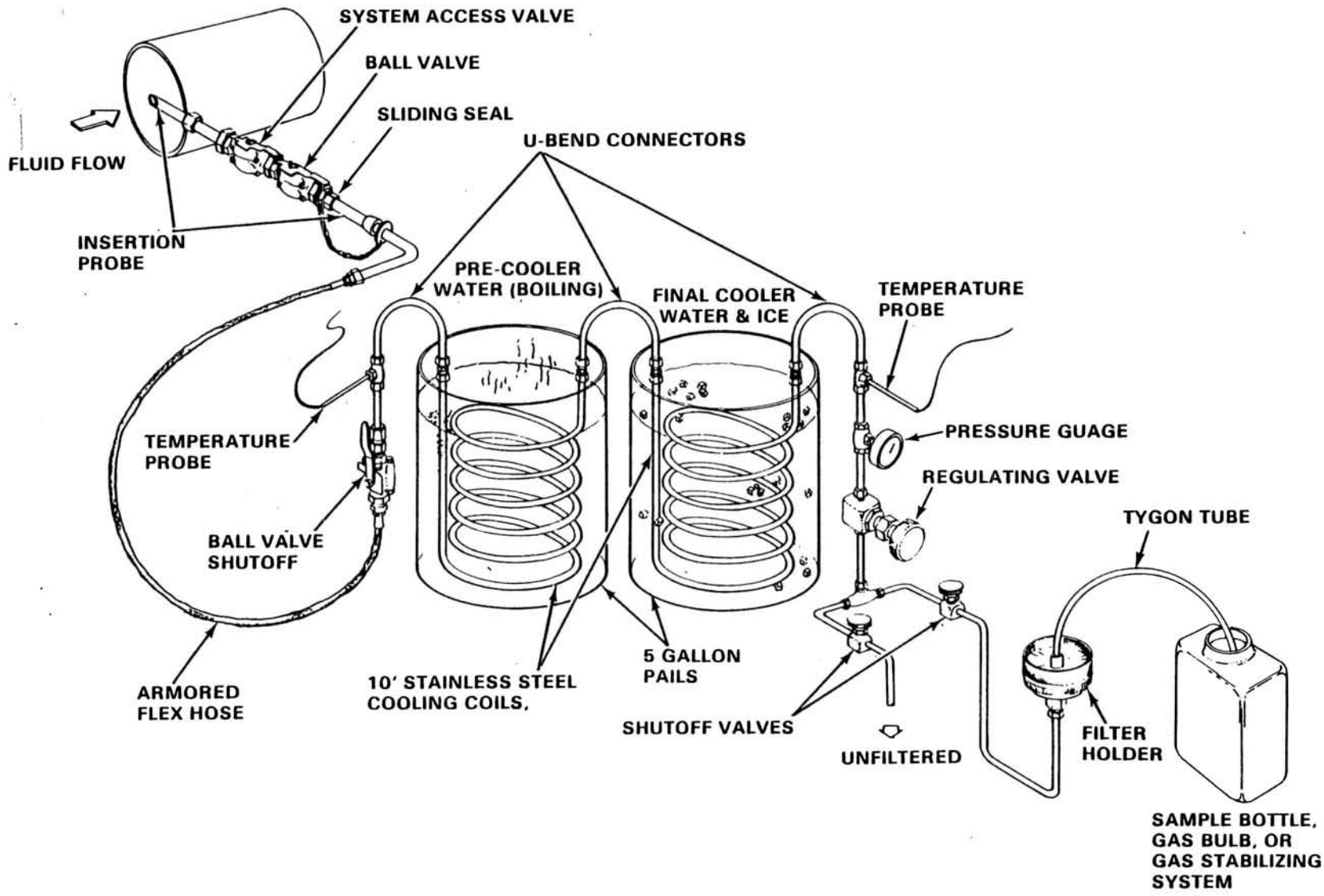

Figure II-9. Geothermal double coil sampling system (From Ref. 1).

tained from an insertable sampling probe and valve assembly. Hot, pressurized fluid is directed to the cooling system using a Teflon-lined, stainless steel flex hose. The hot fluid is then passed sequentially through boiling water and ice bath coolers to quench the fluid. The cooled liquid can then be sampled with or without membrane filtration.

The basic design of Figure II-9 is a workable and reliable system for sampling hot, pressurized systems. The design as shown, however, can be modified to improve convenience of use and safety. The insertable probe offers advantages even when sampling a single phase (liquid or gas) stream by minimizing wall effects. However, a fixed probe of appropriate geometry can be used in most instances. A conventional sampling valve with appropriate fittings to mate with the flex hose can then be attached to the fixed or insertable probe. The valve should be located toward the bottom of the flow line and it should be ideally angled upward at about a 45 degree angle. The greatest utility of an insertable probe would be in conjunction with the sampling of a two phase process stream. However, even in the case of a two phase stream, the use of a static probe does not really represent a great problem. If the sampling location is a horizontal pipe, and if the static probe is inserted upward at a 45 degree angle from the bottom of the pipe so that the tip of the probe is centered in the lower portion of the pipe up about one third the diameter of the pipe from the bottom of the pipe, it should be possible to obtain reasonable samples for analysis. The problem with the insertable probe is that one does not know what setting of the probe yields the best sample. Therefore, it would be necessary to obtain many samples at various probe settings and average the results. It is unlikely that the reliability of the data would be much of an improvement as compared

to samples taken using a static probe that had been located well within the single phase liquid region. The best step that could be taken to improve reliability of samples is to provide the facility for obtaining a single phase sample. This can be accomplished by sampling immediately downstream of a large separator or by use of a small sampling separator such as the Webre unit described in Ref. 9.

The safety aspects associated with the sampling system of Figure II-9 should be carefully considered. Use of stainless steel armored flex hose represents a real danger in some high pressure/temperature sampling systems. Experience has shown that the armore can fail with simultaneous catastrophic failure of the inner Teflon lining[a]. The problem is caused by wetting of the armore by chloride-rich geothermal fluid and subsequent rapid failure due to cracking of the strands of stainless steel that are used to form the armore. Experience at a hypersaline geothermal resource in Southern California indicated that flex hoses used to sample high pressure/temperature single phase brine and noncondensable gases failed after about 10 days of use. The failures were undoubtedly caused by the wetting of the stainless steel by hypersaline brine spray. Prudence would suggest that safe use of this type of hose necessitates use of a protective covering for the flex hose or use of some other more corrosion resistant armore material. The Hose Products Division of Parker Fluid Connectors (Wickliffe, Ohio) can provide a firesleeve for flexhose. The sleeve is flexible and has a thermal resistance beyond 500°F. End connectors and assembly tools to seal the firesleeve at the ends of the flexhose are also available.

The sampling of two phase brine/gas stream suggests the possibility of obtaining noncondensable gases at the sample collection point downstream of

the membrane filter. Noncondensable gases with a relatively high proportion of hydrogen sulfide could alter the composition of collected brine samples by the precipitation of metal sulfides. The safety aspects should also be considered since the operators of the smpling train would be exposed periodically to hydrogen sulfide gas. A simple means of segregating noncondensable gases from the quenched liquid stream is to incorporate a small low pressure separator in the sampling system downstream of the coolers. A device with this facility is described subsequently. A sampling train equipped with a separator and used in conjunction with either an insertable probe or two sample taps located in the single phase (liquid and gas) positions along the bottom and top, respectively, of a horizontal flow line would offer the ability to segregate samples for subsequent analysis. The same type of sampling train would also be of obvious utility in the characterization of single phase steam and noncondensble gas flows. It should be emphasized again, however, that the sampling of a two phase mixture at in-situ conditions using a Webre separator or similar device is preferable to the use of a sampling train that permits interaction of quenched liquid and gas.

II-5-2. Brine and Gas Sampling Train

Figure II-10 illustrates the appearance of a brine and gas sampling train based on Battelle, PNL design of Figure II-9. This sampling system was built by Terra Tek Research, Salt Lake City, Utah for hypersaline geothermal brine service . The system includes a boiling water heat exchanger coil fabricated from Inconel 600 to provide superior corrosion resistance. The heat exchanger coil was placed in a stainless steel pot of five gallon capacity. The second stage, ice bath cooler was constructed using a stainless steel heat exchanger contained in a five gallon capacity polyethylene bucket. The ice bath cooler was constructed with stainless because of the low pressure/temperature oper-

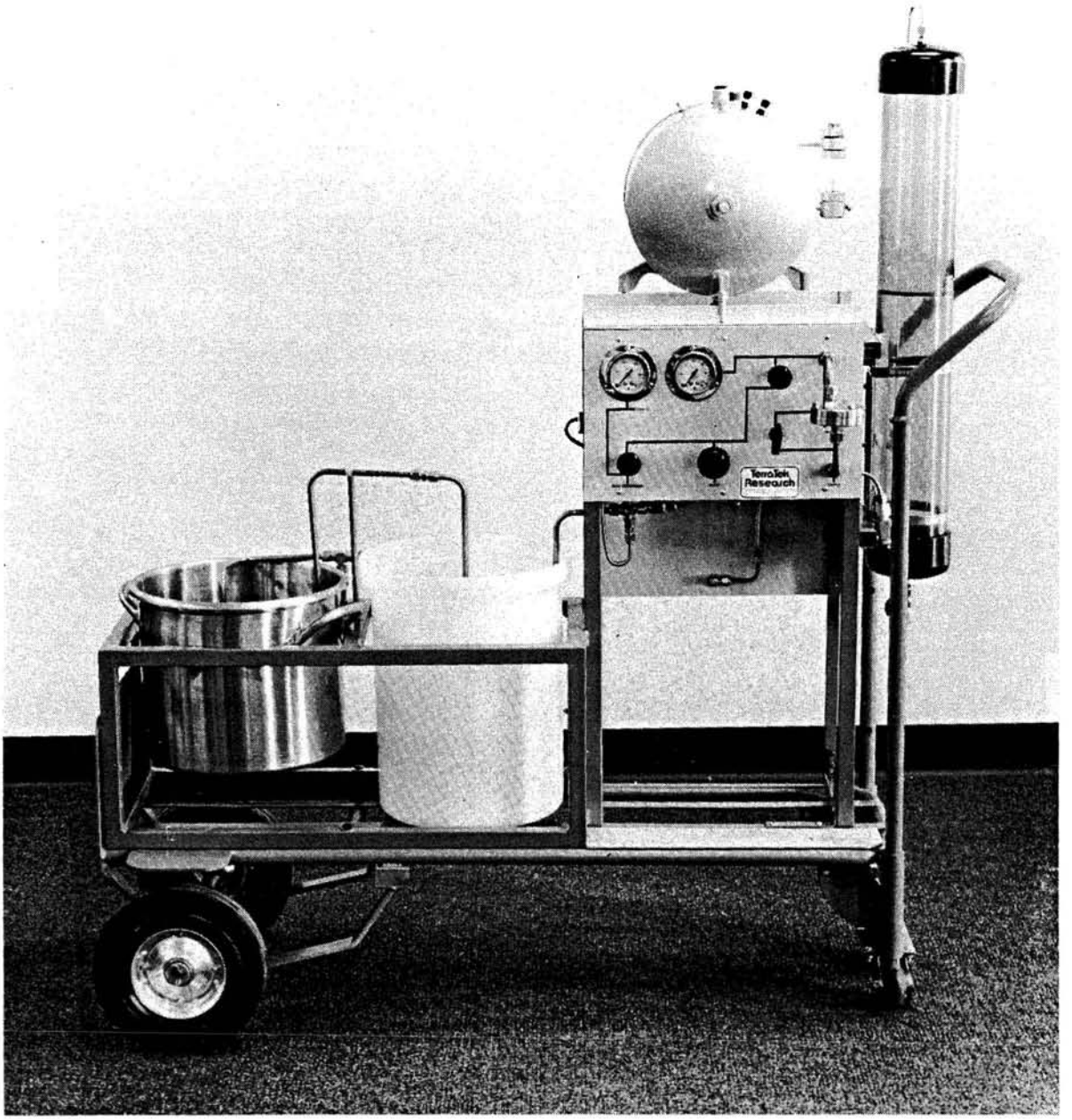

Figure II-10. Terra Tek Research Brine and Gas Sampling Train. The long, vertically-mounted transparent tube located on the right side of the unit is a tongential entry separator.

ating conditions of this unit. All tubing and valving on the downstream portion of the sampling train were built using stainless steel hardware. Needle-type control valves should not be used to sample a brine with a high scale formation tendency if plugging problems are to be avoided. Valve plugging can occur within seconds of exposure to, for example, a hypersaline geothermal brine. Large orifice valves should be used and all tubing, including the heat exchangers, should have a 1/4 inch I.D. at the minimum.

The long, transparent tube located on the right side of the sampling train illustrated in Figure II-10 is a tangential entry separator constructed from 4 inch diameter thick walled plastic tubing. The endcaps should be threaded on to eliminate the potential for leaks. In similar fashion, the pass through fittings on the endcaps should be threaded in to avoid leaks. Gas samples are collected using a bomb connected to the top end of the separator. Condensate or entrained brine is collected from a drain located on the bottom of the separator. The separator can be eliminated from the sampling train if sampling is restricted to single phase brine. The front panel contains an in-line high pressure membrane filter holder to permit the collection of prefiltered and quenched liquid samples. A useful modification to the sampling train shown in Figure II-10 would be to substitute larger diameter pneumatic tires in place of the tires shown to increase the maneuverability of the unit.

Operation of the sampling train is straightforward: The system is connected to a sampling valve using a length of flex hose (of adequate corrosion resistance). The sampling valve is slowly opened and flow is admitted to the coolers. It is most convenient to use block ice, if available from local suppliers, rather than crushed ice or ice cubes in the ice bath cooler. The liquid flow should be maintained to waste for a few minutes prior to sample

collection to insure that the train has been adequately cleaned. Prefiltered samples should be collected for quantitative chemical analysis. If the membrane filter (0.45 micron pore size) has been preweighed, then suspended solids collected by the filter can be weighed after careful washing and drying to yield an accurate measurement of the concentration of suspended solids in the sampled fluid provided that the total volume of filtered fluid has been measured. Immediately before sampling, a vacuum should be pulled on the membrane filter to purge it of any trapped air. A hand operated vacuum pump is convenient for this purpose. Alternatively, a purge valve can be installed on the top of the membrane filter holder and trapped air can be purged by passing a fluid stream through the purge valve. Isolation valving would have to be installed upstream and downstream of the filter to enable use of a vacuum pump. Liquid purging requires the use of one downstream isolation valve. It is important to operate the sampling train at a throughput rate that produces quenched liquid well below its boiling point to avoid altering collected sample compositions by evaporative losses.

Sampling of steam with noncondensable gases is also straightforward. The condensate sample is collected from the bottom of the sampling train separator. Gas samples at essentially ambient atmospheric conditions are collected in Supelco or equivalent gas chromatography glass, gas sampling bulbs with greased glass stopcocks (Figure II-11). A bulb with a volume of 250 ml is adequate. The bulb should be evacuated prior to use and then purged with noncondensable gas for at least 10 minutes prior to the trapping of a sample. The glass sampling bulb can preserve hydrogen sulfide gas for several days to several weeks. Thus, it is possible to consider post-collection analysis of noncondensable gas samples at a distant analytical facility. For safety purposes, the gas bulb should be placed in a metal cylinder during the sample

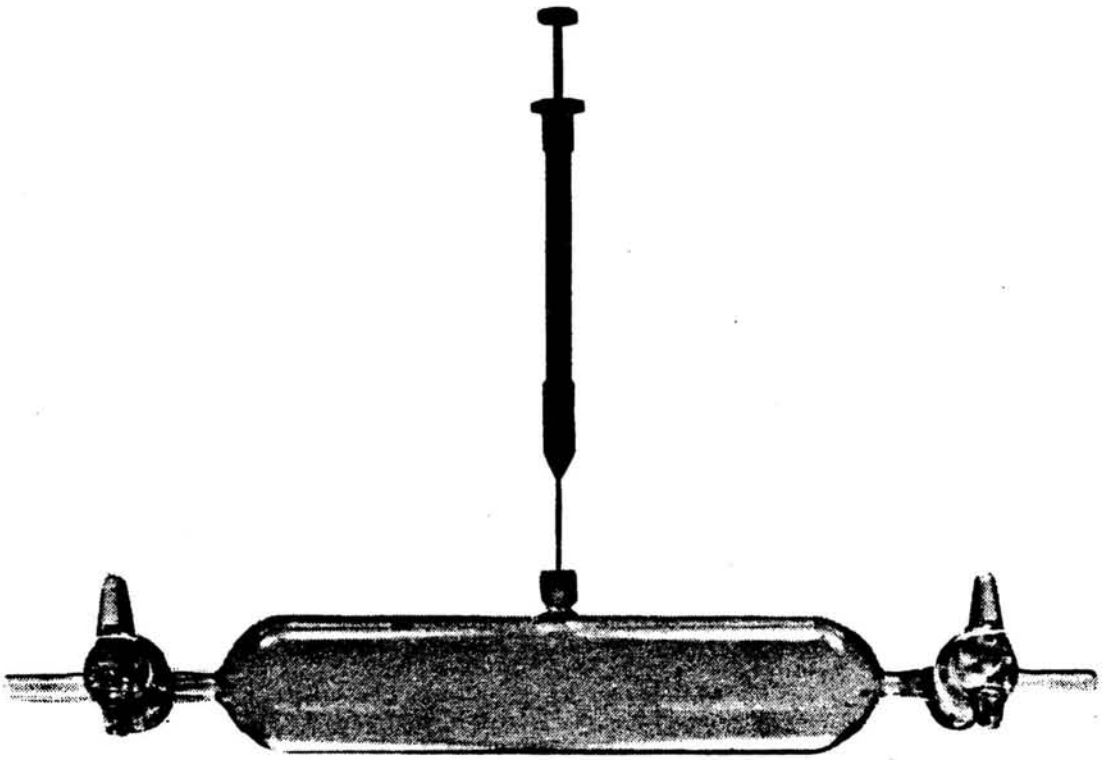

Figure II-11. Gas sampling bulb. These glass bulbs make it conveninet to trap a gas sample, and to subsequently remove an aliquot through the plug-type septum.

collection process. The trapping of gas samples at 10-12 psig can be safely accomplished using the Supelco bulbs. At the time of analysis, the internal pressure in the sampling bulb should be measured and compared to the pressure at the time of collection (with adequate regard to difference in ambient temperature and barometric pressure) to demonstrate that leakage of sample has not occurred. Alternatively, one can collect gas samples in citrate-type glass bottles. A sampling procedure is described in Appendix II-1.

An important task, as described in detail in a subsequent section, is the measurement of total noncondensable gas in a geothermal reservoir. The sampling train equipped with a separator provides a very simple but accurate method for accomplishing this task. Condensate volume is measured by simply draining the separator liquid contents into a volumetric cylinder. The total gas volume can be measured using either a wet test meter or a calibrated rotometer.

If a sampling program is to be set up for both geothermal liquid and gas samples, it will, in most instances, be preferable to use separate liquid and gas sampling trains. This precaution will eliminate the possibility of contamination of low salinity condensate samples by higher salinity residual brine or water. Sampling trains should be cleaned after use. Steam condensate is an excellent source of cleaning solution if available. An auxiliary peristalic pump can be used to clean sampling trains with potable water. The Horizon Ecology Corp. of Chicago, Illinois[1] supplies a suitable battery operated pump. Certain sample preservation techniques for noncondensable gases requires that noncondensable gases be bubbled through preserving solutions. If insufficient pressure is available, the portable peristalic pump can be used to advantage. The pump can also be helpful when insufficient pressure is available to filter samples.

II-5-3. Webre Separator

To reiterate, the best method for characterizing high temperature/pressure two phase discharge is to sample the separated liquid and gas flows produced by a full scale separator. In the absence of a large separator, the next best two phase sampling procedure is based on the use of a small sampling separator. The Webre cyclone separator (Figure II-12) described in Ref. 9 has been used for a number of years with great success. The unit may be used to sample discharges over a pressure range of about 22 to 440 psia and an enthalpy range of 190-475 cal/g. If actual discharge enthalpies are lower or in excess of the nominal operating range of the sampler, it is not possible to obtain cleanly separated water and gas samples at one specific setting of the valves. In these instances, the sampler is adjusted to produce either pure steam or pure water. Detailed operating instructions for the Webre separator are described in Ref. 9.

II-5-4. Downhole Samplers

In some instances, a production well taps several zones which produce geothermal water and gas. The use of a downhole sampler affords the opportunity of obtaining samples at known depths. Such samples can be used to identify and characterize production zones. The samplers are wireline tools which are lowered into a well by a cable and winch assembly. In most instances, it is desirable to flow the well during sampling. In hot, deep geothermal wells, the use of a downhole sampler entails some risk of damage to the well if the tool becomes stuck or the wireline breaks. Breakage of the wireline is a real concern, especially in the case of wells which produce highly corrosive brine. Sticking a tool is also a real possibility.

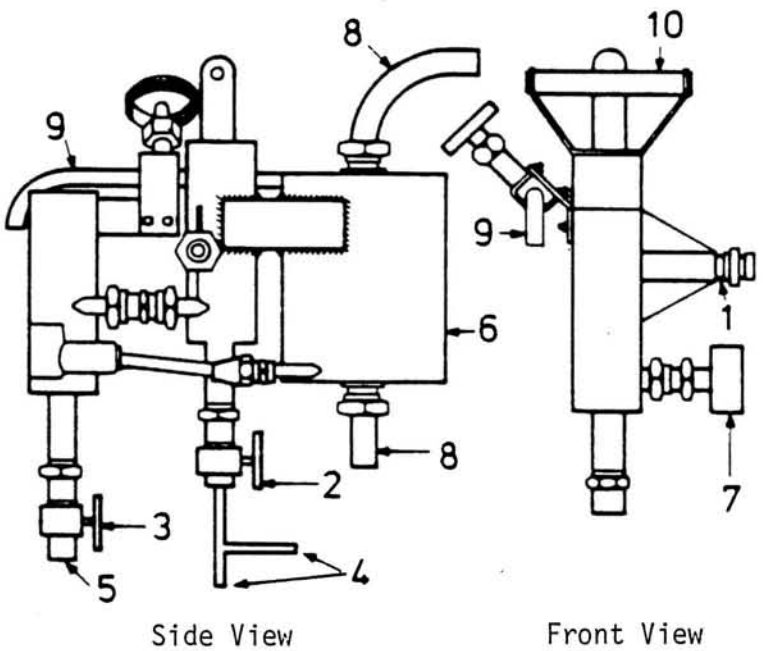

Figure II-12. Webre cyclone separator for collecting steam and water samples under pressure from a discharging geothermal well. 1, steam-water inlet; 2, valve for controlling steam discharge on first separator; 3, valve for controlling steam discharge on second separator; 4, dry steam outlet on first separator, 5, dry steam outlet on second separator; 6, separated water cooler; 7, pressure gage fitting; 8, cooling water inlet and outlet; 9, outlet for cooled separated water; 10, handle. (From Ref. 9).

The decision to attempt to retrieve a downhole sample is usually addressed on a case by case basis. Several samplers are available and commercial wireline serices can run downhole sampling tools. A basic downhole sampler is illustrated in Figure II-13. This device is fully described in Ref. 9.

II-5-5. Miscellaneous Types of Samplers

Devices designed to sample solids and sludge are described in Ref. 2. At times it may also be necessary to sample the discharge from a pipe that is delivering brine, for example, to a holding pit. It may not be possible to conveniently reach the discharge because of distance or the possibility of burning ones hand when attempting to sample a hot fluid with a hand held bottle or beaker. The extended reach dipper sampling device illustrated in Figure II-14 is simple to fabricate and indispensable under the right circumstances for obtaining either sludge, solids or liquid samples.

Sampling sludge from a sedimentation tank may on occasion be necessary. The preferred way to obtain this type of sample is by means of sampling ports installed at varying heights above the bottom of the tank. In the absence of such ports, the sampling devices shown in Figures II-15 and 16 can be used. Both types of devices can be obtained from commercial suppliers. The Coliwasa should be built using transparent plastic tubing to facilitate visual estimation of suspended solids concentrations as a function of height above the bottom of a sedimentation tank. This type of data is quite useful in determining how well a sedimentation tank is performing.

II-6. Geothermal Brine Characterization

For the sake of convenience, the term brine will be used in reference to the characterization of liquid samples other than steam condensate. In most

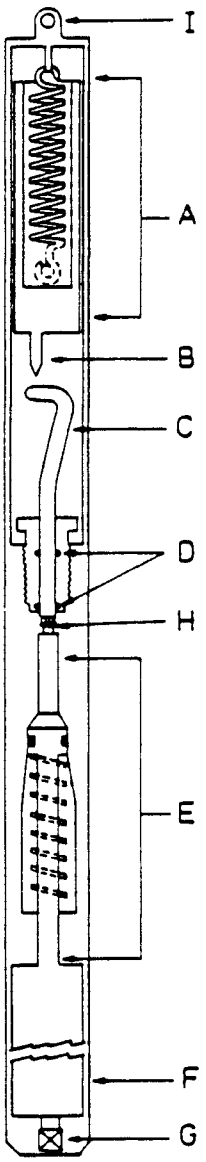

Figure II-13. Downhole sampling bottle. A, inertia mechanism; B, striker; C, break-off tube; D, seal gland for break-off tube; E, nonreturn valve (valve stem is of triangular cross section, allowing transfer of sample fluids); F, sample vessel; G, sample release valve; H, filters; I, wire suspension. (From Ref. 9).

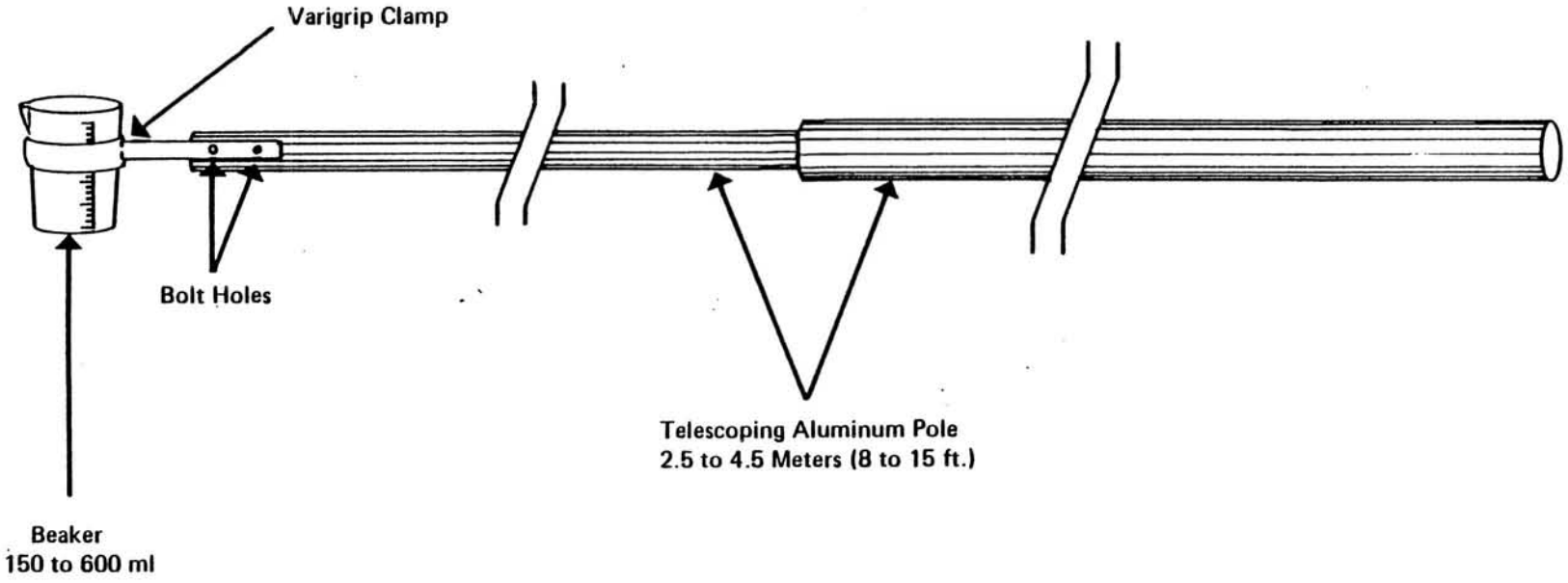

Figure II-14. Extended reach dipper sampling device (From Ref. 2).

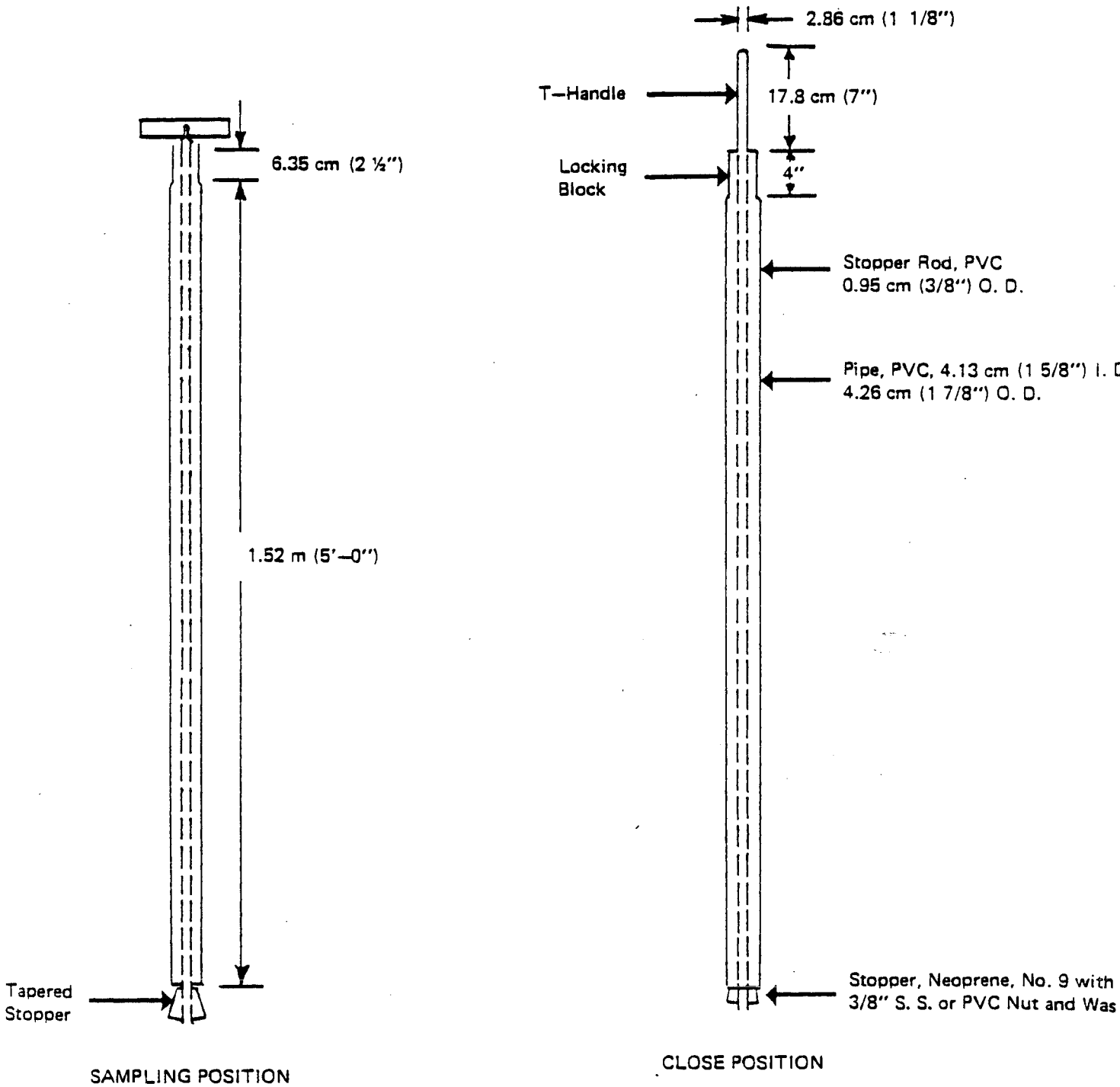

Figure II-15. Composite liquid waste sampler (Coliwasa) (From Ref. 2).

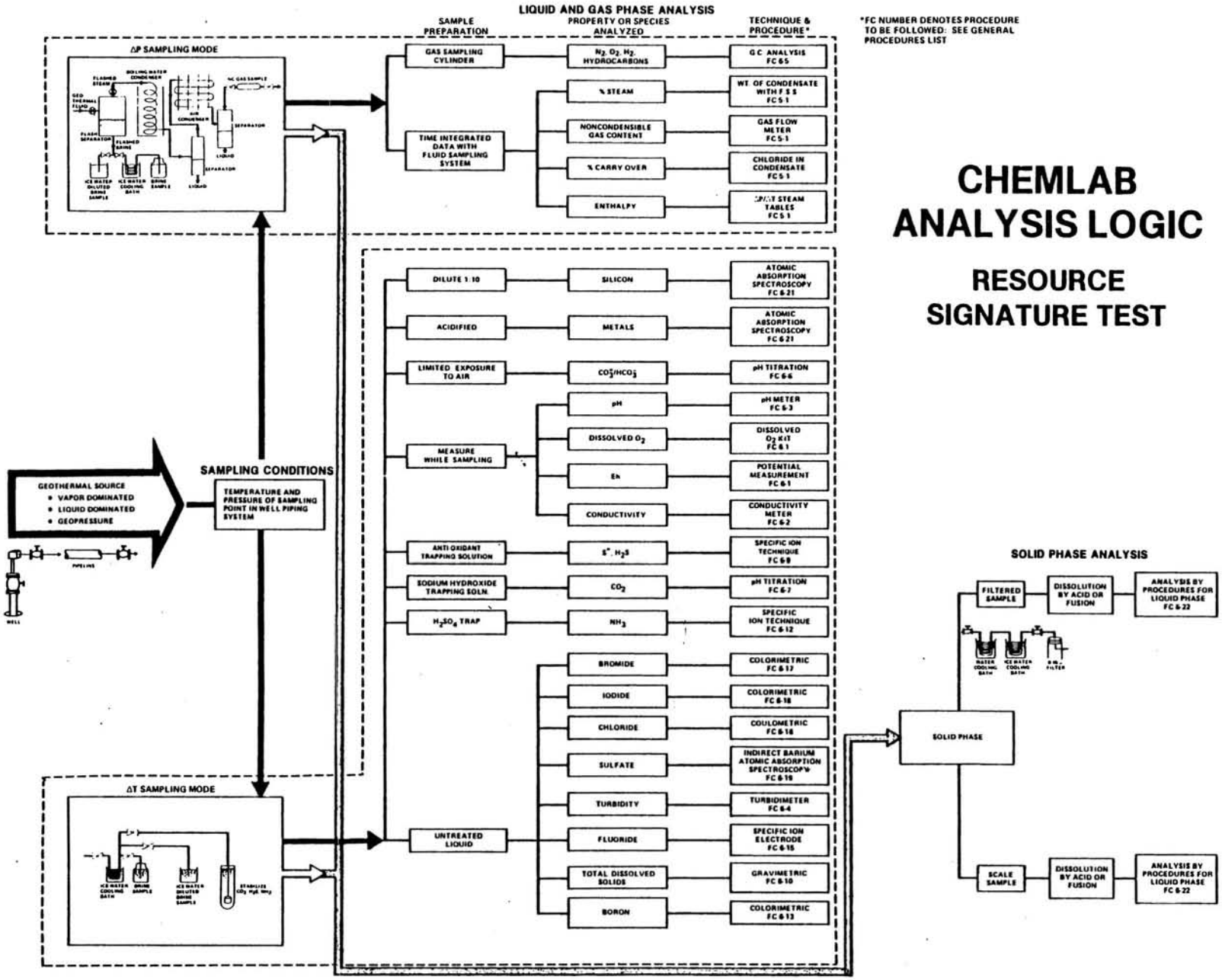

Figure II-16.(From Ref. 13).

instances, geothermal waters have a salinity in excess of potable water (greater than ~1000 mg/l). Resources with a sufficiently elevated temperature to be considered for electric power production may encompass a broad range of brine salinity. The low salinity brine may have a total dissolved solids (TDS) content that falls between 1000 to about 30,000 mg/l. High salinity or hypersaline brine have TDS values ranging between 100,000 to 300,000 mg/l. Moderate salinity brines have TDS values intermediate between the low salinity and high salinity brines. The characterization of a geothermal brine involves several steps which including sampling, sample preservation, determination of physical properties and determination of chemical properties.

II-6-1. Sampling a Brine Source

Sampling devices are described in Section II-5. Adequate characterization of a brine will require that a requisite volume of sample be obtained consistent with the analytical requirements. Reference to Figure II-1 illustrates in a general sense, volumetric requirements for various kinds of analyses. Figure II-16 illustrates a similar sampling and analytical scheme utilized by the Electric Power Research Institute (EPRI) Mobile Laboratory. Brine samples are obtained using a dual cooler device. Gas samples are obtained using a combination of separators and boiling water and air condensers. The appropriate amount of sample for a particular test will depend to a large extent on the actual concentration of the dissolved species or the chemical parameter which is to be determined. For example, the measurement of TDS in a clean steam condensate sample might require several hundred ml of sample to achieve a desired accuracy. The same level of accuracy could most probably be achieved for a hypersaline brine with only 1 ml of sample. It should be borne in mind that obtaining a representative sample is the first step in obtaining an accurate analytical result. In the case of an analytical procedure that

required a sample size of 1 ml, it would obviously be best to obtain a large sample (>100 ml) from which a 1 ml aliquote was subsequently taken for analysis than to attempt to take a 1 ml sample from the brine source.

Depending upon the type of characterization a particular sample is to be subjected to, preservation and/or filtration of the sample may or may not be needed. The guidelines summarized in Figure II-1 cover most contingencies. In general, samples taken for subsequent quantitative analysis must be both prefiltered and preserved. Samples taken for TDS or density determinations should be prefiltered, but not preserved. In subsequent portions of this section, recommended procedures for sampling, preservation and subsequent analysis of geothermal brine will be described. Essentially all of the recommended procedures have been successfully implemented in the characterization of hypersaline geothermal brine[8] and thus should be relevant to almost any geothermal brine or water.

The interested reader should review a compilation of potentially applicable analytical techniques for the characterization of geothermal fluids and gas by Watson[10] and relevant material in the Geothermal Resources Council Technical Training Course No. 6[11].

II-6-2. Sample Stabilization

Special handling requirements for liquid analysis are summarized in Table II-3. Polyethylene bottles can be used exclusively for geothermal liquid samples. Unstable species should either be determined in the field immediately after sampling or preserved according to standard procedures[1-4]. Silica-bearing samples must be diluted at the time of collection to prevent post-collection precipitation. If field anlytical facilities are avilable, the analytical characterization program should have capabilities for the following types of evaluations:

TABLE II-3. SUMMARY OF SPECIAL SAMPLING AND SAMPLE HANDLING REQUIREMENTS

Determination	Container†	Minimum Sample Size, *ml*	Storage and/or Preservation
Acidity	P, G(B)	100	24 hr; refrigerate
Alkalinity	P, G(B)	200	24 hr; refrigerate
BOD	P, G	1,000	6 hr; refrigerate
Boron	P	100	—
Carbon, organic, total	G(brown)	100	Analyze as soon as possible, refrigerate or add HCl to pH≤2
Carbon dioxide	P, G	100	Analyze immediately
COD	P, G	100	Analyze as soon as possible; add H_2SO_4 to pH≤2
Chlorine dioxide	P, G	500	Analyze immediately
Chlorine, residual	P, G	500	Analyze immediately
Chlorophyll	P, G	500	30 days in dark; freeze
Color	G	500	—
Cyanide	P, G	500	24 hr; add NaOH to pH 12; refrigerate
Fluoride	P	300	—
Grease and oil	G, wide-mouth, calibrated	1,000	Add HCl to pH≤2
Iodine	P, G	500	Analyze immediately
Metals	P, G	—	For dissolved metals separate by filtration immediately; add 5 ml conc HNO_3/l
Nitrogen			
Ammonia	P, G	500	Analyze as soon as possible; add 0.8 ml conc H_2SO_4/l; refrigerate
Nitrate	P, G	100	Analyze as soon as possible; add 0.8 ml conc H_2SO_4/l; refrigerate
Nitrite	P, G	100	Analyze as soon as possible; add 40 mg $HgCl_2$/l and refrigerate or freeze at -20 C
Organic	P, G	500	Analyze as soon as possible; refrigerate or add 0.8 ml conc H_2SO_4/l
Odor	G	500	Analyze as soon as possible; refrigerate
Oxygen, dissolved	G, BOD bottle	300	Analyze immediately
Ozone	G	1,000	Analyze immediately
Pesticides (organic)	G(S)	—	—
pH	P, G(B)	—	—
Phenol	G	500	24 hr; add H_3PO_4 to pH≤4.0 and 1 g $CuSO_4 \cdot 5H_2O$/l; refrigerate
Phosphate	G(A)	100	For dissolved phosphates separate by filtration immediately; freeze at ≤-10 C and/or add 40 mg HgCl/l
Residue	P, G(B)	—	—
Salinity	G, wax seal	240	Analyze immediately or use wax seal
Silica	P	—	—
Sludge digester gas	G, gas bottle	—	—
Sulfate	P, G	—	Refrigerate
Sulfide	P, G	100	Add 4 drops 2*N* zinc acetate/100 ml
Sulfite	P, G	—	Analyze immediately
Taste	G	500	Analyze as soon as possible; refrigerate
Temperature	—	—	Analyze immediately
Turbidity	P, G	—	Analyze same day; store in dark for up to 24 hr

*See text for additional details. For determinations not listed, no special requirements have been set: use glass or plastic containers, preferably refrigerate during storage, and analyze as soon as possible.
†P=plastic (polyethylene or equivalent); G=glass, G(A) or P(A)=rinsed with 1+1 HNO_3; G(B)=glass, borosilicate; G(S)=glass, rinsed with organic solvents. (From Ref. 3).

Physical Properties	Chemical Properties
Density	pH
Temperature	Acidity/Alkalinity
Suspended Solids	Chloride
Conductivity	Sulfate/Sulfide
Turbidity	Ammonia
	Dissolved Oxygen
	Total Dissolved Solids

The detailed multi-element quantitative analysis of major and trace species in brine and other liquid samples is accomplished using field preserved samples. The laboratory should, therefore, have sufficient equipment and supplies on hand to facilitate field preservation of samples.

The analyst can accomplish the goals of the field characterization program in many ways. However, in considering a particular analytical procedure one should balance the required level of accuracy for the determination with the degree of difficulty in carrying out the procedure. For this reason the use of HACH portable field equipment and methods is recommended for those tests that must be carried out either immediately or within 24 hours of sample collection. A further advantage of the HACH equipment are the comprehensive HACH water analysis manuals and the use of premixed and prepackaged reagents. The HACH methods are all in accordance with standard practices for water analysis and the use of their portable equipment and prepackaged reagents significantly simplifies field analytical work.

We recommend that the laboratory at the minimum be equipped with a HACH Digital Titrator (16900-01), delivery tubes and the appropriate reagents for chloride and alkalinity/acidity tests. A more comprehensive field analytical capability can be created by use of the HACH DREL series of portable laboratories which contain high quality spectrophotometers and conductivity meters. The units can also be obtained with an integral pH meter. However, we would suggest the use of a separate, high quality laboratory grade pH meter. The

HACH Water Analysis Handbook[12] is keyed to the use of their portable laboratories and prepackaged reagents.

Brine samples should be obtained using procedures and equipment discussed previously. Samples taken for quantitative analysis must be prefiltered immediately before dilution and preservation. Failure to remove suspended particulates will cause erratic analytical results since it is impossible to determine what fraction of the suspended solids, if present, were dissolved by acid preserving solutions. Independent characterization of recovered suspended particulates is easily accomplished. The standard preserving solution for geothermal liquid samples is 1 ml of concentrated reagent grade nitric acid per 100 ml of liquid sample. Total sample volumes can vary from 125 ml to 500 ml depending upon the scope of subsequent analytical characterization. The larger sample volumes provide the opportunity of obtaining a somewhat more representative sample. However, use of a dual cooler sampling train with a high volumetric throughput rate can yield representative samples by virtue of operating a bypass line to waste during the sampling procedure. In many instances, sample volumes of 125 ml will prove to be entirely satisfactory.

The recommended dilution factor for stabilizing dissolved silica is at least 10:1. If an estimate of the silica content of a brine stream is available at the time of sampling, the sample should be diluted to a silica value of 90-100 mg/l. Therefore, it may be appropriate to obtain separate samples for silica analyses to avoid reducing trace element concentrations to below detection limits as might occur by significant dilution of samples. Several methods are available for actually obtaining a stabilized sample. EPRI[13] collects samples in a 500 ml capacity polyethylene bottle which has been prescribed with a 500 ml volumetric calibration. The sample bottle is preloaded with 5 ml of concentrated nitric acid preservative added with a high

precision buret. The geothermal sample is then taken by placing the mouth of the sample bottle directly underneath the quenched brine discharge. During the subsequent laboratory analysis of the sample, the dilution factor due to addition of 5 ml of nitric acid is accounted for. The chemical purity of the dilution water must be known so that blank corrections can be applied to the analytical data. Normally, one would subject a sample(s) of dilution water to the same analytical procedures that are to be applied to the geothermal samples. Hypersaline brines of the Imperial Valley of southern California contain high concentrations of dissolved manganese. These brines should be stabilized with concentrated hydrochloric acid rather than nitric acid to avoid precipitation of manganese.

Alternatively, one can weigh an appropriate amount of preserving solution into a preweighed sample bottle. The geothermal liquid sample is collected as described above and the weight of the liquid sample determined. The equivalent volumes of the preserving solution and brine solution are then obtained from the measured density of each fraction. Other combinations of procedures are obviously possible.

II-6-3. Physical Property Determinations

II-6-3a. Density - Density is defined as the weight of a sample divided by its volume:

$$d = A/v \qquad \text{(II-5)}$$

where: A = sample weight (grams)

v = sample volume (ml)

Specific gravity is dimensionless. It is the ratio of the density of a sample to the density of water at 4°C. Alternatively, specific gravity can be de-

fined as the weight of a sample of known volume divided by the weight of distilled water of the same volume:

$$\text{sp gr} = A/B \qquad \text{(II-6)}$$

where: A = weight of the sample of volume V

B = weight of distilled water of volume V

Accurate determination of specific gravity can be accomplished using a hydrometer or the ASTM Methods D1429, Test for Specific Gravity of Industrial Water. The ASTM method involves an accurate gravimetric determination using a water pycnometer in which a known volume of water is weighed at 60°F. The reported accuracy of this method is ±0.0005. This method can be used to measure density as follows:

1) Preweigh a 10 ml capacity volumetric flask.

2) Fill the flask to the mark with the sample.

3) Reweigh the flask.

Required Calculations:

Weight of Flask + Sample = B
Weight of Flask = A
Weight of Sample = B-A
Density = B-A/10 ml (gm/ml)

The ultimate accuracy of the technique will depend on how well the sample temperature was known. Use of hydrometers with the appropriate measurement range is also an accurate and convenient method for determining specific gravity. An advantage of the hydrometer method is that an analytical balance is not needed. The temperature at which a density or specific gravity measurement was made should always be reported.

The determination of density or specific gravity of a hypersaline brine or a low salinity water with a high dissolved silica content is complicated by precipitate formation at ambient temperature. For example, sodium chloride precipitates from flashed hypersaline geothermal brine at a temperature of 30-35°C. Silica may also precipitate from water after cooling. In hypersaline geothermal brines, dissolved iron will also precipitate upon exposure of the brine to air. In these cases, the sample should be diluted prior to measurement of density.

The following procedure may be used to measure density of a solution which will form precipitates after being cooled to the ambient temperature. The procedure is based on the dilution of the sample with distilled water (referred to as water):

1) Add a known weight of water to a 10 ml volumetric flask.

2) Add a known weight of sample to the volumetric flask.

3) Mix well.

4) Dilute to the mark with a known weight of water.

5) Measure the density of the water.

Required Calculations:

Weight of Flask + Aliquote of Water = A (gm)
Weight of Flask = B (gm)
Weight of Aliquote of Water = A-B = C (gm)

Weight of Flask + Water + Sample = D (gm)
Weight of Sample = D-B-C = E (gm)

Weight of Flask + Water + Sample +
Additional Water = F (gm)
Total Weight of Water = F-B-E = G (gm)

Volume of Water at Measurement Temp. = G/density of water = V1 (ml)
Volume of Sample at Meas. Temp. = 10 ml-V1 = V2 (ml)

Density of the Sample = E/V2 = ds (gm/ml)

Sp Gr of the Sample = ds/density of H_2O (4°C)

The use of pipets with hot fluids (temperature > 25-30°C) is not appropriate and significant errors will occur due to expansion of the liquid sample. Plastic tips for mechanical pipets will also have a tendency to swell when contacted by a hot solution, but this type of volume expansion is irrelevant. However, in a piston actuated pipet, temperature-induced air expansion above the liquid level in a plastic tip can lead to transfer of less-than-the-intended volume of liquid.

II-6-3b. Temperature - Temperature measurements are needed to document density determinations and for the correction of pH and electrical conductivity if auto-temperature compensating devices are not available. During the sampling process it is also desirable to document sampling temperature. The measurement of temperature is highly developed and adequate accuracy can be obtained by several means. However, the accuracy of the thermometer should be checked periodically . If a standard or reference thermometer is not availalbe in the field, thermometers can be checked using ice and boiling water baths. Digital thermometers are now commonly available and they can also be used with less concern about susceptibility to damage. Conventional thermometers should be stored in metal or cardboard tubes to prevent damage. Several thermometers should be on hand in a field laboratory to allow for breakage.

II-6-3c. Suspended Solids - Determination of suspended solids or total filtratable residue is described in Standard Methods 208 D^3. Suspended solids

obtained during the operation of in-line sampling trains is accomplished as follows:

1) Label a glass fiber or Millipore type HA or Nucleopore membrane filter with nominal pore size of 0.45 microns with a ballpoint pen. The label should be inscribed along the outer perimeter of the filter that will subsequently be covered by a mounting O-ring.

2) Predry the membrane filter at 103 to 105°C for 10-15 minutes (Millipore type HA filters should not be heated to temperatures in excess of about 60°C).

3) Allow the filter to cool in a desiccator.

4) Obtain the tare weight of the filter.

5) Mount the filter in a high pressure, in-line membrane filter holder (Millipore or equivalent). Be sure to place a fibrous prefilter pad beneath the membrane filter to enhance filtration rates.

6) Run the sampling train to waste for a minute or so to clean the lines.

7) Pass at least 100 ml of geothermal water through the filter. Measure the filtrate volume using a graduated cylinder.

8) Remove the filter assembly and take into laboratory.

9) Remove the top of the filter assembly and connect a vacuum system to the bottom drain line of the filter assembly. The filter can be held by a ringstand.

10) Repeatedly wash the filtered residue with 0.45 micron prefiltered deionized water. After each washing allow the water to drain completely.

11) Remove the filter from the filter assembly, <u>after</u> first breaking the vacuum, using membrane forceps. Transfer the filter to a watch glass. Remove and discard the prefilter pad.

12) Dry the filter in a vacuum oven at 103-105°C for 1 hour or longer depending upon the quantity of residue (Millipore type HA filters should not be heated to temperatures in excess of about 60°C).

13) Cool the filter and residue in a desiccator and then reweigh.

14) In the initial part of a study, reheat the residue several time and reweigh until a constant weight is achieved. Modify the procedure as necessary for subsequent analysis.

Required Calculations:

Weight of Filter + Residue = A (gm)
Weight of Filter = B (gm)

Volume of Filtrate = V (ml)

Total Suspended Solids (mg/l) = (A-B)x1,000/V

II-6-3d. Conductivity - The electrical conductivity of a solution is proportional to the amount of ionizable species present in the solution. Thus, conductivity measurements are a convenient way to index the total dissolved solids (TDS) content of a sample. The standard method for measurement of TDS, which involves evaporation of a sample to dryness and weighing the residue, could require 24 hours or longer to complete. Single electrical conductivity measurements can be accomplished in a few minutes. Conductivity measurements can be made on a continuous basis using a small sidestream and data logger or strip chart recorder. This capability can be particularly useful in certain instances. For example, the monitoring of steam condensate as an indicator of steam purity.

Conductivity is not a particularly good way to characterize high salinity or hypersaline solutions, however. The method is useful in characterizing low to moderately high salinity fluids. Conductivity is measured with a conductivity meter, preferably a unit that provides automatic temperature compensation to eliminate the need for application of correction factors. Samples should be neutralized prior to measurement of specific conductance owing to the high conductance per unit weight of hydrogen and hydroxide ions. In high purity samples such as steam condensate, dissolved gases can significantly influence conductance. Appropriate methods for dealing with dissolved gases are discussed in Ref. 14.

Conductivity meters generally have an operating range of from 0 to 20,000 micromhos/cm. More concentrated solutions require dilution prior to measurement of conductivity. The sample dilution procedure is described in Ref. 12. All conductivity meters utilize a measurement cell with a finite volume. Sample dilution is accomplished by partially filling the measurement cell with sample and then diluting to the mark with low conductivity (deionized or distilled water) diluent. The dilution should be performed with a graduate or a pipet. The dilution factor is simply the ratio of the conductivity cell volume (the total measurement volume) to the sample volume. For example:

Measurement Volume = 25 ml

Sample Volume = 10 ml

Dilution Factor = 25/10 = 2.5

The corrected conductivity is equal to the conductivity times the dilution factor:

Corrected Conductivity = Measured Conductivity x Dilution Factor

If samples are diluted with water having a significant conductivity, then the effect of the conductivity of the diluent must be removed for the highest possible accuracy. The following equation can be used to correct for both the volume and conductivity of a dilution water[12]:

$$\text{Conductivity (Micromhos/cm)} = (100 \times A) - \{B \times (100 - V)\} / V \qquad \text{(II-7)}$$

where: A = measured conductivity (micromhos/cm)

B = conductivity of dilution water (micromhos/cm)

V = sample volume (ml)

II-6-3e. Turbidity - Turbidity is a measure of the concentration of suspended particulates in water. The measurement is based on the amount of scattered

light which reaches one or more photocells as compared to standards of known turbidity. The most commonly employed measurement unit is the NTU or Nephelometer Turbidity Unit. A nephelometer is a turbidity instrument in which scattered light intensity is measured in a direction 90 degrees from the incident light beam. The most stable and accurate Nephelometers are ratio devices which incorporate two or more photodetectors to provide high sensitivity and stability. The HACH Ratio Turbidimeter (18900-10) is a typical laboratory grade nephelometer with a detection limit of 0.01 NTU. The unit can be provided with a flow-through cell for continuous monitoring.

Turbidimeters are calibrated using Formazin polymer suspensions that can be prepred following guidelines in Ref. 3. HACH supplies premixed polymer suspensions that can be diluted to desired strength. The real utility of turbidity measurements is that a good relative estimate of the concentration of suspended solids in a sample can be obtained in less than a minute as compared to the 24 hours or more that is required in implementing the standrd filtration-gravimetric suspended solids methodology. The relationship between NTU's and the measured concentration of suspended solids is based on an empirical correlation developed between both types of measurements for samples obtained at the same sampling point by the same method. An arbitrary number of samples (say 10) are obtained and the suspended solids concentration levels are determined by the filtration-gravimetric method. The turbidity of the samples is also determined prior to filtration. The relationship between turbidity and mg/l suspended solids can then be derived by least squares approximation and subsequently determined turbidity values can be converted to an equivalent suspended solids concentration.

If a highly turbid solution is to be measured, it is useful to dilute the sample solution before performing the measurement. The dilution should be

carried out using volumetric glassware. The true turbidity of a diluted sample is calculated as follows[3]:

$$\text{Actual Turbidity (NTU)} = A \times (B + C) / C \qquad \text{(II-8)}$$

where: A = turbidity of diluted sample (NTU)
B = volume of dilution water (ml)
C = sample volume before dilution (ml)

Turbidity measurements obtained on a continuous basis are an excellent means of monitoring water quality immediately upstream of an injection well or for assessing the performance of clarifiers, filters and sedimentation tanks. In practice it is inconvenient and sometimes impossible to obtain acceptable quality turbidity readings using grab samples. In the process of letting down a pressurized sample to atmospheric conditions a multitude of tiny bubbles may form. Since it may be inappropriate to wait sufficiently for the bubbles to evolve before measuring turbidity, turbidity measurements using grab samples may not be useful. Small bubbles are detected as suspended solids during the turbidity measurement and the presence of bubbles can lead to erroneous inferrences regarding the turbidity of the process stream being monitored. Continuous measurements using flow-through cells are an acceptable and practical way to measure turbidity of hot pressurized process streams.

The HACH surface scatter turbidimeters are designed for continuous monitoring of process streams. The instrument operates on the principle of surface scattering of light by suspended solids as shown in Figure II-17. An advantage of this type of instrument is that the process stream does not come in physical contact with any part of the turbidimeter's optics. A disadvantage of this system for geothermal applications is that the surface of the fluid being monitored is exposed to the atmosphere. Thus, a possibility exists for the generation of extraneous precipitates and anomalously high

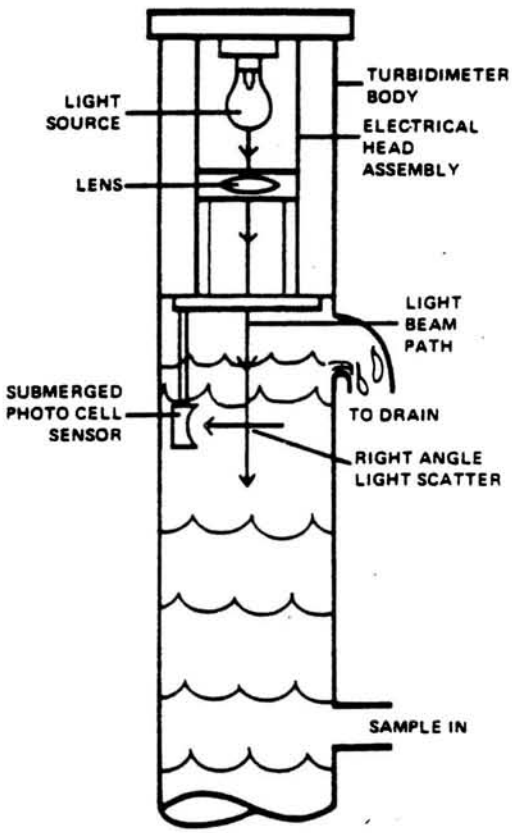

Figure II-17. Surface scattering turbidimeter(HACH Model 1720A).

turbidity readings. Fogging of the instrument's optics is another potential problem that might be encountered in monitoring a hot fluid with this instrument. The merits of this particular type of device would have to be established for a particular application. Both a low to high range instrument (15625-41) and an ultra low instrument (1720A) are available from HACH.

True ratio type turbidimeters are available for continuous monitoring duty from HACH, Fisher Scientific, VWR and other sources. H.F. Instruments, DRT-200 turbidimeter (available through Fisher Scientific) is designed for field use and was successfully integrated into an injection well monitoring system installed at the South Brawley geothermal test site operated by MCR Geothermal Corporation[8]. The basic methodology for operation of a continuously recording in-line turbidimeter is illustrated in Figures II-18 and 19. Figure II-18 illustrates the use of a flow-through cell with the HACH Ratio Turbidimeter (not shown). Since the HACH instrument is intended primarily for laboratory use we do not recommend on-line monitoring in a field situation. Figure II-19 illustrates the H.F. Instruments DRT-200 system. The sensing module is provided as an independent unit. The indicator electronics are mounted in a separate environmentalized package which can be remotely mounted from the sensing module. The indicator can be obtained with either a digital or analog display. The DRT-200 or similar device is the better choice for field applications that require continuous turbidity monitoring.

In geothermal applications, two problems are likely to be experienced. The flow-through cell of the DRT-200 has a maximum pressure limitation of 60 psi at 120°F. Other turbidimeters with flow-through cells have similar limitations. Thus, some precautions have to be taken by operators to prevent accidental dmage to the sensing cells due to overpressure or excessive temperature. The presence of bubbles in the influent brine will lead to erroneously

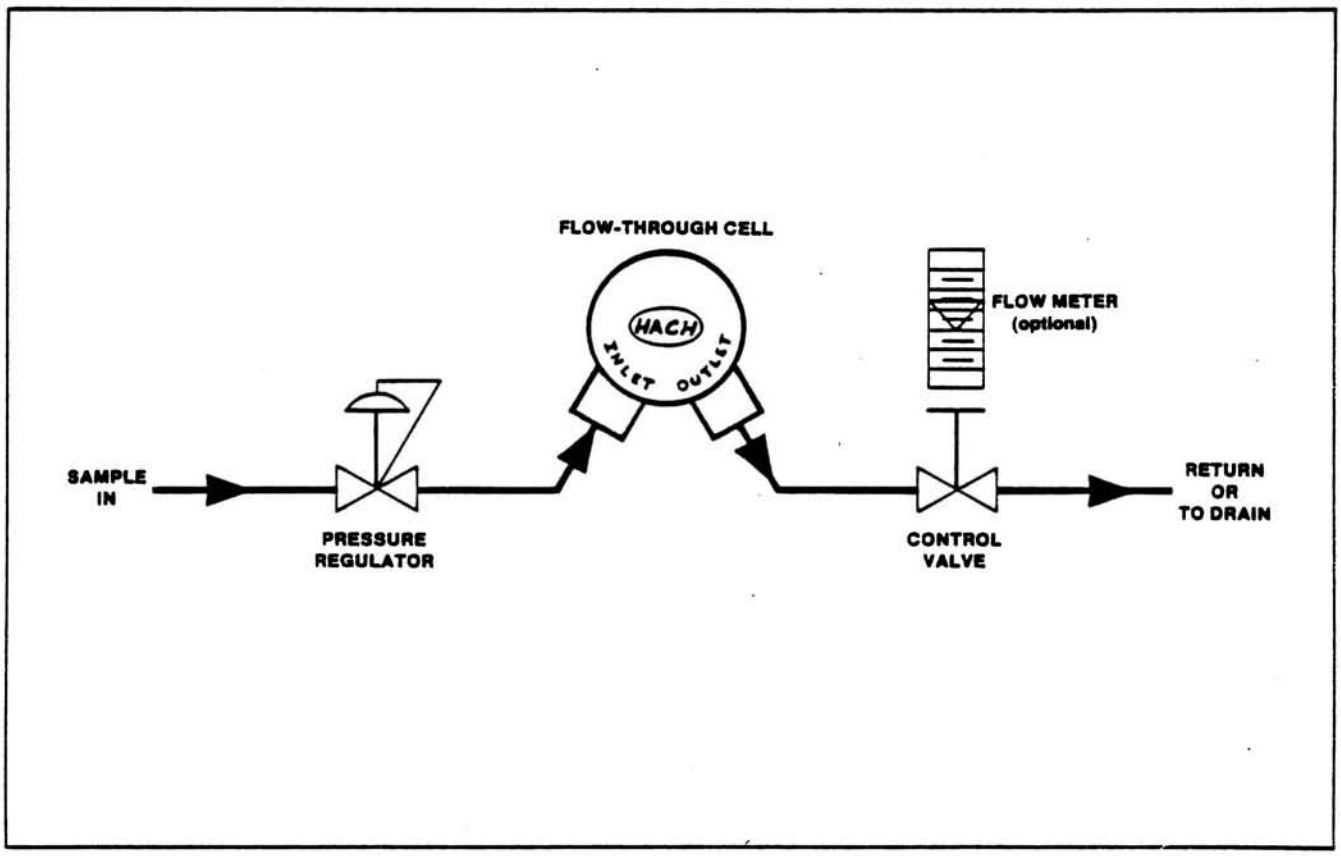

Figure II-18. HACH flow-through cell for continuous turbidity monitoring.

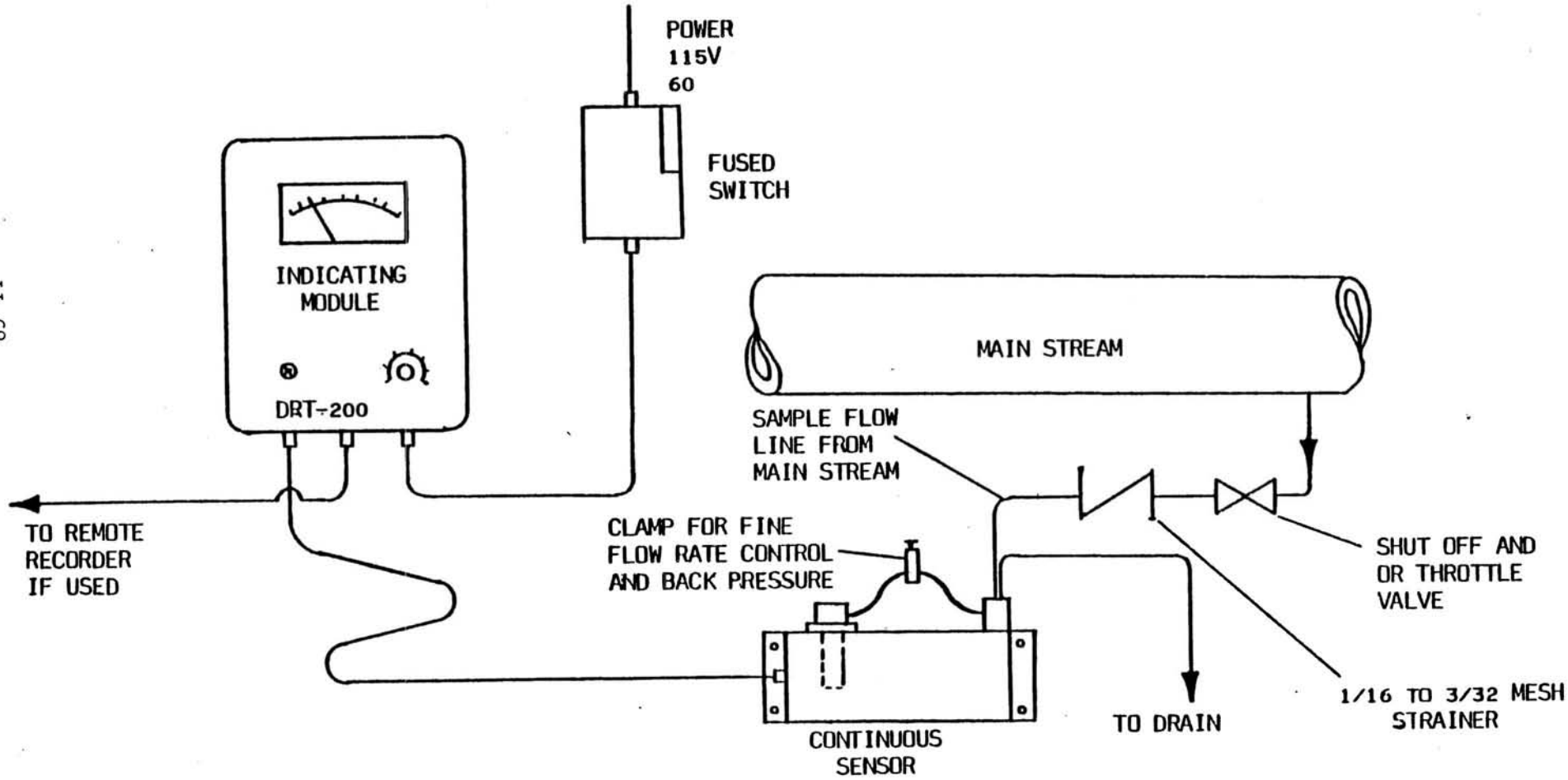

Figure II-19. H.F. Instruments continuous recording turbidimeter with flow-through cell.

high turbidity readings. A bubble trap, as shown in Figure II-20, is normally used to eliminate bubbles. The overflow from the bubble trap should be directed to waste.

Control of influent brine pressure and temperature is controlled by use of a small air cooler and pressure control valves. A small water cooler could also be used but at the inconvenience of having to supply a source of cooling water. We do not recommend use of a conventional pressure regulator in a scaling environment. A better procedure would be to use a relief valve in conjunction with a control valve. Use of a flow meter is not essential as flow through the sensing cell can be checked periodically by direct measurement using a graduate. The flow system should be equipped with a pressure gauge as an aid in setting the correct operating pressure. The output of the indicator module can be periodically manually logged or a remote recorder can be used. Several spare flow-through glass cells should be on hand in the event of accidental breakage or optical impairment due to deposition of silica or other deposits on the glass. Spare bulbs for the flow-through sensor should also be on hand.

II-6-4. Chemical Characterization of Geothermal Brine

II-6-4a. Measurement of pH - pH is a basic property of geothermal fluids that influences the behavior of certain dissolved species, such as silica and iron, and the corrosivity of the fluid. Certain analytical determinations, such as acidity and alkalinity, are based on measurement of chemical consumption as a function of pH. Such analytical determinations require accurate and stable pH meters. The measurement of pH can easily be accomplished in the field. For high quality work, use of a laboratory grade pH meter is essential. Since it may also be necessary to utilize other specific ion electrodes, as for the

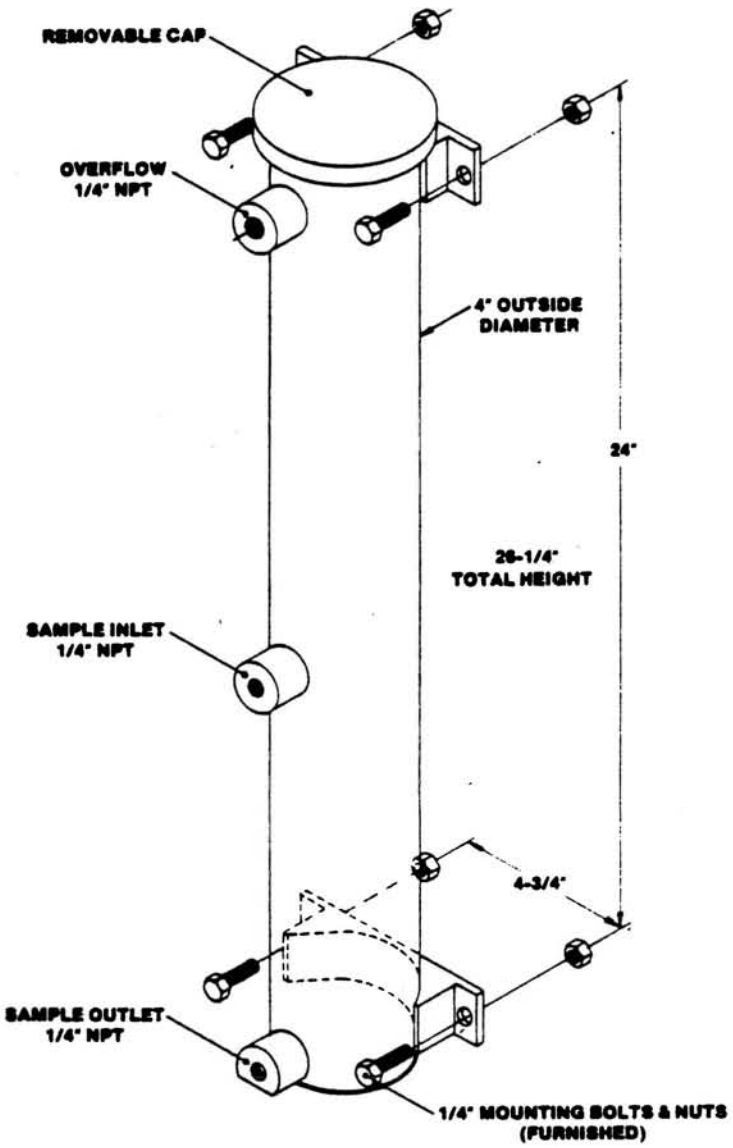

Figure II-20. HACH(Model 3563-03) Bubble trap for use immediately upstream of an in-line turbidity monitor.

determination of dissolved ammonia and dissolved sulfide, it is desirable to obtain a high quality instrument that provides both pH and mv functions.

It is also useful to consider low cost battery operated digital pH meters which are rugged and useful if it becomes necessary to measure pH immediately after sampling especially in conjunction with the operation of brine processing equipment. Shannon[15] has discussed the proper operation of portable pH meters. A high quality pH meter should be equipped with high quality electrodes. The use of combination electrodes and a separate automatic temperature compensating (ATC) electrode is most convenient. The field laboratory should be equipped with several sets of spare electrodes and an adequate supply of buffer solution for calibration purposes. The manufacturer's instructions for proper operation and calibration of a particular pH meter should be followed. Buffer powders can be obtained from the chemical supply houses. It is best to mix one liter quantities of buffer solution in polyethylene bottles for use as needed. Samples should be stirred while measuring pH. Use of a combination hot plate-magnetic stirrer is recommended. High quality electrodes reach equilibrium within about 30 seconds. Continued stirring of a solution will result in a slow but continuous rise in pH as dissolved gas (CO_2) are liberated. Therefore, all pH readings should be made after a given mixing time of 30 to 60 seconds.

II-6-4b. Acidity/Alkalinity - Acidity and alkalinity are quantitative indicators of a water's ability to neutralize a strong base and a strong acid, respectively to a designated pH. Both factors are commonly expressed in mg/l as $CaCO_3$. Rapid determination in the field of both factors is readily accomplished using a HACH digital titrator and the appropriate HACH reagents. The APHA Standard Methods, keyed to the HACH Digital Titrator and HACH reagents

are summarized in Ref. 12. The conversion of concentration units from mg/l (ppm) as $CaCO_3$ to mg/l of an ion such as HCO_3 is accomplished as follows:

$$\text{ppm of ion} = \frac{\text{equivalent weight of ion}}{\text{equivalent weight of } CaCO_3} \times \text{ppm of ion} \qquad \text{(II-9)}$$

$$\text{where: equivalent weight} = \frac{\text{atomic weight or molecular weight}}{\text{valence}}$$

Calcium carbonate conversion factors are summarized in Table II-4. Equivalent weight for some elements, ions and compounds are listed in Table II-5.

II-6-4c. Chloride - The concentration of dissolved chloride in geothermal brine is a factor of fundamental importance in the characterization of reservoir fluids and their energy content or enthalpy because chloride is basically the dominant anion. Chloride concentrations and the changes in ratios of residual scale components to chlorice concentration can be used as a chemical tracer in evaluating precipitate formation and the degree of steam flashing. The chloride content of steam condensate has important ramifications with respect to the suitability of separated steam for use in turbines. A high level of chloride in steam condensate may indicate inadequate performance of steam separation equipment or the need for auxillary steam scrubbers.

Determination of chloride is straightforward and easily accomplished in the field. The HACH methodology based on titration of samples with mercuric nitrate is fast, accurate and free of interferences even in the case of hypersaline brines from the Salton Trough[8]. The APHA Standard Methods procedure described in Ref. 12 is keyed to the use of HACH prepackaged reagents and the HACH digital titrator. Accuracy and reproducibility of the method can be checked by titration of a standard sodium chloride solution. The method of standard additions can also be used to verify analytical results. In general, two aliquots of sample should be independently titrated to establish measurement precision and to identify faulty analytical data. If a wide diversion

Table II-4

Calcium Carbonate Conversion Factors
(From Ref. 16)

To Convert From	To	Ion	Multiply By
ppm as $CaCO_3$	ppm	Ca^{++}	0.400
	of the	Mg^{++}	0.243
	Ion	K^{+}	0.782
		Na^{+}	0.460
		Ba^{++}	1.374
		Sr^{++}	0.876
		Fe^{++}	0.558
		Fe^{+++}	0.372
		Cl^{-}	0.709
		HCO_3^{-}	1.220
		OH^{-}	0.340
		$SO_4^{=}$	0.960
		$CO_3^{=}$	0.600

$$\text{Conversion Factor} = \frac{\text{Equivalent Wt. of Ion}}{\text{Equivalent Wt. of } CaCO_3}$$

$$= \frac{\text{Equivalent Wt. of Ion}}{50}$$

Table II-5

Equivalent Weights of Some Elements, Ions and Compounds

Element, Ion or Compound	Atomic or Molecular Weight	Valence	Equivalent Weight
Hydrogen (H)	1	+1	1
Oxygen (O)	16	-2	8
Calcium (Ca^{++})	40	+2	20
Bicarbonate (HCO_3^-)	61	-1	61
Carbonate (CO_3^{--})	60	-2	30
Ferrous Iron (Fe^{++})	56	+2	28
Ferric Iron (Fe^{+++})	56	+3	18.7
Sulfate (SO_4^{--})	96	-2	48
Chloride (Cl^-)	35.5	-1	35.5
Calcium Carbonate ($CaCO_3$)	100	2*	50
Calcium Sulfate ($CaSO_4$)	136	2*	68
Sodium Chloride (NaCl)	58.5	1*	58.5
Hydrochloric Acid (HCl)	36.5	1*	36.5

*The concept of valence does not apply to compounds. The denoted valence is the total valence of cations or anions in the compound.

between duplicate determinations is noted, another sample aliquot should be titrated.

In some cases, it will be necessary to dilute samples prior to analysis. For example, in the case of hypersaline brines, it may be necessary to use sample dilutions of up to 1000 times. Sample dilution can, in most instances, be accomplished using precision pipets and volumetric flasks. If a brine forms salt precipitate upon cooling, dilution will have to be made at somewhat higher temperatures based on the weight of sample actually added to a volumetric flask. The sample weight can be subsequently converted to an equivalent volume using measured density data.

An alternative analytical procedure that has been used successfully to measure chloride in geothermal waters including hypersaline brines is based on coulometric titration[13]. The Potentiometric Method for chloride is described in Ref. 3 (APHA Standard Method 408 C). Chloride is determined by potentiometric titration with silver nitrate solution using a glass and silver-silver chloride electrode system. The potential of the reaction is monitored using a high quality voltmeter. The mv function of a laboratory grade pH meter is acceptable for this determination. Usually practice, however, is to use an apparatus designed for the potentiometric titration of chloride. Suitable equipment is described in Fisher Scientific, VWR and other scientific equipment supply catalogs. If many determinations for chloride are to be made, the use of cmmercial potentiometric equipment with auto-titration features becomes desirable, although the initial cost in setting up the procedure is significantly higher than for the mercuric nitrate titration.

Neither the mercuric nitrate or potentiometric titration methods distinguish between bromide and iodide that might be present in a sample. Geothermal brines may commonly contain bromine, for example, that will be directly

titrated as chloride. Corrections for dissolved bromine and iodide must be based on independent determinations for these halogens. In hypersaline brines, bromine is present at relatively high concentrations (a few hundred ppm). The bromine concentration is low, however, in comparison to typical chloride concentrations. Iodine may also be present, but at a much lower concentration. Thus, determination of chloride in the field should be considered as indicative of total halogen content (chloride + bromide + iodide) until such time as other halogens which may be present are quantified. The independent determination of bromide and iodide is described in Ref. 3. Chromate, ferric, sulfite and sulfide also interfere when present at concentration levels in excess of 10 mg/l. These interferring species are easily controlled by diluting geothermal samples before analysis. In almost all cases, the concentration of dissolved chloride will be greatly in excess of the corresponding concentration of interferring species. HACH supplies a special prepackaged reagent to control sulfide interference.

II-6-4d. Sulfate - Dissolved sulfate is an important parameter in geothermal waters because of the potential for calcium and strontium sulfate scale formation. More commonly, the presence of high sulfate levels in geothermal waters is an indication of mixing with non-geothermal waters and/or indicative of production well casing leaks that allow cooler waters to comingle with the hotter geothermal fluids in the wellbore. For example, anomalously high sulfate levels in brine produced by the Woolsey No. 1 well in the Salton Sea Geothermal Field, Southern California was the first indication of a probable leak in the well casing . The leak was subsequently confirmed by means of a downhole spinner/temperature survey.

Dissolved sulfate is measured by the Turbidimetric method[3,12]. The determination is easily performed in the field using HACH prepackaged reagents and a HACH spectrophotometer. The method involves precipitation of barium sulfate crystals of uniform size. The amount of precipitate is subsequently quantified by use of a transmission spectrophotometer. Silica in excess of 500 mg/l interferes and suspended particulates, if present in the water, must be removed by filtration. Chloride, in excess of 40,000 mg/l and magnesium in excess of 10,000 mg/l may also interfere[12]. These interferences species, if present, can usually be controlled by dilution of the sample.

II-6-4e. Sulfide - Hydrogen sulfide gas is produced at many geothermal resources in association with separated steam. The level of residual sulfide ion in produced geothermal water is important in establishing total sulfide content of the reservoir fluids and in assessing the potential for formation of sulfide scale deposits. Since sulfide ion is a toxic species, it may be necessary to monitor sulfide levels in certain process streams for compliance with environmental regulations. The sulfide determination is also useful in quantifying the amount of hydrogen sulfide gas trapped by scrubbing with sodium hydroxide in conjunction with the standard procedure for quantifying CO_2 in noncondensable gases.

Sulfide is determined by the conversion of N,N-dimethyl-p-phenylenediaminine oxalate to methylene blue by reaction with hydrogen sulfide. The quantity of methylene blue formed by the reaction is determined using a spectophotometer at a wavelength of 665 nm. The HACH procedure used in conjunction with a HACH portable chemistry laboratory greatly simplifies the field determination of sulfide.

II-6-4f. Ammonia - Ammonia is commonly present in geothermal discharges. The ammonia, by virtue of a relatively high solubility in water redistributes between steam condensate and the residual noncondensable gases after flashing if the noncondensable gases are allowed to contact the condensate. Ammonia is a weak base that is stabilized in the liquid phase by reaction with CO_2 (CO_2 + NH_3 + H_2O -> NH_4HCO_3). Redissolution of ammonia in steam condensate can increase the pH of the condensate:

$$NH_3 + H_2O <-> NH_4 + OH \qquad \text{(II-10)}$$

Utilization of condensate as make-up water for injection may result in the mixing of condensate, with an elevated pH, with spent brine, of lower pH. Depending upon the heavy metal content of the spent brine, remixing could enhance the potential for precipitation of hydrated metal oxides such as $Fe(OH)_3$. Elevation of spent brine pH could also promote precipitation of dissolved silica.

The Nessler method is a standard laboratory procedure for determination of ammonia [3,12]. However, the procedure is susceptible to interference which causes precipitation of the reagent. Usual practice is to remove interferring iron and sulfide by distillation of the sample to purify ammonia prior to analysis. The Salicylate method is more sensitive than the Nessler method but it is also susceptible to interferring species[3,12]. Some of the interferring species (Ca and Mg) present in geothermal waters may greatly exceed the concentration of ammonia. In these cases, sample dilution may offer no relief from the interferring species.

The specific ion electrode method for ammonia is the only practical approach to field analysis of ammonia[18]. The Orion model 95-10 ammonia electrode has been successfully used to measure ammonia in steam condensate produced at the South Brawley Geothermal Field in Southern California[8]. The resource produces a hypersaline brine[7]. Detailed instructions provided with the electrode should be followed. Standard ammonia solutions are available from Orion as an aid in calibrating the electrode response. The electrode method is accurate and rapid.

II-6-4g. Dissolved Oxygen - Geothermal waters normally are deficient in dissolved oxygen, but they can become enriched in dissolved oxygen upon exposure to air. If air exposure occurs, the residual dissolved oxygen content of geothermal waters can have a significant impact on the corrosivity and chemical stability of the waters. Oxygen content can be measured in several ways including the Winkler wet chemistry method[3,12], the specific ion electrode[18] and the colorimetric method based on the reaction of Rhodazine D with dissolved oxygen. Of the above methods, the colorimetric method is preferred due to its accuracy, sensitivity, simplicity and rapidity.

The colorimetric test for dissolved oxygen as packaged by CHEMetrics, Inc., Warrenton, Virginia contains evacuated glass vials prefilled with the appropriate quantity of reagent. After immersion of the vial i the sample solution, the tip of the vial is snapped off. A quantity of liquid is immediately pulled into the vial. The vial is removed from the solution, capped and agitated by hand for a few seconds. The color development due to the presence of dissolved oxygen in the sample is compared to color standards provided with the kit to quantify oxygen concentration. Several kits covering a variety of dissolved oxygen concentrations are available. Precautions should be taken to avoid contamination of samples by atmospheric oxygen during sampling and subsequent comparison of standard solutions with the sample. In general, samples obtained from a sampling valve should be taken as follows:

1. Connect a length of plastic tubing to the sample valve.
2. Insert the free end of the tubing well into a 125 ml or larger Erlenmeyer flask.
3. Insert a CHEMet vial into the provided plastic sampling tube (Figure II-20).
4. Continuously flow sample liquid into the Erlenmeyer flask allowing the flask to overflow. The flask can be held over a large bucket to contain the overflowed liquid.
5. Immerse the plastic sampling tube well into the sample solution while continuously flowing fresh sample into the Erlenmeyer flask.
6. Snap the tip of the CHEMet vial by pressing downward on the top of the vial. Allow the vial to fill with sample, but remove the vial in less than 5 seconds to avoid loss of reagent.
7. Remove the CHEMet vial from the solution and immediately cover the broken tip with a finger. Mix the vial contents by repeated inversion of the covered tube.
8. The oxygen content of the sample is determined by comparison with supplied color standards.

Proper sampling procedure is essential in obtaining accurate results. Allowing water to free flow into a sampling flask is sufficient to permit significant atmospheric contamination of the sample. It is for this reason that the sample should be conveyed to a sampling flask via a length of tubing. As an alternative procedure, sample can be conveyed directly into the plastic sample holder (Figure II-21) via plastic tubing. The sample holder can be gripped with a pair of laboratory tongs during the sampling procedure.

II-6-4h. Total Dissolved Solids - The actual quantity of dissolved constituents in a geothermal water or total dissolved solids (TDS) is an extremely important factor in assessing reservoir enthalpy[11,19,20]. TDS variations are also indicative of the degree of steam flashing along a process stream. Reservoir engineering assessments of production and injection require information about TDS in order to compute probable trends in chemistry of produced water after a specific period of injection has occurred. TDS data may also be needed to demonstrate compliance with environmental regulations. Flashed brine that is ultimately injected may have a TDS value 20 percent or more higher than the produced water. Ultimately, more concentrated brine may be produced with potentially detrimental effects on scale deposition and, perhaps, corrosivity of the produced fluids as injected brines break through to production wells.

The determination of TDS is described in APHA Standard Methods Procedure 208 A[3]. Use of VYCOR or porcelain evaporating dishes is recommended in lieu of platinum due to the difficulty of maintaining proper control of valuables in the field. For most geothermal waters, the procedure described in 208 A is adequate. We have found, however, that significant changes in the procedure are required for the accurate analysis of hypersaline brine[8]. The standard procedure requires a sample size such that ultimately, the minimum residue

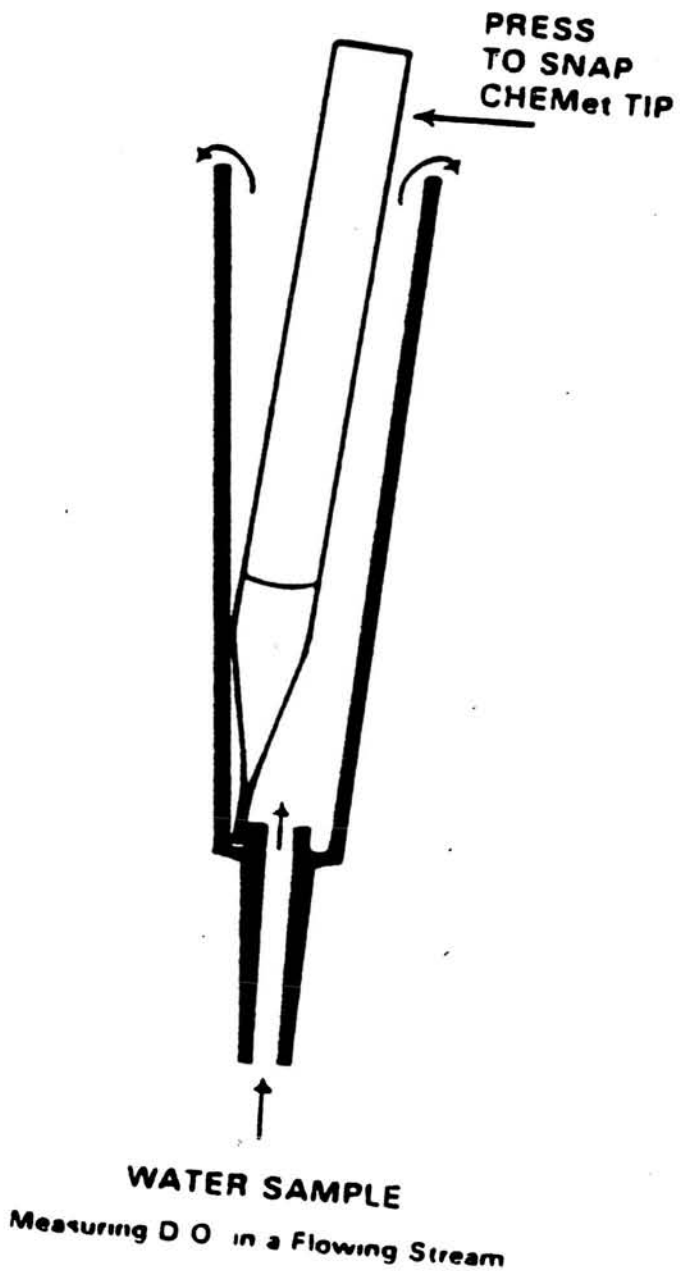

Figure II-21. CHEMetrics water sampling tube and CHEMet vial.

weighs between 25 to 250 mg. For a hypersaline brine, this translates to a sample volume of from 0.5 to 1.0 ml. We recommend the following procedure for TDS determinations of hypersaline brines:

1. Transfer the requisite sample volume to a 5 ml capacity VYCOR beaker. The sample should be accurately weighed into the beaker.
2. Place the beaker with the sample on a hot plate and heat to dryness on a low temperature setting to avoid splattering.
3. Slowly increase the temperature setting of the hot plate, over a two hour period, to eliminate all traces of residual moisture.
4. Transfer the sample to a vacuum oven and heat for two hours at 103-105°C.
5. Allow the sample to cool in a desiccator and reweigh.
6. Repeat steps 4 and 5 to demonstrate attainment of constant weight.

Required Calculations:

$$\text{mg/l TDS} = \frac{(A-B) \times 1{,}000}{C} \qquad \text{(II-11)}$$

where: A = weight of sample + beaker (gm)
B = weight of beaker (gm
C = sample volume (ml)

This procedure has been found to yield highly reproducible results with a mean standard deviation of better than 2 percent for duplicate TDS determinations for 33 hypersaline brine samples[8]. If a vacuum oven is used for the final drying of hypersaline TDS samples, the same procedure should be used for other samples to permit direct comparisons of analytical results. Samples used for TDS determinations must be prefiltered using a 0.45 micron membrane filter prior to analysis. Hot, pressurized geothermal fluids should be prefiltered on-line simultaneously with sampling. It has been our experience that standard methodology for measurement of TDS of hypersaline brine does not yield acceptable data and the length of time required for a single determination is

objectionable. The modified procedure utilizing a vacuum oven as described above is recommended.

II-6-4i. Quantitative Analysis - Field preserved liquid samples can be characterized using either atomic absorption spectrophotometry (AA) or inductively-coupled plasma spectrometry (ICP). The ICP procedure is preferred for rapid, low cost multi-element analysis. Furthermore, the ICP determination of certain cations such as sodium is free of matrix interferences that complicate conventional AA determinations. A modern ICP facility can provide for the essentially simultaneous determination of up to 40 elements or more in a single sample. Table II-6 illustrates working detection limits and calibration ranges for a typical ICP installation. It should be borne in mind that the ICP characterization of a sample may require one or more sample dilutions to place all sample constituents within the appropriate measurement range. Thus, several runs on the ICP may be necessary for complete characterization of a sample.

The recommended ICP wavelengths for sample characterization are summarized in Table II-7. Once an analytical procedure has been set-up for a particular category of sample, for example, a hypersaline brine, synthetic brine samples of known composition should be prepared and analyzed to demonstrate the validity of the analytical procedure. Selection of an appropriate commercial laboratory for analysis of samples, if such analysis cannot be accomplished in-house, should be based to a large extent on the demonstrated ability of the laboratory to perform the work successfully rather than on price per analysis. Bad analytical data is worthless.

A unique characteristic of the hypersaline geothermal brines of Southern California's Salton Trough is the presence of anomalously high concentrations of heavy metals including silver. Harrar and Raber[21] evaluated various analy-

ELEMENT	WORKING DETECTION LIMIT (ppm)*	CALIBRATION RANGES (ppm)
Na	1.25	3-3000
K	2.5	2-2000
Ca	0.25	2.5-2500
Mg	0.5	2-2000
Fe	0.025	.02-100
Al	0.625	.4-2000
Si	0.25	.93-467
Ti	0.125	.1-500
P	0.625	.5-500
Sr	0.013	.02-20
Ba	0.625	.5-500
V	1.25	1-1000
Cr	0.05	.2-200
Mn	0.25	2-2000
Co	0.025	.1-100
Ni	0.125	.2-200
Cu	0.063	.06-300
Mo	1.25	.5-500
Pb	0.25	.3-300
Zn	0.125	.04-200
Cd	0.063	.02-100
Ag	0.05	.04-200
Au	0.1	.05-50
As	0.625	.4-400
Sb	0.75	.6-600
Bi	2.5	2-2000
U	6.25	1-1000
Te	1.25	.5-500
Sn	0.125	.2-200
W	0.125	.2-100
Li	0.05	.04-200
Be	0.005	.004-20
B	0.125	.1-100
Zr	0.125	.1-100
La	0.125	.1-500
Ce	0.25	.4-400
Th	2.5	1-1000

*Note:

The working detection limit shown represents the lower limit of quantative determination for an element in solution with other elements. Much lower detection limits are of course possible when only a single element in solution is involved.

Table II-6. Typical detection limits and calibration ranges for an inductively coupled plasma spectrometer.

Table II-7

Recommended ICP Wavelengths (From Ref. 1)

Element	Wavelength (A)	Element	Wavelength (A)
Al	3092	Na (high conc.)	3303*
Ag	3280	Na (low conc.)	5896
As	1936	Ni	2316 x2
B	2497	P	2149 x2
Ba	4934	Pb	2203
Ca	3179	Sb	2175
Cd	2265	Se	1960
Co	2286	Si	2881
Cr	2677	Sn	1899
Cu	3247	Sr	4215
Fe	2599	Th	2837
K (low conc.)	7664*	Ti	3349
K (high conc.)	4047	Tl	3775
Li	6707	U	3859
Mg	3832	Zn	2062 x2
Mn	2576	Zr	3391
Mo	2020		

*Better choice for single wavelengths.
x2 indicates 2nd order.

tical techniques for the analysis of silver content in hypersaline brine. They found that the limits of detection for the fire assay technique, which involves collection of silver in a gold carrier followed by AA determination of silver[22], is 0.5 mg/l at the 3 σ level. They concluded that solvent extraction of silver, with dithizone, followed by AA determination of silver was the best available method for quantifying silver in brine.

II-6-5. Steam Loss Corrections

The reduction of analytical data to a common basis is desirable as a means of facilitating intersample comparisons. Usually, one is interested primarily in the actual chemical composition of reservoir brines. The reduction of data to atmospheric pressure and the boiling temperature of the brine is also of interest. The computational methods used to reduce analytical data to a common basis can be used for any given set of conditions desired. Various computational techniques may be employed in recalculating analytical data. In the simplest case, liquid single phase samples are obtained for analysis from a separator. If the percent steam flash is known from direct measurement of the mass fractions of produced brine and steam discharged from a separator, then the correction applied to analytical data for recalculation to a preflash reservoir condition is applied as follows:

$$\text{Steam Flash Fraction} = \frac{\text{Steam Mass Rate}}{\text{Steam Mass Rate + Brine Mass Rate}} = F \qquad \text{(II-12)}$$

and Percent Flash = 100 F

and $x_o = x_i\ (1-f)$

where: x_o = concentration of a dissolved species in the reservoir

x_i = concentration of a dissolved species in residual brine effluent

Alternative methods for applying steam loss corrections are described in Refs. 9 and 10. The pre-flash concentration of a dissolved species may be computed by noting that the flash fraction is a function of the adiabatic part of the temperature change experienced by the reservoir liquid :

$$F = \frac{(H_o - L) - H_v}{H_L - H_v} \qquad \text{(II-13)}$$

or

H_o = enthalpy of reservoir brine at reservoir conditions

L = conductive heat losses between the reservoir and the point of steam separation

H_v = enthalpy of steam at steam separation conditions

H_L = enthalpy of residual liquid at steam separation conditions

F = fractional steam flash

A tabulation of heat capacities and heats of vaporization for ideal sodium chloride solutions is provided as Tables II-8 and 9. An example of the calculation of steam loss effects on dissolved solids concentration is provided in Ref. 10.

The concentration of a dissolved species can be recalculated to any basis if the following information is available[9]:

1. E = Enthalpy of reservoir fluid (C)
2. L = Latent heat of evaporation of reservoir fluid (cal/g)
3. H = Enthalpy of fluid at sampling conditions (cal/g)
4. F = Dryness factor (fractional steam flash)
5. Xo = Concentration of dissolved species in reservoir fluid (mg/l)
6. Xi = Concentration of Xo at the desired steam separation condition (mg/l)

The source fluid enthalpy at reservoir conditions is given by:

$$E = H + F \qquad \text{(II-14)}$$

The fractional flash is given by:

$$F = \frac{E-H}{L} \qquad \text{(II-15)}$$

TABLE II-8. (From Ref. 10)

Heat Capacities (cal $deg^{-1}g^{-1}$) for solutions containing various weight percentages of NaCl

Temp.		% NaCl	Cp							
			0	5	10	15	20	25	30	35
°C	°F									
80	176		0.996	0.936	0.874	0.809	0.740	0.664		
85	185		0.997	0.937	0.876	0.812	0.745	0.671		
90	194		0.997	0.938	0.878	0.815	0.749	0.678		
95	203		0.998	0.939	0.880	0.818	0.754	0.684		
100	212		0.998	0.940	0.882	0.821	0.758	0.690		
105	221		0.999	0.941	0.883	0.824	0.762	0.696		
110	230		0.999	0.942	0.884	0.826	0.765	0.701		
115	239		0.999	0.943	0.892	0.839	0.786	0.729		
120	248		1.000	0.945	0.892	0.839	0.786	0.730		
125	257		1.001	0.945	0.892	0.840	0.786	0.730		
130	266		1.001	0.946	0.893	0.840	0.786	0.731		
135	275		1.002	0.946	0.893	0.840	0.786	0.731		
140	284		1.003	0.946	0.893	0.840	0.786	0.731		
145	293		1.003	0.947	0.893	0.840	0.786	0.731		
150	302		1.004	0.947	0.893	0.840	0.786	0.730		
155	311		1.005	0.948	0.893	0.839	0.786	0.730		
160	320		1.006	0.948	0.893	0.839	0.785	0.730	0.669	
165	329		1.007	0.949	0.893	0.839	0.785	0.729	0.668	
170	338		1.008	0.949	0.894	0.839	0.784	0.728	0.668	
175	347		1.009	0.950	0.894	0.839	0.784	0.728	0.667	
180	356		1.011	0.951	0.894	0.839	0.784	0.727	0.666	
185	365		1.012	0.951	0.894	0.839	0.783	0.726	0.665	
190	374		1.014	0.952	0.895	0.839	0.783	0.726	0.664	
195	383		1.015	0.953	0.895	0.838	0.782	0.725	0.663	
200	392		1.017	0.954	0.895	0.839	0.782	0.725	0.663	
205	401		1.018	0.955	0.896	0.839	0.782	0.724	0.662	
210	410		1.020	0.956	0.897	0.839	0.782	0.724	0.661	
215	419		1.022	0.957	0.897	0.839	0.782	0.724	0.661	
220	428		1.024	0.959	0.898	0.840	0.782	0.724	0.661	
225	437		1.026	0.960	0.899	0.840	0.783	0.724	0.661	
230	446		1.028	0.962	0.900	0.841	0.783	0.725	0.661	
235	455		1.031	0.963	0.901	0.842	0.784	0.726	0.662	
240	464		1.033	0.965	0.903	0.843	0.785	0.727	0.664	
245	473		1.036	0.967	0.904	0.845	0.787	0.728	0.665	
250	482		1.038	0.969	0.906	0.846	0.789	0.731	0.668	
255	491		1.041	0.971	0.908	0.848	0.791	0.733	0.671	
260	500		1.044	0.974	0.910	0.851	0.794	0.737	0.675	0.599
265	509		1.047	0.976	0.913	0.854	0.797	0.741	0.680	0.605
270	518		1.050	0.979	0.916	0.857	0.801	0.746	0.687	0.613
275	527		1.054	0.982	0.919	0.861	0.806	0.752	0.682	0.622
280	536		1.057	0.985	0.923	0.866	0.812	0.759	0.704	0.633
285	545		1.061	0.989	0.927	0.871	0.819	0.768	0.715	0.646
290	554		1.065	0.993	0.932	0.877	0.827	0.779	0.728	0.663
295	563		1.069	0.997	0.937	0.884	0.837	0.791	0.744	0.682
300	572		1.073	1.002	0.944	0.893	0.848	0.806	0.763	0.706
305	581		1.077	1.007	0.951	0.903	0.861	0.824	0.786	0.734
310	590		1.082	1.013	0.959	0.915	0.877	0.845	0.813	0.768
315	599		1.087	1.019	0.969	0.929	0.896	0.870	0.845	0.808
320	608		1.092	1.027	0.980	0.945	0.919	0.901	0.884	0.857
325	617		1.098	1.035	0.993	0.964	0.946	0.937	0.931	0.916

TABLE II-8. (From Ref. 10)

Heat Capacities (cal $deg^{-1}g^{-1}$) for solutions containing various weight percentages of NaCl

Temp.		% NaCl	Cp							
			0	5	10	15	20	25	30	35
°C	°F									
80	176		0.996	0.936	0.874	0.809	0.740	0.664		
85	185		0.997	0.937	0.876	0.812	0.745	0.671		
90	194		0.997	0.938	0.878	0.815	0.749	0.678		
95	203		0.998	0.939	0.880	0.818	0.754	0.684		
100	212		0.998	0.940	0.882	0.821	0.758	0.690		
105	221		0.999	0.941	0.883	0.824	0.762	0.696		
110	230		0.999	0.942	0.884	0.826	0.765	0.701		
115	239		0.999	0.943	0.892	0.839	0.786	0.729		
120	248		1.000	0.945	0.892	0.839	0.786	0.730		
125	257		1.001	0.945	0.892	0.840	0.786	0.730		
130	266		1.001	0.946	0.893	0.840	0.786	0.731		
135	275		1.002	0.946	0.893	0.840	0.786	0.731		
140	284		1.003	0.946	0.893	0.840	0.786	0.731		
145	293		1.003	0.947	0.893	0.840	0.786	0.731		
150	302		1.004	0.947	0.893	0.840	0.786	0.730		
155	311		1.005	0.948	0.893	0.839	0.786	0.730		
160	320		1.006	0.948	0.893	0.839	0.785	0.730	0.669	
165	329		1.007	0.949	0.893	0.839	0.785	0.729	0.668	
170	338		1.008	0.949	0.894	0.839	0.784	0.728	0.668	
175	347		1.009	0.950	0.894	0.839	0.784	0.728	0.667	
180	356		1.011	0.951	0.894	0.839	0.784	0.727	0.666	
185	365		1.012	0.951	0.894	0.839	0.783	0.726	0.665	
190	374		1.014	0.952	0.895	0.839	0.783	0.726	0.664	
195	383		1.015	0.953	0.895	0.838	0.782	0.725	0.663	
200	392		1.017	0.954	0.895	0.839	0.782	0.725	0.663	
205	401		1.018	0.955	0.896	0.839	0.782	0.724	0.662	
210	410		1.020	0.956	0.897	0.839	0.782	0.724	0.661	
215	419		1.022	0.957	0.897	0.839	0.782	0.724	0.661	
220	428		1.024	0.959	0.898	0.840	0.782	0.724	0.661	
225	437		1.026	0.960	0.899	0.840	0.783	0.724	0.661	
230	446		1.028	0.962	0.900	0.841	0.783	0.725	0.661	
235	455		1.031	0.963	0.901	0.842	0.784	0.726	0.662	
240	464		1.033	0.965	0.903	0.843	0.785	0.727	0.664	
245	473		1.036	0.967	0.904	0.845	0.787	0.728	0.665	
250	482		1.038	0.969	0.906	0.846	0.789	0.731	0.668	
255	491		1.041	0.971	0.908	0.848	0.791	0.733	0.671	
260	500		1.044	0.974	0.910	0.851	0.794	0.737	0.675	0.599
265	509		1.047	0.976	0.913	0.854	0.797	0.741	0.680	0.605
270	518		1.050	0.979	0.916	0.857	0.801	0.746	0.687	0.613
275	527		1.054	0.982	0.919	0.861	0.806	0.752	0.682	0.622
280	536		1.057	0.985	0.923	0.866	0.812	0.759	0.704	0.633
285	545		1.061	0.989	0.927	0.871	0.819	0.768	0.715	0.646
290	554		1.065	0.993	0.932	0.877	0.827	0.779	0.728	0.663
295	563		1.069	0.997	0.937	0.884	0.837	0.791	0.744	0.682
300	572		1.073	1.002	0.944	0.893	0.848	0.806	0.763	0.706
305	581		1.077	1.007	0.951	0.903	0.861	0.824	0.786	0.734
310	590		1.082	1.013	0.959	0.915	0.877	0.845	0.813	0.768
315	599		1.087	1.019	0.969	0.929	0.896	0.870	0.845	0.808
320	608		1.092	1.027	0.980	0.945	0.919	0.901	0.884	0.857
325	617		1.098	1.035	0.993	0.964	0.946	0.937	0.931	0.916

TABLE II-9

Heats of vaporization (cal g^{-1}) for solutions containing various weight percentages of NaCl

Temp.		Wt. % NaCl	0	5	10	15	20	25	30	35
°C	°F					ΔH				
80	176		551.2	556.1	561.1	566.4	572.0	578.2		
85	185		548.2	553.3	558.6	564.1	569.9	576.3		
90	194		545.1	550.5	556.0	561.7	567.8	574.4		
95	203		542.0	547.7	553.4	559.4	565.6	572.4		
100	212		538.9	544.8	550.7	556.9	563.4	570.4		
105	221		535.7	541.9	548.1	554.5	561.1	568.3		
110	230		532.5	538.9	545.4	552.0	558.9	566.2		
115	239		529.2	535.7	541.9	548.1	554.5	561.3		
120	248		525.9	532.7	539.2	545.7	552.4	559.4		
125	257		522.5	529.6	536.5	543.3	550.3	557.6		
130	266		519.1	526.5	533.7	540.8	548.1	555.7		
135	275		515.6	523.4	530.9	538.3	545.9	553.8		
140	284		512.0	520.2	528.0	535.8	543.7	551.9		
145	293		508.5	517.0	525.1	533.2	541.4	549.9		
150	302		504.8	513.7	522.2	530.6	539.1	548.0		
155	311		501.1	510.3	519.2	527.9	536.8	546.0		
160	320		497.2	506.9	516.1	525.2	534.5	544.0	554.4	
165	329		493.3	503.4	513.0	522.5	532.1	542.0	552.8	
170	338		489.3	499.8	509.8	519.7	529.6	539.9	551.1	
175	347		485.2	496.1	506.5	516.8	527.2	537.8	549.4	
180	356		481.0	492.4	503.2	513.4	524.6	535.7	547.7	
185	365		476.7	488.5	499.8	510.9	522.1	533.5	546.0	
190	374		472.3	484.6	496.3	507.9	519.4	531.3	544.2	
195	383		467.8	480.6	492.8	504.7	516.7	529.0	542.3	
200	392		463.2	476.5	489.1	501.5	513.9	526.7	540.4	
205	401		458.4	472.3	485.4	498.2	511.1	524.2	538.4	
210	410		453.5	467.9	481.5	494.9	508.2	521.7	536.4	
215	419		448.5	463.5	477.6	491.4	505.1	519.1	534.3	
220	428		443.4	458.9	473.5	487.8	502.0	516.4	532.0	
225	437		438.1	454.2	469.3	484.1	498.7	513.6	529.6	
230	446		432.6	449.3	465.0	480.2	495.3	510.6	527.1	
235	455		427.0	444.3	460.5	476.2	491.8	507.5	523.8	
240	464		421.2	439.1	455.8	472.1	488.1	504.3	521.6	
245	473		415.2	433.8	451.0	467.8	484.2	500.8	518.5	
250	482		409.1	428.3	446.1	463.3	480.1	497.1	515.2	
255	491		402.7	422.6	440.9	458.6	475.8	493.1	511.6	
260	500		396.2	416.7	435.5	453.7	471.3	488.9	507.6	530.2
265	509		389.4	410.5	429.9	448.5	466.5	484.3	502.9	526.2
270	518		382.4	404.2	424.1	443.0	461.3	479.4	498.5	521.6
275	527		375.1	397.6	417.9	437.2	455.8	474.0	493.2	516.4
280	536		367.6	390.7	411.5	431.1	449.8	468.1	487.2	510.5
285	545		359.8	383.5	404.7	424.6	443.4	461.7	480.6	503.6
290	554		351.7	376.1	397.6	417.6	436.5	454.5	473.1	495.8
295	563		343.3	368.3	390.0	410.1	428.8	446.6	464.6	486.7
300	572		334.6	360.1	382.0	402.0	420.4	437.6	455.0	476.2
305	581		325.5	351.4	373.4	393.3	411.2	427.6	443.9	463.9
310	590		316.1	342.4	364.3	383.7	400.8	416.2	431.1	449.5
315	599		306.2	332.8	354.4	373.1	389.3	403.2	416.2	432.5
320	608		296.0	322.7	343.7	361.4	376.2	388.2	398.8	412.3
325	617		285.2	311.9	332.0	348.4	361.2	370.7	378.3	388.2

Reference

Haas, J. L., Jr. Preliminary "Steam Tables" For NaCl Solutions U.S. Geological Survey, Reston, VA 1975 Document No. USGS-OFR-75-675. Values in Table above were calculated from USGS values.

TABLE II-9

Heats of vaporization (cal g^{-1}) for solutions containing various weight percentages of NaCl

Temp.		Wt. % NaCl	0	5	10	15	ΔH 20	25	30	35
°C	°F									
80	176		551.2	556.1	561.1	566.4	572.0	578.2		
85	185		548.2	553.3	558.6	564.1	569.9	576.3		
90	194		545.1	550.5	556.0	561.7	567.8	574.4		
95	203		542.0	547.7	553.4	559.4	565.6	572.4		
100	212		538.9	544.8	550.7	556.9	563.4	570.4		
105	221		535.7	541.9	548.1	554.5	561.1	568.3		
110	230		532.5	538.9	545.4	552.0	558.9	566.2		
115	239		529.2	535.7	541.9	548.1	554.5	561.3		
120	248		525.9	532.7	539.2	545.7	552.4	559.4		
125	257		522.5	529.6	536.5	543.3	550.3	557.6		
130	266		519.1	526.5	533.7	540.8	548.1	555.7		
135	275		515.6	523.4	530.9	538.3	545.9	553.8		
140	284		512.0	520.2	528.0	535.8	543.7	551.9		
145	293		508.5	517.0	525.1	533.2	541.4	549.9		
150	302		504.8	513.7	522.2	530.6	539.1	548.0		
155	311		501.1	510.3	519.2	527.9	536.8	546.0		
160	320		497.2	506.9	516.1	525.2	534.5	544.0	554.4	
165	329		493.3	503.4	513.0	522.5	532.1	542.0	552.8	
170	338		489.3	499.8	509.8	519.7	529.6	539.9	551.1	
175	347		485.2	496.1	506.5	516.8	527.2	537.8	549.4	
180	356		481.0	492.4	503.2	513.4	524.6	535.7	547.7	
185	365		476.7	488.5	499.8	510.9	522.1	533.5	546.0	
190	374		472.3	484.6	496.3	507.9	519.4	531.3	544.2	
195	383		467.8	480.6	492.8	504.7	516.7	529.0	542.3	
200	392		463.2	476.5	489.1	501.5	513.9	526.7	540.4	
205	401		458.4	472.3	485.4	498.2	511.1	524.2	538.4	
210	410		453.5	467.9	481.5	494.9	508.2	521.7	536.4	
215	419		448.5	463.5	477.6	491.4	505.1	519.1	534.3	
220	428		443.4	458.9	473.5	487.8	502.0	516.4	532.0	
225	437		438.1	454.2	469.3	484.1	498.7	513.6	529.6	
230	446		432.6	449.3	465.0	480.2	495.3	510.6	527.1	
235	455		427.0	444.3	460.5	476.2	491.8	507.5	523.8	
240	464		421.2	439.1	455.8	472.1	488.1	504.3	521.6	
245	473		415.2	433.8	451.0	467.8	484.2	500.8	518.5	
250	482		409.1	428.3	446.1	463.3	480.1	497.1	515.2	
255	491		402.7	422.6	440.9	458.6	475.8	493.1	511.6	
260	500		396.2	416.7	435.5	453.7	471.3	488.9	507.6	530.2
265	509		389.4	410.5	429.9	448.5	466.5	484.3	502.9	526.2
270	518		382.4	404.2	424.1	443.0	461.3	479.4	498.5	521.6
275	527		375.1	397.6	417.9	437.2	455.8	474.0	493.2	516.4
280	536		367.6	390.7	411.5	431.1	449.8	468.1	487.2	510.5
285	545		359.8	383.5	404.7	424.6	443.4	461.7	480.6	503.6
290	554		351.7	376.1	397.6	417.6	436.5	454.5	473.1	495.8
295	563		343.3	368.3	390.0	410.1	428.8	446.6	464.6	486.7
300	572		334.6	360.1	382.0	402.0	420.4	437.6	455.0	476.2
305	581		325.5	351.4	373.4	393.3	411.2	427.6	443.9	463.9
310	590		316.1	342.4	364.3	383.7	400.8	416.2	431.1	449.5
315	599		306.2	332.8	354.4	373.1	389.3	403.2	416.2	432.5
320	608		296.0	322.7	343.7	361.4	376.2	388.2	398.8	412.3
325	617		285.2	311.9	332.0	348.4	361.2	370.7	378.3	388.2

Reference

Haas, J. L., Jr. Preliminary "Steam Tables" For NaCl Solutions U.S. Geological Survey, Reston, VA 1975 Document No. USGS-OFR-75-675. Values in Table above were calculated from USGS values.

The recalculated concentration of dissolved species Xi is given by:

$$Xi = \frac{Xo}{1 - F} \qquad \text{(II-16)}$$

Examples illustrating utilization of this calculational technique are provided in Ref. 9.

II-6-6. Chemical Geothermometry

The concentrations of dissolved alkali and alkaline-earth elements in a geothermal brine are controlled in part by the dissolution of feldspars and clay minerals in the geothermal reservoir. Similarly, dissolved silica in geothermal brines is contributed by the partial dissolution of quartz and amorphous silica present in the reservoir rocks. The dissolution reactions are temperature dependent and several geochemical models have been devised to equate the dissolution of reservoir minerals with the reservoir temperature and corresponding concentration levels of certain key dissolved species[23-34]. The evaluation of subsurface temperature based on the use of the Na-K and Na-K-Ca geothermometers is preferred in systems which produce two phase mixtures of brine plus steam. The calculations are independent of steam flashing because ratios of the elemental indicators are utilized. If no selective precipitation occurs, flashing has minimal effect on the utility of these temperature indicators. If, however, massive precipitation of calcium carbonate occurred upstream of the sampling point, utilization of the Na-K-Ca geothermometer might yield erroneous results. The deviation between predicted temperatures and measured flowing bottomhole temperatures could, however, be interpreted in terms of the partial precipitation of calcium.

The silica geothermometers are also susceptible to erroneous temperature predictions due to partial precipitation of silica as scale or in the form of suspended solids. If flashing occurs prior to sampling, the concentration of

dissolved silica would have to be adjusted for steam flash-induced changes in brine concentration. The solubility of dissolved silica is also proportional to the total dissolved solids concentration of a brine. Therefore, estimates of subsurface temperature based on the use of distilled water silica solubility data will yield erroneous results in the case of a hypersaline brine.

Recently, all of the presently available chemical geothermometers were evaluated in conjunction with an extended test of a hypersaline brine well in the South Brawley Geothermal Field, Southern California[8]. The flowing bottomhole temperature in the test well was known from direct measurement. The most consistently accurate estimates of bottomhole temperature were obtained using the Na-K-Ca with Mg correction geothermometer[30], the Na-K-Ca geothermometer[29], and the Na/K geothermometers[31,33] based on the analysis of 33 flash-corrected (~8% steam flash) brine samples. Silica-based estimates of bottomhole temperature were significantly low and the Na-Li and Li geothermometer estimates were significantly high. The Na/K[33] and Na-K-Ca, Mg-corrected geothermometers yielded accurate estimates of bottomhole temperature even when the estimate was based on the analysis of brine flashed to atmospheric conditions.

The utility of accurate estimation of bottomhole temperature, beyond the obvious evaluation of resource temperature is the ability to check the validity of chemical analyses. In the case of hypersaline geothermal brines, the total of sodium, potassium and calcium represents the major portion of total dissolved solids (along with chloride) in the brine. Accurate temperature estimation is a good indication that the concentration of these species is correct. Attainment of charge and mass balances, in similar fashion, would suggest that the concentration of chloride has also been correctly determined.

II-7. Characterization of Geothermal Steam and Noncondensable Gases

A major objective of a geochemical engineering assessment of a new geothermal prospect is the accurate determination of total noncondensable gas content in the source brine or at production wellhead conditions. Total noncondensable gas content is extremely important if a flash steam energy conversion cycle is proposed for a particular site. High noncondensable gas loading to a steam turbine contributes to the turbine backpressure necessitating additional capital expenditures and energy penalties that correspond to the installation and operation of steam-jet ejectors or vacuum pumps[35]. Evolution of CO_2 as a consequence of steam flashing in production wells and surface equipment can also result in significant carbonate scale formation. The ultimate selection of a particular energy conversion cycle will depend in an important way on the accurate assessment of total noncondensable gas loading.

It is straightforward to demonstrate that the bulk of noncondensable gases originally present in the source reservoir are separated from the liquid phase at relatively high temperature and pressure. CO_2 represents the predominant noncondensable gas component in almost all geothermal systems. The distribution of CO_2 and H_2O between liquid and gas phases is defined by the Ostwald coefficient (λ) or by the A coefficient[35] as follows:

$$\lambda = \frac{\text{grams } CO_2/\text{ml (liquid phase)}}{\text{grams } CO_2/\text{ml (vapor phase)}} \qquad \text{(II-17)}$$

and $$A = (n^v_{H_2O} n^l_{CO_2})/(n^l_{H_2O} n^v_{CO_2})$$

where n^v = number of moles in gas phase
n^l = number of moles in liquid phase

Both coefficients yield essentially the same results. The separation factor ($SF\text{-}CO_2$) defines the fraction of the original CO_2 which is transferred to the vapor phase after flashing and FF defines the fraction of the original fluid flashed to steam as follows:

$$SF_{CO_2} = \frac{1/A}{(1/FF-1) + 1/A} \qquad \text{(II-18)}$$

Values of 1/A are tabulated in Table II-10. The calculation yields an approximation of CO_2 behavior because the liquid phase is assumed to be a pure sodium

Table II-10

Values of 1/A for Water and
Different Salt Solutions (From Ref. 37)

Temperature (°C)	Molarity of NaCl Solution			
	Water	0.5 M	1.0 M	2.0 M
150	1349	1479	1660	1995
160	1047	1122	1318	1585
170	813	871	1023	1230
180	631	676	794	955
190	490	525	617	759
200	380	427	479	588

chloride solution and kinetic effects are ignored. Since essentially all of the CO_2 is flashed during the initial pressure reduction, selection of energy conversion cycle is really a direct function of the total noncondensable gas load. In some cases, for example, the San Diego Gas and Electric Company/U.S. DOE Geothermal Loop Experimental Facility operation at the Salton Sea Geothermal Field, levels of CO_2 in the reservoir dramatically declined over a relatively short period of time necessitating redesign of the energy conversion cycle[36]. It is extremely important that sufficient pre-development testing be

carried out prior to committing to a particular conversion cycle. Unless the system parameters are well understood, accurate economic forecasting will not be possible.

The characterization of steam and noncondensable gases is more complicated than analysis of liquid streams. Sampling problems must be overcome and the instability of gaseous components must be adequately dealt with. The basic parameters of interest in assessing geothermal steam are:

1. Total noncondensable gas load
2. Steam condensate composition
3. Noncondensable gas composition

The accurate determination of noncondensable gas composition is necessary to predict possible hydrogen sulfide emission problems and corrosivity of produced gases. Steam condensate composition is important both from the point of view of corrosivity and scale deposition difficulties in turbine components and condensers.

II-7-1. Total Noncondensable Gas Concentration

Several methods are available for the routine determination of total noncondensable gas concentration in geothermal steam. The classical method involves the direct measurement of separated steam and brine mass flowrate. This type of determination is usually carried out using a large capacity separator feed by the total production of a geothermal well. The method offers a high degree of accuracy in large part due to the representative flow of reservoir brine and gases and the high efficiency of separation. Metering of brine and steam flows is most usually accomplished using orifice-type flowmeters. Alternative methods for assessing total noncondensable gas content involve the use of low flow capacity sidestream sampling and gas separation-condensing

FIGURE II-22. TYPICAL FACILITY FOR THE CHARACTERIZATION OF A GEOTHERMAL WELL DISCHARGE.

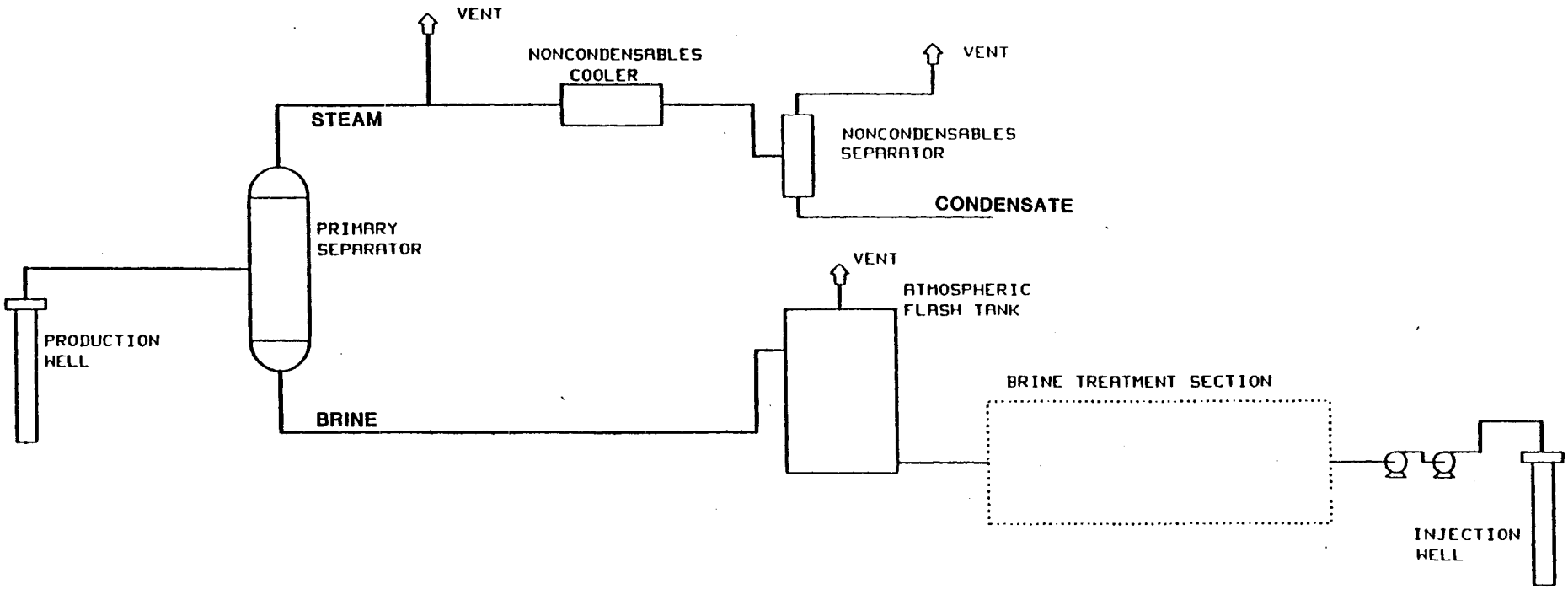

devices. One novel method uses a probe inserted in the high pressure/temperature steam line to measure directly the enthalpy of the steam and noncondensable gas phases as compared to the enthalpy of pure water at the same temperature and pressure conditions.

II-7-1a. Production Well Testing Facility - A typical design for a full-scale production well testing facility is shown in Figure II-22. Fluid and gas from the geothermal reservoir are admitted to a primary steam separator. The separated brine is let down to atmospheric conditions in an atmospheric flash tank. The spent brine, after appropriate treatment, is reinjected. This type of facility is designed to permit long-term testing of a well. A short-term test could be accomplished without the atmospheric flash tank or the brine treatment system by directing the separated brine discharge produced by the primary separator directly to a brine pit. Periodically, the pit could be emptied by reinjection of untreated brine.

The separated steam and noncondensable gases are directed to a vent. Depending upon the mass flowrate, a rather substantial steam silencer stack would be needed to control noise. A portion of the high temperature/pressure steam is sampled using a combination cooler and separator. The noncondensable separator produces steam condensate and noncondensable gas streams which can be independently characterized. The sidestream mass flow rate from the steam line could be relatively low to support use of a sampling train of the type described previously in Section II-5. The sidestream, under these conditions is operated periodically, on an as-needed basis, to permit characterization of the steam condensate and noncondensable gases. Alternatively, the sidestream can be operated on a continuous basis at a relatively high mass flowrate. A large air or water cooled condenser and an appropriately sized noncondensable

separator would then be used for the continuous metering of steam condensate and noncondensable gas production rates.

Operation of the primary separator can be controlled in such a way to reduce the severity of scale deposition during the test period. This is accomplished by operating the separator at wellhead pressure for effective separation of noncondensable gases. The high pressure/temperature operation suppresses scale formation that might be enhanced if the produced brine experienced a large pressure drop in the primary separator. In this fashion, stable operation of the entire system can be realized thereby facilitating detailed characterization of the thermodynamic and chemical properties of the goethermal resource. A relatively long period of stable production is also required for the reservoir engineering assessment work needed to define the size and hydraulic properties of the resource. The facility illustrated in Figure II-22 is typical of a well designed test facility that would be installed for the large-scale, long-term testing of a resource. Depending upon the desired mass flowrates, the test facility could be skid mounted to facilitate the testing of several wells.

The characterization of noncondensable gas content based on the facility illustrated in Figure II-22 proceeds as follows:

$$Wg = Wt - Wc \qquad \text{(II-19)}$$

where: Wt = total mass flow of steam to the noncondensable cooler-separator (lbs/hr)

Wg = mass flowrate of noncondensable gas vented by the noncondensable separator (lbs/hr)

Wc = mass flowrate of condensate discharged by the noncondensable separator (lbs/hr)

It is assumed that the steam input to the noncondensable cooler (Wt) has a total dissolved solids content (TDS) of zero. The CO_2 concentration in steam produced by the primary separator is given by:

$$(CO_2)t = \{Wc \times (CO_2)c + Wg \times (CO_2g\} / Wt \qquad \text{(II-20)}$$

where: $(CO_2)t$ = weight fraction of CO_2 in steam produced by the primary separator

$(CO_2)c$ = weight fraction of CO_2 in steam condensate produced by the noncondensable gas separator

$(CO_2)g$ = weight fraction of CO_2 in noncondensable gases vented from the noncondensable gas separator

The value of $(CO_2)c$ may be measured by titration of a sodium hydroxide scavenged condensate sample or calculated using Henry's Law. $(CO_2)g$ can be determined in similar fashion or by analysis of a collected gas sample. A small amount of CO_2 originally in the production wellhead product remains in the brine produced by the primary separator. The content of CO_2 in separated brine can either be calculated or measured as noted above. In the remainder of this discussion, the fraction of the total CO_2 dissolved in brine is ignored.

The use of Henry's Law to evaluate CO_2 distribution between steam condensate and noncondensable gas proceeds as follows:

$$X_{CO_2} = \frac{P_{CO_2}}{K_H} \qquad \text{(II-21)}$$

where: K_H = Henry's Law constant

Pco_2 = partial pressure of CO_2 in the gas phase

Xco_2 = mol fraction of CO_2 in the liquid phase

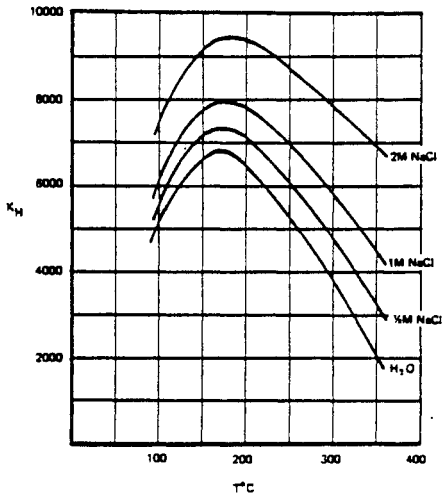

K_H vs. temperature for different salinities.

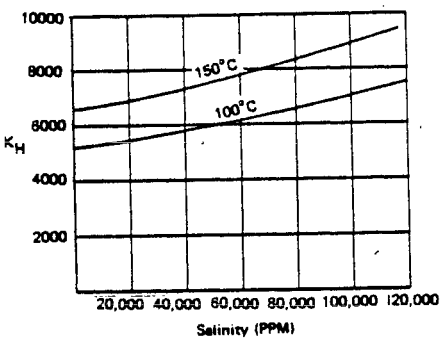

K_H vs. salinity for different temperatures.

Figure II-23. Values of Henry's Law Constants as a function of temperature and sodium chloride concentration (From Ref. 35).

Values of K_H are tabulated as a function of temperature and sodium chloride concentration in Table II-11. A graphical representation of Henry's Law constants for various temperatures and sodium chloride compositions is shown in Figure II-23. The mol fraction of CO_2 in the liquid phase is then calculated by an iteration process based on appropriate values of K_H and the calculated estimates for Pco_2. Examples of the application of Henry's Law are provided in Refs. 35 and 38.

Table II-11

Tabulated Values of the Henry's Law Constant K (From Ref. 37)

	Temperature - °F (°C)					
Solvent	212 (100)	302 (150)	392 (200)	482 (250)	572 (300)	662 (350)
Water	5200	6000	6400	5300	3900	2100
0.5 M NaCl	5600	7150	7100	6000	4800	3300
1.0 M NaCl	6150	7800	7800	7000	5850	4400
2.0 M NaCl	7450	9200	9400	8700	7800	6500

The mass balance for the primary separator is given by:

$$Wp = Wb + Wt \qquad \text{(II-22)}$$

where: Wp = mass flow of the production wellhead product to the primary separator (lbs/hr)

Wb = mass flow of the separated brine effluent from the primary separator (lbs/hr)

Determination of the total mass flow from the production well is usually based on orifice metering data obtained in the gas and brine legs from the primary separator. It is not possible to obtain accurate flow data using orifice

meters for wellhead production if the wellhead product consists of a two phase mixture of brine plus steam and noncondensable gases as is usually the case.

The CO_2 concentration in the steam leg of the primary separator is equal to $(CO_2)t$. The concentration of CO_2 in the brine effluent from the primary separator is assumed to be zero, but the actual concentration can be measured or estimated as noted above.

The total CO_2 content of the wellhead product is calculated by means of a simple mass balance:

$$(CO_2)p = (CO_2)t \times Wt / Wp \qquad \text{(II-23)}$$

where: $(CO_2)p$ = weight fraction of CO_2 in the total production wellhead product

The TDS content of the production wellhead product can be measured, using quenched samples of brine from the primary separator and recalculated to wellhead conditions using the methods of Section II-6. Alternatively, TDS can also be estimated for the produced brine at wellhead conditions based on a simple mass balance:

$$(TDS)p = (TDS)s \times \frac{Wb}{Wp} \times [1 / (1 - (CO_2)p)] \qquad \text{(II-24)}$$

where $(TDS)s$ = measured TDS in separated brine (mg/l)

This calculation assumes that there is no carryover of dissolved species in separated steam produced by the primary separator. The calculated value of production wellhead TDS is thereby derived on a gas-free basis.

II-7-1b. Measurement of Total Noncondensable Gas Using Small Sampling Trains - The noncondensable gas sampling train depicted in Figure II-22 could, as noted previously, represent either a large continuously operating gas separation

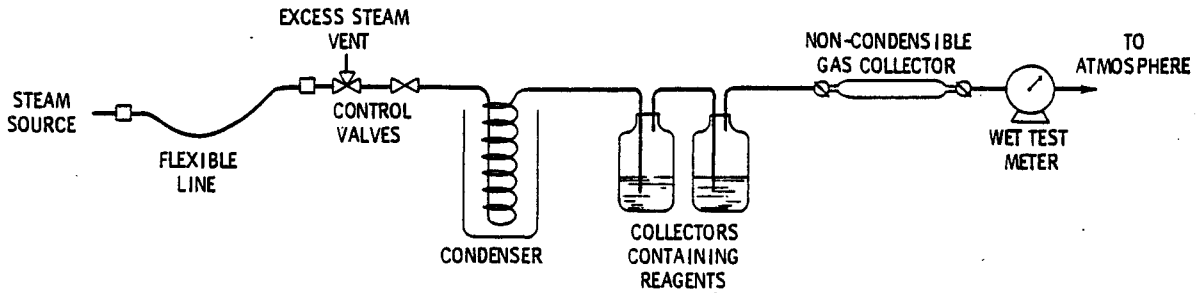

Figure II-24. Basic steam sampling apparatus (From Ref. 39).

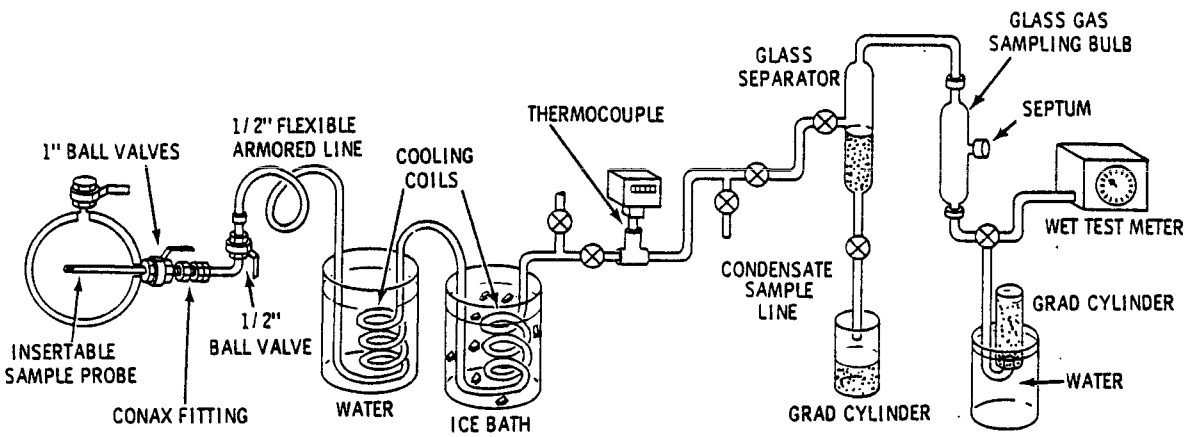

Figure II-25. Wet test meter method used in field test to sample noncondensables in steam line (From Ref. 10).

system or it could represent the several components that comprise a small sampling train of the type described in Section II-5. The basic high temperature steam sampling train was described by Christoffersen, et al.[39]. The systems, illustrated in Figures II-23 and 24, were used to characterize steam produced at the Geysers geothermal field in Northern California and at the Baca geothermal field in New Mexico. The basic system (Figure II-23) consisted of a single coil ice water bath condenser, chemical scavenger solutions for the collection and stabilization of reactive noncondensable gas species such as CO_2 and H_2S, a gas sampling bulb, and a wet test meter to quantify the volume of noncondensable gas produced during a sampling interval. The elaboration of this basic system as described in Section II-5, in Ref. 1 and in Figure II-24 yields a reliable and simple to operate integrated sampling system for the determination of important properties of a geothermal steam flow.

When a steam flow is sampled in the manner depicted in Figures II-24 and 25, a volume of condensate and a corresponding volume of noncondensable gases will be produced. The condensate volume is quantified by collecting the sample in a weighted bottle or by draining a separator into a volumetric cylinder, the measured volume of condensate subsequently converted to an equivalent mass based on the density of the condensate. Suitable separators are shown in Section II-5 and in Ref. 1. The volume of noncondensable gas produced by the sampling train can be quantified using a wet test meter, a rotometer or by displacement of a measured volume of water from a large drum.

Use of a wet test meter is straightforward. The manufacturer's instructions should be carefully followed. The raw volume data produced by a wet test meter must be reduced to an equivalent volume at STP. This data reduction requires a value of local barometric pressure at the time of measurement. A worksheet keyed to the reduction of volumetric data obtained with a Preci-

Table II-12

Wet Test Meter
Calculation of Total Volumetric Gas Flow

Date _____ Time _____

Sample No. _____ Sample Location _____

Sample Description _____

$$V_m' = \frac{P_m'}{P_s} \frac{T_s}{T_m} V_m$$

where: V_m = measured volume (liters)

V_m' = corrected measured volume (liters)

V_s = volumetric gas flow @ STP

P_s = standard pressure = 760 mm Hg.

T_s = standard temperature = 273.16°K

T_m = measured temperature (°C)

P_m = measured pressure (inches water)

P_m' = corrected pressure (mm Hg)

P_{sat} = saturated water vapor pressure from steam tables (MPa)

P_{bar} = barometric pressure (psi)

T_m = _____°C + 273.16 = _____°K

P_m = _____ inches water x 1.8694 = _____ mm Hg

P_{bar} = _____ psi x 51.7149 = _____ mm Hg

P_{sat} = _____ MPa x 7502.68 = _____ mm Hg

$P_m' = [(P_{bar} + P_m) - P_{sat}]$

$$V_m' = (0.3594) \frac{P_m'}{T_m} V_m$$

Submitted by _____

Table II-13

Saturation Pressures (From Ref. 40)

Pressure MPa - p	Temp. °C - t	Pressure MPa - p	Temp. °C - t	Pressure MPa - p	Temp. °C - t
.0006113	.01	.0075	40.29	.075	91.78
.0007	1.89	.0080	41.51	.080	93.50
.0008	3.77	.0085	42.67	.085	95.14
.0009	5.45	.0090	43.76	.090	96.71
		.0095	44.81	.095	98.20
.0010	6.98	.010	45.81	.100	99.63
.0011	8.37	.011	47.69	.105	101.00
.0012	9.66	.012	49.42	.110	102.31
.0013	10.86	.013	51.04	.115	103.58
.0014	11.98	.014	52.55	.120	104.80
.0015	13.03	.015	53.97	.125	105.99
.0016	14.02	.016	55.32	.130	107.13
.0017	14.95	.017	56.59	.135	108.24
.0018	15.84	.018	57.80	.140	109.31
.0019	16.69	.019	58.96	.145	110.36
.0020	17.50	.020	60.06	.150	111.37
.0021	18.28	.021	61.12	.155	112.36
.0022	19.02	.022	62.14	.160	113.32
.0023	19.73	.023	63.12	.165	114.26
.0024	20.42	.024	64.06	.170	115.17
.0025	21.08	.025	64.97	.175	116.06
.0026	21.72	.026	65.85	.180	116.93
.0027	22.34	.027	66.70	.185	117.79
.0028	22.94	.028	67.53	.190	118.62
.0029	23.52	.029	68.33	.195	119.43
.0030	24.08	.030	69.10	.200	120.23
.0032	25.16	.032	70.60	.205	121.02
.0034	26.19	.034	72.01	.210	121.78
.0036	27.16	.036	73.36	.215	122.53
.0038	28.08	.038	74.64	.220	123.27
.0040	28.96	.040	75.87	.225	124.00
.0042	29.81	.042	77.05	.230	124.71
.0044	30.62	.044	78.18	.235	125.41
.0046	31.40	.046	79.27	.240	126.10
.0048	32.15	.048	80.32	.245	126.77
.0050	32.88	.050	81.33	.250	127.44
.0055	34.58	.055	83.72	.255	128.09
.0060	36.16	.060	85.94	.260	128.73
.0065	37.63	.065	88.01	.265	129.37
.0070	39.00	.070	89.95	.270	129.99

Interpolation Formula

$$P = \frac{(T-T_1)}{(T_2-T_1)} (P_2-P_1) + P_1$$

sion Scientific Co., wet test meter is provided as Table II-12. Table II-13 provides a tabulation of water saturation vapor pressures from the Steam Tables[40]. An interpolation formula is also provided in Table II-13. The volumetric flow requirement should be carefully assessed before purchase of a wet test meter to avoid overranging problems. Sampling trains, depending upon their design, must operate at a minimum throughput rate to avoid gas stripping and resulting erroneous gas to condensate volume ratios. During an actual run, the operating instructions discussed in Ref. 39 should be adhered to. It is particularly important to flow gas through the wet test meter for a period of time prior to commencing a run to insure that the meter is equilibrated with CO_2 and other gases in the gas stream.

Wet test meters are expensive and susceptible to damage either due to mechanical shock or by the action of corrosive gases. Rotometers provide an accurate means of metering gas flows using a relatively inexpensive device. The rotometer can be used as a gas metering device by simply connecting an apprpriate unit to a gas sampling train in place of the wet test meter. Whereas the wet test meter measures the total volume of gas produced, the rotometer measures the gas flowrate. A total volume is subsequently obtained by integration of the flowrate data. As received from the manufacturer, rotometers are calibrated for air and pure water flow. The air calibration is inappropriate for the metering of CO_2 or mixtures of CO_2 and other noncondensable gases. However, the calculation of accurate calibration curves for any gas or mixture of gases is straightforward. For example, complete instructions for recalculating calibration curves for Fischer and Porter (Warminster, Pennsylvania) variable area flowmeters and selection guidelines for the proper application of rotometers are described in Refs. 41 to 44.

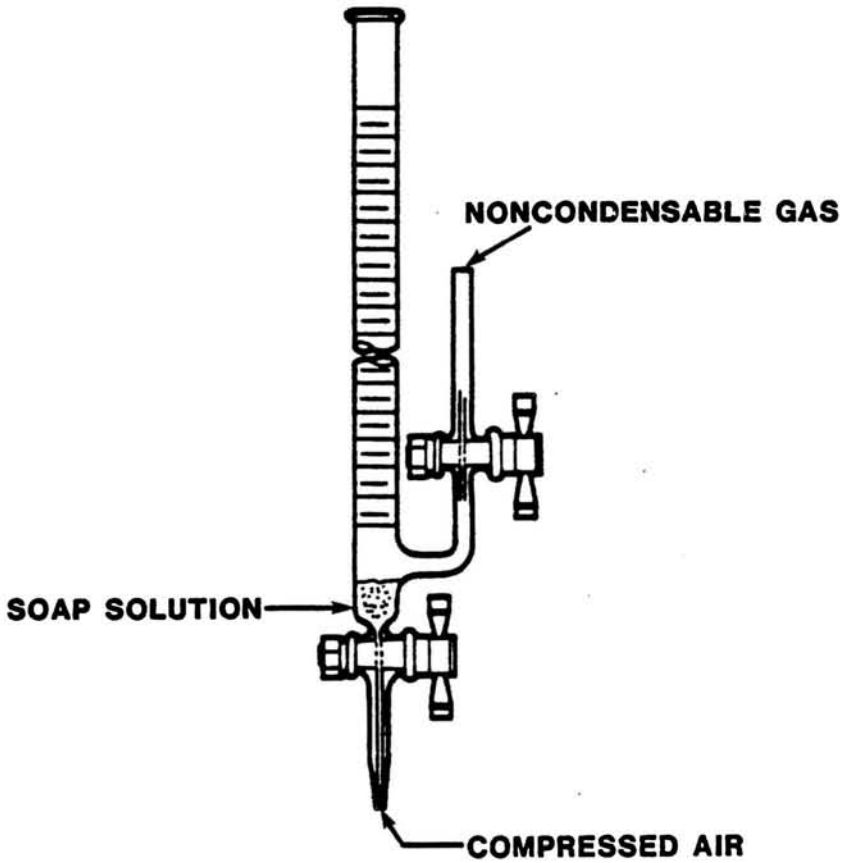

Figure II-26. Construction of a soap buble flowmeter using a 50 ml buret with a side filling tube and stopcocks. (Fisher Scientific 03-722-10)

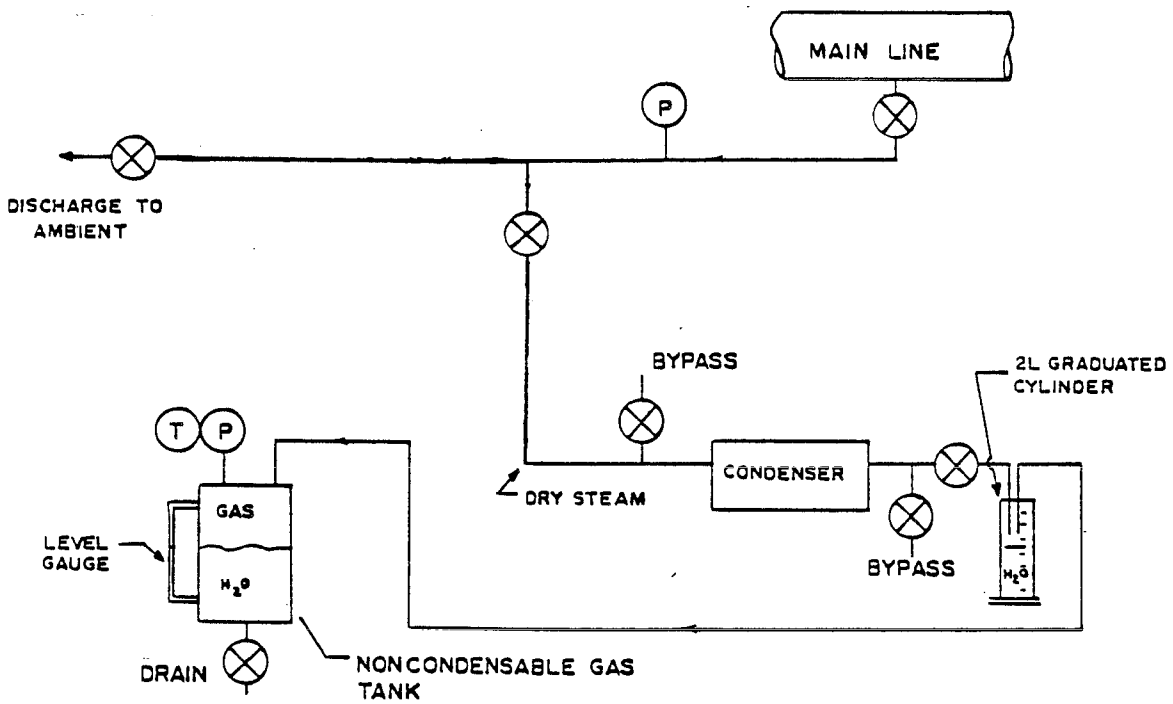

Figure II-27. Water displacement method of measuring noncondensable gas flowrate. (From Ref. 45)

It is always beneficial to directly check the calibration of a rotometer prior to use. Calibration checks can easily be accomplished using a soap bubble flow meter. Construction of a suitable flowmeter is illustrated in Figure II-26. The flowmeter is built using a Fisher Scientific (or equivalent) 50 ml buret with a side filling tube and stopcock. Noncondensable gas is passed through the rotameter and then into the side arm of the buret. The lower portion of the buret is filled with a soap solution. Snoop solution used to check for gas leaks works well. The soap solution level should be just below the side arm input port as shown in Figure II-26. A short burst of compressed air (from a small compressor or a rubber bulb) is injected into the bottom of the buret through the drain pipet. Soap bubbles are immediately formed and lifted up above the noncondensable gas injection side port. The rate at which soap bubbles are swept up towards the top of the buret by the continuous stream of noncondensable gas is determined by noting the time required for a bubble to travel an arbitrary distance in the buret. The distance is quantified using the volume calibration of the buret.

An alternative method for quantifying noncondensable gas flowrate is depicted in Figure II-27. High temperature/pressure steam is passed through a condenser and separator, to remove steam condensate, and the noncondensable gases are then used to displace water from a fifty gallon drum. The volume of water displaced from the drum is equivalent to the total noncondensable gas volume injected into the drum. This method is very accurate. The 2 liter graduated cylinder used as a condensate-noncondensable gas separator can be designed as shown in Figure II-28.

II-7-1c. Alternative Method for Calculating Total Noncondensable Gas Concentration - The methodology described in Section II-7-1a for calculating total noncondensable gas concentration produced by a geothermal well was based on a mass balance. An alternative methodology[45], based on the application of

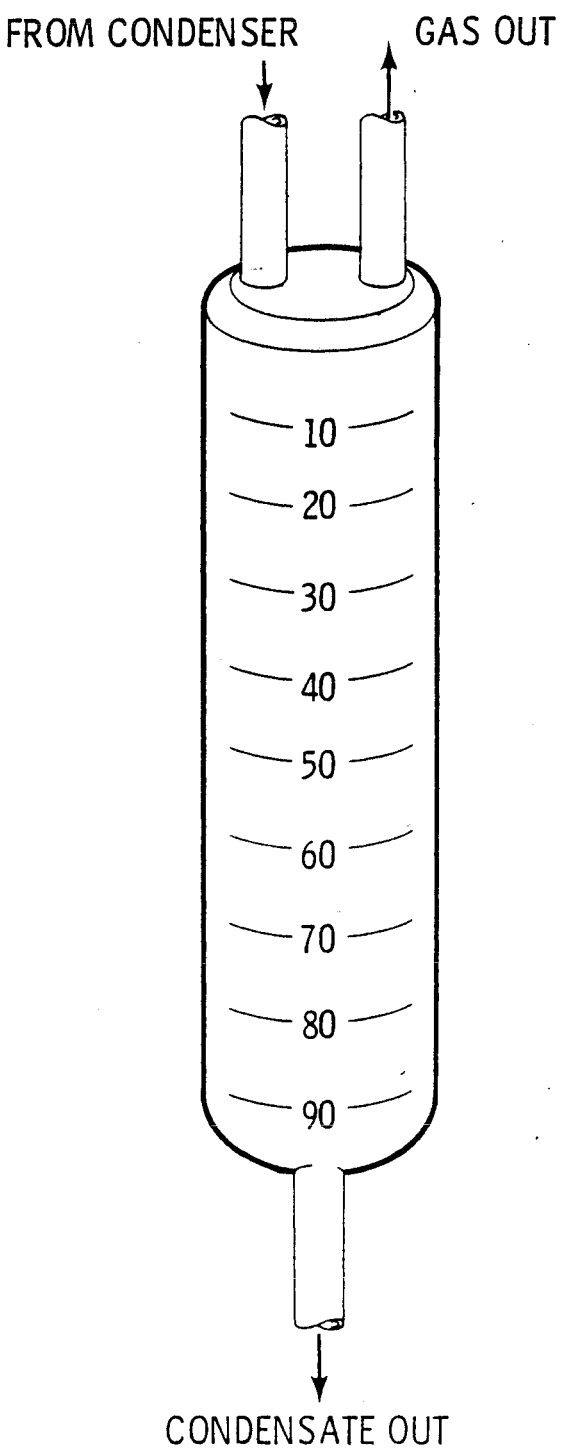

Figure II-28. Steam-gas separator modified from a 100 ml graduated cylinder. (From Ref. 10)

Dalton's rule for partial pressures and Amagat's rule for partial volumes, is particularly applicable to the volumetric data produced by small sidestream sampling devices. The noncondensable gas concentration is calculated as follows:

Idealizing the noncondensable gas/steam mixture as a mixture of perfect gases:

$$P_t V = N_t RT \qquad \text{(II-25)}$$

where: P_t = total pressure of mixture
V = volume of mixture
N_t = number of moles in mixture
R = gas constant
T = mixture temperature

Utilizing Dalton's rule for partial pressures:

$$P_s = N_s \frac{RT}{V} \qquad \text{(II-26)}$$

$$P_g = N_g \frac{RT}{V} \qquad \text{(II-27)}$$

Where subscripts denote:

s = steam properties
g = noncondensable gas properties

$$\frac{P_g}{P_s} = \frac{N_g \frac{RT}{V}}{N_s \frac{RT}{V}} = \frac{N_g}{N_s} \text{ (Molar Ratio)} \qquad \text{(II-28)}$$

Utilizing Amagat's rule for partial volumes:

$$V_g = \frac{N_g RT}{P} \qquad \text{(II-29)}$$

$$V_s = \frac{N_s RT}{P} \qquad \text{(II-30)}$$

$$\frac{V_g}{V_s} = \frac{N_g \frac{RT}{P}}{N_s \frac{RT}{P}} = \frac{N_g}{N_s} \text{ (Volume Ratio)} \qquad \text{(II-31)}$$

$$\frac{P_g}{P_s} = \frac{N_g}{N_s} = \frac{V_g}{V_s}$$ Ratio of partial pressures equals molar and partial volume ratio

To account for non-ideal behavior of gases, the compressibility factor can be introduced to the perfect gas equation of state as follows:

$$P_t V = Z N_t R T \tag{II-32}$$

where: Z = compressibility factor
Other variables as previously defined

Utilizing Dalton's rule for partial pressures:

$$P_s = \frac{Z_s N_s R T}{V_t} \tag{II-33}$$

$$P_g = \frac{Z_g N_g R T}{V_t} \tag{II-34}$$

(subscripts as previously defined)

$$\frac{P_g}{P_s} = \frac{\frac{Z_g N_g R T}{V_t}}{\frac{Z_s N_s R T}{V_t}} = \frac{Z_g N_g}{Z_s N_s} \tag{II-35}$$

or
$$\frac{N_g}{N_s} = \frac{P_g}{P_s}\,\frac{Z_s}{Z_g} \tag{II-36}$$

On a molar volume basis:

$$V_s = \frac{V_t}{N_s} \tag{II-37}$$

$$V_g = \frac{V_t}{N_g} \tag{II-38}$$

where: V_s = molar volume of steam
V_g = molar volume of gas

or
$$\frac{V_s}{V_g} = \frac{V_t/N_s}{V_t/N_g} = \frac{N_g}{N_s} \tag{II-39}$$

Thus:
$$\frac{N_g}{N_s} = \frac{P_g}{P_s}\,\frac{Z_s}{Z_g} = \frac{V_s}{V_g} \tag{II-40}$$

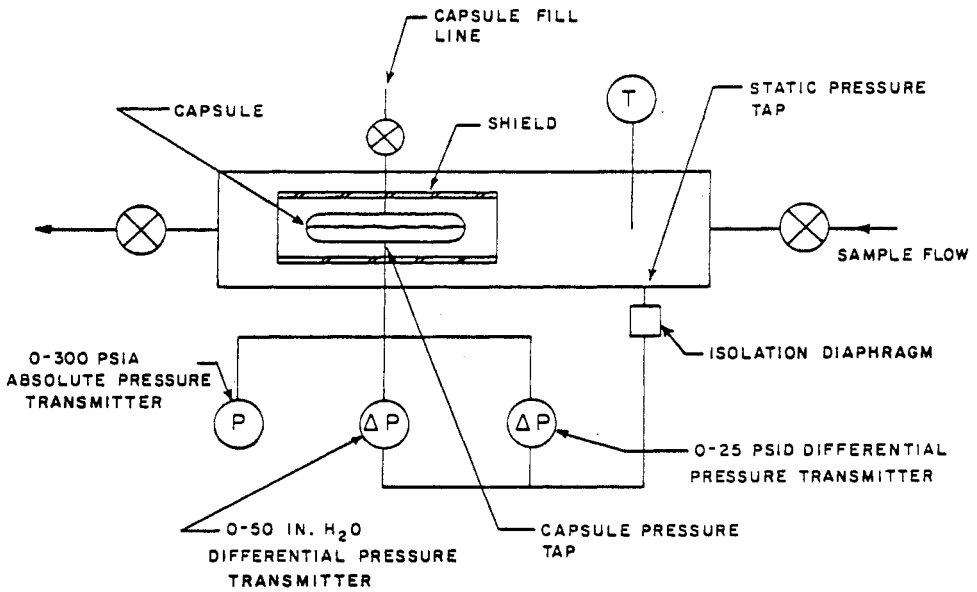

Figure II-29. Probe for the measurement of total Noncondensable Gas Concentration. (From Ref. 45)

Utilizing Amagat's rule for partial volumes:

$$V_g = \frac{Z_g N_g RT}{P_t} \qquad \text{(II-41)}$$

$$V_s = \frac{Z_s N_s RT}{P_t} \qquad \text{(II-42)}$$

$$\frac{V_g}{V_s} = \frac{Z_g N_g RT/PT}{Z_s N_s RT/PT} = \frac{Z_g}{Z_s} \frac{N_g}{N_s} \qquad \text{(II-43)}$$

If the molar weights of the constituents are known, then:

$$\frac{N_g}{N_s} \times \frac{M_g}{M_s} = \frac{W_g}{W_s} \qquad \text{(II-44)}$$

where: M = molar weight of component
W = mass of component
Subscripts as previously defined

II-7-1d. Noncondensable Gas Concentration Measurement Probe - McDowell[46] and Blair and Harrison[45] have described a device for the continuous monitoring of total noncondensable gas concentration in geothermal steam. The measurement principle is based on the measurement of the partial pressures of gases in the discharge in relation to the vapor pressure of pure water at the sampling pressure. A schematic diagram of the device is shown in Figure II-29. The molar ratio of noncondensable gas to steam is determined by measuring the static pressure of the system and the vapor pressure exerted by the pure water in a sealed capsule when heated to the system temperature. The device can also be used to measure the enthalpy of a two phase sample flow. The enthalpy estimation technique, based on measurements taken at two or more sampling conditions, and the calculational procedures are fully described in Ref. 45. If one assumes that the noncondensable gas content of geothermal steam is CO_2, then the calculation of total noncondensable gas in steam, based on use of the probe, is given by[46]:

$$W = \frac{144 \times M \times Pg \times Vs}{1545 \times T} \qquad \text{(II-45)}$$

where: W = pounds of noncondensable gas per pound of steam
Pg = partial pressure of noncondensable gas (psi)
Vs = specific volume of steam at the vapor pressure of the production water or brine (ft^3/lb)
T = temperature (°F)
M = molecular weight of the noncondensable gas

An advantage of the noncondensable gas probe is its capability for providing continuous data on the concentration of noncondensable gases in geothermal steam.

II-7-2. Chemical Characterization of Geothermal Steam Condensate

Analytical methods for the chemical charcterization of geothermal steam and noncondensable gases are described in Refs. 10, 11, 37, 39 and 47. Sampling procedures for hot, pressurized steam systems involve the use of small sampling trains as described in Section II-7-1b. The basic features needed in a sampling train are a condenser and a separator for fractionating noncondensable gases and steam condensate. The analytical characterization of steam condensate proceeds in analogous fashion to the analytical characterization of geothermal brine[3,5]. Steam produced by a full size steam separator is usually very clean. If brine carryover has been minimized by use of the appropriate separator design and, where necessary, steam scrubbers, total dissolved solids content of separated steam will usually be less than 100 mg/l. The characterization of noncondensable gases requires sample stabilization procedures to preserve reactive gas components such as H_2S and CO_2. Scavenging techniques are also required to effectively capture reactive dissolved gas components in steam condensate for subsequent quantification.

The basic procedure for the sampling and analysis of geothermal steam and its several components is designed to obtain samples of gas and condensate for characterization. Gas samples can be obtained in glass bulbs for quantification of components by gas chromatography and mass spectrometry. Reactive gas

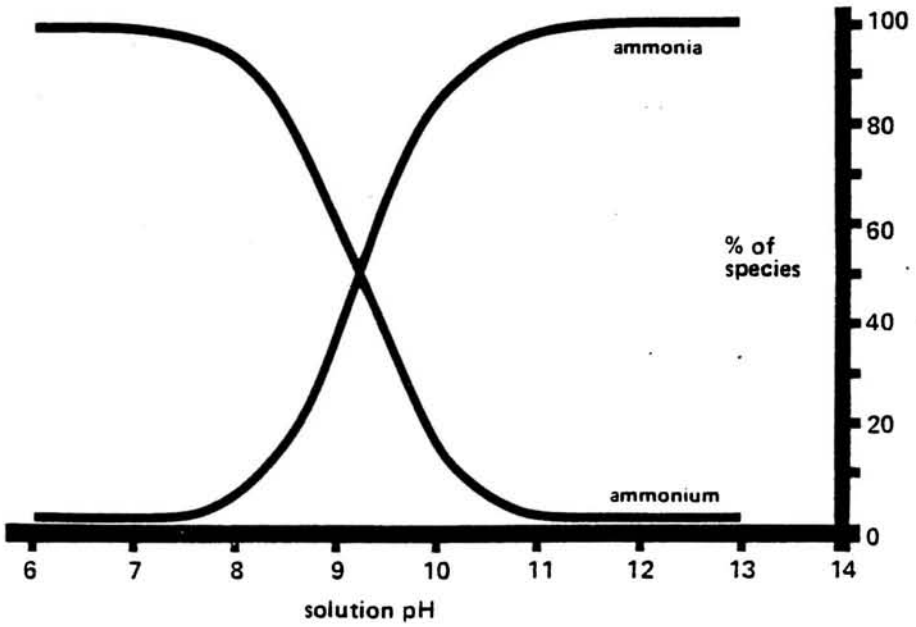

Figure II-30. Distribution of Ammonium and Ammonia ions in solutions. (From Ref. 49)

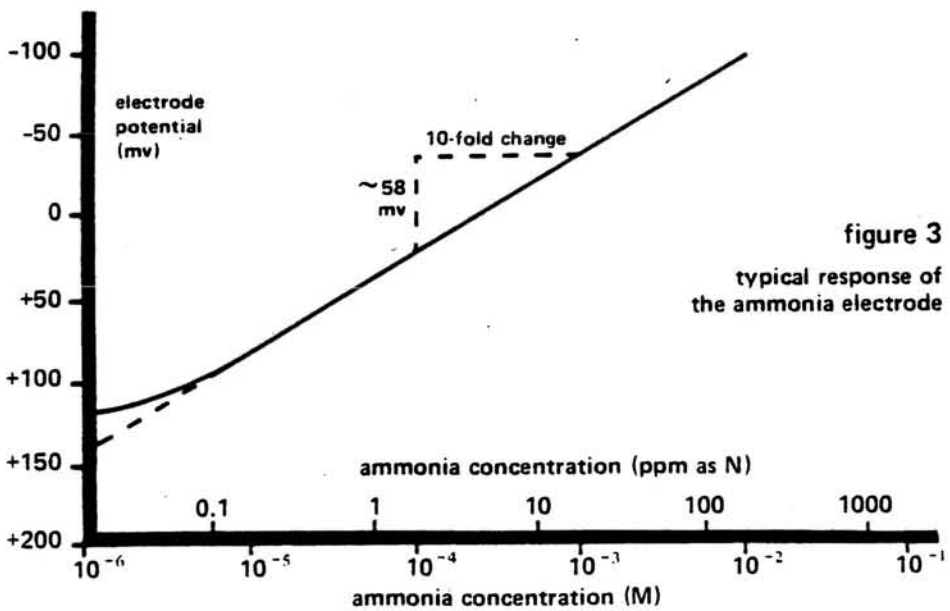

Figure II-31. Calibration curve for Orion Model 95-10 Ammonia Electrode. (From Ref. 49)

components are collected for analysis using specially formulated preserving and scavenging solutions. Condensate is obtained directly and stabilized with nitric acid. Dilution of condensate is not desirable owing to its low TDS content. Steam purity is usually expressed in terms of the separation efficiency[48].

II-7-2a. Analysis of Steam Condensate - Samples are obtained directly from a sampling train separator. Stabilization with 1 mg/l of concentrated nitric acid per 100 ml of sample is recommended. Determination of the residual concentration of dissolved noncondensable gases (ammonia, carbon dioxide and hydrogen sulfide) in condensate should proceed as follows:

II-7-2b. Ammonia - Samples should be analyzed as soon after collection as possible. It is assumed that the ammonia concentration will be determined using an Orion Model 95-10 ammonia electrode. The distribution of ammonia and ammonium ions in solution is shown in Figure II-30. The solution at time of measurement should have an adjusted pH of between 11 to 14. The measurement should be made immediately after sample collection if preservation techniques are not use. According to the Orion instruction manual[49], 50 percent of the original ammonia in a 100 ml sample, stored in a 100 m beaker, is lost after six hours of stirring at room temperature. Preservation of samples is accomplished by acidifying samples to a pH of about 6 using hydrochloric acid. Ref. 3 recommends the addition of 0.8 ml concentrated sulfuric acid per liter of sample and refrigeration. The determination of ammonia must be made at a constant temperature. The standards must be at the same temperature as the sample. A temperature change of 1°C gives rise to an analytical error in ammonia concentration of 2 percent when the ammonia concentration is 10^{-3} M (17 mg/l). Immediately before the determination of ammonia, the pH of samples

is elevated by the addition of 10 M NaOH. Direct determination of ammonia is based on generation of a calibration curve using a standard solution of 0.1 M ammonium chloride diluted as necessary to bracket the ammonia content of the sample (Figure II-31). The method of standard additions, which involves adding a standard of known concentration to the sample and redetermining the ammonia content of the mixture can also be used. Complete instructions for the use of the ammonia electrode is provided in Ref. 49.

II-7-2c. Carbon Dioxide - The CO_2 concentration in steam condensate depends upon sampling temperature and total CO_2 gas concentration. One method for measuring the concentration of CO_2 in condensate involves bubbling the condensate through 2N NaOH. A sparger should be used to insure good contact between the condensate and the sodium hydroxide solution. The total CO_2 content may then be determined by titration (APHA Standard Method 407 B[3]), by use of nomograms and measured alkalinity data (APHA Standard Methods 407 A[3]) or gravimetrically by scavenging CO_2 with strontium nitrate or barium hydroxide solution[10]. Alternatively, CO_2 may be determined directly by precipitation with concentrated ammonium hydroxide saturated with strontium chloride[50]. Alkalinity is conveniently measured using the HACH digital titrator and prepackaged sulfuric acid titrant. The nomographic technique is extremely useful because any or all of the alkalinity forms and CO_2 can be determined if the solution pH, total alkalinity, temperature and total dissolved solids content are known. The nomographic method is based on the interrelationship of ionization equlibria for the carbonate species and water. The relationships are valid only if the carbonate species control the titration behavior of the sample solution.

II-7-2d. Hydrogen Sulfide - The dissolved concentration of H_2S in steam condensate is determined by scavenging H_2S at the time of sampling using a solution of cadmium sulfate[39] or zinc acetate (APHA Standard Methods 428 B[3]) followed by acid solution of the cadmium or zinc sulfide precipitate and determination of the sulfide concentration using the methylene blue method (APHA Standard Methods 428 C[3,12]) or by the iodine titrimetric method (APHA Standard Methods 428 D[3]). Alternatively, H_2S can be scavenged using cadmium chloride solution[50] with subsequent quantification of sulfide based on the weight of the cleaned and dried cadmium sulfide precipitate.

II-7-3. Chemical Characterization of Noncondensable Gases

The characterization of noncondensable gas constituents in geothermal steam proceeds in analogus fashion to procedures described in Section II-7-2 for the characterization of steam condensate. A small sampling train with integral separator is used to provide a gas sample. The noncondensable gases are then bubbbled through scavenging solutions for the removal of CO_2 and H_2S. Alternatively, the noncondensable gases can be collected in an evacuated glass bulb for subsequent quantification by gas chromatography and mass spectrometry (see Appendix I). The scavenged reactive gases are quantified as per methods described in Section II-7-2. Ammonia-bearing solutions should be immediately stabilized by acidification if analysis is delayed.

II-7-4. Separation Efficiency

The carryover of dissolved solids with steam during the steam separation process is a measure of the separation efficiency. Separation efficiency is defined by Awerbuch, et al.[51] as follows:

$$\text{Separation Efficiency} = 1 - \frac{\text{Na in Steam}}{\text{Na in Brine Discharge}} \times 100 \qquad \text{(II-46)}$$

In similar fashion, separation purity can be defined as[51]:

$$\text{Separation Purity} = \frac{\text{Na in Steam}}{\text{Na in Brine Discharge}} \times \text{TDS (ppm) in Brine} \qquad \text{(II-47)}$$

Separation efficiencies of better than 99 percent can be achieved with adequately designed separators even in the case of hypersaline geothermal brine without the need for secondary steam scrubbers. One concern with regard to steam purity, however, is the carryover of volatile constituents. For example, a small amount of boron may be volitized during the flashing process and redistributed into steam condensate. Of greater concern is the carryover of dissolved silica which could promote turbine scaling. Silica volatility at the conditions commonly encountered in geothermal applications is low. However, volatile species of silica do exist (for example, as fluoride and boron complexes). In addition, colloidal silica present in flashed brine may be carried over with separated steam and subsequently redissolved in condensate[52]. The presence of silica in separated steam can lead to turbine scaling and, therefore, the need for control processing.

The maximum allowable silica concentration in steam produced in a conventional fossil-fuel or nuclear power plants is 0.025 mg/l[53]. The partitioning of silica between boiler feed water and steam is described by the distribution ratio which defines the ratio of silica concentrations in boiling water and the evolved steam. As shown in Figure II-32, the silica distribution ratio rapidly increases at pressures in excess of 1000 psi. If we assume a silica concentration of 500 mg/l in geothermal brine at a pressure of 500 psi, the corresponding silica distribution ratio and silica concentration in separated steam (from Figure II-32) are 0.005 and 2.5 mg/l, respectively.

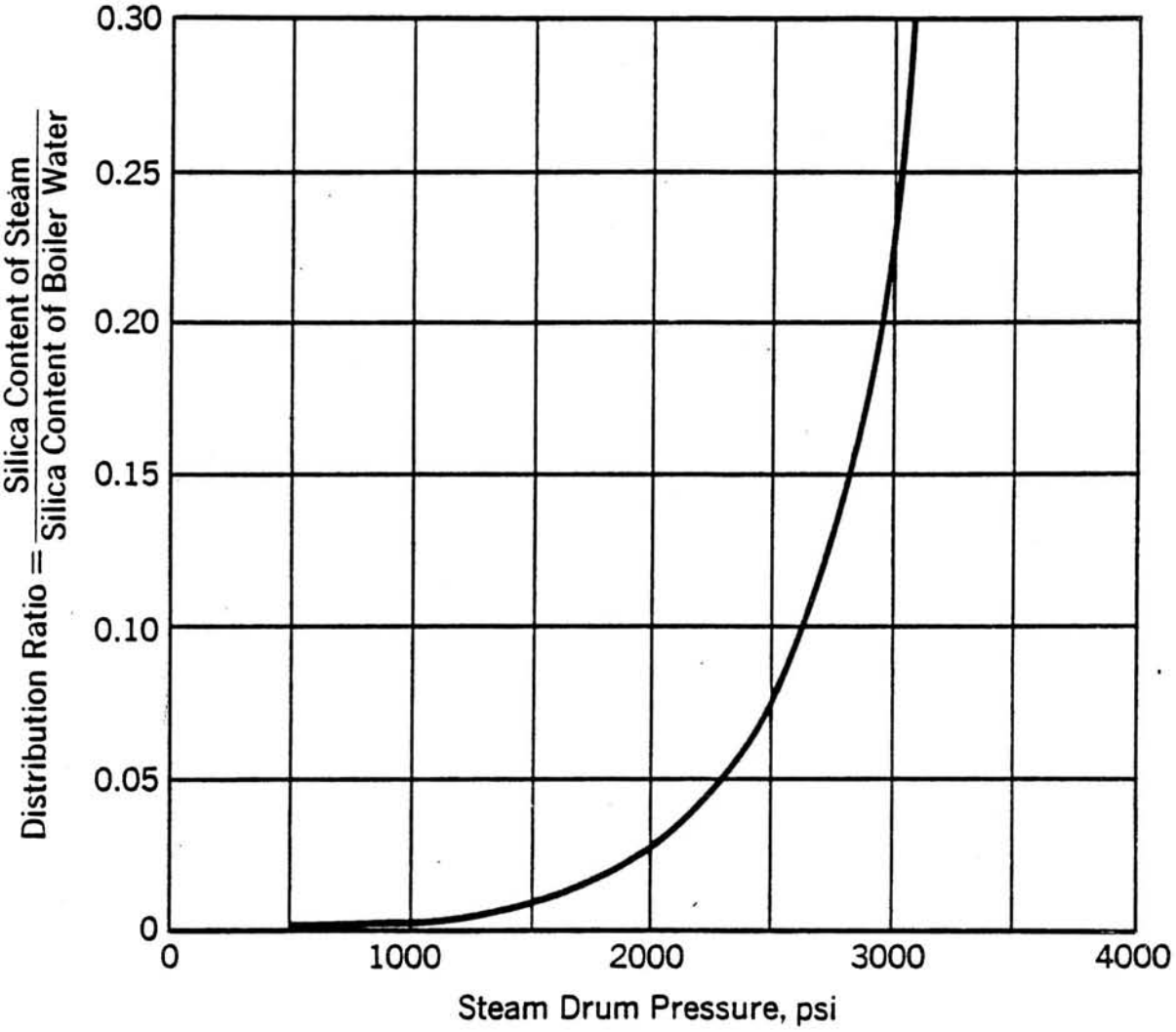

Figure II-32. Effect of pressure on silica distribution ratio. (From Ref. 53).

The requirement for field evaluation is to determine scaling characteristics in separated steam. This could be accomplished by use of preweighed scaling coupons placed in the steam line. Demonstration of the existence of a scaling problem may necessitate the installation of steam scrubbing equipment. Steam scrubbing is accomplished by washing steam with high purity water to redistribute silica species. Steam condensate would most likely be used as the source of washing water. It would be necessary to pretreat the condensate to remove dissolved silica prior to scrubbing the steam. It is common experience in geothermal power plants to clean turbine components periodically by sandblasting or other techniques. The various options that may be utilized at a particular site to maintain turbine operation have to be selected in part by the determination of scale deposition potential and by operating experience.

II-8. Thermodynamic Properties of Geothermal Brine

Evaluation of a geothermal prospect has as one of the primary goals the accurate determination of the energy content of the produced fluids and the equivalent electric power production potential of the resource. In the early stages of an investigation, short duration flow from a single well may be the only means of measuring production fluid enthalpy. The most commonly employed configuration for the testing of wells which produce a mixture of steam and hot water is shown in Figure II-33. The flow of separated steam and brine is metered using orifice meters. Calculation of equivalent volumetric and mass flowrates based on observed differential pressure drops across orifice plates requires accurate values for density and viscosity of the flow streams.

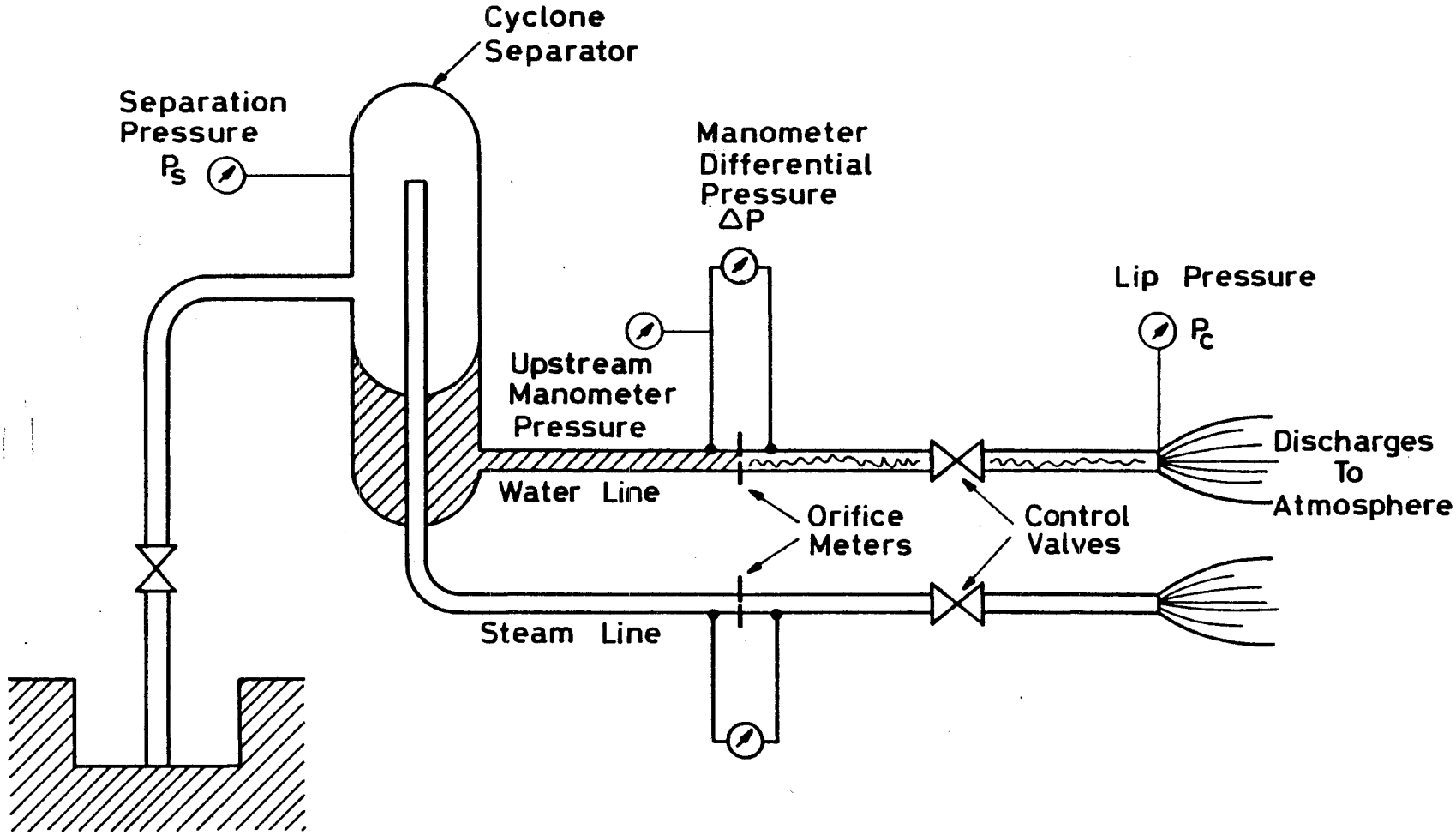

Figure II-33. Arrangement for measuring separated steam and water from geothermal well. (From Ref. 54).

Reservoir engineering assessments of a geothermal resource require accurate values for reservoir fluid density, viscosity and enthalpy in order to predict long-term performance of a reservoir under a variety of production-injection conditions.

II-8-1. Physical Methods for Estimating Enthalpy and Density

A simple method, based on measurement of lip pressure, for the estimation of the electric power potential of a geothermal well is described in Refs. 55 and 56. As shown in Figures II-34 and 35, lip pressure is measured at the end of a vertical discharge pipe of known ID. Lip pressure (Pc) is measured with the well throttled to a wellhead pressure of 175 psig while discharging through a vertical pipe. For environmental reasons, the method is only applicable in those cases where discharge of geothermal water or brine to the land surrounding the well does not pose a hazard.

For steam-water discharges where the enthalpy varies between 400 and 600 btu/lb, the electric power potential of the well is given by:

$$MW(e) = \frac{P_c^{0.96} d_c^2}{287.08} = P_c^{0.96} \frac{d_c^2}{16.94} \qquad \text{(II-48)}$$

where: P_c = the lip pressure (psig)
d_c = internal diameter of the discharge pipe (in)

The thermal efficiency of the power conversion process is assumed to be 0.10. Net power is estimated by reducing the calculated value of MWe by an additional 5 percent to account for parasitic losses associated with the operation of the energy conversion process. The overall accuracy of the estimation method is believed to be ±5 percent. The equivalent estimate of power production potential from a dry steam well is given by:

$$MW(e) = \frac{P_c^{0.96} d_c^2}{209.81} = P_c^{0.96} \frac{d_c^2}{14.48} \qquad \text{(II-49)}$$

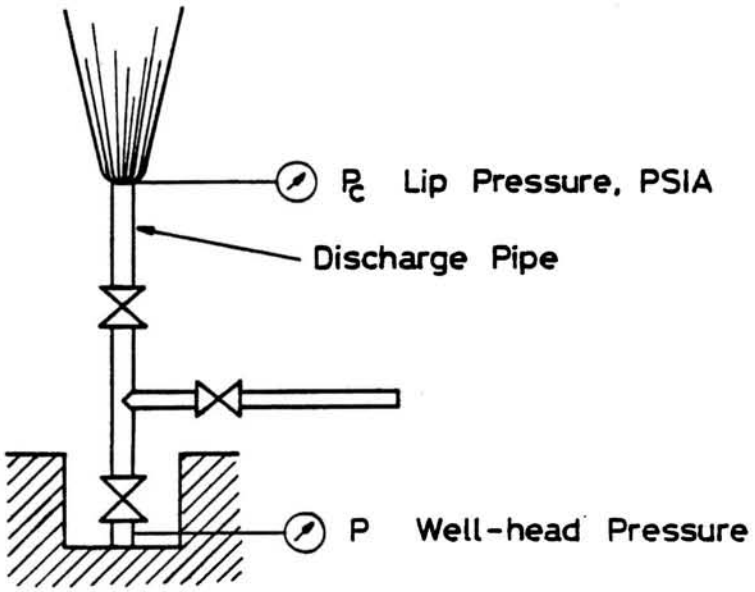

Figure II-34. Geothermal well discharging to the atmosphere via a vertical pipe. (From Ref. 56).

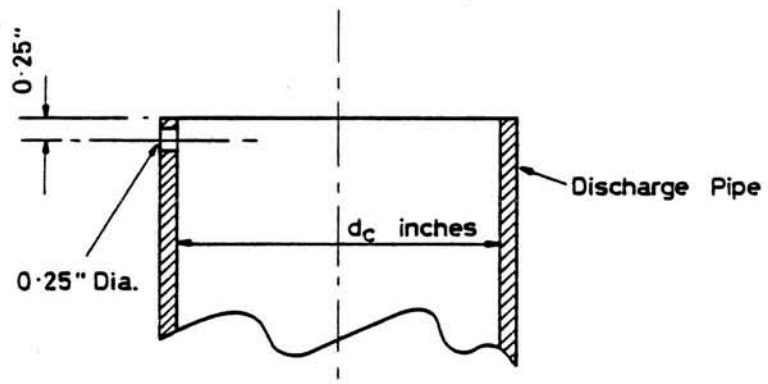

Figure II-35. Lip pressure assembly detail for a vertical discharge pipe. (From Ref. 56).

Enthalpy, downhole resource temperature, density of the production fluid at wellhead conditions, percent steam flash or dryness fraction and the velocity of a produced steam-water mixture at wellhead conditions can be deduced from the measurement of maximum discharging-pressure obtained at production wellhead conditions[57]. The temperature-depth relationship for a reservoir with a boiling mixture to a depth below which pressurized hot water exists is given by:

$$C = 69.56\ L^{0.2085} \text{ for } 30 < L < 3{,}000 \qquad \text{(II-50)}$$

where: C = boiling water temperature (°C)
L = depth of boiling (meters)

The percent steam flash is given by the expression:

$$q\% = \frac{P_m}{4} \qquad \text{(II-51)}$$

where: q% = percent steam flash
P_m = maximum discharge pressure at the wellhead (bars)

The total mass flowrate of a well operated at its maximum discharge pressure is given by:

$$W = 2.5\ h\ d^2 \qquad \text{(II-52)}$$

where: W = flowrate (t/h)
h = boiling water enthalpy at temperature °C (kj/kg)
d = wellbore diameter (meters)

The velocity of the steam-water mixture at wellhead conditions is given by:

$$u_{sw} = \frac{h}{188.5} \qquad \text{(II-53)}$$

where: u_{sw} = the velocity of the steam-water mixture at wellhead conditions (m/s)

The estimation of boiling water enthalpy as described above assumes that the water is pure and enthalpy values obtained from the Steam Tables are

adequate to describe the system. The presence of dissolved salts in water has a profound effect on enthalpy of the salt solution. Data plotted in Figure II-36, based on least squares linear approximations described in Ref. 20, illustrate how enthalpy varies as a function of temperature and salinity. Brine enthalpy can be measured using a calorimeter. However, estimation procedures and an energy balance offer a much simpler, but accurate method for determining enthalpy.

II-8-2. Enthalpy Determinations

Using the methods of Section II-7-1a and an energy balance it is straightforward to compute production wellhead specific enthalpy. The calculation is based on the availablility of a test facility of the type shown in Figure II-33. The enthalpies of the separated brine and gas streams from the separator are calculated. The brine enthalpy is corrected for salinity using the techniques described in Refs. 20 and 58 (see also Figure II-36). The enthalpy of the steam-noncondensable gas stream from the separator is obtained for pure component properties using the Steam Tables[40] and for CO_2 gas properties from Refs. 59-60. If quantitative data on the composition of noncondensable gases are available, the total enthalpy of the gas mixture may be computed. Otherwise, the noncondensable gases are assumed to consist entirely of CO_2. In most instances, the assumption of 100 percent CO_2 for the noncondensable gases is reasonable given that CO_2 accounts for 90 to 95 percent of the total noncondensable gases at most geothermal resources.

The enthalpy of steam plus noncondensable gases (CO_2) produced by the separator shown in Figure II-33 is given by:

$$Hv = Wv \{Hco_2 \times Xco_2 + Hs(1-Xco_2)\} \qquad \text{(II-54)}$$

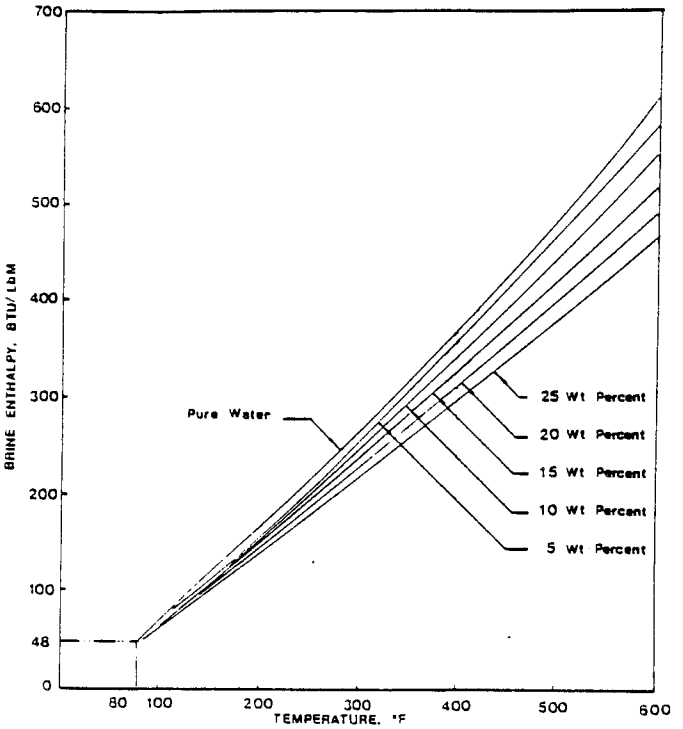

Variation of Enthalpy with temperature and salinity based on a least squares linear approximation. (From Ref. 20)

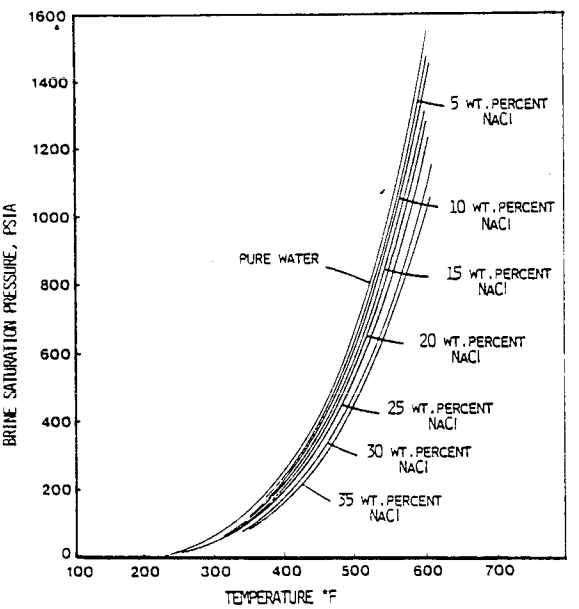

Figure II-36. Calculated brine saturation pressure curves as a function of sodium chloride concentration and temperature. (From Ref. 20)

where: Hv = enthalpy of the steam + noncondensable gas produced by the separator (btu/lb)

Wv = total mass flowrate of the steam + noncondensable gases (lb/hr)

Hco_2 = enthalpy of CO_2 (btu/lb)

Xco_2 = fractional weight percent CO_2

Hs = enthalpy of the steam (btu/lb)

The enthalpy of the brine produced by the separator of Figure II-31 is given by:

$$Hb = Wb \times Hb \qquad \text{(II-55)}$$

where: Hb = enthalpy of brine (btu/lb)

Wb = mass flowrate of brine (lb/hr)

Brine enthalpy is derived using the methods of Refs. 20 and 58 based on the measured value of total dissolved solids in the separated single phase brine.

The wellhead enthalpy is computed as the sum of the enthalpies of the steam and brine flows produced by the separator:

$$Hp = Hv + Hb \qquad \text{(II-56)}$$

II-8-3. Geochemical Methods for Evaluating Brine Properties

A detailed tabulation of brine properties for every conceivable brine composition that might be encountered is, in general, not available. The experimental determination of brine properties is also inconvenient. The utilization of estimation procedures for evaluating brine properties such as density, viscosity and enthalpy provides accurate values which are based on analysis of the available data base for sodium chloride and mixed brine solutions. For example, accurate estimates for the equation of state of complex geothermal brines is possible using estimation procedures such as the methodology described in Refs. 20 and 53 for the calculation of important thermophysical properties of brine as a function of temperature and salt content.

The methodology of Refs. 20 and 53 can be used to compute estimates for brine saturation pressure, liquid and vapor density, enthalpy and entropy.

II-8-3a. Estimation Procedures for Brine Saturation Pressure - Figure II-36 illustrates the variation of brine saturation pressure[20] as a function of temperature and sodium chloride concentration. The estimate was based on regression analysis of data by Hass[61] which led to the following approximation:

$$PSATB(T) = a_1 \times PSAT(T) \qquad \text{(II-57)}$$

X_s, Wt. Percent	a_1
5	0.969
10	0.934
15	0.894
20	0.847
25	0.794

where: PSATB(T) = brine saturation pressure (psia)

a_1 = regression coefficients for sodium chloride brines of varing concentration (X_s)

PSAT(T) = pure water saturation pressure (psia)

T = temperature (°F)

II-8-3b. Estimation Procedures for Calculating Brine Density - Regression analysis[20] of data from Ref. 61 yielded the following relationship for estimating brine density:

$$RHOB(T) = a_2 \times T + a_3 \qquad \text{(II-58)}$$

X_s, Wt. Percent	a_2	a_3
5	-0.043	72.60
10	-0.039	73.72
15	-0.035	74.86
20	-0.032	76.21
25	-0.030	77.85

where: RHOB(T) = calculated brine density (lbs/ft^3)

T = temperature (°F)

X_s = weight percent NaCl

a_2;a_3 = regression coefficients

Brine density is plotted as a function of sodium chloride concentration and temperature in Figure II-37. The calculated density values coincide with pure water density at temperatures between 250 to 575°F. Above and below these temperatures, the calculated density values are in error.

Cramer[62] described a method for estimating hypersaline brine density based on the regression analysis of density data compiled in Ref. 63. The approximation for brine density is given by:

$$P_b = P_\omega + [0.03378 + 0.05622 \times 10 \exp T/66.0\}] \qquad \text{(II-59)}$$

where: P_b = calculated brine density (gm/cc)
P_ω = density of vapo saturated pure water at temperature T (gm/cc)
T = absolute temperature (°K)

The approximation is accurate over the temperature range 0 to 275°C with a standard deviation of ±1%. The accuracy of the approximation is reported as ±0.012 gm/cc.

Hass[63] derived the following expression for the calculation of the density of vapor-saturated brine solutions:

$$d = \frac{1000 + xW_2}{1000v_0 + x\phi} \qquad \text{(II-60)}$$

$$\phi = \phi^* + kx^{0.5} \qquad \text{(II-61)}$$

$$\phi^* = c_0 + c_1v_0 + c_2v_0^2 \qquad \text{(II-62)}$$

$$k = (c_3 + c_4v_0)\,[v_0/(v_c - v_0)]^2 \qquad \text{(II-63)}$$

where: d = density of brine solution (gm/cc)
W_2 = molecular weight of sodium chloride (58.4428 g/mol)
v_0 = vapor-saturated specific volume of liquid water at the temperature of the brine solution (cm^3/g)
x = concentration of sodium chloride in the brine solution (mol NaCl/Kg H_2O - molal)
c_0 = -167.219 c_1 = 448.55 c_2 = -261.07 c_3 = -13.644
c_4 = 13.97 v_c = 3.1975

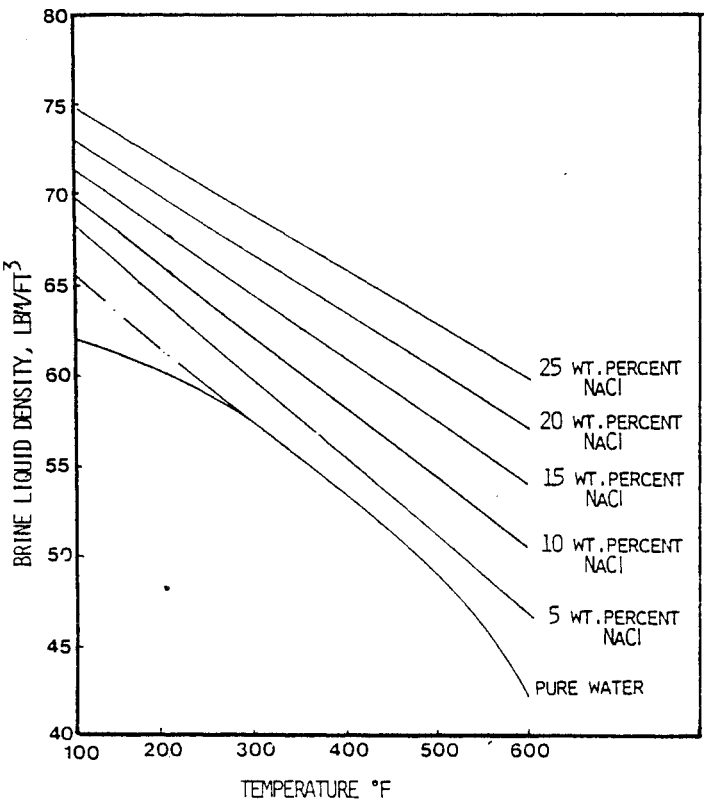

Figure II-37. Calculated values of Brine Density as a function of sodium chloride concentration and temperature. (From Ref. 20)

The precision and accuracy of density estimates was determined to be ±0.002 gm/cc and ±0.006 gm/cm, respectively.

Potter and Brown[64] derived expressions for the calculation of vapor-saturated brine density over the temperature range 0 to 500°C for brine concentrations of up to 8 molal (Tables II-14 and 15). They also derived an expression that describes the density of brine solutions at pressures up to 2000 bars. Preliminary steam tables for sodium chloride solutions are available in Refs. 63 and 65. Potter and Hass[66] describe a model for the calculation of the density of a complex brine solution with an arbitrary number of components. They show that the solution density is proportional to the densities of each component and the ratio of the concentration of each component to the total concentration of salts in the solution. They provide an example for the calculation of the density of a hypersaline geothermal brine over the temperature interval from 25 to 300°C based on estimates of component densities using regression analysis techniques.

An alternative approach for the calculation of a complex brine solution density is described by Potter[11]. The method involves calculation of an equivalent sodium chloride concentration for the brine, based on its total chloride concentration, and then utilizing Tables II-14 and 15 from Ref. 64 to determine the density of the equivalent sodium chloride solution at the desired temperature. Equivalent sodium chloride concentration is defined as follows:

$$eNaCl = (7.577\alpha + 0.03546\alpha^2) \frac{1}{1000 + \alpha} \qquad \text{(II-64)}$$

where: α = chloride concentration (gm/l)

In the case of brines containing significant dissolved sulfate, α is defined as:

TABLE II-14. DENSITIES OF VAPOR-SATURATED NaCl SOLUTIONS, g/cm^3 (From Ref. 64).

[The uncertainties in the densities are: 5-place figures $\pm 10^{-5}$, 50° data $\pm 10^{-4}$, 75° data $\pm 5 \times 10^{-4}$, 3-place figures ± 0.005, 2-place figures ± 0.05.]

	Molality															
Temp °C	0.5	1.0	1.5	2.0	2.5	3.0	3.5	4.0	4.5	5.0	5.5	6.0	6.5	7.0	7.5*	8.0*
0	1.02190	1.04244	1.06206	1.08086	1.09891	1.11625	1.13292	1.14895	1.16437	1.17920	1.19347	1.20719	--	--	--	--
25	1.01710	1.03621	1.05458	1.07227	1.08932	1.10576	1.12162	1.13691	1.15167	1.16591	1.17964	1.19288	--	--	--	--
50	1.0074	1.0259	1.0437	1.0609	1.0775	1.0936	1.1092	1.1242	1.1389	1.1530	1.1667	1.1801	--	--	--	--
75	0.9941	1.0126	1.0304	1.0477	1.0645	1.0807	1.0963	1.1115	1.1263	1.1405	1.1543	1.1677	--	--	--	--
100	0.978	0.997	1.014	1.031	1.046	1.062	1.078	1.093	1.107	1.122	1.136	1.151	1.165	--	--	--
125	0.961	0.980	0.998	1.013	1.028	1.044	1.060	1.075	1.089	1.104	1.118	1.133	1.147	--	--	--
150	0.941	0.960	0.979	0.993	1.008	1.024	1.040	1.055	1.070	1.084	1.099	1.114	1.128	1.143	--	--
175	0.916	0.937	0.957	0.971	0.985	1.003	1.018	1.034	1.049	1.064	1.079	1.094	1.108	1.123	1.14	--
200	0.888	0.910	0.932	0.947	0.961	0.979	0.996	1.011	1.027	1.042	1.057	1.072	1.088	1.103	1.12	1.14
225	0.856	0.880	0.903	0.920	0.934	0.955	0.971	0.987	1.004	1.019	1.035	1.050	1.066	1.081	1.10	1.12
250	0.820	0.846	0.872	0.890	0.905	0.928	0.945	0.962	0.980	0.996	1.012	1.027	1.043	1.058	1.08	1.10
275	0.780	0.810	0.838	0.859	0.874	0.899	0.918	0.936	0.954	0.971	0.987	1.003	1.019	1.034	1.05	1.08
300	0.736	0.769	0.801	0.824	0.842	0.869	0.889	0.908	0.927	0.945	0.962	0.978	0.994	1.009	1.03	1.05
325	0.689	0.726	0.760	0.788	0.807	0.837	0.859	0.880	0.899	0.917	0.935	0.952	0.968	0.984	1.00	1.02
350	0.637	0.679	0.717	0.749	0.770	0.804	0.827	0.849	0.870	0.889	0.907	0.925	0.941	0.957	0.97	0.99
375	0.56	0.629	0.671	0.708	0.730	0.768	0.794	0.818	0.839	0.860	0.878	0.896	0.913	0.929	0.94	0.95
400	--	0.56	0.621	0.665	0.689	0.731	0.760	0.785	0.808	0.829	0.849	0.867	0.884	0.900	0.90	0.91
425	--	--	0.569	0.619	0.646	0.693	0.724	0.751	0.775	0.797	0.818	0.837	0.854	0.869	0.87	0.87
450*	--	--	--	0.57	0.60	0.65	0.67	0.72	0.74	0.76	0.79	0.81	0.82	0.84	0.83	0.82
475*	--	--	--	--	--	0.61	0.65	0.68	0.71	0.73	0.75	0.77	0.79	0.81	0.79	0.77
500*	--	--	--	--	--	--	0.61	0.64	0.67	0.70	0.72	0.74	0.76	0.77	0.75	0.72

*Extrapolated values

TABLE II-15. DENSITIES OF VAPOR-SATURATED NaCl SOLUTIONS, g/cm^3(From Ref.64).

[The uncertainties in the densities are: 5-place figures $\pm 10^{-5}$, 50° data $\pm 10^{-4}$, 75° data $\pm 5 \times 10^{-4}$, 3-place figures ± 0.005, 2-place figures ± 0.05.]

	Weight percent													
Temp °C	1	3	5	7	9	11	13	15	17	19	21	23	25	30*
0	1.00755	1.02283	1.03814	1.05354	1.06908	1.08476	1.10060	1.11660	1.13276	1.14906	1.16551	1.18210	1.19880	--
25	1.00411	1.01823	1.03247	1.04688	1.06146	1.07624	1.09122	1.10639	1.12176	1.13732	1.15307	1.16900	1.18509	--
50	0.9948	1.0085	1.0222	1.0362	1.0503	1.0647	1.0793	1.0942	1.1093	1.1247	1.1403	1.1561	1.1722	--
75	0.9816	0.9952	1.0090	1.0229	1.0372	1.0516	1.0663	1.0813	1.0965	1.1119	1.1277	1.1436	1.1598	--
100	0.963	0.979	0.993	1.007	1.021	1.035	1.049	1.063	1.078	1.093	1.109	1.125	1.142	--
125	0.947	0.962	0.976	0.990	1.003	1.017	1.031	1.045	1.060	1.075	1.091	1.107	1.124	--
150	0.926	0.942	0.956	0.970	0.984	0.997	1.011	1.025	1.040	1.055	1.071	1.088	1.105	--
175	0.901	0.917	0.932	0.947	0.961	0.975	0.989	1.003	1.018	1.034	1.050	1.067	1.085	1.14
200	0.871	0.889	0.905	0.921	0.936	0.950	0.965	0.980	0.995	1.011	1.028	1.046	1.064	1.12
225	0.836	0.857	0.875	0.892	0.908	0.923	0.939	0.955	0.971	0.988	1.005	1.023	1.041	1.10
250	0.797	0.822	0.842	0.860	0.878	0.894	0.912	0.928	0.945	0.963	0.981	0.999	1.018	1.07
275	0.753	0.782	0.805	0.825	0.845	0.863	0.882	0.900	0.918	0.937	0.955	0.974	0.994	1.05
300	0.705	0.739	0.765	0.787	0.809	0.830	0.850	0.870	0.890	0.909	0.928	0.948	0.968	1.02
325	0.652	0.692	0.721	0.745	0.771	0.794	0.817	0.838	0.859	0.880	0.901	0.921	0.942	1.00
350	0.594	0.641	0.675	0.701	0.730	0.756	0.781	0.805	0.828	0.850	0.872	0.893	0.914	0.97
375	0.532	0.586	0.624	0.654	0.686	0.716	0.744	0.770	0.795	0.819	0.841	0.864	0.886	0.93
400	--	--	0.571	0.603	0.640	0.674	0.704	0.733	0.760	0.786	0.810	0.833	0.856	0.90
425	--	--	--	0.550	0.591	0.630	0.663	0.694	0.724	0.752	0.778	0.802	0.825	0.87
450*	--	--	--	--	0.54	0.58	0.62	0.65	0.69	0.72	0.74	0.77	0.79	0.83
475*	--	--	--	--	--	--	--	0.61	0.65	0.68	0.71	0.74	0.76	0.79
500*	--	--	--	--	--	--	--	--	0.61	0.64	0.67	0.70	0.73	0.75

*Extrapolated values

$$\alpha = Cl^{-} + \sqrt{SO_4^{=}} \qquad \text{(II-65)}$$

where the concentration units for chloride (Cl^{-}) and sulfate ($SO_4^{=}$) ions are in grams per liter (gm/l).

II-8-3c. Estimation Procedures for Total Enthalpy - Numerical approximations for brine enthalpy are provided in Ref. 67. Potter[11] provides an excellent example which illustrates the geochemical basis for the estimation of total enthalpy of a pressurized brine at production wellhead conditions. The example utilizes data for a production well at the Cerro Prieto geothermal field located in Northern Mexico. The calculation is based on the availability of analytical chemistry data for the separated and quenched brine and measurements of the separated steam and brine mass flowrates and the separation pressure:

Example Illustrating the Estimation Procedures for Calculation of Total Flow Enthalpy:

1. Chemistry and Production Data

Well M-30 (1-29-74) Cerro Prieto

Separator Pressure = 7.8 bars
Steam Flow = 81.8 ton/hr
Water Flow = 231.5 ton/hr
Na = 8655 mg/l
K = 2033 mg/l
Li = 27.2 mg/l
Ca = 567 mg/l
Cl = 16,000 mg/l
SiO_2 = 920 mg/l

2. Evaluation of the Percent Steam Flash

$$\text{Steam Flash} = \frac{\text{Steam Mass Rate}}{\text{Steam Mass Rate + Brine Mass Rate}} \qquad \text{(II-66)}$$

$$\text{Steam Flash} = \frac{81.8}{81.8 + 231.5} = 0.261 \qquad \text{(II-67)}$$

Percent Steam Flash = 26.1

3. Calculation of the Equivalent Sodium Chloride Concentration

$$eNaCl = [(27.577\alpha + 0.03546\alpha^2)] \frac{1}{1000 + \alpha} \quad \text{(II-68)}$$

$$eNaCl = [(27.577 \times 16) + (0.03546 \times 16^2)] \frac{1}{1000 + 16} \quad \text{(II-69)}$$

$$eNaCl = 0.443 \text{ molal}$$

4. Calculation of the Steam Separation Temperature

The separation temperature corresponding to an equivalent sodium chloride concentration of 0.443 molal at a separation pressure of 7.8 bars is determined by interpolation of data presented in Tables 1 and 2 of Ref. 65. Find the temperature in Tables 1 and 2 which brackets the observed separation pressure of 7.8 bars as follows:

	P1	P2
Temp °C	0 molal NaCl	0.5 molal NaCl
170	7.920 bars	7.786 bars

Let Px = the separation pressure for a 0.443 molal sodium chloride solution. Then:

$$Px = P1 - \frac{P1-P2}{5} \times 4.43 \quad \text{(II-70)}$$

$$Px = 7.80 \text{ bars}$$

The separation temperature is, therefore, 170°C. The calculated separation temperature can be compared to the actual measured separation temperature, if available.

5. Calculate the Enthalpy of the Steam and Brine Flows

The enthalpy of brine and steam at 170°C and 7.8 bars is obtained by interpolation from Tables 1 and 2 of Ref. 65:

Brine		Steam	
H_1^L	H_2^L	H_1^G	H_2^G
0 molal NaCl	0.5 molal NaCl	0 molal NaCl	0.5 molal NaCl
12938 J/mol	12499 J/mol	49871 J/mol	49891 J/mol

Let H_x^L = enthalpy of 0.443 molal NaCl at 170°C and 7.8 bars

$$H_x^L = H_1^L - \frac{H_1^L - H_2^L}{5} \times 4.43$$

$$H_x^L = 12549 \text{ J/mol}$$

Let H_x^G = enthalpy of steam

$$H_x^G = H_1^G + \frac{H_2^G - H_1^G}{5} \times 4.43$$

$$H_x^G = 49889 \text{ J/mol}$$

6. Enthalpy Units Conversion

The units of enthalpy from Tables 1 and 2 of Ref. 65 may be converted to btu/lb as follows:

$$H = \frac{J/mole}{MW \times 4.1868} \times 1.8 = btu/lb \qquad (II-71)$$

where: H = specific enthalpy (btu/lb)
MW = molecular weight (gm/mole)

For the steam phase, specific enthalpy is computed with MW equal to the molecular weight of pure water as follows:

$$H_s = \frac{49889}{18.0152 \times 4.1868} \times 661.4 \text{ cal/gm} \times 1.8 = 1190.6 \text{ btu/lb} \qquad (II-72)$$

For the brine phase, an adjusted molecular weight must be computed as follows:

$$f = \frac{x}{1000/MW_{H_2O} + x} \qquad (II-73)$$

where: f = mole fraction of NaCl in solution
x = NaCl molality
MW_{H_2O} = molecular weight of pure water (gm/mole)

The adjusted molecular weight of the solution is then computed:

$$MW_B = (F)(MW_{NaCl}) + (1-f)(MW_{H_2O}) \qquad (II-74)$$

where: MW_B = molecular weight of the brine (gm/mole)
MW_{NaCl} = molecular weight of sodium chloride (58.4428 gm/mole)

Therefore:

$$MW_B = 18.335$$

and

$$H_B = \frac{12549}{18.335 \times 4.1868} \times 1.8 = 294.3 \text{ btu/lb} \qquad (II-76)$$

7. Calculation of the Enthalpy of the Total Flow

The calculation of total flow specific enthalpy (Hp) proceeds as follows:

$$Hp = (q \times H_S) + [(1-q)(H_B)] \qquad (II-77)$$

where: Hp = specific enthalpy at reservoir conditions (btu/lb)
q = fractional percent steam flash

For the Cerro Prieto example:

$$Hp = (0.261)(1190.6) + [(1-0.261)(294.3)] \quad \text{(II-78)}$$

$$Hp = 528.2 \text{ btu/lb}$$

II-8-3d. Approximation Techniques for Estimating Brine Viscosity - According to Wahl[67] electrostatic forces in an ionic solution contribute to the transmission of shear forces throughout the fluid thereby contributing to an increase in viscosity relative to pure water. The viscosity of water is also temperature dependent and the variation in viscosity with temperature can be described for pure water with the following equation:

$$\log \mu_w = 2.03 + \frac{560}{T} \quad \text{(II-79)}$$

where: T = temperature (°K)

μ_w = viscosity (cp)

A viscosity approximation for a typical low to moderate salinity geothermal brine in which sodium, potassium and calcium are the principal cationic species is described by the following equation from Ref. 68:

$$\mu = \mu_w (1+0.021w_t + 0.00027w_t^2) \quad \text{(II-80)}$$

where: μ = viscosity of the brine solution (cp)

μ_w = viscosity of pure water at the temperature of the brine solution (cp)

Ref. 68 also provides approximations for the estimation of surface tension, enthalpy, vapor pressure, heat capacity and density of brine solutions.

The viscosity of geothermal brines can be estimated using methods described in Refs. 67 and 69. Ref. 69 describes an empirical correlation that allows the existing viscosity data for sodium chloride solutions to be extrapolated to temperatures as high as 325°C.

Viscosity estimates with an accuracy of 1.5 percent up to a temperature of 300°C can be obtained using the approximation technique described in Ref. 67. The viscosity of pure water is given by:

$$\log \frac{\mu_w\ (T)}{\mu_w\ (20)} = \frac{20 - T}{96 + T} [1.2378 - 1.303 \times 10^{-3}\ (20 - T)] + 3.06 \times 10^{-6}\ (20 - T)^2 + 2.55 \times 10^{-8}\ (20 - T)^3 \qquad \text{(II-81)}$$

The viscosity of a brine solution is given by:

$$\log \frac{\mu\ (T,m)}{\mu_w\ (T)} = A(m) + B(m)\ \log \frac{\mu_w\ (T)}{\mu_w\ (20)} \qquad \text{(II-82)}$$

where: $A(m) = 0.3324 \times 10^{-1}\ m + 0.3624 \times 10^{-2}\ m^2 - 0.1879 \times 10^{-3}\ m^3$

$B(m) = -0.3961 \times 10^{-1}\ m + 0.102 \times 10^{-1}\ m^2 - 0.702 \times 10^{-3}\ m^3$

$$m = \frac{1000\ X}{58.44\ (1 - X)}$$

and μ = brine viscosity, micro-pascal

μ_w = water viscosity, micro-pascal

m = brine salinity, NaCl equivalent molality

T = brine temperature, °C

$\mu_w\ (20)$ = 1002 micro-pascal

X = the NaCl weight fraction

Viscosity expressed as micro-pascals (μ Pas) may be converted to centipoise (cp) units as follows:

$$cp = 1000\ \mu\ Pas$$

The use of an equivalent NaCl concentration, as described in Section II-8-2c, will yield an accurate representation of the viscosity of a geothermal brine.

A graphical representation of sodium chloride viscosity data is available in Ref. 70 for temperatures up to 400°F. These data are shown in Figure

II-38. The effect of pressure on brine viscosity can be modelled using the procedure described in the insert on Figure II-38.

Viscosity estimation procedures for mixed sodium, potassium and calcium chloride geothermal brines are described in Ref. 71. The procedure, which is based on laboratory data, can accurately describe mixed brine viscosity for equivalent sodium chloride brine concentrations from 0.99 to 16.667 weight percent and temperatures up to 275°C.

Viscosity of sodium chloride, calcium chloride and potassium chloride brine solutions are summarized in Tables II-16 to 18, respectively. For a given potassium chloride or calcium chloride concentration, C_1, with a corresponding viscosity, μ, at Temperature T_1, a multiplier is derived to relate the mixed brine viscosity to the equivalent concentration of a sodium chloride solution with the same viscosity as μ, at the same temperature T_1. The multiplier is defined as the ratio of C_2/C_1 where C_2 is the equivalent sodium chloride concentration. Table II-19 summarizes multipliers for potassium chloride and sodium chloride solutions. A brine viscosity may be estimated using the following analytic expression:

$$\mu = 10^{-4}\left[\alpha+\beta t+\gamma T^2+\delta t^3+241.4\times10^{247.8/(T-140)}\right] \qquad \text{(II-83)}$$

where: $\alpha = 0.7543564E+04 + 0.1585416E+04\cdot C - 0.2153238E+03\cdot C^2 + 0.1311786E+02\cdot C^3$

$\beta = -0.4203004E+02 - 0.8313187E+01\cdot C + 0.1260422E+01\cdot C^2 - 0.7739334E-01\cdot C^3$

$\gamma = 0.81770676E-01 + 0.15072873-01\cdot C - 0.2354586E-02\cdot C^2 + 0.1479379E-03\cdot C^3$

and $\delta = -0.5509047E-04 - 0.8906202E-05\cdot C + 0.1396191E-05\cdot C^2 - 0.9156521E-07\cdot C^3$

T is temperature in degrees Kelvin and C is the equivalent sodium chloride concentration in weight percent.

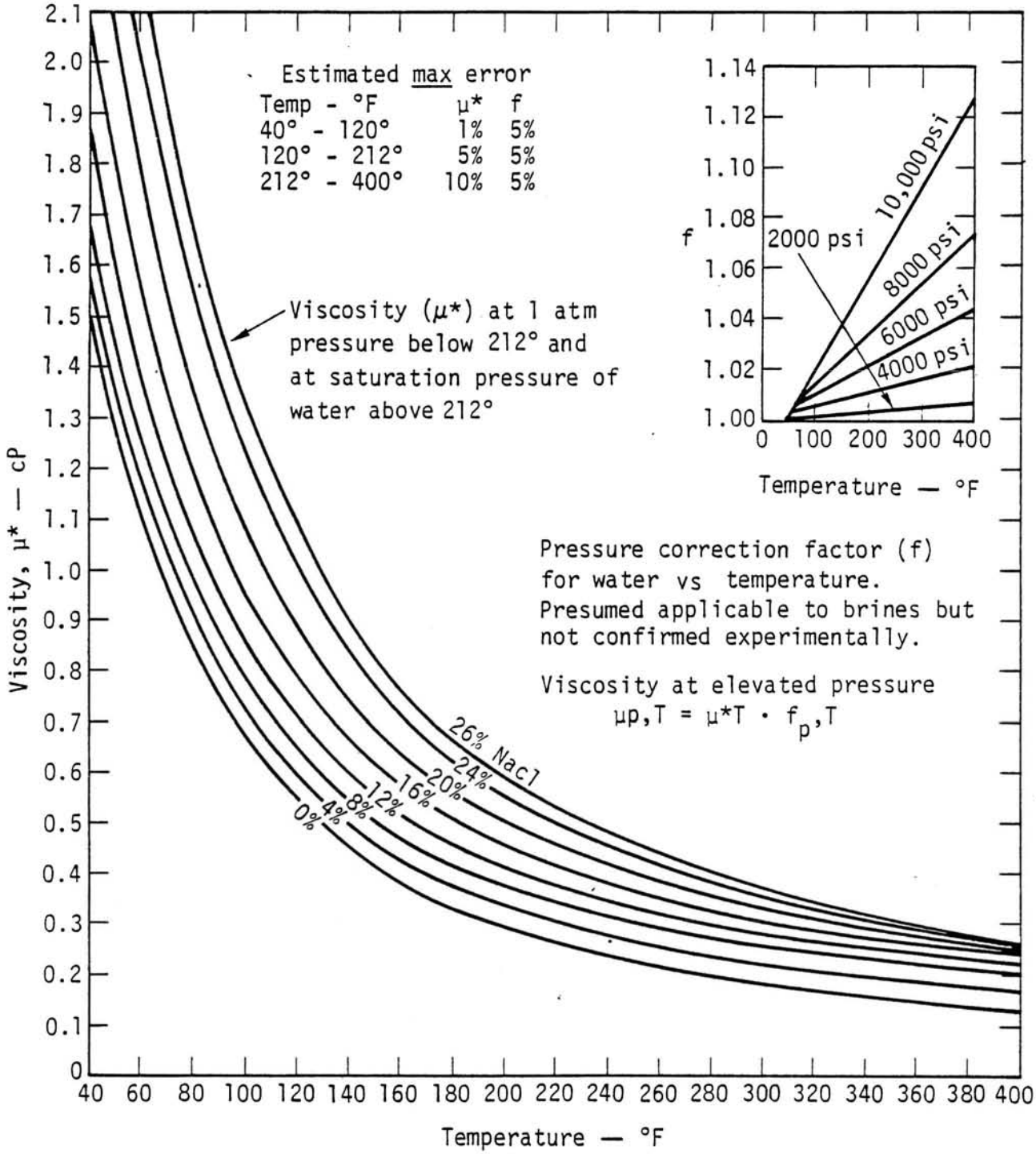

Figure II-38. Water viscosities for various salinities and temperatures. (From Ref. 70)

Temperature (°C)	Concentration (wt%) 1.0	3.0	9.0	13.0	17.0
25	0.892	0.962	1.079	1.182	1.350
30	0.825	0.869	0.979	1.096	1.241
40	0.711	0.749	0.847	0.948	1.070
50	0.625	0.658	0.743	0.825	0.940
60	0.556	0.588	0.659	0.724	0.836
70	0.498	0.526	0.595	0.651	0.750
80	0.444	0.470	0.543	0.592	0.672
90	0.399	0.420	0.493	0.542	0.618
100	0.359	0.379	0.452	0.500	0.568
110	0.331	0.342	0.416	0.452	0.521
120	0.288	0.309	0.380	0.428	0.483
130	0.258	0.280	0.352	0.398	0.450
140	0.227	0.251	0.328	0.370	0.418
150	0.206	0.229	0.304	0.345	0.390
160	0.188	0.220	0.283	0.325	0.364
170	0.172	0.198	0.266	0.306	0.348
180	0.168	0.181	0.251	0.288	0.328
190	0.148	0.172	0.237	0.275	0.312
200	0.139	0.165	0.228	0.264	0.294
210	0.130	0.154	0.218	0.252	0.285
220	0.126	0.150	0.210	0.242	0.272
230	0.120	0.145	0.204	0.232	0.261
240	0.115	0.142	0.199	0.224	0.252
250	0.113	0.139	0.195	0.215	0.241
260	0.110	0.136	0.190	0.210	0.232

Table II-16. Viscosity of NaCl solutions (cp).

Temperature (°C)	Concentration (wt%) 1.0	3.0	9.0	13.0	17.0
25	0.975	1.079	1.229	1.500	1.790
30	0.886	0.975	1.150	1.296	1.621
40	0.735	0.808	0.930	1.055	1.258
50	0.626	0.688	0.800	0.904	1.028
60	0.538	0.586	0.700	0.792	0.841
70	0.476	0.515	0.620	0.705	0.790
80	0.421	0.459	0.560	0.632	0.720
90	0.379	0.416	0.500	0.570	0.651
100	0.339	0.376	0.452	0.518	0.590
110	0.309	0.339	0.420	0.472	0.540
120	0.278	0.310	0.381	0.435	0.499
130	0.259	0.287	0.350	0.400	0.465
140	0.237	0.269	0.332	0.372	0.430
150	0.221	0.252	0.302	0.348	0.400
160	0.219	0.238	0.290	0.326	0.380
170	0.199	0.226	0.274	0.308	0.360
180	0.190	0.218	0.261	0.290	0.342
190	0.181	0.209	0.250	0.276	0.320
200	0.175	0.200	0.240	0.264	0.301
210	0.172	0.196	0.230	0.255	0.292
220	0.165	0.190	0.221	0.246	0.280
230	0.158	0.186	0.216	0.239	0.270
240	0.152	0.181	0.210	0.232	0.260
250	0.150	0.178	0.204	0.230	0.252
260	0.146	0.175	0.200	0.255	0.249

Table II-17. Viscosity of $CaCl_2$ solutions (cp).

Temperature (°C)	Concentration (wt%) 1.0	3.0	9.0	13.0	17.0
25	0.890	0.929	1.030	1.160	1.114
30	0.798	0.846	0.930	0.965	1.050
40	0.668	0.712	0.790	0.822	0.899
50	0.566	0.606	0.679	0.718	0.785
60	0.495	0.518	0.600	0.638	0.700
70	0.435	0.458	0.531	0.576	0.631
80	0.389	0.409	0.475	0.522	0.571
90	0.349	0.370	0.430	0.476	0.522
100	0.313	0.332	0.390	0.435	0.480
110	0.280	0.301	0.354	0.402	0.450
120	0.256	0.278	0.322	0.372	0.415
130	0.238	0.255	0.300	0.345	0.388
140	0.220	0.240	0.279	0.320	0.362
150	0.208	0.221	0.260	0.298	0.340
160	0.190	0.209	0.242	0.280	0.320
170	0.179	0.198	0.230	0.262	0.300
180	0.170	0.186	0.215	0.249	0.283
190	0.159	0.175	0.205	0.234	0.265
200	0.150	0.169	0.192	0.219	0.252
210	0.141	0.160	0.186	0.212	0.242
220	0.135	0.154	0.178	0.202	0.231
230	0.130	0.150	0.172	0.198	0.225
240	0.125	0.145	0.165	0.190	0.218
250	0.120	0.140	0.158	0.181	0.209
260	0.115	0.138	0.152	0.176	0.201

Table II-18. Viscosity of KCl solutions (cp).

Concentration (wt%)	Temperature (°C)	Multiplier	
		KCl	$CaCl_2$
1	50	0.200	1.100
	100	0.400	0.900
	150	1.100	1.400
	200	1.500	2.000
	250	1.600	2.900
3	50	0.233	1.733
	100	0.267	1.067
	150	0.800	1.667
	200	1.330	2.333
	250	1.167	2.667
5	50	0.400	1.660
	100	0.480	1.040
	150	0.700	1.200
	200	1.200	1.600
	250	1.000	1.800
7	50	0.429	1.571
	100	0.500	1.143
	150	0.714	1.286
	200	0.857	1.357
	250	0.714	1.429
9	50	0.556	1.333
	100	0.611	1.056
	150	0.667	1.111
	200	0.778	1.278
	250	0.722	1.444
11	50	0.636	1.273
	100	0.682	1.091
	150	0.909	1.045
	200	0.727	1.136
	250	0.545	1.318
13	50	0.569	1.231
	100	0.615	1.077
	150	0.692	1.031
	200	0.769	1.154
	250	0.654	1.231
15	50	0.633	1.200
	100	0.667	1.067
	150	0.933	1.080
	200	0.733	1.093
	250	0.600	1.111
17	50	0.706	1.118
	100	0.765	1.059
	150	0.824	1.029
	200	0.735	0.988
	250	0.647	1.029

Table II-19. Multipliers of KCl and $CaCl_2$

II-9. Characterization of Geothermal Scale Deposits

Formation of scale deposits in wells and surface facilities is a common operational problem associated with the geothermal energy conversion process. The definition of the physical and chemical characteristics of scale is important from the points of view of defining the magnitude of the problem and establishing remedial treatments or procedures for controlling the problem. In addition, scale depsotion upstream of the point where brine samples are obtained for chemical characterization represent a partial fractionation of dissolved species originally present in the reservoir fluid. Complete characterization of the production fluid requires that corrections be made for the removal of dissolved species as scale. This is especially important in the case of deep wells operating in a high scaling environment as the total mass of scale in a wellbore can be quite substantial after as little as one month of operation.

The obvious steps in the characterization of scale is to first determine the rates of scale formation in various parts of a facility including production and injection wells and the composition of the scale deposits. It is also important to properly evaluate scale formation in surface elements of the facility at temperature-pressure conditions that will most likely be experienced during the operation of a full-sized facility. It is important, therefore, to operate pilot facilities over the full range of anticipated operating conditions so that scale formation rates and the properties of scale depsits can be determined. It is also useful in identifying scale deposits to begin consideration of possible abatement procedures as well as methods for removing scale deposits if complete suppression by chemical additive additions or careful control of operating conditions is not entirely effective in preventing scale formation.

II-9-1. Characterization of Scale

The important elements in the complete characterization of scale are:

1. Determination of the rates of formation.
2. Scale mineralogy.
3. Scale chemistry.
4. Bulk density and porosity.

The above properties should always be established. Scaling rates are measured directly by determining the thickness of scale accumulation in various parts of a test facility. The rate of formation can be easily computed if total production corresponding to the measured scale thicknesses has been determined. Scale deposition in a wellbore can be established by the use of caliper logs run before and after a long-term flow period. Alternatively, a wireline scraper-bailer device can be used to collect samples of scale. The samples provide important information regarding both the formation rates and the identity of scale phases. Some scales are particularly adherent and hard such as the heavy metal sulfide and iron-rich siliceous scales characteristic of the hypersaline resources of southern California. It is difficult to completely remove these deposits from a wellbore using a scraper device. In these cases it is most useful to utilize data from calipers, if available, in conjunction with the recovered scale samples.

Mineralogy of scale deposits is obtained by the combination of x-ray diffraction analysis and optical petrographic techniques. It is sometimes useful to supplement these types of investigations with scanning electron microscopy analyses to better define microstructural attributes of the scales and as an aid in identifying fine-grained scale phases not identifiable by standard x-ray diffraction techniques. The use of EDAX-SEM capabilities is particularly good in identifying fines in a scale sample. The EDAX or energy

dispersive x-ray analysis yields qualitative microchemistry data for samples obtained in conjunction with an SEM analysis.

Chemistry of scale samples is more difficult to establish than the chemistry of a brine sample. The scale sample must be placed into solution prior to analysis. In the case of heavy metal sulfide scales containing large amounts of lead this is sometimes quite difficult as the lead and other heavy metals have a tendency to reprecipitate. Once a sample is in solution, analysis by ICP, AA or other techniques is straightforward. The preferred analytical scheme for scale samples is as follows:

1. Wash crushed samples repeatedly with distilled water to remove extraneous salts.

2. Dry the sample thoroughly in a vacuum oven and then obtain the sample weight.

3. Determine the acid solubility of the sample using hydrochloric acid. Ths is accomplished by treating a weighed amount of pulverized sample with concentrated hydrochloric acid and then determining the residual sample weight after filtration and drying. The insoluble residue is characterized subsequently.

4. Dissolution of samples for subsequent quantitative analysis is accomplished using concentrated hydrochloric acid in the case of acid soluble phases such as the carbonates. Heavy metal sulfide scales are dissolved in a hot mixture of hydrochloric, nitric, hydrofluoric and perchloric acids. Silica must be determined separately on a different sample split. Silica is determined after lithium metaborate fusion[72-73] of a sample and subsequent dissolution of the fusion cake with 3 percent nitric acid. The silica concentration is usually determined colorimetrically[3]. Analytical data are reported in units of ppm by weight (μg/gm).

In order to insure reliable results it is important to carefully homogenize samples prior to chemical analysis. Samples should be dried and then pulverized to 100 mesh or finer and then homogenized on a roller table. Precious metal content of heavy metal sulfide samples can be determined by a combination of fire assay and AA techniques. If samples are to be sent to commercial analytical laboratories for analysis, it should be noted that finely pulver-

ized heavy metal sulfide samples represent a potential combustion hazard due to the spontaneous ignition of oxidized sulfides. These samples should be shipped in waterfilled polyethylene bottles.

Density and porosity of scale samples may be determined using techniques described in Ref. 74-75. Bulk density is readily etermined using the water immersion or gas pycnometer techniques.

II-9-2. Treatment of Scale Analytical Data

It is useful to convert chemical analytical data obtained for scale samples to the equivalent scale compounds. This is more than a mere academic effort since it serves as an excellent means of checking the validity of the analytical data as well as providing important insights into the scaling phenomena. The technique also provides the basis for ultimately correcting reservoir brine compositions for deficiencies caused by the formation of scale.

The conversion of elemental concentrations (μg/gm) to the equivalent weight percent of scale forming compounds is accomplished as follows:

$$X_C = (X_E \cdot F)/10^4 \qquad \text{(II-84)}$$

where: X_C = the weight percent of a compound in the scale
X_E = the elemental concentration in the scale (μg/g)
F = M/An
M = the molecular weight of a scale compound
A = the element X_E atomic weight
n = number of moles of element X_E per mole of scale compound

The selection of appropriate scaling phases with which to represent the actual scale deposits should be selected on the basis of petrographic and x-ray diffraction analysis of the scale samples. Bearing in mind the inherent limitations of x-ray diffraction techniques in elucidating fine-grained low

abundance mineralogies in a complex mixture of crystalline and amorphous phases, some judgemental decisions will be necessary in defining the scale mineralogy. However, one check on the selected mineralogical abundances will be obvious after summing the total percent of calculated mineral oxides, sulfides, carbonates, etc.

A certain percentage of the dissolved brine constituents originally present in the reservoir brine are partitioned into scale. In order to determine the actual reservoir fluid composition it is necessary to correct the brine compositions at the sampling point for scale deposition. It is also of interest to compute an overall material balance for a geothermal flow test that accounts for the total fluid production and the total mass of scale formed during the test. The calculation of a material balance is straightforward:

1. Determine the mass of scale forming elements in the production well and surface facilities back to the injection well.
2. Correct the average reservoir brine composition, derived from steam flash-corrected analyses of brine samples and total noncondensable gases, for the deposition of scale.
3. Correct the average composition of injection wellhead brine for total steam loss including evaporative losses in the brine treatment facility.
4. The change in brine composition between the geothermal reservoir and the injection wellhead should be balanced by the formation of scale and sludge in various parts of the production and surface facilities.

The mass of each scale-forming compound up to the location of the first sample for analytical characterization is computed as follows:

$$Ms = (V_s)\cdot(\rho_s)\cdot(K)\cdot(1-\phi)\cdot(Q_s) \qquad \text{(II-85)}$$

where: V_s = calculated volume of scale compound (ft^3)

ρ_s = scale density (g/cc)

K = density conversion factor (62.43)

ϕ = fractional scale porosity

Q_s = fractional percent scale abundance

M_s = mass of a given scale compound (lbs)

The elemental mass in each scale compound may be computed as follows:

$$M_E = (M_S)(1/F) \qquad \text{(II-86)}$$

where: M_E = elemental mass (lbs)

M_S = scale compound mass (lbs)

F = molecular weight of scale compound/(atomic weight of element · n)

n = number of moles of element X_E per mole of scale compound

The production reservoir brine composition is corrected for scale formation between the reservoir and the location of the brine sampling station used to obtain primary brine samples for characterization of the ultimate reservoir brine composition. The correction is applied as follows:

$$P_{Tc} = \sum_{i=1}^{n} [(P_{Ti})(1x10^{-6})(Q) + P_{Si}] \,/\, (Q)(1x10^{-6}) \qquad \text{(II-87)}$$

where P_{Tc} = scale corrected total dissolved solids concentration (µg/g) in the production reservoir brine

P_{Ti} = concentration (µg/g) of ith dissolved element in the production reservoir brine

P_{Si} = mass (lbs) of ith element in scale deposited between the production reservoir and the brine sampling location

Q = total mass (lbs) of produced brine from the resevoir

The total mass balance is computed as follows:

$$[(P_{TC})\cdot(Q)\cdot(k)] - [(I_T)\cdot(1-f)\cdot(Q)\cdot(k) - M_1 - M_2 - M_3\ M_n] = 0 \qquad \text{(II-88)}$$

where: P_{TC} = scale-corrected prouction reservoir total dissolved solids (µg/g)

Q = total brine mass flow - $212x10^6$ lbs

k = 1x0^{-6} lbs/lb - converts µg/gm to lbs/lbs

I_T = injection wellhead brine total dissolved solids (µg/gm)

f = fractional steam flash plus evaporative losses

M_1, M_2, M_3, M_n = mass of solids and scale formed in various parts of the surface facility between the location of the brine sampling station and the injection wellhead (lbs)

II-10. References

1. Kindle, C.H. and Woodruff, E.M., 1981, Techniques for Geothermal Liquid Sampling and Analysis: Battelle Rpt. PNL-3801.

2. Test Methods for Evaluating Solid Waste Physical/Chemical Methods, (1982): U.S. EPA, SW-846, 2nd Edition.

3. Standard Methods for the Examination of Water and Wastewater (1975): 14th Edition, APHA-AWWA-WPCF.

4. Part 31, Water (1982): Annual Book of ASTM Standards, ASTM, Philadelphia, Pennsylvania.

5. Kopp, J.F. and McKee, G.D., 1978, Methods for Chemical Analysis of Water and Wastes: U.S. EPA Rept. PB-297686.

6. Part 41, General Test Methods, Nonmetal; Laboratory Apparatus; Statistical Methods; Space Simulation; Durability of Nonmetallic Materials (1982): Annual Book of ASTM Standars, ASTM, Philadelphia, PA.

7. Vetter, O.J. and Kandarpa, V., 1982, Integrated Geothermal Well Testing Part III: U.S. DOE/DGE Report.

8. Owen, L.B. and Burton, F.M., 1983, Milestone II Long-Term Test of Lacy 2-28 Volume IV: Chemistry and Corrosion Assessment: Terra Tek Research Rept. TR 83-24, Submitted to MCR Geothermal Corporation in Two Volumes.

9. Ellis, A.J. and Mahon, W.A.J., 1977, Chemistry and Geothermal Systems: Academic Press.

10. Watson, J.C., 1978, Sampling and Analysis Methods for Geothermal Fluids and Gases: Battelle, PNL Rept. PNL-MA-572.

11. Geochemical Fundamentals for Geothermal Exploration and Reservoir Evaluation, 1980: Technical Training Course No. 6, Geothermal Resources Council, Davis, California.

12. HACH Water Analysis Handbook, 1981: HACH Company No. 2504-08.

13. Jamin, M.E. and Nealy, C.L., Mobile Laboratory: Results from the First Year: Proc., 5th Annual Geothermal Conference and Workshop, EPRI Rept. EPRI AP-2098, 5C-17-5C-32.

14. Hamilton, C.E., Editor, 1978, Manual on Water: ASTM Special Technical Publication 442A.

15. Shannon, B., 1982, Drilling Fluid pH: How to Get Accurate Field Measurements: Petroleum Engineer, International, March, 98-104.

16. Patton, C.C., 1977, Oilfield Water Samples: Campbell Petroleum Series, Norman, Oklahoma.

17. Kasameyer, P., Morse, J. and Owen, L.B., 1977, Evaluation of Magmamax 1 and Woolsey 1 Production Wells: University of California, Lawrence Livermore National Laboratory Geothermal Energy Program Highlights Report ATHS/ISP-8.

18. Handbook of Electrode Technology, 1982, Orion Research, Inc., Cambridge, Massachusetts.

19. Grens, J.Z., 1975, The Effect of Salinity on Geothermal Well Performance: University of California, Lawrence Livermore National Laboratory Rept. UCID-16791.

20. Dittman, G.L., 1977, Calculation of Brine Properties: University of California, Lawrence Livermore National Laboratory Rept. UCI-17406.

21. Harrar, J.E. and Raber, E., 1983, Chemical Analyses of Geothermal Waters and Strategic Petroleum Reserve Brines for Strategic and Precious Metals: University of California, Lawrence Livermore National Laboratory Rept. UCRL-88575 Preprint.

22. Beamish, F.E. and VanLoon, J.C., 1977, Analysis of Noble Metals: Academic Press, New York, NY.

23. Fournier, R.O. and Rowe, J.J., 1966, Estimation of Underground Temperatures From the Silica Content of Water from Hot Springs and Wet-Steam Wells: American Journal of Science, V. 264, 685-697.

24. Truesdell, A.H. and Fournier, R.O., 1977, Procedure for Estimating the Temperature of a Hot-Water Component in a Mixed Water by Using a Plot of Dissolved Silica Versus Enthalpy: Jour. Research, U.S. Geol. Survey, V. 5, No. 1, 49-52.

25. White, D.E., 1970, Geochemistry Applied to the Discovery, Evaluation and Exploration of Geothermal Energy Resources: U.N. Symposium on the Development and Utilization of Geothermal Resources, Section V, Pisa, Italy.

26. Ellis, A.J., 1979, Chemical Geothermometry in Geothermal Systems: Chemical Geology, 25, 219-226.

27. Fournier, R.O., White, D.E. and Truesdell, A.H., 1974, Geochemical Indicators of Subsurface Temperature - Part I, Basic Assumptions: Jour. Research, U.S. Geol. Survey, V. 2, No. 3, 259-262.

28. Fournier, R.O. and Truesdell, A.H., 1974, Geochemical Indicators of Subsurface Temperature - Part 2, Estimation of Temperature and Fraction of Hot Water Mixed with Cold Water: Jour. Research, U.S. Geol. Survey, V. 2, No. 3, 263-270.

29. Fournier, R.O. and Truesdell, A.H., 1973, An Empirical Na-K-Ca Geothermometer for Neutral Waters: Geochimica et Cosmochimica Acta, V. 37, 1255-1275.

30. Fournier, R.O. and Potter, R.W., 1979, Magnesium Correction to the Na-K-Ca Chemical Geothermometer: Geochim. Cosmochim. Acta, V. 43, 1543-1550.

31. Fournier, R.O., 1979, A Revised Equation for the Na/K Geothermometer: Geoth. Res. Council Trans., V. 3, 221-224.

32. Reed, M.J., 1975, Chemistry of Thermal Water in Selected Geothermal Areas of California: California Division of Oil and Gas, Rept. No. TR15.

33. Fournier, R.O., 1981, Application of Water Chemistry to Geothermal Exploration and Reservoir Engineering: in L. Rybach and L.J.P. Muffker, Geothermal Systems, Principles and Case Histories, John Wiley and Sons, New York, NY.

34. Fouillac, C. and Michard, G., 1981, Sodium/Lithium Ratios in Water Applied to Geothermometry of Geothermal Reservoirs: Geothermics, V. 10, 55-70.

35. Kestin, J., DiPippo, R., Knalifa, H.E. and Ryley, D.J., Editors, 1980, Sourcebook on the Production of Electricity from Geothermal Energy: U.S. DOE Rept. DOE/RA/4051-1, 285-286.

36. Jacobson, W.O., 1978, Operational History of the Geothermal Loop Experimental Facility at the Salton Sea KGRA: Geothermal Resources Council, Trans., V. 2, 325-326.

37. Ellis, A.J. and Golding, R.M., 1963, Solubility of Carbon Dioxide Above 100°C in Water and Sodium Chloride Solutions: Amer. Jour. Science, V. 261, No. 47.

38. Blair, C.K. and Owen, L.B., 1981, Utah State Prison Space Heating With Geothermal Heat: DOE/ET/27027-4.

39. Christoffersen, D.J., Wheatley, R.N. nd Baur, J.A., 1975, Union Oil Company of California's Geothermal Sampling Techniques: Proceedings, 1st Workshop on Sampling Geothermal Effluents, Oct. 20-21, Las Vegas, Nevada, EPA-600/9-76-011.

40. Steam Tables, 1967, ASME, New York, NY.

41. Tri-Flat Variable-Area Flowmeters: Handbook 10A9010, Fisher and Porter Company, Warminster, Pennsylvania, 1975.

42. Variable Area Flowmeter Handbook - Volume 1, Basic Rotameter Principles: Catalog No. 10A1021, Fisher and Porter Company, Warminster Pennsylvania, 1982.

43. Variable Area Flowmeter Handbook - Volume II, Rotameter Calculations: Catalog No. 10A1022, Fisher and Porter Company, Warminster, PA, 1977.

44. Variable Area Flowmeter Handbook - Volume III, Rotameter Selection Guide: Catalog No. 10A1023, Fisher and Porter Company, Warminster, PA, 1977.

45. Blair, C.K. and Harrison, R.F., 1980, Development of an Instrument to Measure the Concentration of Noncondensable Gases in Geothermal Discharges: Univ. of Calif., Lawrence Berkeley National Laboratory Rept. LBL-11499.

46. McDowell, G., 1974, Geothermics, V. 3, p. 100.

47. Giggenbach, W.F., 1975, A Simple Method for the Collection and Analysis of Volcanic Gas Samples: Bull. Volcanology, V. 39, No. 1, 1-14.

48. Awerbuch, L., May, S. and Soo-Hoo, R., 1981, Geothermal Steam Separator Evaluation: EPRI Rept. EPRI AP-2098, 5B-31-5B-33.

49. Instruction Manual, Ammonia Electrode Model, 95-10: Orion Research, Cambridge, MA (1979).

50. Nehring, N.L. and Truesdell, A.H., 1977, Collection of Chemical, Isotope, and Gas Samples from Geothermal Wells: Proc. 2nd Workshop on Sampling Geothermal Effluents, U.S. EPA Rept. EPA-600/7-78-121, 130-140.

51. Awerbuch, L., Van der Mast, V.C. and McGrath, D.P., 1982, 6th Annual EPRI Geothermal Conf., Snowbird, Utah.

52. Weres, O., Tsao, L. and Iglesias, E., 1980, Mexican-American Cooperative Program at the Cerro Prieto Geothermal Field: Univ. of Calif., Lawrence Berkeley National Laboratory Rept. LBL-10166.

53. Steam - Its Generation and Use: Babcock and Wilcox, New York, NY (1972).

54. James, R., 1975, Possible Serious Effect of the Presence of Steam on Hot-Water Flow Measurements Utilizing an Orifice Meter: Proc., 2nd U.N. Symposium on the Development and Use of Geothermal Resources, 1703-1706.

55. James, R., 1962, Steam-Water Critical Flow Through Pipes: Inst. Mech. Engrs. Proc., V. 176, No. 26, p. 741.

56. James, R., 1975, Rapid Estimation of Electric Power Potential of Discharging Geothermal Wells: Proc., 2nd U.N. Symposium on the Development and Use of Geothermal Resources, 1685-1687.

57. James, R., 1980, Significance of the Maximum Discharging Pressure of Geothermal Wells: Proc. 6th Workshop, Geothermal Reservoir Engineering, Stanford Geothermal Program, Stanford University Rept. SGP-TR-50, 145-149.

58. Miller, A., 1980, Brine-Steam Properties Computer Program for Geothermal Energy Calculations: University of California, Lawrence Livermore National Laboratory Rept. UCRL-52495.

59. Perry, R.H. and Chilton, C.H., 1973, Chemical Engineer's Handbook: 5th Edition, McGraw-Hill, New York, NY.

60. Gas Machinery

61. Hass, J.L., Jr., 1971, The Effect of Salinity on the Maximum Thermal Gradient of a Hydrothermal System at Hydrostatic Pressure: Economic Geology, V. 66, 940-946.

62. Cramer, S.D., 1978, A Simplified Equation for Calculating the Density of Vapor-Saturated Sodium Chloride Brines: Geothermal Energy Magazine, V. 6, No. 7, 22-24.

63. Hass, J.L., Jr., 1976, Physical Properties of the Coexisting Phases and Thermochemical Properties of the Component in Boiling NaCl Solutions: U.S.G.S. Bulletin 1421-A, 73 p.

64. Potter, R.W., II, and Brown D.L., 1977, The Volumetric Properties of Aqueous Sodium Chloride Solutions From 0° to 500°C at Pressures Up to 2000 Bars Based on a Regression of Available Data in the Literature: U.S.G.S. Bulletin 1421-C, 36 p.

65. Hass, J.L., Jr., 1976, Thermodynamic Properties of the Coexisting Phases and Thermodynamic Properties of the NaCl Component in Boiling NaCl Solutions: U.S.G.S. Bulletin 1421-B, 71 p.

66. Potter, R.W., II, and Hass, J.L., Jr., 1978, Models for Calculating Density and Vapor Pressure of Geothermal Brines: Jour. Research, U.S. G.S., V. 6, No. 2, 247-257.

67. Michaelides, E.E., 1981, Thermodynamic Properties of Geothermal Fluids: Geothermal Resources Council, Transactions, V. 5, 361-364.

68. Wahl, E.F., 1977, Geothermal Energy Utilization: John Wiley and Sons, New York, NY.

69. Potter, W.R., II, 1978, Viscosity of Geothermal Brines: Geothermal Resources Council, Trans., V. 2, 543-544.

70. Matthews, C.S. and Rossell, D.G., 1967, Pressure Build-Up and Flow Tests in Wells: Monograph, V. 1, H.L. Doherty Series, Soc. of Petroleum Engineers.

71. Ershaghi, I., Abdassah, D., Bonakdar, M.R. and Ahmad, S., 1983, Estimation of Geothermal Brine Viscosity: Journal of Petroleum Technology, V. 35, N. 3, 621-628.

72. Ingamells, C.O., 1970, Lithium Metaborate Flux in Silicate Analysis: Anal. Chem. Acta, V. 52, 323-334.

73. Suhr, N.H. and Ingamells, C.O., 1966, Solution Technique for Analysis of Silicates: Anal. Chemistry, V. 38, No. 6, 730-733.

74. API Recommended Practice for Core-Analysis Procedure: Amer. Pet. Institute, API RP40 (1960).

75. Rall, C.G., Hamontre, H.C. and Taliaferro, D.B., 1954, Determination of Porosity by a Bureau of Mines Method: U.S. Bureau of Mines Rept. of Investigations 5025.

APPENDIX II-1 - ALTERNATIVE PROCEDURE FOR GAS WELL SAMPLING USING CITRATE TYPE BOTTLES*

A. • Samples are best taken from a meter outlet valve with 1/4x18 NPT female threads.
• Screw threaded polyethylene tube into valve.
• Insert tube into short section of zip-lok bag (long section of zip-lok held closed by a staple).

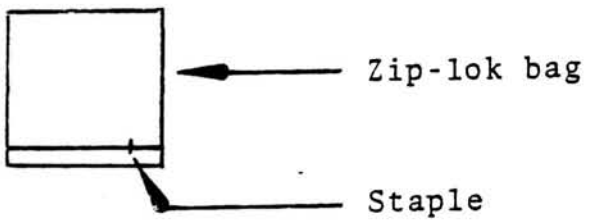

B. • Invert bottle (citrate-type or Grolsch beer bottle), open bottle cap and insert tube to the bottom of the bottle.

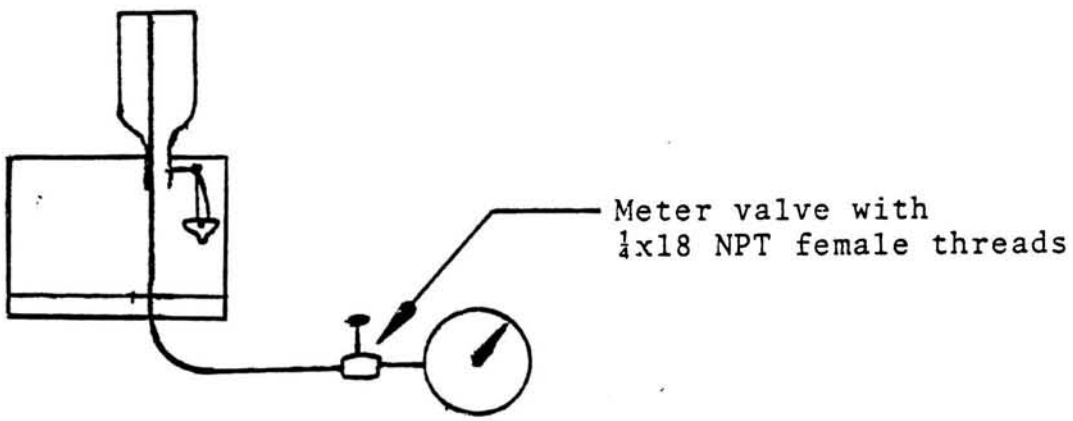

C. • Allow gas to flow into the bottle.
• Gas escaping from the bottle will fill the bag like a balloon.

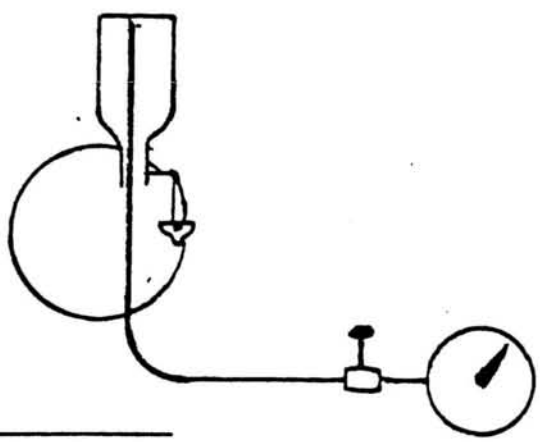

*Global Geochemistry Corp., Canoga Park, California

D. • With gas still flowing into the bottle, squeeze gas out of the bag.

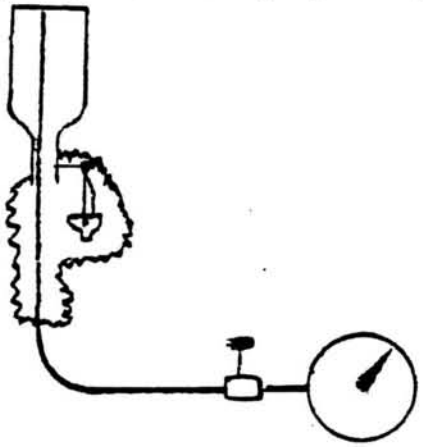

E. • Let the bag fill again and squeeze it empty. Repeat filling the bag and squeezing it empty five (5) times. This procedure will keep any air from getting into the sample.
• With gas still flowing, gently withdraw the tube from the mouth of the bottle.

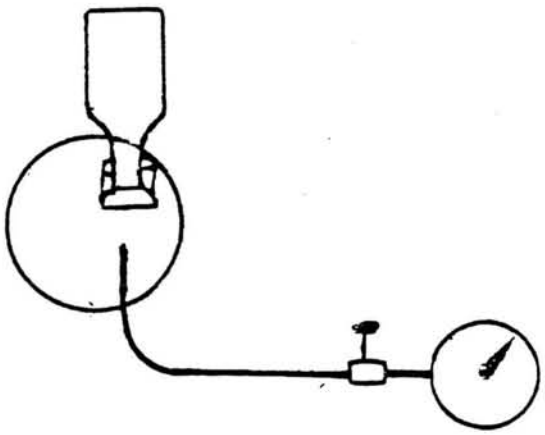

F. • While still letting gas flow into the bag, close the bottle cap.
• Turn off gas and remove the tube from the bag.
• Remove the bag from the neck of the bottle.
• Wrap masking tape around the metal clamp of the bottle to prevent it from accidentally opening.
• Label the bottle and fill out the log sheet.

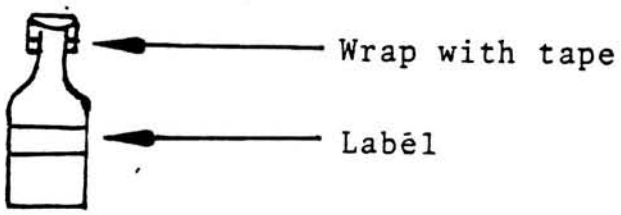

• Collect duplicate samples for each well.

Chapter III

SCALE AND SOLIDS CONTROL

III. SCALE AND SOLIDS CONTROL

III-1. Chapter Summary

Most freshly produced brines tend to deposit scales on pipes and valves at rates too high for practical operations. Deposition may be controlled partly by engineering design, by restrained conditions of production, by adding chemicals, or by periodic shut-downs for descaling by a combination of chemical and mechanical means. Decisions in this area are among the most important in an entire development program since failure to adequately control scale and sludge will result in premature shut-down of the plant. Although considerable effort has been directed at chemical inhibition of scale deposition and solids control very few inexpensive, effective solutions have resulted. Noteable success with the control of carbonate scales has, however, been achieved. The problems seem to be difficult partly because the context of geothermal fluid production has little counterpart in industrial or laboratory chemistry and partly because experimentation is awkward especially on siliceous scale. The use of high temperature/high pressure crysstallizers, however, offers an efficient means of controlling scale deposition downstream of production wells.

III-2. Introduction

The rapid temperature drop of flashing geothermal brines leaves residual liquids that have inordinately large chemical instabilities which sometimes yield unpredictable and novel solid deposits. In those cases where chemical properties of the brine are indefinite, sampling and taking experimental sidestreams can initiate behaviors that are not representative of the fluid's behavior in the main flowstream. This yields confusing results and practical

issues require experimentation on the full-flow streams. That in turn involves treating, handling, and disposing of up to 500,000 lbs of brine per hour. Thus, even simple experimental objectives can become very costly.

The indefiniteness of a brine's behavior depends on its composition which derives from its temperature and history of water-rock interactions. Moderate temperature liquids of low salinity (>150°C) generally yield $CaCO_3$ scale by prompt reactions and offer few experimental complications. Hotter liquids of low salinity commonly yield silica scale in a sluggish fashion. Hotter liquids of high salinity have exceedingly complex behaviors due to many minor components.

A description of chemical behavior of these brines requires a description of the process stream as much as a description of the ordinary chemical factors. A useful point of view is to imagine oneself moving with the brine as it enters the wellbore after being in chemical equilibrium with the rocks of the production zone. Then, by "travelling" up the wellbore with the fluid and through the plant, one "observes" the continuous changes in the physical nature of the brine and the evolution of chemical tendencies which yield solids. Following the brine through the system in this way should continue to where the brine is chemically "stabilized" prior to injection for disposal, and then, continue onto the injection zone, where the brine will again be out of chemical equilibrium with the rocks. It is important to consider the entire flow path as an entity within which there are continuus and extreme changes, but often limited times for chemical reactions to be completed before the reactants move on.

By contrast, sampling the stream, taking sidestreams for experiments, and injecting chemicals are operations done at fixed points along the flow path. The transient fluids with which these points are in contact will appear to change in character due to many reasons. These effects cause the fluid to

appear to be variable when it is not and to amplify real varitions in the composition of brine which enters the wellbore. Sampling, experimentation, and chemical treatments must accommodate both real and apparent variability.

III-3. Descriptions of Scale-Forming Reactions

Classifications of scale might be based on any of several criteria, e.g. composition, temperature of formation, solubility in acids, relative hardness, etc. The approach used here aims instead at the chemical behavior of the fluid and conditions which initiate those behaviors. The intention of this approach is to present scale and other solids as logical consequences of upsetting the brine's physical conditions. Understanding scale deposition this way yields a rationale for selecting chemical or procedural "fixes" for scale problems.

III-3-1. Prompt Reactions

Some scale depositions occur quickly and approach thermodynamic equilibrium closely. The most significant example is $CaCO_3$ deposition. Additionally, multiple production zones tapped by wells may contain liquids that are chemically reactive with one another. Also, reduced temperatures due to flash cooling and conduction will cause simple compounds to become supersaturated. The ionic varieties will deposit promptly.

III-3-1a. Calcium Carbonate Deposition - The most important prompt reaction is the deposition of calcium carbonate. It is initiated first by the flashing of steam from the brine and has a second stage which is more intense than the first. The first stage yields calcite (the common rhombohedral form of $CaCO_3$) and the second often yields aragonite (the orthorhombic form of $CaCO_3$). Only mild supersaturations of $CaCO_3$ develop due to exhalation of CO_2 within the first several degrees of flash cooling. Most geothermal brines are highly

charged with CO_2 with the result that the suite of carbon species is dominated by $CO_2(aq)$ and HCO_3^-; H_2CO_3 and $CO_3^=$ are scarce. Most of the CO_2 is partitioned into new-formed steam within the first few percents of steam flashing (ΔT = 20°F or less). Equation III-1 describes the major process at this stage:

$$CO_2(aq) \rightarrow CO_2(g) \qquad \text{(III-1)}$$

Additional links in a chain of events include breakup of H_2CO_3 since its concentration, though minor, is directly proportional to the concentration of $CO_2(aq)$. Equation III-2 describes the process. It yields a trivial fraction of the total CO_2 since the ratio $CO_2(aq)/H_2CO_3$ has a value in the range of 200 to 690 in the temperatures of interest[1].

$$H_2CO_3 \rightarrow H_2O + CO_2 \qquad \text{(III-2)}$$

Loss of H_2CO_3 by equation III-2 stimulates a consumption of acidity due to the availability of HCO_3 ion:

$$H^+ + HCO_3^- \rightarrow H_2CO_3 \qquad \text{(III-3)}$$

but the molar amount of H^+ consumed is less than the amount of H_2CO_3 lost via equation III-2.

Subsequently, some HCO_3^- ionizes:

$$HCO_3^- \rightarrow H^+ + CO_3^= \qquad \text{(III-4)}$$

but not enough, quantitatively, to make up for the H^+ consumed by reaction III-3. Thus, there is no significant change in the overall HCO_3^- concentration due to reactions III-3 and 4.

However, this ionization sequence simultaneously yields $CO_3^=$ in small amounts that are highly significant as compared to the initial CO_3 ion concen-

tration before flashing. The CO_3 is available to react with Ca. If the liquid had been in equilibrium with calcite of the reservoir rocks, a common circumstance, then $CaCO_3$ will deposit promptly. The mild supersaturation at this stage is conducive to growth of well-formed crystals of calcite which may reach millimeter dimensions within a few hours where they are attached to stationary pipe walls and nourished by the flowing, activated liquid. Under steady production, well-formed crystals of calcite several centimeters long may develop over weeks or months, defining a radial pattern of growth on pipewalls as the unfavorably oriented crystals terminate against their radially aligned neighbors.

High temperatures favor the mild supersaturation because the ratio of $CO_3^{=}/HCO_3^{-}$ is then small, on the order of 0.001 or less. In this stage $CaCO_3$ deposition in small amounts can have large effects on the $CO_3^{=}/HCO_3^{-}$ ratio, even in the face of large losses of $CO_2(aq)$.

As flashing continues the temperature declines and an increase in the $CO_3^{=}/HCO_3^{-}$ ratio occurs due to its substantial dependence on temperature. Equation III-5 expresses the process at this stage:

$$2HCO_3^{-} \rightarrow H_2O + CO_2 + CO_3^{=} \qquad \text{(III-5)}$$

The CO_2 is expelled efficiently and continuously by boiling and the HCO_3^{-} concentration may be reduced by 10 to 30 percent, compared to only one percent, or so, via the process of reaction III-4.

The contrasts between equation III-4 and 5 define the two stages of $CaCO_3$ deposition that occur upon flashing. They differ most significantly in the amounts of $CO_3^{=}$ formed. Reaction III-5 can yield more than ten times as much $CO_3^{=}$ in nominal circumstances[2] and dominates the overall consumption of Ca ions.

High final pH values, exceeding 9, may result from reaction III-5 due to hydrolysis of some of the newly-formed $CO_3^=$:

$$CO_3^= + H_2O \rightarrow HCO_3^- + OH^- \qquad \text{(III-6)}$$

The HCO_3^- formed via equation III-6 enters the relatively large pool of HCO_3^- already in the brine, a negligible outcome which completes the chain of reactions that are the $CaCO_3$ deposition mechanism. It is accurate to perceive the final pH as a consequence of the $HCO_3^-/CO_3^=$ behavior, in contrast to colloquial and inaccurate expressions that pH "controls" carbonate scale deposition.

In brines where the Ca concentrations are small, aragonite will develop instead of calcite during the late-stage flashing. Apparently the calcite crystal growth mechanism is clogged by an excess of $CO_3^=$ but, aragonite can form in the presence of excess $CO_3^=$[4]. It often appears as needle-like crystals a few to several micrometers long.

The fast-forming aragonite crystals may grow into porous mats that give a venturi-like shape to the inside of the pipe where the deposition occurs. Upon drying, the mats are soft, chalky and display textures related to their growth processes. These mats are commonly, but incorrectly, ascribed as being due to the impact and adhesion of earlier-formed crystals onto the locations where they are found[5,6].

III-3-1b. Mixing Brines in Wellbores - Prompt reactions are also possible when a well taps two liquids of different chemical character. For example, a highly saline brine may stably underlie a fresher brine due either to a large density contrast or a physical barrier that prevents convective intermixing. A well completed across the interface will result in mixing of the fluids in the wellbore when the well is produced. This situation occurs in the Salton Sea KGRA[7] and there the highly saline brine contains heavy metals and is high in barium and strontium. The dilute brine is typical of shallower waters and contains substantial bicarbonate.

Particulate solids can result from blending dissimilar brines and they may adhere to the wellbore or casing near the upper zone inflow points, partially plugging them. Also, particles suspended in the upward-moving fluid tend to settle so they spend longer periods in the zone of active growth than the liquids do. These particles can grow and eventually settle out to accumulate in the bottom of the well, potentially building up to interfere with lower zone production.

These reactions can occur without substantial inducements by temperature change or by flashing. The mineral siderite ($FeCO_3$) is sometimes observed and its presence suggests mixing. Substantial concentrations of iron can be carried only in liquids of moderately low pH (5 or less), a condition which admits CO_2 and HCO_3^-, but not $CO_3^=$. Siderite, once formed, is stable at pH 5 however. $PbCO_3$ has also been reported[8] and is insoluble even in hydrochloric acid. Siderite can form under other circumstances so interpretations about fluid blending should be done cautiously[9].

Brines that differ substantially in pH tend to neutralize one another and in at least one case this appeared to have a beneficial result[7]. In the Salton Sea field, a well co-produced hypersaline chloride brine (250,000 ppm TDS) and a dilute brine (60,000 ppm) that was suspected to have contained substantial HCO_3, but apparently little to no sulfate. Since the acid capacity of the hypersaline brine greatly exceeded the base capacity of the dilute brine the mixture appeared much like a dilute version of ordinary hypersaline brine, even though the dilute member constituted 2/3 of the total production.

Dilution assured that NaCl in the hypersaline brine would not deposit as a scale, a factor of important concern with some fully-flashed hypersaline brines at temperatures below atmospheric boiling. Additionally, the lowered salt content may have partly suppressed the deposition of wellbore scale which

was composed mainly of heavy metals and silica in combination. The deposition rate is normally higher from saltier waters.

Once a field is known to contain contrasting brines, the blending of them can constitute a development strategy. However, the blending ratio is crucial. If the acid capacity of the hypersaline brine is exceeded then the large amount of iron would form massive amounts of solids. These would interfere with production of both zones, as described earlier. To cure a well impaired by those latter circumstances one could drill deeper to obtain more production of the hypersaline brine. This would be a preferred alternative to closing off some of the shallower, dilute brine production.

III-3-2. Simple Supersaturation - Some hypersaline wells yield brines so concentrated that NaCl is supersaturated after flashing. The thermodynamic drive for solids formation is due to temperature drop and to higher concentrations due to flashing of steam, but not to sequences of chemical reactions as in the case of $CaCO_3$. In the case of Cesano #1 brine, the solid is mainly sulfates of sodium and potassium[10]. Since the deposition potential may be hundreds of mg per kg of brine, massive deposits can develop in a few hours. They are favored by locations which yield more efficient cooling of the brine such as valves and smaller diameter pipes. Although these scales develop late in the flashing process, they are categorized here as "prompt" because their massive character can quickly create acute problems for field operations.

Control might be achieved by injecting fresh water upstream of the deposition zone, but induced deposition of other materials, e.g. gypsum, would be unacceptable for anything except a field expedient. Alternatively, the well's production rate might be reduced, causing more heat loss via conduction by the wellbore and elsewhere, resulting in a smaller degree of flashing and thus a smaller rise in concentration. In a power plant context, brines from multiple

wells can be blended before final stage flashing if they are not all susceptible to the problem.

Although silica also forms a solid due to simple saturation the more significant feature of its deposition is its sluggishness. It will be discussed in a subsequent section.

III-3-3. Intermediate Reactions

III-3-3a. Heavy Metal Sulfide Deposition - When flashing occurs, two competing effects can take place which affect the deposition of heavy metal sulfides. If the brine is mildly acidic some of the sulfide enters the vapor phase in the form of H_2S, depleting the availability of $S^{=}$ in the residual brine which leads toward desirable undersaturation of heavy metal sulfides. Contrastingly, the slight rise in pH due to exhalation of CO_2 and hydrolysis of $CO_3^{=}$ (equations III-3 and 6) converts some HS^- to $S^{=}$ which favors deposition of heavy metal sulfides. The framework of chemical events for H_2S is very similar to that for deposition of the carbonates. The $H_2S(g)$, $H_2S(aq)$, HS^-, and $S^{=}$ are nearly exact analogues of the corresponding carbon species, responding to H^+ in qualitatively the same ways. Since the availabilities of sulfur forms is usually much less than their carbon counterparts, pH effects are driven by the carbon reactions (III-1 - III-6) which thereby control the H_2S-$S^{=}$ distributions as well.

Additionally, most heavy metal sulfides are less soluble at lower temperatures even at constant pH or $S^{=}$ availability[11]. The temperature change of flashing favors their deposition and this is converse to the situation with carbonates. The interplay of these factors tends to spread deposition of heavy metal sulfides over a considerable length of the fluid's flow path.

There seldom, if ever, is a sudden buildup of deposition potential which results in heavy deposition in a short zone, as in the examples for aragonite and NaCl depositions described earlier.

Since heavy metal sulfides are only slightly soluble under most conditions, the intensity of deposition will be modest, though in some cases, still serious. For the cases where H_2S, $HS^=$, and $S^=$ are only modestly available, the potential amount of deposition is small -- a few ppm at most. Deposition will be most noticeable in wellbores and may form tenacious scales that have few other components. Further along the flow path the heavy metal sulfides may continue to deposit at comparable rates, but appear less significant

The heavy metal sulfide scales may cease to develop when their actively growing surfaces are overtopped by deposition of other scales, e.g. silica, which come to form more rapidly. Several examples of banded scales have been discovered that seem not to be due to simple shifting of deposition conditions along the flow path. Alternatively, heavy metal sulfides may nucleate within a predeposited layer of siliceous scale[17]. A commonly observed property of Salton Sea-type sulfide-siliceous scale is the occurrence of a thin band of silica-rich material between the steel host upon which the scale formed and the overlying much thicker layer of heavy metal sulfide scale. The presence of a thin iron-rich siliceous layer can be recognized as a stable corrosion product[15].

Control of some complex silica scales has been obtained by adding acid to lower brine pH[12,13]. Ostensibly this decreases the rate of silica deposition, an issue described later, but the effect on heavy metal sulfides is also relevant. The acid retards deposition of sulfides by reducing $S^=$ availability. Additionally, there is a synergistic effect for situations where banded scales form due to a partial denial of a suitable surface on which one component can nucleate.

In solutions where HS^- and $S^=$ are abundant, heavy metals can be carried in high concentrations as sulfide complexes such as HgS_2^{2-}, $Zn(HS)_3^-$, $Cd(HS)_4^{2-}$, and others[11]. Such complexes increase the amount of heavy metal in solution with increased availability of $S^=$, the opposite effect of normal solubility relations for sulfide minerals. Such solutions would appear to have a very large potential for solids formation. Although these relations are suspected to be important in the genesis of ore deposits, there are few commercially interesting geothermal sites, if any, where they are significant. These complexes appear only in a narrow range of circumstances -- substantially basic pH conditions and uncommonly high total sulfur contents. Data about them comes mainly from laboratory studies. They will not be considered further in this report.

III-3-3b. Heavy Metal-Silica Scales - Hypersaline brines from the Imperial Valley yield scales in wellbores and surface equipment that develop upon the fluid's cooling only a few tens of degrees due to flashing. The silica fraction of the scale increases as flashing progresses, but silica deposition occurs at higher temperatures and upon smaller temperature changes than are required to yield silica scale from simple brines and laboratory solutions. These scales are tenacious and hard, they seriously interfere with valve functions, and they form soon after flashing is initiated, fouling wellbores as well as surface equipment.

The presence of heavy metals, prominently iron but also lead and copper, has lead to suggestions that the material is an amorphous iron silicate[15], rather than a mechanical mixture of iron and silicon oxides and their hydrated forms. The distinction, if true, could be important to controlling the effects of scale. If deposition of the silica fraction could be delayed until after the fluid gets beyond the wellhead the accumulated thicknesses in wellbores

IN SOLIDS, Si ALWAYS COORDINATES WITH 4 OXYGEN ATOMS;
Fe WITH 4 OR 6, AS IN THESE DIAGRAMS WHERE Fe AND Si RESIDE
IN THE CENTERS OF CAGES.

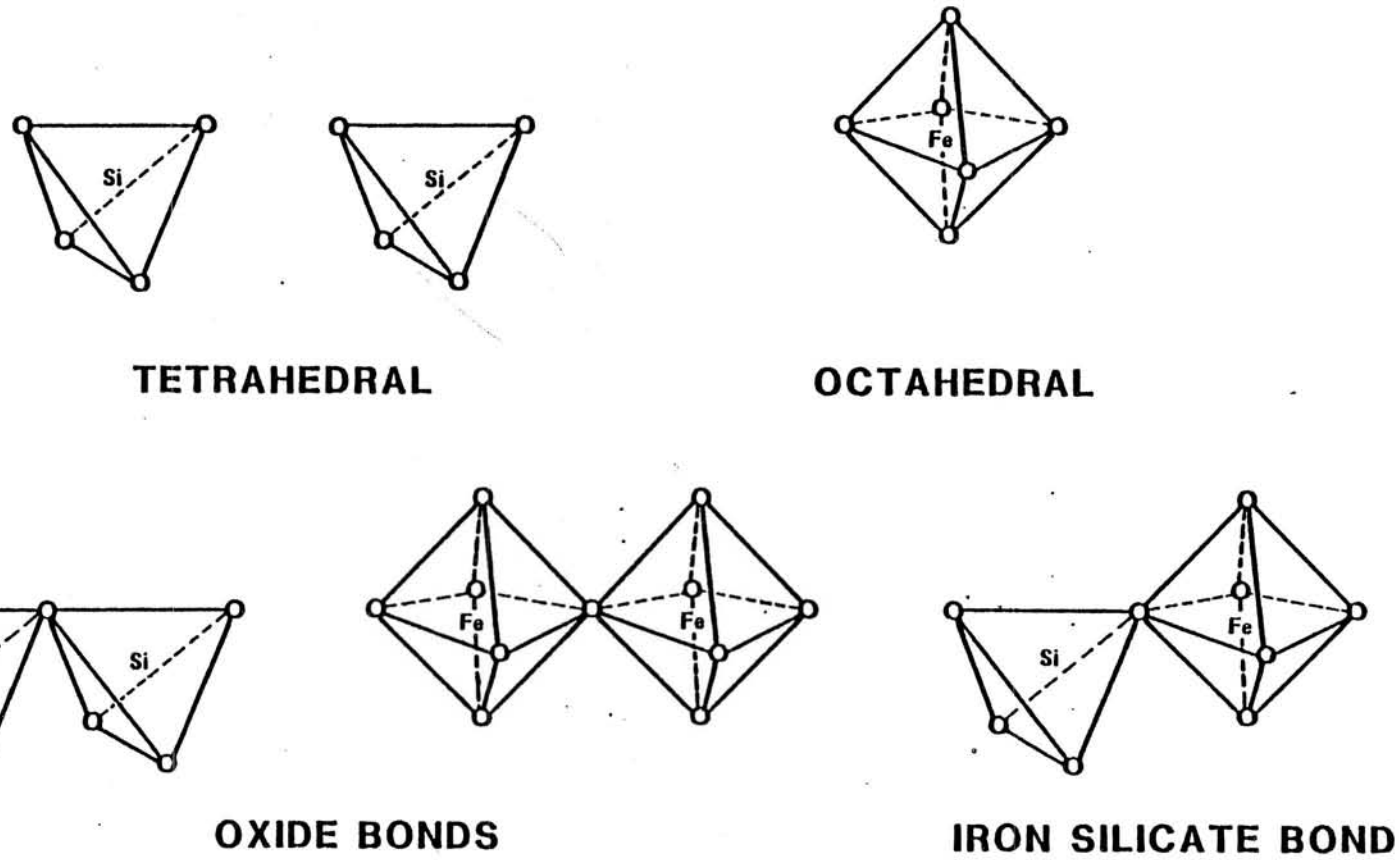

Figure III-1. Iron silicate vs mixed oxide bonds.

would then require mechanical reaming at less frequent intervals, saving maintenance costs and wear on casing. Figure III-1 shows the distinction between the iron silicate bond and the counterpart bonds in a simple mechanical mixture of solids.

Little evidence deals clearly with this issue. Injection of OH^- into a hot, partly flashed hypersaline brine caused reductions in the amount of silica contained in solids which were subsequently filtered from the treated liquid[7].

The iron content of siliceous solids was increased by OH^- dosages to the brine before the solids formed, but the silica was decreased. If iron silicate were the dominant form one might expect an additive to change the total amount of deposition, but the iron and silica would then change in the same, not opposite senses. The observed opposite responses are exactly what one would expect from iron and silica responding independently to increased OH^- availability. Thus, the experiment can be interpreted to indicate against the concept of amorphous iron-silicate. However, if one suggests that the OH^- is merely a better competitor for separate association with iron and silica than silica is for iron (and vice versa) the concept of iron silicate-type bonding can be saved, arguing that iron silicate bonding requires a relative scarcity of OH^-, which is the case in hypersaline brines (pH's 4 to 5.5).

It is most probable that adjustments in brine pH simply cause deposition of the appropriate thermodynamically stable species[15]. Whereas deposition of amorphous iron-silicates appears to be favored from acidic solutions, hydrated oxides of iron precipitate from more basic solutions. The primary effect of elevated brine pH on silica deposition is to enhance rates of silica polymerization and hence precipitation. The apparent decrease in silica precipitation at higher pH may be the result of enhanced ion precipitation.

The micro- and macro-structural features of heavy metal sulfide and iron-rich siliceous scale are reminiscent of Liesegang rings, as they commonly

occur in the form of alternate bands of light and dark material. Jackson and Hill[16] have discussed the possible interaction of siliceous scale forming species with metal ions and sulfur species. They suggest that the metal ions and aluminum promote the aggregation of silica sol particles and thereby help to form a rigid gel structure. The formation of heavy metal sulfide, bridges that link silica particulates, may be the initiation mechanism for the subsequent growth of well crystallized heavy metal sulfides and their characteristic structures such as the well known dendrite growths found in hypersaline brine, high temperature scale deposits. This mechanism suggests the nucleation of heavy metal sulfide scale follows initial deposition of siliceous scales. Evidence to support this mode of heavy metal sulfide scale formation is found in Refs. 15-19. A suggested reaction pathway for the formation of heavy metal sulfide scale deposits is provided in Figure III-2. An interesting discussion of the mineralogy of heavy metal sulfide and siliceous scale deposits from the Salton Sea Geothermal Field is provided in Ref. 19. It is shown in Ref. 19 that a significant fraction of the iron and sulfur in the scale is not present in the form of sulfides thus supporting the contention that these species serve to promote adhesion of silica sol particles.

The distinction between independent and cooperative behavior of scale components is very significant to the search for chemicals to control scale deposition. If each component is truly independent then a separate chemical control method may be needed for each and a complete system could be unworkably complicated. However, there are indications of cooperative behaviors of scale components and these might be upset by a single chemical additive and a simple injection plan. For example, the basis for development of the acidification procedure for the control of siliceous scales[12] was predicated on the complex interaction of sulfide scale forming species with mechanistic views of

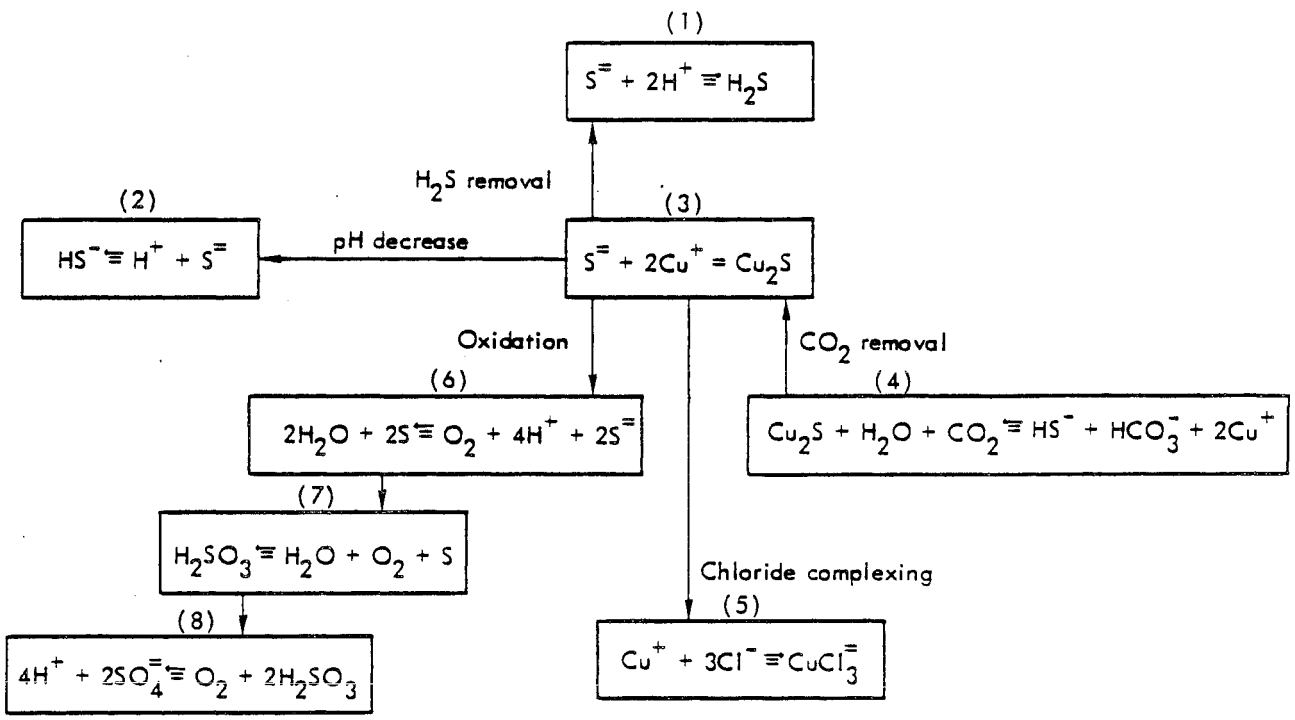

Figure III-2. Schematic diagram of typical reactions in sulfide scale formation (From Ref. 15).

silica scale formation. It was concluded that suppression of silica scale deposition should have a pronounced impact on heavy metal sulfide scale formation. Field test results[13,14] confirmed the hypothesis.

III-3-4. Delayed Reactions

This category concerns solids which develop mainly after the last stage of flashing when the temperatures are reduced to the atmospheric pressure/temperature boiling point of a geothermal brine. The most prominent delayed deposition is of silica, but the brine's opportunities to interact with the atmosphere can yield additional complications.

III-3-4a. Silica Deposition - The classic behavior of supersaturated silica in cooled solutions has been described in Refs. 14 and 21-23. Useful graphs which show the interplay of temperature, silica content, degree of supersaturation, and deposition rate are available[24]. Essentially, solubility and kinetic factors operate in opposition. A larger degree of supersaturation increases the deposition rate at any temperature, and a decrease in temperature increases the supersaturation at any (nonequilibrium) silica content. However, a lower temperature severely reduces the intrinsic molecular rates of the solids-forming reaction. The consequence is a maximum in silica precipitation at the appropriate temperature-silica concentration (Figure III-3). A family of curves is, therefore, required to show the relationship among the four factors (solubility, degree of supersaturation, temperature and kinetics) that control silica precipitation. Thus, silica deposition spans the boundary between intermediate and delayed categories, but most of the total deposition occurs after the last stages of flash cooling.

Harrar, et al.[8] speculate that from hypersaline brines above 125°C, silica deposition on stationary surfaces proceeds by addition of monomer units

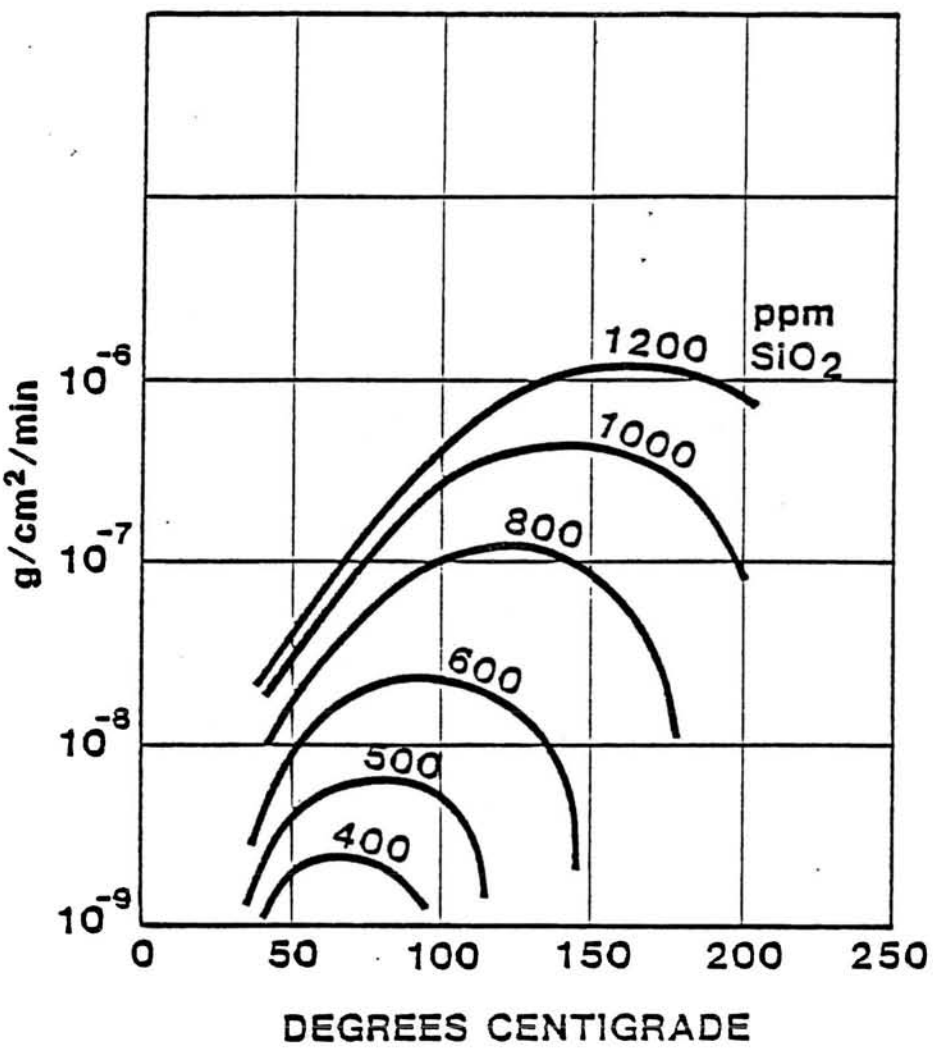

Figure III-3. Heavy curves represent the rate of deposition of amorphous silica from a simple aqueous solution. At any temperature, the rate is greater for larger supersaturations. The limits of extension of curves on the right side is determined by the silica solubility vs. temperature. On the left, the intrinsic sluggishness of the deposition mechanism results in decreased and more nearly equivalent rates for the various supersaturations. Figure is based on O. Weres, ref. 16.

of dissolved silica. At lower temperatures they suggest that deposition on stationary surfaces proceeds by sticking and aggregation of colloidal-sized silica polymers. This latter process would be greatly influenced by turbulence and other macro details of transport in the liquid phase. Figure III-4 shows the uniform silica scale thickness observed at a flange joint in a pipe carrying two-phase hypersaline brine near a wellhead at a temperature greater than 180°C. The absence of hydrodynamic effects is consistent with monomeric deposition wherein the rate is controlled by some atomic-scale step on the surface. The scale in this case was black and rich in iron with traces of other heavy metals. In hypersaline brines, the rate of silica precipitation and scaling tendency are directly proportional to the total chloride content [25].

In less salty brines, colloidal particulates of silica are also alleged to form in the homogeneous liquid without necessity of wall surface contact [21]. Presumably these particulates adhere for subtle reasons of surface electrical charges, perhaps becoming welded in place by additional monomer deposition from the solution. The result in many locations is a pale vitreous scale that builds up slowly, and is tenacious and chemically resistant [26]. It continues to develop for many hours after the brine has flashed, but at diminishindirates due jointly to additional cooling and partial consumption of the supersaturation. The situation can be eased, but not resolved, by providing additional residence time for the reactions to operate before injection [27]. For the chemically simple brines, the rate of silica deposition can remain low, but finite, for times on the order of many hours.

Silica deposition reactions are substantially faster for the hypersaline brines of the Imperial Valley (Southern California) than for chemically simple brines. In the near-wellhead zone, observed deposition rates can be 10,000

times faster than rates for the same silica concentrations and temperatures determined in laboratory studies. The relatively high reaction rates for silica in partly flashed hypersaline brines continues through lower temperatures. Residual silica concentrations reach 200 ppm post-flash (from 600 ppm pre-flash) within about an hour. The higher reaction rates are undoubtedly influenced by the high salt contents, but the function of heavy metals may be significant. As deposition temperature declines, the proportions of nonferrous components in scale also decline, but do not reach zero. The sludges which develop contain alulminum, which is very scarce in the initial brine, plus sodium, potassium, and iron, but little to no calcium. Such a compositiional pattern suggests that some kind of proto-mineral is forming that is an analogue of some alumino-silicates (the sludges are generally x-ray amorphous). Monovalent sodium and postassium can balance the charge deficit due to substitution of aluminum in a silicate lattice, but divalent calcium cannot. To a degree, iron, perhaps a minor part of which becomes oxidized to ferric state (Fe+++) due to atmosphere contact, can substitute for aluminum.

The great bulk of silica will be amorphous and few quantitative remarks can be made about it. In contrast to crystalline materials which have rigid structural features and precise energy relationships among components, the structural and energy features of amorphous silica are modest ranges rather than quantum-precise values. For this reason, mathematical models based on equilibrium concepts fail because there is no definite energy content to assign to the siliceous solid that actually develops. In practical terms, the structure of amorphous silica is very forgiving of the presence of other materials. The few structural regularities that are describable depend more on the local compositional environment than on the structure limitations of silicon-to-oxygen bonding.

The silica supersaturation can be more quickly consumed by providing increased surface area for deposition and providing the highest brine temperatures consistent with engineering requirements [28; see also Chapter IV]. The silica-rich solids form a brown (iron-rich) floc which helps provide surface for additional deposition. This principle has been exploted by recycling some sludge, removed from a liquid clarifier unit, into a second-stage flash vessel [29; se also Chapter IV]. In this context, the silica surface appears to greatly exceed the surface area of the vessel with the result that negligible deposition is reported to occur on the vessel walls.

Once the suspended solids have been separated from the brine the loss rate of dissolved silica from the brine approaches zero because the available surface is then limited to the walls of pipes and vessels. In a well-operated reactor-clarifier the silica supersaturation should be reduced to such a degree that amorphous silica is no longer a candidate phase to form [30]. Under these conditions, the residual brine will be still supersaturated in quartz and in other minerals. Reactions to form other minerals are possible if limiting components, such as aluminum or atmospheric oxygen can be made available, but without such additives the brine is then stable in a practical sense.

Injection of spent brine recreates opportunities for abundant contact between the brine and surfaces. The practical consequences will vary depending on whether the injection zone is made of fractured or porous rock. Those circumstances differ greatly in regard to the ratio of available rock surface area to volume of injectate. In this realm of water-rock interaction, the description of the water's condition is not sufficient to predict the outcome. Details of the tests for injectivity would best be planned according to the rock characteristics. Although few details are available about fluid behavior

upon injection, the issue is important, especially if the rock porosity/permeability has little capacity to absorb a chemical insult from the brine.

The temperature regime upon injection may be complicated, especially if the rocks are hotter than the injected brine. Eventually, the brine will chill the fluid flow path, but the fluid's temperature will tend to rise as it moves away from the wellbore. If there is residual saturation in amorphous silica, there may be a tendency for deposition along the cooled flow path. The zone of deposition in the rock moves away from the wellbore as injection continues, but it never actually disappears. Viewed from the brine, deposition does eventually cease because loss of silica reduces supersaturation and rising temperature eliminates it. This circumstance is likely to be a non-problem with regard to amorphous silica, but other reactions cannot be ruled out. One needs to know the nature of reactive minerals that are near the flow path.

If injection is interrupted, then the injectate already in place will mix with local waters and be warmed on a different pattern than if injection had continued. Generally, one would expect the injected water to sink, if flow paths were open, because it is likely to be more dense than the native fluids due to lower temperature and perhaps to concentration due to steam removal. Thus, the native fluids would likely reenter rocks near the injection bore if a shutdown lasted long enough. Upon restart of injection, most of the same set of reactions that occurred during the first injection could occur again. If these involved depositions, then an additional layer of deposits in the injection zone should be expected after each shutdown. Perhaps, more importantly, interruptions in injection allow volumes of brine in the wellbore to age providing sufficient residence time in some cases for the appearance of additional precipitates. Shutdowns also provide the opportunity for atmospheric oxygen contamination that can encourage additional precipitation.

III-3-4b. Atmospheric Reactions and Consequences - Geothermal liquids under reservoir conditions are so poor in dissolved oxygen that concentrations cannot be measured, only calculated on the basis of some suite of minerals for which the thermodynamic relationships are known. Results of these considerations yield calculated oxygen chemical activites of 10^{-20} to 10^{-40} atmospheres This is equivalent to less than one oxygen molecule in all the deep geothermal reservoirs of the Imperial Valley. As a corollary, all of the hypersaline brines have an inordinate potential reactivity when exposed to the oxygen of the atmosphere.

Absorption of oxygen by the brines will be limited in rate by the molecular processes at the brine-atmosphere boundary, hence the reactions will appear to develop slowly and continue for substantial periods of time -- probably until injection once again isolates the liquid. Steam caps on large vessels are commonly used to retard atmosphere ingress in a power plant context.

The capacity of the liquid to react with atmospheric oxygen will depend on the availability of oxidizable components in the brine. Principle among these are H_2S, and ferrous iron (Fe++). Typical major components, alkali and alkaline earth metals and halides, have only one available oxidation state and thus do not react with oxygen.

The apparent corrosiveness of geothermal brines is greatly accelerated by the interaction of high chloride concentrations with dissolved oxygen at the air-metal interface. The chloride assists the oxidation reaction between O_2 from the atmosphere and the metal by stabilizing the iron ions in solution as they are produced by oxidization. Complexing enables iron molecules to diffuse away from the site of O_2 attack, enhancing the access of new O_2 to the site. The effect is similar to that in seawater, but quantitatively different

because O_2 is less soluble in saltier brines, a factor which reduces the instantaneous corrosion intensity. But the higher chloride concentrations make iron complexes more stable, effectively removing the reaction products and increasing the net rate of corrosion which may be sustained by continued contact with the atmospheric oxygen[15].

The hypersaline brines of the Imperial Valley typically contain more than 1500 ppm of ferrous iron (Fe^{++}), most of which is susceptible to oxidation. Oxygen which does enter the brine is chemically reduced quickly by Fe^{++} with formation of Fe^{+++}.

The oxygen consumption progresses through multiple stages. In the first stage the oxidized iron reacts with water to form a brown solid of iron hydroxy-oxide indicated by Equation III-7:

$$\tfrac{1}{2}O_2 + 2Fe(II) + 3H_2O \rightarrow \underline{FeOOH} + 4H^+ \qquad \text{(III-7)}$$

Eventually, the co-generated acidity builds up and the earlier formed iron precipitate may be dissolved according to Equation III-8.

$$FeOOH + 3H^+ + nCl^- \rightarrow Fe(Cl)_n^{+3-n} + 2H_2O \qquad \text{(III-8)}$$

Oxidation can continue and pH values may become less than 1. Exposures yielding such low pHs may also involve intense evaporation so that NaCl and perhaps KCl deposits. In a pond situation, the deposits of NaCl may insulate early-formed FeOOH from late-formed acid.

The brines at this stage are exceedingly corrosive to metals. Fe^{+++} is more effective at attacking metallic iron than is oxygen. Additionally, the high H^+ content prevents the buildup of a protective rust layer while the high

Cl^- content provides complex-forming capacity to reduce the chemical activity of the Fe^{++} products of the corrosion.

In extreme cases of desiccation and oxidation, the residual liquid will be mainly $CaCl_2$. As H_2O is lost by evaporation, the liquid approaches a molten salt in character. In this condition the fluid is very hazardous. It can desiccate skin by the combination of acid attack and osmotic tension of the concentrated $CaCl_2$ solution. The potential for eye damage by splashed droplets seems large. However, they should not be compared to superficially similar brines developed in the course of commercial $CaCl_2$ production where the absence of iron and application of minor treatments yields a product that is nearly pH neutral.

These oxidized, desiccated brines are awkward to handle in large quantity. In addition to severe corrosivity they are dense (sp.g ~1.6), viscous, and hard to filter, as in preparation for disposal by injection. Modest dilution with water may cause the pH to rise with a concomitant formation of FeOOH precipitate which can further frustrate attempts at filtering. Attempts to evaporate these concentrated brines to solids are difficult due to the hydroscopic nature of $CaCl_2$. They are handled best by never allowing them to form.

III-5. Scale Control

Genuine prevention of scale by the use of chemical inhibitors is now possible only for carbonates and salts in the sense that the appropriate chemical additives prevents their deposition anywhere in the system. Silica scale deposition can be suppressed by the process of acidification using hydrochloric acid as the chemical additive. Silica and sulfide scales can be partially suppressed or their deposition displaced to other locations in the system, where dealing with them is more convenient by careful control of temperature-pressure conditions. Effective control of silica and heavy metal

sulfide scales is accomplished using crystallization and reaction clarification processes. These treatment systems are discussed in Chapter IV. This section describes methods for dealing with carbonate scales, particularly the $CaCO_3$ polymorphs calcite and aragonite. Several chemical additives are available for them and other approaches also work. For NaCl and other soluble salt deposits, dilution appears practical. Work performed to date indicates some potential benefits may be derived from the use of certain organic compounds as silica inhibitors in low to moderate salinity brines.

III-5-1. Dilution-Prevention of Soluble Scales

The most straightforward way of reducing soluble salt supersaturation is by blending fluids of contrasting composition. This is applicable to NaCl scales and perhaps to sulfide scales, but practical opportunities are limited. For the slow reaction of silica, dilution might be made in a somewhat timely way after the heat removal step but this would not avoid some early deposition of silica (see Chapter IV).

Dilution can protect the downstream part of the plant system, including the injection well, from deposition due to NaCl. However, the reservoir rocks of the injection zone would be jeopardized if the blended liquid could deposit $CaSO_4$ which upon heating has a lower solubility.

Requirements for 100% injection of produced fluids may be enforced in certain locations as a subsidence mitigating measure. This would involve blending geothermal residual brines with locally available (surface) water or steam condensate irrespective of the plant's need to dilute for purposes of chemical control.

Blending requires a reliable source of diluent water and extraneous solid reaction products must be accommodated, probably by filtering. Chemical

mixing models would be useful in this context in order to optimize a blending schedule. This would help in predicting the potential for secondary solids formation or in minimizing the complications due to forming them. Credibility of the chemical mixing models will be favored by the lower temperatures for which solubility data are of higher quality. However, high ionic strengths remain troublesome in attempting to utilize chemical equilibrium models.

Direct measurements of solids yielded by blending brines and/or diluents over the operating range of steam flash and conductive cooling prior to disposal is the best method for assessing potential problems. These would require equipment no more sophisticated than filtering apparatus, an analytical balance, and a means to control evaporation or drying of samples (see Chapter II). Data should be collected for individual wells in order to accurately approximate an average brine composition that might be produced as a spent effluent by a power plant.

III-5-2. Prevention of Carbonate Scales

Several principles of carbonate scale control are possible, but not all are equally practical in the geothermal context. They may be described as:

- Interfering with the crystal growth processes at the crystal surface.
- Reducing calcium ion chemical activity by use of sequestering agents.
- Reducing availability of carbonate ion by:
  - a) producing fully pressured brine using downhole pumps
  - b) downwell injection of CO_2
  - c) downwell injection of strong acid

III-5-2a. Crystal Growth Inhibition - This approach provides the cheapest and most chemically elegant method now available for controlling carbonate and sulfate scale deposition. It deserves to be considered in all contexts of steam flashing. Tests have been made under a variety of conditions[31-35] and

all have shown impressive success. At least two families of chemicals are functional, phosphonates and maleic acid derivatives. They are available from multiple sources. Colloquially they are known as "threshold inhibitors" due to their activity on crystal nuclei and on the surfaces of scale crystals. It is necessary to add the chemical to the fluid upstream from the place where flashing (bubble point) begins.

The effectiveness of threshold inhibitors at low concentrations in liquids is due to their deposition on the surfaces of growing crystals. Atomic structures of scale minerals are somewhat like a 3-dimensional checkerboard. The fluxes of (+), (-) components alternates in time during growth as well as in space. Furthermore, the growth process is mostly constrained to atomic scale steps on the otherwise nearly perfect crystal surface. Accordingly, at any one moment during normal growth of a scale crystal, only a small fraction of the total surface area is receptive to addition of another (+) or (-) component.

Threshold inhibitors are moderately large molecules that attach to the growing crystal surface. They mechanically block the atomic processes, which lay up the (+)(-) alternating structure, by occupying a growth-active site. Yet, they do not provide an adequately prepared site for the next ion to fit into a structurally correct position of the crystal. These inhibitors are effective when they occupy far less than a molecular monolayer on the growing crystals. Because their affinity for surfaces is great, adequate surface populations can be supported by strikingly low concentrations in the liquid phase. Figure III-4 is the molecular structure of one phosphonate inhibitor, illustrating how it occupies a position on a calcite surface.

Significantly, in this method, the thermodynamic drive to form solid $CaCO_3$ is not relieved. The solution remains supersaturated because the inhibitor molecules deny the mechanism which normally relieves the supersaturation.

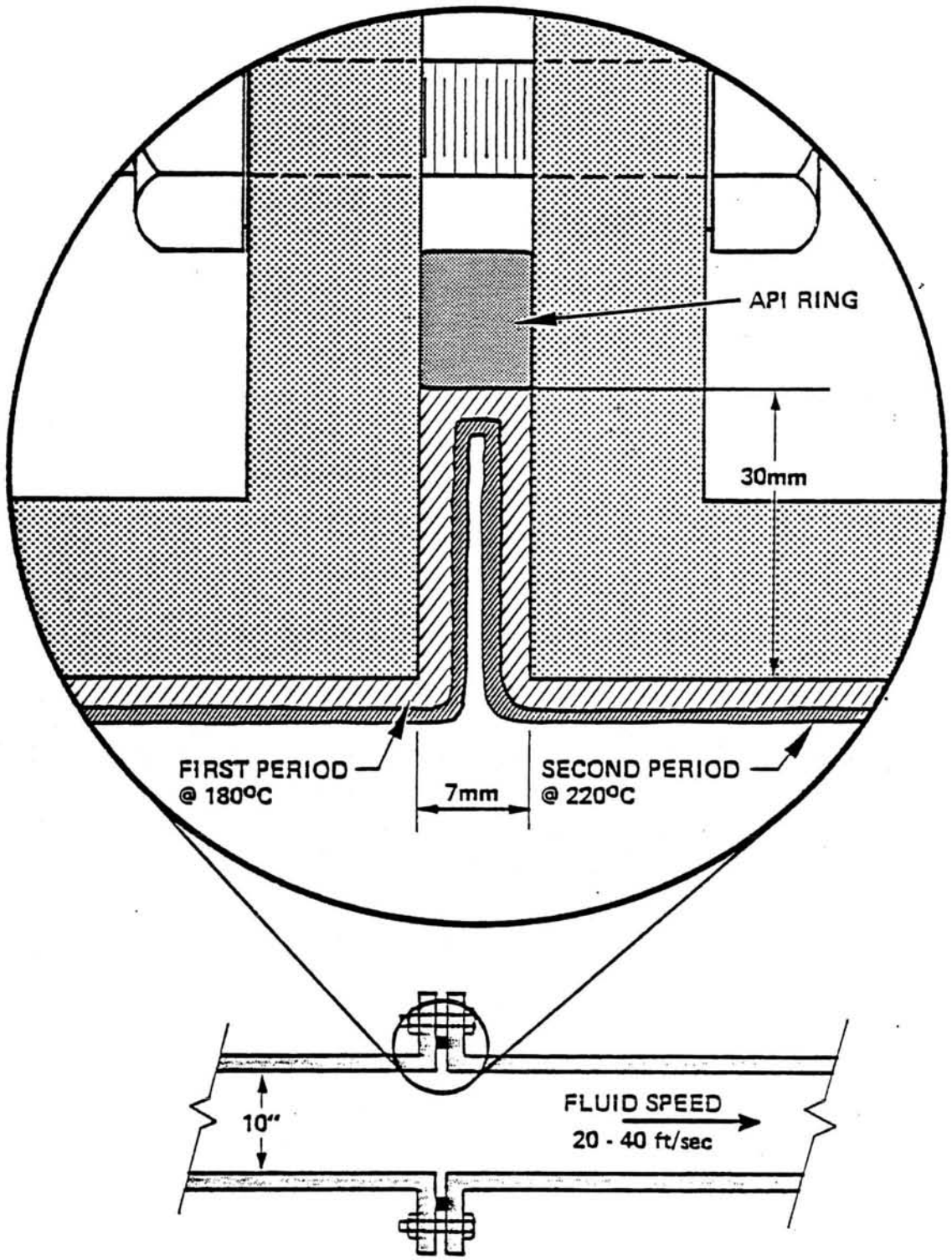

Figure III-4. Siliceous scale at a flange joint deposits with uniform thickness on available surfaces. Equal deposition in and out of crevices shows that hydronamics is irrelevant to the deposition rate. Two test periods differed in well production rate and in temperature at this flange joint.

Eventually (in a statistical sense) the inhibitor molecules will detach from the crystal's surfaces or be slowly overgrown by $CaCO_3$. When either of those happens, growth continues in an ordinary way. However, the crystal surface always is vulnerable to the effect of the threshold agent. Growth can remain inhibited due to residuals from a first dosage of the inhibitor or renewed by additional dosages.

Disposal of inhibited brines by injection into wells places the fluids into a place where the inhibitor will eventually fail, perhaps by sorption onto formation minerals, eventual overgrowth by components of the brine, decomposition due to temperature in the subsurface, or by other means. The longevity of injection wells depends on how far the fluid moves from the wellbore before inhibitor failure occurs. In some circumstances it would be a non-problem, but engineering assessments of this issue are apparently scarce.

Fortunately, concentrations of growth inhibitors can be very small in the fluid in order to sustain a functional population on the crystals. Concentrations below 1 ppm in the liquid are effective under some circumstances[35-36]. This is equivalent to less than one phosphonate molecule (in the liquid) per 100 Ca ions. By comparison, sequestering Ca ions requires more than one sequestering molecule per Ca ion in order to be similarly effective.

Thermal stability of threshold inhibitors is the major drawback to their use in suppressing scale formation in production wells. The highest recorded temperature (180°C) for successful threshold inhibitor application is described in Ref. 32. The use of these inhibitors at higher temperatures is a function of residence time and ultimate thermal stability of the compound. High temperature applications will require experimentation to determine efficacy. A drawback to the use of phosphonate inhibitors is the potential for production of calcium phosphonate scales or pseudo scales[31]. Careful control of inhibitor concentration is mandatory in preventing pseudo scale formation.

Equipment for placing crystal growth inhibitors into the pre-flash liquid is superficially the same as for adding sequestering agents but can be physically smaller due to the volumes of injectate required.

III-5-2b. Sequestration and Calcium Complex Ions - Ionic components of scale can be effectively removed from the scale deposition reaction by incorporating them in soluble complexes. In effect, a competition is set up between soluble and insoluble forms of the scale component as shown in Equation III-9:

$$C + AB \rightleftarrows A^+ + B^- + C \rightleftarrows AC^+ + B^- \qquad \text{(III-9)}$$

A and B represent ionic scale components and C represents a complex former for component A. At low or zero concentrations of C, the equilibria will be described by the left 2/3 of Equation III-9, but if enough C is present, the complex AC^+ will form, causing solid AB to dissolve, or fail to form.

In this circumstance there is no change in the absolute availabilities of A or B except for the trivial dilution due to addition of C and a carrier liquid. However, the thermodynamic drive to form AC^+ exceeds that to form solid AB. Thus, there are no unstable non-equilibria implied in the relationships of equation III-9, a feature which is not true for crystal growth inhibitors described earlier.

A very large variety of complexing materials are available. In practice, selection of one requires consideration of several chemical and economic factors. Among these are:

- thermal stability of the complex former (C),
- pH range over which (C) functions with the target,
- thermal stability of the formed complex (CA),
- possibility that a solid form of the complex can develop (pseudo scale)
- solubility of (C) in the brine,
- compatibility of (C) stock with the brine (if it is nonaqueous),

- capability of (C) to form complexes with nontarget ions,
- stability of CA compared to AB at expected levels of B,
- availability of (C) in a practical form for injection,
- availability of a practical means to inject (C) into the brine upstream from scale-prone areas,
- acceptably low thermal burden on the geothermal brine due to injection of (C) and its carrier,
- vulnerability of the injection means to malfunction,
- serviceability of the injection means,
- security of an adequate supply of (C),
- forecastability of costs for obtaining (C).

The list above comprises a formidable set of hurdles for applying sequestration to geothermal brines. The list applies to all additives, including threshold inhibitors. However, the cost items are especially significant for sequestrants due to the chemical (stoichiometric) requirement for each ion of A to associate with one molecule (or ion) of C in the liquid phase. Dosages of sequestrants could be in the range of hundreds of ppm. There is the probability that very large volumes of brine must be treated without recycling the sequestrant. Additionally, there may be a requirement for pH control in order to make the complex selective for Ca or to be more durable. Although sequestration is workable in a technical sense, there would seem to be no context where it would be a superior practical choice over crystal growth inhibitors.

It is pertinent to note that one successful example of carbonate scale inhibition by the use of EDTA in oil wells has been described[37]. EDTA was used to remove carbonate scale from production zones immediately adjacent to completion intervals in production wells. Although scale removal by use of hydrochloric acid was possible, EDTA provided superior performance because its use prevented reprecipitation of calcium as the acid treatment spent and rapid rescaling of wells occurred after production resumed.

III-5-3. Reducing $CO_3^=$ Availability

From equations III-1 - III-6 it is clear that $CaCO_3$ scale deposition coincides with the buildup of $CO_3^=$ from the reservoir of HCO_3^- carried by the brine. Thus, additional methods of scale control have focussed on mitigating $CO_3^=$ buildup, as an alternative to reducing Ca^{++} availability. Three variants of this objective are considered here:

- Downwell pumping of the liquid in order to eliminate or displace the flashing.
- Downwell injection of CO_2 into a producing well wherein steam flashes in the wellbore.
- Downwell injection of strong acid into a producing well below the level of flashing.

The governing equation which describes carbonate scale inhibition by total pressure or CO_2 gas partial pressure maintenance is given by:

$$Ca^{++} + 2(HCO_3^-) \rightarrow CaCO_3\downarrow + CO_2\uparrow + H_2O \qquad \text{(III-10)}$$

Release of CO_2 gas by flashing encourages carbonate precipitation.

III-5-3a. Downwell Pumping - Pumping a geothermal well permits the liquid to be withdrawn without flashing in the wellbore. Above ground, the liquid can then be used in a surface heat exchanger-Rankine cycle[38] so that neither flashing nor CO_2 release is allowed. Alternatively, the liquid could be flashed into a direct contact heat exchanger-Rankine cycle or directly flashed to drive a steam turbine[38-40].

The effect on $CaCO_3$ scale deposition for these options can be described through Figure III-6. The flash-cooling process indicated by the heavy line from upper right to lower left of Figure III-6 decreases the capacity of a brine to carry Ca^{++} and HCO_3^-/CO_3^{--} as described by equations III-1 - III-6.

However, conductive cooling of the brine, indicated by the heavy line on the right side of Figure III-6 increases the capacity of a brine to carry Ca^{++} and $HCO_3^-/CO_3^=$, hence no $CaCO_3$ scale would form. Conductive cooling without flashing can be achieved by combining downwell pumping with a surface heat exchanger-Rankine cycle. This method has been demonstrated successfully in a 10 megawatt electric plant at East Mesa, Imperial County, California[41], and a commercial size plant of similar design is now being constructed at the nearby Heber site[42].

This mechanical approach to solving a chemical problem succeeds because $CaCO_3$ has an inverse solubility with temperature that is sufficient to overcome the reduction in CO_2 activity that results from cooling. It is not necessary to add any chemicals to the brine so long as the CO_2 is retained in amounts commensurate with the diagram of Figure III-6.

An economic comparison of pumping vs. adding chemical inhibitors cannot be made in a straightforward way. Decisions about which method to use would be dictated by design features of the very different kinds of plants that are used to exploit flashed vs. unflashed brine. For example, the use of downwell pumps permits some wells to yield twice, or more, the fluid that natural artesian flow would yield. Thus, from an operational point of view, a downwell pump may be equivalent to a second production well but is only a fraction as costly to install.

The energy inputs to downwell pumps can be compensated by the higher thermodynamic efficiencies of turbines that result from the higher wellhead temperatures of pumped wells compared to the alternative of flashing downwell. Thus comparisons of running costs for pumping vs. chemical inhibition are not straightforward either, but may favor pumping. The long-term reliability of downhole pumps in a high temperature, moderate to high salinity environment,

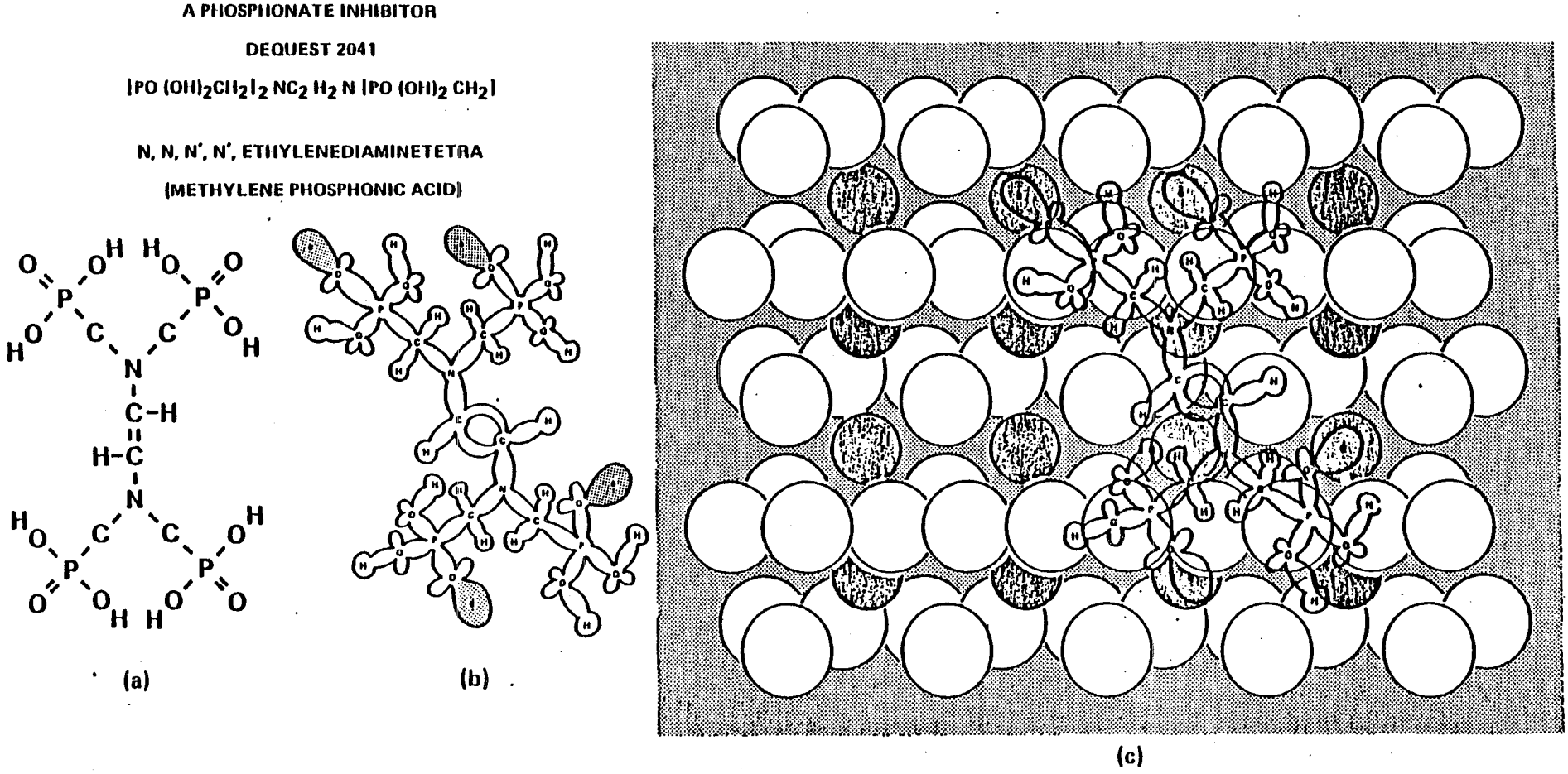

Figure III-5. A compositional diagram of DEQUEST 2041 is given in 4a. 4b represents a possible, nearly planar, configuration of the molecule drawn approximately to scale. The outline represents the electron clouds, with emphasis on the electron-rich doubly bonded oxygens attached to the phosphorous atoms. Figure 4c shows how the configuration of (b) fits onto an atomic plane of calcite where the dark circles represent calcium ions. Electrostatic attachment of electron-rich oxygen ligands to the calcium, pins the DEQUEST on the calcite at four locations. Decoration of DEQUEST across atomic steps in a nonplanar calcite surface can occur readily due to flexibility of the DEQUEST skeleton. In either case, the span of attachment is enough to interfere with growth processes that would otherwise add calcium and carbonate ions as extensions to the crystal structure.

is an issue, however, that must be considered very carefully. The costs involved in operation and maintenance of a downhole pump can rise dramatically if operational difficulties are experienced. A manufacturer of a downhole pump must be able to demonstrate reliable long-term operation before any decision to purchase can be made. Overall, consideration of maintenance costs favor chemical injection, because installation and repair of a pump and its auxiliaries are much more demanding than the counterpart for a downwell injection tubing with a surface-mounted pumping system.

Once pumped brine is at the ground level plant, there are additional options that bear on the useability of inhibitors. Direct contact heat exchange (mixing of produced brine with the organic Rankine fluid) may not require a chemical scale inhibitor because the precipitation of carbonates may provide sufficient surface area to effectively eliminate carbonate (and other species) deposition. As mentioned above, a surface heat exchange-type Rankine cycle does not require inhibitor if it is used alone, but hybrid units which take a small brine flash upstream of the Rankine unit require use of an inhibitor. The hybrid system gains an increment of thermodynamic efficiency from the enthalpy carried by the flashed steam.

Not all wells are suited to being pumped. Temperatures above 175°C currently deny electrical submersible pumps of large size due to breakdown of electrical insulation at those temperatures in brine. Development is underway to improve this, however. Shaft-driven pumps are workable, in principal, at much higher temperatures, but serious complications occur in applications approaching 200°C, especially for setting depths deeper than 300 meters. Bearing clearances and lubrication are disturbed by temperature effects and normal wellbore deviation makes it difficult to provide adequate clearance between moving parts of the pump in response to shaft elasticity and thermal expansion.

The wells to be pumped must be highly productive so that large increments of production rate may be gained from relatively small increments in drawdown of the well's bottomhole pressure or of setting depth of the pump[43].

III-5-3b. Downwell Injection of CO_2 - Many geothermal wells that yield electrical quality fluids are too hot or flash too deeply for pumping to be a practical alternative. For them, control of $CaCO_3$ scaling in the wellbore requires a more direct chemical approach. Downwell injection of CO_2 in modest amounts may have several advantages. Control of $CaCO_3$ scale is one of these [44]. The method has had a recent successful demonstration[45] with respect to suppression of carbonate scaling.

Higher production rates for geothermal fluid may be possible due partly to a gas-lift effect[46], but field data on this aspect are not now available. Additionally, the wellhead temperatures may be higher with CO_2 injection[44, 47], even at the same rates of geothermal fluid production.

In principle, adding CO_2 to the flashing geothermal stream can sustain the CO_2 pressure above the level required for the brine to retain all of its Ca^{++} in a dissolved form. Figure III-6 is useful for showing a process pathway. The amount of CO_2 required for injection does not need to sustain all the CO_2 pressure that was present initially, only enough to make up the difference represented by the distance between the left and middle process lines. Specifically, the difference between the adiabatic flash process and a process which yields a constant Ca^{++} solubility. This pressure is called the Kuwada pressure in recognition of the inventor of the process.

The required amount of CO_2 for scale control can be computed for any percentage of steam flash and temperature that a given resource might yield. The maximum amount of CO_2 required to suppress scaling over the temperature

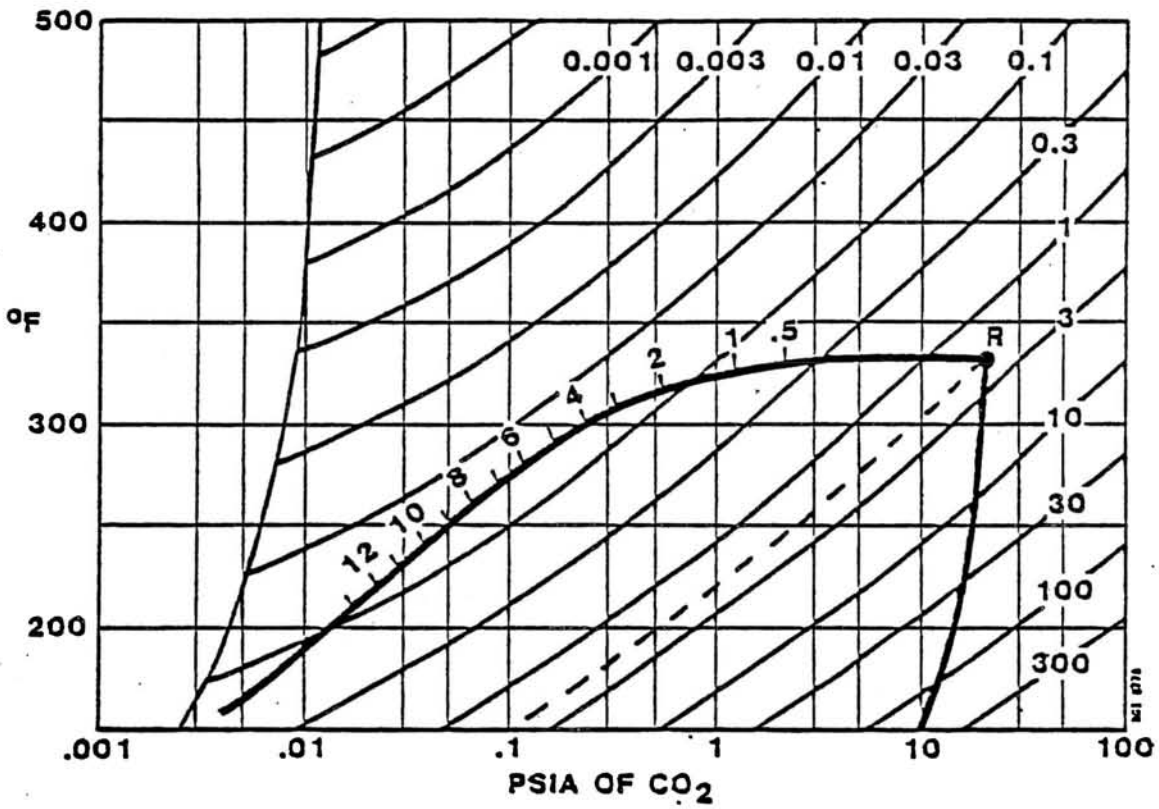

Figure III-6. Relative capacity of a brine to hold calcium.

Isopleths represent relative concentrations of calcium in equilibrium with calcite when the concentration of HCO_3^- is substantially greater than calcium. A brine having a reservoir condition represented by point R can be cooled by conduction during confinement (heavy line extending downward from R) or by steam flashing (heavy line extending leftward from R). Tic-marks on the flash line represent weight percent of fluid converted to steam. The abscissa represents the Henry's Law pressure of CO_2(aq) which begins at R. During flashing, the CO_2 is partitioned between the liquid and vapor phases, but during conductive cooling, it remains wholly in the CO_2(aq) form. The dashed line from R represents the Kuwada pressure of CO_2 which is just adequate to prevent $CaCO_3$ deposition as the fluid is cooled, e.g. by steam flashing.

range for wellbore flashing is a design parameter that can be evaluated for an engineering application. A method for making these calculations is provided in Section III-5-3c. Injection of CO_2 in amounts much in excess of the calculated minimum amounts might be justified on the basis of increased production rate due to gas lift effects, or of higher turbine efficiencies due to higher wellhead temperatures.

III-5-3c. Calculation of CO_2 Injection Pressure -- To engineer the Kuwada process and apply it to a flowing geothermal well, one needs, among other things, to calculate a required injection rate for CO_2. That rate can be related to a multiple of the concentration of native CO_2 in the resource. The objective of this section is to derive that multiplier from chemical principles.

In practice, the minimum pressure of CO_2 which sustains Ca^{++} and $CO_3^{=}$ as soluble species during flashing is called the Kuwada pressure and is designated P_k. It is greater than the pressure (P_n) due to the native CO_2 content. The required CO_2 concentration needed to make the Kuwada process fully effective is defined as follows:

$$CO_2 = (P_k/P_n) \times (CO_2)_o \qquad \text{(III-11)}$$

where $(CO_2)_o$ = reservoir CO_2 concentration

Carbonate scale control is achieved by injecting an amount of CO_2 that is defined as the product of total fluid production rate and the CO_2 concentration defined by equation III-11.

Before flashing begins, the CO_2 pressure can be represented by combining some of the equations for carbonate equilibria, yielding:

$$P_o = (44h_oK''/K'K_{sp})_o\,[HCO_3]_o^2[Ca]_o \qquad \text{(III-12)}$$

In equation III-12, subscript o refers to preflash conditions, K' and K" to first and second dissociation constants for carbonic acid, K_{sp} is the solubility product for calcite, and h is the Henry's Law solubility of CO_2.

During flashing for a Kuwada-type process, HCO_3^- and $Ca^=$ ions are conserved in the residual liquid. Their concentrations rise during flashing by the factor 1/(1-F) where F is the mass fraction of liquid converted to steam. Thus, the Kuwada counterpart to equation III-12 is given by equation III-13 wherein the activity coefficients, γ, change during the process. Subscript k refers to the "Kuwada" conditions during flashing where CO_2 pressure sustains the solubility of calcium and carbonate:

$$P_k = (44hK''/K'K_{sp})_k \, ([HCO_3]_o^2 \, [Ca]_o/[1-F]^3) \, (\gamma_{-1}^2 \, \gamma_{+2})_k/(\gamma_{-1}^2 \, \gamma_{+2})_o \qquad \text{(III-13)}$$

The ratio of P_k/P_o is given by equation III-14 which contains no concentration terms:

$$\frac{P_k}{P_o} = \frac{(K''/K'K_{sp})_k}{(K''/K'K_{sp})_o} \; \frac{h/ho}{(1-F)^3} \; \frac{(\gamma_{-1}^2 \, \gamma_{+2})}{(\gamma_{-1}^2 \, \gamma_{+2})_o} \qquad \text{(III-14)}$$

In equation III-14, the first term of the right side, consisting entirely of equilibrium constants, varies strongly with temperature; $K''/K'K_{sp}$ ranges from about 10^9 at 250°C to 10^6 at 125°C. The middle term does not vary much from unity. The third term, comprised of activity coefficients, varies modestly with flashing; the ratio for k/o terms increases, from unity toward ten across the geothermally interesting range of temperature. Thus, the Kuwada pressure approaches smaller values as flashing progresses and CO_2 pressures as little as a few percent of the initial pressure can be effective in suppressing scale. Unfortunately, the pressure due to native CO_2 is even smaller so that scale is not suppressed by it.

In the next stage of the derivation, it is useful to trace the change of CO_2 pressure, during flashing, which is due to just the native CO_2. This can be done through the Henry's Law relationship:

$$P = Ch \tag{III-15}$$

Parameter C represents the concentration of $CO_2(aq)$ and h has the units of force/concentration. The force is the vapor pressure of CO_2. Nominally, P is about three atmospheres when C is one gram $CO_2(aq)$ per kg of liquid. Initially:

$$P = C_o h_o \tag{III-16}$$

After flashing begins, the concentration of $CO_2(aq)$ diminishes sharply as the CO_2 enters the vapor phase. The vapor component of CO_2 is presumed to be in equilibrium with the residual $CO_2(aq)$ of the liquid phase such that:

$$P_n = C_n h_n \tag{III-17}$$

where: P_n = CO_2 pressure in the vapor and liquid phases

n = unmodified native or reservoir fluid at any condition of flashing

Alternatively, the $CO_2(g)$ pressure can be calculated from the gas laws as follows:

$$P_n = nRT/V \tag{III-18}$$

When correlated with a unit mass of preflash liquid, V is identical to the volume of H_2O vapor that develops during flashing. It is computed as the product of flash fraction and specific volume, v, of the steam:

$$V = F(v) \tag{III-19}$$

The number of moles, n, of gas-phase CO_2 is given by the amount originally present in a mass of liquid less the amount remaining there at any stage of flashing:

$$n = \frac{C_o - (1-F)(P_n/h_n)}{44} \qquad \text{(III-20)}$$

Combining equations III-18 to 20 yields:

$$P_n = \frac{C_o h}{(44/RT)\ (Fvh) + (1-F)} \qquad \text{(III-21)}$$

and the ratio of P_n/P_o is given by combining equations III-21 and 17 to yield:

$$\frac{P_n}{P_o} = \frac{h/h_o}{(44/RT)\ (Fvh) + (1-F)} \qquad \text{(III-22)}$$

The ratio P_k/P_n is given by combining equations III-22 and III-14 to yield:

$$P_k/P_n = \left[1 + \frac{44\ Fvh}{RT(1-F)^3}\right] \left[\frac{(K''/K'K_{sp})_k}{(K''/K'K_{sp})_o}\right] \left[\frac{1}{(1-F)^2}\right] \left[\frac{\gamma_{-1}^2\ \gamma_{+2})_k}{\gamma_{-1}^2\ \gamma_{+2})_o}\right] \qquad \text{(III-23)}$$

Equation III-23 yields the multiplier to apply to the native CO_2 concentration for computing the amount (C_k) of CO_2 to inject for the Kuwada process, as shown below:

$$C_k = C_o\ (P_k/P_n) \qquad \text{(III-24)}$$

III-5-3d. Numerical Example for the Kuwada Principle - For a numerical example, consider a liquid resource initially at 200°C flashing to 125°C in the surface equipment and having an initial ionic strength of one, corresponding to a total dissolved salt content near 50,000 ppm. Required equilibrium constants are summarized in Table III-1. With some allowances for heat losses, the net flash fraction will be about 0.13. In reference to equation III-23, the first term in brackets will take a value near 29, the second 0.12, the third 1.62, and the last 1.8. Overall, P_k/P_n = 10.1.

Table III-1

Selected Constants for Carbonate Equilibria

°C	-log K"	-log K'	-log K_{sp}	+log K"/K'K_{sp}	°F
0	-10.61	-6.53	-8.24	4.16	32
25	10.33	6.37	8.36	4.40	77
50	10.18	6.31	8.61	4.74	122
75	10.14	6.33	8.96	5.15	167
100	10.14	6.41	9.38	5.65	212*
125	10.21	6.54	9.84	6.17	257*
150	10.34	6.71	10.34	6.71	302*
200	10.71	7.13	11.40	7.82	392*
250	11.20	7.66	12.51	8.97	482*
300	11.78	8.26	13.63	10.11	572
350	12.43	8.11	14.74	10.42	662

*In this practical temperature range, log (K"/K'K_{sp}) = 3.012 + 0.0123°F.

If such a resource contained 5,000 ppm CO_2 then a total of 50,500 ppm of CO_2 on a total fluid basis would be required to make the Kuwada process operate. For a nominal production rate of 180,000 kg of resource fluid per hour, about 9,000 kg of CO_2 would be required per hour, injected downwell.

As a matter of perspective, the vapor phase for this example, at 125°C, would contain about 28 weight percent CO_2. Special accommodations for CO_2 removal and recovery must be made if the steam is intended for use in condensing turbines. For example, a steam reboiler unit might be needed (see Chapters IV and V). Chemical scale inhibitor for $CaCO_3$ might also be required at the point where CO_2 separation takes place.

The depth at the injection point and the pressure there can be calculated in principle, but require models of two-phase wellbore flow that are adapted to the high noncondensable gas contents. Such models have not yet been demonstrated. Additionally, corrosion due to CO_2 may require the well to be constructed using alloy steel casing.

In most applications, the steam will eventually be separated from the liquid. If the separated liquid is subsequently flashed again, then $CaCO_3$ scale would form. Some other chemical inhibitor could be added before then, of course. Details of energy recovery schemes using this method have not been widely distributed but a few variants are possible.

Comparison of costs with the alternative of injecting a threshold inhibitor downwell have not been explored. Obviously, the installation of a CO_2 injection system will be more costly because it uses larger injection tubing and compressors of much higher capacity. In principle, the wellbore casing must be larger, too, in order to accommodate the higher fluid flow (geothermal fluid plus injected CO_2) and the injection tubing. However, the higher wellhead temperatures imply smaller specific volumes for the H_2O vapor phase component, an off-setting factor. Any net incremental cost for refurbishing

the basic well deserves to be charged against the installation of the CO_2 injection system.

On the other hand, CO_2 is a ubiquitous component of geothermal resources and the makeup supply for recycled CO_2 can come from the geothermal fluid itself. This eliminates one running cost for chemicals. It simultaneously makes the system invulnerable to external loss of supply of a key component required for sustained operations.

There is no temperature nor depth limitation on the resource to which this method might be applied. Enhanced corrosion by the CO_2-charged liquids is a potential problem that might be solved by using low alloy chromium-molybdenum alloys for downwell tubulars. These casing materials are at least twice as costly as conventional tubulars and could significantly impact the cost of a well.

III-5-4. Downwell Injection of Strong Acid

Although the concept of acid effects on bicarbonate solutions is simple and broadly recognized, its application downwell may be difficult to control and risks serious malfunctions. Consideration of this method should recognize two classes of brine which can yield $CaCO_3$ scale; those in which calcium content exceeds bicarbonate vs. those in which the converse is true. For the latter, the amount of strong acid required to reduce the bicarbonate sufficiently would likely be too costly owing to the effects of carbonate buffering. Significantly, the scale potential for them is only slightly affected by destruction of modest amounts of bicarbonate. These kinds of resources are more common than the other.

However, a few geothermal resources contain smaller concentrations of bicarbonate than calcium and partial destruction of that bicarbonate gives a directly proportional reduction in $CaCO_3$ scale potential. These brines may be economically treatable with strong acid.

The intention of this treatment is to bring the pH of freshly flashed brine into the range of 5.5 to 7.5; $CaCO_3$ is soluble below pH 8.3 against atmospheric CO_2. For comparison, some bicarbonate-dominated brines have pH above 9 after flash. This method is distinct from a similar recommendation [12-14] to acidify in order to control the rate of silica deposition in which the pH target of 3.5 to 5.0 may yield a seriously corrosive liquid.

Obviously, over-treatment in this approach may cause a serious increase in brine acidity which would yield high corrosion rates. Accurate monitoring and injection control would, therefore, be required. Volatilization of hot acid is a potential difficulty with respect to corrosion of turbine components.

Compared to injecting threshold inhibitors, strong acids would not leave the brine in a thermodynamically poised condition. There would be no risk of precipitating $CaCO_3$ in the injection formation due to warmup that diminishes $CaCO_3$ solubility. To the degree that such fluids were overdosed with acid, they might increase the injectivity of rock formations which receive them.

The acid injection system for a production well would be similar to that for downwell injection of a threshold inhibitor. Major differences would be in selecting metals to contact the respective liquid injectates.

The volumes of liquid involved with the two methods would be more similar than the dose rates might imply. For example, 50 ppm of HCO_3^- in the resource would suggest a dose rate of 30 ppm of concentrated HCl vs. 1 ppm of threshold inhibitor. However, the inhibitor must be injected with a carrier liquid whereas the HCl can go in as concentrated acid.

Continuous use of strong acid to routinely control carbonate scale by downwell injection is not practiced. However, acid commonly is injected into oil wells and some geothermal wells in massive amounts to treat wellbore scale or clogged porosity of adjacent rock[48]. Thus, experience for handling acids is available and there is no fundamental reason to avoid a non-massive routine

use of them. However, compared to the broad applicability of threshold inhibitors and the scarcity of dangers in their misuse, injection of small amounts of strong acid may seldom be a preferred alternative.

III-5-5. Calcium-Deficient Carbonate Scales

Strontium (Sr^{++}) forms a carbonate mineral structure (strontianite) that is isomorphous with aragonite. Strontium can also occupy Ca^{++} positions in the aragonite structure. No complications with strontium-containing scales are known to this writer, despite Sr^{++} occurrences as a minor component in most aragonite scales.

Iron forms a mineral (siderite) which has a calcite-like structure that is stable at moderately low pH (~4 or less) in simple solutions. Siderite is reported in several contexts, but none are very similar to calcite. Siderite can be a corrosion product when carbonic acid reacts with metallic iron. Whether iron deposits as siderite or remains solvated may depend on the level of CO_2 pressure. High CO_2 partial pressures can yield pH values in the vicinity of pH = 4, hence the stability of siderite. Siderite may form as an alteration of millscale present on pipe at the time of installation. When present as a component of scale, the scale is generally thin and tenacious and may contain magnetite or siliceous scale components.

Siderite can form by mixing dissimilar brines in a wellbore and deposits in such a case could be heavy. Several other minerals could form simultaneously and their collective volumes can form rapidly and even prevent satisfactory tests of wells. Such mixed production is not likely to reach a commercial stage of development -- some other accommodation would be implemented first -- so that continuous inhibition of siderite in a power plant context is not likely to be required. No data is available about whether the threshold inhibitors that work on $CaCO_3$ also work on siderite, however, the structural

similarities of the minerals are strikingly suggestive that such inhibitors would be effective.

Cerussite, $PbCO_3$, has been reported[8], but conditions for its development are obscure. No data are available on its response to threshold inhibitors. Once formed, it must be removed mechanically since it is insoluble in HCl. However, it has never been reported as a major component of geothermal scale.

III-6. Prevention of Silica Scale

III-6-1. Control of Supersaturation of Amorphous Silica

True prevention of silica scale is practical only in limited applications and these do not involve chemical methods. Prevention techniques currently depend on solubility of the amorphous form of silica and sluggishness of its deposition reaction, especially at lower temperatures.

The interplay of temperature, silica content and degree of supersaturation are commonly described in terms of Figure III-7. The two solid-line curves represent the saturation concentrations of dissolved silica in equilibrium with quartz and with amorphous silica[49]. Almost all high temperature geothermal liquids that enter wellbores are saturated with respect to quartz. Moreover, the position of the quartz-line in Figure III-7 is not seriously affected by any factors of liquid composition except the chemical activity of water, which is influenced by highly saline circumstances, and by pressures that correspond to only the deepest of geothermal wells[50].

The curve for amorphous silica is less well defined despite the precision of its representation in Figure III-7. Amorphous silica commonly is an aggregation of microspheres of silica that can vary in size and composition[23] according to conditions of formation. All are fairly open structures in both senses, space among the aggregated microspheres and the structurally imprecise

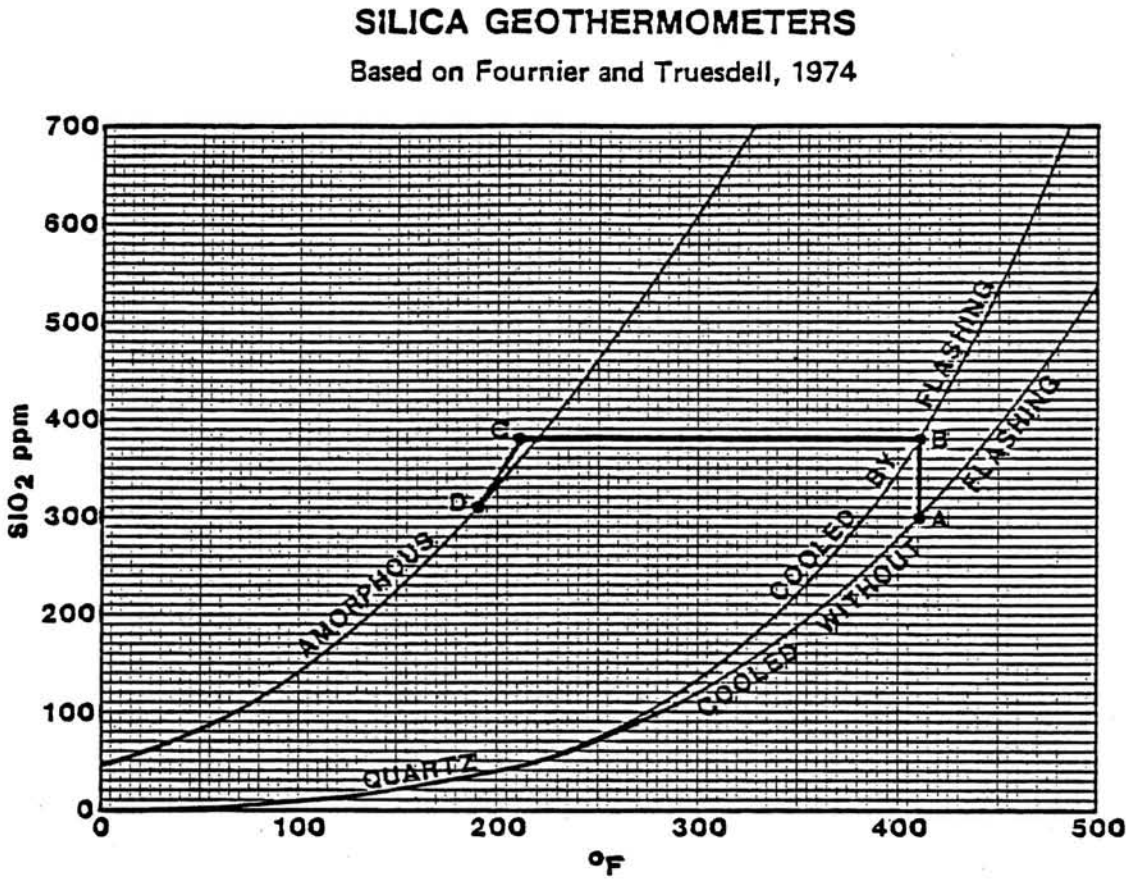

Figure III-7. Silica deposition tendencies of a hypothetical resource at 420°F are identified through the points A-D. A pre-flash concentration of 300 ppm (point A) corresponds to quartz equilibrium in the reservoir. Flash cooling to the temperature of C would yield a residual concentration of 380 ppm indicated by B. Amorphous silica solubility would not be exceeded until the last stages of the flash process, below about 220°F. Additional cooling, toward point D, an injection temperature, would result in deposition of amorphous silica.

The amount of deposition potential is given by the difference between amorphous silica solubilities at temperatures C and D, approximately 70 ppm according to the diagram above. For a well delivering 500,000 pounds of fluid per hour, the 70 ppm deposition would yield more than 480,000 pounds of solid silica scale per year with a volume exceeding 3,600 cubic feet. Note that the residual silica concentration at D exceeds the numerical concentration of silica in the unexploited resource represented by A.

silica polymer of the individual microspheres. There is much tolerance for irregularities of composition and structure, hence solubility is not thermodynamically defined.

The factors affecting deposition of quartz are well known from laboratory work and commercial growth of large single crystals of quartz has been routine for many years. However, conditions of geothermal exploitation always are far from favoring quartz deposition.

The possibility of depositing quartz is usually disregarded as being trivial. Thus, the quartz-line in Figure III-7 is relevant only with regard to the amount of silica initially dissolved in a brine. The dashed-line curve in Figure III-7 (labeled "cooled by flashing") represents the silica concentration available in residual brine upon flashing from the reservoir temperature to atmospheric conditions. The corresponding saturation temperature for amorphous silica can be read from the graph, just to the right of point C.

Prevention of silica scale from chemically simple brines can be achieved simply by designing a process that limits the amount of steam flashing and provides disposal of brine at temperatures near the solubility of amorphous silica[51]. Although that approach to scale control is simple and workable, it may have an immense cost in terms of revenues foregone.

For example, a liquid resource with a temperature of 480°F (250°C) would require rejection temperatures of 330°F (165°C); thus foregoing about 12 percent of steam flash. The "useable" flash interval 250 to 165°C yields about 17 percent flash, theoretically, but would probably be nearer a net of 13 percent in practice. Allowing for the different thermodynamic efficiencies of the two increments of steam flash, the foregone steam would represent more than 40 percent of the useable energy produced by such wells.

For a power plant of net 50 MWe and receiving 100 mils/kwh, generated by the high temperature steam alone, control of silica scale by rejecting brine at 165°C would cost about $16 million per year in foregone revenues, clearly a desperation attempt at control of scale.

Such calculated costs diminish fairly rapidly as resource temperatures approach 185°C for which flashing to atmosphere seldom yields a problem with silica scale. However, lower temperature resources are tempting to develop with Rankine cycles that yield brine rejection temperatures of 120 to 160°F (50-70°C). The corresponding resource temperature to yield a silica-free operation should then be no higher than 160-180°C.

III-6-2. Chemical Interference with Silica Polymerization and Aggregation - More than one hundred organic compounds have been evaluated for their effects on silica scale and sludge formation in hypersaline brines. The results of these studies are summarized in a paper by Harrar and others of Lawrence Livermore National Laboratory[52]. Some related information on silica deposition from less saline and cooler water is given by Iller[23]. Use of hydrochloric acid to inhibit silica scale from hypersaline brines has been proposed and successfully tested[12-14,52-53] and the concomitant effects on metal corrosion rates are described[54].

No organic additives are completely effective in hypersaline brines but several cause reductions in the rate of silica scaling of up to 80 percent. Results of these early studies are also encouraging because some patterns have emerged which suggest reasonable follow-on experiments. Significantly, the organic additives appear to act only on discrete particles of silica, colloidal or microcellular nature, decreasing their rate of aggregation in the homogeneous liquid brine and their rate of deposition on a fixed surface. Whether these effects are due to steric hindrance by the adsorbed organic molecules or to stabilization of electrical charges has not been determined.

The organics show no apparent effect on the deposition of silica monomers nor on the polymerization of monomers, nor on monomer additions to oligomers or colloidal-sized particles. Hydrochloric acid does reduce the deposition of monomers, presumably by depleting the already small population of reactive $H_3SiO_4^-$ ions, or their oligomeric counterparts, by simple protonation.

Unfortunately, the organics tested so far allow continuous and substantial formation of solid particles to occur for more than two hours after dosing, at the incubation temperature used (90°C). Since that time frame is near or greater than the typical residence time of brine through a geothermal electric plant and the injector wells, the utility of these additives is doubtful. However, the experiments were run in hypersaline brine which has very fast silica deposition compared to more common silica scaling brines. Thus, if comparable percentage reductions of silica deposition rate could be achieved in the slower-responding brines, then the organics might be useful after all. Relevant experiments have not been reported. Ref. 14, for example, indicates that significant reduction in silica scaling and particulate production rates can be achieved by acidification of a moderate salinity brine to pH 5-5.5.

The currently successful method of dealing with silica scale from hypersaline brines involves promoting disposition of silica onto particles which aggregate into a floc which then settles at practical rates in a reactor-clarifier system, perhaps preceded with a flash-crystallizer unit (see Chapter IV). Most of the "effective" organics tested so far would seem to interfere with such a system, although a few were reported to enhance flocculation. This latter aspect would seem to be a useful avenue for development. Reactor-clarifiers are large vessels, 30 to 100 feet in diameter by 10 to 30 feet tall. Substantial costs could be saved if chemical additives permitted the use of smaller vessels.

III-7. Scale Removal

Removal of adherent scale from pipes, valves, or vessels requires much vigor, either chemical or mechanical. Breakup or dissolution of the scale with acceptably small insult to the substrate can be a serious problem in balancing tradeoffs. Mechanical methods are easier to control.

Strong mineral acids are effective for removing $CaCO_3$ scale but they must contain inhibitors to slow their action on steels. Frothing due to formation of CO_2 gas may create problems for getting the acid to efficiently contact the scale. Cold mineral acids with the exception of hydrofluoric acid are not effective on silica or sulfide scales[55]. Use of acid treatment methods for wellbore and formation deposits is fully described in Ref. 56.

Chelating chemicals are ineffective because of the large volumes of liquid required and the inherently slow reaction rates. The chemicals are expensive as well. The batch approach required by chemical removal methods is inefficient in the use of time compared to the alternative of using chemicals to inhibit deposition. The use of acid pH EDTA treatment for removal of carbonate wellbore and completion zone scale is practical and effective[37].

Mechanical methods are most effective for the removal of non-carbonate scales because their energy can be focussed on the place where the scale exists and withdrawn when the scale is removed, unlike the chemical methods. At least four classes of mechanical methods are available: a) reaming with rotary equipment, especially in wellbores, b) scraping, as with pigs forced through liquid-filled pipelines, c) hydroblasting the scale with a jet of high-pressure water while the scale is open to the atmosphere. This is useful in dismantled or disconnected pipes, valves, and vessels and yields variable sized fragments of scale as a waste product, and d) cavitation descaling in which a high pressure and high speed jet of water is introduced into a liquid-

filled pipe or vessel so as to create cavitation bubbles. When the bubbles collapse near the scale, the scale is broken into fine particles.

None of the mechanical methods is usefully augmented with chemicals that are simultaneously applied, so they will not be discussed further.

III-8. Chemical Modeling and Predicting Scale Deposition

Forecasting scale deposition and other chemical features of brines affects geothermal developments at two levels. At an economic level, models provide data which affect cost estimates for scale mitigation, solids handling, effects of gases on net energy outputs, and requirements for environmental impact controls. The outputs of those models become reflected in requirements for capital investment and, eventually, in the economic rates of return on the investments. At a technical level, the chemical modeling must deal with rates of scale buildup in the system under specific conditions of flow, with and without attempts to mitigate that buildup.

The direct value of a chemical model lies in the marginal cost savings which result from using it to make the chemical control methods more effective or less costly in an engineering sense, or in selecting a plant design which yields a more economic output than its alternative. Indirect values of chemical models result from an improved understanding about the behavior of real and imagined brines. Such understanding hopefully could be extended to other endeavors, not necessarily geothermal, which become more successful as a consequence.

III-8-1. Engineering Utility of Models

The utility of chemical models depends on their applicability, accuracy, and credibility which are the subjects of this section. Although all models and approaches to modeling have defects, some of which are serious from a

technical point of view, they deserve to be treated as a set of tools. As when selecting wrenches from a box to choose a wrench that fits a particular nut, some chemical models fit a resource better, or more simply than do others.

Chemical models range from simple to the hopelessly complex. The task of a geochemical engineer is to select, or invent, an appropriate model that works with data that can be made available in a timely and practical way.

The term "chemical model" often is aimed at complex computerized calculational systems based on thermodynamic principles of chemical reactivity. Here the term will be used without regard to relative complexity or whether the model has any basis in chemical theory. Any calculational method which yields an output about the quantity of solids that may form from a brine, or their rates of formation, has a utility in forecasting scale deposition and deserves to be considered. The emphasis on rates and amounts of deposition is appropriate for the engineering focus when applying a model.

From that point of view, some of the large computerized thermodynamic models are seen to have low utility when they only predict tendencies of solid forms to precipitate without also estimating rates or amounts. Although such models can function in a way to provide some insight about a brine's chemical behavior, such output often is too little or too late. Appropriate data are difficult to specify before a well is drilled, for example, but a new well at once yields some direct evidence about the issue of solids deposition. To the degree a model ignores kinetic factors, and many do, its output has an uncertain credibility in regard to the dynamism of geothermal production.

General chemical models which have a sound thermodynamic basis and incorporate kinetic factors and predict amounts of deposition and predict where the deposition will be located in a power plant have become available, partly through a process of evolution[57]. Unfortunately, the models cannot be fully

tested by comparison with measured deposits in real geothermal systems. Partly this is because no single well provides all the categories of chemical possibilities that a generalized computer model can consider. But neither will a complete, yet scale-prone system be built and purposely allowed to function in all detrimental modes that a computer model has been designed to represent. Thus, complete calibration of a complex model seems hard to realize.

The experimental alternative, of course, is to build small, temporary systems that allow direct experimentation with portions of a fluid's flow path, using data from them to calibrate or verify the models. This is equivalent to testing small, or partial chemical models, an alternative that is more tractable conceptually as well as experimentally. Thus, small, focussed, narrow chemical models can have substantial utility because they can be designed relevant to immediate situations. Furthermore, their validity can be established in practical experiments.

III-8-2. History of Chemical Models

The conceptual evolution of general computerized models can be traced to systems of equations designed by R. M. Garrels[58] and M. J. N. Pourbaix[59]. Their systems showed how the equations for chemical equilibrium constants could be combined with equations for mass balance and electrical charge balance. Such a set of equations plus one other measured (or assumed) quantity permitted numerical evaluation of all the unknowns through solving the equations simultaneously. For example, Garrels' system for carbonate equilibria in water used six equations which are easily solved by hand. Similarly tractable models can be readily put together for sulfides, silicates, etc. All serious students of scaling phenomena deserve to work out a few examples by hand in order to become sensitive about how the concentrations of components

trade off against one another in the mathematics of chemical equilibria. The same principles are used to generate systems with more than 200 equations that can only be solved by computers, often using specially adapted algorithms, such as by Newton-Raphson iteration.

The first models of large size dealt only with the issue of chemical equilibrium via the concentrations of dissolved components and the presence of several minerals in unspecified amounts. They were developed by H. C. Helgesen and his coworkers mainly after 1965[60-64]. The original purposes were in regard to genesis of ore deposits for which the concepts of long times and steady temperature and pressure are appropriate.

By the mid 1970's the programs incorporated estimates of specific activity coefficients vs ionic strength and temperature as well as accounting for material being distributed between solids and solutes. In principle, that provides for complete thermodynamic descriptions of the issue in the form of closed mathematical solutions. A bibliography, which includes 48 listings describing the sequence of code development, is available[65]. A thorough exposition of state of the art chemical modeling is given in Ref. 66 and comparisons of computerized chemical models for equilibrium calculations in aqueous systems is provided in Ref. 67.

The factor of chemical equilibrium, which makes valid the mathematical framework of these models, large and small, also is the issue which provides the most trouble in applications to industrialized geothermal systems. Equilibrium in the laboratory sense generally means long time intervals at constant and uniform temperature with no change in total mass of the system. A flowing geothermal well has none of those features.

The counterpart of "equilibrium" in a flowing system is the "steady state" conditions of temperature and pressure that "occur" at fixed points

along the flow path when the system moves stably at a constant throughput rate. Conceptually, this yields stable concentrations of reactants in the (local) brine even though deposition is occurring there due to chemically unstable (nonequilibrium) concentrations.

Often this is a useful point of view but subtle mismatches occur with reactions that are of the intermediate and delayed categories described in the previous sections. In those cases, chemical events at one location can depend on other events that happened far upstream destroying the specificity that the quasi-equilibrium assumption requires. Thus, some features of patterns along the flow path may not simply expand or contract with changes in the length of flow path, they may even be lost if crucial time-at-temperature conditions are forced out of the flow path by mechanical means that cause abrupt changes in temperature.

With the fundamental principles of the mathematical basis unmet in real systems, one is more justified in being surprised by matches between calculations and direct observation than by mismatches. Some matches do occur, particularly for "prompt" reactions and especially for the carbonate equilibria which involve chemical reaction mechanisms fueled by relatively simple ions and triggered by such events as sudden loss of CO_2 or temperature changes which elicit changed proportions of components, like $HCO_3^-/CO_3^=$. These components are connected by reaction mechanisms which are seldom inhibited and are complete within half-lives often measured in fractional seconds.

Sulfide equilibria appear similarly fast and are only a little more complicated, hence some calculation results are practically accurate. However, the metal ions which are involved in the formation of sulfide scales are generally hard to characterize in regard to gross concentration and distribution among multiple complexed forms. Consequently, calculated results are

frequently in error due to inaccurate inputs or ill-fit of the model, rather than violations of the equilibrium assumption or inherently slow reaction rates.

Silica deposition in wells and plants cannot be calculated accurately by thermodynamic models. Partly this is because the reactions which tend to take place after a triggering event generally occur with half-lives of minutes to days. Reasons for variability involve at least temperature, gross salt content, and availability of an assortment of minor components. The relationships among those are poorly characterized at present. Furthermore, silica, whether in an amorphous or crystalline form, provides an atomic structure that is very forgiving of irregularities in composition. Thus, siliceous solids are poorly definable in thermodynamic terms apart from being largely undefined at the present time. There would seem to be no hope of building theoretical models to successfully quantify deposition of amorphous silica-rich scales. Since silica is a common scale in geothermal systems, and often the dominant one, the poor applicability of theory is unfortunate. Build-up of silica-rich scales from unmodified brines, and effects on the scale due to additives must be approached via direct experimentation on fluids from individual wells.

The idealism of an assumption for equilibrium has other troublesome aspects. In equilibrium theory, no consequences are assigned to unequalness in the concentrations of dissolved components which tend to form solids of a definite stoichiometry. For example, the development of calcite and aragonite from the same parent brine at different stages of flashing was described earlier. Similarly, laboratory recipes for preparing calcite, aragonite, and vaterite (a third polymorph of $CaCO_3$) involve specific techniques of blending reactive solutions so that mechanical factors become involved with the chemical ones, yielding non-equilibirum polymorphs. These mechanical interactions

with chemical phenomena are legion in number, many form the basis for patents. The mathematical models ignore those mechanical aspects and this is a great peril to their accuracy.

When equilibrium-type chemical models are applied to the dynamic, non-equilibrium context of geothermal exploitation their validity is not certain. However, models do provide some insight about a system's sensitivities to a few factors, especially relative concentrations, and they deserve to be used since they provide a tentative basis for planning. However, their accuracy cannot be judged well in advance. They must always be backed up by direct experimentation before commitments are made about engineering designs of geothermal projects.

Chemical modeling of geothermal brines in flowing systems should be regarded as more art than science. Simple models that can be worked by hand may require clever insight about the chemical system. Simplifying assumptions must be selected with care and this requires astute subjectivity in order to be successful. On the other hand, generalized computer models require inputs of data that are not always available from field tests or are obtained with serious numerical uncertainties. To compensate, one again needs the astute judgement of people who know the vagaries of the program as it occurs in a specific computer as well as knowing the vagaries due to sampling, analysis, and natural geochemical behavior of crucial components. These combinations of talent are difficult to arrange.

There is no limit to "the pitfalls for the unwary" in using chemical models of any degree of complexity, thus no attempt will be made here to provide a comprehensive check-list of do's or don'ts. However, it is useful to convey a sense for how subtle differences in the set-up of chemical models can lead to substantial contrasts in the outcomes of the calculations, sug-

gesting how severely the real system can be misrepresented by unwary acceptance of calculated results. Two examples will be given, both in regard to carbonate equilibria for which the most successful models exist.

The first example is taken from Garrels[58] who considers five methods of equilibrating calcite with water; two of which are: a) the water is equilibrated with the atmosphere before the calcite is introduced, whereupon the system is closed to the atmosphere; b) the water is equilibrated with calcite while open to the atmosphere and the atmospheric CO_2 component ($\sim 10^{-3.5}$ atm).

Equilibrium pH's for cases (a) and (b) are 9.9 and 8.4 respectively. Equilibrium Ca^{++} concentrations are 0.14 and 0.40 millimolar. Thus, the simple aspect of when the system is open to the atmosphere yields a 3-fold difference in calculated calcium content and a 30-fold difference in calculated hydrogen ion (H^+) concentration. Subtle and partially obscure presumptions are commonly made when setting up the mathematical framework of models. Being certain that the framework properly represents the real system demands an intimate knowledge of both.

The second example illustrates one effect of the contrast between laboratory perspective and circumstances of geothermal production. It illustrates both an inappropriate use of the equilibrium concept and an (apparently) unexamined simplification about the system.

Upon writing the equation for dissolution of calcite:

$$CO_2 + H_2O + CaCO_3 \rightleftarrows Ca^{++} + 2HCO_3^- \qquad \text{(III-25)}$$

one can simplify the equilibrium constant, as in Equation III-26, by noting that in equation III-25 the concentration of HCO_3^- appears to be twice that of Ca^{++}:

$$K = \frac{[Ca][HCO_3]^2}{(PCO_2)[H_2O][CaCO_3)} = \frac{4[Ca]^3}{PCO_2} \qquad \text{(III-26)}$$

This outcome is usually expressed as the calcium concentration being proportional to the cube root of the CO_2 pressure. It was originally pointed out in 1929[68]. It has been repeated by chains of successive authors up to the present time and is included as part of some geochemical/geothermal models.

Unfortunately, that perspective misrepresents geothermal chemistry at two levels. At an operational level, natural concentrations of Ca^{++} and HCO_3^- are seldom, if ever, present in the proportions of 1:2. They can be greatly different from that in either direction, a feature which destroys the proportionality in equation III-26.

The cube root proportionality over-simplifies real geologic systems. For example at East Mesa, California the proportions of Ca^{++}:HCO_3^- are near 1:35 and a fuller analysis of equations III-25 and 26 show that Ca^{++} concentration there is proportional to the first power of the CO_2 pressure, not the one-third. In contrast, at the Salton Sea Geothermal Field, the Ca^{++}:HCO_3^- ratio is nearly 450:1 and Ca^{++} concentration is analytically invariant with changes in CO_2 pressure of several tens of atmospheres.

The reason for those outcomes has two parts. The mechanistic connection between CO_2 and Ca^{++} is tripply indirect since at substantial CO_2 pressures the series of chemical reactions is:

$$CO_2(g) \leftrightarrows CO_2(aq) \leftrightarrows HCO_3^- \leftrightarrows CO_3^= \leftrightarrows CaCO_3 \qquad \text{(III-27)}$$

Equation III-27 emphasizes that only the $CO_3^=$ form of carbon is directly involved with $CaCO_3$. The solubility product constant, K, involves only the ions Ca^{++} and $CO_3^=$. When the concentration of one of those is much larger than the other, removal (or addition) of equal dissolved amounts, as in pre-

cipitation (or dissolution) has a large effect on the value of K with only a negligible effect on the concentration of the major component.

At a theoretical level, the laboratory model represents an approach toward equilibrium through the process of dissolution. This displaces the subsequent $Ca^{++}:HCO_3^-$ ratio toward 1:2, irrespective of the starting conditions. By contrast, in the case of flashing geothermal brine, the new chemical equilibrium is approached through a process of deposition. This fact of life displaces the subsequent $Ca^{++}:HCO_3^-$ ratio from 1:2. Although the [presumption of] 1:2 proportions in the incremental and overall Ca^{++} and HCO_3^- concentrations is appropriate for the laboratory context of calcite dissolution it is not appropriate for the field conditions and deposition in an open system. Thus, even though carbonate reactions are intrinsically fast enough that equilibrium is an acceptable approximation, not all the corollaries of equilibrium can be utilized in setting up the mathematical models. Unfortunately, this over-simplification currently is entrenched in the geochemical literature (see for example, Refs. 69-71).

III-8-3. Available Geochemical Models

With the limitations of computational models for analysis of geochemical systems in mind, it is appropriate to consider available computational capabilities. In this section, a tabulation of modeling capabilities is provided. Application of these models must be carefully considered in terms of the conditions for which the models were originally intended to deal with and the particular application to which they are to be applied.

III-8-3a. Geochemical Models - Computer codes for the calculation of reservoir chemistry based on chemical analysis of surface samples and estimates or measurements of total enthalpy are described in Refs. 72-75. The code de-

scribed in Refs. 72 and 73 provides a capability for calculating reservoir temperature, pH, gas pressure and ion activities if the specific enthalpy of the total production (liquid + gas) and chemical analyses of the produced water and gas, collected at known pressures, are available. Alternatively, given the availability of a single phase liquid sample obtained with a downhole sampler, the code calculates reservoir chemistry and properties without a measured or estimated value for total enthalpy.

The computer code described in Refs. 74 and 75 is a large data base with the following capabilities.

1. Stores steam and brine analytical data in disk files.
2. Calculates downhole (reservoir) chemistry, temperature, chemical ratios, gas pressures and specified chemical equilibria.
3. Generates tables and graphs of input data and calculated parameters.

III-8-3b. Silica Geochemical Model - A computer code called SILNUC, described in Refs. 21 and 76, models the homogeneous nucleation and growth of colloidal particles of amorphous silica. The code is applicable to 150°C and pH values of 8 or less. The code accounts for base and fluoride catalysis of monomeric silica polymerization. Scale deposition rates are not computed. The code assumes that the brine solution consist of sodium chloride, sodium fluoride and dissolved silica (initially present as the monomer). More complex brine solutions are accounted for by first computing an equivalent sodium chloride concentration which is equal to the molar concentration of chloride and bicarbonate at room temperature. A complete description with history of the code, which is written for the MNF4 FORTRAN Compiler and the CDC 7600 computer, is provided in Ref. 76.

Type curves for manually computing polymerization behavior of dissolved silica are provided in Ref. 24. This reference provides empirical equations

for calculating molecular deposition rates of silica as a function of silica concentration at temperatures to 150°C and sodium chloride concentrations up to 1 M (mol/kg).

III-8-3c. Estimation Procedures for Reservoir Temperature - A description of estimation procedures for evaluating production reservoir temperature is provided in Chapter IV. The interested reader should also review Refs. 77 and 78.

III-8-3d. Thermodynamic Equilibrium Codes - A comparative discussion of equilibrium models is provided in Ref. 67. These codes calculate distribution and activities of dissolved species on the assumption that thermodynamic equilibrium is attained in the aqueous phase. Calculation of speciation then permits consideration of complex interactions between liquids, gases, and reservoir rocks and the effects of these interactions on liquid and gas chemistry.

Jackson[79] described a predictive model for calculating noncondensable gas composition, brine pH and concentrations of scale-forming species in brine given the calculated reservoir brine chemistry and steam-flash history of the brine. The data for equilibrium constants and activity coefficients needed to model scale formation were extrapolated from data in Ref. 80.

Miller, et al.[81] describe an attempt to utilize the Helgeson-Herrick equilibrium code to predict precipitation of scale forming species from hypersaline brine. The code predicted, for a given set of conditions, a much larger number of precipitating phases than actually observed. In a qualitative sense, the code provided some indication of brine behavior at changing temperature, pressure and pH conditions especially for sulfide phases. Predictions of silica behavior were not closely related to observations of actual precipitation reactions.

Wolery[65, 82] describes the capabilities of a complex equilibrium code that can be used to predict the ramifications of heating or cooling of an aqueous solution and solution-rock interactions. The code predicts mineral phase precipitation reactions and the quantity of mineral phases that precipitate. An example is presented in Ref. 65 that describes the consequences of reheating Salton Sea water to 220°C as part of an evaluation of the use of Salton Sea water as a source of injection make-up water. The EQ 3/6 code developed by Wolery is presently used in the assessment of underground storage of nuclear waste. The data base has been significantly extended and work is proceeding to provide kinetic data for modelling of reaction rates.

Shannon, et al.[57] and Lessor and Kreid[83] describe what is perhaps, at the present time, the most complete integrated computational package for the description of geothermal chemistry and scaling reactions. The code consists of four parts as follows:

- EQUILIB - provides chemical equilibrium computations for a brine as a function of thermodynamic state
- FLOSCAL - provides kinetics of deposition and corrosion processes for specified flow geometry and conditions
- PLANT - provides a steady-state geothermal power plant model with provision for scale specifications at key points
- GEOSCALE - is an executive routine that calls the other codes to generate a time-dependent geothermal power plant model

Ref. 83 provides examples of the application of the code. Simulation of hypersaline brine scaling processes must relie upon approximations for equilibrium constants, activity coefficients and reaction rates since experimental data are lacking. Calibration of the code based on carefully controlled field experiments is one method that could significantly improve the site specific predictive capabilities of the codes in those instances where experimental

data needed to describe the thermodynamic behavior of a geothermal fluid are lacking. Refs. 85 and 86 describe a new approach to the prediction of mineral solubilities at high ionic strength ($\leq$20 m) and temperatures to 300°C.

III-8-3e. Carbonate Scaling Equilibria - Calculation of $CaCO_3$ saturation in brine solutions at elevated temperature and pressure is described in Ref. 84. The method is an extension of the Langelier and Stiff-Davis techniques for calculating a carbonate saturation index[87-88]. The new method described in Ref. 84 permits calculation of saturation index and pH at elevated temperature and pressures without the need for activity coefficients. Examples of the application of the new method are provided.

Application of the Langlier saturation index to the prediction of carbonate and sulfide scale formation is described in Refs. 89 and 90. Ref. 90 provides excellent instructive examples of the utilization of this relatively simple method for predicting scale formation at modest temperatures and salinities.

III-9. References

1. Kern, D.M., 1960, The hydration of carbon dioxide: Jour. Chem. Ed., V. 37, N. 1, p. 14-23.

2. The ratio of $CO_3^{=}/HCO_3^{-}$ varies jointly with temperature and CO_2 pressure, but in flashing systems the CO_2 pressure diminishes rapidly. Graphic descriptions of the relationship are shown in Michels, D.E., 1981, CO_2 and Carbonate Chemistry applied to geothermal engineering: Lawrence Berkeley Laboratory, Rpt. LBL-11509, 27 pp.

   It can be shown that $(CO_3^{=}) = (HCO_3^{-})^2\ K''/K'HPCO_2$ where h is the Henry's law coefficient for $CO_2(aq)$ and K' and K'' are the first and second dissociation constants for carbonic acid. For all geothermally reasonable temperatures and HCO_3^{-} concentrations the concentration of $CO_3^{=}$ remains small until the CO_2 pressure becomes substantially less than 0.1 atm. Such small CO_2 pressures correspond to substantial amounts of steam flash.

3. Significantly, the amount of CO_2 expelled in the second stage is small compared to the earlier exhalation of CO_2 that was initially present as unionized molecules of $CO_2(aq)$. At temperatures below 300°F, for example, the $CO_3^{=}/HCO_3^{-}$ ratio will become established at values greater than 0.1 in well-flashed systems. Thus, a nominal initial concentration of 500 ppm HCO_3^{-} would then yield about 42 ppm of $CO_3^{=}$, enough to cause severe supersaturation of $CaCO_3$. The associated amount of CO_2 expelled would be only 30 ppm. By comparison, release of 500 ppm of $CO_2(aq)$ due to early stage flashing could cause a change in the CO_3/HCO_3 ratio from 0.0005 to 0.005 which yields only 2.5 ppm of $CO_3^{=}$.

4. Michels, D.E., 1980, Deposition of $CaCO_3$ in porous materials by flashing geothermal fluid: Lawrence Berkeley Laboratory Rept. LBL-10673, 28 pp.

   Evidence that aragonite mats are not impact-deposited crystals includes two experiments which used fluid from the East Mesa geothermal resource. The $CaCO_3$ deposition potential was about 15 mg/kg of brine; the initial concentrations of Ca and HCO_3 were about 6 and 500, respectively. Zoned deposition occurred in a porous matrix. In microscopic view of thin sections prepared from the matrix, the calcite can be readily distinguished from the aragonite because of their crystal shapes, rhombs vs. needles. Calcite occurs in the flow path at positions slightly down-flow from the point of initial flashing. Aragonite occurs in further downstream parts of the flow path where calcite is scarce to absent.

5. Michaelides, E.E., 1981, The effect of magnus force on the scale deposition in geothermal systems: Jour. of Energy Resources Tech., V. 103, p. 352-354.

   A computational method shows that forces on small particles in a laminar sublayer having a steep velocity gradient yield a depositional context. No comment is made about the origin of the particles nor how they came to be suspended in the liquid, but the concept could apply to debris from the production zones or to aragonite (e.g.) particles sloughed from their places of formation in the casing or piping. The possibility that the

particles could form homogeneously within the liquid has no support by data and some data are available which show clearly that growth of the $CaCO_3$ particles occurs at fixed locations along the fluid's flow path. That is, nucleation and growth occurred at the places they were found. Moreover, evidence for substantial sloughing due to mechanical buffeting by the flowing fluid appears absent.

6. Republic Geothermal, Inc., internal reports.

   Sequential deposition of calcite, then aragonite also occurred in a horizontal test loop which contained the full flow of a geothermal well. A series of orifice plates was installed in the loop to establish a cascade of temperature-pressure conditions in order to outline the conditions for onset of scale deposition. On one of these, aragonite-free calcite scale, that was dense and tenacious, decorated the upstream surface of the orifice plate and the adjoining pipe surfaces. By contrast, the pipe walls downstream of the orifice plate acquired a thick venturi-shaped mat of aragonite. X-ray analysis of the mat indicated virtually 100% aragonite, the calcite peak was diffuse and barely resolvable. The thickness of the upper-face calcite layer was about 2 mm and uniform, the aragonite zone reached a maximum thickness of 50 mm about one meter downstream of the orifice plate.

   The fluid in the test loop section where aragonite deposited was in a mistflow condition, as indicated by the uniformity of macro characteristics of the scale deposit around the pipe's circumferences. The size of mist droplets can be estimated by calculation to be less than 5 micrometers in diameter. Since that dimension is smaller than the aragonite crystals, the crystals could not have formed enroute from the orifice plate to the points where droplets impacted.

   The promptness of the aragonite deposition mechanism can be indicated by simple considerations of the test loop example. The fluid speed below the orifice was calculated to be about 60 meters/sec, yet the maximum deposition occurred only one meter further along the flow path -- about 15 milliseconds. In that time interval, the thermodynamic potential for deposition developed (re: $CO_3^=$ buildup) and the transport of the reactants to the walls and crystal growth sites occurred via droplet impact.

7. Michels, D.E., 1982, Chemical experiments with fresh, hot, party-flashed hypersaline brine: Geothermal Resources Council Trans., V. 6, p. 297-300.

8. Harrar, J.E., et al., 1979, Incipient processes in the corrosion of mild steel in 90° hypersaline geothermal brine: J. Corr. Sci., V. 19, p. 819-833.

9. e.g., siderite can develop as a corrosion product or conversion from iron oxide (as pipe rust) when contacted with oxygen-scarce CO_2-rich geothermal fluid.

10. Calamai, A., et al., 1975, Preliminary report on the Cesano hot brine deposit (Northern Latium, Italy): 2nd U.N. Symposium, San Francisco, V. 1, p. 305-313.

11. Barnes, H.L. and G.K. Czamanske, 1967, Solubilities and transport of ore minerals: In Geochemistry of Hydrothermal Ore Deposits, H.L. Barnes, ed., Holt, Rinehart and Winston, New York, p. 334-381.

12. Owen, L.B., 976, Precipitation of amorphous silica from high temperature hypersaline geothermal brine: Univ. of Calif., Lawrence Livermore National Laboratory Rept. UCRL-51866.

13. Grenz, J.Z. and L.B. Owen, 1977, Field evaluation of scale control methods; Acidification: Geothermal Resources Coun. Trans., V. 1, p. 119-121.

14. Rothbaum, H.P., Anderton, B.H., Harrison, R.F., Rohde, A.G. and Slatter, A., 1979, Effect of silica polymerization and pH on geothermal scaling: Geothermics, V. 8, 1-20.

15. Goldberg, A. and Owen, L.B., 1979, Pitting, corrosion and scaling of carbon steels in geothermal brines: Corrosion, V. 35, N. 3, 114-124.

16. Jackson, D.D. and Hill, J.H., 1976, Possibilities for controlling heavy metal sulfides in scale from geothermal brine: Univ. of Calif., Lawrence Livermore National Laboratory Rept. UCRL-51977.

17. Owen, L.B., 1977, Properties of siliceous scale from the Salton Sea geothermal field: Geothermal Resources Council, Trans., V. 1, 235-238.

18. Austin, A.L., Lundberg, A.W., Owen, L.B. and Tardiff, G.E., 1977, The LLL geothermal energy program status report - January 1976 - January 1977: Univ. of Calif., Lawrence Livermore National Laboratory Rept. UCRL-50046-76.

19. Skinner, B.J., White, D.E., Rose, H.J. and Mays, R.E., 1967, Sulfides associated with the Salton Sea geothermal brine: Economic Geology, V. 62, 316-330.

20. Bohlman, E.G., Mesmer, P.H. and Berlinski, P., 1980, Kinetics of silica deposition from simulated geothermal brines: Soc. Pet. Engr. Jour., p. 239-248.

21. Weres, O., Yee, A. and Tsao, L., 1980, Kinetics of silica polymerization: Jour. Coll. and Interface Sci., V. 84, N. 2, p. 379-402.

22. Rimstidt, J.D. and H.L. Barnes, 1980, The kinetics of silica water reactions: Geochim. et Cosmochim. Acta, V. 44, p. 1,683-1,699.

23. Iler, R.K., 1979, The chemistry of silica: John Wiley and Sons, New York, NY.

24. Weres, O., Yee, A. and Tsao, L., 1982, Equations and Type Curves for Predicting the Polymerization of Amorphous Silica in Geothermal Brines: Soc. Pet. Eng. Jour., 9-16.

25. Harrar, J.E., et al., 1980, On-line tests of organic additives for the inhibition of the precipitation of silica from hypersaline geothermal brine iv. Final tests of candidate additives: Univ. of Calif., Lawrence Livermore National Laboratory Rept. UCID-18536, 47 pp.

26. Ozawa, T. and Y. Fujii, 1970, A phenomenon of scaling in production wells and the geothermal power plant in the Maksujkawa area: U.N. Symposium, Pisa, V. 2, p. 1,613-1,618.

27. Yanagase, T. et al., 1970, The properties of scales and methods to prevent them: U.N. Symposium, Pisa, V. 2, p. 1,619-1,623.

28. Featherstone, J.C., R.H. VanNote and B.S. Pawlowski, 1979, A cost-effective treatment system for the stabilization of spent geothermal brine: Geothermal Resources Council Trans., V. 3, p. 201-204.

29. VanNote, R.H., 1981, Geothermal Brine Treatment: U.S. Patent 4,320,328 assigned to Envirotech Corp., Menlo Park, California.

30. Featherstone, J.C. and D.R. Powell, 1981, Stabilization of highly saline geothermal brines: Jour. Pet. Tech., V. 33, p. 727-734.

31. Vetter, D.J. and D.A. Campbell, 1979, Scale inhibition in geothermal operations. Experiments with DEQUEST® 2060 phosphonate in Republic's East Mesa field: Lawrence Berkeley Laboratory Report.

32. Auerbach, M.H. and R.A. Reimer, 1982, A calcium carbonate scale inhibitor for direct contact binary geothermal service: Soc. Pet. Engrs., Paper SPE 10607, Int'l. Symp. on Oil Field and Geothermal Chemistry, Dallas, Jan. 25-27, 1982, p. 151-160.

33. Oddo, J.E., et al., 1982, Inhibition of $CaCO_3$ precipitation from brine solutions. A new flow system for high-temperature and pressure studies: Jour. Pet. Tech., V. 34, p. 2,409-2,422.

34. Cowan, J.C. and Weinttritt, D.J., 1976, Water-formed scale deposits: Gulf Publishing Co., Houston, Texas.

35. Casper, L.A. and Pinchback, T.R., 1980, Geothermal scaling and corrosion: ASTM, STP717.

Nancollas, G.H. and M.M. Reddy, 1974, The kinetics of crystallization of scale-forming minerals: Soc. Pet. Engr. Jour., p. 117-126, SPE-AIME Oilfield Chemistry Symposium, Denver, May 24-25, 1973.

36. Nancollas, G.H. and Sawada, K., 1982, Formation of scales of calcium carbonate polymorphs: The influence of magnesium ion and inhibitors: Jour. Pet. Tech., 645-652.

37. Shaughnnessy, C.M. and Kline, W.E., 1983, EDTA removes formation damage at Prudhoe Bay: Jour. Pet. Tech., 1783-1791.

38. Kestin, J., DiPippo, R., Khalifa, H.E. and Ryley, D.J., Editors, 1980, Sourcebook on the production of electricity from geothermal energy: U.S. DOE Rept. DOE/RA/4051-1.

39. Hlinak, A.J., J.L. Lobach, and K.E. Nichols, 1981, Operational and field test results from the 500 KW direct contact pilot plant at East Mesa: Geothermal Resources Council Trans., V. 5, p. 429-432.

40. Sheinbaum, I., 1976, Power generation from hot brines: U.S. Patent 3,988,895.

Hutchinson, A.J.L., 1977, Working fluids and systems for recovering geothermal or waste heat: U.S. Patent 4,057,964.

41. Shannon, D.W., et al., 1981, Monitoring the chemistry and materials of the Magma binary cycle generating plant: Battelle, Pacific Northwest Laboratory Rept. PNL-4123.

42. Lacy, R.G. and T.T. Nelson, 1982, Heber binary project-binary cycle geothermal demonstration power plant: Geothermal Resources Council Trans., V. 6, p. 359-362.

43. Michels, D.E., 1981, CO_2 and carbonate chemistry applied to geothermal engineering: Lawrence Berkeley Laboratory, Rpt. LBL-11509, 27 pp.

44. Kuwada, J.T., 1974, Geothermal hot water recovery process and system: U.S. Patent 3,782,468, assigned to Rogers Engineering Co., San Francisco.

45. Kuwada, J.T., 1982, Field demonstration of the EFP system for carbonate scale control: Geothermal Resources Council Bul., V. 11, N. 9, p. 3-9.

46. Berg, C.H., 1977, Geothermal brine production: U.S. Patent 4,189,923.

47. Michels, D.E., in progress. A temperature-drop model for 2-phase flow in geothermal wellbores.

48. Bélteky, L., 1975, Problems related to operating thermal wells subject to scaling in Hungary: Geothermics, V. 4, Nos. 1-4, 57-65.

49. Fournier, R.D. and J.J. Rowe, 1977, The solubility of amorphous silica in water at high temperatures and high pressures: Amer. Miner., V. 62, p. 1052-1056.

50. Fournier, et al., 1982 The solubility of quartz in aqueous sodium chloride solution at 350°C and 100 to 500 bars: Geochem. et Cosmochim. Acta, V. 46, p. 1975-1978.

51. Arnørsson, S., 1981, Mineral deposition from Icelandic geotherml waters: Environmental and Utilization Problems: Jour. Pet. Tech., 181-187.

52. Harrar, J.E., Locke, F.E., Otto, C.H., Jr., Lorensen, L.E., Monaco, S.B. and Frey, W.P., 1982, Field tests of organic additives for scale control at the Salton Sea Geothermal Field: Soc. Pet. Eng. Jour., 17-27.

53. Harrar, et al., 1979, Studies of brine chemistry, precipitation of solids, and scale formation at the Salton Sea geothermal field: Lawrence Livermore National Laboratory Rept. UCRL-52640.

54. McCright, R.D., et al., 1979, Corrosion resistance of metals in hypersaline geothermal environments - electrochemical and weight loss determinations: AIME Metallurgical Soc., New Orleans, Feb.

55. Deutscher, S.B., Ross, D.M., Quong, R. and Harrar, J.E., 1980, Studies of the dissolution of geothermal scale: Univ. of Calif., Lawrence Livermore National Laboratory Rept. UCRL-52897.

56. Williams, B.B., Gridley, J.L. and Schechter, R.S., 1979, Acidizing fundamentals: Soc. Pet. Eng. (AIME) Monograph, Vol. 6, Henry L. Doherty Series.

57. Shannon, D.W., Walter, R.A. and Lessor, D.L., 1978, Brine chemistry and combined heat/mass transfer: EPRI Rept. ER-635.

The Electric Power Research Institute through Battelle Pacific Northwest Laboratories has developed a set of computer models that operate to simulate scale and corrosion in wells, pipes, heat exchangers, etc., of a test facility or plant. The codes predict scaling in a flashing well or across an orifice, they predict precipitation when two or more brines are mixed, and they simulate acid injection for scale inhibition or removal. Their successful use requires substantial attention by persons who are knowledgeable about chemistry and about the computer programs.

58. Garrels, R.M., 1960, Mineral Equilibria: Harper and Bros., New York, 254 pp.

Garrels, R.M., and C.L. Christ, 1965, Solutions, minerals and equilibria: Freeman, Cooper and Co., San Francisco, 450 pp.

59. Pourbaix, M.J.N., 1949, Thermodynamics of dilute solutions: Edward Arnold & Co., London, 136 pp.

60. Helgesen, H.C., 1967, Thermodynamics of complex dissociation in aqueous solution at elevated temperatures: J. Phys. Chem., V. 71, N. 10, p. 3121-3136.

61. _____, 1969, Thermodynamics of hydrothermal systems at elevated temperatures and pressures: Amer. J. Sc., V. 267, p. 729-804.

62. _____, et al., 1976, Calculation of mass transfer in geochemical processes involving aqueous solutions: Geochim. et Cosmochim Acta, V. 34, p. 569-592.

63. _____, and D.H. Kirham, 1974, Theoretical prediction of the thermodynamic behavior of aqueous electrolytes: Amer. J. Sci. (Geology), V. 274, N. 10.

64. _____, and D.H. Kirham, 1976, Theoretical prediction of the thermodynamic behavior of aqueous electrolytes at high pressures and temperatures III. Equation of state for aqueous species at infinite dilution: Amer. J. Sci., V. 276.

65. Wolery, T.J., 1979, Calculations of equilibrium between solution and minerals - The Equation 3/6 Software Package: Lawrence Livermore Laboratory Rept. UCRL-52658.

66. Jenne, E.A., 1979, Chemical modeling in aqueous systems: Amer. Chem. Soc. Symposium Series No. 93, 914 pp.

67. Nordstrom, D.K., et al., Comparison of computerized chemical models for equilibrium calculations in aqueous systems: Amer. Chem. Soc. Symposium Series No. 93, 857-894.

68. Frear, G.L. and J. Johnston, 1929, The solubility of calcium carbonate (calcite) in certain aqueous solutions at 25°: Jour. Amer. Chem. Soc., V. 51, p. 2082-2093.

69. Stumm, W. and J.J. Morgan, 1970, Aquatic chemistry: John Wiley and Sons, p. 182.

70. Holland, H.D., 1978, The chemistry of the atmosphere and oceans: John Wiley and Sons, p. 18.

71. Vetter, O. and V. Kandarpa, 1980, Prediction of $CaCO_3$ scale under downhole conditions: Soc. Pet. Engr., Paper SPE 8991, Int'l. Symp. on Oilfield and Geothermal Chemistry, Stanford, May 28-30, 1980, p. 158.

72. Truesdell, A.H. and Singers, W., 1974, The calculation of aquifer chemistry in hot-water geothermal systems: Jour. Research, U.S. Geol. Survey, V. 2, N. 3, 271-278.

73. A PL-1 computer code, discussed in Ref. 72, is available from National Technical Information Service, U.S. Dept. of Commerce, 5285 Port Royal Road, Springfield, VA 22161, Document PB-219.

74. Palmer, R.A., 1977, Computer Storage, Processing and Display of Geothermal Data: Geothermics, V. 6, 31-37.

75. Palmer, R.A., 1976, GEODATA User's Guide and Program Description: N.Z. Dept. of Scientific and Ind. Research.

76. Weres, O., Yee, A. and Tsao, L., 1980, Kinetics of silica polymerization: Univ. of Calif., Lawrence Berkeley National Laboratory Rept. LBL-7033.

77. Fournier, R.O., 1980, Application of water geochemistry to geothermal exploration and reservoir engineering: In Geothermal Systems: Principles and Case Histories, Rybach and Muffler, ed., John Wiley and Sons, Ltd., 109-143.

78. Geochemical fundamentals for geothermal exploration and reservoir evaluation: Geothermal Resources Council, Technical Training Course No. 6 (1980).

79. Jackson, D.D., 1977, Computation of gas-liquid equilibria in high-salinity geothermal fluids:

80. Helgesen, H.C., 1967, Thermodynamics of complex dissociation in aqueous solutions and elevated temperatures: Jour. Phys. Chem., V. 71, N. 10, 3121-3136.

81. Miller, D.G., Piwinskii, A.J. and Yamanchi, R., 1977, Geochemical equilibrium codes: A means of modelling precipitation phenomena in the Salton Sea geothermal field: SPE 6604.

82. Wolery, T.J., 1980, Chemical modeling of geologic disposal of nuclear waste: Progress Report and a Perspective: Univ. of Calif., Lawrence Livermore National Laboratory Rept. UCRL-52748.

83. Lessor, D.L. and Kreid, D.K., 1980, Computer Simulation of Scale Formation: Proc., 4th Annual EPRI Geothermal Conf. and Workshop, EPRI Project RP653-3, 3-65 to 3-77.

84. Oddo, J.E. and Tomson, M.B., 1982, Simplified calculation of $CaCO_3$ saturation at high temperatures and pressures in brine solutions: Jour. Pet. Tech., 1583-1590.

85. Harvie, C.E. and Weare, J.H., 1980, The prediction of mineral solubilities in natural waters: The Na-K-Mg-Ca-Cl-SO_4-H_2O system from zero to high concentrations at 25°C: Geochim. Cosmochim. Acta, V. 44, 981-997.

86. Weare, J.H. and Moller, N., 1984, Progress Report on Geothermal Solution Modeling Program: Report Submitted to U.S. DOE/SAN.

87. Langelier, W.F., 1946, Chemical equilibrium in water: Jour. Amer. Water Works Assoc., V. 38, 169-178.

88. Stiff, H.A. and Davis, L.E., 1952, Method for predicting the tendency of oilfield waters to deposit calcium carbonate: Trans., AIME, V. 195, 213-216.

89. Hausler, R.H., 1978, Predicting and controlling scale from oilfield brines: The Oil and Gas Journal, Sept. 18, 146-154.

90. Patton, C.C., 1977, Oilfield water systems: Campbell Petroleum Series, Norman, Oklahoma.

Chapter IV

PROCESSING SPENT BRINE FOR REINJECTION

IV. PROCESSING SPENT BRINE FOR REINJECTION

IV-1. Chapter Summary

Subsurface disposal of spent brine effluents will, in most instances, be a necessary part of hydrothermal resource exploitation. Although a large body of technical literature and practical experience has been generated in conjunction with "conventional" oil-field and industrial operations, field geothermal requirements can be more stringent owing to chemical instability of injected fluids. Nonetheless, methods developed, primarily in the oil fields, for assessing injection requirements, specifying and operating injection systems and evaluating reasons for injection well failure and implementing injection well restoration procedures are well documented and compatible with geothermal operational requirements. Technology developed primarily for municipal water treatment facilities, especially reaction clarification and filtration methods are also applicable and amenable to geothermal operations.

In general, geothermal fluids must be stabilized prior to injection to eliminate possibilities of post-injection generation of precipitates or scale deposits. All treatment methods should be designed to provide a stable effluent for injection. Removal of suspended particulates may be insufficient if the injected fluids react with in-situ reservoir fluids or forms extraneous precipitates or solids due to delayed reactions resulting from slow precipitation of dissolved species such as iron or silica. Oxidation of iron-bearing fluids can be quite damaging as hydrated iron oxides are among the most damaging particulates.

This chapter considers methods for assessing the compatibility of injected effluents with injection formations as well as methods of treating effluents to render them compatible with the injection formation. Emphasis is

placed on describing methods for assessing fluid injectability. Descriptions of the most likely methods for treating effluents, their operational characteristics and methods of evaluating system performance are also provided.

IV-2. Introduction

Oil field injection practice has been summarized by Campbell, et al[1]. The petroleum industry has been injecting oil field brines in the subsurface for more than 45 years. It has been estimated that more than 45,000 brine injection wells were in operation within the continental United States in 1978[2]. Of these, over 20,000 wells were in Texas and Louisiana. The number of satisfactory and successful installations of high-volume deep-injection wells is growing at an increased rate. The popularity of underground injection and storage has increased substantially in the last few years as petroleum and industrial operations have become more complex and as state and federal agencies have imposed more stringent surface water quality requirements and regulatory criteria.

Conventional well injection systems, however, have their limitations. All areas of the United States are not suitable for injection well systems. Experience has shown that the subsurface geological conditions necessary for economically viable waste injection systems are zones of sufficient permeability and hydraulic capacity to readily accept the volume to be injected. Such geological conditions are found in about one-half of the land area of the United States, predominantly in the Central Plans states and the coastal areas of the Southeast. These injection systems are heavily concentrated in the northcentral and Gulf Coast areas of the United States.

In the entire Gulf Coast region of Texas and Louisiana, there is a minimum of 1000 feet of highly permeable sandstone intervals within the zone between 2000 and 6000 feet deep. Extensive exploratory drilling in this re-

gion has yielded sufficient subsurface information to permit adequate mapping of subsurface structure and general reservoir characteristics. Sufficient information is also available to establish, within reasonable limits, the anticipated drilling conditions. Thus, injection practice for Gulf Coast Geopressured-Geothermal applications is well developed especially if injection of spent fluids is planned for relatively shallow, normally pressured formations. The situation for more conventional hydrothermal resources characteristic of the western United States is less certain. Some of these resources may be characterized by reservoirs of high matrix permeability such as the Heber Known Geothermal Resource Area (KGRA) and the shallower portions of the East Mesa KGRA in Southern California's Imperial Valley. However, many of the high temperature hydrothermal reservoirs are either fracture dominated or are characterized by a combination of fracture and matrix permeability. Oil field injection experience with these types of reservoirs is less abundant given the effects of high in-situ temperatures and potential chemical instability of spent geothermal fluids.

It is nonetheless instructive to consider that high-volume subsurface injection has been frequently demonstrated in the oil fields. This is an important observation given that geothermal production rates for electric power production applications can be enormous, thereby imposing a critical demand on the availability of a high efficiency reinjection system. High-volume injection has been frequently demonstrated in the Gulf Coast region. There are several examples of individual well injection rates of 35,000 bbl/d or more[1]. Over 75 active injection wells in Louisiana have had injection rates of over 25,000 bbl/d since 1968.

Most high-rate injection systems have been properly designed and operated. Several high-volume injection wells have been failures as a result of poor

knowledge of the subsurface conditions, such as low sand/shale ratios and faulting of the selected injection intervals. Poor well design and construction are also indicated factors in subsequent well failures[3]. In addition, at least 25 percent of high rate wells have been plugged and abandoned because of improper or nonexistent surface treatment facilities. In general, it has seldom been possible to inject large volumes of untreated brine over an extended period. Thus, pretreatment such as surface filtration is universally accepted by the oil industry as one of the most important requirements to insure success of a brine injection program.

Injection well life is normally a function of the ability of the operator to backwash, acid treat, or perofrm other remedial operations to maintain or improve the injectability of the injection interval[4]. In almost all cases regarding brine injection in Texas and Louisiana, pretreatment of brine and backwashing operations are common practices. The formations in the area have the capability of accepting large quantities of brine. The principal operational objective is to maintain the permeability in and around the wellbore. Backwashing of the injection interval is periodically accomplished in all successful operations and is routinely initiated when wellhead pressures increase to a predetermined level. With backwashing performed in a proficient manner, individual injection zones have been known to accept high-volume fluids for more than 10 years.

Data from nearby wells in a region of interest are useful for anticipating drilling conditions and injection well design planning. Specific reservoir data are normally obtained from all prospective intervals before casing is set in the initial well drilled. In addition to logging, core samples are required to establish reservoir characteristics throughout the proposed injection zone or zones. The samples are normally analyzed for sand grain size,

permeability, porosity, and silt and clay contents. Formation fluid samples must also be taken for compatibility studies. Fluid samples are taken before any injection by backwashing or by producing the well to obtain a sufficient volume of uncontaminated formation water. Following an initial backwash operation, a static bottomhole pressure is generally measured with a pressure bomb in the hole after the final injection test. Based on these data, the initial flow capacity of the well is determined for evaluating future well performance. Potential injection reservoirs are selected from an evaluation of engineering and geological data obtained after the first test injection well of the field is drilled.

The deepest zone penetrated by the test well is usually selected as the initial injection zone. This procedure allows recompletion in the next shallower zone if performance of the deeper zone deteriorates because of formation damage or excessive injection pressures. The second well drilled might be completed in the next sand above the deepest zone initially completed, depending on the distance between wells and other factors. This procedure also allows for secondary completion zones, if required. Economic considerations must be made, however, because well cost depends directly on well depth.

The volume of fluid to be injected and the estimated injection pressure dictate the diameter of the tubing required. The tubing material should be corrosion resistant. In conventional oil field injection wells where high temperatures are not a consideration, the annular space between the tubing and the casing is filled with a noncorrosive fluid. Clean brine with a corrosion inhibitor additive is a commonly employed annular fluid. The use of a screen and/or liner and packer is the preferred completion practice in the Gulf Coast region because it provides minimum pressure and flow restriction to the fluid injection. The gravel pack design restricts formation sand from caving and

entering the well during remedial back-flushing operations. The use of a packer allows positive pressure control and keeps injection pressure away from the casing. The annular pressure is not constant since the injection tubing is subject to expansion and contraction, and temperature and pressure change. It is generally desirable to maintain annular pressure at a fixed differential above injection pressure (100 psi, for example). The physical condition of the tubing is of critical importance in all successful injection programs involving corrosive fluids.

Proper selection of drilling mud is extremely important to minimize hole washout and formation damage[5]. The mud should have sufficient water loss to maximize hole support but should not excessively invade and damage a potential injection formation.

A factor that must be considered in detail during the early stages of a brine injection program is the quality of the brine to be injected. Solids content, chemical stability, temperature and pressure conditions, and corrosion and scaling potential must be established to determine the relative compatibility between the formation fluid and the brine to be injected and between the brine and the well equipment with which the brine will be in contact. Injection fluid compatability with the indigenous formation fluid is mandatory to avoid subsequent formation plugging[6]. Casing and cementing programs must be designed to meet corrosion protection requirements. Corrosion protection is normally planned and designed to protect both surface and downhole equipment[4].

A surface filtration system is required when fluid injection is anticipated in a porous medium reservoir. In a fractured reservoir, however, filtration may not be required. The function of a filter system is to trap solids. Hence, periodic backwashing of the surface filter system removes the

trapped solids before such solids can enter the injection well and seriously reduce injection capacity. It should be emphasized that backwashing of the surface filter system, or even replacing it, is economically preferable to backwashing the formation. A surface filter is easier to clean than a plugged injection interval thousands of feet below the surface. The formation is the final filtration system, and its functional longevity depends directly on the extent to which solids have been removed at the surface via filtration systems.

In considering surface filtration system requirements, two major features are examined: 1) the maximum particle dimensions the injection formation will accept, and 2) the maximum total-solids content that the surface filtration system is capable of removing economically. The design of the surface filtration system is also affected by the following factors:

1. physical characteristics of the solids contained in the brine both before and after surface filtration;
2. density of the solids in the brine;
3. chemical characteristics of the brine (e.g., pH, salinity, dissolved species, etc.);
4. volume of fluid to be injected; and
5. filtration temperature.

Surface facilities are designed so a nonplugging, compatible fluid is injected into the target formation or sections thereof. The following subsystem design features are normally incorporated in brine injection systems:

1. closed system with oxygen scavengers (to remove O_2 from the brine and control corrosion of piping and tubing);
2. gas separation (to prevent two-phase segregation in the injected formation);
3. chemical treatment (to reduce incompatibility between formation brine and matrix and the brine to be injected);

4. filtration to reduce solids content of brine to be injected;

5. chemical treatment (to improve brine filtration characteristics); and

6. equipment utilizing corrosion resistant materials (to increase wll systems longevity and maintain formation injectability).

Brine quality, injection pressure, temperature, corrosion inhibitors, and injection volumes must be rigorously monitored in both surface and downhole systems. It should be reemphasized that the formation is the final filtration system, and its longevity and utility in addition to the longevity and utility of the injection well equipment are solely dependent on the characteristics of the fluids to be injected and the solids they contain. Surface systems designed to reduce solids content are periodically backwashed while subsurface systems, which include the screened or perforated intervals of the well structure are backwashed or acidized only as a final attempt to improve injectability and to prolong the functional life of the system. The most economically feasible surface filtration systems will pass certain quantities of solids with time, resulting in plugging that cannot be removed via backwashing or acidizing.

In general, the capacities of injection wells deteriorate with time. This is usually the result of plugging in the formation with mineral precipitates, solids and with other materials carried in the water after surface filtration systems have either failed, or have been improperly maintained or have been bypassed during downtime of filtration systems.

Scale deposits in the tubing have been shown to increase the friction and reduce the capacity of injection well systems. Case histories report that scale deposits have been found in certain parts of wells exposed to brine, i.e., on tubing interior, on screens, and on the face or within the injection formation. This can be a result of the commingling of two or more brines of different chemical compositions or as a result of changes in temperature or

pressure or both. Some of these deposits are calcium carbonate, introduced or precipitated iron oxide, iron sulfide, silica, barium sulfate, strontium sulfate, calcium sulfate, and various other forms, some of which are precipitated as a result of bacterial activity (e.g., iron oxidizing and sulfate-reducing species).

Comprehensive and accurate records and appropriate supervision, such as maintaining accurate injection rate and pressure information is normally practiced to monitor formation response characteristics. For example, when injection pressure rises to a predetermined level, immediate action should be taken. Remedial expense can be minimized by backwashing or acidizing before serious formation plugging has occurred. Thus, expensive workover operations can be generally eliminated. The potential for scaling can be estimated by previously conducted compatibility tests. Once the relative potential is established, a remedial program can be designed and implemented if required. This predetermines the probable method for treating the well and often eliminates trial-and-error remedial methods. Without sound baseline data on original physio-chemical conditions of the brine to be injected and of the environment into which the brine is to be injected, remdial programs must of necessity be based on time consuming and costly trial-and-error methods.

Formation backwashing is the normal response to declining injectability. Nitrogen or compressed air lift to create high-velocity backwashing is in common use. If the interval is relatively shallow and if the casing is of sufficient diameter, submergible pumps can be employed to achieve cleaning. Excellent results have been achieved by backwashing with compressed air. The effectiveness of such workovers, however, cannot be established as long as brine with high solids content is injected after a workover has been completed.

A common chemical workover technique is the injection and backwashing of hydrofluoric or hydrochloric acids in an attempt to improve well injectability. This technique assumes that the deposits are acid-soluble and are treated in the early stages of formation plugging. Hydrofluoric or mud acid will dissolve clay and mud around the injection well. Special additives can be used with the acid to prevent the dissolved material from precipitating and being redeposited in the formation. Sulfates of barium, strontium, calcium, and iron are generally insoluble in acid and must be removed mechanically. Therefore, it is necessary to ensure that such mineralization does not occur within the well structure or formation.

The recommended types and sizes of acid treatment methods vary in different areas and geological conditions. Experience and local conditions determine the remedial procedures best suited for a particular well.

Where the formation or gravel pack face is severely plugged, treating with acid through a jet tool is normally more beneficial than with conventional and acid backwashing techniques. The entire length of the zone is treated with acid, and the position of the jets is adjusted from the bottom to the top of the injection interval[7]. This procedure is advantageous in cased hole completions where scale or deposits may form in the screen or perforations and cannot be reached by other mechanical means.

Acid is normally pumped with a pump pressure of 1000 psi or more if conditions warrant. Normal acid concentrations of 15 percent are used for jetting purposes. Sometimes it is more advantageous to use large volume treatments. The concentration may be reduced and the volume increased for approximately the same treating cost as a smaller more concentrated treatment. This procedure is often more successful than high concentration applications.

Acidizing may be ineffective in improving the injectability of a well because of the insoluble characteristics of the plugging materials. Overpres-

suring may be more effective in certain wells. This procedure can create partings in the porous medium. These partings allow new zones of higher permeability to be developed through plugged intervals into zones of the formation where plugging has not occurred or is minimal. Furthermore, the procedure may force the solids farther away from the wellbore relieving some of the restriction.

Brine is generally used as the overpressuring fluid. Other fluids may not be compatible with the brine to be injected and may cause deposits to form when the two are mixed. Best results have been obtained when using large volume treatments and high injection rates.

Corrosion inhibitors are used in many injection wells to protect equipment and to prevent the formation of corrosion products that could plug the injection formation and surface and downhole pipe. The inhibitor is often injected continuously into the well by means of a chemical pump or periodically into the surface filtration systems, water line, or injection well. Work is still underway by industry to determine the effects of corrosion inhibitors in treating injection wells. It is apparent at this time that some advantage may be obtained from the sequestering and surface-tension reducing characteristics inherent in certain chemicals under development.

From the preceeding discussion it might be concluded that planning and execution of injection programs in modern oil-field operations is a well developed art and this is certainly the case. However, a cursory review of the literature reveals that as recently as 1963 insufficient attention was paid to proper design of oil field injection operations with resulting significant injection well impairment[8]. The stringent requirements for development of an adequate treatment system for processing of sea-water as an injection fluid in an offshore pressure maintenance project is illustrated in Figure

IV-1. The various elements of this system include primary and secondary filtration units, a biocide treatment unit and a corrosion inhibitor injection unit. The steps that must be completed to permit design of a system of the type illustrated in Figure IV-1 are the subject of the remainder of this chapter. Emphasis will be placed on those aspects of injection technology most pertinent to hydrothermal operations.

IV-3. Geothermal Injection Experience - A Review

In 1982, five hydrothermal resources were in production in Japan[9]. Spent fluid from all of the resources was injected. The Japanese geothermal production represents more than half of the liquid-dominated operating resources in the world. At four of the five resources, fracture-dominated reservoirs caused rapid breakthrough of cool injected waters to production wells resulting in a detrimental impact on production water enthalpy. Aside from providing a convenient means for the disposal of large volumes of waters not compatible with surface disposal methods, water reinjection provides the potential for maintenance of reservoir pressure and recovery of additional heat stored in the reservoir formations. Horne[9] has summarized the Japanese geothermal injection experience as follows:

1. Breakthrough of cool injected fluids to production wells, separated by distances of hundreds of meters, has been observed to occur within a few hours to a few days at Wairaikei (New Zealand), Ahuachapan (El Salvador), and Kakkonda and Hatchobaru (Japan).

2. Reinjection wells and production wells should be sufficiently far apart to preclude premature thermal breakthrough.

3. Vertical separation of production and reinjection wells does not preclude premature thermal breakthrough.

4. Limiting thermal breakthrough should take precedence over pressure maintenance programs.

5. Sufficient exploratory drilling, geologic and geophysical work and preliminary well testing should occur to define the subsurface flow

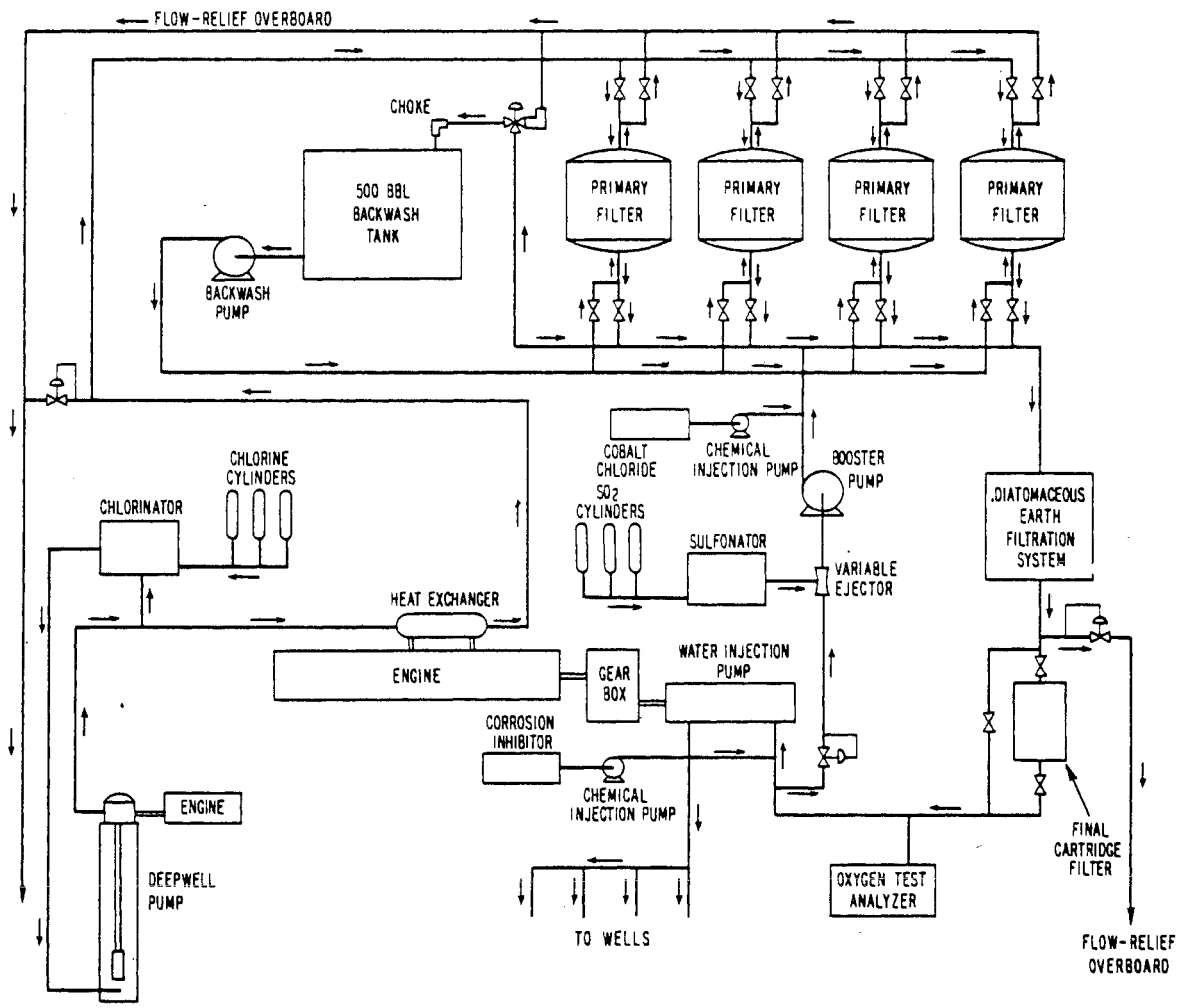

Figure IV-1. Injection unit schematic diagram.

paths in fracture dominated reservoirs before committing to the construction of an operational injection system.

Although thermal breakthrough problems are a major concern in injection operations at Japanese geothermal resources, impairment of injection wells due to scale deposition has also been experienced. The Hatchobaru facility includes a double-stage flash system that produces relatively low temperature effluents for reinjection. Injectivity declines have been experienced due to silica deposition. Similar problems have been experienced at Otabe. The Otabe fluids contain arsenic which necessitates reinjection. Injectivity loss due to silica deposition will require wastewater treatment facilities to remove excess silica. Work on development of effective arsenic removal methods in this instance would eliminate the environmental motivation for subsurface disposal. Thus, at Otabe, pressure maintenance has been subjugated by the economic realities associated with wastewater treatment needed to prevent loss-of-injectivity due to mineral deposition. The foreign geothermal injection experience is summarized in Refs. 10-26.

The high temperature hypersaline liquid-dominated resources of the Imperial Valley of southern California are extremely important since they represent the greatest electric power production potential of any U.S. hydrothermal resource. Injection of spent hypersaline brine has proven to be difficult. Messer, et al.[27] described the successful use of a mixed acid treatment program that restored injectivity impairment caused by deposition of silica. Jorda[28] described injectivity impairment of a hypersaline brine injection well located in the Salton Sea KGRA, southern California. This well was ultimately abandoned by the operator, Imperial Magma Power Co. Operation of low salinity injection wells at the Raft River KGRA has also been problematic. But, in this case, difficulty was due to reservoir constraints[29]. Shallow injection

wells at Raft River apparently are in hydraulic communication with overlying aquifers that are tapped locally as a source of agricultural water. Injection into these wells results in contamination of the overlying aquifers. Deeper injection wells tap a reservoir of apparently limited volume. Estimates suggest that brine injection, at a rate of 2500 gpm, into the deeper reservoir might only be possible for two to four months before reservoir pressure would build up and exceed the fracturing gradient.

General geothermal injection practice in the past has been somewhat lax with regard to insuring trouble-free operation. Most experience in the United States with subsurface injection has taken place in conjunction with resource evaluation operations. Comprehensive treatment of spent geothermal fluids, consistent with oil-field methods, has seldom been practiced. Usually, operators have been willing to sacrifice injection well performance as an expedient in defining resource productivity. Enough information is available, however, to suggest that long-term injection of untreated spent brine will not be possible.

IV-4. Evaluation of Geothermal Reinjection

The design and construction of a successful geothermal injection system while straightforward, requires input from a number of technical disciplines. The various factors that should be included in a reinjection program are:

1. Reservoir Engineering Assessment
2. Reservoir Geology and Structure Assessment
3. Well Design
4. Well Completion
5. Comprehensive Records
6. Well Testing Program
7. Characterization of Reinjected Fluid Quality
8. Pre-Injection Fluid Processing Requirements
9. Monitoring Activities
10. Workover Plans
11. Economic Factors

IV-5. Reservoir Factors

Reinjection wells will ultimately show declines in injectivity. Implementation of an injection program along the lines outlined above are useful in determining the impairment and identifying remedial actions. From the preceeding discussion, major sources of injectivity difficulty in geothermal operations are premature mass breakthrough of cool injected waters to production wells and injectivity impairment due to particulate and scale deposition. Avoidance of the former type of difficulty requires that careful attention be paid to injection well placement. Avoidance of the latter source of difficulty is not possible without a comprehensive review of water quality factors and implementation of the necessary remedial processing to upgrade water quality to an arbitrarily defined standard. The term arbitrary is not used in a derogatory sense. Each operator will have to consider project requirements that represent the best trade-off between useful injection well performance life between planned workovers and economic factors. The required water quality and pre-injection processing necessary to achieve that water quality can then be specified.

IV-6. Well Placement

A cursory review of the technical literature suggests that there is no way to predict with 100 percent reliability, the migration behavior of injected fluids after reinjection. A number of sophisticated codes are available for calculating mass and thermal breakthrough times. However, the codes cannot consider short circuiting unless reservoir, geologic, structural and hydraulic data are available to indicate the probability of rapid migration of injected fluids to production wells. In new field development projects, placement of initial injection wells and analysis of test data is one way to influence placement of subsequent wells. But, the operator runs the risk of

losing the utility of the initial injection wells. In general, one would like to provide the greatest possible lateral spacing between production and injection wells consistent with leaseholdings and costs associated with construction of the surface facilities. Thus, input from reservoir engineers and careful consideration of reservoir geology and structural data, obtained from an analysis of well cutting, core samples, and surface expressions and familiarity with subsurface operations in nearby areas are important factors to consider before committing to a production-injection well placement plan.

A simplified method for estimating mass breakthrough of injected fluids is given by Jorda[28] using the following expression:

$$r_e = \frac{22{,}300 \times q \times t}{\phi \times S_w \times h}^{\frac{1}{2}} \qquad \text{(IV-1)}$$

where q = injection rate - gallons per minute
t = time - years
ϕ = fractional porosity of the injection formation
S_w = fractional water saturation index
h = net thickness of the injection interval - feet
r_e = radius of injected fluid front at any time - feet

Equation IV-1 assumes infinite permeability and cylindrical symmetry with no permeability anisotropy due to the presence of natural fractures. Use of this expression is only justified as a simple approximation for a layered matrix-type reservoir. The effect of permeability on fluid front migration velocity[30] is of the form:

$$r_e = \frac{0.029\sqrt{kt}}{\phi\mu\, C_t} \qquad \text{(IV-2)}$$

where: k = formation permeability - md
t = time - hours
ϕ = fractional porosity
μ = viscosity - cp
C_t = system total compressibility - psi^{-1}

In a fractured reservoir, injected fluid fronts can migrate at relatively high velocities. References 30-34 should be consulted for information concerning the analysis of reservoir engineering data. Review of technical papers published in the Journal of Petroleum Technology and the Society of Petroleum Engineers Journal (both published by the Society of Petroleum Engineers, Dallas, Texas) are useful sources of additional information on the evaluation of reservoir engineering data. Proceedings and technical papers published by the Stanford University Geothermal Program, and the Lawrence Berkeley National Laboratory Geothermal Program in the general discipline of geothermal reservoir engineering should also be consulted.

It is instructive to consider how injected fluid front migration is influenced by the thickness of an injection interval. If we assume infinite permeability (Equation IV-1), 30 percent formation porosity, 100 percent water saturation, a 20 year injection interval, and an injection rate of 40,000 bpd (barrels per day), the radius of an injected water pressure front is as shown in Figure IV-2. Increasing the injection formation thickness by 100 percent results in a decrease in the radius of injection of about 30 percent. Thus, providing as great an injection interval as possible, by completing the injection well over as large an interval as possible, is one effective method of diminishing chances for premature fluid breakthrough to production wells. It should also be evident that even qualitative estimates of reservoir performance based on the use of sophisticated computer codes are critically dependent upon knowledge of the areal distribution of intrinsic formation properties such as permeability and porosity. Formation properties are usually developed from analysis of core samples, well logs and well test data. Another obvious control on injection radius is the rate of injection. Prudence would suggest that projects include additional injection capacity as a contingency in the event of loss-of-injectivity or outright failure of one or more injection wells.

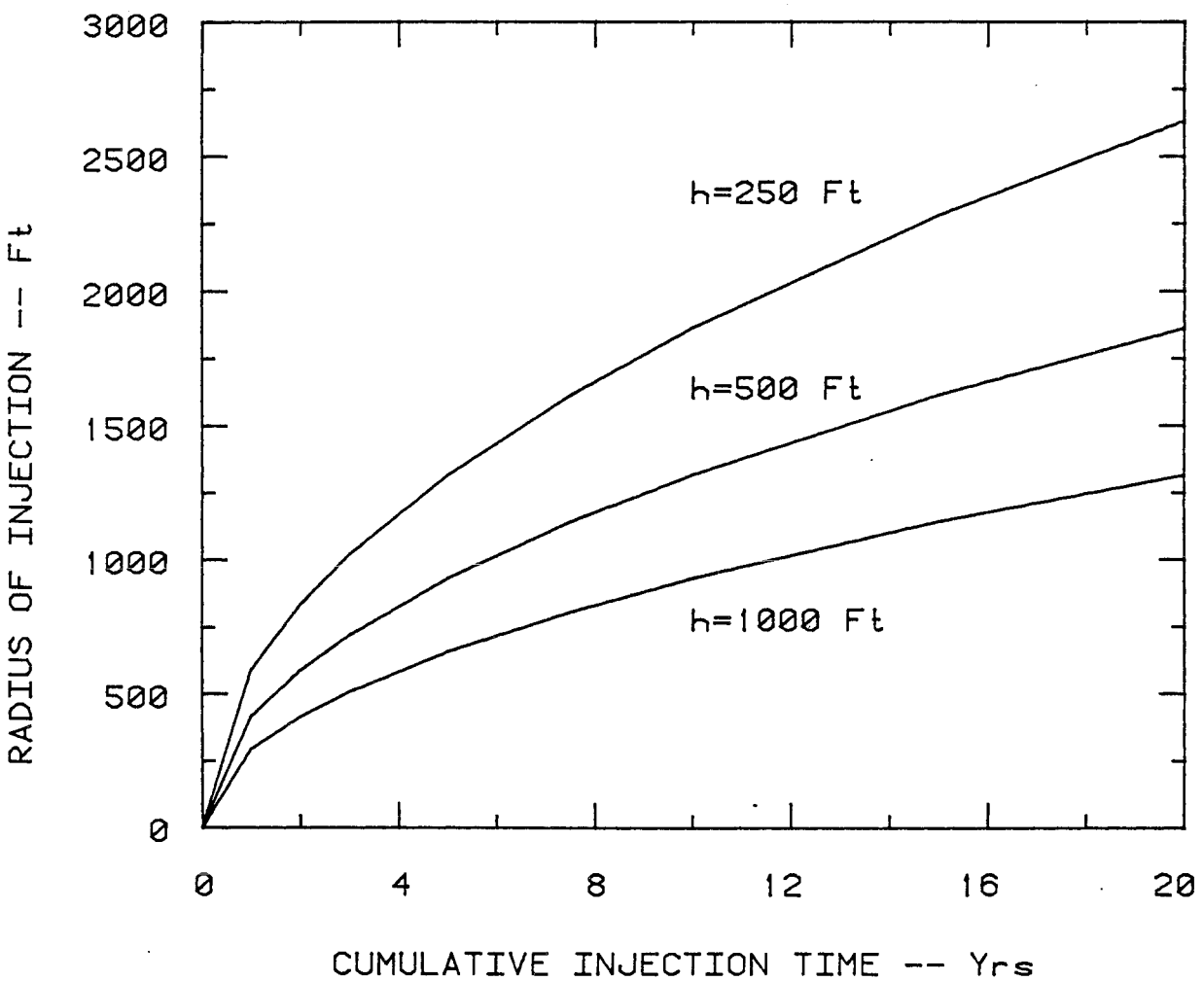

Figure IV-2. Influence of injection interval thickness on the radius of the injection pressure front.

IV-7. Estimating Bottomhole Injection Temperature

Knowledge of the time-dependent variation of bottomhole injection temperature is important for several reasons. Accurate predictions of reservoir performance requires that fluid viscosity and its time-dependence are known. Downhole precipitation and scaling phenomena are also critically dependent upon time-dependent changes in injected fluid temperature. Estimating the extent of damage zones or skin about a wellbore requires some insight into the nature of the damage mechanisms and means of evaluating the probable extent of damage. Since scaling and precipitation may be examples of coupled time-temperature dependent phenomena, it would be helpful to be able to estimate the most probable damage radius about an injection well.

The various factors which must be considered in estimating bottomhole injection temperature are summarized in Figure IV-3. First, as fluid with a surface temperature (τ_0) is injected, heat loss via conduction will occur through the wellbore. Thus, a small time lag will exist, depending primarily upon the depth of the well and the injection rate, before the bottomhole temperature of the injected fluid (T_B) reaches a steady-state equilibrium temperature. The time lag is on the order of a few days. As fluid with a temperature T_B flows into the reservoir, additional heat loss (or gain) occurs from the injected fluid to the reservoir and from the reservoir to the overlying and underlying formations. The injected fluid can either heat up or cool off depending on whether the injection formation is at a higher or lower temperature than the injected fluid. If reinjection occurs back into the geothermal reservoir which is the usual practice, the injected fluids will be at a lower temperature than the reservoir fluids and would tend to cool a reservoir zone adjacent to the injection well. In geopressure-geothermal applications, most reinjection will probably occur into shallower, cooler

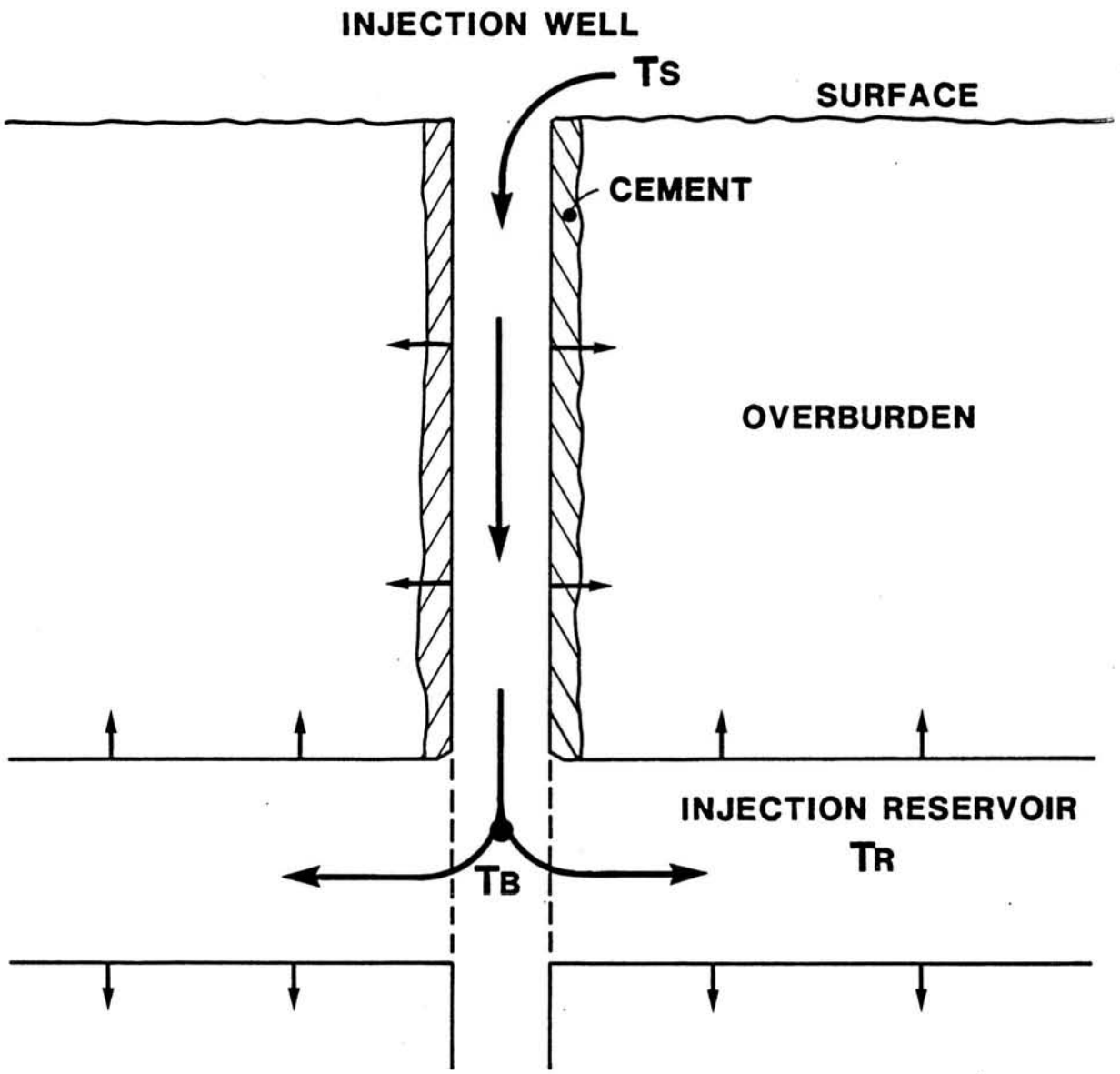

Figure IV-3. Sources of heat loss and gain in a typical geothermal injection system.

horizons as a cost saving step. In these cases, the injection formation adjacent to the injection well will be heated by the injected fluids. Deep reinjection of geopressured-geothermal fluids might, at some point, also be practiced as a means of prolonging reservoir productivity[35].

Estimating Bottomhole Temperature

The most direct approach to estimation of bottomhole temperature is by direct measurement using an appropriate temperature logging tool. The temperature tool need not be an elaborate device. Well operators could either purchase a commercial tool or build their own using off-the-shelf items. Unfortunately, it might not be possible or desirable to leave instrumentation in the injection wellbore on a continuous basis and it could, under certain circumstances, be inconvenient for well operators to run their own temperature surveys. Thus, estimation procedures that utilize measured temperature values for reinjected fluids at wellhead conditions to compute bottomhole temperature are of obvious interest.

Temperature transients in a flowing injection well due primarily to conductive heat losses to the cement and formations penetrated by the well have been modeled by Hanson[36]. Figure IV-4 illustrates the nature of temperature transients in an injection well as a function of injection rate. These results indicate the general time dependence of thermal perturbations. At high injection rates, cooling to the wellhead temperature occurs rapdily, within a few days of the start of injection. At lower injection rates, lesser degrees of cooling occur but quasi-steady state conditions are still rapidly attained.

Kasameyer[37] presented analytical solutions for radial flow temperature perturbations assuming that:

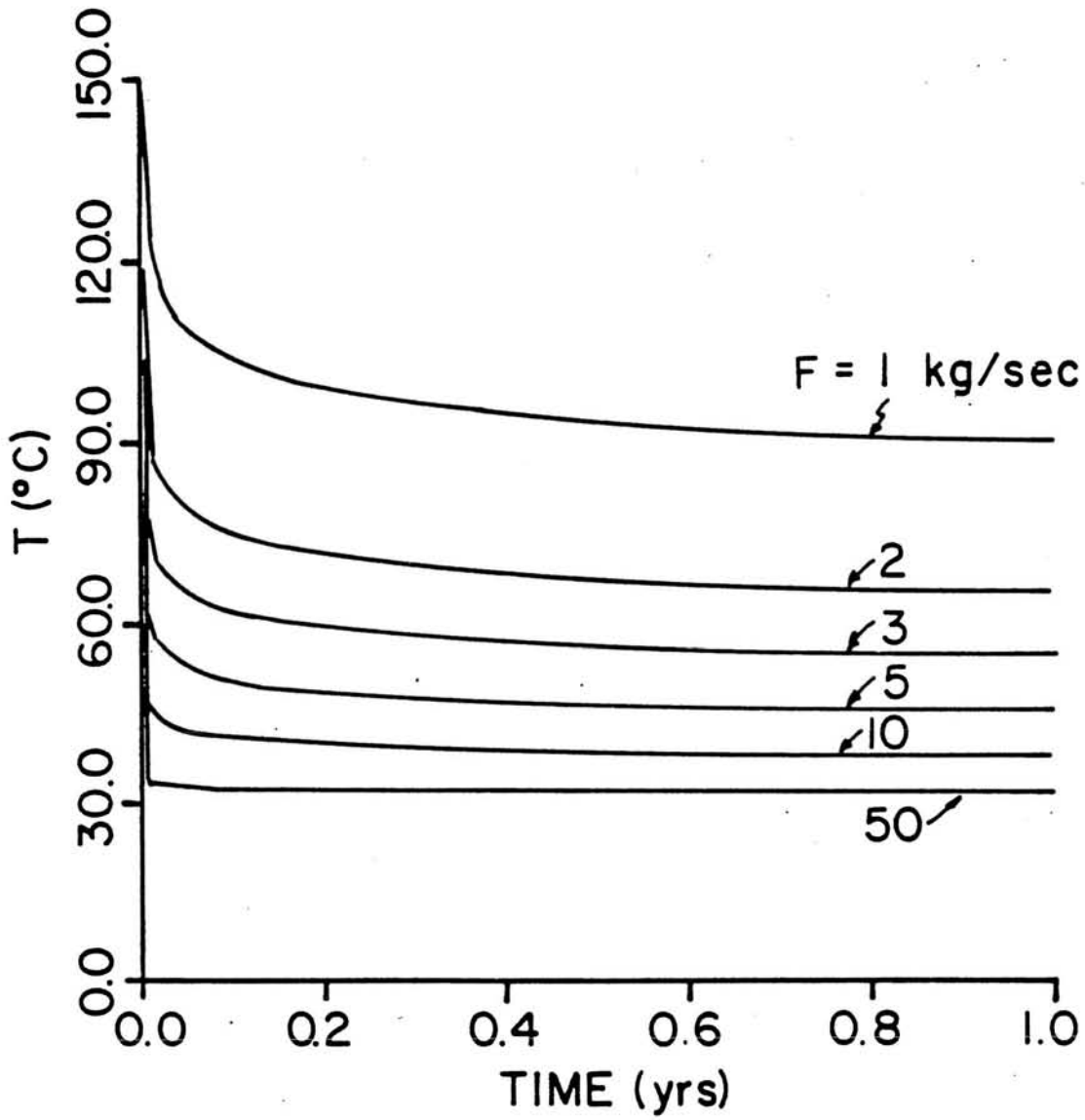

Figure IV-4. Temperature transients in an injection well for various constant injection rates F at the casing formation interface. In this example, the temperature of the injected fluid at the wellhead was 30°C and the rock formation temperature was 150°C.

1. The fluid is injected at a constant volumetric flow rate Q into a layer of uniform permeability (k) of height H from a line source perforated through its entire length. Gravity is ignored so that the flow is radial.

2. The fluid moves away from the source without mixing. The flow from any time interval displaces the shell of fluid from previous intervals outward away from the source. Consequently, the flow rate through a small area A (normal to the flow) at a distance r from a well is $QA/2\pi rh$, and the flow rate per unit area decreases as $1/r$.

3. The fluid is assumed to flow in small pores in the rock matrix and to reach thermal equilibrium with the rock matrix in a negligible time. Consequently, only the thermal properties of saturated rock need be considered. The saturated rock is initially at temperature T_q, and the fluid is injected at temperature T_0.

4. The compressibility and thermal expansion of the rock and fluid are ignored.

Use of this model allows one to calculate the distance from the injection interval to temperature and injected fluid particle fronts. An example calculation is illustrated in Figure IV-5. The calculation illustrated in Figure IV-5 was based on reservoir and injection parameters tabulated in Table IV-1. The significance of the temperature front is illustrated in Figure IV-6.

The model calculations indicate that relatively cool injected fluid when reinjected into a hot porous resevoir will not be reheated immediately, but will remain cool for approximately one-fourth of the time that the well has been used for injection. For the case of injection wells that have been in operation on a continuous basis for an extended period of time, reinjected fluids will remain cool for many years. The converse situation will also pertain for the case where spent geothermal fluid is injected into shallower,

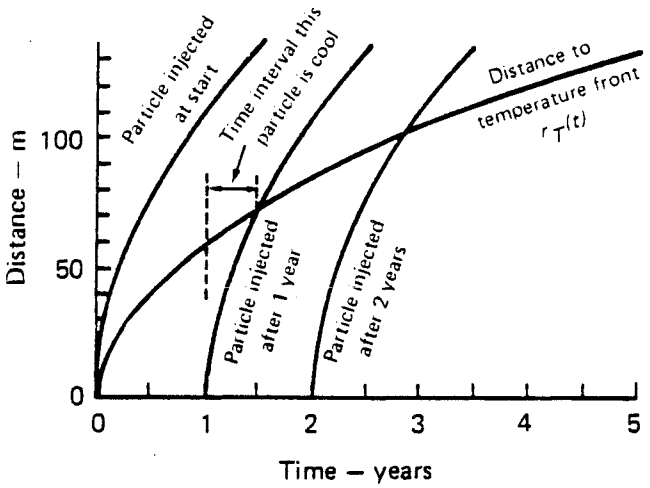

Figure IV-5. Location of temperature front and fluid particles injected at different times. (From Ref. 37)

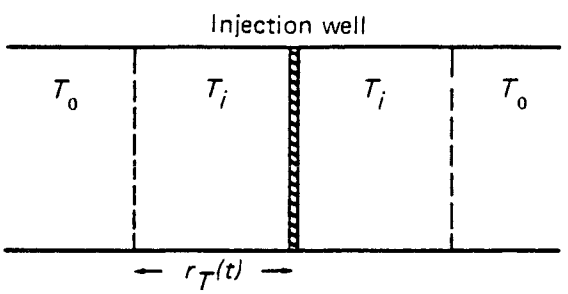

Figure IV-6. Cross section of permeable layer, showing temperature front at distance $r_T(t)$ from injection well. (From Ref. 37)

Table IV-1

Reservoir and Injection Parameters Used to Evaluate
The Thermal Model Illustrated in Figure IV-5

Parameter	Old Units	S.I. Units
Flow Rate Q	400,000 lb/hr at 62.4 lb/ft^3	0.0504 m^3/sec
Permeability k	500 millidarcys	5 x 10^{-13} m^2
Thickness h	660 ft	200 m
Conductivity K_s	0.58 Btu/hr-ft^2-°F	3.29 W/m-K
Heat Capacity C_R	0.256 Btu/lb-°F	1070 J/kg-K
Heat Capacity C_F	1.0 BTu/lb-°F	4180 J/kg-K
Viscosity μ	0.2 cP	2 x 10^{-4} Pa-sec
Density ρ_f	62.4 lb/ft^3	1000 kg/m^3
Porosity ϕ	0.20	0.20
Density ρ_R	144 lb/ft^3	2300 kg/m^3

cooler formations as is the usual case for disposal of spent geopressured-geothermal brines.

A Useful Computer Code

A practical and relatively simple analytical method for predicting injection formation temperature and heating or cooling rates was described by Hanson and Kasameyer[38]. It was demonstrated that the length of time required for an injected fluid element to heat to a given temperature is independent of the streamline path taken by the injected fluid element. This statement is valid for both the case where there is no conductive transport from the rock mass bounding the aquifer and for the case where there is conductive transport in the direction perpendicular to the aquifer.

Derivation

Consider a homogeneous and isotropic aquifer of thickness h and porosity ϕ in the (x,y) plane (Figure IV-7). A fully penetrating well intersects the aquifer at Σ_o, where Σ_o is a point in the (x,y) plane. Let Γ be a line corre-

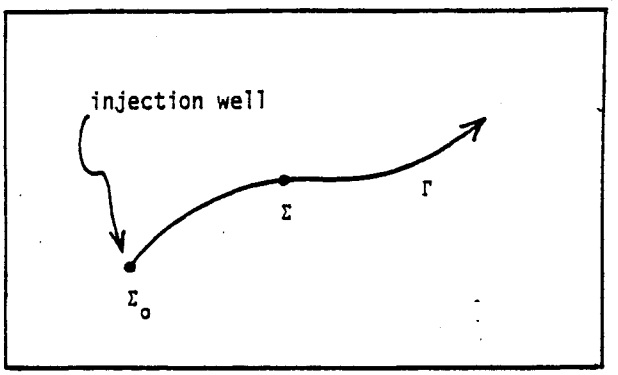

Figure IV-7. Streamline path of an injected fluid element.

sponding to an arbitrary flow streamline and Σ be an arbitrary point on the streamline.

The heat transfer equation for an arbitrary position in the (x,y) plane is given by:

$$\phi\rho_f\sigma_f\delta h\partial_t T_f + h\phi\sigma_f\rho_f v\nabla_2 T_f = 2\, k_r \partial_z T_r \Big|_{Z\downarrow o} \qquad \text{(IV-3)}$$

where: $\delta = 1 + \dfrac{\rho_r\sigma_r(1 - \phi)}{\rho_f\sigma_f\phi}$

The left hand side of Equation IV-3 represents the change in temperature of the wet rock (1st term) and the convective transport along the streamline (2nd term) and the right hand side is the conductive transport from the rock bounding the aquifer. It is assumed that the interstitial fluid temperature T_f in the aquifer is equal to the aquifer rock matrix temperature and that the aquifer temperature is a function only of (x,y) (i.e., isothermal in the z coordinate). T_r (x,y,z,t) is the temperature of the rock bounding the aquifer and is assumed to be governed by the 1-D diffusion equation:

$$\frac{1}{a_r}\partial_t T_r - \partial_{zz} T_r = o \qquad \text{(IV-4)}$$

Laplace transforming (IV-4) with respect to t:

$$T_r\ (X,\ Y,\ Z,\ S) = A(X,\ Y,\ S)\ e^{-\frac{S}{a_r} Z} + \frac{T_o}{S} \qquad \text{(IV-5)}$$

where s is the transform variable corresponding to t and the "^" denotes the Laplace transformation. Inserting (IV-5) into the Laplace transform of (IV-3) and assuming the <u>fluid velocity is stationary in time</u>:

$$K(S)\ A\ (X,\ Y,\ S) + v \cdot \nabla_2\ A\ (X,\ Y,\ S) = 0 \qquad \text{(IV-6)}$$

where $$K(S) = S\delta + \frac{2\ k_r}{h\ \phi \rho_f \sigma_f}\ \ \frac{S}{a_r}$$

Equation IV-6 is valid if one considers only points along the streamline $[(x,y) = \Sigma_1]$. Upon this restriction, (IV-6) can be written as:

$$K(S)\ A(\Sigma_1,\ S) + v(\Sigma_1)\ \frac{\partial A(\Sigma_1 S)}{\partial \Sigma_1} = 0 \qquad \text{(IV-7)}$$

where $\partial/\partial\Sigma$ is the differential operator along the streamline. Now

$$d\Sigma = v(\Sigma)\ dt_p(\Sigma_1)$$

where $dt_p(\Sigma_1)$ is the infintestimal time span for the fluid particle to go from Σ_1 to $\Sigma+d\Sigma$ on the streamline. Therefore Equation IV-7 can be written as:

$$K(S)\ A(\Sigma_1 S)\ \frac{dt_p(\Sigma_1)}{d\Sigma_1} + \frac{\partial A(\Sigma_1,\ S)}{\partial \Sigma_1} = 0$$

or

$$K(S)\ dt_p(\Sigma_1) + \frac{dA(\Sigma_1,\ S)}{A\ (\Sigma_1,\ S)} = 0$$

Integrating the above expression from Σ_{10} to an arbitrary point Σ_1 along the streamline, it can be shown that:

$$A(\Sigma_1, S) = A(\Sigma_{10}, S)\, e^{K(S)\,[t_p(\Sigma) - t_p(\Sigma_0)]} \qquad \text{(IV-8)}$$

Inserting (IV-8) into (IV-5), the Laplace transform of the fluid temperature along the streamline is obtained:

$$T_f(\Sigma_1, S) = \frac{(T_i - T_o)}{S}\, e^{-K(S)\, t_p(\Sigma_1)} + \frac{T_o}{S} \qquad \text{(IV-9)}$$

The following initial and boundary conditions have been used:

1. $T_r(0, 0, S) = T_i$
2. $t_p(\Sigma_{10}) = 0$
3. $T_r(\Sigma_1, 0, S) = T_f(\Sigma_1, S)$

The inverse Laplace transform of Equation IV-9 yields:

$$T_f(\Sigma, t) = (T_i - T_o)\, \text{erfc}\, \frac{k_r t_p(\Sigma)}{h\phi\rho_f\sigma_f \sqrt{a_r \tau}}\, U(\tau) + T_o \qquad \text{(IV-10)}$$

where

$$\tau = t - t_p(\Sigma_1)\delta$$

and

$$U(\tau) = \begin{matrix} 0, & \tau < 0 \\ 1, & \tau < 0 \end{matrix}$$

Equation (IV-10) is a generalization for an arbitrary streamline. Defining $R(\Sigma, t) = T_o - T_f(\Sigma,t)/T_o - T_i$, (IV-10) can be rewritten as:

$$R(\Sigma_1,t) = \text{erfc}\, \frac{k_r t_p(\Sigma)}{h\phi\rho_f\sigma_f \sqrt{a_r \tau}}\, U(\tau) \qquad \text{(IV-11)}$$

It should be emphasized that t is the time after initiation of flow in the system and $t_p(\Sigma)$ is the length of time <u>after injection</u> that it takes a parti-

cle to reach the position Σ on the streamline. Therefore, the particle was injected at time $t_{inj} = t - t_p(\Sigma)$. In terms of t_{inj}, Equation IV-11 can be written:

$$R(\Sigma_1, t_{inj}) = \text{erfc} \frac{k_r \alpha t_p(\Sigma_1)}{h\phi\rho_f\sigma_f\alpha \sqrt{a_r \tau^*}} U(\tau^*) \qquad \text{(IV-12)}$$

$$t^* = t_{inj} - \alpha t_p(\Sigma_1)$$

where $\alpha = (\delta - 1)$ is a new reservoir parameter. Equation IV-12 may be recast in dimensionless format to define the characteristic time T as:

$$T = \frac{\alpha^2\sigma_f{}^2\rho_f{}^2h^2d\phi^2a_r}{k_r{}^2} = \frac{\rho_r{}^2\sigma_r{}^2}{k_r{}^2}(1-\phi)^2 h^2 a_r)$$

and define the dimensionless times

$$t_p(\Sigma) = \frac{\alpha t_p(\Sigma)}{T}$$

$$t_{inj} = \frac{t_{inj}}{T} \qquad \text{(IV-13)}$$

Therefore,

$$R(\Sigma, t_{inj}) = \text{erfc} \frac{t_p(\Sigma)}{\sqrt{t_{inj} - t_p(\Sigma)}} U[t_{inj} - t_p(\Sigma)] \qquad \text{(IV-14)}$$

The time it takes an injected particle to heat up the initial formation temperature (R=0) is shown by (IV-14) to be

$$t_p(\Sigma) = \frac{t_{inj}}{\alpha} = \frac{\sigma_f\rho_f\phi}{\sigma_r\rho_r(1-\phi)} t_{inj}$$

This is precisely the result obtained by Kasameyer[37] for the case of no conductive transport from the rock bounding the aquifer (i.e. piston-like thermal front with no trailing transition zone). For the case in which 1-D conduction

is included, the transition zone behind the front is clearly shown by expression IV-14 by the existence of the complimentary error function.

Consider a particle injected at dimensionless time t_{inj} and that the following question is posed: What is the (dimensionless) time t_p required for the particle to reach an isotherm at Σ defined by $R(\Sigma, t_{inj}) = R_0 = \text{const.}>0$? The solution is easily computed from IV-14 and is found to be:

$$t_p = \frac{-B^2 + \sqrt{B^4 + 4B^2 t_{inj}}}{2} \qquad \text{(IV-15)}$$

where B satisfies the functional $\text{erfc}(B) - R_0 = 0$. It is evident that IV-15 generates a family of curves where the choice of isotherm R_0 determines the curve. As expected, for R>0 (isotherms less than the initial formation temperature T_0), the length of time it takes a particle to heat up is less than for the case in which conduction from the bounding rock mass is ignored (i.e., R=0). A unique aspect of this analytical solution is that the time required for an injected element of fluid to reheat is independent of injection rate for the stated assumptions.

A fully documented code written for the HP-67 calculator is provided, as Appendix IV-1, for the estimation of injection temperatures based on Reference 38. The methodology has been extended to calculate both the heating time and the travel distance for an injected element. Consider the following example:

Let: thermal diffusivity (A) = 10^{-6} m^2/sec = 3.6×10^{-4} m^2/hr
fractional porosity (P) = 0.1
thickness of injection zone (H) = 100 m
injection formation temperature (T0) = 200°C
injection fluid temperature (T1) = 30°C
desired isotherm temperature (T9) = 190°C

Question: How long will an injected element of fluid take to reheat to 190°C? How far will the injected fluid element travel before reheating to 190°C?

Solution

$$R = \frac{200 - 190}{200 - 30} = 0.0588$$

Solve: erfc (X) = R

Now let: density of rock (D1) = 2.7×10^3 kg/m^3
heat capacity of rock (H1) = 7.8×10^2 J/Kg·°C
density of fluid (D2) = 1×10^3 kg/m^3
heat capacity of fluid (H2) = 4.2×10^3 J/kg·°C

Solving: $\delta = 1 + [(D1 \cdot H1)(1-P)]/(D2 \cdot H2 \cdot P)$

$$\delta = 1 + \frac{1.90 \times 10^6}{4.20 \times 10^5}$$

$$\delta = 5.52$$

$$\alpha = \delta - 1 = 4.51$$

$$T = (1 - P)^2 \, H^2/A$$

$$T = (0.9)^2 \, (100)^2/3.6 \times 10^4 \text{ m}^2/\text{hr}$$

$$T = 2.25 \times 10^7 \text{ hr}$$

hence $t_{inj} = 24/2.25 \times 10^7$

$$t_{inj} = 1.067 \times 10^{-6}$$

and

$$t_p = t_p \cdot T/\alpha = (1.067 \times 10^{-6})(2.25 \times 10^7 \text{ hr})/4.513$$

$$\boxed{t_p = 5.3 \text{ hrs}}$$

where t_p is the time required for an injected element of fluid to reheat to 190°C.

The distance traveled by an element of injected fluid to a point where it reheats to the specified temperature is calculated assuming a Darcy-type of radial flow:

$$Qt_p = D2 \cdot \pi \cdot R1^2 \cdot H \cdot P$$

where Q = mass flow rate - kg/sec

t_p = travel time

Therefore: $R = \sqrt{Qt}_p/\pi \cdot H \cdot D2 \cdot P$

If Q = 50 kg/sec, then:

$$r = \frac{\left[(1.8\times10^5 \text{ kg/hr})(5.317 \text{ hr})\right]^{\frac{1}{2}}}{(0.1)(\pi)(100)(1\times10^3 \text{ kg/m}^3)}$$

$$\boxed{r = 5.52 \text{ m}}$$

IV-8. Injection Well Hydraulics

Successful operation of an injection well requires that the reinjection reservoir have a capacity to accept fluid at the desired injection rate and that sufficient surface pumping capacity is available. In general, the absolute upper limit on surface pumping pressure is governed by the minimum pressure necessary to hydraulically fracture the reinjection reservoir. If the fracturing pressure limit is exceeded, injected fluid may migrate out of the injection formation in an uncontrolled and in an unpredictable manner. Alternatively, hydraulic fracturing could be desirable as an effective means of breaking down near wellbore skin that would otherwise interfere with injection well performance. Skin damage is usually the result of drilling and well completion efforts and it results in degraded well performance. Methods for estimating skin damage are described by Earlougher[30], Hawkins[39], and Brons[46]. Fracturing may also be a useful means of linking an injection well with an adjacent natural fracture system. Thus, the benefits of hydraulically fracturing an injection well must be considered on a case by case basis.

Formation breakdown pressures are equal to the pressure required to fracture the rock plus the effective overburden pressures. Breakdown pressures shown in Figure IV-8 are typical of the Gulf Coast area[33].

Fresh water injection tests of two geothermal wells (Magmamax No. 2 and 3) located in the Salton Sea Geothermal Field (southern California) resulted in hydraulic fracturing of the injection formations[41]. The peak downhole pressure at the midpoint of the perforations for both injection wells is shown in Figure IV-9 superimposed on a plot of bottomhole fracturing pressure versus

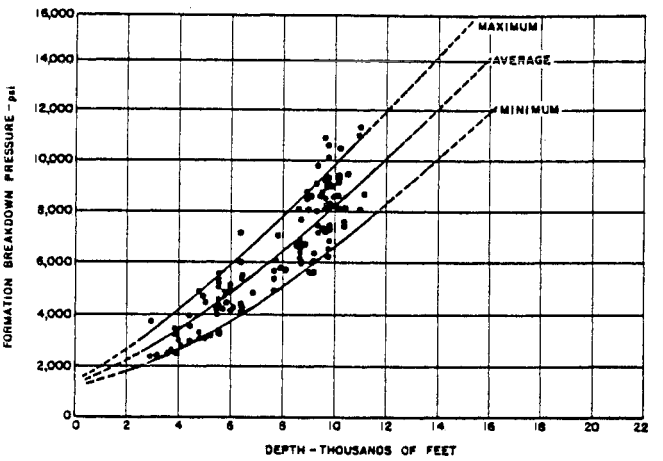

Figure IV-8. Formation Breakdown Pressures[33]

versus depth[42]. The injection tests showed an initial high pressure and correspondingly low injection rate. Subsequently, the pressure suddenly decreased with a concurrent increase in injection rate. This type of response was considered to be indicative of initiation of hydraulic fractures.

Formation breakdown pressure establishes the absolute injection pressure limit. Another more pragmatic control on surface injection pressure is the available pumping capacity. Pump sizing considerations are important because of capital and O&M costs associated with use of a specific pump. Thus, the manner in which an injection well is sized and completed has significant impacts on costs and useful life of the well. Optimization of an injection well design involves selecting the appropriate tubing sizes to yield the desired volumetric injection capacity, consistent with formation injectivity. Other factors which must be taken into consideration include the effects of scale deposition and corrosion over the planned life of the well. If the well is initially sized without consideration given to scale deposition and corrosion effects, surface pumping requirements may eventually exceed the capacity of installed equipment.

The optimization of injection well performance requires calculation of the necessary bottomhole driving pressure to maintain a desired injection

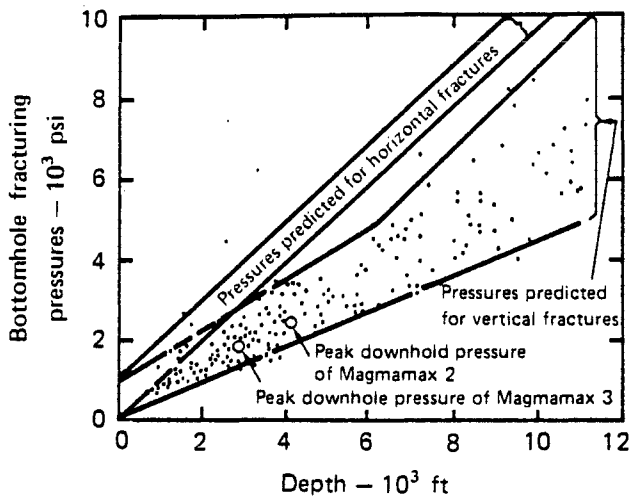

Figure IV-9. Theoretically predicted bottomhole fracturing pressures and field data. The experimental peak downhole pressures for the Magmamax wells are shown by the open circles[41].

rate. A parametric analysis is carried out to establish the optimum tubing size consistent with expected scale deposition, which causes a reduction in wellbore volume, corrosion product formation, which causes an increase in the wellbore friction factor, and the desired injection rate.

Bottomhole driving pressure may be calculated assuming radial Darcy flow and laminar flow conditions[28] as follows:

$$P_1 - P_2 = \frac{q\,\mu\,\ell n\,(r_e/r_w)}{0.007087\,hk} \qquad \text{(IV-16)}$$

where: P_1 = wellbore pressure (psia)
P_2 = static reservoir pressure (psia)
r_e = interference radius (feet)
r_w = wellbore radius (feet)
q = water injection rate (b/d)
μ = water viscosity (cp)
h = net injection interval height (feet)
k = effective formation permeability (md)

The hydrostatic head is calculated as follows:

$$P_h = \rho\ g\ h\ c \qquad \text{(IV-17)}$$

where: P_h = hydrostatic head (psi)
ρ = injected fluid density (g/cm^3)
g = gravitational constant (980 cm/sec^2)
h = well depth (feet)
c = unit conversion factor (4.76x10^{-4})

The injection wellhead pressure[28] is given by:

$$P_w = P_1 - P_h + P_f$$

where: P_w = injection wellhead pressure (psi)
P_f = pressure drop due to friction (psi)

The frictional pressure drop (P_f) is determined using the Darcy-Weisbach equation[28] as follows:

$$P_f = (0.9019)\ \rho \cdot (100/C)^{1.85} \cdot (q^{1.85}/di^{487}) \qquad \text{(IV-19)}$$

where: P_f = frictional pressure drop in injection tubing (psi)
ρ = specific gravity of injected fluid
C = constant
q = injection rate (gpm)
di = internal diameter of injection tubing (inches)

The constant C for non-corroded steel pipe varies from 120 (new pipe) to 90 (25 year old pipe). Severely corroded pipe has a C value of about 60.

A parametric analysis must be completed to establish injection wellhead pressure as a function of tubing diameter. As an example, Figure IV-10 illustrates the effects of tubing diameter and injection rate on surface injection pressure. The change in surface injection pressure due to corrosion of a 5½ inch diameter tubing string is shown in Figure IV-11. Thus, while a 5½ inch uncorroded tubing string might be adequate for an injection rate of 40,000 b/d, a larger diameter tubing string would be needed to compensate for the

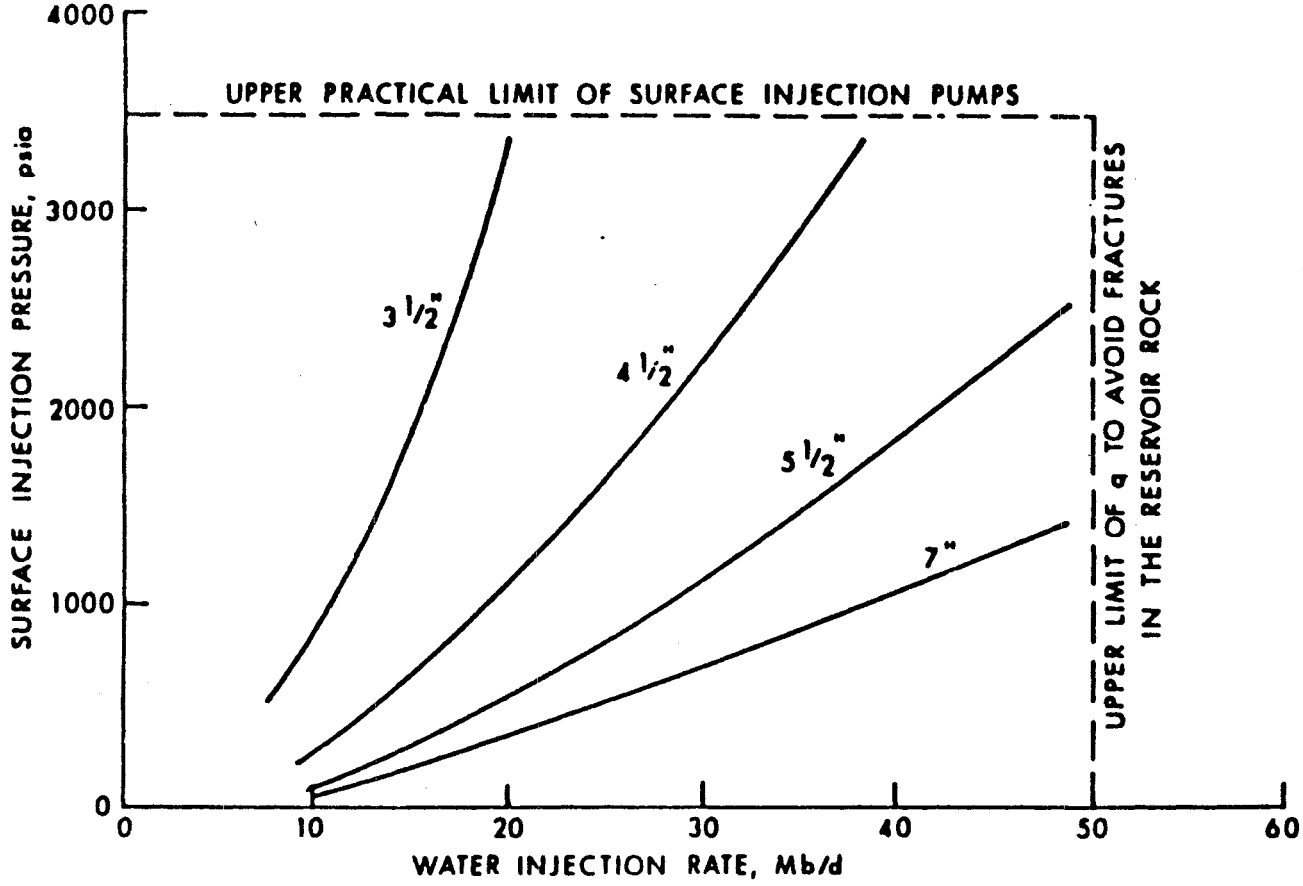

Figure IV-10. Influence of tubing size and injection rate on surface injection pressure.

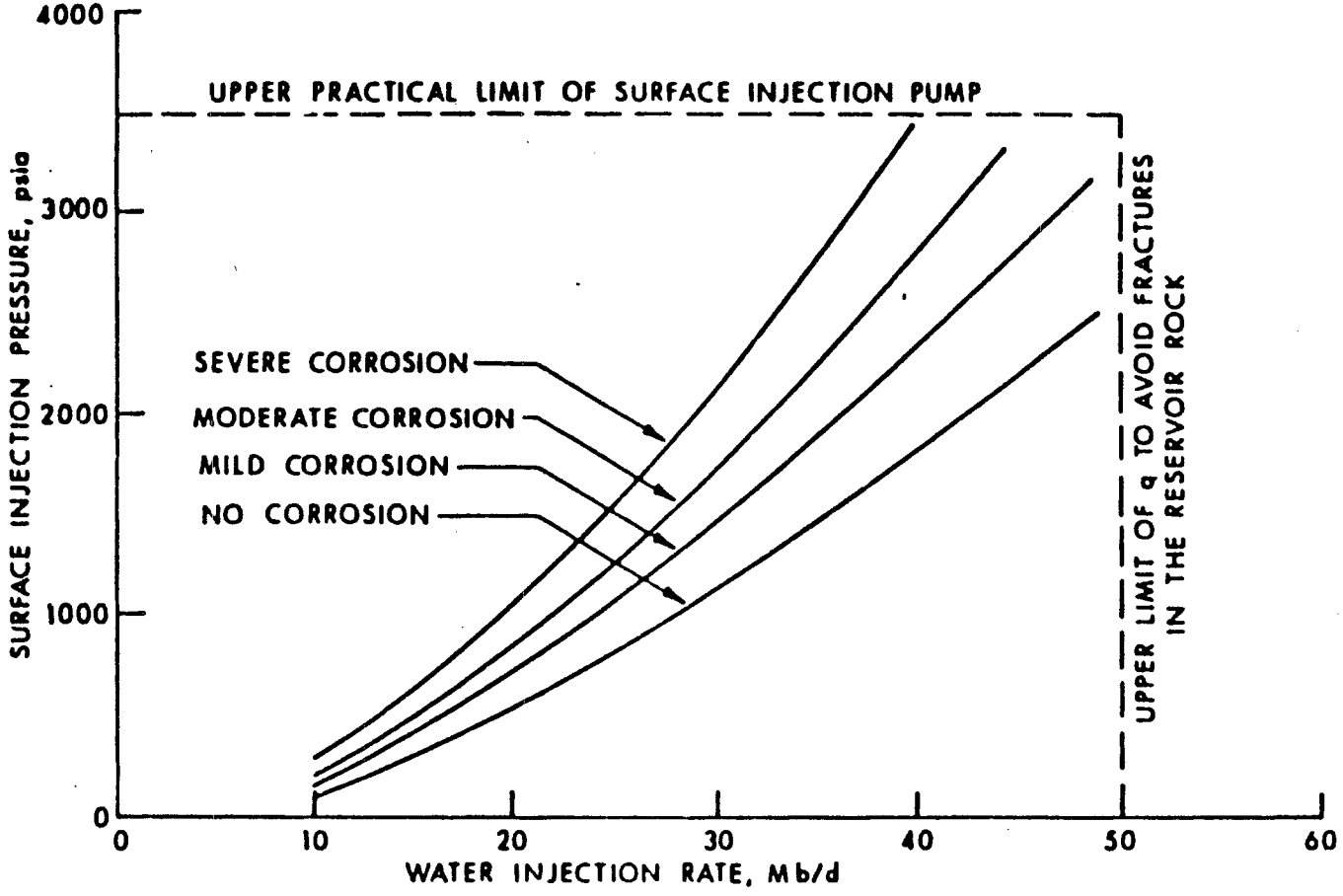

Figure IV-11. Effect of corrosion on surface injection pressure for various injection rates using a 5½ inch diameter tubing string.

frictional pressure losses caused by corrosion induced surface roughening. In the case of scale deposits, pressure drops due to both wellbore volume changes and increased frictional losses must be considered. The constant C in equation IV-19 is about 75. The effect of scale deposition on surface injection pressure is illustrated in Figure IV-12.

An alternative method for analysis of injection power requirements was described by Blair and Owen[35]. Wellhead injection pressure can be determined from the injection formation pressure by use of the energy equation as follows:

$$\frac{P_2}{\gamma} + \frac{V_2^2}{2g} + Z_2 = \frac{P_3}{\gamma} + \frac{V_3^2}{2g} + Z_3 + \text{losses}_{2-3} \qquad \text{(IV-20)}$$

where: P = pressure (lb/ft^2)
γ = specific weight (lb/ft^3)
V = fluid velocity (ft/sec)
g = gravitational constant (ft/sec^2)
Z = vertical distance from datum point (ft)
Subscripts denote properties at state point.

State points for analysis of injection pumping power requirements are depicted in Figure IV-13. For a constant diameter well, $V_2 = V_3$, and for an elevation datum point at the wellhead, Equation 3.1 yields the following expression for wellhead pressure:

$$P_2 = \gamma \frac{P_3}{\gamma} - Z + \text{losses}_{2-3} \qquad \text{(IV-21)}$$

The losses from point 2 to 3 consist of wellbore frictional losses. Frictional losses are determined from the Darcy-Weisbach Equation[43]:

$$h_f = f \frac{L}{D} \frac{V^2}{2g} \qquad \text{(IV-22)}$$

where: h_f = head loss (ft)
L = well length (ft)
D = well diameter (ft)

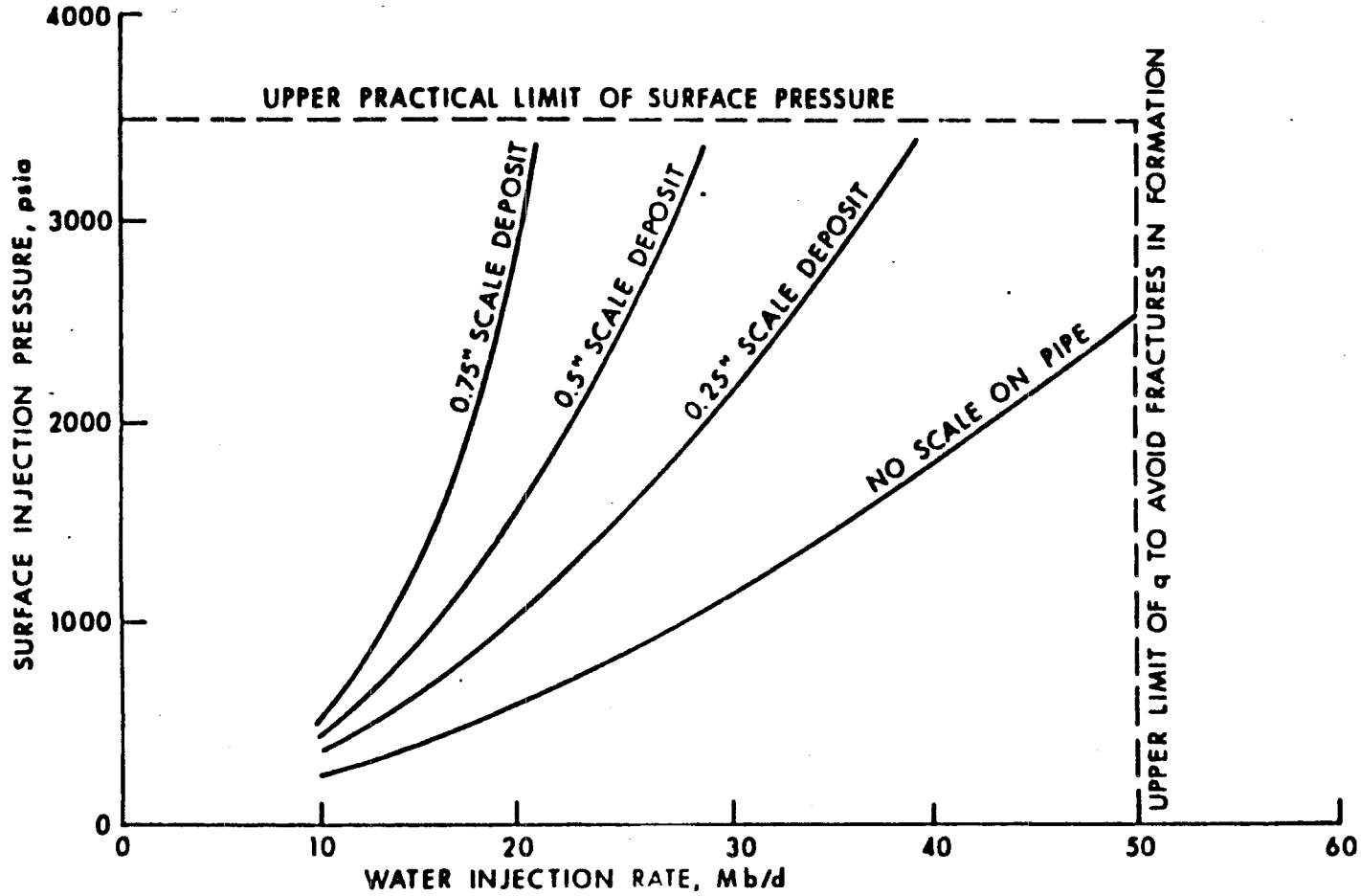

Figure IV-12. Surface injection pressures as a function of injection rate and scale deposition in a 5½ inch diameter tubing string.

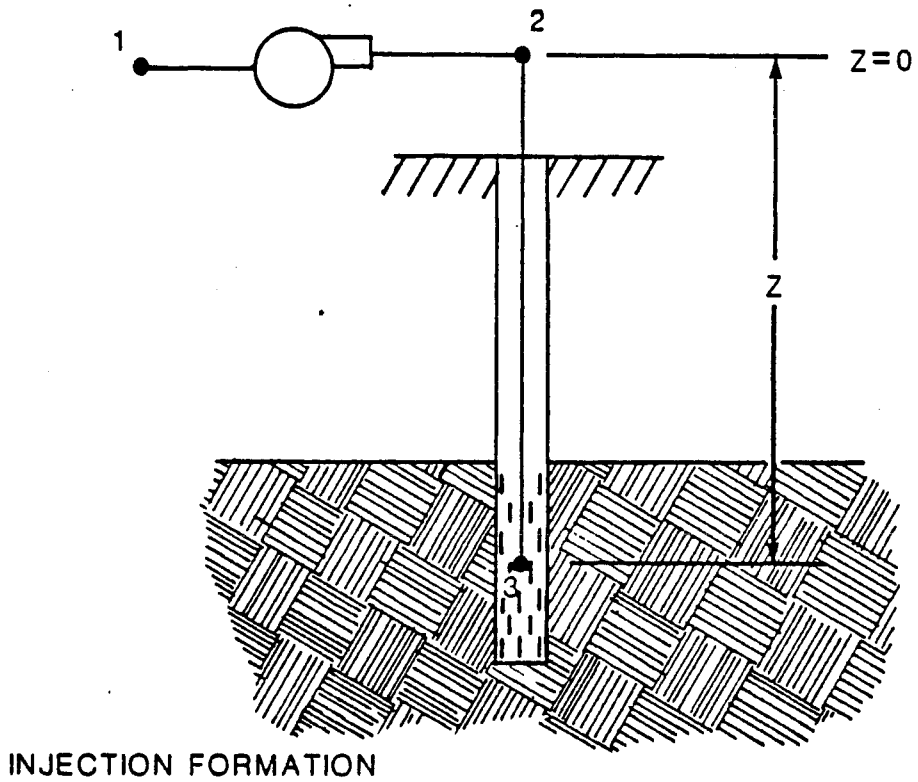

Figure IV-13. State points for calculation of injection surface pressure and injection power requirements.

Upon determination of the required wellhead pressure for the given injection flow rate, energy requirements for injection[44] are determined as follows:

$$\text{Power(HP)} = \frac{S\ Q\ \Delta H_{1-2}}{3960\ \eta} \qquad \text{(IV-23)}$$

where: S = fluid specific gravity

Q = flow rate (gal/min)

ΔH_{1-2} = required pump head increase from point 1-2 (ft)

η = pump efficiency (80% assumed)

Consider the following example as an illustration of the computation of injection pumping power:

Parameters:

Well diameter = 0.5 ft

Flow rate = 40,000 bbl/day

μ = 0.30 cp

$\rho = \gamma = 1.05 \times 60.1 = 63.1$ lb/ft^3

$$V = \frac{M}{\rho A} = \frac{40{,}000}{(63.1 \text{ ft}^3)\ \pi\ \frac{0.5 \text{ ft}^2}{4}} \times 42 \times 0.13368 \times 63.1 \times \frac{1}{24} \times \frac{1}{60} \times \frac{1}{60}$$

$$= 13.24 \text{ ft/sec}$$

$$Re = \frac{V\Delta\rho}{\mu} = \frac{(13.24)(0.5)(63.1)}{0.30 \times 0.000672} = 2.07 \times 10^6$$

$$\varepsilon/D = \frac{0.00015}{0.5} = 0.0003 \quad \text{(Relative Roughness)}$$

$$= f = 0.0155 \quad \text{(Moody Diagram)}$$

$$h_f = (0.0155\ \frac{1 \text{ ft}}{0.5 \text{ ft}}\ \frac{(13.24 \text{ ft/sec})^2}{(Z)\ 32.2 \text{ ft/sec}^2} = 0.0844 \text{ ft per foot of well}$$

Pumping Power:

Assume P_1 = 300 psi

$$P = \frac{SQH}{3960\ \eta}$$

where: P = pumping power (hp)

S = fluid specific gravity

Q = flow gpm

H = pump head (ft)

η = pump efficiency (80% assumed)

IV-9. Injection Well Completion

Injection well design and completion techniques are factors of obvious importance. The injection well must be designed to yield fluid handling capacities that are consistent with planned production and injection pumping requirements. Allowance should also be made for scale deposition and surface roughening of the tubulars due to corrosion and the effects of these factors on pumping requirements. It is reasonable and desirable to assume that some

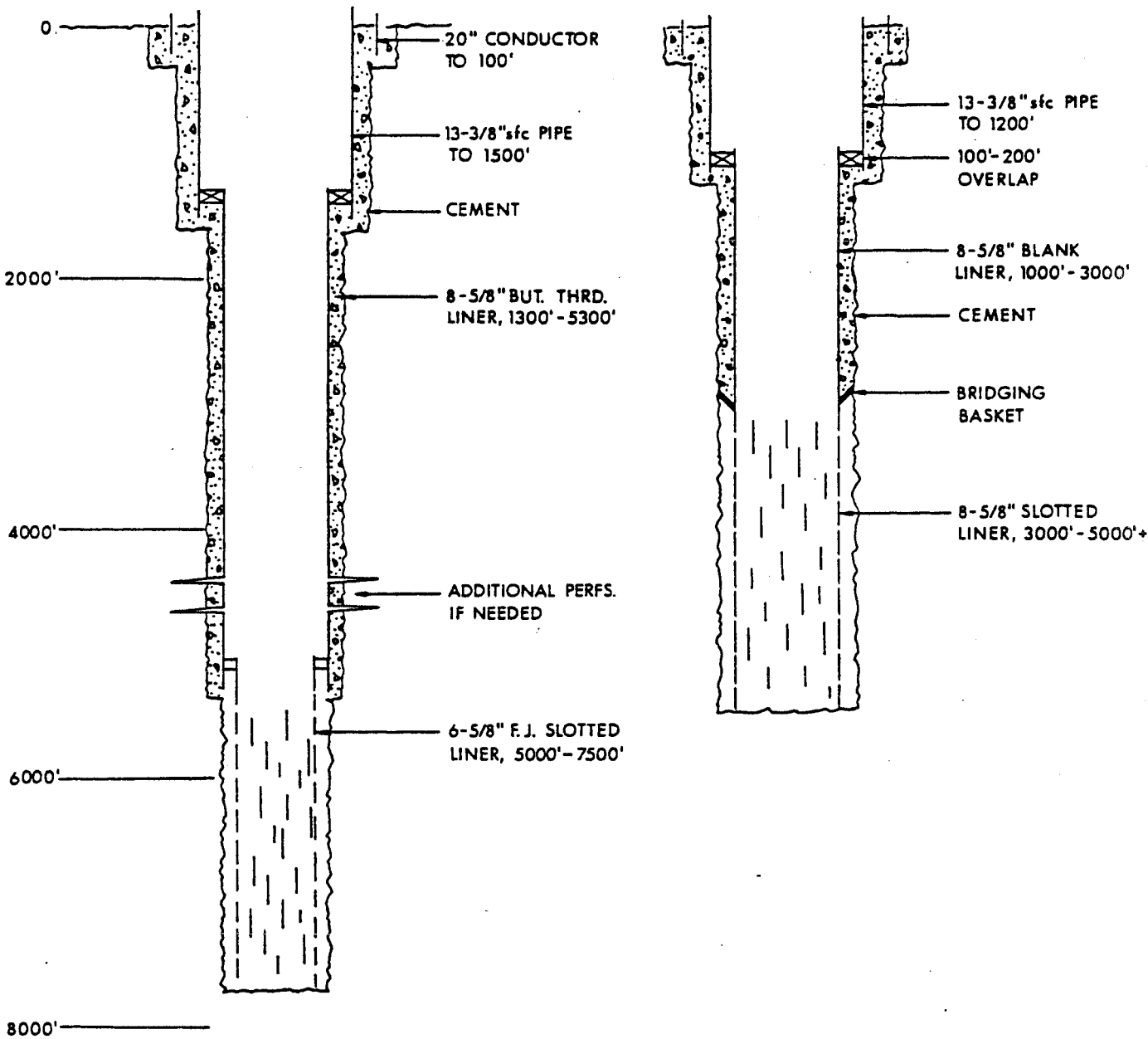

Figure IV-14. Typical Imperial Valley completions for two well depths. Full casing strings or tie back casing would be required as tubing for injection wells (from Ref. 45).

sort of workover will ultimately be necessary to maintain injectivity. Therefore, the well design should not preclude use of desired workover techniques. In geothermal injection wells, relatively frequent bailing may be required, as an example, to remove suspended particulates from the wellbore. The presence of a rat hole would be of obvious importance. Descaling operations and perforation cleaning may also generate extraneous particulates which could also be trapped in a rat hole.

Geothermal well completions have been reviewed by Snyder[45]. Typical Imperial Valley hydrothermal well completions are schematically illustrated in Figure IV-14. A major area of concern with respect to completion of a well in the injection interval is avoidance of drilling and completion fluid-induced damage. The appropriate drilling fluids must be selected from the point of view of thermal stability and chemical compatibility with in-situ fluids. If injection reservoir fluids are available, chemical compatibility tests should be carried out. These tests can be as simple as contacting aliquots of both fluids at ambient conditions and observing any tendency for formation of precipitates. The mixture can also be filtered and the precipitated particulates weighed to quantify the incompatibility reactions. Recovered precipitates can also be chemically analyzed to identify the reacting species. Core and cutting material, if available, can be quite useful in establishing or or predicting formation response to drilling, completion and workover fluids. Petrographic, x-ray diffraction and scanning electron microscopy can be used to establish bulk mineralogy, clay mineralogy, matrix and microstructural aspects, presence of fracture and other factors that may impact injectivity. Swelling tests performed with formation core samples at ambient conditions can be used to screen potential drilling and completion fluids. Laboratory permeability tests, measurements of porosity and pore size distribution can also be

extremely useful in locating the "best" injection zones and in establishing minimum requirements for surface treatment of spent fluids[46-49]. A comprehensive well logging program will also contribute to development of an extensive data base as field development activities continue. The combination of laboratory derived formation properties based on analysis of core and cuttings and well log derived formation properties are the first logical steps in defining the in-situ pre-development condition of the injection reservoir.

IV-10. Records

Availability of comprehensive records are essential for each injection well drilled on a project. At some point during future operations, a particular injection well may become impaired. Questions will immediately arise as to the origin of impaired performance. In diagnosing the source or sources of difficulty, it would be extremely helpful if detailed information concerning injection reservoir properties, drilling and completion fluid properties, in-situ injection reservoir fluid properties, composition and pre-injection treatment history of all injected fluids, and injection rate-pressure data were known. Maintenance of detailed records for each well is not difficult, but compilation of adequate records requires time and commitment. However, the value of such records when contemplating a workover, for example, cannot be overemphasized.

Care should be exercised in preventing haphazard or unauthorized disposal of any fluids. For example, drilling crews should not be allowed to empty pits into a completed injection well without first considering the ramifications of such actions. A senior site employee should be given authority to control injection well operation especially during early phases of any project. Periodic review of compiled records especially with regard to injection pressure perturbations would be helpful in anticipating potential difficulties. A

typical data sheet format is illustrated in Figure IV-15 as a convenient means of documenting injection well operational practices while at the same time providing a data basis that may be invaluable at a future time in diagnosing reasons for impaired well performance.

IV-11. Testing an Injection Well

The methodology for testing oil field injection wells has been summarized by Earlougher[30]. Technical papers bearing on this subject are also published periodically in The Journal of Petroleum Technology. Proceedings of technical symposia published by The Geothermal Resources Council[50], by Lawrence Berkeley National Laboratory[51], and the Stanford University Geothermal Programs[52] are excellent sources of additional information. All completed injection wells should be adequately tested to determine reservoir hydraulic properties, initial injection pressure, or injectivity and skin factors. Long-term injection tests of weeks to months duration would ultimately be needed to determine interwell interference effects and ultimate reservoir response to injection. At some point, relatively sophisticated numerical or analytical modelling may be needed to plan injection/production well placement to optimize utilization of the resource. Failure of injection wells or impaired injectivity during initial well testing activities can be caused by improper pre-treatment of injected waters. Thus, even at this early stage of injection well utilization, it is important to carefully monitor and control reinjected fluid properties.

IV-12. Water Quality

Reinjected water can cause impairment of injection zones for any one of several reasons. The collective characteristics of reinjected waters with respect to the potential for causing loss-of-injectivity are referred to as "water quality". Physical and chemical properties of an injected water that

INJECTION WELL OPERATIONS LOG

_____

(Well Identification)

Date		Time		Total Time (hrs)	Source of Injected Influent	Pre-Injection Treatment	Injection Rate (gpm)	Injection Press./Temp. (psig/°F)	Total Inj. Vol. (gal)	pH	Remarks
Start	Finish	Start	Finish								

Figure IV-15. Typical Injection Well Operations Log

govern water quality include: a) chemical composition, b) presence of suspended solids, c) presence of free gas, d) temperature of injected water, and e) density/viscosity of injected water.

The specific chemical composition of a reinjected water can cuase impairment of an injection zone as follows:

a. A chemically unstable water may form precipitates that can mechanically plug an injection zone.

b. A chemically stable water may form precipitates when mixed with in-situ formation waters. Precipitates can then mechanically plug an injection zone.

c. A chemically stable water may cause corrosion of injection well tubulars leading to production of corrosion product particulates that can mechanically plug an injection zone.

d. Reinjected waters may react with formation materials causing production of fine-grained particulates, collapse of matrix pore structure or chemical precipitates.

Suspended solids, either organic or inorganic, can cause a loss-of-injectivity by forming an impermeable cake on the formation face, by invading the pore structure of a formation to form an internal filter cake, by plugging gravel packs, screens or perforations or by filling the wellbore with impermeable sludge. The type of damage mechanism leading to impairment by suspended solids is governed by the properties of the solids and the pore structure of the injection zone formation. Particle size and pore diameter are of obvious importance. The presence of only colloidal sized particulates in an injected water does not completely rule out the possibility of mechanical plugging of an injection zone because the surface potential of small particles could, under certain circumstances, lead to plugging.

Free gas in a reinjected water is detrimental because of the potential for vapor blocks in the pore structure of the injection zone. Unless the gas is redissolved at depth because of higher hydrostatic pressure, vapor blocking

is a real possibility. This is a direct result of the higher mobility of gas relative to liquid and relative permeability effects. Dissolved gases, such as oxygen or hydrogen sulfide can also be a source of indirect difficulty due to their effect on corrosion of tubulars and possible incompatibility reactions in the injection zone leading to precipitation of solids from in-situ waters.

The natural driving force for injection is ultimately related to the density contrast between injected waters and in-situ waters. Depending upon well depth and water temperature, a specific hydrostatic head will result that may be sufficient in many cases to permit disposal of reinjected waters without use of surface injection pumping equipment. The flow of water through a porous matrix is described by Darcy's law. Fluid flow is inversely proportional to fluid viscosity. Thus, temperature of injected water is important because of the effect on fluid density and viscosity.

IV-13. Evaluating Water Quality

In considering the various factors that can adversely impact injectivity, the presence of suspended particulates and their size distribution is extremely important. The general behavior of uniform, rigid, spherical suspended solids in water flowing through an ideal rigid porous medium consisting of spherical grains of uniform size is summarized in Figures IV-16 and 17. Particles, which on simple size considerations alone, that are smaller than the pore size of the porous medium may not pass through without forming an internal filter cake. For example, colloidal silica has a finite negative surface potential and would be susceptible to deposition in the pore structure if the appropriate surface charge was present on the rock surfaces. Ultimate demonstration of the injectability of an effluent should be based on use of core and membrane filter tests as described in a subsequent section. Nonethe-

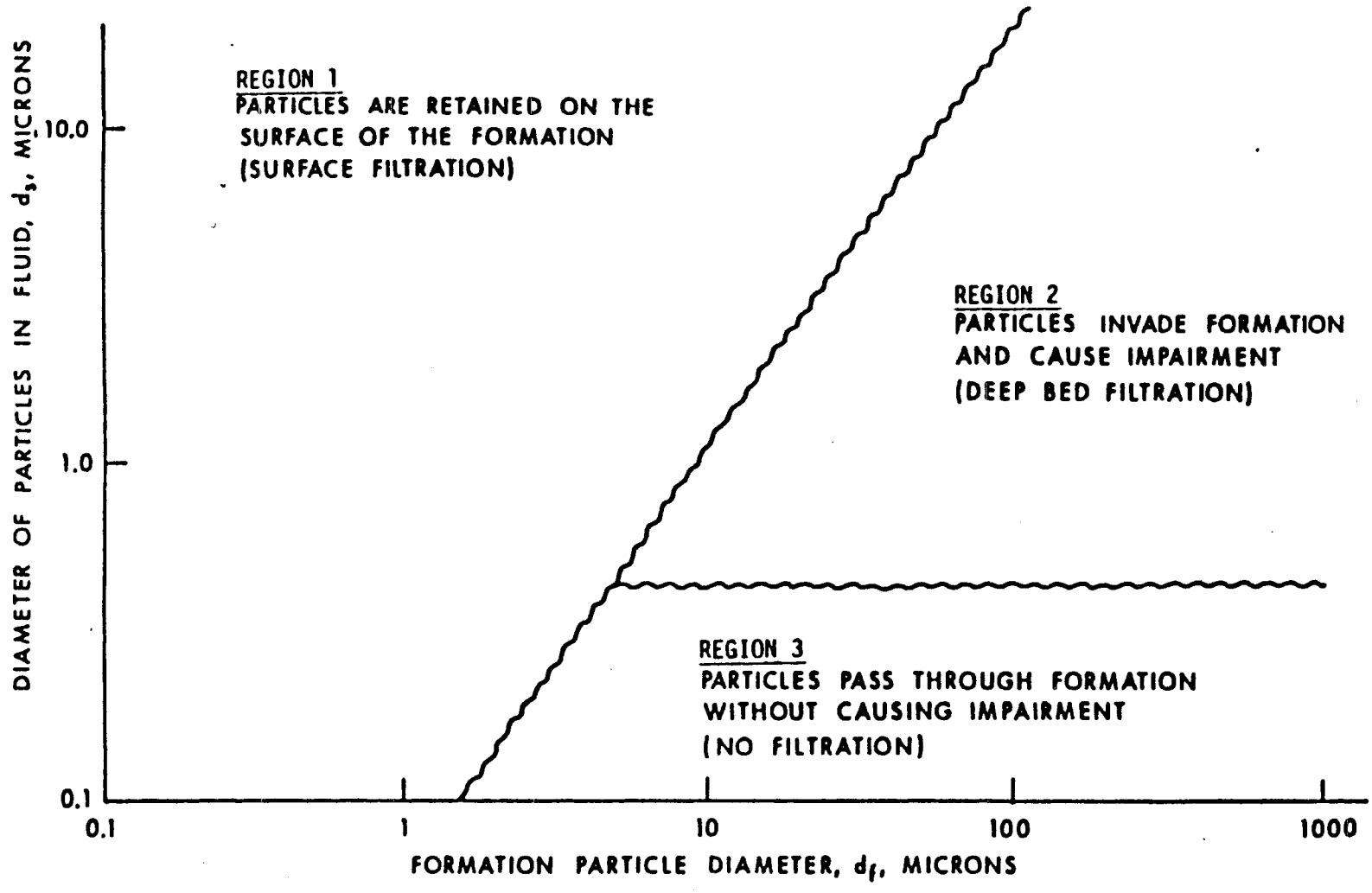

Figure IV-16. Particle distribution in systems where the particles in the fluid and the reservoir are spheroids. (From Ref. 53)

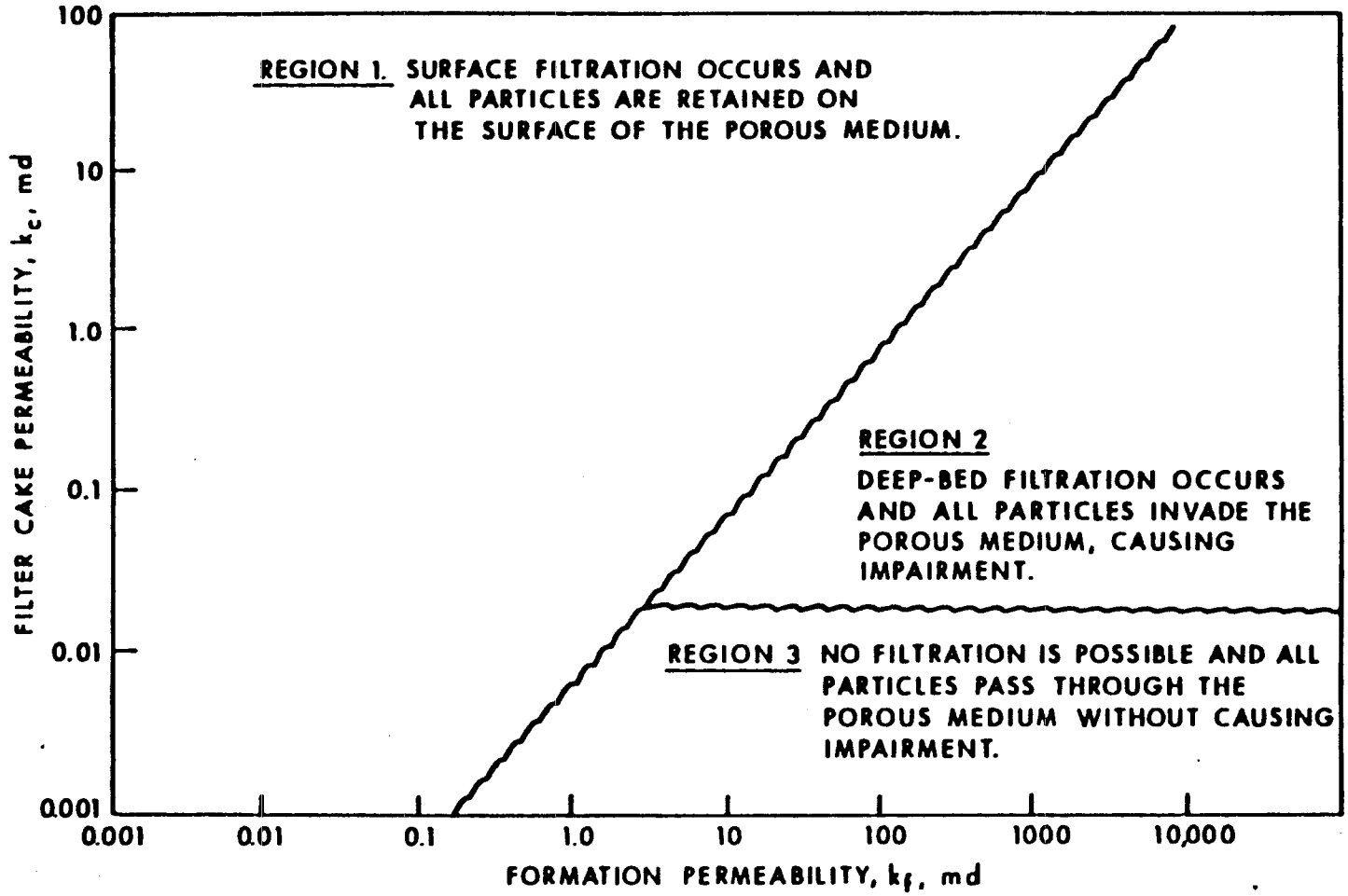

Figure IV-17. The relationship between filter cake and formation permeabilities in the flow of particle-laden fluid through porous media. (From Ref. 53)

less, the relationship shown in Figure IV-16 can be used in a general sense to assess injectability provided that samples of injected waters and injection zone core material are available for analysis. The size distribution of suspended solids can be measured using serial membrane filtration techniques or particle counters. Formation particle size distribution can be estimated on the basis of pore size estimates derived from capillary pressure data[46,47] or by granulometric analysis of thin sections[54,55]. If the reservoir rock is poorly consolidated, standard sieve analysis techniques[56] could also be used after disaggregating the core material.

Serial membrane filtration is best carried out using Millipore high pressure stainless steel membrane filter holders and filtration media with a range of pore sizes. Conventional membrane filters are available with pore sizes ranging from the submicron range to 12 μm. Large pore size filters can be made from Spectra/Mesh (Fisher Scientific) polymer squares or similar material. If the temperature of a reinjected process stream is about 100°C or less than almost any filtering medium will be acceptable. In the authors' experience, Nucleopore membrane filters are usable to about 120-130°C. Millipore (Type HA) membrane filters deteriorate above about 70°C in geothermal brine. Silver membrane filters are useful at high temperatures. The silver membrane should be used if filtered residues are to be subsequently analyzed by x-ray diffraction. However, the presence of dissolved sulfide ion in the filtered brine will cause adverse reactions with the silver membrane. Other filter types produce x-ray diffraction patterns which complicate analysis of the filtered solids. Glass filter membrane filters can also be used at high temperature but they are available in a limited range of pore sizes. All membrane filters should be placed on top of a pre-filter fiber pad supplied by numerous manufacturers. These pads prevent permeability decline in the membrane filters when they are pressurized. They also promote clean removal of the filters from the holder O-rings.

Direct measurement of particle size of suspended solids in a liquid can be accomplished using particle counting instrumentation. Coulter counters are used routinely in the oil fields to measure particle size distributions of injected waters. This type of instrumentation is relatively costly and complex. However, the instrument can be used in the field if suitable laboratory space is made available. Laser scattering devices such as the SPECTREX Corp. particle counters are also available. These devices have been used successfully in the field to measure particle size distributions in hypersaline brines[57-58]. SPECTREX Corp. also manufactures a particle profiling attachment which produces complete particle size distributions in graphical format automatically. Sophisticated x-ray particle size analyzers (Micromeritics) are also available, but these devices are not amenable to routine field use.

All particle size analyzers require discrete samples at ambient conditions (the laser particle counters can accept samples at any temperature below boiling). A useful procedure would be collection of a known volume of a water sample and immediate dilution with a known volume of deionized water to prevent additional formation of chemical precipitates. The measured particle distribution can then be corrected by use of a simple material balance.

The relationship shown in Figure IV-17 can also be used to assess relative injectability of a reinjected water. Formation permeability is readily obtained from core tests or well tests. Filter cake permeability can be estimated using techniques described in a subsequent section of this chapter.

The objective of water quality measurements is to establish the probable response of the subsurface injection formation to long-term reinjection. An operator is faced with the question of establishing how long an injection well will perform adequately given a specific water quality and assuming that there are no hydraulic limitations in the reservoir. Water quality testing provides

one method of evaluating injection well performance. Repetitive measurements can also be used to evaluate potential improvement in well performance due to installation of water treatment systems such as filters, clarifiers, settling tanks, chemical treatment, etc. The relationship between water quality measurements and design of an injection water treatment system is shown schematically in Figure IV-18[59]. Preliminary core flooding, filtration and chemical stability tests are used to establish the injectability of reinjected waters [8,60-67]. Identification of probable reservoir impairment mechanisms leads to subsequent development of water processing systems to condition reinjected water. Pilot processing facilities are designed and subsequently reevaluated using water quality testing methods. These procedures minimize damage to injection wells during initial field development and permit estimates to be made of the expected operating lifetime of disposal wells.

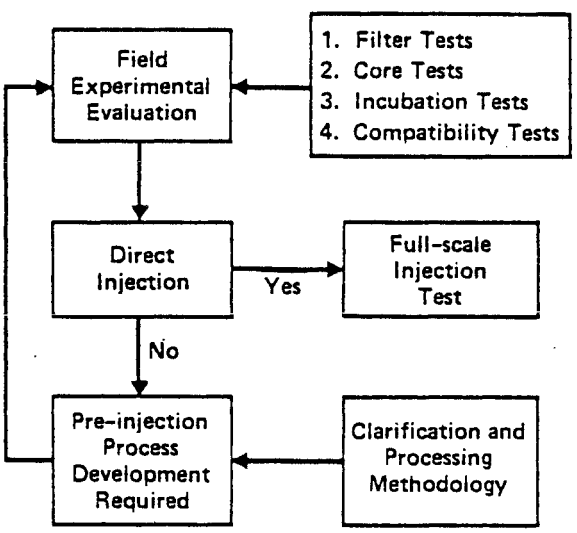

Figure IV-18. Injection Evaluation Methodology[59]

Water quality tests are most frequently used in a qualitative sense to show relative improvement resulting, for example, from installation of a filtration system. Thus, a core flooding test might show better permeability maintenance with prefiltered water relative to unfiltered water. In recent years, a number of researchers have discussed analytical models which attempt to relate water quality experimental data to actual performance of injection wells[53,65,68-69].

IV-14. Impairment Mechanisms

Four types of injection wellbore impairment[65] caused by suspended solids are illustrated in Figure IV-19. Wellbore narrowing occurs when injected solids are filtered out on the face of the injection formation and form a surface filter cake. Perforation plugging is an accelerated case of wellbore narrowing in which injected solids form a filter cake in the open perforations. Failure of the injection well due to perforation plugging occurs more rapidly than in the case of wellbore narrowing because of the smaller formation surface area available for filter cake formation. Invasion occurs when fine particulates invade the pore structure of the injection formation. At some radial distance from the wellbore, solids will settle and form an internal filter cake. This type of damage can be quite serious because of the difficulty in removing the damage during a workover. Wellbore fill-up occurs when solids deposit within the wellbore as a sludge. Cleaning of the well would be necessary when the sludge level builds up through the injection zone. The presence of a relatively deep rat hole would be advantageous with respect to wellbore fill-up and also as a receptacle for extraneous solids generated during well workovers.

IV-15. Evaluating Injection Well Performance

Wellbore narrowing can be evaluated using simple core flooding or mem-

1. WELL BORE NARROWING

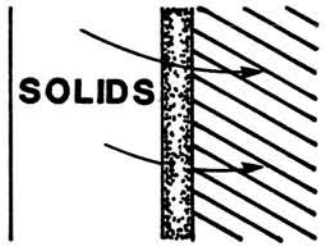

2. INVASION

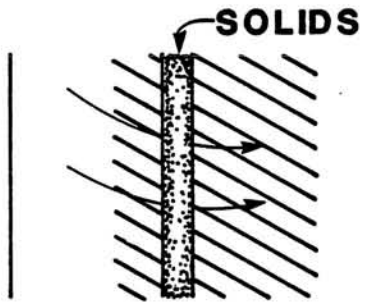

3. WELL BORE FILL UP

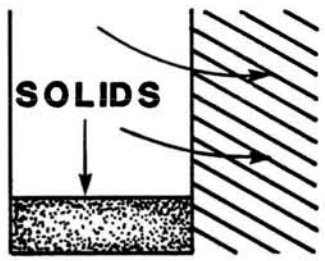

4. PERFORATION PLUGGING

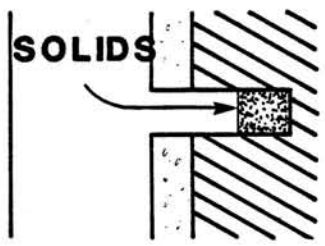

Figure IV-19. Types of wellbore impairment caused by suspended solids. (From Ref. 65)

brane filtration tests. Jorda[53] described a simple linear flow analytical model for computing the pressure drop across a filter cake and the resultant impact on injection rates. The flow model is illustrated in Figure IV-20. The system behavior may be described as follows:

$$dP_t = \frac{q\, l_c\, \mu}{A\, K_c} + \frac{q\, l_f\, \mu}{A\, K_f} \qquad \text{(IV-24)}$$

where: dP_t = pressure drop across system (atm)
q = instantaneous flowrate (ml/sec)
l_c = filter cake thickness - time varing (cm)
l_f = membrane filter or core sample thickness (cm)
μ = reinjection water viscosity (cp)
A = cross sectional flow area (cm^2)
K_c = filter cake permeability

Filter cake thickness (l_c) is determined as follows:

$$l_c = \frac{wV}{\rho_c A} \qquad \text{(IV-25)}$$

where: w = suspended solids concentration in reinjection water (gm/l)
ρ_c = filter cake bulk density - measured (g/cm)
V = total filtrate volume (ℓ)

Substituting:

$$dP_t = \frac{q\, w\, V\, \mu}{A^2\, \rho_c\, K_c} + \frac{q\, l_f\, \mu}{A\, K_f} \qquad \text{(IV-26)}$$

Rearranging:

$$K_c = q\, w\, V\, \mu \,/\, (A^2\, \rho_c)\, \left(dP_t - \frac{q\, l_f\, \mu}{A\, K_f}\right) \qquad \text{(IV-27)}$$

Filter cake permeability can be calculated because all other variables can be directly measured or estimated. The permeability of a filter cake depends upon the chemical and physical properties of the suspended solids. K_c values may be generalized as follows[53]:

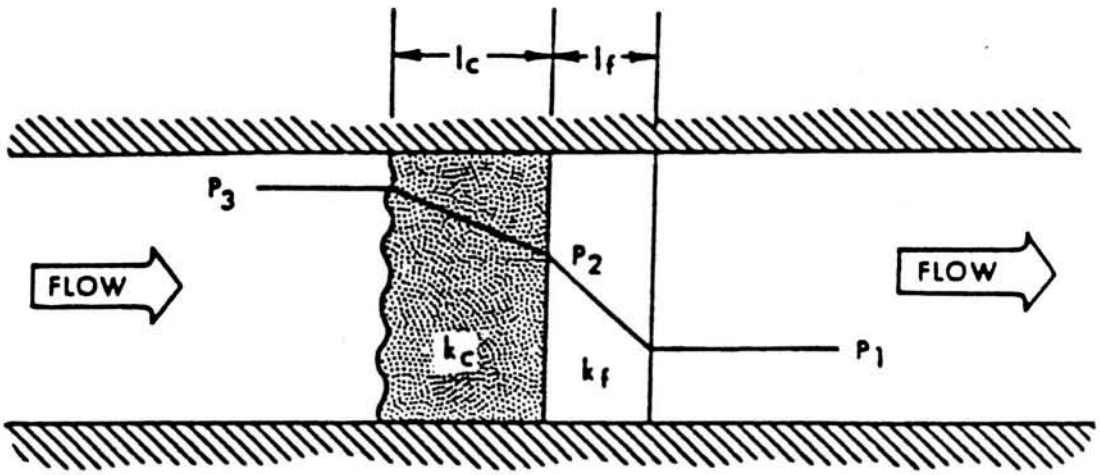

Figure IV-20. The linear flow model from which k_c, the permeability of a close-packed filter cake, can be determined using a membrane filter or core test. l_c and l_f are the filter cake and core or membrane filter thicknesses. k_c is the filter cake permeability and the pressure drops through the system are defined by $P_1 - P_3$.

1. Flocced materials (iron hydroxides, etc.) and water-borne organic matter often result in K_c values in the fractional millidarcy range.

2. Iron sulfides produce K_c values of less than one millidarcy.

3. Non-hydrated corrosion products, other than iron sulfide, produce K_c values of 1-10 millidarcies.

4. Fine sandy-type solids produce K_c values in the tens of millidarcies.

Once K_c has been evaluated, using data obtained from relatively simple membrane filter or core flooding tests, injection well response can be calculated. Jorda[53] derived the following analtyical model:

Given:

1. The water enters the reservoir uniformly, with even distribution over the injection interval.

2. The wellbore narrowing impairment mechanism is accurately reflected by uniform deposition of solids on a membrane filter or core sample.

3. The filter cake in the injection well is not fractured.

4. Sloughing of the filter cake does not take place.

5. Filter cake build-up occurs in the form of a right circular cylinder.

Then:

$$r_c = \frac{\pi r_w^2 h - \bar{q}w/\rho_c}{\pi h}^{\frac{1}{2}} \qquad \text{(IV-28)}$$

where: $\bar{q}$ = cumulative volume of water injected (liters)

r_w = wellbore radius (cm)

r_c = inner radius of deposited cake (cm)

h = injection interval height (cm)

w = suspended solids content of water (gm/l)

ρ_c = filter cake bulk density (gm/cc)

The pressure drop through the filter cake is given by:

$$dP = q_i \mu \ell n\ (r_w/r_c)/2\pi k_c h \qquad \text{(IV-29)}$$

where: dP = pressure loss through the filter cake (atm)

q_i = water injection rate (cc/sec)

If we assume a hypothetical injection well having the following properties:

q = 10,000,000 barrels = 1590 x 10^6 liters

r_w = 5 inches = 12.7 cm

h = 250 feet = 7620 cm

w = 1 ppm = 0.001 gm/l

ρ_c = 3 gm/cc

q_i = 73,605 cc/sec (40,000 b/d)

The, r_c = 11.79 cm and dP = 457 psi or 137,131 psi values of k_c of 3 md and 0.01 md, respectively. Thus, the impact of filter cake permeability on injectability becomes obvious. The method outlined above is extremely useful in evaluating the time dependent increase in bottomhole injection pressure for a constant water quality injection stream.

Jorda[53] also described a simple analytical model for calculating decline injection rate again using data obtained from a membrane filter or core flooding test:

$$\frac{1}{q} = \frac{\mu \, \ell n(r_e/r_w)}{2\pi k_f h(P_1-P_2)} + \frac{\mu \, \ell n(r_w/r_c)}{2\pi k_c h(P_1-P_2)} \qquad \text{(IV-30)}$$

where: q = water injection rate (cc/sec)

μ = water viscosity (cp)

r_e = well interference radius (cm)

r_w = wellbore radius (cm)

r_c = inner filter cake radius (cm)

k_f = formation permeability (darcies)

k_c = filter cake permeability (darcies)

h = injection interval height (cm)

P_1 = bottomhole injection pressure (atm)

P_2 = static reservoir pressure (atm)

If the bottomhole injection pressure (P_1) is set to the maximum possible considering surface injection pumping equipment capability and the fracturing gradient, then equation IV-30 yields an estimate of the maximum possible injection rate assuming uniform build-up of a filter cake with known permeability.

IV-16. Barkman and Davidson Model

Injection Well Half-Life Estimates

Half-life estimates for a disposal well can be calculated after the method of Barkman and Davidson[65] for a constant pressure drop process. The calculated half-life is the time required for the injection rate to decline to one-half of its initial value. Disposal well impairment models are described for the cases of wellbore narrowing, invasion, wellbore fill-up and wellbore narrowing or invasion with a perforated completion. The most realistic estimates of injection well performance, however, are based on use of the open hole completion wellbore narrowing and invasion models.

Wellbore narrowing results when a filter cake forms on the sand face and then builds inward eventually partially filling the wellbore. The invasion model accounts for penetration of the disposal formation by fine suspended solids which ultimately form an internal filter cake within the disposal formation. For each mechanism, the half-life is given by the product:

$$T_{\frac{1}{2}} = (F)(G) \qquad \text{(IV-31)}$$

Relevant formation and injection parameters that are needed to develop half-life estimates are provided in Table IV-2. The F-factor is a constant given by:

$$F = (1.723 \times 10^4) \frac{\pi \cdot r_w^2 \cdot h \cdot \rho_c}{i_o \cdot w \cdot \rho_w} \qquad \text{(IV-32)}$$

Table IV-2

Data Required to Calculate Injection Well Performance Using the Barkman and Davidson Method

Water Density
Water Viscosity

Injection Rate
Radius of Injection Tubing
Vertical Extent of Injection Interval

Injection Formation Permeability
Injection Formation Porosity
Radius of Effect
Invasion Radius

Filter Cake Density
Exposed Area of Membrane Filter*
Estimate of Formation Pore Size Distribution

* NOTE: The first 10 mm or so of any membrane filter, as measured inward from the circumference of the membrane filter, is sealed by an O-ring. Thus, this portion of the membrane filter is not part of the surface area of the filter exposed to fluid flow. The sealed portion of a membrane filter can be measured by sealing a filter inside the filter holder and then subsequently measuring the width of the O-ring indentation left on the membrane.

where: F = time to fill the wellbore with solids at the initial flow rate (years)

r_w = wellbore radius (meters)

h = injection interval (meters)

i_o = initial injection rate (STBD)

w = concentration suspended solids (μg/g)

ρ_c/ρ_w = density ratio, filter cake brine

Estimates of the permeability of filter cakes are developed from calculation of the water quality ratio given by:

$$\frac{w}{K_c} = (8166.11)\ \frac{1}{S^2}\ \frac{2\rho_c A^2 \Delta P}{\mu \rho_w} \qquad \text{(IV-33)}$$

where: w = weight concentration of solids in water (μg/g)

K_c = filter cake permeability (md)

S = slope of cumulative volume vs. square root of time (ml/√min)

ρ_c = bulk density of filter cake (gm/cm^3)

ρ_w = density of water (gm/cm^3)

A = exposed area of filter cake (cm^2)

ΔP = total pressure differential across filter (psi)

μ = fluid viscosity (cp)

G-factors for wellbore narrowing and invasion are estimated as follows:

$$\text{Wellbore narrowing: } G = 1 + \frac{1}{2\ln\theta} - \frac{1}{\alpha} + \frac{1}{2\ln\theta}\ \theta^{2(\alpha-1)/\alpha} \qquad \text{(IV-34)}$$

where: α = 0.5

$\theta = (r_e/r_w)^{k_c/k_F}$

r_e = radius of effect

r_w = wellbore radius

k_c = filter cake permeability

k_F = formation permeability

$$\text{Invasion:}\quad G = \frac{r_a^2\phi^2}{r_w^2}\left[1 + \frac{\beta}{2\ln\theta} - \frac{1}{\alpha} + \frac{\beta}{2\ln\theta}\right]\theta^{2(\alpha-1)/\alpha\beta} \qquad \text{(IV-35)}$$

where: r_a = invasion radius

$\beta = 1-(k_c/k_F)$

ϕ = fractional porosity

Filtration data are reduced in the form of linear coordinate plots of cumulative volume versus the square root of time (Figure IV-21). If the membrane filter becomes impaired by formation of a filter cake, either on the surface of the membrane or within its pore structure, the filtration curve approaches a straight line. The slope of the linear portion of the filtration curve is porportional to the water quality ratio, $W(ppm)/K_c(md)$, defined as the ratio of suspended solids concentration to the permeability of the filter cake formed on or within the membrane filter. Since the suspended solids concentration is known (measured during the membrane filtration test), the filter cake permeability can be calculated and a half-life estimate can then be developed for the injection wells. The actual performance of an injection well will depend in part on whether suspended solids are filtered out at the sandface or invade some distance before bridging pores and constructing an internal filter cake. The extrapolation of the linear portion of the filtration curve allows an estimate of invasion to be made; a negative intercept indicates no invasion while a positive intercept indicates invasion.

Barkman and Davidson emphasize that half-life estimates are semi-quantitative at best because of the uncertainty in fixing the injection parameters and in determining the true time-average of the water quality ratio from spot measurements. Furthermore, a membrane test only resolves injection well impairment resulting from deposition of suspended solids or scale formation. The actual improvement in injection that might be realized as a result of

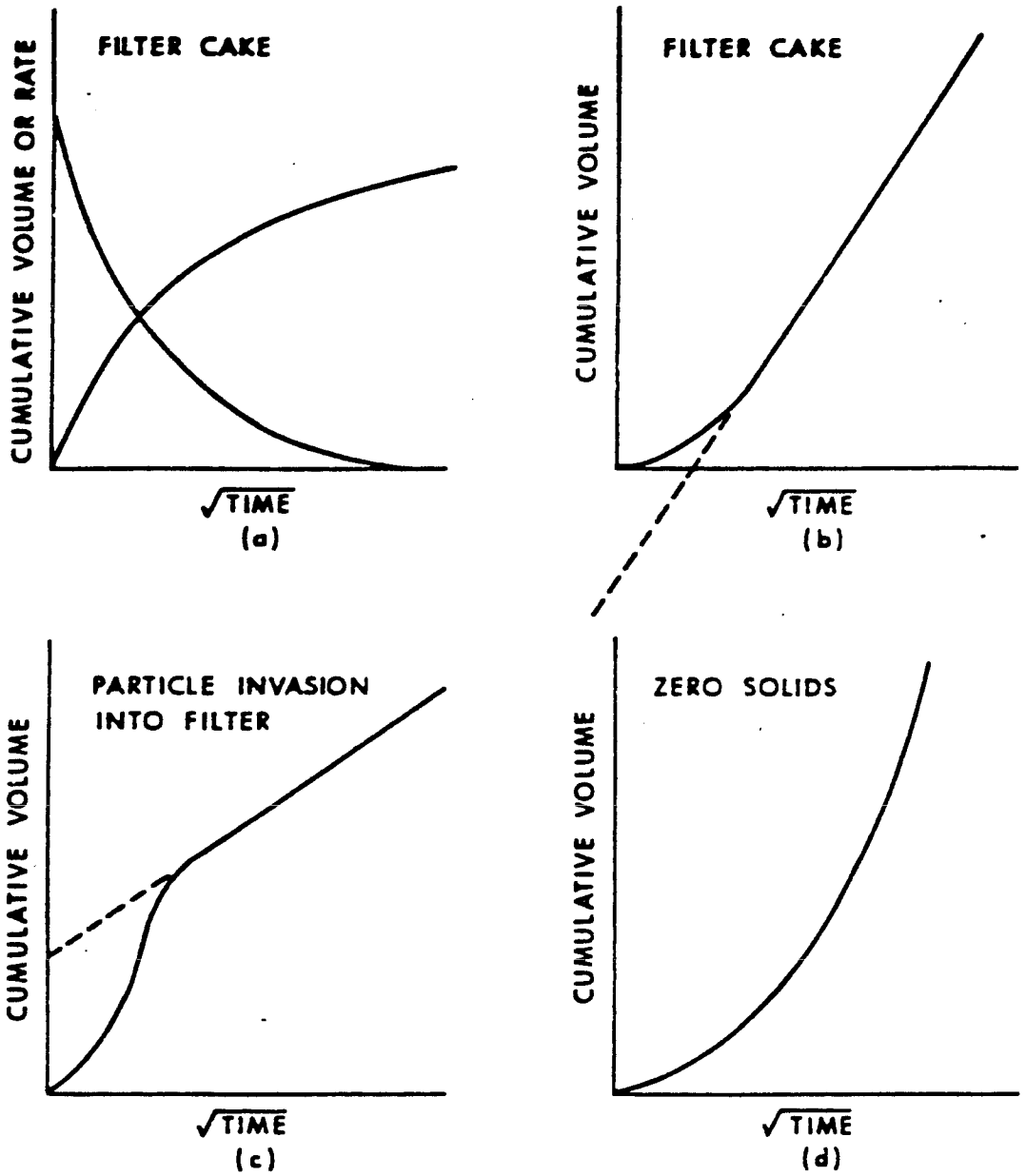

Figure IV-21. Types of curves obtained from membrane filter tests. (From Ref. 65)

prefiltering brine, for instance, prior to injection cannot be accurately estimated since deficiencies in injection reservoir properties, well completion practices or poor operating procedures may be in part responsible for injection difficulties. These types of impairment mechanisms cannot be resolved by membrane filtration tests except indirectly when test results indicate no potential for particulate-induced damage. A detailed reservoir assessment and careful control of drilling and operational practices are essential elements of a properly functioning injection system.

Another deficiency of the Barkman and Davidson method is due to the fact that water quality data are obtained under constant differential pressure conditions. Experience has shown that this model tends to underestimate injection well performance. It is extremely important to use a membrane filter with the appropriate pore size to best simulate the injection formation. The effect of particulate size distribution on the permeability of a porous matrix is shown in Figure IV-22. Champlin, et al.[70] suggested the following expression is useful in relating formation porosity and permeability to the mean pore diameter of an injection zone.

$$D = 4(1 - \phi)/[(\phi \times 10^3)/5k]^{\frac{1}{2}} \qquad \text{(IV-36)}$$

where ϕ is porosity, K is permeability (md), and D is the mean pore diameter. They subsequently demonstrated, by means of core tests, that the largest size particle passing through core samples was about 25 percent smaller than the calculated mean pore size (Figure IV-23). The Kozeny relationship can also be expressed as follows:

$$k = \frac{d^2\phi^3}{(1-\phi)^2} \qquad \text{(IV-37)}$$

or

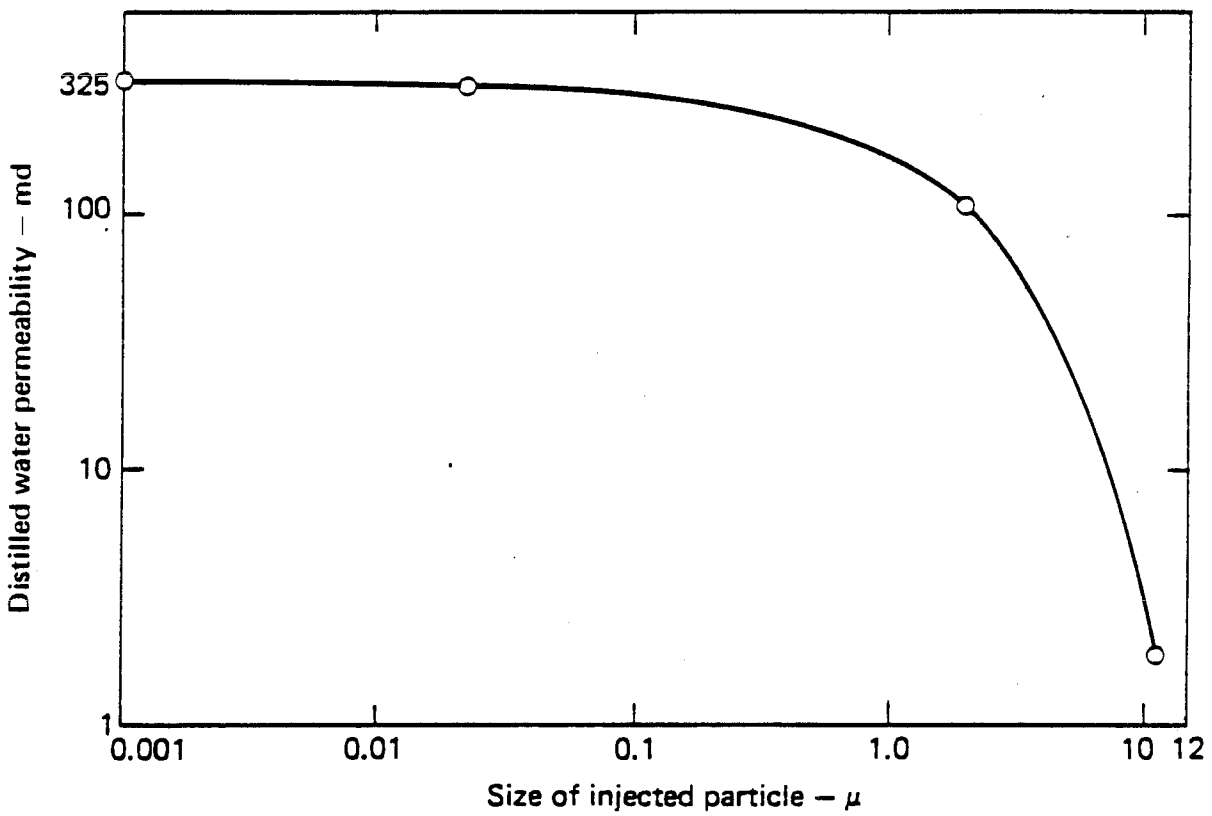

Figure IV-22. Effect of particle injection on the permeability of selected sandstone cores. (From Ref. 70)

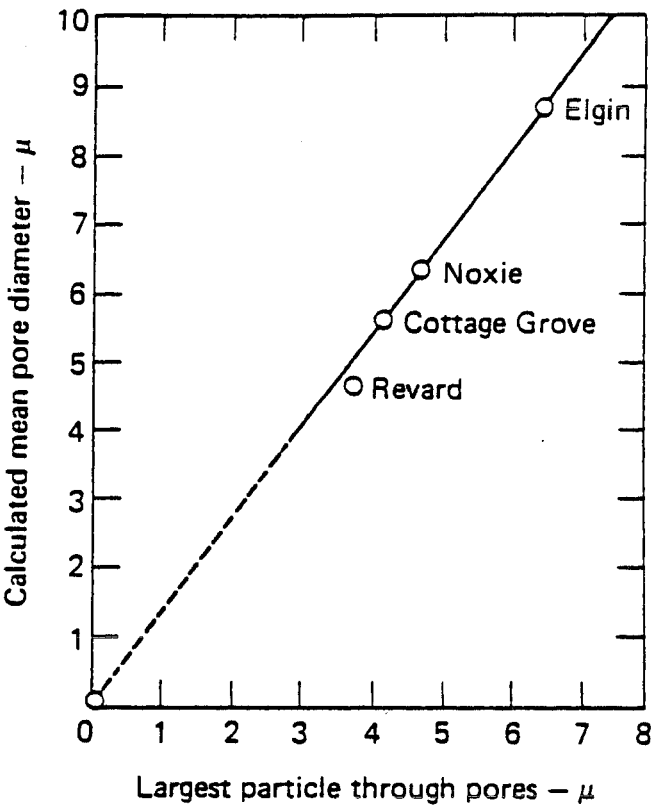

Figure IV-23. Relationship of calculated pore diameter to the largest particle passed through selected core samples. (From Ref. 70)

$$k \cong \frac{d^2}{14.44} \qquad \text{(IV-38)}$$

where: k = permeability (md)

d = median grain diameter (μm)

ϕ = fractional porosity

Usual practice is to estimate pore size distribution of the injection formation using some form of the Kozeny equation or laboratory capillary pressure data and then select the most appropriate membrane filter for water quality testing. Membranes with pore size distributions of 10 μm to 12 μm are most commonly used. Total suspended solids estimates are always based, however, on use of 0.4 or 0.45 μm membrane filters.

Calculation of half-life estimates for injection wells based on the Barkman and Davidson model is straightforward but time consuming. A code, written for the Hewlett-Packard Model 67 (HP-67) calculator, is provided as Appendix II. This code calculates injection well half-life using either the wellbore narrowing or invasion models.

Simplified Half-Life Estimates

In order to utilize the Barkman and Davidson method for estimating injection well half-life, it is first necessary to measure a suspended solids concentration for the water being evaluated. Field measurement of suspended solids concentration, while not difficult, is laborious. A simple method can be used to eliminate the necessity of measuring suspended solids concentrations. This method also eliminates the necessity of estimating the filter cake to brine density ratio.

The basis for simplified wellbore narrowing half-life estimates can be developed as follows:

$$T_{\frac{1}{2}} = (F)(G)$$

For $\frac{k_c}{k_f} < 0.05$

$$G \cong 3 \frac{k_c}{k_f} \ln \frac{r_e}{r_w}$$

Since $$F = \frac{\pi r_w^2 h}{i_o w} \frac{\rho_c}{\rho_w}$$

$$T_{\frac{1}{2}} = \frac{k_c}{w} \frac{\rho_c}{\rho_w} \frac{\pi r_w^2 h}{i_o} \frac{3}{k_F} \ln \frac{r_e}{r_w}$$

But $$\frac{k_c}{w} = \frac{S^2 \mu}{2A^2 \Delta p} \frac{\rho_w}{\rho_c}$$

where S is the slope of the cumulative volume vs. the square root of time curve

Substituting:

$$T_{\frac{1}{2}} = \frac{S^2 \mu}{2A^2 \Delta p} \frac{\pi r_w^2 h}{i_o} \frac{3}{k_F} \ln \frac{r_e}{r_w} \qquad \text{(IV-39)}$$

IV-17. Davidson Method

One explanation for overly conservative estimates of injection well performance by the Barkman and Davidson method is due to the uncertainty in specifying invasion radius. If the invasion radius could be better defined, then the Barkman and Davidson invasion model could be better utilized in estimating well performance. Another difficulty with the Barkman and Davidson methodology results from the constant differential pressure requirement. A more recent paper by Davidson[68] discusses the utility of the constant flow methodology in estimating injection well performance.

Invasion

According to Davidson, the minimum injection rate (Q_c) required to prevent deposition (i.e. support deep invasion of suspended solids) is given by:

$$Q_c = 3.6 \left(\frac{\delta \rho}{\rho}\right)^{\frac{1}{2}} \frac{d_o}{a^{\frac{1}{2}}} \qquad \text{(IV-40)}$$

where: suspended solids are greater than 1 μm in size and

Q_c = B/D/FT required to prevent deposition

$\Delta\rho$ = (density of suspended solids) - (density of brine), g/cc

ρ = density of brine, g/cc

d_o = initial formation pore diameter, μm

a = particle diameter of suspended solids, μm

Injection formation pore diameter (d_o) can be estimated using laboratory capillary pressure data or empirical relationship between porosity and permeability as described previously. Equation (IV-40) implies that the velocity required to prevent deposition decreases as particle size increases because larger particles protrude into regions of higher velocity adjacent to pore boundaries than do smaller particles.

Invasion Radius

Invasion radius is given by:

$$r_a = \frac{K_F}{d_B}^{0.75}_{3} \qquad \text{(IV-41)}$$

where r_a = invasion radius in terms of the number of wellbore radii

$\bar{d}_B = 3\ a/d_o$

$\bar{K}_F$ = the constant flowrate asymptotic permeability

Estimating K_F presents some difficulty. The significance of K_F is shown in Figure IV-24. Type (a) curves represent internal pore bridging or the start of surface filtration whereas Type (c) curves indicate formation of non-retaining beds (i.e. deep invasion). The parameter $\Delta p/\Delta p$ is the relative differential pressure change and Y_w is the asymptotic value of $\Delta p/\Delta p$. Since permeability is inversely proportional to differential pressure, Y_w can be

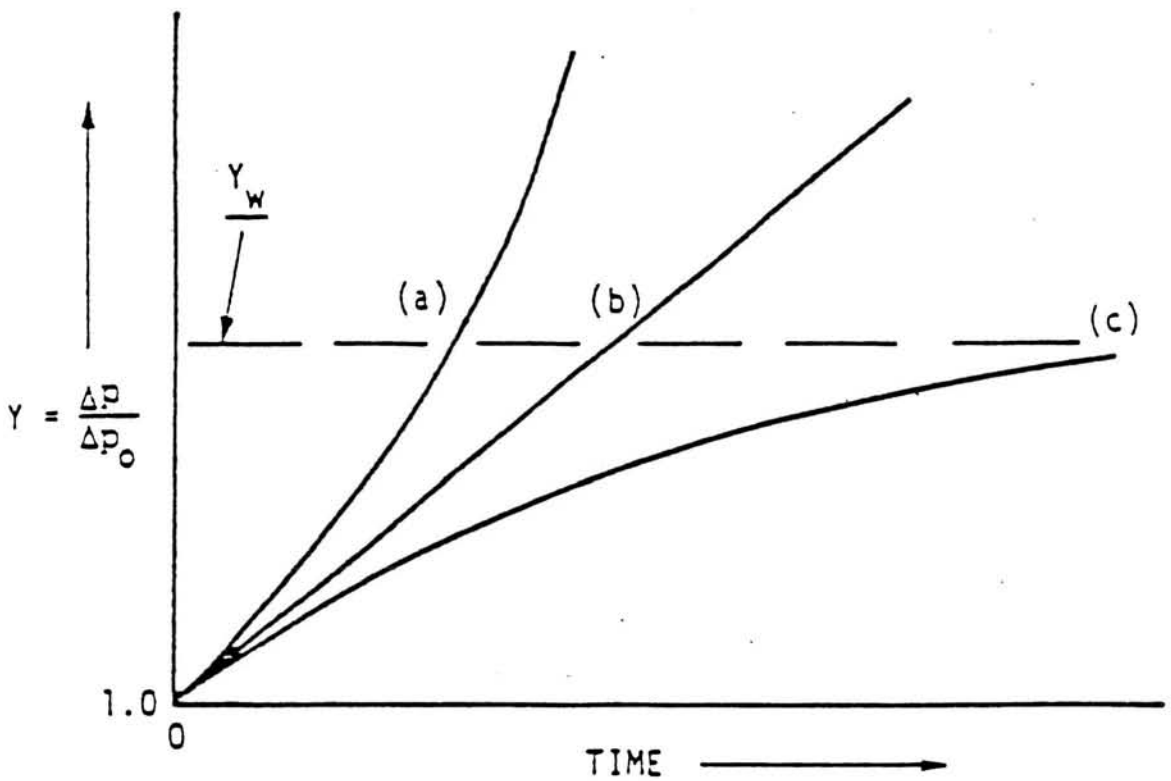

Figure IV-24. Constant Rate Impairment Curves. (From Ref. 68)

used to calculate K_F. Y_w is estimated on the basis of a core test run at constant flow where the core is characteristic of the injection formation.

Half-Life Estimates

An estimate of the time in years required to attain a 2 to 1 reduction in effective injection formation permeability ($t_{\frac{1}{2}}$), assuming a > 1 micron, can be obtained from:

$$t_{\frac{1}{2}} \sim [Q_C]\,[(3.6)(\rho_s)/(\Delta P)(w)(a)] \qquad \text{(IV-42)}$$

where w = solids concentration, ppm

ρ_s = suspended solids density, g/cc

IV-18. Measuring Water Quality

The NACE standard (TM-01-73)[71] for measuring water quality is discussed by Patton[72]. The test consists of passing a known volume of injection water through a membrane filter under constant pressure and recording the flow rate and cumulative volume of water at intervals. The test is qualitative in nature and indicates the relative quality of injected water. Data is usually represented in the form of a graph of flow rate versus cumulative volume of water filter. The standard calls for the use of a 47 mm diameter, 0.45 μm membrane filter. The various configurations for carrying out a filter test are shown in Figures IV-25 to 27.

The basic test system configuration is shown in Figure IV-25. A reservoir is filled with injection water and pressurized with nitrogen. Fluid is then forced through a membrane filter mounted in an appropriate holder. A vent valve is used on he filter assembly to purge any trapped air before the filtration test is initiated. The filter assembly can also be purged using a vacuum pump as shown in Figure IV-26. For geothermal applications the system shown in Figure IV-27 is preferable since the properties and quantity of suspended solids could be significantly influenced by temperature, aeration and, to a lesser extent, pressure drop.

Temperature effects can be extremely significant in carrying out water quality measurements. Spent geothermal waters may commonly be saturated or supersaturated with respect to dissolved silica. Temperature decline would tend to promote additional silica precipitation. Calcium carbonate (calcite) has an inverse temperature solubility. Therefore, cooling a water or brine sample prior to and during testing may actually improve water quality with respect to the suppression of carbonate precipitation. Introduction of air

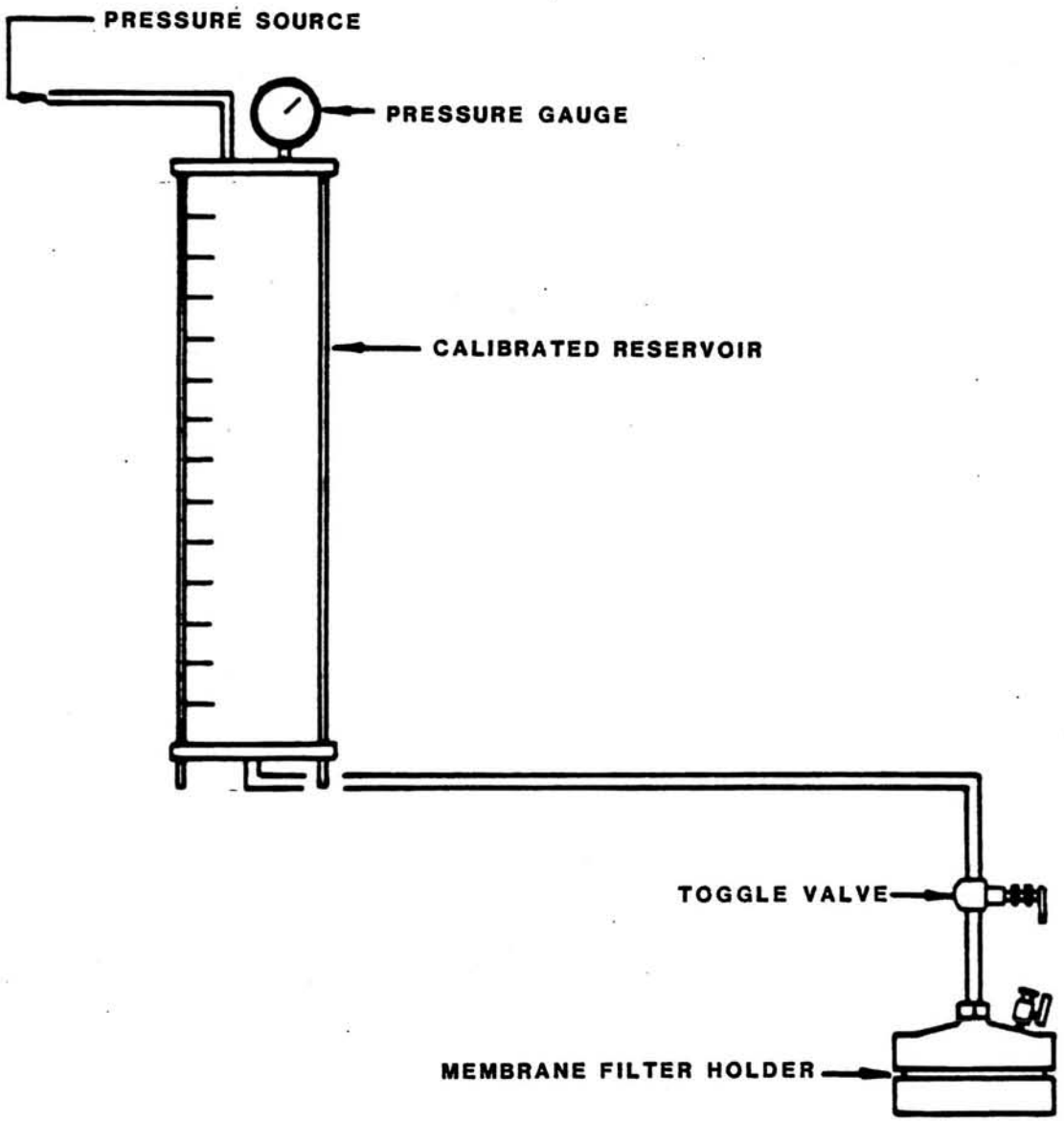

Figure IV-25. A two-stage apparatus with pressure gauge and regulator for repressuring and testing a sample collected in a reservoir rather than from the water handling system as in Figure IV-27. This apapratus is used primarily when the sample point cannot be readily adapted to on-stream application. To ensure that test conditions correspond with those of Figure IV-27, nitrogen gas is used to raise reservoir pressure to 20 psig.

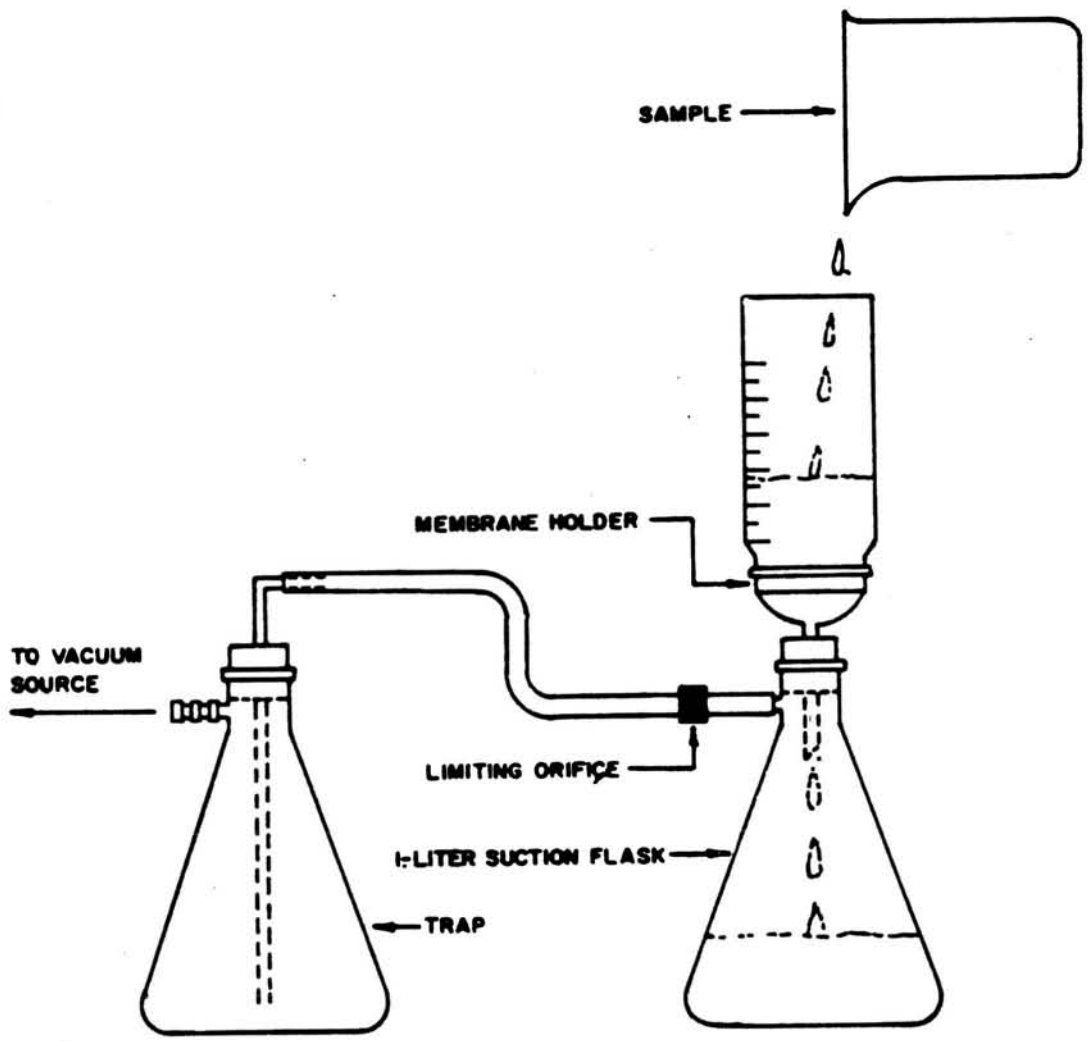

Figure IV-26. Apparatus for testing aged samples(secondary suspended solids) by vacuum filtration. The sample is poured into the cylinder over the holder, which contains a pre-weighed membrane filter. The vacuum source may be either a vacuum pump or water aspirator.

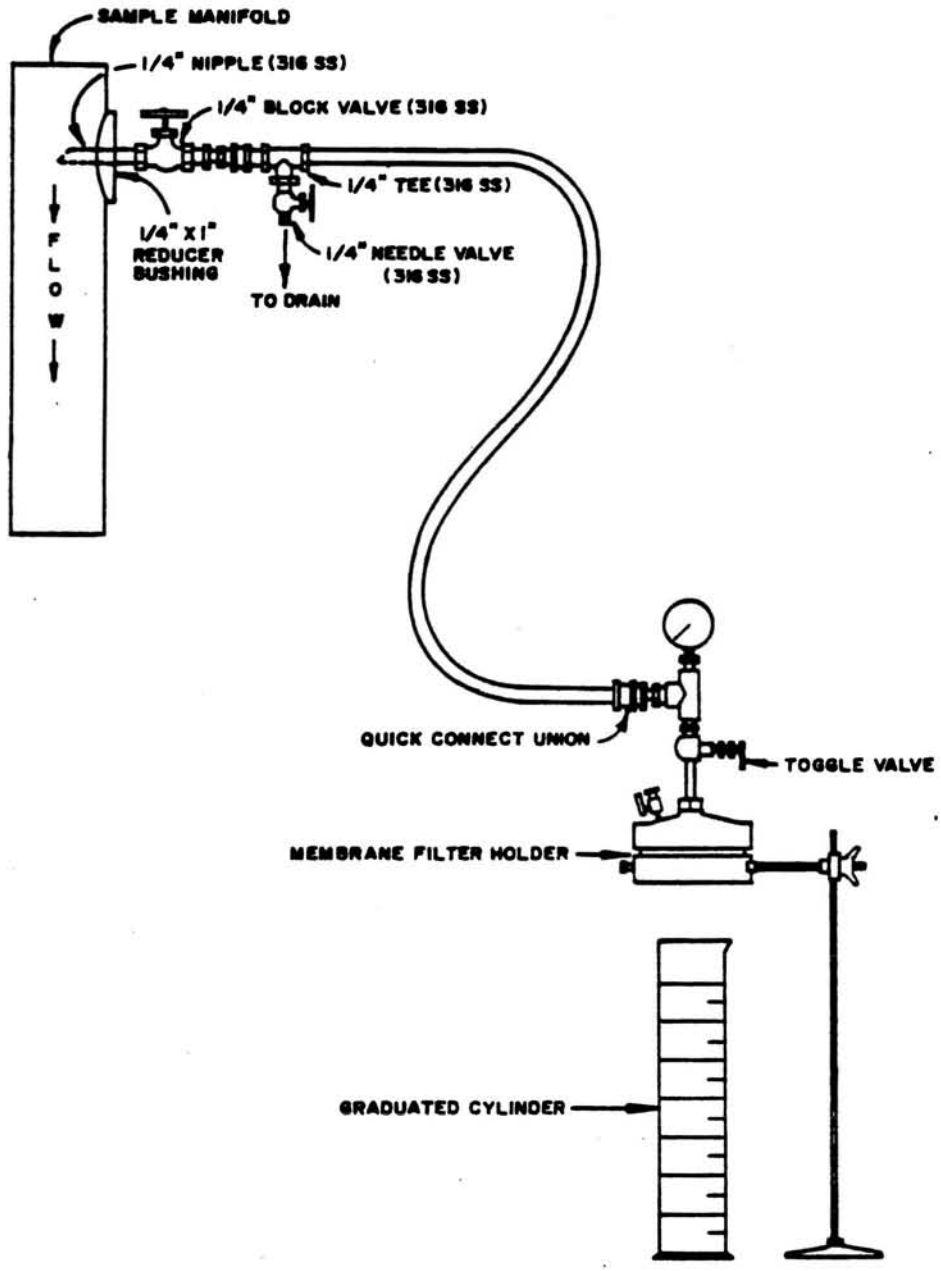

Figure IV-27. Membrane filter test apparatus showing a membrane filter holder connected to a water supply system. The ¼" block valve and needle valve shown near the top of Figure IV-27 control system pressure within prescribed limits. Just above the filter holder is a quick-opening type toggle valve to permit immediate, full-stream flow essential to timing accuracy.

into a sample could induce precipitation of dissolved iron that could manifest itself as a significant reduction in apparent water quality. In general, the sampling and water quality measuring technique should be designed to minimize or eliminate changes in the basic injection water properties. In this regard, the ability to sample directly from a flowing reinjection stream and to perform the filtration test at or near in-situ temperature would be highly desirable.

The influence of temperature on water quality is shown graphically in Figures IV-28 to 31. Membrane filtration, injectability, or water quality test results obtained at the University of Minnesota Seasonal Thermal Energy Storage (STES) test facility[73] are summarized in Figures IV-28 and 29. Test results indicated that fluid injectability decreased significantly as a function of increasing temperature. Subsequent analysis of filter cakes formed on 0.4 and 10 micron membrane filters indicated that permeability impairment was due primarily to deposition of calcite ($CaCO_3$). The injectability test results are consistent with geochemical models which predicted that calcite precipitation would occur when reservoir fluids were heated to temperatures in excess of about 18°C. A water conditioning system is now being installed at the University of Minnesota STES facility to control calcite precipitation. If the water quality tests had been performed at ambient temperature, an overly optimistic conclusion would have been reached concerning ultimate fluid injectability.

Field core flooding test results are summarized in Figure IV-30[74]. Permeability of flashed (atmospheric pressure) hypersaline brine from the Magmamax No. 1 well, Salton Sea Geothermal Field was used to flood core samples of Kayenta sandstone at temperatures between 28 and 70°C. The brine was prefiltered, using a 1 μm pore size cartridge filter, immediately before

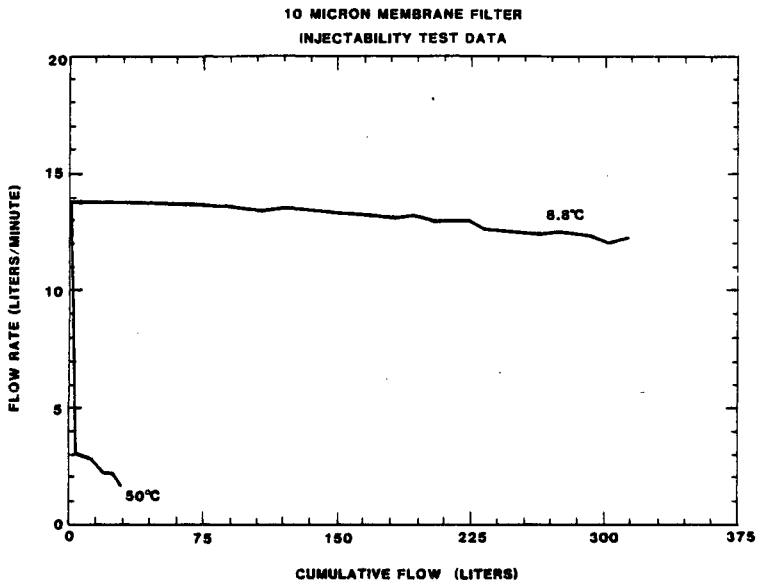

Figure IV-28.

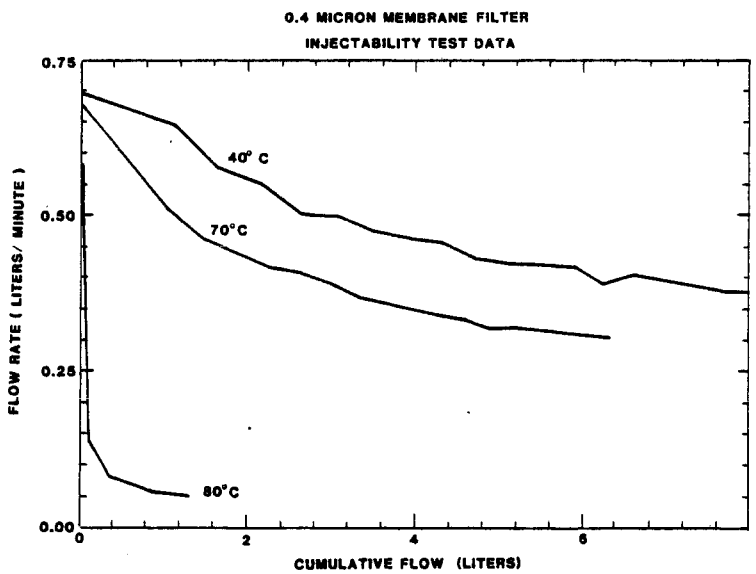

Figure IV-29.

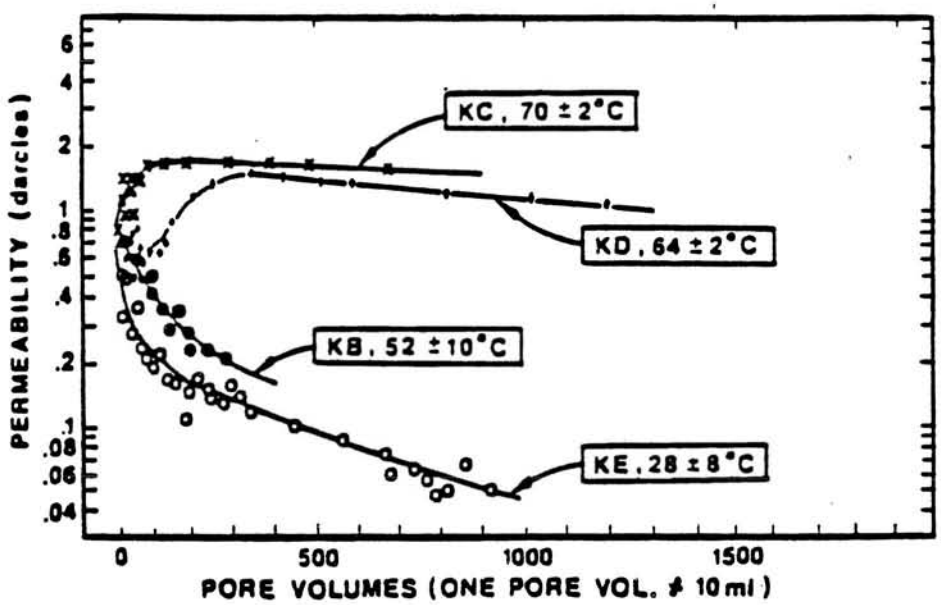

Figure IV-30. Plot of permeability versus volume of throughput for four cores of Kayenta sandstone at various brine temperatures. All runs were with prefiltered (1 μm) acidified (pH ≤ 4.6) brine and cores at 500 psi confining pressure.

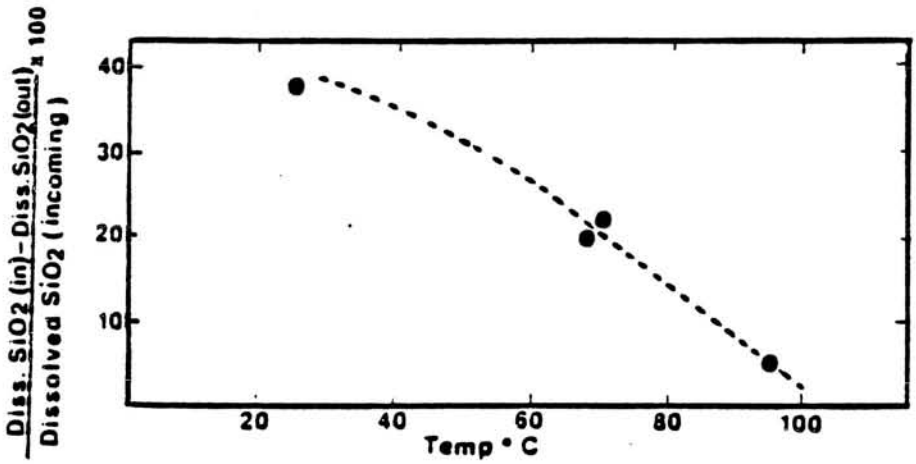

Figure IV-31. Percentage of dissolved silica precipitated in core for runs of Kayenta sandstone at various temperatures.

flowing into the core samples. The temperature dependence of core permeability is obvious. The cause of permeability impairment was deposition of dissolved silica as shown in Figure IV-31.

In carrying out membrane or core flooding water quality tests, the differential pressure set against the reservoir analog is of some importance because compression of filter cakes that may form during a test influence filter cake hydraulic properties. The NACE standard is 20 psig ± 10%. Jorda[53] emphasizes that a differential pressure of 80 psig should be used in all cases. In an actual injection well of several thousands of feet depth, the hydrostatic head is such that filter cakes are compressed by pressures of hundreds to thousands of psig. In selecting an appropriate differential pressure for a water quality test, one should select the highest possible pressure consistent with experimental conditions. The preferred method of testing is to bypass injection water directly from a pressurized injection flow line to the water quality testing apparatus. This method eliminates the need for external pumps or sources of pressurized inert gases. Core testing should be carried out in a manner that precludes turbulent non-Darcy flow within the core sample.

Water Quality Testing Equipment

Water quality testing systems have been described by several authors [8,53,60,62,64,71,72]. Field methods for obtaining water quality data on geothermal process streams are described by Netherton and Owen[75], Hasbrouck, et al.[76], Hauer, et al.[77] and Owen, et al.[73,78-80]. The geothermal testing systems range from relatively simple, manually operated devices to complex automated or semi-automated systems that represent a significant investment in both time and money. In general, the simpler manual system can provide reasonable results at very modest cost. Embellishments that add to convenience

of use involve use of automated flow measuring devices. In systems which operate on a pressurized bypass line, throughput rates through a core sample or membrane filter may be so high as to make use of 2 liter graduated cylinders awkward. A simple mass flowmeter is described in Ref. 75 for use with geothermal brines. This system makes use of a calibrated load cell from which is suspended a large capacity (20 gallon bucket). Turbine flowmeters are not recommended for geothermal field service owing to their fragile nature and susceptibility to corrosion. Sophisticated mass flowmeters with totalizers manufactured by Micro Motion, Boulder, Colorado, have been successfully used in conjunction with the assessment of geopressured geothermal brines and Seasonal Thermal Energy Storage waters.

A simple apparatus for carrying out water quality tests using membrane filters is shown in Figure IV-32. This system employs a pump to permit testing unpressurized process streams. Any suitable pump may be used. The gear pump, if used, should be equipped with an electronic speed control. The pump should also be mounted on a sound isolation stand as it is quite noisy. Differential pressure across the filter is controlled with the combination of the filter ball valve and the by-pass control valve. Total filtrate volume can be measured using a 2-liter plastic graduated cylinder or a flowmeter. The by-pass discharge fluid should be dumped to a tank or pit. The system should also be mounted on a sound isolation stand as it is quite noisy. adjacent to the filter holder which is a standard Millipore 47 mm diameter high pressure membrane filter holder. Alternatively, the filter holder may be mounted inside of a clam-shell type of heater. The heater can be controlled using any standard heater controller unit. Materials of construction should be corrosion resistant. Use of 316 stainless steel fittings and valves in conjunction with Inconel 600 tubing may be a reasonable configuration in most

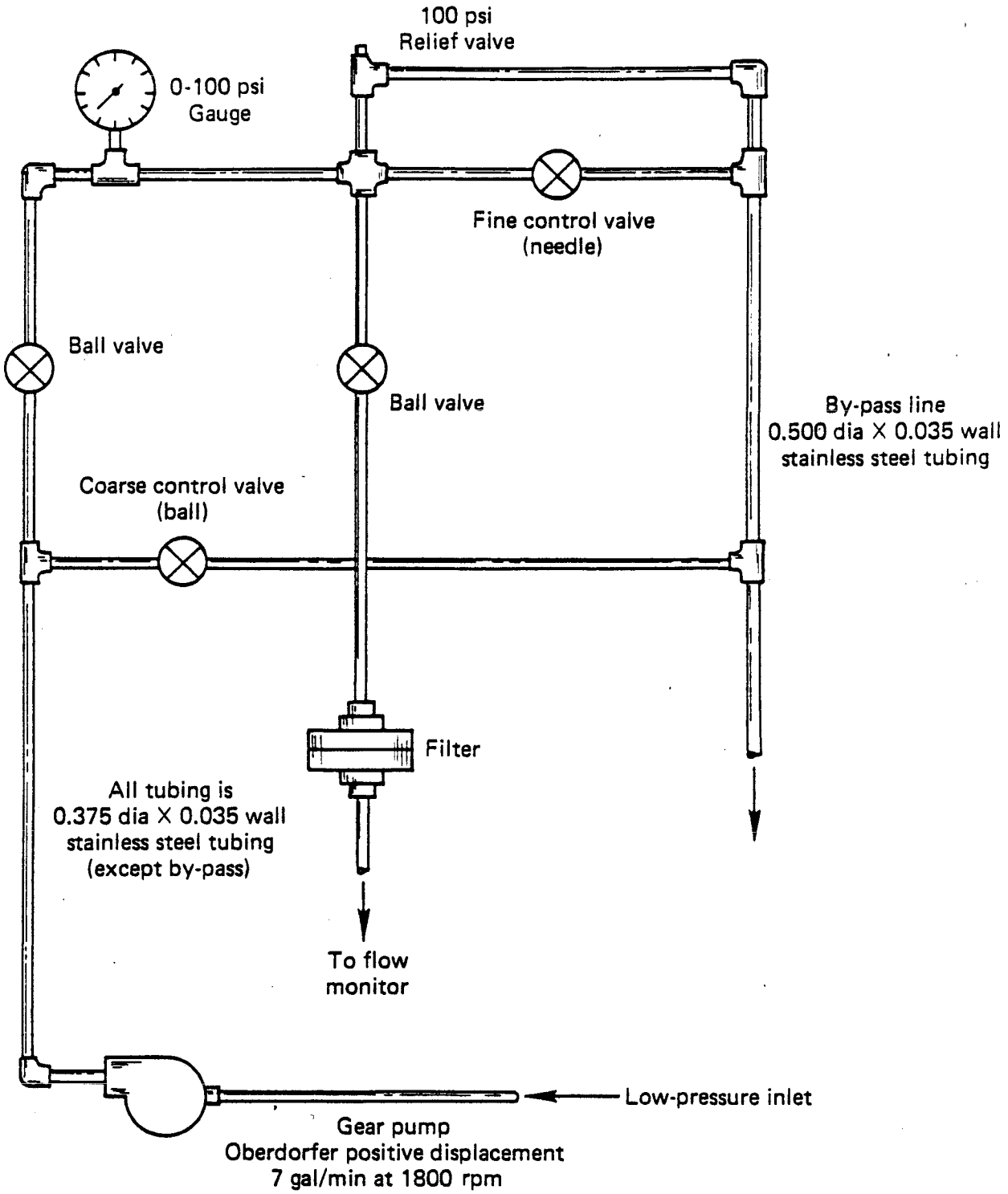

Figure IV-32. Simple membrane filtration water quality testing apparatus. (From Ref. 80) The apparatus can be mounted on an aluminum or steel stand-alone frame.

instances. However, one should be familiar with the potential for generation of small amounts of corrosion product particulates that could affect measured water quality. Safety considerations are also of obvious importance.

A more elaborate water quality testing apparatus which includes a prefilter assembly is shown in Figure IV-33. The prefilter permits evaluation of the effect of brine processing on water quality. Cartridge filters with pore sizes ranging between 1 and 10 μm can be used. Pressure relief valves maintain safe pressure levels in the test system. Differential pressure across the membrane filter is maintained using the by-pass control valves. This system should also be adequately insulated.

A combination core flooding-membrane filter water quality testing apparatus that was successfully used to evaluate hypersaline brine from the Salton Sea Geothermal Field is described by Netherton and Owen[75]. This system employed a pressure vessel for core samples that had a capability for applying confining stress to the core sample via hydraulic oil. A Tygon sleeve was used to isolate the core sample from the hydraulic fluid. The details of the pressure vessel are shown in Figure IV-34. The vessel can be constructed using low carbon steel. Fluid feed throughs should beconstructed using corrosion resistant materials. Low carbon steel end caps were found to corrode (rust) in the humid field environment. They were subsequently replaced with Ti-6Al-4V alloy end caps and the corrosion problem was eliminated.

Core Samples

Core holders, modeled after the Millipore high pressure membrane filter assembly can be easily fabricated. The holder consists of a central ring in which a core sample is cemented and two end caps. A core holder built by Terra Tek Research[73] accepts 1 inch diameter core by 1.5 inches long with a

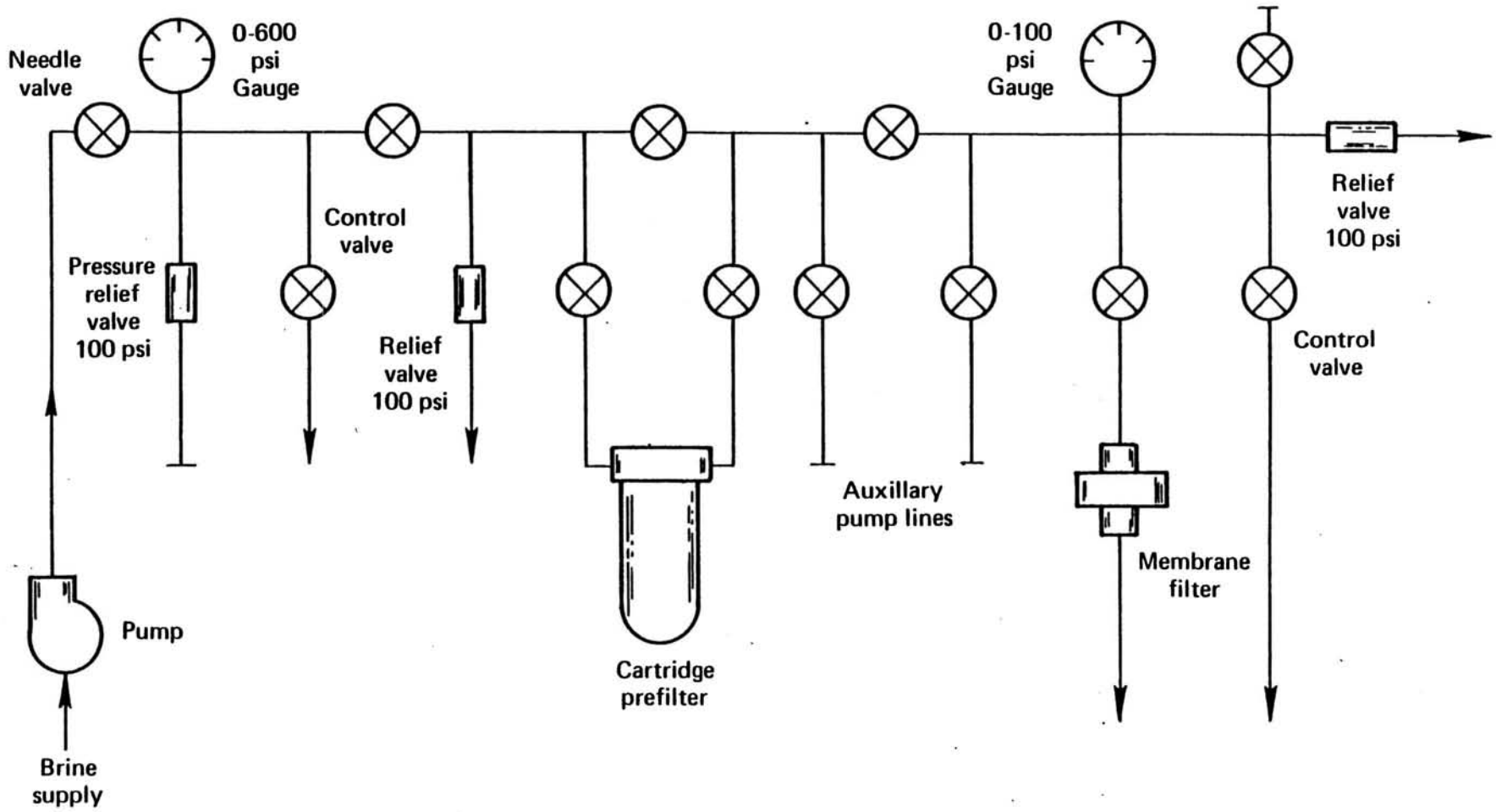

Figure IV-33. Injectivity test apparatus for membrane filtration water quality tests. (From Ref. 80)

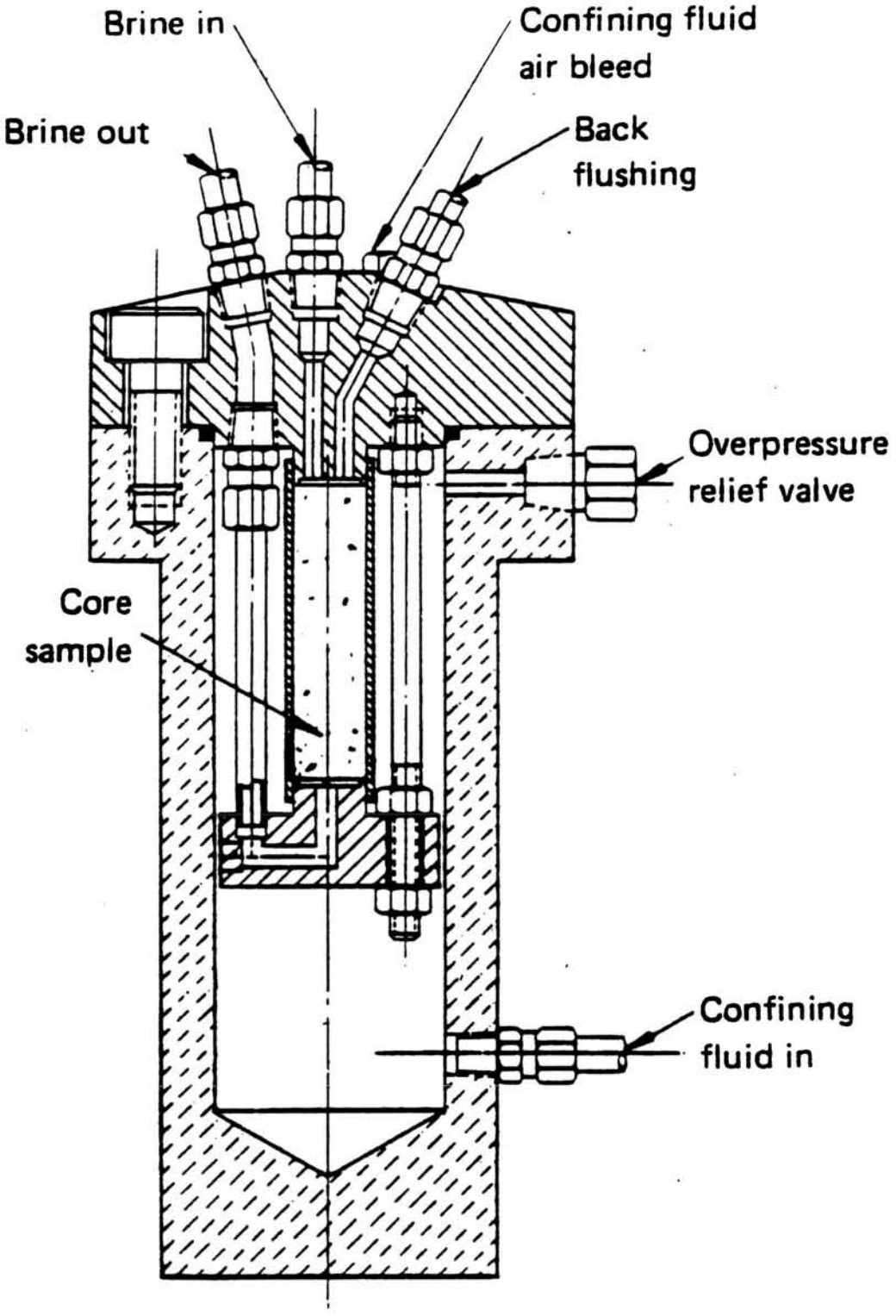

Figure IV-34. Core flooding pressure vessel.

tapered longitudinal section. Stainless steel screens are placed on each end of the core to insure uniform distribution of fluid.

Core samples are placed in the cylindrical center section of the core holder. The annulus is then filled with DURALCO 700 epoxy available from Coltronics Corporation. A mixture consisting of 8 parts hardener to 100 parts resin was found to be satisfactory. This mix will harden at room temperature in about 2 hours. Heating the mixed epoxy will decrease its viscosity and accelerate the curing time. To facilitate the flow of the epoxy around the sample and to insure that there will be minimum voids in the potting material, the sample and sample holding ring can be preheated to approximately 80°C.

Alternatively, the hardener/resin mixture can be heated in an oven at 100°C for 10 to 15 minutes. Periodically, the mixture should be stirred to insure good mixing. The epoxy may then be flowed into the annulus as described above.

The core sample holder and epoxy mount were pressure tested at temperatures to 175°C as follows:

•	Nitrogen:	Steel Sample,	200 psi @ 175°C (4 hrs)
		Sandstone,	200 psid @ 175°C (2 hrs)
•	Water:	Steel Sample,	2000 psid @ 175°C (3 hrs)
		Sandstone,	200 psi @ 175°C (3 hrs)
			4500 psi @ 175°C (3 hrs)
			400 psi @ 175°C (1 hr)(steady flow)

Massillon sandstone was used in the above tests. A steady-state flow rate of 1 ml/min was used for the dynamic test. Conventional low viscosity epoxies were found unsatisfactory because they tended to infiltrate the core sample to an excessive extent.

IV-19. Chemical Stability Tests

A primary source of injection well impairment results from injection of

waters that are either chemically unstable or capable of forming chemical precipitates when mixed with in-situ formation waters. An injected water, after passing through a processing system that might include various types of filtration and other kinds of processing may appear to the casual observer as being clear and particle free. However, certain dissolved species may precipitate if given sufficient residence time or if subjected to a temperature change. The purpose of chemical stability tests is to determine the long-term stability of reinjected waters.

Typical data pertaining to the chemical stability of dissolved silica in hypersaline brine is illustrated in Figures IV-35 and 36[81,82]. In most instances, dissolved silica and iron in various forms will be the most important precipitating species. However, precipitation of other cations such as calcium and barium as carbonates and sulfates, should also be considered. For example, Raber, et al.[83] found that water from the Salton Sea, when mixed with flashed hypersaline geothermal brine, produced copious amounts of sulfate precipitates.

Chemical stability tests are performed by placing samples of water in air tight containers and incubating the samples for varying periods of time at a desired temperature while maintaining anaerobic conditions. Introduction of air can cause precipitation of dissolved iron species and thus should be avoided. At the end of the incubation period samples are rapidly filtered and the stability of the water or brine is based on the amount of recovered precipitate and the chemical composition of both the precipitate and the residual filtrate. Chemical compatibility of two waters is established using the same basic technique described above after mixing the two waters in any desired ratio. Hill, et al.[81] describe a testing procedure which involves incubation of sample waters in glass ampules that are pressurized with nitrogen and then

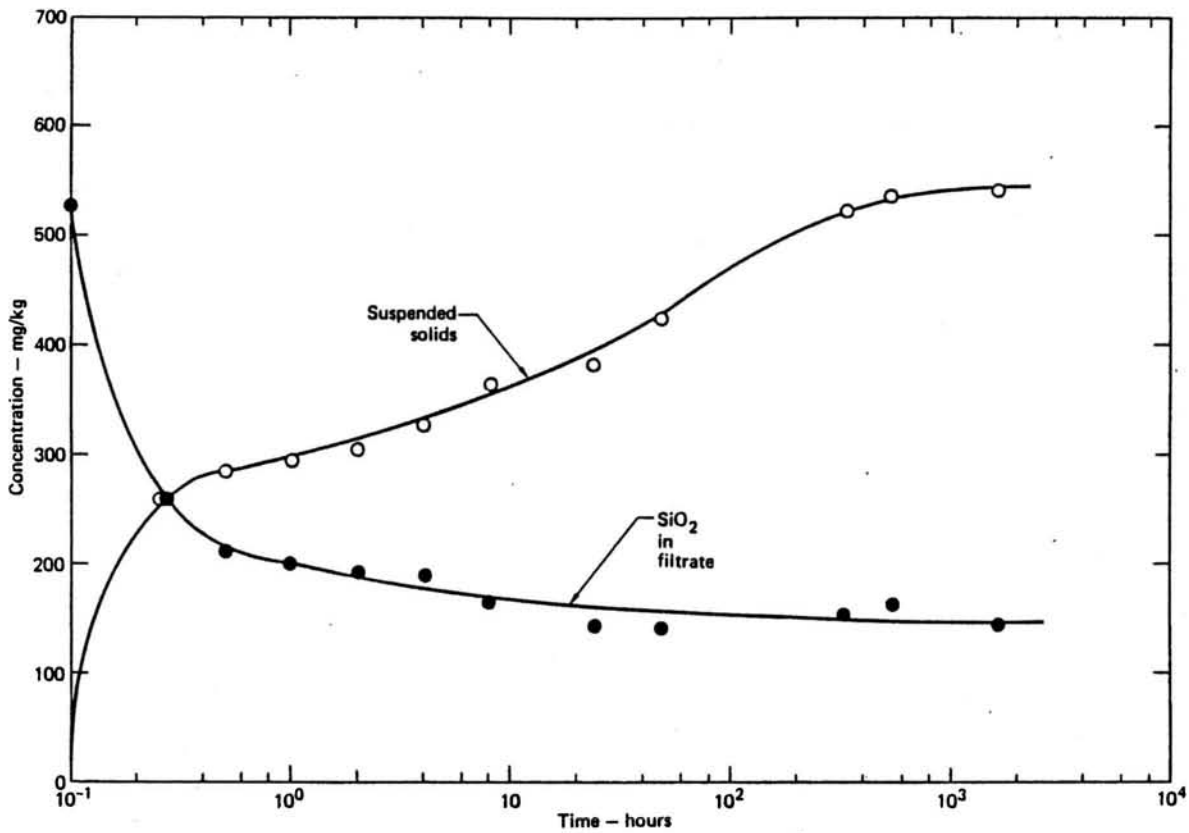

Figure IV-35. Concentration of suspended solids and dissolved SiO_2 in effluent hypersaline geothermal brine after incubation at 90°C. (From Ref. 81)

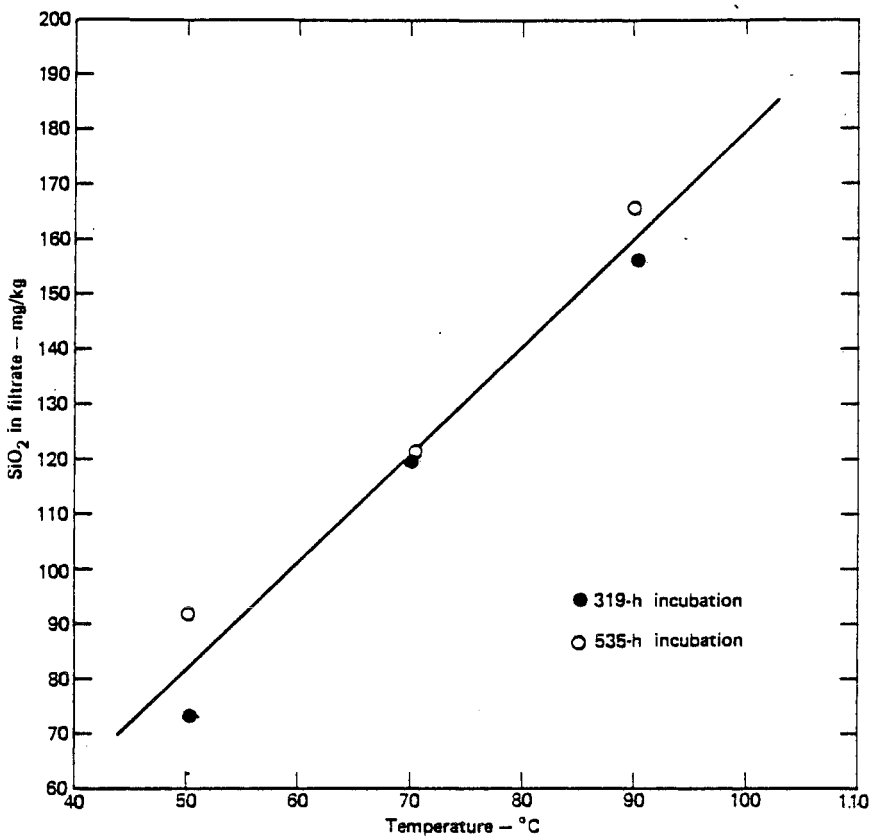

Figure IV-36. Solubility of SiO_2 in hypersaline geothermal brine. (From Ref. 81)

sealed by melting the narrow neck of the container with the flame from a small torch or bunsen burner. After the incubation run is completed, the ampule is opened using a special hot wire device described in Ref. 81.

A much easier procedure has been successfully used by the authors in the evaluation of hypersaline brine from the Imperial Valley. Samples are obtained initially in a 1 gallon capacity thermos jug. The jug is quickly taken into a field laboratory where 100 ml plastic bottles are filled, sealed and then placed in a vacuum oven preheated to the desired temperature. The thread mouth of the bottles is heavily wrapped with teflon tape before securing the caps. Samples placed under vacuum show no tendency to oxidize. At temperature of 100°C, plastic bottles tend to soften. To avoid tipping bottles use of aluminum support sleeves is recommended. When the samples are sequentially withdrawn from the oven, they are rapidly filtered using a 0.45 μm membrane vacuum filtration system. When sufficient liquid has been filtered for chemical analysis, an aliquot is taken and immediately stabilized using procedures dissolved in Chapter II. The remainder of the sample is rapidly filtered and the suspended solids, after being washed with deionized water and dried under vacuum, are weighed.

IV-20. Brine Treatment

Geothermal systems which require subsurface disposal of spent brine usually must include treatment facilities for insuring that injected brines are compatible with the subsurface injection formations. The major objectives of the brine treatment systems are to remove extraneous suspended particulates, which can cause mechanical plugging of the injection formation, and to insure that the brine is chemically stable to prevent formation of precipitates downhole or within the injection formation. Control of biological activity is usually not a concern in geothermal operations owing to the effects of high

temperatures and moderate to high salinities. However, standard techniques can be employed to assess the potential for downhole problems due to bacterial agents[103]. The corrosivity of injected effluents is a matter for concern if accelerated corrosion of casing and plugging of the injection formation by corrosion products is to be avoided (see Ref. 104). Usual practice is to operate the injection system as a closed system to avoid contamination by atmospheric oxygen. Introduction of air can cause additional precipitation of dissolved constituents as well as increase the corrosivity of the injected brine.

the following processing units:

1) gravity settling
2) flotation
3) centrifical separation
4) filtration
5) clarification/crystallization
6) chemical treatment

Most geothermal treatment systems will need filtration systems to pretreat injected waters. Depending upon the level of particulate matter n the water sedimentation units might or might not be required. The purpose of the sedimentation units is to reduce the particulate loading to downstream filters. The length of time a filter can be operated before backwashing of filter elements or replacement of filter elements is required is an important operating parameter that significantly influences operating costs. In certain geothermal systems such as the hypersaline resources of Southern California, suspended solids concentrations in brine flashed to atmospheric pressure can range between 500 to 2000 mg/l. In these cases, direct operation of filtration systems is not practical and some form of settling system is mandatory for economic water treatment operations.

For the most part, particulate matter formed during the geothermal energy conversion process consist of chemical precipitates which tend to be fine-grained. These particulates may adsorb evolved gases which tends to further diminish their settling rates. Effective removal of this type of material by use of settling systems may necessitate chemical treatment schedules and mechanical agitation to encourage flocculation of discrete particles into larger, more dense masses.

Clarification systems are used in geothermal operations to enhance precipitation of supersaturated species dissolved in the goethermal water while simultaneously promoting flocculation of particulates and particle removal by a combination of gravity sedimentation and filtration. These units are intended to produce an overflow effluent which is chemically stable at the treatment conditions with less than 50 mg/l of suspended particulates. In order to function as gravity settling tanks, the units must be physically large. It is also necessary to operate the units under closed-system conditions to preclude air contamination and post-processing precipitation of additional solids. The clarified overflow is polished by means of a high efficiency filtration system to produce an effluent that might contain between 0.5 to 1.0 mg/l suspended solids.

The important components of an integrated reaction-clarification system include the reaction zone, where mechanical agitation is used to promote particle growth by enhancement of liquid phase-solid phase contact, the gravity settling basin, where density segregation of particulates is accomplished, and the sludge bed filtration zone where liquid is forced to flow through settled sludge to achieve additional particle removal by the filtration properties of the settled sludge.

Crystallization is a high temperature/pressure version of reaction clarification process. Whereas reaction clarification is employed at atmospheric or near atmospheric pressure and temperature. Crystallizers can be operated at much higher temperature and pressure. Obviously, mechanical consideration will be more stringent since the crystallizer operates as a pressure vessel. In operation, the crystallizer is intended to reduce supersaturated species dissolved in the geothermal water to saturation levels in order to limit or eliminate scale deposition downstream of the crystallizer unit. Patented designs now are available which permit the crystallizer to function as both a scale control system and as a steam separator. Provision can also be made for recovery of precipitated sludge directly from the crystallizer while it is operating. Alternatively, precipitated material can be allowed to pass through to downstream water treatment components where the suspended solids can be removed at atmospheric conditions. High temperature recovery of precipitated solids could be desirable under certain conditions. For example, mineral recovery schemes for separation of heavy metals from hypersaline brines would benefit from the ability to segregate concentrates at their point of formation.

All processing systems which concentrate suspended solids by sedimentation processes produce a water-rich sludge which must be further processed prior to ultimate diposal. The processing consists of additional steps that reduce the water content of the sludge. These steps might include use of centrifuges, thickeners and filter presses in combination or alone. Descriptions of the mechanical components used to reduce water content of sludge can be found in Ref. 84. Direct recovery of suspended solids from a geothermal effluent using high speed centrifical separators is in general not practical owing to low solids to liquid ratios and the low density of the suspended material.

In the following sections, the most commonly employed brine treatment systems will be discussed in more detail. The design of an integrated water treatment system must be carefully planned in order to control costs. The least amount of processing required to yield an injectable effluent is the desired goal. The water quality testing methods described previously become very important in defining water treatment standards and in assessing the relative merits of a particular treatment system during bench and pilot testing activities. Additional testing methods that address the evaluation of gravity settling systems and chemical treatment programs are also discussed in the following sections.

IV-20-1. Gravity Settling

Settling velocities of spherical particles can be described by Stokes Law:

$$v = \frac{g(\rho_s - \rho)}{18\ \mu}\ d^2$$

where: v = settling velocity of a spherical particle -- cm/sec
g = gravitational constant -- 981 cm/sec
= specific gravity of the settling particle
= specific gravity of the liquid
= dynamic viscosity of the liquid -- cp
d = diameter of the partice -- cm

Deviations of settling time based on Stokes' Law can result from surface or convection currents, and density and eddy currents induced by the specific operating parameters of a settling system. In geothermal processes where relatively hot water is treated, convection currents can be a serious disruptive factor. Convection is minimized by use of adequate insulation on settling tanks. Surface and eddy currents can be controlled by careful design of influent geometries and by use of covers in conditions where wind-generated

currents may be a concern. Density currents caused by a disparity in solids loading between influent and effluent portions of the settling system can be minimized by adequate sizing of the settling tank.

The basic elements of a settling system consist of the settling tank or basin, a means of directing solids ladened water into the settling system, a means for recovering settled solids and a means for separating clarified overflow. Although sedimentation can be accomplished using either batch or continuous operations, most processes are continuous flow. However, the use of holding pits as settling basins can be considered if cooling of the treated water is not a great concern. An advantage of a large batch holding area represented by a large pit is that supersaturated dissolved species or dissolved species with a strong solubility-temperature dependence can be removed from the water. In an open pit, water would become oxygenated. Subsequent processing might be needed to remove the residual oxygen from the water prior to subsurface disposal. In the case of the hypersaline geothermal brines of Southern California, oxygenation is controlled by the dissolved iron content of the brines. In this instance it might only be necessary to provide sufficient post-settling residence time under anerobic conditions to insure complete removal of excess iron by precipitation of ferric iron. Iron precipitates could be removed by a downstream polishing filter.

In a settling tank, solids can be removed by an underdrain system. In a holding pit it would be necessary to periodically dredge the pit of deposited solids. The basic forms of settling basins are illustrated in Figure 37. Operation of a continuous settling process requires that a reasonable density contrast exist between the particulate matter and the liquid phase. The ability to remove particulates will, therefore, depend on the drag forces exerted on the particles by the liquid as it moves through the basin, the

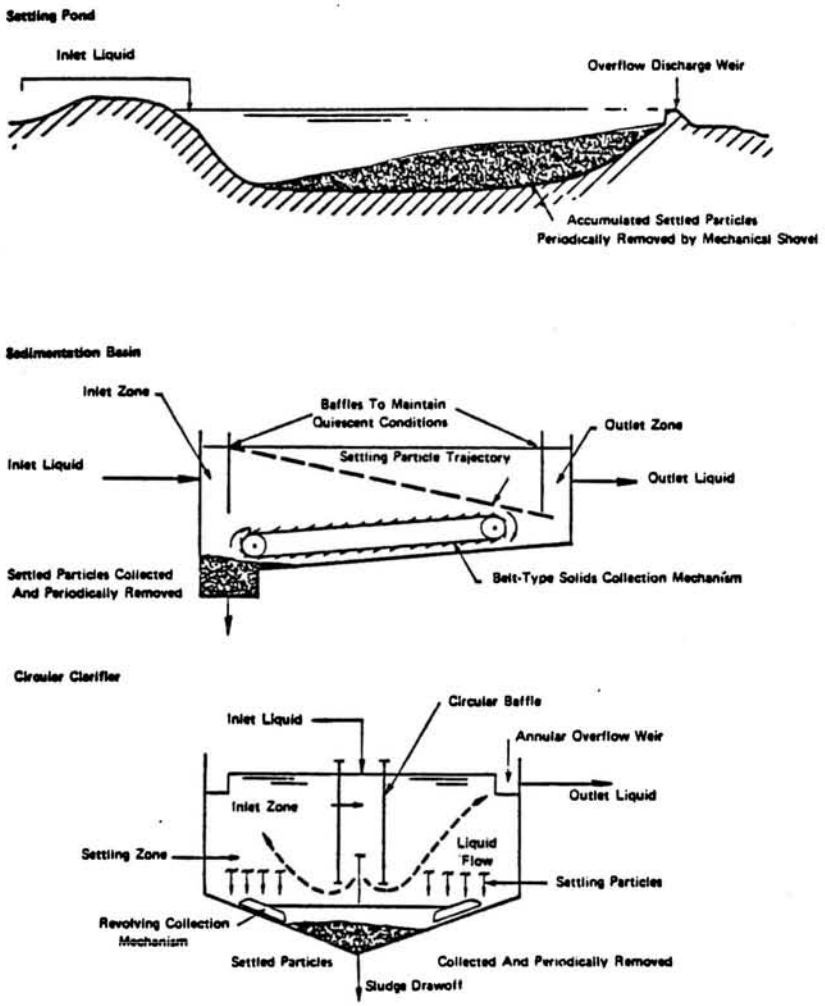

Figure IV-37. Representative types of sedimentation. (From Ref. 85)

downward acting gravitational forces, and parasitic forces due to convection or eddy currents that may act to counterbalance the gravitational forces. The long-tube method can be used to assess the operational characteristics of a sedimentation basin. This method is suitable for all suspended particulates that settle without a well defined interface. Systems in which particulates are particularly dense or have high flocculation tendencies can be evaluated using jar testing methods.

Long-Tube and Jar Testing Methods

According to Ref. 84, the long-tube apparatus consists of a three inch I.D. tube, with a length of eight feet. The tube is equipped with sampling taps located at one foot intervals. For hot liquids, sufficient insulation of the tube is required to eliminate disturbances due to convection. Removal of insulation or use of sufficient insulation to simulate thermal losses from a settling tank is a useful way to use the long-tube apparatus to simulate heat loss effects on performance of the scaled-up settling tank. The apparatus must be filled with process water that is to be treated. Samples are withdrawn beginning at the top of the tube at timed intervals and the concentration of suspended solids is determined. The settling time and basin depth required to yield an overflow of the desired clarity is readily determined from the suspended solids data.

Jar testing methods can be used to evaluate the added benefits, if any, that may be realized by use of mechanical agitation and chemical flocculation. A typical jar testing apparatus, available from Fisher Scientific, HACH and other suppliers, is capable of rapidly assessing mechanical flocculation characteristics of suspended solids by use of a bank of motor driven blade-type stirrers. The test water is contained within glass beakers. For hot solutions, small hot plates can be used to maintain solution temperature.

Utilization of the apparatus is basically governed by the operators perception of the degree to which suspended solids have flocculated and settled. A more scientific appraisal of performance can be obtained by withdrawing liquid samples from a prescribed depth from each beaker after a prescribed reaction time and measuring the turbidity of the samples using a turbidimeter. Samples can be withdrawn from the sample containers using a pipette.

Direct observation of flocculation tendency in a long-tube apparatus is feasible if transparent plastic tubing is used. The mechanical agitation of the sample and admixture of a chemical flocculation agent would have to be accomplished using an outboard mixing apparatus. A pump might also have to be provided to subsequently transfer the mixed sample to the long-tube apparatus.

The assessment of performance of an operating settling system can be readily accomplished using a method analogous to the long-tube method. The settling tank should be provided with multiple sampling valves which provide the means of testing water clarity as a function of depth in the tank. In addition, sampling valves should be provided on the inlet and overflow drain of the tank to permit evaluation of percent solids removal by the settling system and to ascertain the clarity of the overflow. As noted previously, use of an underdrain system is desirable in the case of fine, easily dispersed solids. The underdrain, operated as either a continuous or batch process provides the means of removing settled solids before they can be redispersed by eddy or convection currents within the settling tank. The underdrain is usually set so as to provide a particular density of accumulated solids at a particular depth in the tank. The set point can be determined by using the solids sampling valves, as noted previously.

The overall efficiency of the settling system will be dependent in a significant manner on the size distribution of solids which are carried into

the tank. The density of the suspended solids is also of obvious importance. The size distribution of suspended solids in the inflow stream to the settling system should be measured using one of the techniques described previously. The simplest method is to perform serial filtration using membrane and mesh-type filters. The measurement of suspended solids size distribution in the overflow from the settling system provides a simple means of assessing the efficiency of the system. Density of suspended solids can be measured by capturing suspended solids via the sampling valves and using an appropriate measurement technique such as the water immersion, heavy liquid or pycnometer techniques. The chemical composition of the suspended solids is also of interest. Samples can be obtained of the solids for multi-element chemical characterization and mineralogical characterization by x-ray diffraction techniques. The underdrain, if used, will deliver settled solids to a holding tank or pit. It is of interest to measure or estimate the total mass of settled solids removed by the settling system as a function of the total liquid throughput. Cumulative suspended solids data can be obtained by integrating suspended solids data taken periodically from settling tank overflow as compared to the influent suspended solids concentration. The use of automated turbidity monitors on the influent and effluent lines can also be considered since the response of the turbidity meters can be calibrated in terms of suspended solids concentration.

IV-20-2. Filtration

In geothermal operations, filtration is considered for the removal of suspended solids from spent effluents prior to injection. Filtration equipment may also be employed in the dewatering of sludge produced by sedimentation units, clarifiers or other filters. Depending upon the particulate load in waters to be treated, one or more stages of filtration may be needed. The

prefilter stage is useful in removing the bulk of coarser particulates. Polishing filters can then be used to remove residual fines. Geothermal service imposes constraints on filtration systems not usually encountered in other industrial applications. Geothermal waters are usually hot, at or near the boiling point. The waters are also commonly supersaturated with respect to one or more dissolved species. Precipitation of solids within the matrix of a porous filter media may degrade or prevent effective backwashing and necessitate more frequent replacement of the filter elements. For this reason, prefilters in geothermal applications are usually granular media systems which are periodically fluidized with air or clean water to remove trapped solids. Thermal limitations can also narrow the potential selection of removable or backwashable elements for use in polishing filters.

Filter Systems

Media Filters - The physics of the filtration process and a summary of various types of filtration systems, operating parameters and cost information are discussed in Ref. 84. The most commonly used filtration systems for treatment of spent geothermal waters are the granular media filter and the cartridge-type of filter unit. A typical commercial media filter unit is shown in Figure 38. This unit is a downflow filter which consists of graded beds of anthracite, garnet and rock. Other materials such as graded fractions of sand, can also be used. The various materials that make up the filter media are selected so that the average density of constituents comprising each layer is such that when the bed is fluidized during backwashing cycles, the materials will rearrange themselves under quiesent conditions. For example, properties of a typical granular filter media are as follows:

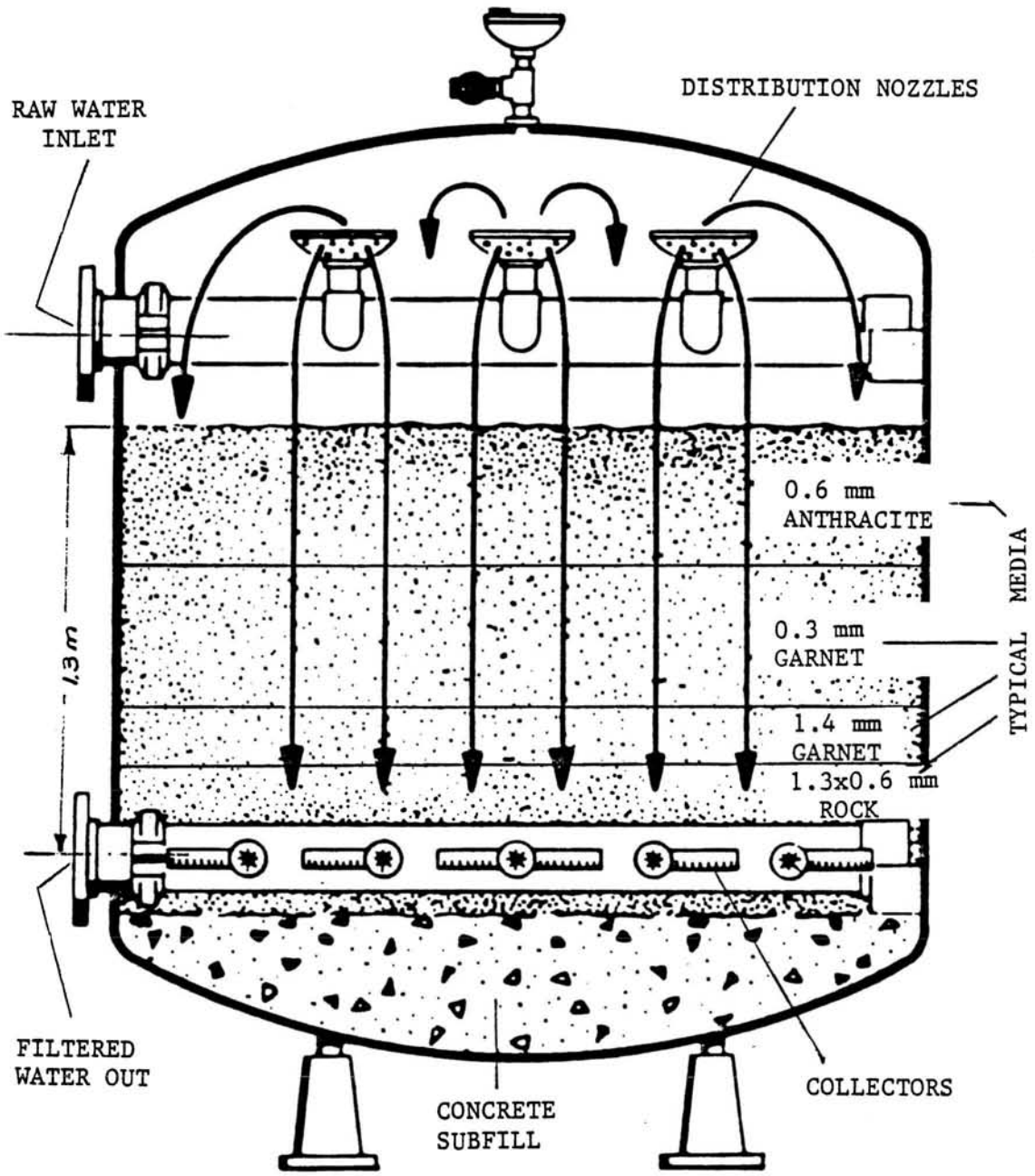

Figure IV-38. Multimedia high rate downflow filter. (From Ref. 86)

Layer	Material	Specific Gravity	Typical Layer Thickness
Top	Coarse Anthracite	1.5	30 cm
Middle	Fine Sand	2.6	150 cm
Bottom	Coarse Garnet	4.2	30 cm

The higher density, coarser material provides no filtration function. This material serves to support the finer-grained, lower density filter media.

Granular media filters are available as downflow units, upflow units and as dual flow units in which one half of the raw water is admitted through the top of the unit and one half of the raw water is admitted through the bottom of the unit. This type of system is basically a downflow, coarse-to-fine filter and an upflow coarse-to-fine filter in series with a centrally located drain for removal of filtrate. The properties of media filters are summarized in Table IV-3.

Conventional graded bed filters have relatively low filtration efficiency with respect to the removal of fine-grained particulates. However, they are effective as prefilters and they are relatively simple devices. As shown in

Table IV-3

Operating Parameters of Granular Media Filtration Systems

Filter Type	Rated Flow Capacity ($m^3/hr/m^2$)	Backwash Rate ($m^3/hr/m^2$)	Particle Removal Without Coagulant	Efficiency with Coagulant (μm)
Conventional Graded Bed Filter	6.0	24-37	25-50	---
High Rate, Deep Bed, Upflow Filter	15-20	37-50	5-10	1
High Rate, Deep Bed, Downflow Filter	25-50	30-37	7-10	1-2
Dual Flow Filter	50-100	---	---	---

(Data from Ref. 72)

Figures 39 and 40, this type of system can be provided as a completely self-contained unit in the form of a large open or closed tank fitted with the apprpriate plumbing system to facilitate backwashing operations. The system shown in Figure 40 can easily be adapted for geothermal use by converting a standard Baker tank (20,000 gallon capacity) for use as a filter.

The high rate upflow, downflow and dual flow commercial filter units have been optimized to provide high throughput rates with excellent filtration efficiency. Particle removal down to 10 μm can be realized without the use of chemical coagulants. When chemical filter aids are employed, particle removal down to 1 μm can be achieved and suspended solids concentration in filtered effluent can be reduced to less than 1 mg/l. The high rated flow capacity of the dual flow filter is achieved by operating two conventionally sized media filters simultaneously as shown in Figure 41. In general, high rate downflow filters operate at higher flux rates than upflow units and often can be cleaned using relatively low backwash rates.

Evaluation Techniques

The selection of a particular media filtration system requires some insights as to the nature and properties of the particulate matter which is to be removed from geothermal waters. Often it is not practical to specify a particular filtration system without some field evaluation. The problem is most serious in the case of polishing filters which may be expected to have reasonably long operating periods before the need for backwashing occurs. Since the main purpose of filtration is to render a spent effluent suitable for subsurface injection, careful attention should be paid to the selection

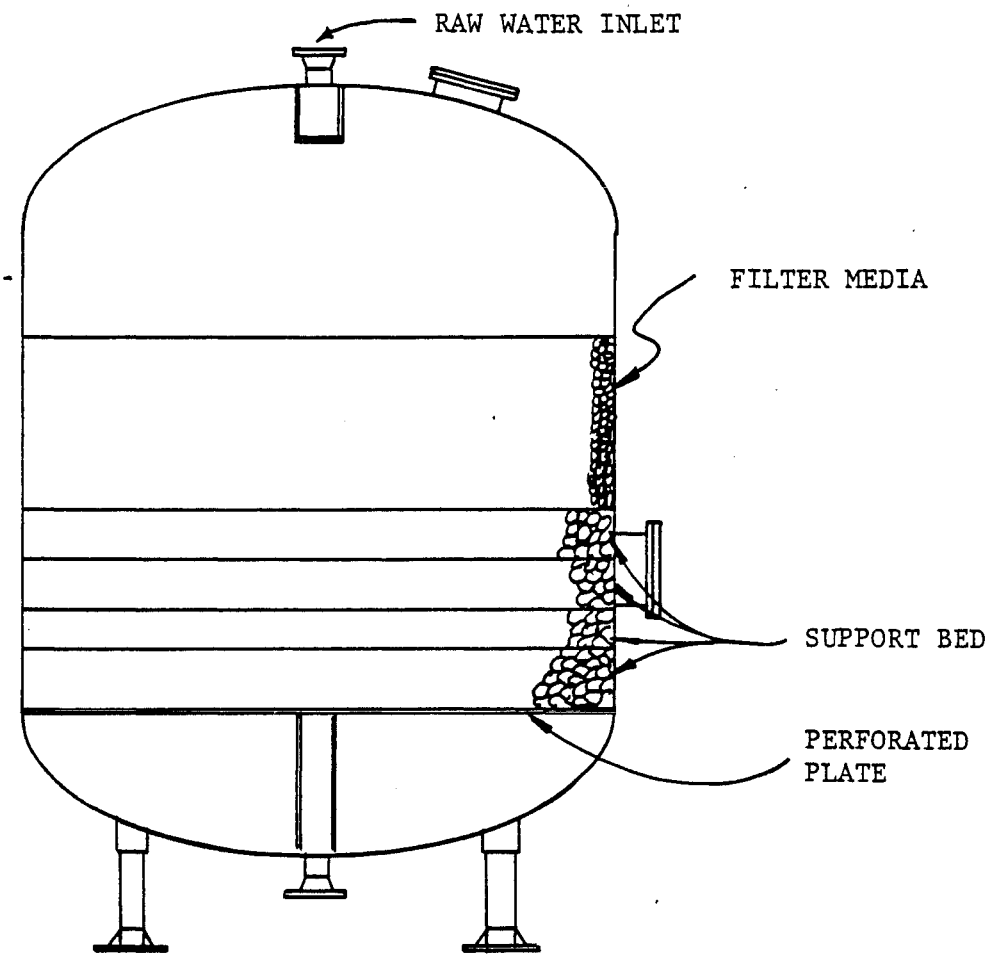

Figure IV-39. Graded bed filter. (From Ref. 72)

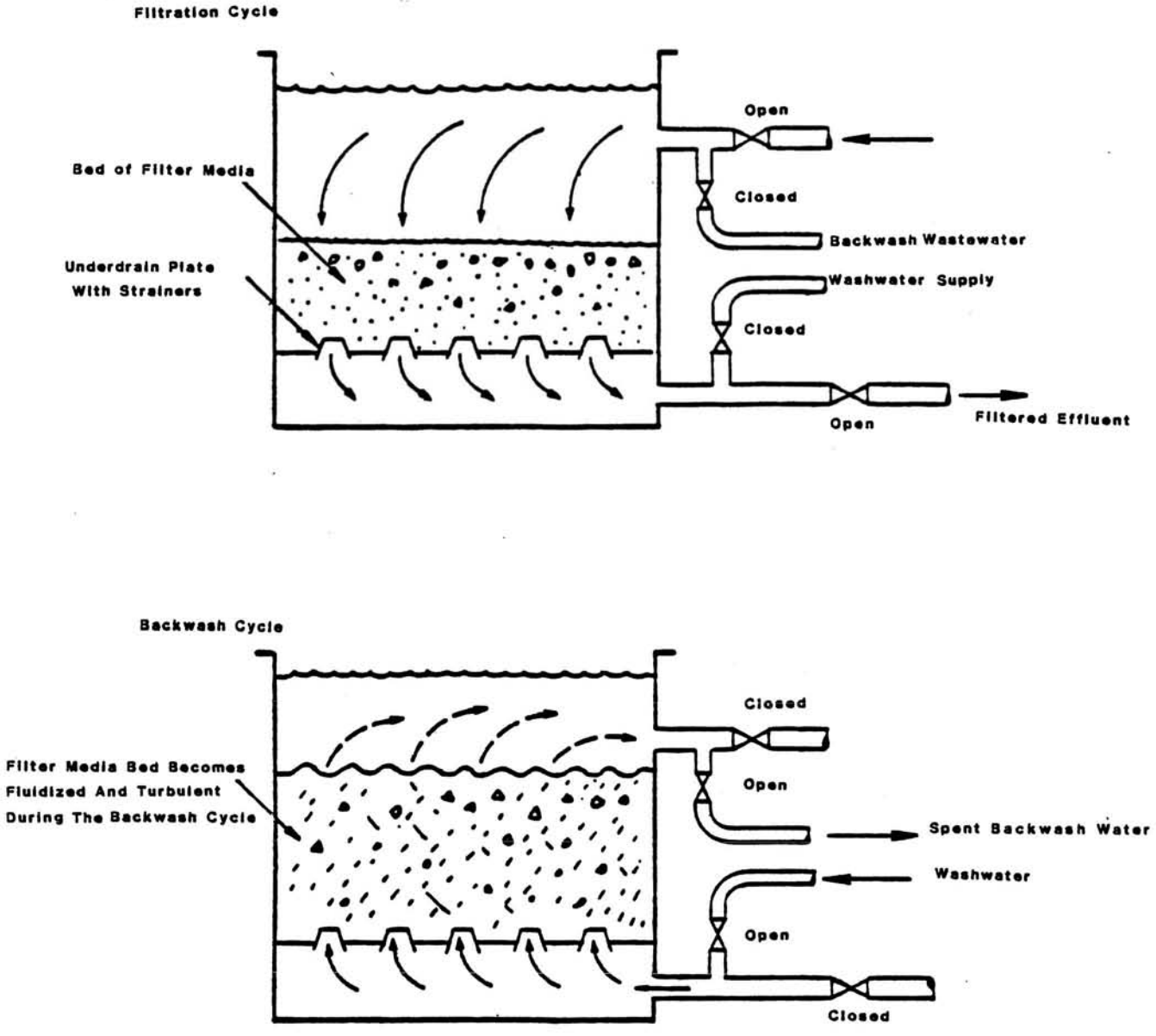

Figure IV-40. Graded media filtration system in open tank. (From Ref. 85)

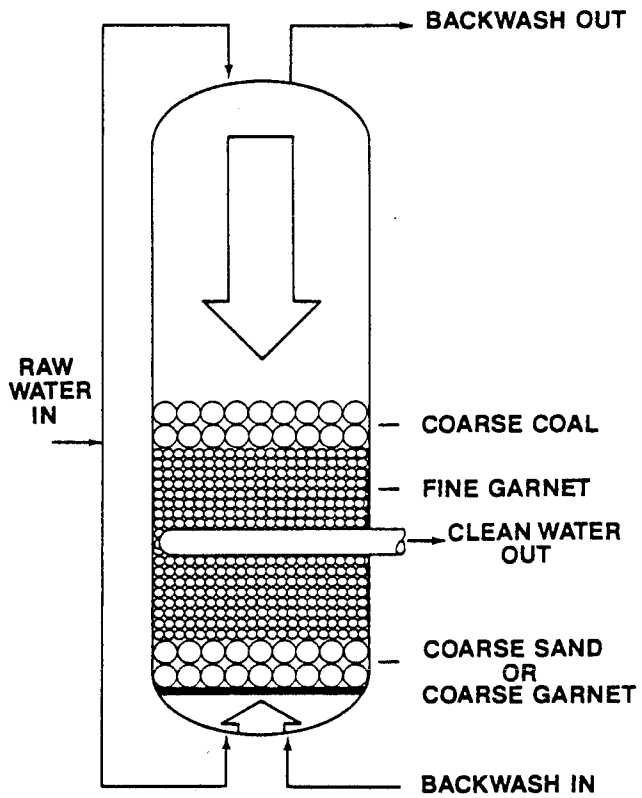

Figure IV-41. The dual flow (dfx) filter. (From Ref. 72)

criteria or the risk of injection well damage or other significant field problems may be encountered.

The best means of evaluating one or more filtration systems is to arrange for field tests so that the filtration units may be operated under actual conditions. Selection of chemical filter aids, which improve shear resistance of particulates and provide for increased floc sizes, can be performed in a preliminary way by means of jar tests. These tests should be carried out in a way that closely simulates the actual operating conditions, temperature being a significant variable. The brine and suspended solids should accurately duplicate actual effluents that will be produced by the geothermal facility. These conditions imply that field evaluation is preferable to laboratory simulations. The final selection of chemical aids is best accomplished in conjunction with tests involving operation of pilot sized or full sized filtration systems. Contact should be made with filter system suppliers to determine if field test units are available for testing and evaluation purposes. The jar testing procedure serves as a good screening test which can aid in rapidly selecting chemicals for filter tests. Use of chemicals implies an economic penalty so that the various options available to an operator should be carefully evaluated. For example, in lieu of separate pre- and polishing filtration units, it might, under rigorously controlled conditions, be possible to optimize performance of a media filter with the appropriate chemical additive to directly produce an injectable effluent.

The selection of filtration systems and the identification of coagulants or flocculants, if needed, can be approached with the aid of filtration system manufacturers and service companies that specialize in providing chemicals for water treatment services. One should also speak with other geothermal operators of water treatment facilities that may be located in the same area as the

proposed geothermal facility to determine if some operational experience might be shared. At the minimum, manufacturers of equipment used to treat similar types of geothermal effluents should be identified and approached for additional information.

In geothermal operations, waste water disposal is a high cost item in the overall energy conversion system. Water treatment and injection well costs can represent a signficiant increment in the cost of produced energy. Therefore, operators have a real incentive to reduce costs by installing the minimum treatment capacity necessary to produce injectable water that will provide for a reasonable injection well operating life. Completion of lengthy field evaluations of filtration systems may not be practicable in many cases. Therefore, the ability to simulate media filter performance under field conditions using inexpensive and simple to operate equipment is desirable. One such type of media filtration simulator that has been used extensively in field evaluation programs is shown in Figure 42. This unit may be constructed using high temperature transparent plastic tubing. The system is designed to simulate filtration and backwash cycles. Chemical additives can be easily injected into the raw water stream to evaluate impact on filtration. Injection of chemicals is readily accomplished using a peristaltic pump with a speed control or almost any type of metering pump. For high pressure applications the entire system can be constructed using steel tubing. A commercial version of the test filter has been available from National Technical Services, Corvallis, Oregon.

In many applications it would be appropriate to provide several test filters to permit rapid assessment of filtration media and chemical additives. The cost of these units either when purchased prefabricated or built by a geothermal operator is minor in comparison to full sized field filtration

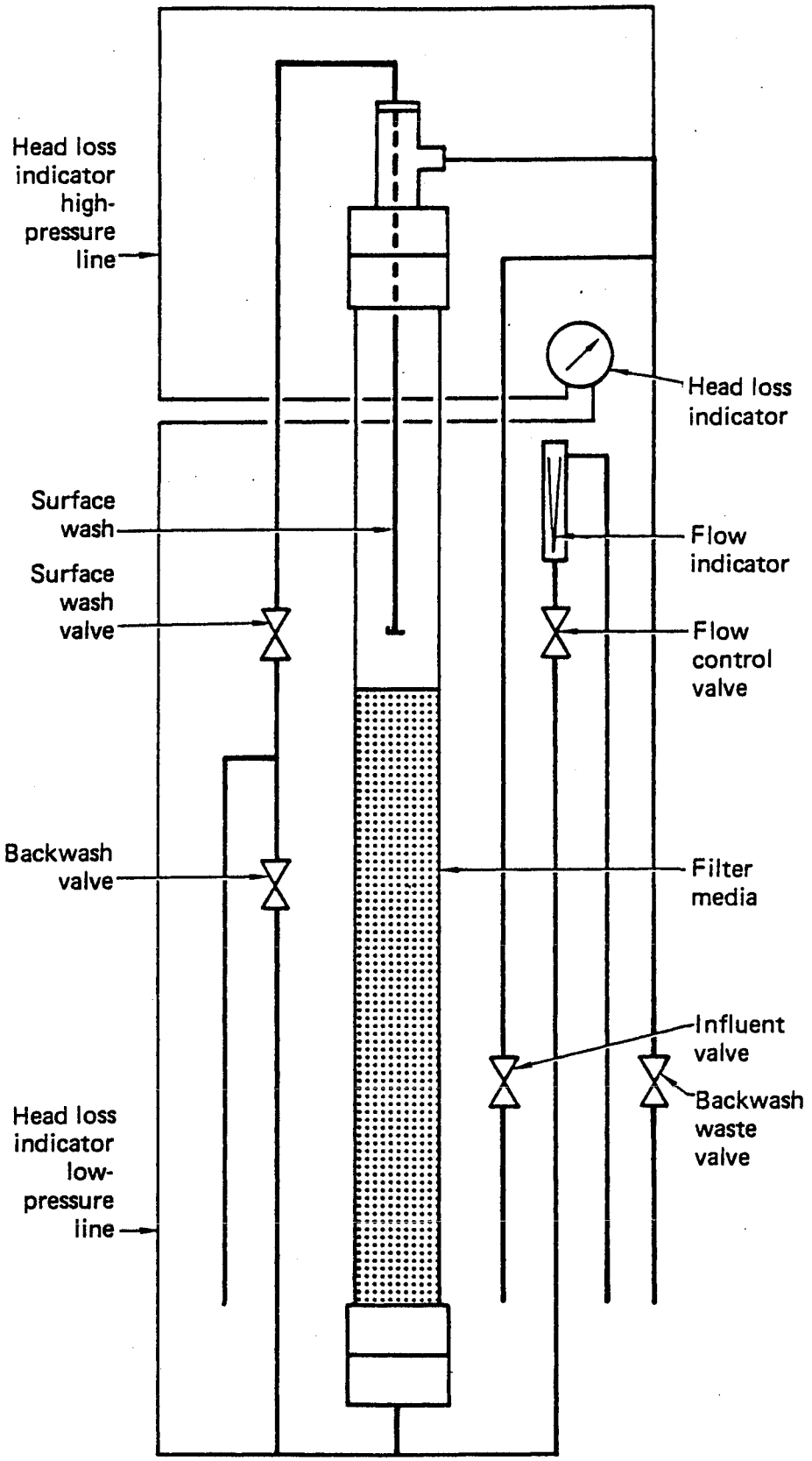

Figure IV-42. Schematic diagram of a 4-inch-diameter pilot filter. (From Ref. 80)

tests. The basic procedures used to evaluate filtration systems which make use of media filter simulators are described in Refs. 80 and 86.

The basic evaluation procedure involves jar testing to rapidly screen chemical floculating agents coupled with baseline filtration tests using the model filtration systems. The initial baseline filtration tests define optimum media composition and filtration efficiency. Subsequent filtration tests using chemical additives permit evaluation of ultimate attainable filtration efficiency in the presence of the most active additives.

The chemical additive prescreening procedure is carried out using the following procedure described in Ref. 80:

1. Use a standard jar testing apparatus.
2. Obtain samples of the raw process water containing suspended solids.
3. Add known amounts of chemical additive to the raw water.
4. Mix solution, at ambient process temperature, for two minutes at a constant speed of 100 rpm. Continue mixing for an additional 10 minutes at a constant speed of 20 rpm.
5. Filter solution using a Whatman #2 filter paper.
6. Immediately measure the turbidity of the filtrate using a ratio-type of analytical turbidity meter. The HACH Model 18900-00 turbidimeter or similar device is satisfactory.
7. Rank additives with respect to the measured turbidity. The best additives will produce an effluent with the lowest turbidity. Compare quality of effluents with and without additive treatment.

A typical data set obtained in conjunction with the screening of additives for use in the filtration of hypersaline brine from U.S. Gulf Coast Strategic Petroleum Reserves is shown in Table IV-4. The development of filtration data with and without the use of chemical additives using procedures described in Ref. 80 could be used to establish with a reasonable degree of accuracy flow capacity, the time dependence of differential pressure increase, concentration

Table IV-4

Prescreening of Coagulants and Flocculants as Filter Aids (From Ref. 80)

Coagulant or Flocculant	Amount Added (ppm)	Description	Effect on Turbidity at Indicated Site [a]		
			West Hackberry	Bayou Choctaw	Bryan Mound
Cationics					
Alum	1-300	Inorganic, short-chained, high-charged; used with Cyfloc 4500	E	R	E
$FeCl_3$	1-50	Inorganic, short-chained	R	-	-
Cat Floc-T	0.5-10	Low molecular weight (0.5 m)	N	N	-
Calgon					
Cyanamid					
Magnafloc 507C	0.5-3	Low molecular weight, high-charged; used with 3340	N	N	-
Cyanamid					
Magnafloc 581C	0.5-10	---	N	N	-
Cyanamid					
Magnafloc 1561C	0.5-10	---	-	N	-
Cyanamid					
Magnafloc 1563	0.5-10	---	-	N	-
Nalco Vx-740	0.5-5	High molecular weight (7-10 m)	-	-	N
Visco 3317	0.5-3	$AlCl_3$ cationic polymer; used with anionics (834A, 1820A, 3340)	N	R	R
Visco 3342	1-20	---	N	-	-
Visco 3347	0.5-10	Alum; cationic polymer	N	N	-
Visco 3349	0.5-10	---	N	N	-
Zimmite 2T68	1-20	---	N	-	-
Zimmite 2T653	0.5-20	---	N	-	-

a - N = no change in turbidity;
R = reduced turbidity to some degree;
E = excellent turbidity reduction.

and size distribution of particulates in the filtered effluent and the backwash cycle requirements for a filter with a particular media construction.

The evaluation of the performance of a media filter proceeds in a manner similar to the jar testing procedure. Filtered effluent turbidity, suspended solids concentration (as measured with a 0.45 μm membrane filter) and particle size distribution in reference to the influent or raw water properties serves as the most direct means of assessing performance. These properties will vary primarily as a function of filtration rate, the presence or absence of chemical additives, the media composition and the properties of the raw water. The same physical properties are also used as diagnostics in determining the requirements for stisfactory backwashing of fouled filters.

Illustrative examples taken from Ref. 80 and 86 readily show the value of small scale filtration tests in designing a filtration system suitable for the treatment of hypersaline brine (nearly saturated sodium chloride solution). For example, Figure 42 shows the effect of filtration rate on the quality of effluent based on periodic measurements of filtrate turbidity. Two filter simulators with different media compositions were operated during these tests. Both process streams were treated with a Nalco chemical additive. As can be seen, the higher filtration rate of the A1 filter resulted in premature penetration of suspended solids.

Figure 43 illustrates the effect of different chemical treatments on effluent turbidity produced by media filters of identical composition. This test sequence clearly demonstrated the detrimental effects of dissolved chlorine. In similar fashion, Figure 44 illustrtes the impact of alum usuage ($A_{12(SO4)}3 \cdot H_2O$) on the turbidity of filter effluent. These data were obtained at the same filtration rate for filters with identical media construction.

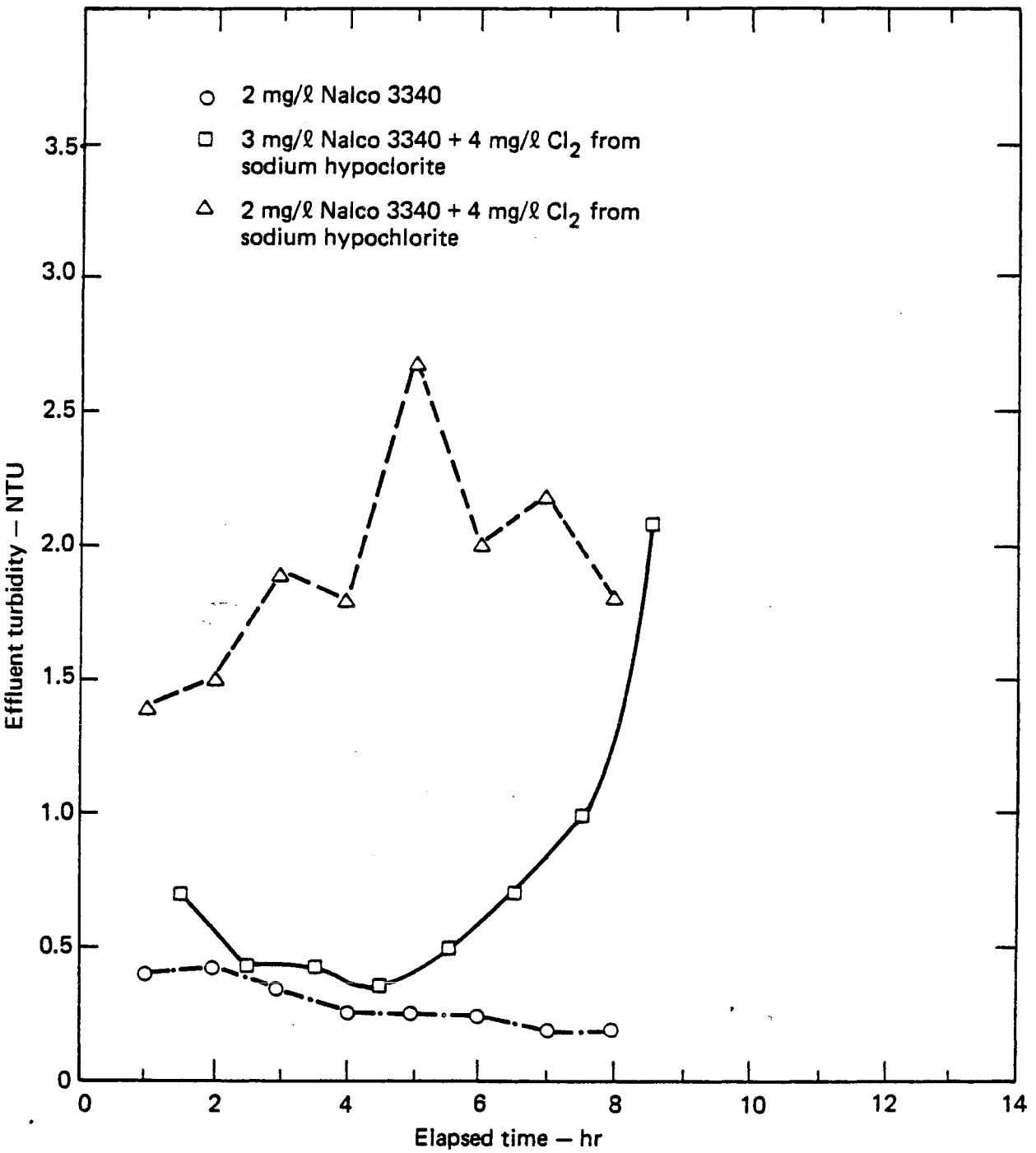

Figure IV-43. Comparison of Filter Effluent Turbidity Using Nalco 3340 With and Without Chlorine (from ref. 80).

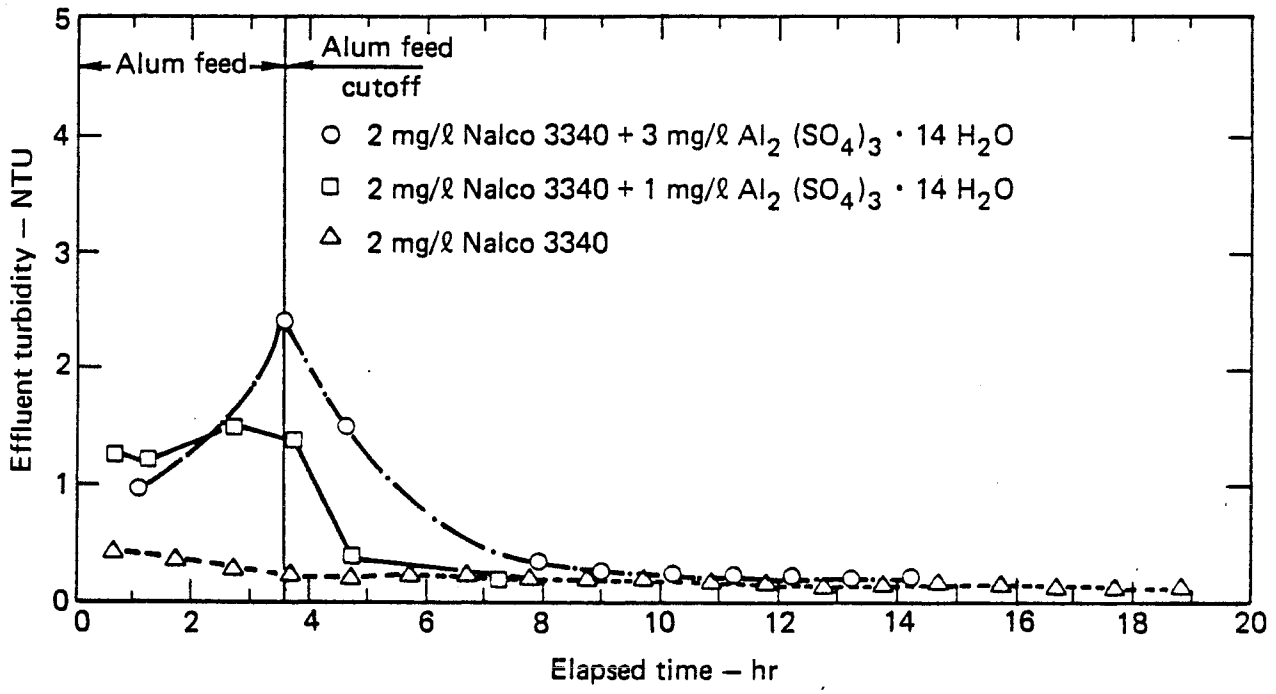

Figure IV-44. Comparison of effluent turbidity using Nalco 3340 with and without alum. (From Ref. 80)

Figure 45a compares filtered effluent turbidity in the cases of chemical injection and no chemical injection. As can be seen, the turbidity of properly treated media filtered brine compared favorably with the effluent produced by a high efficiency ultrafilter. The ultrafilter is an absolute cartridge filtration system with the capability of removing submicron particulates (>0.1 μm). Figure 45b illustrates the relative improvement in water quality obtained by use of media filtration or ultrafiltration as compared to the raw water. These data are presented in terms of the reltive permeability impairment of a 10 μm pore size membrane filter which was used in a manner discussed in Section IV-18.

Figure 46 illustrates how measurements of suspended solids particle size distribution can be used to assess filter performance. These data were obtained using a Spectrex laser particle counter equipped with a particle profile attachment.

The use of chemical additives as filtration aids must be carefully considered because certain additives have the potential for impairing injectability of disposal wells. Figure 47 illustrates the influence of an anionic polymer on the permeability of membrane filters of various pore sizes. As can be seen, impaired permeability was experienced in all filters with a pore size below 10 μm. The impairment resulted from deposition of high molecular weight polymer molecules. The same impairment mechanism could adversely impact the pore structure of an injection zone. Thus, control of residual polymer content in filtered water and an assessment of the plugging potential of such water should be part of an overall water treatment assessment program. Other chemical additives such as alum or chlorine should also be assessed with respect to the potential for post-filtration precipitation and possible impairment of injection horizons. Since geothermal brines may be chemically

(From Ref. 80)

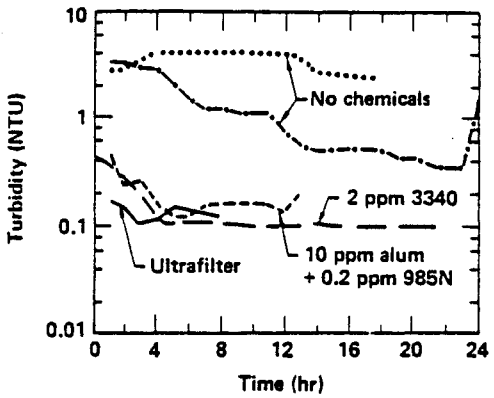

Figure IV-45a. Comparisons of effluent quality with and without chemical treatment. Comparitive data for an ultrafilter is also provided.

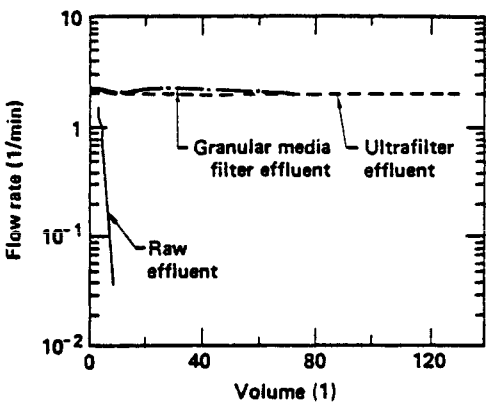

Figure IV-45b. Improved brine injectability with filtration as indicated by water quality tests using 10 μm pore size membrane filters.

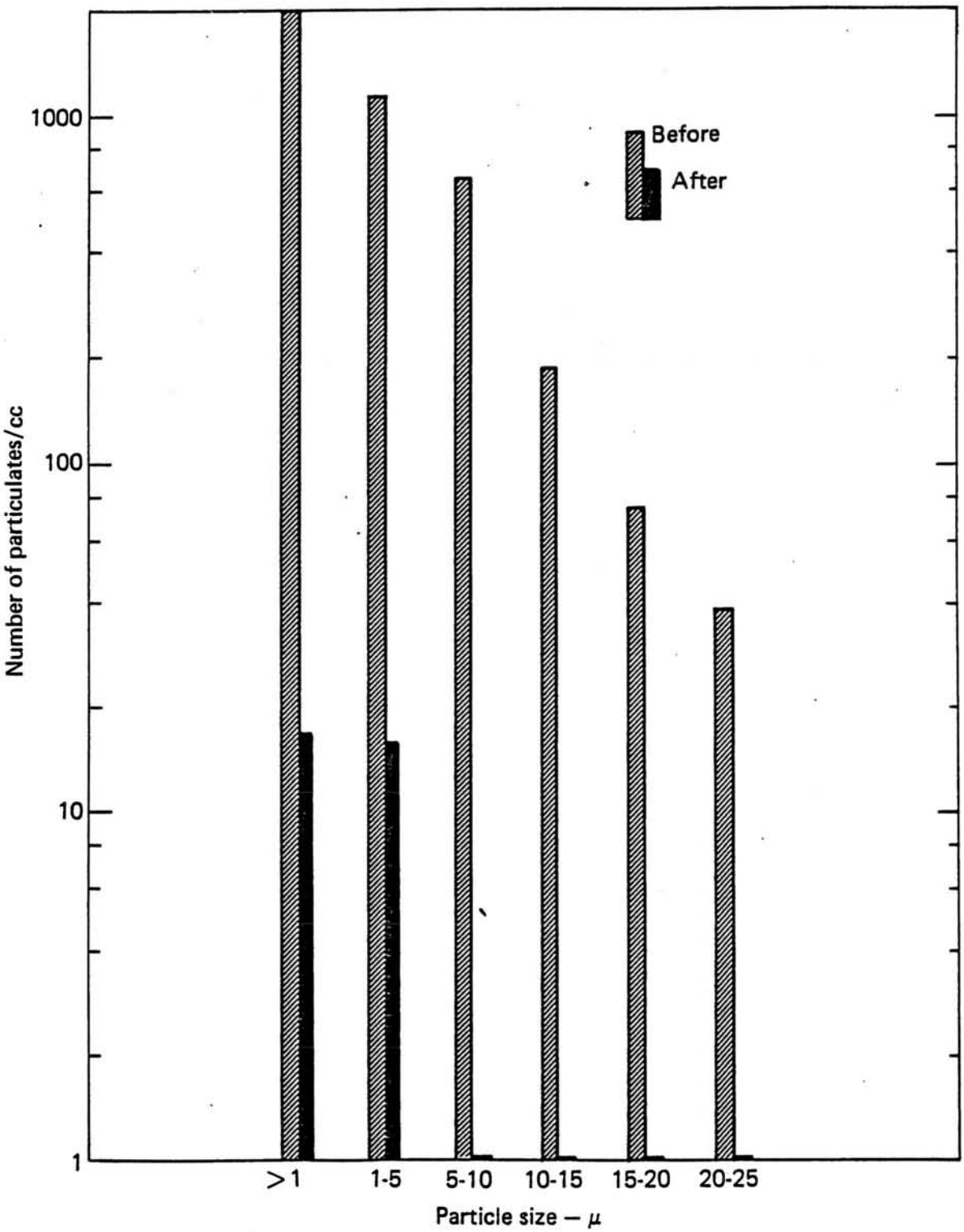

Figure IV-46. Change in particle size distribution produced by granular media filtration. (From Ref. 80)

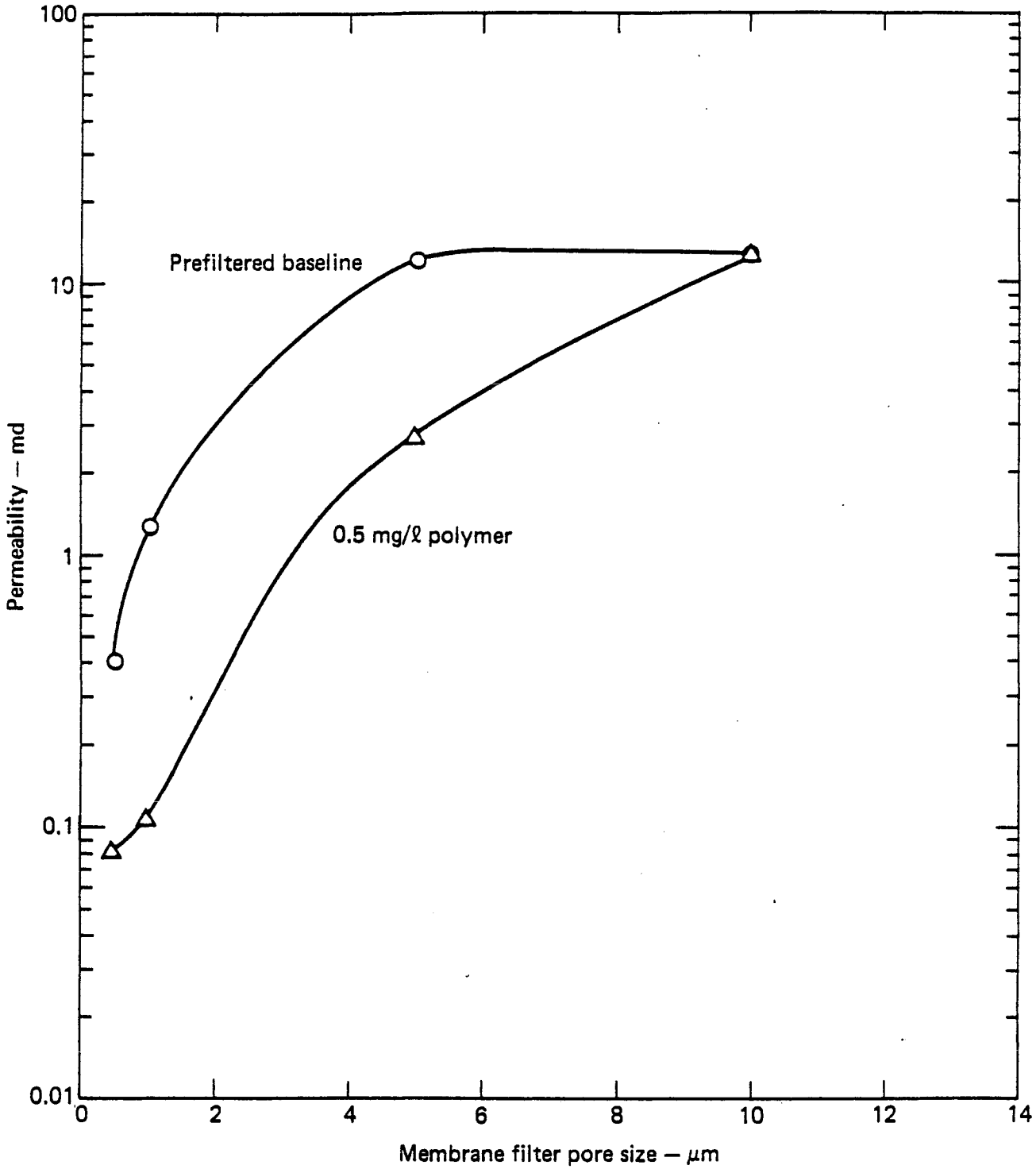

Figure IV-47. Effect of anionic polymer (after 30 minutes of flow) on the permeability of various pore size membrane filters. (From Ref. 80)

complex (for example, the hypersaline brines of the Southern California Imperial Valley), the potential for unfavorable interaction of additives with the process water should be evaluated. Incubation tests and water quality tests should be carried out to assess potential problems.

Ref. 86 includes a description of a 250,000 B/D downflow media filtration system. The downflow filter was selected for analysis based on pilot field tests which showed that the downflow filter had much better headloss characteristics than either upflow or dual flow units (Figure 48). Depening upon the characteristics of the raw water process stresm, other filter types might prove superior. For the particular application discussed in Ref. 86, the optimized filtration plant shown in Figure 49 was designed with an estimated installed cost of $840,000 in 1981 dollars. It was also estimated that approximately 20 to 24 weeks would be required for installation of the filtration plant. An advantage of this type of installation is that the system is automated and therefore requires minimum operator attention. In lieu of an automated backwash recycle system, an alarm function can be provided to alert operators to the need for initiating a backwashing cycle.

Precoat Filters -- Diatomaceous earth (DE) can be used as a coating material in conjunction with a wire or cloth mesh or perforated plate support structure to form a very effective filtration system. Diatomaceous earth consists of diatomes which are single-celled marine organisms with siliceous tests or shells. The fossilized remains of these animals are processed to produce well sorted DE for use in filtration applications. The DE is applied as a coating to the support structure and the filtration of suspended solid occurs directly within the porous DE network. Backwashing of a precoat filter is relatively easy as the DE layer with its load of trapped solids is readily removed from the support structure. When properly operated,there is little

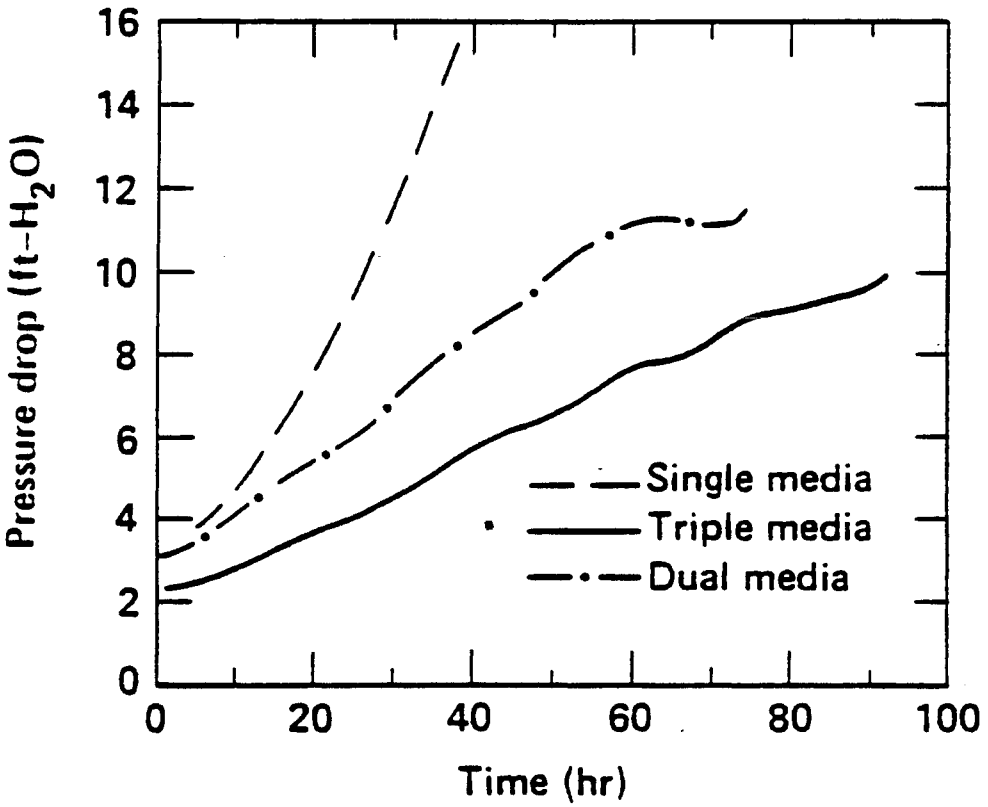

Figure IV-48. Evaluation of headloss vs. time for granular media filtration. (From Ref. 86)

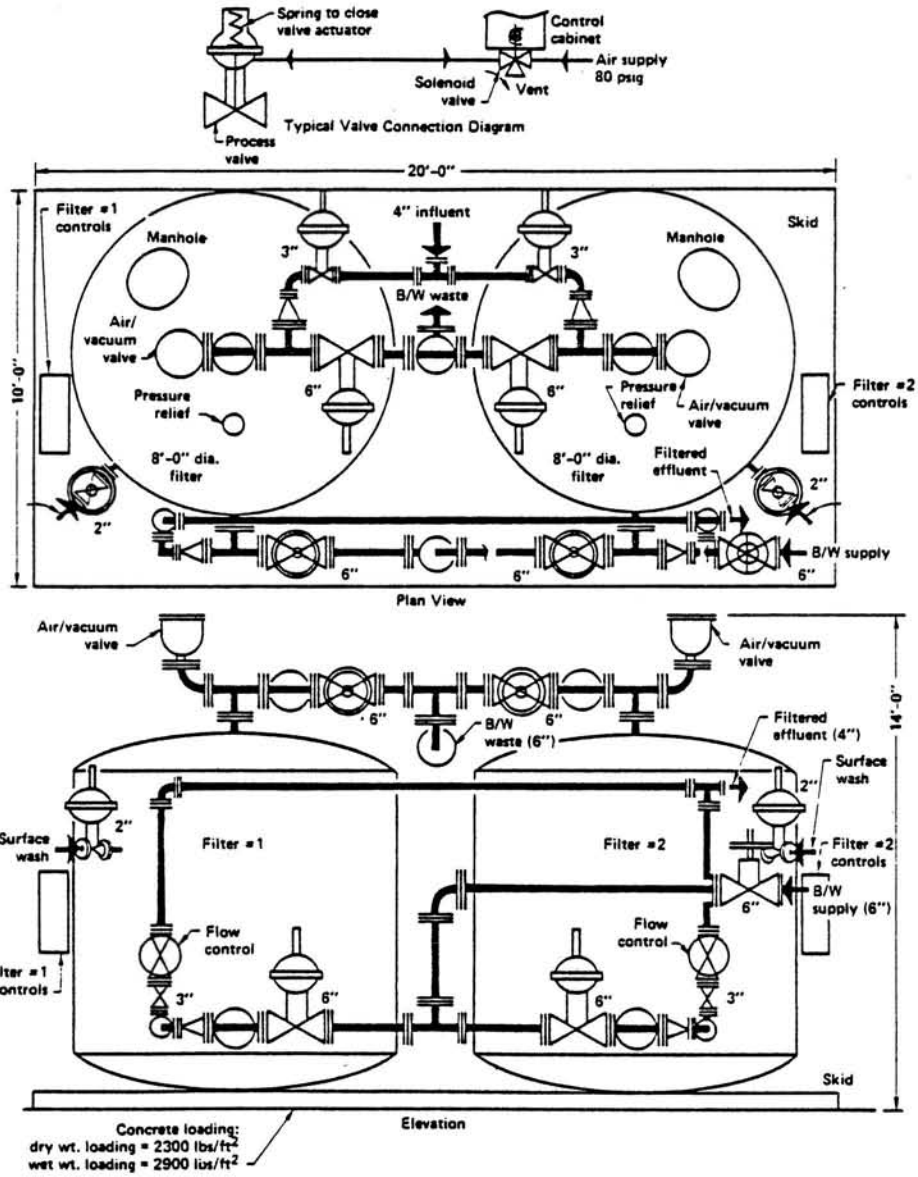

Figure IV-49. Design schematic for a high rate downfall media filtration system. (From Ref. 86)

danger of plugging the precoat filter support structure. Commonly, a continuous stream of DE is injected into the raw water feedstock to prevent rapid formation of low permeability filter cakes and thereby extend operating cycles. This type of operation is called body feed. The use of body feed with other types of filters can be practiced. However, care must be exercised to prevent loss of DE from the filter. DE is an extremely damaging solid which can easily impair injection zones.

Patton[72] has discussed the operational characteristics of precoat filters in the context of oilfield operations. He has summarized the following rules of thumb for operating this class of filter:

(a) DE filters are the most complicated filters to operate of those used in the oilfield.

(b) They are economically feasible only when the suspended solids do not exceed 30-50 mg/l.

(c) The "average" DE filter is operated at a rate of 2.5 $m^3/hr/m^2$, with a maximum rating of about 5.0 $m^3/hr/m^2$. However, overall space requirement is less than for conventional or high-rate filters.

(d) DE filters will remove entrained oil from water, but this results in rapid fouling of the bed.

(e) They will remove very fine suspended particles - down to as small as 0.5 μm in diameter.

(f) DE can and usually does bleed through the filter and is an excellent formation plugging material. Downstream cartridge filters are strongly recommended to catch any bleed-through.

(g) Diatomaceous earth must be supplied and constitutes a logistical problem. Also, disposal of the used DE and the associated filtered solids can prove to be an operational difficulty.

Item (g) above is of no practical concern in geothermal operations since the DE disposal will only represent a very small fraction of the particulate matter recovered from treated water. DE does not represent an environmental hazard from the point of view of landfill disposal. Any arrangements made for

the disposal of recovered particulate matter from a geothermal water will, therefore, also be satisfactory for the disposal of spent DE. Similarly, item (d) above is of no practical concern in geothermal operations.

Results of comparative pilot-scale tests of precoat and media filters were reported by Quong, et al.[87] for hypersaline geothermal brine. Their results are summarized in Table IV-5. The influent brine to the filters was produced by a pilot-size reaction clarifier. The brine suspended solids load ranged between 25 to 340 mg/l. It was estimated that approximately 135 ft^2 of filter area would be needed to treat a one well flow of 550 gpm. Operation of the precoat filter was very simple. About three minutes were required to initially coat the filter with DE and a similar amount of time was needed to perform the backwash cycle.

Cartridge Filters -- Cartridge filtration systems are commonly used in geothermal operations. This type of unit is an absolute filter which will remove essentially all particulates down to a rated size. The filter may operate by surface filtration in which case solids greater than a particular diameter cannot penetrate the filter. Alternatively, the filter may operate as a depth filter which will permit penetration of solids into the body of the filter. Invasion phenomena may, however, be detrimental, if chemical precipitates form. Precipitates can readily plug filters and are, therefore, undesirable.

Typical cartridge filtration systems are illustrated in Figures 50 and 51. These types of systems are available with replaceable or backwashable filter elements. Care must be exercised befor installing a cartridge filtration system with backwashable elements since the ability to effectively clean filter elements will depend to some degree on the nature of the particulate matter. Field tests under actual operating conditions are essential before committing to the installation of a large system.

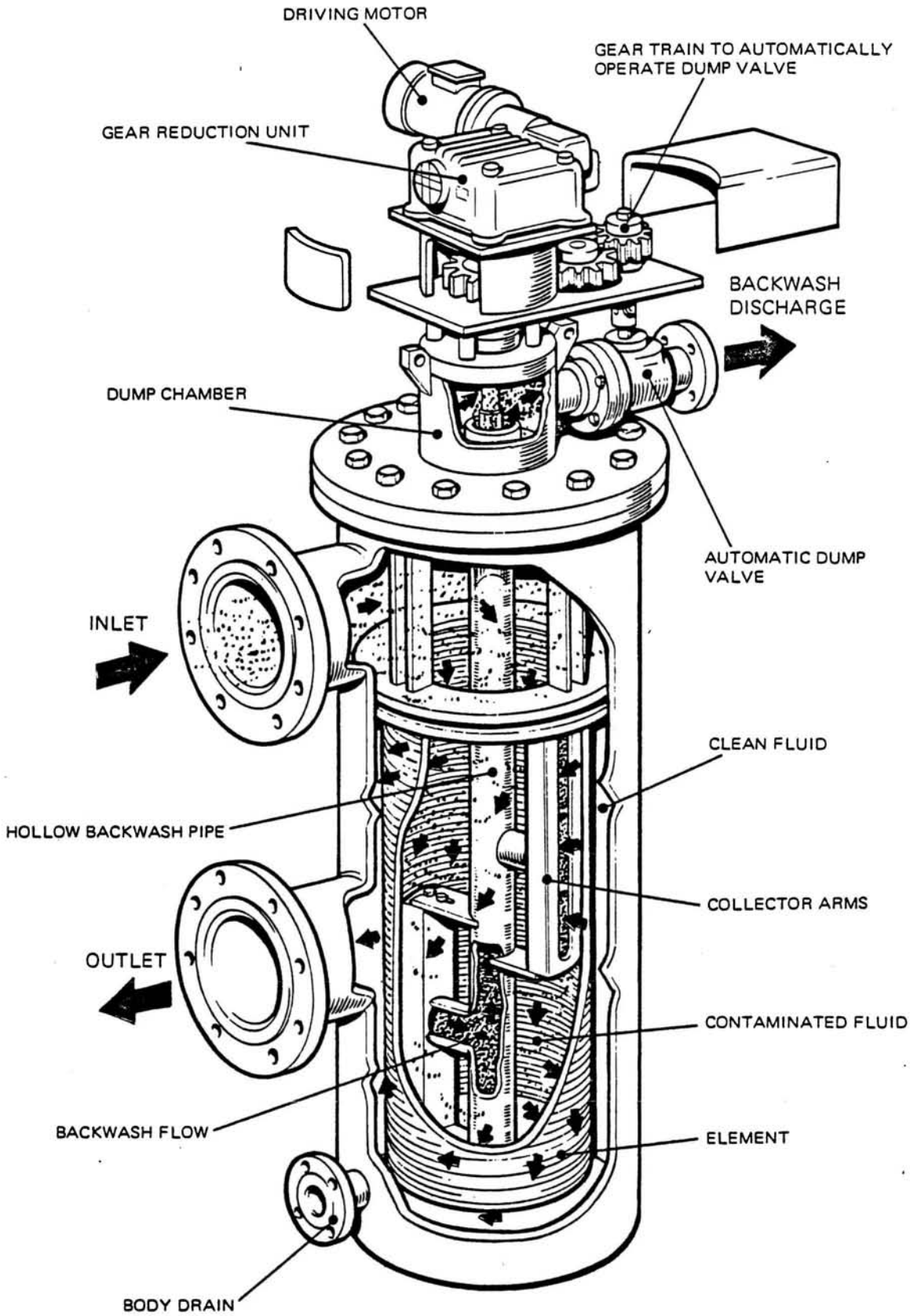

Figure IV-50. Plenty and Son, Ltd. automatic backflushing cartridge filter. (From Ref. 72)

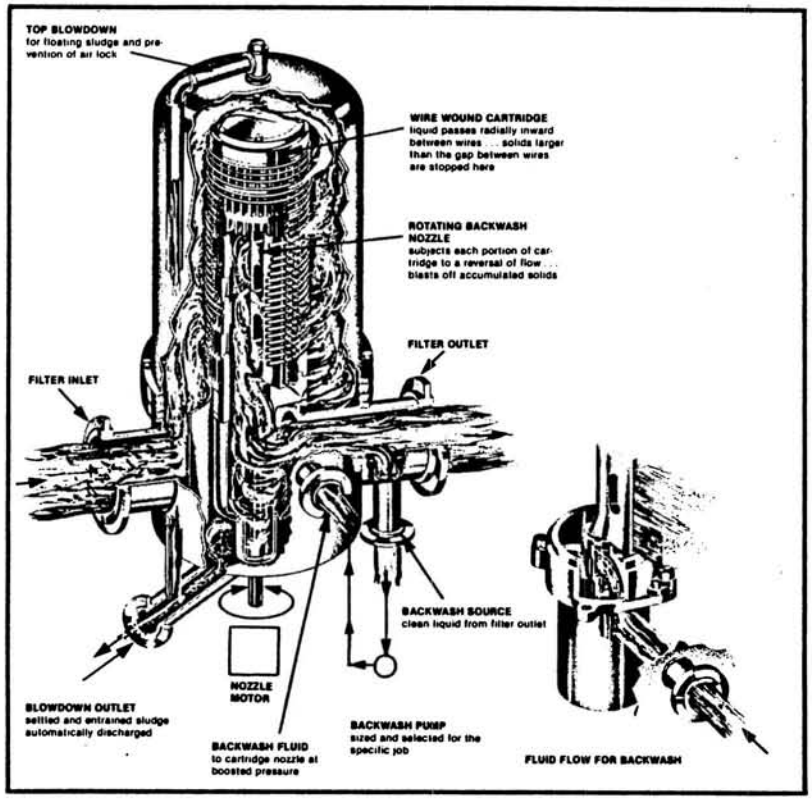

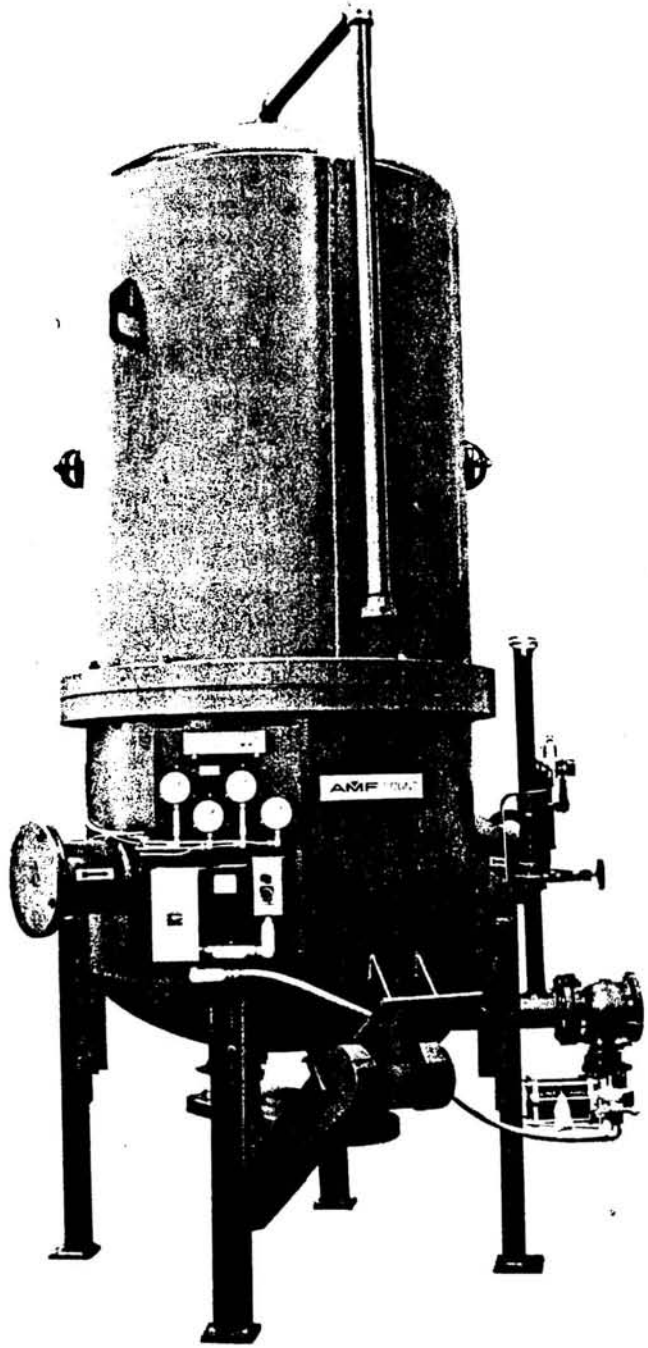

Figure IV-51. AMF Cuno metal element high capability cartridge filtration system with continuous backwash capability.

Table IV-5

Results of Hypersaline Geothermal Brine Filtration Tests
(From Ref. 87)

Results of Precoat Pressure Filtration Tests on Niland Brine Effluents

Test No.	Conditions[a]	Cycle Time to 30 psi ΔP (hrs)	Avg. Solids Conc. (ppm) In	Avg. Solids Conc. (ppm) Out	Flowrate (gpm/ft^2)	Cost Filter Aid Mils/kWh/ppm[b] Brine Solids
1	Precoat: JM Hyflo Super-Cel (Medium Grade)	4.0	108	<5	1.1±0.2	0.0054
2	Precoat: JM Hyflo Super-Cel Bodyfeed: 150 ppm	2.0	292	1	1.1±0.2	0.0078
3	Precoat: JM 545	2.2	340	<5	1.1±0.2	0.0038

a - Precoat layer: 0.2 lbs/ft^2 JM: Johns-Manville Celite Diatomite filter aid.
b - Filter aid cost: $7/100 lbs 100# brine → 1 kWh

Mixed Media Sand[a] Filtration of Niland Brine Effluents

Cycle[b]	Cycle Duration (hrs)	ΔP Across Bed (psi) Initial	ΔP Across Bed (psi) Final	Avg. Turbidity, NTU In	Avg. Turbidity, NTU Out	Average Temp (°C) In	Average Temp (°C) Out	Flow Rate (gpm/ft^2)
1	8.5	0.3	1.6	28	0.6[c]	81	79	4.2±0.4
2	23.0	0.3	46.6	33	0.5	81	79	4.2±0.4
3	14.5	1.0	16.6	28	0.5	77	75	4.2±0.4

a - Mixed media: 18" anthracite coal
9" silica sand
3" garnet sand
3" garnet support
b - Filter was backwashed with filtrate after each cycle
c - 1 NTU = 2-3 ppm suspended solids

Cartridge filters are commonly employed during the conduction of well testing programs. Portable or small scale systems can be obtained as rental units and are convenient when field activities will not be of extended duration. In general, a system with backwashable filter elements will be more convenient to operate and less expensive than similar units with replaceable filter elements. The primary limitation with respect to utility of a particular filter unit on a geothermal project is temperature capability. Injected effluents commonly are at or near boiling temperature. One type of cartridge filter unit that is of potential use in geothermal applications utilizes steel mesh filter elements that are backwashable. For example, Michigan Dynamics, Inc., Garden City, Michigan can supply wire cloth absolute backwashable filter units with flow capacities of up to 12,000 gpm at 500 psi and 600°F. This type of unit would be most attractive as an injection system polishing filter. AMF Cuno also manufactures metal element cartridge filtration systems which include provisions for automatic, continuous backwashing to minimize differential pressure increases. These units are sized for flows to 20,000 gpm. Higher flows can obviously be accommodated by utilizing several filter modules. The metal cartridge filters offer attractive possibilities for geothermal applications especially since chemical treatment of raw waters is not required as may be the case in obtaining optimum performance from a media filter.

IV-20-3. Sludge Dewatering

In geothermal operations, solids recovered by filtration, sedimentation, clarification, etc. must be further treated prior to ultimate disposal in a landfill. Additional treatment is required to reduce the moisture content of the sludge. Reduced moisture content is desirable first because the entrained waters may contain toxic dissolved species, such as boron, soluble chlorides and heavy metals, and secondly because moisture content represents bulk which

will increase transportation costs for delivering sludge to an approved disposal site. Sludge dewatering operations can be readily accomplished using conventional thickener and filter press technology[84].

A thickener is a sedimentation tank equipped with a central cone through which settled solids may be recovered. Depending upon the complexity of the unit, a motor driven rake may be used to direct solids to the central blowdown cone. The solids content of a geothermal sludge can be increased from 1-2 weight percent to as much as 10 weight percent. Thickened sludge is further treated to reduce water content either by the use of special filter assemblies or by centrifuges. Complete descriptions of these types of equipment are provided in Ref. 84. The filter press has been successfully used to treat sludge produced in conjunction with the utilization of hypersaline geothermal brine at the Salton Sea Geothermal Field. The solids content of treated sludge was increased to 65 weight percent from an initial value of 10 percent by use of a plate and frame filter press. Water treatment systems which include reactor-clarifiers incorporate thickeners as part of the clarifier process.

IV-20-4. Flotation

Flotation is a process whereby air bubbles or other gas bubbles are attached to fine-grained particulates so that the particulates, under quiescent conditions, are floated to the top of a sedimentation tank. The process is similar to gravity sedimentation with the obvious difference that the downward force exerted by gravity is overcome by the buoyancy of the gas bubbles. However, the parasitic forces which can disturb gravity sedimentation units must also be considered. In sedimentation units, settled solids are removed by an under drain system and clarified water is recovered using an overflow drain located near the top of the settling tank. In flotation units,

particulates are accumulated at the top of the separation tank and they are removed by means of a traveling rack or some sort of overflow skimming system. Clarified water is captured behind a sludge receiving wier located near the top of the tank.

Flotation is a well developed technology with primary use in the mineral industry for the separation of valuable minerals from tailings. There are no known geothermal flotation applications in the United States. Some interesting pilot scale work has, however, been successfully carried out by New Zealand geothermal researchers[88-89].

Efficient application of flotation requires that suspended particles become attached to levitating gas bubbles. A conditioning process is usually required to achieve particle attachment. The conditioning process involves use of one or more chemical additives that help to collect and secure particles to gas bubbles. For example, Ref. 85 describes the use of a galena collector called xanthate which is very specific for heavy metal sulfide minerals. The xanthate molecule contains a soluble sodium atom attached to an insoluble sulfur-bearing hydrocarbon chain:

$$ROC(=S)SNa \qquad R = \text{hydrophobic hydrocarbon chain}$$

Collection of sulfide particles by xanthate occurs by dissolution of the sodium atom and attachment of the free sulfur atom to a sulfide particulate. The protruding hydrocarbon chains make the sulfide particulate surface hydrophobic which encourages entrainment of the particulates by rising air bubbles. Similar conditioning processes are used to float other types of solids.

The primary difficulty in applying flotation technology to particulate separation from geothermal waters will be in the conditioning area. Geother-

mal waters will be hot and the appropriate chemical aids will have to be identified. Low to moderate salinity geothermal waters may not pose any particular difficulties, but the application of flotation to hypersaline geothermal brines could be problematic. In any case, no data is available to assess the practicality of flotation for a hypersaline brine system. Data are available, however, to indicate that flotation is a technically viable process for the treatment of lower salinity geothermal waters. The precaution noted earlier concerning potential detrimental effects of chemical additives on injectability should also be considered with respect to the use of conditioning aids.

Field Studies of Flotation -- Dissolved air flotation (DAF) is a process whereby bubbles for flotation are produced by dissolving high pressure air in water and then expanding the water through a throttling valve. The resulting bubble size is less than 100 microns and violent agitation of the flotation solution does not occur. For geothermal systems, the floated scum which forms is an advantage because it provides some therml insulation thereby minimizing convection currents.

Shannon and Buisson[88] completed a series of laboratory experiments to evaluate DAF flotation for geothermal applications. They produced iron flocs which were subsequently removed from solution using a laboratory DAF simulator. Their results indicated that:

1. Fine air bubbles for hot water DAF processing can be produced without difficulty.

2. Pumping costs for saturation of hot water with air are comparable to ambient temperature systems because of reduced viscosity and density of water at higher temperatures and lower air solubility.

3. Bubble rise and floc clearance in low viscosity, high temperature water is more rapid thereby favoring more rapid processing of raw water.

4. At 80°C from 70 to 80 percent of $Fe(OH)_3$ precipitate was removed from water using Allied Colloids Magnafloc 351 conditioner and an air-solids ratio as low as 0.05.

5. Less than 2 minutes were required to clear more than 70 percent of an iron floc through a water column 570 mm thick.

6. The capital and operating costs for a hot water DAF process were believed to be comparable to ambient temperature DAF processes.

7. The cost of installing and operating a DAF system has been estimated to be comparable to the costs of conventional sedimentation units of the same capacity.

A subsequent pilot-scale field study by Shannon, et al.[89] substantiated the effectiveness of DAF processing for the removal of particulates from hot geothermal water. In these experiments, hot geothermal water flowing at 6 tons/hour was dosed with ferric sulphate to produce an iron floc. The particulates were subsequently removed in a DAF unit. The overall system is shown schematically in Figure 52. Up to 89 percent of the iron floc was separted with the aid of Allied Colloids Magnafloc 351 and Ciba Geigy Quaternary O surfactant. The separation of iron floc was accomplished in a total treatment time of six minutes. The precipitation of ferric hydroxide in the DAF unit reduced the geothermal water pH from 8 to 4. The pH reduction was intended to stabilize silica in solution to prevent further precipitation. The pH stabilization process was based on work originally reported by Owen[90] and Grens and Owen[91] and subsequently repeated by New Zealand researchers[92]. An initial concentration of 4.5 grams per ton arsenic levels in the geothermal waters was reduced by 98 percent after dosing with 17 grams per ton of iron. The authors concluded that DAF processing was more suitable for removal of suspended solids than a conventional sedimentation unit. The primary advantages were that the hot water DAF process is more efficient than gravity sedimentation, it operates faster and produces a sludge with a higher solids content than settling.

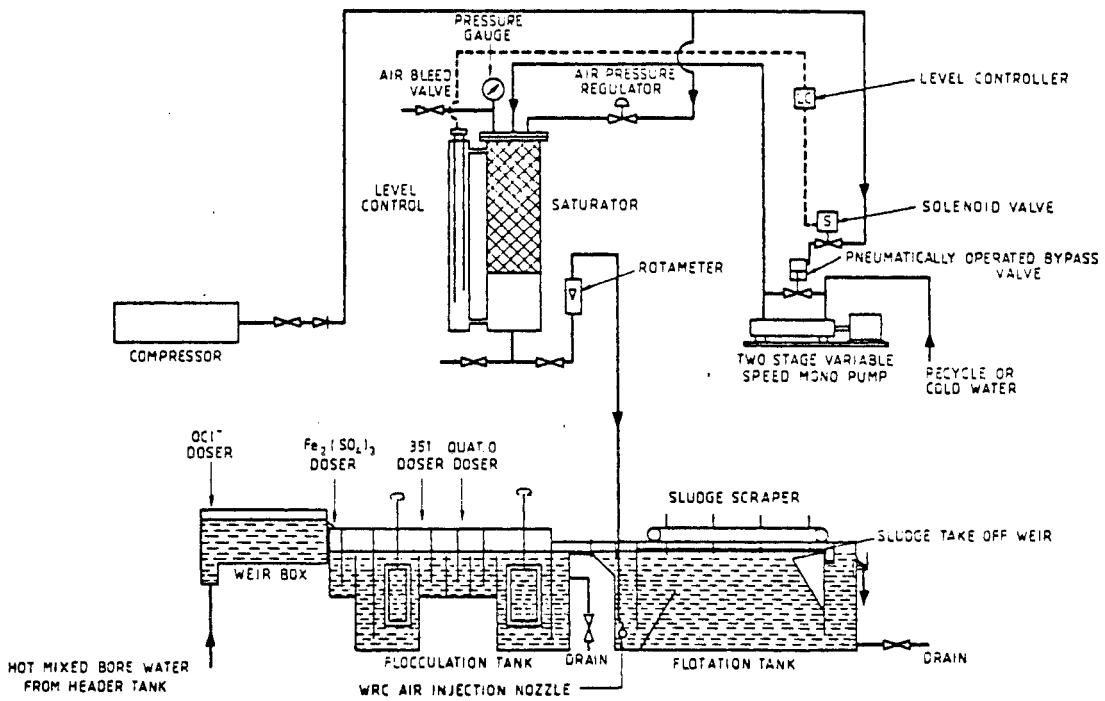

Figure IV-52. Pilot plant for evaluation of a hot water dissolved air flotation process. (From Ref. 89)

IV-20-5. Reaction Clarification

A reactor-clarifier is a device which is routinely used in the treatment of municipal waste streams. The basic system combines the functions of mixing, flocculation and settling in a single tank as shown in Figure 53. The high-rate solids-contact reactor-clarifier is the most efficient type of unit. The best quality overflow is achieved using this type of unit with the minimum amount of chemical additives[84]. Reaction-clarification is used to treat highly turbid waters where coagulation and flocculation are required. The most common applications include lime softening of water, and the treatment of industrial waste streams, and sewage.

A unique feature of a reactor-clarifier is the facility for recirculation of precipitated sludge with incoming raw water. Intimate contact of the water with the circulating sludge results in rapid precipitation of dissolved species which are supersaturated. It is possible, using this method, to more rapidly bring a supersaturated solution to thermodynamic equilibrium at the treatment temperature than would be possible by simply holding the same solution under quiescent periods for the same length of time. The operation of the reactor-clarifier is best understood by referring to Figure 53.

The center cage of the unit contains a high speed turbine mixer. Incoming water is contacted with recirculating sludge precipitated during earlier cycles. Chemical additives are injected into the reactor if needed to improve coagulation and flocculation of particulates. The reacted mixture leaves the central reactor and passes through a quiescent zone where solids are separated by gravity sedimentation. A mechanically operated rake at the bottom of the tank is used to sweep settled solids to a central point where they can be removed from the tank. Clarified effluent is obtained in the overflow from the top of the tank. More efficient clarification of the water can be achiev-

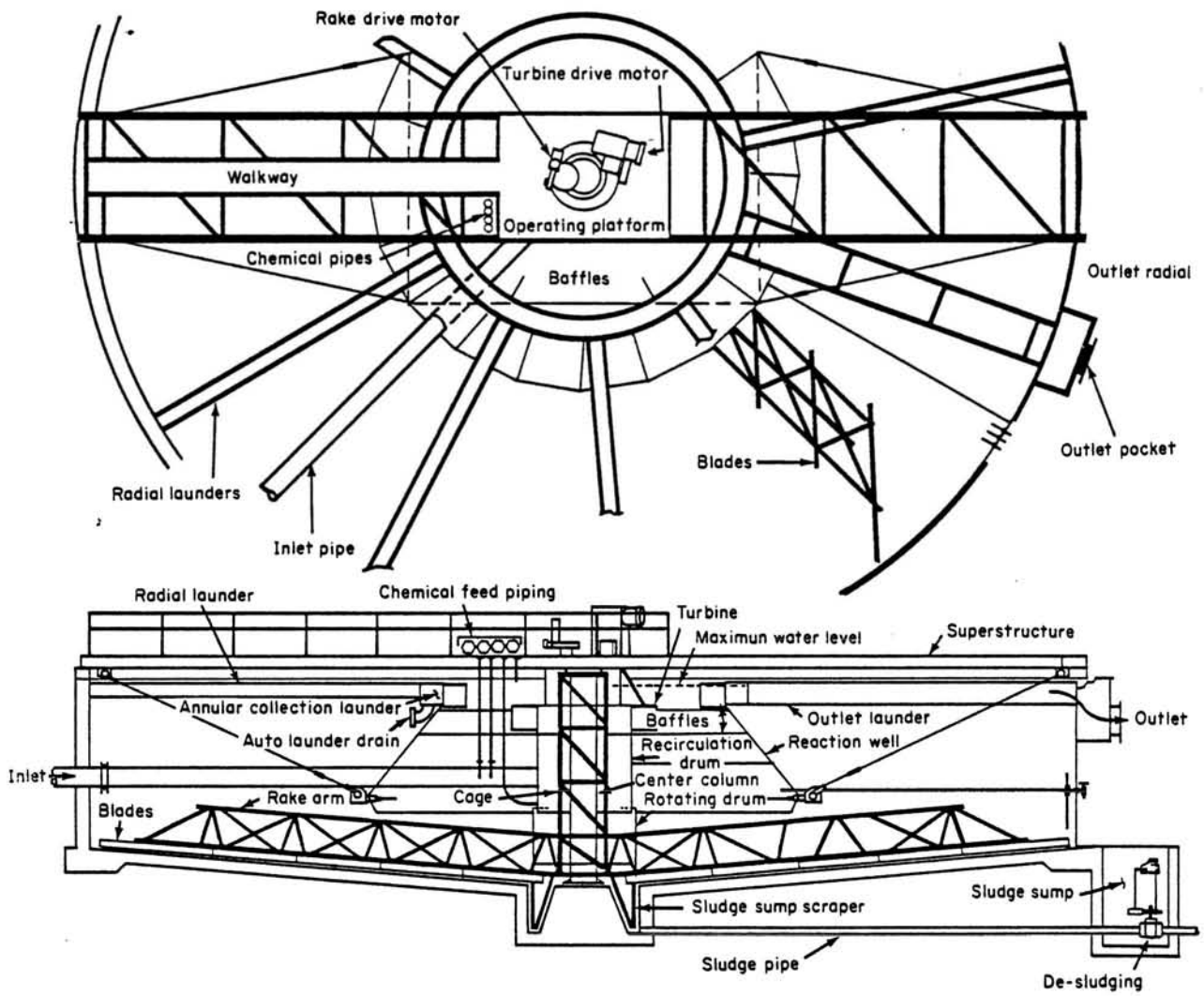

Figure IV-53. Reactor-clarifier of the high-rate, solids-contact type. (From Ref. 84)

ed by forcing the water, after it leaves the reactor zone, to flow through settled sludge, called the sludge blanket. This action results in additional particle removal by sludge blanket filtration.

The first attempt to use a reactor clarifier for the treatment of hot geothermal water was reported by Quong, et al.[93]. These early studies involved attempts to improve the injectability of hypersaline geothermal brine produced by a double flash Geothermal Loop Experimental Facility (GLEF) located in the Salton Sea Geothermal Field (Southern California). The GLEF was a joint operation by the U.S. Department of Energy and the San Diego Gas and Electric Company. Initially, bench condition jar testing was carried out at temperatures to about 90°C to evaluate the settling characteristics and potential for additional precipitation of dissolved species (silica and iron) from flashed brine. As a result of these efforts, important information concerning the behavior of flashed hypersaline brine was discovered:

1. Agitation significantly improved coagulation and flocculation of solids precipitated from hot (85°C) brine.

2. For the chemical additives that were evaluated, temperatures from 45 to 84°C had little influence on performance.

3. Flashed brine at pH 5.5 slowly clouded with silica precipitates. Coagulants did not significantly increase the rate of silica precipitation.

4. It was possible to rapidly precipitate silica in flashed brine by increasing brine pH to 5.9, but this treatment caused precipitation of iron hydroxide.

5. It was possible to rapidly reduce silica in flashed brine to saturation by contacting flashed brine with agitated freshly precipitated sludge (1 to 2 weight percent).

6. Inorganic coagulants and cationic polymers were found to be partially beneficial in combination with sludge contact in reducing treated brine turbidity.

7. Anionic polymers were highly effective flocculents when used in combination with sludge contact. Flocs settled rapidly and supernatant turbidity of 3 NTU was readily achieved.

The most important outcome of the bench scale testing program was the demonstration of the effectiveness of sludge contact in accelerating the precipitation of supersaturated silica and other dissolved species from flashed brine. Figure 54 illustrates the effect of sludge contact on the precipitation of silica from hypersaline brine.

The bench scale tests were followed by a series of pilot scale reactor-clarifier tests which made use of a unit with a brine throughput rate of 10 gallons per minute. The test unit is illustrated schematically in Figure 55. The reaction zone of a conventional reactor-clarifier was simulated using an outboard mixing tank. The residence time was 5 minutes in the mixing tank and 100 minutes in the clarifier. Upflow velocity in the quiescent zone of the clarifier was 0.38 gpm/ft^2. As shown, brine and solids were contacted in the rapid mix tank in the presence of a coagulant aid. The pretreated brine was then transferred to the clarifier where it was subjected to sludge blanket filtration and gravity settling. The sludge blanket was 24 inches thick and it contained 6 to 10 weight percent sludge. The best performance of the unit was achieved using 3 ppmv of Calgon Corp. M-580 coagulant aid (a hydrolyzed polyacrylamide polymer). The overflow effluent contained 44 ppmv suspended solids and dissolved silica was reduced to saturation. The clarification process following the rapid mix tank removed apprximately 80 percent of the suspended solids formed by the sludge contact process. It was further demonstrated that the clarified effluent could be polished using either a precoat pressure filter or a mixed media sands filter to produce an effluent containing less than 5 ppmv of suspended solids. The polished brine was also stabilized with respect to additional precipitation of dissolved silica.

A cost estimate for the brine processing system was generated. Assuming a 50 MWe power plant, the clarification-filtration system would cost 20 cents

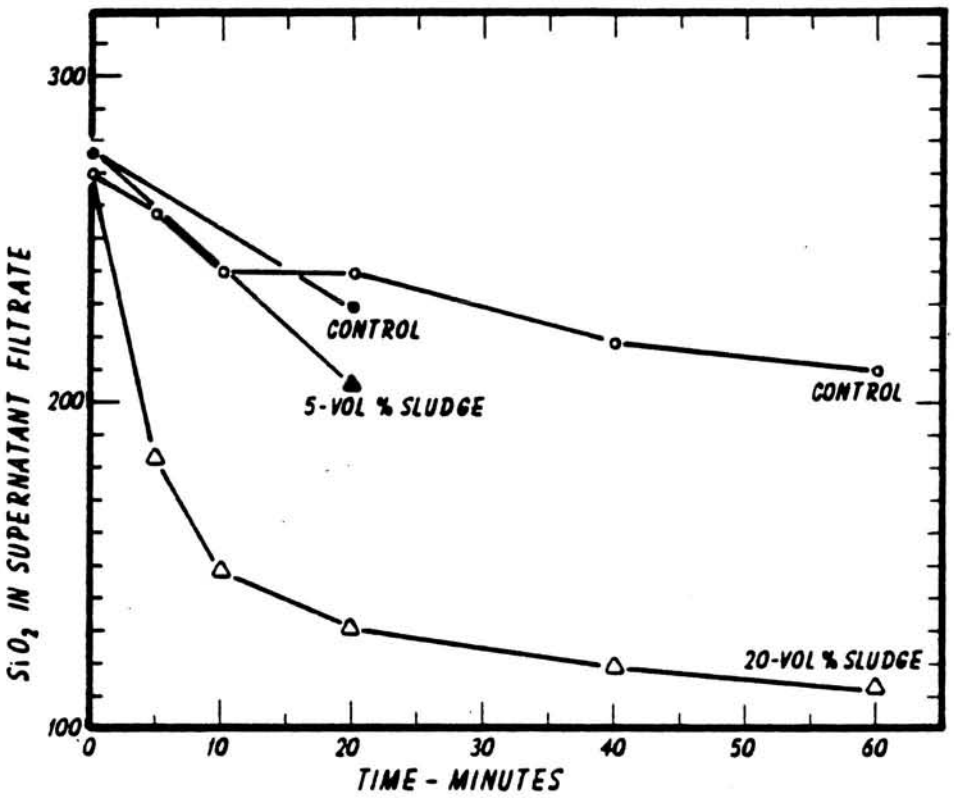

Figure IV-54. The effect of solids (sludge) contact with brine effluent on the precipitation rate of silica. (From Ref. 93)

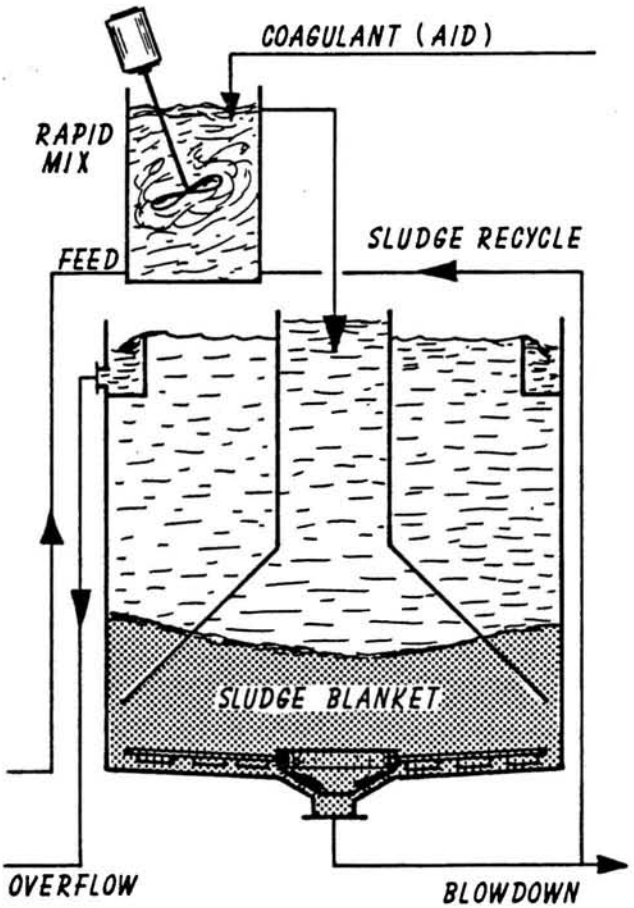

Figure IV-55. Schematic of pilot scale clarifier tested for removal of suspended solids from hypersaline brine. (From Ref. 93)

per 1000 gallons of treated brine. The cost assessment was based on the assumption of 100 lbs of brine per KWh. The treated effluent volume was 10 Mgd. Total costs of 1.7 mils/KWh vary by a few tenths of a mil depending upon the quantities of chemical aids used in the treatment of spent brine, the operating pressure of the filtration system and the water content of the sludge.

Large-Scale Clarifier Tests -- Pilot testing of a 30 gpm reactor-clarifier and filtration system using effluent hypersaline brine from the GLEF were carried out by Magma Power Company in 1978[94-96]. The pilot test unit was located adjacent to an injection well and operated on a continuous basis for a 1.5 month period. Subsequent testing was also carried out using the same unit to develop data for media filtration of clarified overflow and sludge dewatering. Important operating parameters of the integrated brine treatment system were as follows:

1. No chemical aids were used.
2. The upflow reactor-clarifier rate was 0.72 gpm/ft^2.
3. Solids concentration in the reaction well were 2.5 percent.
4. Effluent brine from the clarifier contained 172 mg/l dissolved silica (approximately saturation for the operating temperature) and 44 mg/l suspended solids.
5. Effluent produced by a media contained 5 mg/l suspended solids.
6. Sludge production amounted to 1.7 lbs/day per gpm.
7. Sludge concentrations in various parts of the treatment system were as follows:

    a) reactor-clarifier - 4.5 percent
    b) thickener - 10 percent
    c) filter press - 65 percent

An important outcome of these tests was the determination that conventional thickening-filter press technology could readily produce a filter cake for

landfill disposal with a solids content of 65 percent. The best performance obtained using a centrifuge produced a filter cake with a solids content of 50 percent. The filter press filtrate, which must be returned to the clarifier, was essentially free of suspended solids whereas the filtrate produced by the centrifuge contained up to 1 weight percent suspended solids. Reintroduction of extraneous solids into the reactor-clarifier is detrimental to the performance of the unit.

The reduction of dissolved silica to saturation levels in the reactor zone of the clarifier is a function of the solids concentration in the reactor well. The relationship between solids concentration and silica reduction is shown in Figure 56. Silica stabilization was achieved at a solids concentration of about 2.5 percent. Further increase in the solids concentration had little additional effect on the level of soluble silica in the treated brine. These conditions pervail at the treatment temperature which was between 180 to 200°F. A reduction in brine temperature downstream of the clarifier-filtration system could result in additional precipitation of dissolved silica. Similarly, introduction of air into treated brine could result in post treatment precipitation of dissolved iron and reduction in brine pH.

An estimate of treatment costs lead to the following conclusions:

Brine treatment costs were estimated to be 11 cents per 1000 gallons of brine. The sludge dewatering costs based on the use of thickeners and filter presses was 8 cents per 1000 gallons of brine. The total treatment cost was 19 cents per 1000 gallons of brine or 1.6 mils per KWh. Chemical additions, if needed, would add another 2-5 cents per 1000 gallons of brine to the treatment costs.

Demonstration Tests -- In 1979, a 10 MWe capacity brine treatment facility was built to process the total output of the GLEF. The system design is

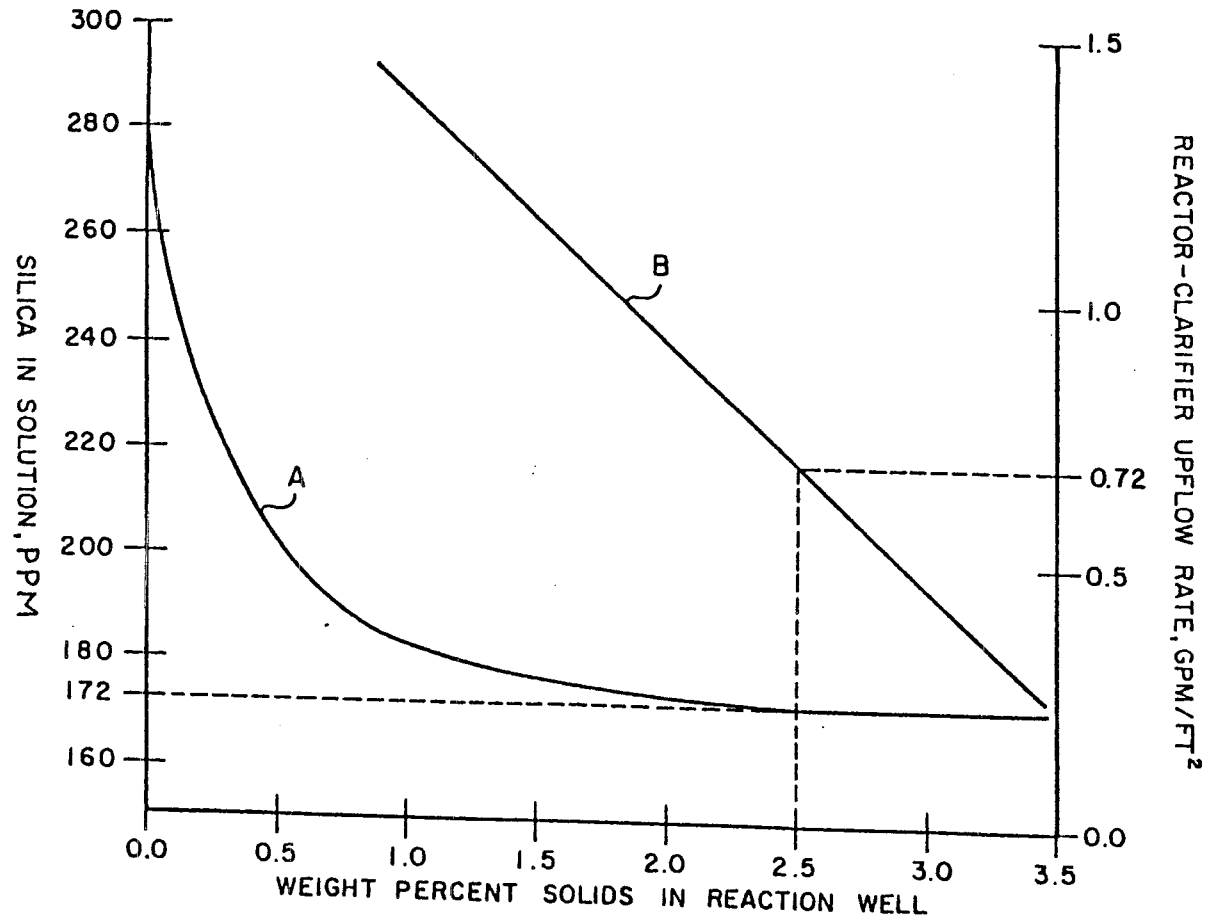

Figure IV-56. Performance characteristics of a reactor-clarifier. Curve A refers to dissolved silica concentrations. Curve B refers to upflow rates. (From Ref. 97)

illustrated in Figure 57. The performance of this unit was similar to results obtained for the 30 gpm pilot system. The detailed operating characteristics and design of the demonstration unit are fully described in Ref. 98. The reactor-clarifier used in the demonstration unit is shown in Figure 58. The unit was supplied by the EMICO Division of Envirotech Corporation. This unit was sized for a brine throughput rate of about 96,000 gallons per hour. A detailed description of the numbered items in Figure 58 is provided in Ref. 98.

IV-20-6. Crystallizer Technology

Successful adaptation of the principle of reaction clarification to treat geothermal effluents for injection led to attempts to carry the process forward in the geothermal energy conversion cycle. One of the major gains in utilizing reactor-clarifiers was the elimination of scale deposition in the clarifier and downstream components. At the GLEF, silica scaling rates of up to 3.5 inches per hour were experienced in the low pressure flash vessel, the atmospheric receiver vessel and in downstream piping[96]. Scale deposition in the higher temperature first-stage flash vessel was lower but still troublesome. Periodic shutdowns were required to mechanically remove scale deposits by hydroblasting. Efforts were, therefore, directed to combine the functions of a flash separator and reactor-clarifier in the same vessel.

Crystallizer technology has been used for years by the chemical processing industry. A comprehensive description of crystallizers is provided in Ref. 84. Crystallizers may be classified in terms of the methods used to suspend the growing product. There are five particle suspension categories as summarized in Table IV-6. In geothermal applications, scale formation is suppressed by providing a large ratio of seed particulates to piping and vessel surface area to preclude scale deposition. The seed material consists of

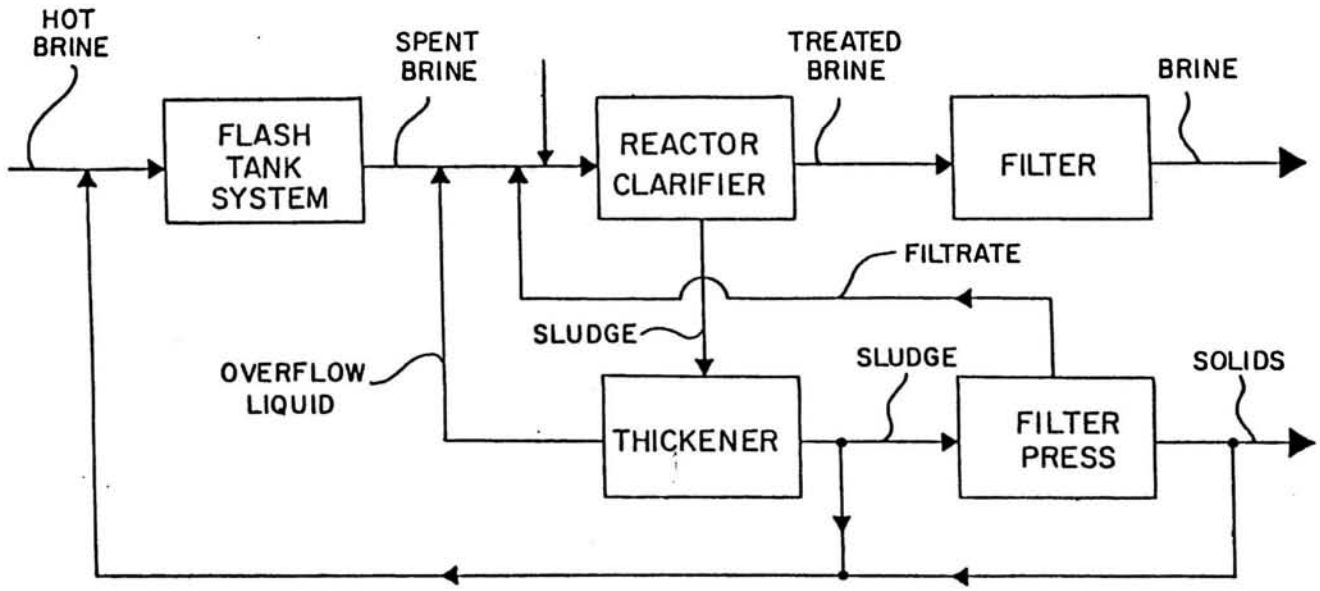

Figure IV-57. Geothermal loop experimental facility (GLEF) brine treatment systems. (From Ref. 97)

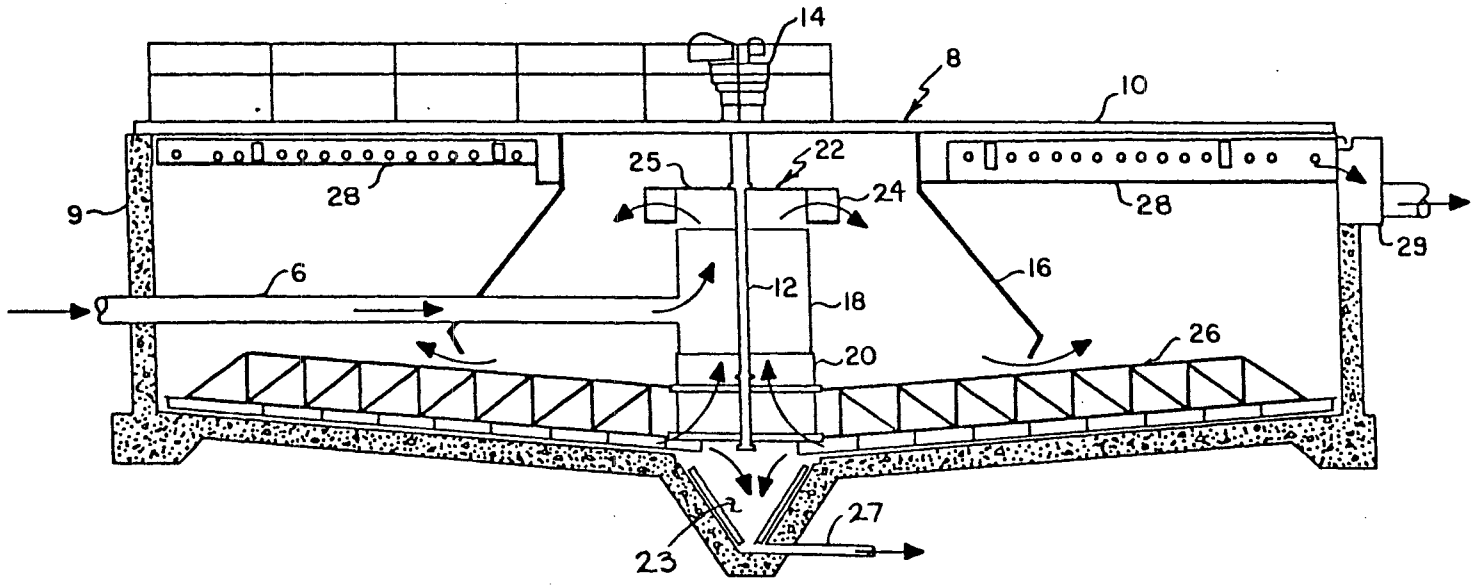

Figure IV-58. EIMCO reactor-clarifier. (From Ref. 98)

Table IV-6

Classification of Crystallizers Based on the Method of Suspending the Growing Product (From Ref. 84)

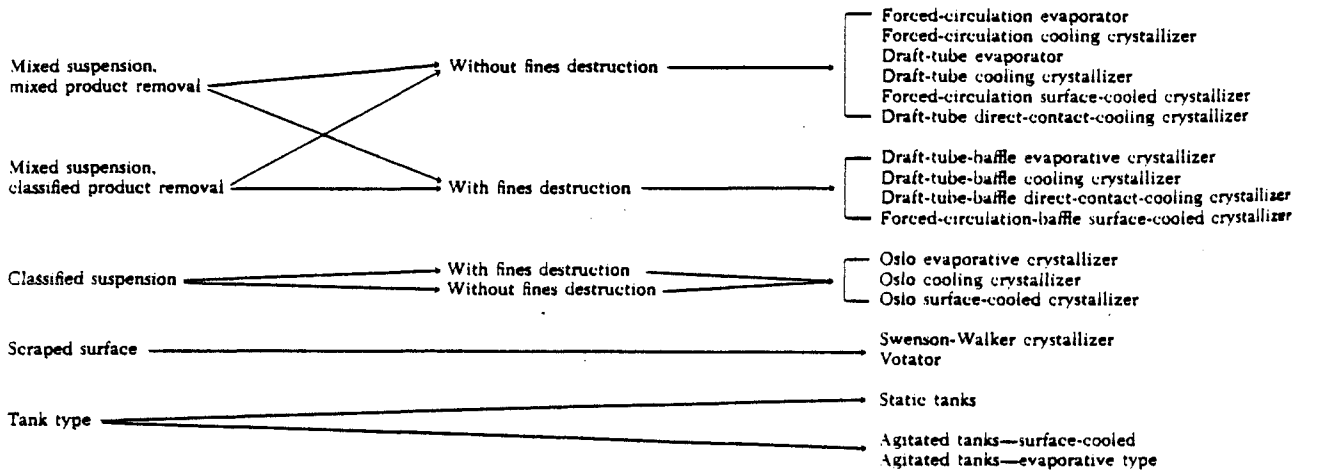

finely divided recycled sludge. The sludge contact reduces supersaturated dissolved species such as silica to saturation levels and thereby reduces the main driving force for scale formation.

The prototype flash crystallizer evaluated for service as a replacement for a low pressure flash steam separator is shown in Figure 59. The unit is similar to a conventional tangential entry flash separator with a provision for recycling sludge produced in a downstream clarifier. The unit has no provisions for removal of precipitated solids. The generated particulates are carried through the system where they are eventually removed by the appropriately sized reactor-clarification system. Operation of this type of unit resulted in essentially complete elimination of scale deposition at the GLEF low pressure steam separator conditions. Chloride carryover in the separated steam was 5 mg/l or less. Brine residence time in the crystallizer was 8 minutes and from 0.5 to 1.0 percent solids recycle concentration was required to control scale deposition. Detailed chemistry assessments made at the GLEF[96] indicated that silica processed brine was slightly supersaturated in

the crystallizer effluent. The solubility of silica in brine for various operating temperatures was as follows:

Average Temperature (°F)	Silica Solubility (mg/l)
263.5	344.4
289.7	369.7
304.9	405.6

Plans developed for a 49 MWe geothermal power plant located at the Salton Sea Geothermal Field involved the use of two first stage flash separators operating at production islands at 200 psia. Scale deposition rates at these conditions were considered acceptable. The separated single phase brine streams were then conveyed to a second stage flash crystallizer operated at 22 psia. The treated brine effluent was then split into two streams and directed to two equal sized reactor-clarifiers. Clarified overflow was split again into two equal streams and then transferred to two media filtration modules for final polishing. The sludge produced by the reactor-clarifier and filters was dewatered using thickeners and a filter press of conventional design.

IV-20-7. Flash Crystallization

The control of scale deposits formed at high temperature and pressure can be achieved by combining recycle seeding and slurry segregation capabilities in a flash steam separator vessel. A series of papers by Awerbuch and others [99-102] describe an integrated flasher-crystallizer-separator (FCS) unit with the capability of eliminating scale deposition while simultaneously producing high purity steam for turbogenerators. The basic FCS unit is shown in Figure 59. Geothermal brine is injected into a centrally located venturi which promotes expansion of the brine to produce steam and simultaneous precipitation of scaling species. The intimate contact of brine with freshly precipi-

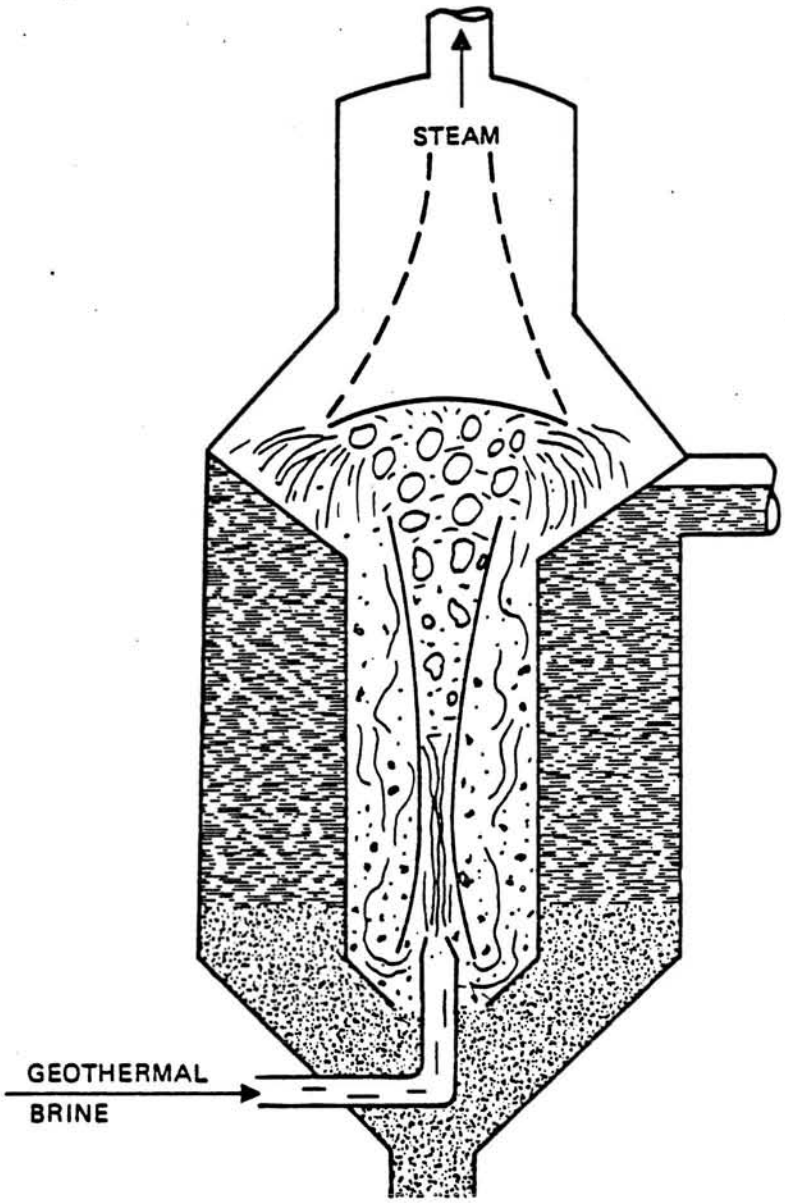

Figure IV-59. The Bechtel flasher-crystallizer-separator unit. (From Ref. 100)

tated particulates promotes rapid precipitation of additional quantities of dissolved scaling species. In the case of silica, reduction of supersaturation by 80 percent causes a substantial increase in the length of time required for attainment of equilibrium. Thus, it is not necessary to achieve silica solubility in the FCS to inhibit silica scale deposition.

The FCS unit shown in Figure 59 incorporates a sludge settling volume and the capability for sludge blanket filtration. This type of unit could potentially be used in a mineral recovery operation where valuable constituents could be segregated from the bulk of solids that would be recovered by a conventional reactor-clarifier. The use of chemicals is not required to prevent scale formation. However, in a combined mineral recovery-scale suppression operation, certain chemical additives might be used to more completely precipitate dissolved species such as the lead, silver or other heavy metals.

The Bechtel FCS process as described in Refs. 99-102 eliminates the need for a downstream reactor-clarifier. The claim is made that silica can be stabilized in solution for injection by diluting and reheating the spent effluent. The integrated process is shown in Figures 60-61. A two-stage FCS system is illustrated with reheat supplied by a thermocompressor (Figure 60) or by a mechanical compressor (Figure 61). The concept of reheating and diluting geothermal brine to stabilize residual silica may be workable at many of the low to moderate salinity resources. However, in the case of the hypersaline resources of the Salton Trough (Southern California), dissolved iron and silica coprecipitate from low pressure flashed brine. Reheat may or may not stabilize silica depending upon the ultimate stability of iron as coprecipitation of both species is probable. In any case the utilization of a downstream reactor-clarifier and filtration system would provide a complete

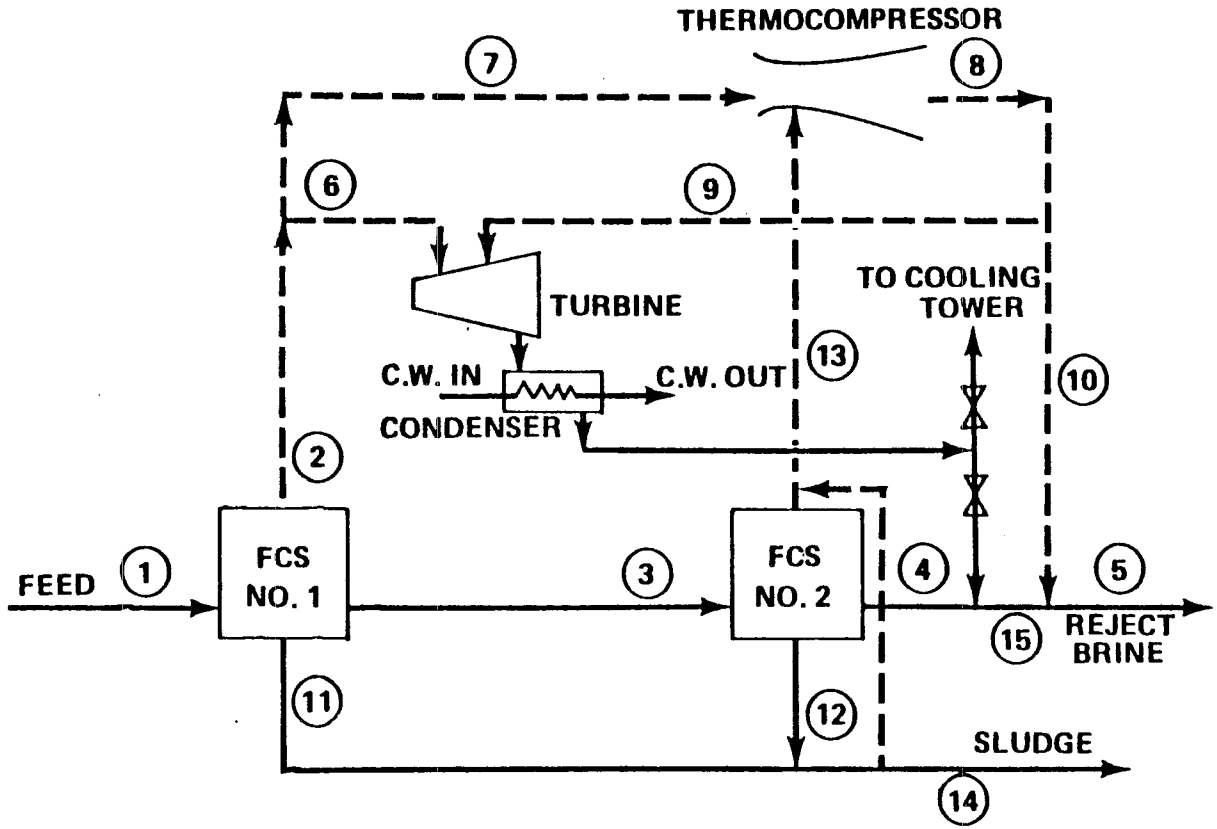

Figure IV-60. Process flow sheet for a dual-stage FCS demonstration plant. (From Ref. 100)

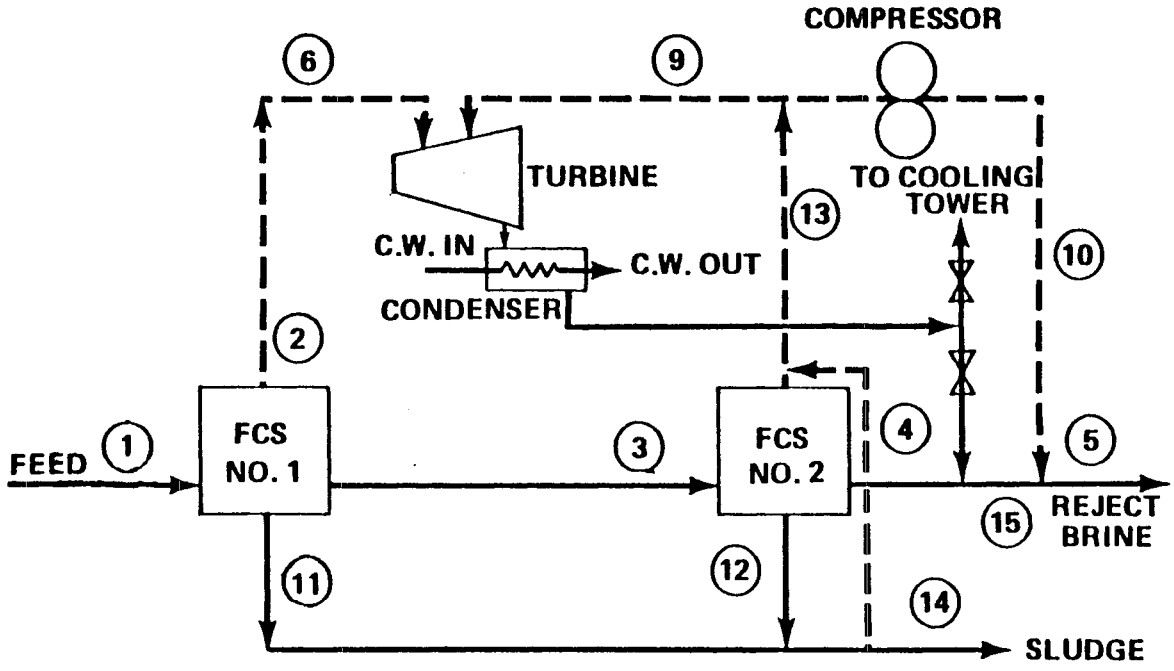

Figure IV-61. Alternate process flow sheet for a dual-stage FCS demonstration plant. (From Ref. 100)

treatment capability for even the hypersaline geothermal brines. A downstream filtration system would be needed even for the reheat FCS system since the overflow from the FCS units would most likely contain objectionable levels of suspended particulates.

The Union Oil Company has been successfully operating a 10 MWe demonstration plant located in the southwestern portion of the Salton Sea Geothermal Field. The plant utilizes a preflash wellhead separator that operates at production wellhead conditions and two Goslin-Burmingham FCS stages. Particulates generated in the FCS stages are carried through the system to a reactor-clarifier followed by a media filter system. Scale abatement in the plant is said to be excellent. It can be concluded on the basis of this experiment that the high temperature/pressure crystallization process when used in combination with a reactor-clarifier makes it possible to utilize hypersaline geothermal brines without major concerns about scaling in surface equipment. By inference, it should, therefore, be relatively easy to treat lower salinity brine systems with the same level of effectiveness.

IV-21. References

1. Campbell, M.D., Mistrot, G. and Towse, D., 1979, Reservoir Assessment: Chap. II - Improving the Performance of Brine Wells at Gulf Coast Strategic Petroleum Reserve Sites: Lawrence Livermore National Laboratory Report UCRL-52829, L. B. Owen and R. Quong, Editors.

2. Knutson, C.F., and C.R. Boardman, 1978, An Assessment of Subsurface Saltwater Disposal Experience on the Texas and Louisiana Gulf Coast for Application to Disposal of Salt Water from Geopressured Geothermal Wells: U.S. Department of Energy, Div. Geothermal Energy, NVO/1531-2.

3. Warner, D.L., 1972, Survey of Industrial Waste Injection Wells, Vols. I and II: U.S. Geological Survey, NTIS AD-756-641, June.

4. Warner, D.L. and Lehr, J.H., et al., 1977, An Introduction to the Technology of Subsurface Wastewater Injection: EPA Environmental Protection Technology Series, EPA-600/2-77 240, 345 p.

5. Campbell, M.D., and G.R. Gray, 1975, Mobility of Well-Drilling Additives in the Ground-Water Systems: EPA Conf. Envirn. Aspects of Chemical Use in Well-Drilling Operations, May 21-23, Houston, Report EPA-560-1-75-004, 45 p.

6. Owen, L.B., 1979, Evaluating Brine Injection for DOE's Strategic Petroleum Reserve Program: Energy and Technology Review, August.

7. Campbell, M.D., and J.H. Lehr, 1973, Water Well Technology: McGraw-Hill, New York (4th Printing, 1977), 601 p.

8. Jordan, C.A., Edmondson, T.A. and Jeffries-Harris, M.J., 1969, The Bay Marchand Pressure Maintenance Project - Unique Challenges of an Offshore, Sea-Water Injection System: JPT, 389-396.

9. Horne, R.N., 1982, Geothermal Reinjection Experience in Japan: JPT, 495-503.

10. Thain, I.A., 1980, Wairakei - The First Twenty Years: Paper Presented at the Electric Power Research Inst. Geothermal Conference, Monterey, CA, May.

11. James, C.R., 1979, Reinjection Strategy: Proc. Fifth Stanford U. Geothermal Reservoir Engineering Workshop, Stanford, CA, 385-389.

12. Chasteen, A.J., 1975, Geothermal Steam Condensate Reinjection: Proc. Second United Nations Symposium on Geothermal Energy, San Francisco, 1335-1339.

13. Gulati, M.S., Lipman, S.C. and Strobel, C.J., 1978, Tritium Tracer Survey at the Geysers: Trans. Geothermal Resources Council, 2, 237-239.

14. Grant, M.A. and Horne, R.N., 1980, The Initial State and Response to Exploitation of Wairakei Geothermal Field: Trans. Geothermal Resources Council, 4, 333-339.

15. Kakkonda Geothermal Power Plant: Japan Metals and Chemicals Co., Ltd., Tokyo (1978) (in Japanese).

16. Nakamura, H., 1981, Development and Utilization of Geothermal Energy in Japan: Trans. Geothermal Resources Council, 5, 33-35.

17. Einarsson, S.S., Vides-R.A., and Cuellar, G., 1975, Disposal of Geothermal Waste Water by Reinjection: Proc. Second United Nations Symposium on Geothermal Energy, San Francisco, 1349-1363.

18. DiPippo, R., 1980, Geothermal Energy as a Source of Electricity: U.S. DOE, Washington, D.C.

19. Ito, J., Kubota, Y., and Kurosawa, M., 1977, On the Geothermal Water Flow of the Onuma Geothermal Reservoir: Chinetsu Enerugii (Geothermal Energy), 14, 15-27 (in Japanese).

20. Koto, K., 1980, A Recent Aspect of Onuma Geothermal Power Plant: Chinetsu Enerugii (Geothermal Energy), 15, 50-51 (in Japanese).

21. Hayashi, M., Mimura, T., and Yamasaki, T., 1978, Geological Setting of Reinjection Wells in the Otake and the Hatchobaru Geothermal Field, Japan: Trans. Geothermal Resources Council, 2, 263-266.

22. Yoshida, K., 1980, Hatchobaru Geothermal Power Plant: Chinetsu Enerugii (Geothermal Energy), 15, 23-49 (in Japanese).

23. Onodera, S. and Fukuda, M., 1976, A Study of the Reinjection at the Otake Geothermal Field: Kogaku Shuho, Technology Report, Kyushu U., 49, 829-835 (in Japanese).

24. Bodvarsson, G., 1972, Thermal Problems in the Siting of Reinjection Wells: Geothermics, 1, 63-66.

25. McCabe, W.J., Manning, M.R., and Barry, B.J., 1980, Tracer Tests - Wairakei: Inst of Nuclear Sciences Report INS-R-275, DSIR, Lower Hutt, New Zealand, July.

26. Ito, J., Kubota, Y. and Kurosawa, M., 1978, Tracer Tests of the Geothermal Hot Water at Onuma Geothermal Field: Japan Geothermal Energy Assn. J., 15, 87-97 (in Japanese).

27. Messer, P.H., Pye, D.S. and Gallus, J.P., 1978, Injectivity Restoration of a Hot-Brine Geothermal Injection Well: JPT, 1225-1230.

28. Jorda, R.M., 1978, An Analysis of Water Reinjection at the Niland Geothermal Test Site: Sandia National Laboratory Report, DOE/DGE Contract No. 05-6199.

29. Ahmed, U., Wolgemuth, K.M., Abou-Sayed, A.S., Schatz, J.F. and Jones, A.H., 1980, Raft River Geothermal Site: A Reinjection Study: Geothermal Resources Council, Trans., V. 4, 385-388.

30. Earlougher, R.C., Jr., 1977, Advances in Well Test Analysis: SPE-AIME, 264 p.

31. Matthews, C.S. and Russell, D.G., 1967, Pressure Build-Up and Flow Tests in Wells: SPE-AIME, 172 p.

32. Craig, F.F., Jr. 1980, The Reservoir Engineering Aspects of Waterflooding: SPE-AIME, 141 p.

33. Howard, G.C. and Fast, C.R., 1970, Hydraulic Fracturing: SPE-AIME, 210 p.

34. Dabe, L.P., 1978, Fundamentals of Reservoir Engineering: Elsevier, 443 p.

35. Blair, C.K. and Owen, L.B., 1981, An Evaluation of Reinjection into Geopressured Reservoirs: Geothermal Resources Council, Transactions, V. 5, 271-274.

36. Hanson, J.M., 1977, Heat Transfer Effects in Forced Geoheat Recovery Systems: Ph.D. Dissertation, Oregon State Univ., 176-186.

37. Kasameyer, P.W., 1977, Thermal History of Injected Effluents: In - The LLL Geothermal Energy Program Status Report, January 1976 - January 1977, Univ. Calif. Lawrence Livermore National Laboratory Report UCRL-50046-76, ed. Austin, et al., 153-156.

38. Hanson, J.M. and Kasameyer, P.W., 1978, Predicting Production Temperature Using Tracer Methods: Geothermal Resources Council, Trans., V. 2, 257-258.

39. Hawkins, M.F., 1956, A Note on the Skin Effect: Petroleum Trans., AIME, V. 207, 356-357.

40. Brons, F., 1961, The Effect of Restricted Fluid Entry on Well Productivity: JPT, 172-174.

41. Morse, J.G. and Schroeder, R.C., 1977, Case Studies, Injection Tests: In - The LLL Geothermal Energy Program Status Report, January 1976 - January 1977, Univ. Calif. Lawrence Livermore National Laboratory Report UCRL-50046-76, Ed. Austin, et al., 165-167.

42. Perkins, T.K. and Kern, L.R., 1961, _____ J. Petroleum Technology, V. 13, 937.

43. Streeter, V.L., 1971, Fluid Mechanics: McGraw-Hill, 5th Edition.

44. Baumeister, T. and Manko, L.S., 1967, Standard Handbook for Mechanical Engineers: 7th Ed., McGraw-Hill.

45. Snyder, R.E., 1978, Geothermal Well Completions - An Overview of Existing Methods in Four Types of Developments: Sandia Laboratories Rept. No. 78-7010.

46. Jorda, R.M., 1980, Use of Data Obtained From Core Tests in the Design and Operation of Spent Brine Injection Wells in Geopressured or Geothermal Systems: Sandia Rept. SAND80-7047.

47. API Recommended Practice for Core Analysis Procedure: American Petroleum Institute, API RP 40 (1960).

48. Donaldson, E.C. and Crocker, M.E., 1977, Review of Petroleum Oil Saturation and its Determination: U.S. DOE, Bartlesville Energy Research Center, BERC/R1-77/15.

49. Anderson, G., 1975, Coring and Core Analysis Handbook: PennWell, 200 p.

50. Transactions, Special Publications and Short Courses, Geothermal Resources Council, P.O. Box 98, Davis, California 95617.

51. Proceedings, Workshop, Geothermal Reservoir Engineering, Interdisciplinary Research in Engineering and Earth Sciences, Stanford Geothermal Program, Stanford University, Stanford, California.

52. Proceedings, International Well-Testing Symposia and Technical Reports, Earth Sciences Division, Lawrence Berkeley National Laboratory, University of California, Berkeley, California.

53. Jorda, R.M., 1978, An Engineering Study of Water Reinjection for Geothermal Systems: Sandia National Laboratory, Rept. SAND78-7009.

54. Rose, H.E., 1968, The Determination of the Grain-Size Distribution of a Spherical Granular Material Embedded in a Matrix: Sedimentology, V. 10, 293-309.

55. VanDerPlas, L., 1962, Preliminary Note on the Granulometric Analysis of Sedimentary Rocks: Sedimentology, V. 1, 145-157.

56. Folk, R.L., 1968, Petrology of Sedimentary Rocks: University of Texas, Geology, 370 K, 383 L, 383 M, 170 p.

57. Grens, J., 1977, Preliminary Tests Using a Laser Particle-Size Analyzer on Geothermal Brine: University of California, LLNL Rept. UCID-17637.

58. Porter, M.C., 1975, A New Particle Counter for Non-Destructive Monitoring of Parenterals: Bulletin of the Parenteral Drug Assn., V. 29, N. 4, 169-182.

59. Quong, R., Owen, L.B., and Tardiff, G.E., 1978, Geothermal Brine Injection Evaluation Methodology: Second Invitational Well-Testing Symposium, Proceedings, University of Calif., Lawrence Berkeley National Laboratory, LBL-8883, CONF-7810170, 78-80.

60. Doscher, T.M. and Weber, L., 1957, The Use of the Membrane Filter in Determining Quality of Water for Subsurface Injection: Drilling and Production Practice, 169-179.

61. Hewitt, C.H., 1963, Analytical Techniques for Recognizing Water Sensitive Reservoir Rocks: Jour. Petroleum Technology, 813-818.

62. Johnston, K.H. and Castagno, J.L., 1964, Evaluation by Filter Methods of the Quality of Waters Injected in Waterfloods: U.S. Bureau of Mines, RI 6426, 14 p.

63. Mungan, N., 1965, Permeability Reduction Through Changes in pH and Salinity: Jour. Petroleum Technology, 1449-1453.

64. Farley, J.T. and Redline, D.G., 1968, Evaluation of Flood Water Quality in the West Montalvo Field: Jour. Petroleum Technology, 683-687.

65. Barkman, J.H. and Davidson, D.H., 1972, Measuring Water Quality and Predicting Well Impairment: Jour. Petroleum Technology, 865-872.

66. McCune, C.C., 1977, On-Site Testing to Define Injection-Water Quality Requirements: Jour. Petroleum Technology, 17-24.

67. Keelan, D.K. and Koepf, E.H., 1977, The Role of Cores and Core Analysis in Evaluation of Formation Damage: Jour. Petroleum Technology, 482-490.

68. Davidson, D.H., 1979, Invasion and Impairment of Formations by Particulates: SPE 8210, Sept.

69. Donaldson, E.C., et al., 1977, Particle Transport in Sandstone: SPE 6905, Oct.

70. Champlin, R.D., Thomas, R.D. and Brownlow, A.D., 1967, Laboratory Testing and Evaluation of Porous Permeable Rock for Nuclear Waste Disposal: U.S. Bureau of Mines, RI 6926, 33 p.

71. Method for Determining Water Quality for Subsurface Injection Using Membrane Filters: National Association of Corrosion Engineers, NACE Standard TM-01-73, 1973.

72. Patton, C.C., 1977, Oilfield Water Systems: Campbell Petroleum Series, Norman, Oklahoma, 252 p.

73. Owen, L.B., Blair, S.C. and Peterson, E., 1982, Field and Laboratory Studies of Subsurface Injection - Seasonal Thermal Energy Storage Program (STES): Proceedings of the DOE Physical and Chemical Energy Storage Annual Contractors Review Meeting, U.S. DOE CONF-820827, Aug. 23-26, Arlington, VA, 96-105.

74. Tewhey, J.D., Chan, M.A., Kasameyer, P.W. and Owen, L.B., 1978, Development of Injection Criteria for Geothermal Resources: Geothermal Resources Council, Transactions, V. 2, 649-652.

75. Netherton, R. and Owen, L.B., 1978, Apparatus for the Field Evaluation of Geothermal Effluent Injection: Geothermal Resources Council, Transactions, V. 2, 487-490.

76. Hasbrouck, R.T., Owen, L.B. and Netherton, R., 1979, An Automated System for Membrane Filtration and Lace Tests: Geothermal Resources Council, Transactions, V. 3, 301-304.

77. Harrar, J.E., Netherton, R., Locke, F.E. and Owen, L.B., 1981, Assessment of the Injectability of Brines Produced by Geopressured-Geothermal Resources of the Gulf Coast: 5th Geopressured-Geothermal Energy Conf., U.S. DOE/Louisiana Geol. Survey/Louisiana State University, Bebout and Bachman, Ed., 145-148.

78. Owen, L.B., Raber, E., Otto, C., Netherton, R., Neurath, R. and Allen, L., 1979, An Assessment of the Injectability of Conditioned Brine Produced by a Reaction Clarification -- Gravity Filtration System in Operation at the Salton Sea Geothermal Field, Southern California: Univ. Calif., Lawrence Livermore National Laboratory, Rept. UCID-18488.

79. Owen, L.B., Blair, C.K., Harrar, J.E. and Netherton, R., 1980, An Evaluation of Geopressured Brine Injectability: Proceedings, Sixth Workshop Geothermal Reservoir Engineering, Stanford Univ., Rept. SGP-TR-50, 98-104.

80. Owen, L.B. and Quong, R., 1979, Improving the Performance of Brine Wells at Gulf Coast Strategic Petroleum Reserve Sites: Univ. of Calif., Lawrence Livermore National Laboratory, Rept. UCRL-52829.

81. Hill, J.H., Harrar, J.E., Otto, C.H., Jr., Deutscher, S.B., Crompton, H.E., Grogan, R.G. and Hendricks, V.H., 1979, Apparatus and Techniques for the Study of Precipitation of Solids and Silica from Hypersaline Geothermal Brine: University of California, Lawrence Livermore National Laboratory Rept. UCRL-52799.

82. Harrar, J.E., Otto, C.H., Jr., Deutscher, S.B., Ryan, R.W. and Tardiff, G.E., 1979, Studies of Brine Chemistry Precipitation of Solids, and Scale Formation at the Salton Sea Geothermal Field: University of California, Lawrence Livermore National Laboratory Rept. UCRL-52640.

83. Raber, E., Owen, L.B. and Harrar, J.E., 1979, Using Surface Waters for Supplementing Injection at the Salton Sea Geothermal Field (SSGF), Southern California: Geothermal Resources Council, Transactions, V. 3, 561-564.

84. Perry, R.H. and Chilton, C.H., 1973, Chemical Engineer's Handbook: Fifth Edition, McGraw-Hill Book Company.

85. Berkowitz, J.B., Funkhouser, J.T. and Stevens, J.I., 1978, Unit Operations for Treatment of Hazardous Industrial Waste: Noyes Data Corp.

86. Raber, E., Thompson, R.E. and Smith, F.H., 1981, Improving the Injectability of High Salinity Brines for Disposal or Waterflooding Operations: SPE 10093.

87. Quong, R., Schoepflin, F., Stout, N.D., Tardiff, G.E. and McLain, F.R., 1978, Processing of Geothermal Brine Effluents for Injection: Geothermal Resources Council, Transactions, V. 2, 551-554.

88. Shannon, W.T. and Buisson, D.H., 1980, Dissolved Air Flotation in Hot Water: Water Research, V. 14, 759-765.

89. Shannon, W.T., Owers, W.R. and Rothbaum, H.P., 1982, Pilot Scale Solids/Liquid Separation in Hot Geothermal Discharge Waters Using Dissolved Air Flotation: Geothermics, V. 11, N. 1, 43-58.

90. Owen, L.B., 1975, Precipitation of Amorphous Silica From High Temperature Hypersaline Geothermal Brine: University of California, Lawrence Livermore National Laboratory Report, UCRL-51866.

91. Grens, J.Z. and Owen, L.B., 1977, Field Evaluation of Scale Control Methods: Acidification: Transactions, Geothermal Resources Council, V. 1, 119-122.

92. Rothbaum, H.P., Anderton, B.H., Harrison, R.F., Rohde, A.G. and Slatter, A., 1979, Effect of Silica Polymerization and pH on Geothermal Scaling: Geothermics 8, 1-20.

93. [LARRY THIS REFERENCE IS THE SAME AS NO. 87]
Quong, R., Schepflin, F., Stout, N.D., Tardiff, G.. and McLain, F.R., 1978, Processing of Geothermal Brine Effluents for Injection: Geothermal Resources Council, Transactions, V. 2, 551-554.

94. Featherstone, J.L., Van Note, R.H. And Pawlowski, B.S., 1979, A Cost-Effective Treatment System for the Stabilization of Spent Geothermal Brines: Geothermal Resources Council, Transactions, V. 3., 201-204.

95. Featherstone, J.L., Powell, D.R. and Van Note, R.H., 1979, Stabilization of Highly Saline Geothermal Brines: SPE 8269.

96. Featherstone, J.L. and Powell, D.R., 1981, Stabilization of Highly Saline Geothermal Brine: Journal of Petroleum Technology, 727-734.

97. Van Note, R.H., 1980, Geothermal Brine Treatment: U.S. Patent 4,304,666.

98. 1980, Final Report on the GLEF: U.S. DOE Report SAN/1137-17.

99. Awerbuch, L. and Rogers, A.N., 1981, Geothermal Scale Control by Crystallization: Fifth Annual EPRI Geothermal Conf., June 23-25.

100. Awerbuch, L. and Rogers, A.N., 1982, Geothermal Scale Control by Crystallization: Sixth Annual EPRI Geothermal Conf., June 29 - July 1.

101. Awerbuch, L., Van der Mast, V. and Rogers, A.N., 1982, Upstream Crystallization for Geothermal Scale Control: International Conf. on Geothermal Energy, Florence, Italy.

102. Awerbuch, L. and Rogers, A.N., 1983, Apparatus and Method for Energy Production and Mineral Recovery from Geothermal and Geopressured Fluids: U.S. Patent 4,370,858.

103. Microbiological Methods for Monitoring the Environment: EPA-600/8-78-017; 1978.

104. Water for Subsurface Injection: ASTM, STP735, 1981.

APPENDIX IV-I

HEWLETT PACKARD CALCULATOR (HP-67) CODE FOR THE CALCULATION OF INJECTION WELL TEMPERATURE DISTRIBUTIONS

User Instructions

Instruction	Input Data/Units	Keys
Key in R value	R	A
Key in ε value	ε	B
Key in Xo value	Xo	C

Registers	Content
0	R
1	ε
2	Xo

Injection Temperature

Step	Key Entry	Step	Key ENTRY
001	*LBLA	052	STOC
002	STO0	053	.
003	RTN	054	4
004	*LBLB	055	7
005	STO1	056	0
006	RTN	057	4
007	*LBLC	058	7
008	STO2	059	x
009	CF1	060	1
010	X>0?	061	+
011	GTOD	062	1/X
012	SF1	063	STOD
013	ABS	064	.
014	*LBLD	065	7
015	GSB1	066	4
016	F1?	067	7
017	CHS	068	8
018	1	069	5
019	-	070	5
020	CHS	071	6
021	RCL0	072	x
022	-	073	.
023	STO6	074	0
024	RCL2	075	9
025	X^2	076	5
026	CHS	077	8
027	e^X	078	7
028	2	079	9
029	x	080	6
030	Pi	081	CHS
031	$\sqrt{X}$	082	+
032	÷	083	RCLD
033	RCL6	084	x
034	X≠Y	085	.
035	÷	086	3
036	RCL2	087	4
037	+	088	8
038	STO4	089	0
039	PSE	090	2
040	RCL2	091	4
041	-	092	2
042	ABS	093	+
043	RCL2	094	RCLD
044	÷	095	x
045	ABS	096	RCLC
046	RCL1	097	X^2
047	X>Y?	098	CHS
048	GOT2	099	e^X
049	RCL4	100	x
050	GTOC	101	CHS
051	*LBL1	102	1

Injection Temperature (Continued)

Step	Key Entry
103	+
104	RTN
105	*LBL2
106	RCL4
107	PRTX
108	RTN
109	R/S

APPENDIX IV-II

HEWLETT PACKARD CALCULATOR (HP-67) CODE FOR EVALUATING THE BARKMAN AND DAVIDSON[65] WELLBORE NARROWING AND INVASION INJECTION WELL IMPAIRMENT MODELS

Primary Storage Registers

* R_0 → W (μgm/gm)

R_1 → Kc (md)

* R_2 → S (mℓ/√min)

---

* R_3 → ρc (gm/cm^3)

* R_4 → ρw (gm/cm^3)

* R_5 → Ac (cm^2)

* R_6 → ΔP_+ (psi)

---

* R_7 → M (cp)

R_8 → F (years)

* R_9 → r_w (M)

* R_A → h (M)

* R_B → i_o (bbl/day)

R_C → G (dimensionless)

R_D → T_α (years)

*Key value into register prior to running program.

Secondary Storage Registers

R_{S0} → G (dimensionless)
R_{S1} → θ (dimensionless)
R_{S2} → K_c/K_f (dimensionless)
* R_{S3} → r_e (M)
* R_{S4} → r_w (M)
* R_{S5} → α (dimensionless)
* R_{S6} → Frac ϕ (dimensionless)
* R_{S7} → r_a (M)
R_{S8} → β (dimensionless)
* R_{S9} → K_f (md)

*Key value into register prior to running program.

Barkman and Davidson (Ref 65) Injectability

Step	Key Entry	Step	Key ENTRY
001	*LBLA	052	RCLO
002	2	053	÷
003	ENT↑	054	RCL4
004	RCL3	055	÷
005	x	056	STO8
006	RCL5	057	R/S
007	ENT↑	058	X=0
008	x	059	GSBB
009	x	060	X>0
010	RCL6	061	GSBC
011	x	062	RCL8
012	RCL7	063	RCLC
013	÷	064	R/S
014	RCL4	065	x
015	÷	066	STOD
016	RCL2	067	RTN
017	ENT↑	068	LBLB
018	x	069	RCL1
019	÷	070	P≠S
020	8	071	RCL9
021	1	072	÷
022	6	073	STO2
023	6	074	RCL3
024	.	075	RCL4
025	1	076	÷
026	x	077	RCL2
027	RCLO	078	Y^X
028	X≠Y	079	STO1
029	÷	080	RCL5
030	STO1	081	1
031	R/S	082	-
032	RCL3	083	2
033	ENT↑	084	x
034	RCLA	085	RCL5
035	x	086	÷
036	RCL9	087	RCL1
037	ENT↑	088	X≠Y
038	x	089	Y^X
039	x	090	RCL5
040	Pi	091	1/X
041	x	092	RCL1
042	1	093	LN
043	.	094	2
044	7	095	x
045	2	096	1/X
046	3	097	+
047	EEX	098	x
048	4	099	RCL1
049	x	100	LN
050	RCLB	101	2
051	÷	102	x

Barkman and Davidson Injectability (Continued)

Step	Key Entry	Step	Key Entry
103	1/X	153	RCL1
104	X≠Y	154	LN
105	-	155	÷
106	1	156	X≠Y
107	+	157	-
108	P≠S	158	1
109	STOC	159	+
110	0	160	RCL6
111	RTN	161	ENT↑
112	*LBLC	162	x
113	RCL1	163	x
114	P≠S	164	RCL7
115	RCL9	165	ENT↑
116	÷	166	x
117	STO2	167	x
118	1	168	RCL4
119	RCL2	169	ENT↑
120	-	170	x
121	STO8	171	÷
122	RCL3	172	P≠S
123	RCL4	173	STOC
124	÷	174	RTN
125	RCL2		
126	Y^X		
127	STO1		
128	RCL5		
129	1		
130	-		
131	2		
132	x		
133	RCL5		
134	÷		
135	RCL8		
136	÷		
137	RCL1		
138	X≠Y		
139	Y^X		
140	RCL5		
141	1/X		
142	RCL8		
143	2		
144	÷		
145	RCL1		
146	LN		
147	÷		
148	+		
149	x		
150	RCL8		
151	2		
152	÷		

Chapter V

CONTROL OF NONCONDENSABLE GAS EMISSIONS

V. CONTROL OF NONCONDENSABLE GAS EMISSIONS

V-1. Chapter Summary

Hydrogen sulfide (H_2S) is a common constituent in geothermal steam and water. Abatement of H_2S emissions during drilling and subsequent resource utilization can be a requirement with respect to satisfying environmental regulations. Beyond compliance with emission standards, however, H_2S control is useful in preventing or minimizing scaling and corrosion of steam turbine components and cooling/condensing equipment. High ambient H_2S levels surrounding a geothermal facility can also drastically accelerate corrosion of exposed electrical devices and contacts, copper being particularly susceptible to this type of attack. This chapter summarizes H_2S environmental standards and H_2S abatement technologies most suitable for use at hydrothermal resources.

V-2. Introduction

The toxicity of H_2S has been well documented (Table V-1). A practical concern regarding H_2S emissions, with respect to human toxicity, is the noxious odor that is detectable at levels as low as 0.03 ppm[2]. The current U.S. Occupational Safety and Health Administration standard for an eight hour continuous exposure period is 10 ppm[3]. Beyond H_2S levels of 20 ppm, respiratory protection is required[2]. Since H_2S is heavier than air, relatively high levels can build up in areas having inadequate ventilation. Extremely dangerous situations can arise in this fashion, in part due to the diminition of odor at elevated H_2S levels and rapidity of onset of severe physiological response and morbidity. Response of local vegetation, especially in cultivated areas, to H_2S exposure is also an important concern. At the present time, California and New Mexico have the most stringent H_2S emission control regulations. The California regulation is 0.03 ppm by volume as a one hour

Table V-1

Effect of Hydrogen Sulfide on Humans

Concentrations (ppm)	Effects
0.0007-0.030	odor threshold
0.33	distinct odor; can cause nausea, headaches
2.7-5.3	odor offensive and moderately intense
20-33	odor strong but not intolerable
100	can cause loss of sense of smell in few minutes
210	smell not as pungent, probably due to olfactory paralysis
667	can cause death quickly due to respiratory paralysis
750	virtually no odor sensation; death can occur rapidly, upon very short exposure

(from Ref. 1)

average. New Mexico's standard is 0.003 ppm. Federal and state H_2S emission standards are described by Hartley[3] and Stephens, et al.[4]. The situation with respect to H_2S emissions at U.S. and foreign geothermal facilities is summarized by Hartly[3] and Pasqualetti[5]. Table V-2, from Layton, et al.[6] summarizes H_2S emissions for hot water and vapor dominated geothermal resources.

V-3. Sources of Hydrogen Sulfide Emissions

Release points for H_2S emissions from geothermal facilities have been described by several authors[1-4]. In general, release points for H_2S may be categorized as pre-energy conversion and as post-energy conversion emissions. Sources of pre-energy conversion H_2S emissions include releases during well drilling and well testing activities, pipeline venting and steam stacking.

Table V-2

Concentrations of Hydrogen Sulfide in Geothermal Fluids and Estimated Emission rates for Hot-Water and Vapor-Dominated Geothermal Reservoirs in the U.S. and Elsewhere

Resource Area	Concentration	Estimated Emissions ($g/MW_e \cdot h$)
	In Liquids (mg/kg)	
Salton Sea, California	3.2	128[a]
Brawley, California	55.1	2,424
Heber, California	0.18	20
East Mesa, California	0.54	60
Baca, New Mexico	60.7	2,125
Roosevelt Hot Springs, Utah	8	304
Long Valley, California	14	826
Beowawe Hot Springs, Nevada	6	348
Wairakei, New Zealand	--[b]	570
Ahuachapan, El Salvador	48	1,580
Otake, Japan	--[b]	542
Matsukawa, Japan	--[b]	5,050-20,800
Cerro Prieto, Mexico	--[b]	32,000
	In Steam (wt. %)	
Larderello, Italy	--[b]	14,300
The Geysers, California	24.5	1,850

a - This emission rate has been recalculated.

b - The hydrogen sulfide concentration associated with the emission rate was not reported.

(From Ref. 6)

Steam stacking is the process whereby steam or hot water bypasses energy conversion equipment and is vented directly to the atmosphere. Steam stacking is necessitated during initial production well start-up and in cases of equipment malfunction when it is impractical or dangerous to attempt rapid shut-in of a well producing hot fluids at high rates. Generally, flow is directed or bypassed around energy conversion equipment and let down to atmospheric conditions using steam silencers, atmospheric flash tanks or by venting directly into holding pits.

Post-energy conversion H_2S emission sources are conversion-process dependent. The most common type of conversion system for producing electricity from liquid dominated geothermal systems is the flashed-steam process. In this process, H_2S emissions occur in the noncondensable gas vent downstream of the steam turbine, during pre-injection treatment of spent fluid and in conjunction with the operation of condensing/cooling units[4]. Similar release points for H_2S also occur in typical direct steam conversion systems in use at steam dominated geothermal resources such as the Geysers in Northern California. Although the ideal binary conversion system produces no H_2S emissions, in practical terms, gas venting to prevent pump cavitation, operation of open system pre-injection spent water treatment facilities or steam stacking operations could be important sources of H_2S emissions[3].

Dispersal of H_2S after atmospheric release is complicated by the relatively high solubility of this gas in water[1,7]. Initial dissolution of H_2S in water droplets condensed from vented steam or in atmospheric mositure results in partial scrubbing of H_2S. However, subsequent dispersal and evaporation of water droplets re-releases H_2S to the atmosphere. Thus, the initial dispersal of H_2S pollutants could in some cases result in a reconcentration of the gas, depending on atmospheric and topographic features, at some distance from the original release point.

V-4. Abatement of Hydrogen Sulfide Emissions

Control technologies for H_2S emissions from geothermal facilities have been extensively reviewed[3-4]. Most work performed to date on a pilot scale has involved emission control at the steam dominated Geysers resource in Northern California. With the exception of the LLNL process[8,9] and the caustic peroxide process[10,11,12], no pilot scale studies of H_2S abatement technologies have been carried out at liquid dominated resources in the United States. Thus, some caution must be exercised in considering the technical viability and economic feasibility of untried abatement methods at the liquid dominated geothermal resources. H_2S control processes which have been developed for industrial applications, such as oil and gas field operations or control of fossil-fuel power plant emissions, are summarized in Table V-3. Many of these processes are inappropriate for geothermal applications because of high costs, complexity, kinetic limitations or the form of the end waste product. A tabulation of H_2S control processes that are amenable to geothermal applications is provided in Table V-4.

A primary difficulty in applying H_2S controls to liquid dominated resources is to insure chemical compatability between the geothermal fluids and the abatement systems. For example, the FMC process requires an alkaline pH and application of the process results in production of dissolved sulfate[10, 11]. Thus, a significant potential exists for precipitation of carbonates, sulfates, silicates, and hydroxides since most high temperature geothermal waters contain abundant dissolved constituents that will react in alkaline, high sulfate solutions. The majority of H_2S control processes are chemical processes with removal of H_2S either by formation of insoluble precipitates (sulfur or heavy metal sulfides) or by formation of water soluble compounds of sulfates or sulfides. The ultimate disposal of H_2S conversion products by an

Table V-3

Industrial Hydrogen Sulfide Abatement Methods

Process	H_2S Removal Principle		End Product	Reference
	Physical Absorption	Chemical Reaction		
ADIP	√		H_2S	4
ALKAZID	√		H_2S	4
Benfield		√	H_2S	4,13,14
Carlstill	√		H_2S	4
Claus		√	S	4,15
Fumaks		√	S	16
Kawada-Uchida	√		Thiosulfuric Acid	16
Mdea	√		H_2S	4
Purisol	√		H_2S	4
Rectisol	√		H_2S	4
Scot	√		H_2S	4
Selexol Solvent	√		S	4
Sivalls		√	FeS_2	17
Stretford		√	S	4,33
Sulfiban	√		H_2S	4
Sulfinol	√		H_2S	4
Takahax		√	S	16

Table V-4

Hydrogen Sulfide Control Processes Potentially Suitable For Application at Hydrothermal Resources

Hydrogen Sulfide Removal	Reference
Pre-Energy Conversion (Upstream):	
o Steam Converters	1, 4
o Steam Condenser-Reboiler	4, 18-20
o EIC Process	2-4, 21-24
o DOW Oxygenation Process	25-26
o UOP Catalytic Oxidation Process	4
o SRI Electrolytic Oxiation Process	4, 27
o Solid Sorbents	28-31
o Deuterium Process	1, 4
Post-Energy Conversion (Downstream):	
o Iron Catalyst	3-4
o Ozone Oxidation	4
o Wackenroder Process	4
Off-Gas (Vent Gas)	
o Hydrogen Peroxide-Sodium Hydroxide Process	4, 10-11
o Selective Caustic Absorption	32
o LLNL Brine Scrubbing Process	4, 8-9
o Stretford	1-4, 33-35
o Claus	2, 15
o Jefferson Lake	2, 15, 36
o Burner-Scrubber	2, 4
o Benfield	4, 37-38
o Ferrox	4
o Sodium Hydrochlorite	4
o Potassium Permanganate	4

off-gas process such as the Stretford Process, if needed, is thus a key consideration in the selection of an appropriate control technology. For example, the pre-energy conversion upstream reboiler process is a potentially important physical H_2S separation technique which involves condensing and reboiling geothermal steam in a specially designed heat exchanger[4]. As the steam condenses, noncondensable gases are partitioned into the vapor phase. During reboiling, steam with less than 90 percent of its original H_2S content is produced. An important subsidiary benefit of this process is the ultimate removal of up to 98 percent of the original total noncondensable gas load. However, the recovered H_2S must then be treated by a subsidiary process such as the Stretford process for final elimination of H_2S emissions.

V-5. Description of Hydrogen Sulfide Control Technologies

Stephens, et al.[4] developed a list of criteria which need to be satisfied by any H_2S abatement technique. The authors note that while most geothermal H_2S emission control techniques have been developed for and tested at the Geysers, the same techniques should be directly applicable to H_2S removal from flashed steam derived from liquid dominated geothermal resources. Unfortunately, this may be a serious understatement of problems arising due to the higher scaling tendency of moderate to high salinity geothermal brines. Chemical incompatability between geothermal brines and H_2S abatement systems may in fact be the major detriment to direct utilization of technologies developed for dry steam dominated resources. Nonetheless, the technical criteria for application of H_2S emission controls from Reference 4 are worth repeating here:

1. The process must be efficient and economical.
2. The process must not increase hazards to the plant workers or to the local environment.

3. Corrosion problems should not be adversely impacted.

4. Dynamic response of the H_2S abatement system should be capable of dealing with fluctuations in H_2S levels.

5. Power conversion efficiency must not be adversely impacted.

6. Solid waste by-products must not cause operational or disposal problems.

7. Chemical compatibility of the abatement process must be verified.

In the following section, potentially useful H_2S emission control systems will be considered with respect to their utility for service in liquid dominated geothermal systems. An attempt will be made to describe potential problem areas that may need additional development work before a particular emission control system could be considered as a viable technique. It is useful to note that of all the control techniques developed for geothermal applications, only the LLNL brine scrubbing method was specifically designed for service at a liquid dominated resource[8,9]. Additional information regarding H_2S detection and abatement are provided in Refs. 41-42.

V-5-1. Pre-Energy Conversion H_2S Abatement Systems

Upstream abatement of H_2S is of primary interest because it protects expensive turbine components from premature failure due to scaling, corrosion and precipitated particulate induced erosion damage. An upstream abatement system would also be helpful in abating H_2S emissions during steam stacking operations. Direct contact condensers are desireable because of their high efficiency and relatively low cost. Pre-energy conversion removal of H_2S would permit realization of direct contact condenser benefits. Several generic types of pre-conversion H_2S control systems have been developed. These systems either physically remove H_2S gas from steam or convert H_2S gas to either stable water soluble species or to stable particulates. Some down-

stream or post-energy conversion abatement systems convert H_2S to reactive water soluble species which must be further treated by a secondary process to prevent re-generation of H_2S gas. Secondary processing is also required to stabilize H_2S gas recovered by physical segregation methods involving use of steam converters or reboilers. A potential problem with all pre-energy conversion H_2S control systems is the likelihood that dissolved species in brine droplets which carryover during the steam separation process may be precipitated by the H_2S control system and thus aggravate scaling and erosion of turbine components.

V-6-1. Steam Converters

V-6-1a. Description of the Method - The basic steam converter process is shown in Figure V-1. The steam converter or primary heat exchanger condenses most of the input steam. As a result of the condensation process, noncondensable gases, comprised of CO_2, NH_3 and H_2S, are segregated from clean condensate and subsequently removed in the gas stripper unit. The heat liberated from the condensing steam is used to reboil clean steam condensate to produce steam that is almost completely free of noncondensable gases[1,4]. The steam converter process was originally developed for use at Lardarello, Italy as part of a boric acid recovery process. The boric acid was concentrated into the small blowdown stream of condensate produced by the gas stripper unit. A modern geothermal power plant equipped with steam converters would require a secondary off-gas process to convert the separated H_2S gas to a stable product. Under favorable conditions it might also be possible to reinject the separated noncondensable gases.

V-6-1b. Hydrothermal Studies - None.

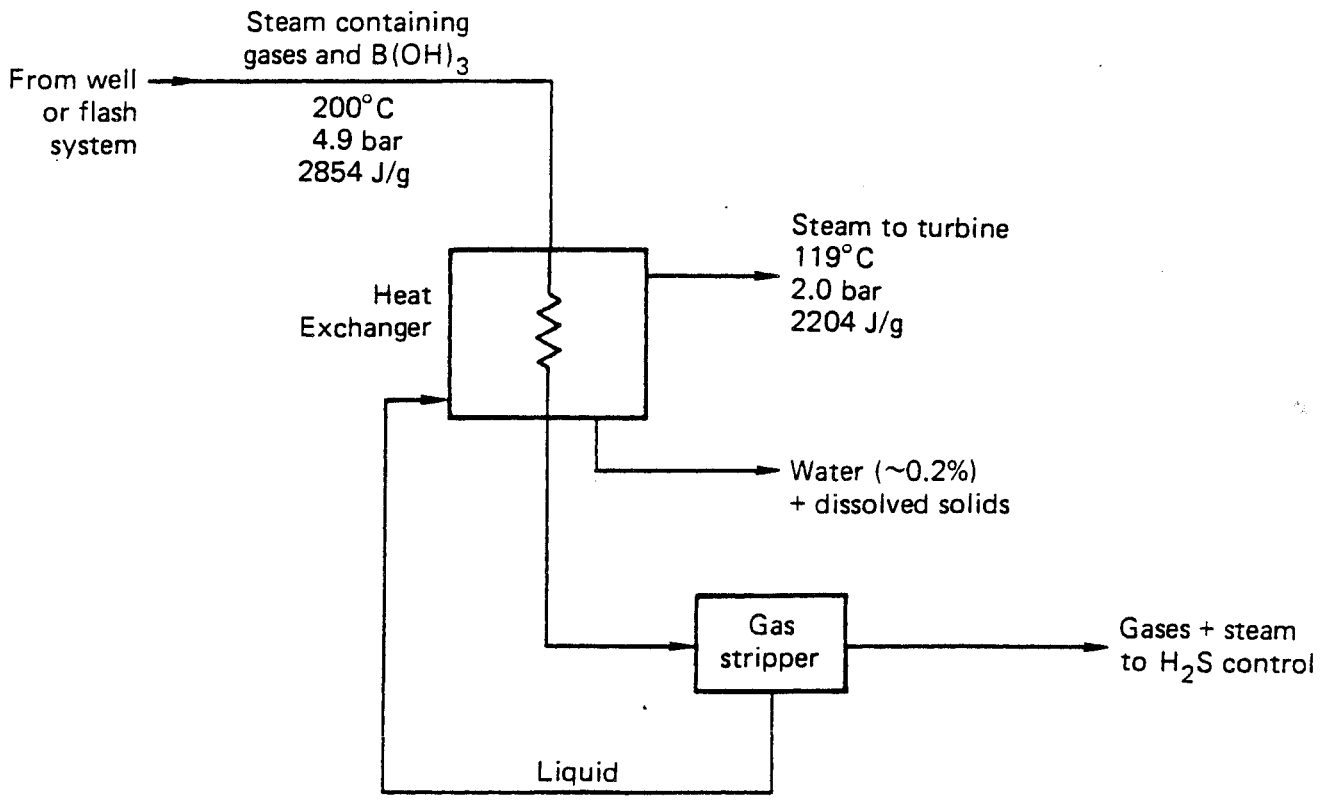

Figure V-1. Schematic of a typical steam converter (From Ref. 4).

V-6-1c. Hydrothermal Applications - According to Ref. 4, the efficiency of steam converters depends on the partitioning of noncondensable gases between liquid and vapor phases. The gas partitioning is dependent upon the pH of the condensate which is controlled by the composition of the noncondensable gases (CO_2 and NH_3 are most important), the temperature and pressure conditions, the volume of produced condensate and the concentration of H_2S in the raw steam. Operation of a steam converter results in loss of enthalpy of the clean steam as compared to the enthalpy of the raw steam. This loss is offset somewhat by the reduction in turbine backpressure due to the almost complete upstream removal of all noncondensable gases which substantially improves turbine efficiency. Upstream removal of noncondensable gases also permits the use of smaller mechanical gas ejectors and direct contact condensers that result in improved efficiency and lower costs. These gains tend to compensate for the enthalpy loss inherent in the overall process. Substantial advances in steam converter technology have been realized over the last several years. These advances (see Section V-6-2) have substantially improved the efficiency of the process. Thus, the use of modern steam reboiler units is now a practical possibility for a hydrothermal facility. The major drawbacks to use of such a unit are the uncertainties regarding mineral deposition or scaling of the reboiler heat exchanger and the resulting loss of thermal efficiency.

V-6-2. Steam Reboilers

V-6-2a. Description of the Process - The basic principles concerning design and operation of a steam condenser-reboiler unit are described in Refs. 18-20. Figures V-2 and 3 illustrate the vertical tube and horizontal tube condenser-reboiler units, respectively. The process can be shown on the basis of equilibrium chemistry to have a theoretical H_2S removal efficiency of greater than 90 percent over a wide range of steam conditions and noncondensable gas con-

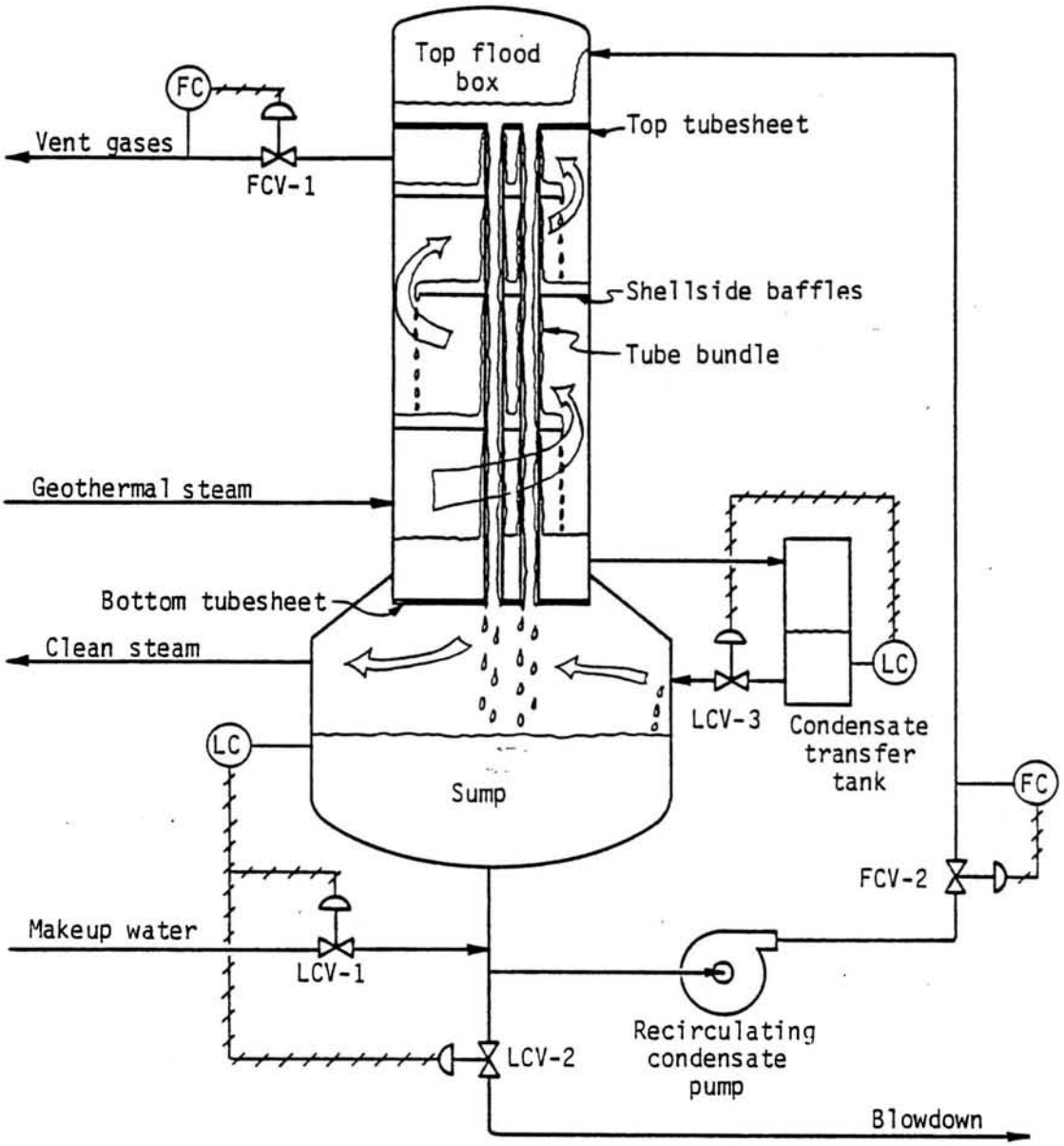

FC - Flow controller

LC - Level controller

FCV - Flow control valve

LCV - Level control valve

Figure V-2. Steam Condenser - Reboiler unit with a vertical tube evaporator baffled shellside configuration (From Ref. 20).

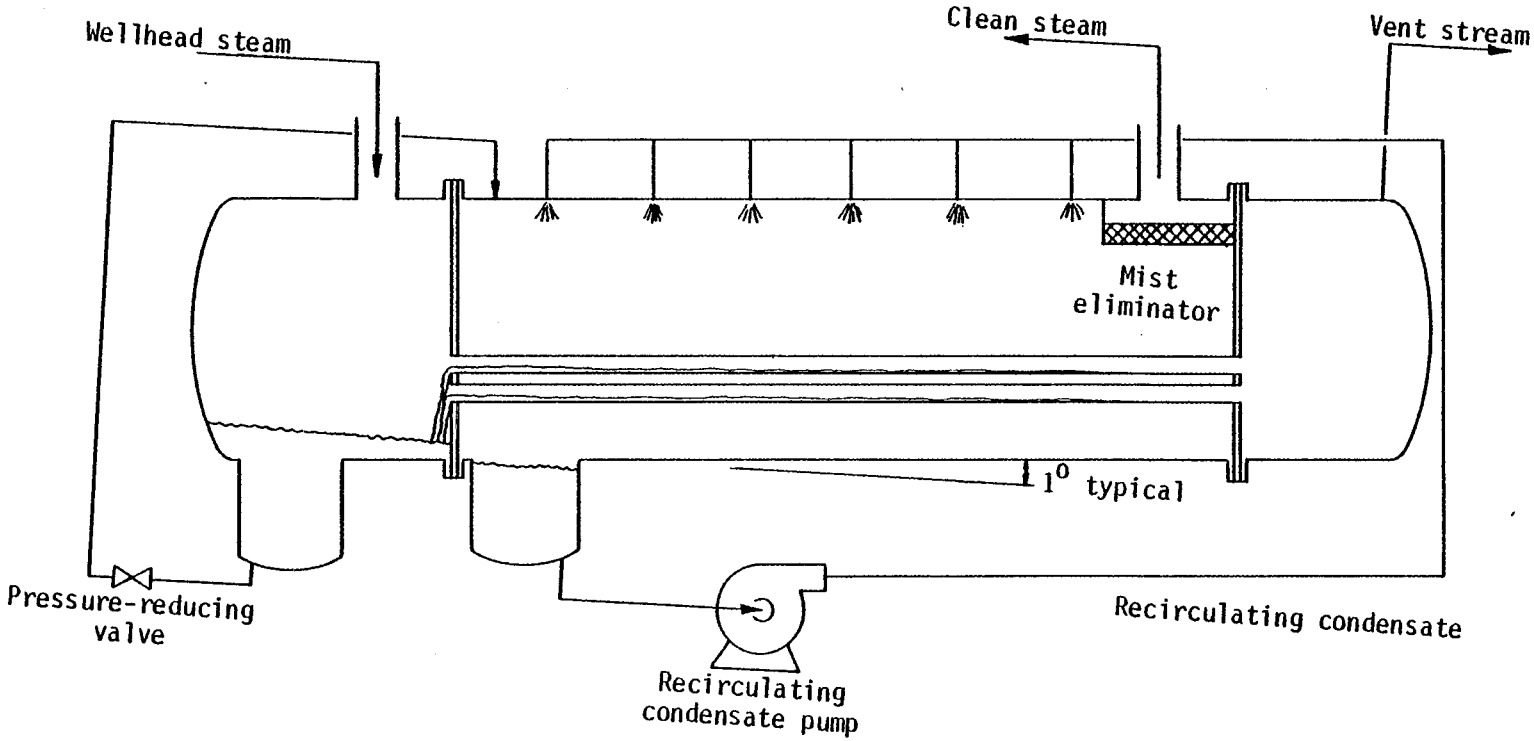

Figure V-3. Steam condenser - Reboiler unit with a horizontal tube evaporator (From Ref. 21).

centrations (NH_3, CO_2 and H_2S mixtures). Referring to Figure V-2, the process operates by continuous condensation-reboiling as follows:

1. Raw steam enters one side of a vertical heat exchanger.
2. All but a small portion of the raw steam is condensed.
3. The noncondensable gases are stripped in a small quantity of noncondensed steam which acts as a carrier.
4. The vent gases are treated in a secondary process such as the Stretford process to stabilize H_2S.
5. The steam condensate undergoes a pressure reduction which causes a corresponding temperature reduction relative to the raw steam.
6. The condensate is passed through the opposite side of the heat exchanger where the temperature difference causes the steam to reboil thereby producing clean, gas-free steam.

The major parameters that control system performance are the temperature, pressure, gas composition and the percent of inlet steam vented. The major cost factors are the amount of noncondensable gas to be removed, the heat transfer area required, the power production penalty for the loss of steam in the vent streams, the power production penalty for the drop in pressure of the clean steam and the credit due to an increase in power production caused by the reduction in steam flow requirements for operation of gas ejectors since the total noncondensable gas load in the system has been reduced. It is shown in Ref. 20 that a 55-MWe steam condenser-reboiler system could be installed at the Geysers for $8.2 million. The cost includes installation of an off-gas Stretford process to stabilize collected H_2S. The cost estimate is based on a two-stage process (Figure V-4). The first stage of the process produces clean steam for the turbine generators. The vent gas from the first stage is then fed to a second stage which is used to produce clean, low pressure steam to operate the jet air ejectors.

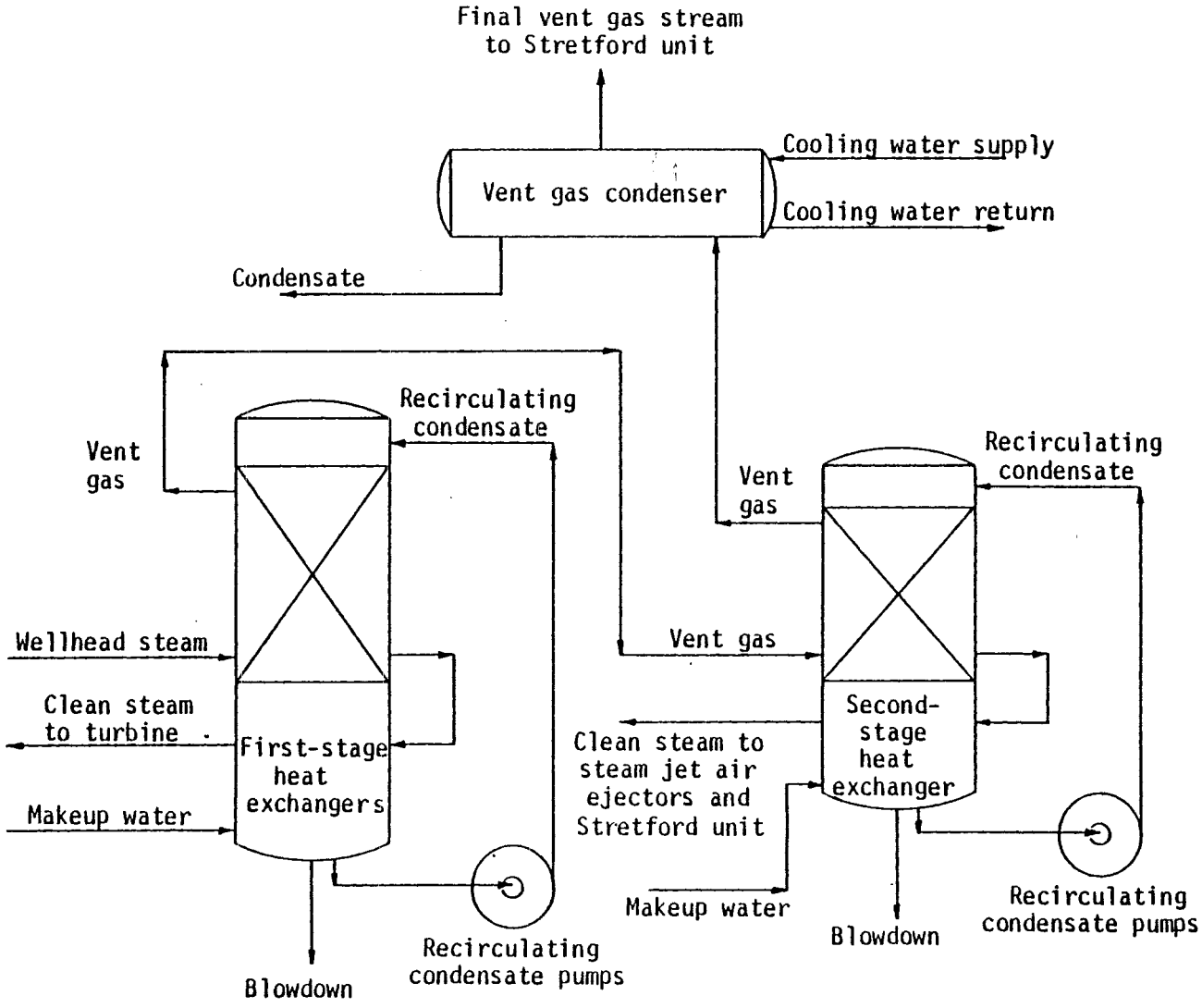

Figure V-4. Process flow schematic for a commercial-scale steam condenser - reboiler process H_2S Abatement System (From Ref. 20).

V-6-2b. Hydrothermal Studies - The Electric Power Research Institute (EPRI) is evaluating steam reboiler technology for possible applications at hydrothermal resources.

V-6-2c. Hydrothermal Applications - The steam reboiler technology can become the preferred method for upstream removal of H_2S if it can be demonstrated that scale deposition within the reboiler unit and resulting degradation of heat transfer coefficients is not an insurmountable problem. Process economics are critically dependent on the maintenance of heat transfer coefficients. Highly efficient boiler design may make it difficult and expensive to clean scaled heat exchanger surfaces.

V-6-3. The Copper Sulfate Process

V-6-3a. Description of the Process - The EIC Copper Sulfate or CUPROSUL process [2-4, 20-25] involves pre-energy conversion scrubbing of geothermal steam using an ammonium sulfate buffered acidic solution of copper sulfate. H_2S is converted to an insoluble copper sulfide precipitate which is subsequently recovered and exposed to a copper sulfate regeneration process. Ultimately, H_2S is converted to either soluble ammonium sulfate or elemental sulfur. Simplified schematics of the copper sulfate process are provided in Figures V-5 and V-6.

Implementation of the Copper Sulfate process proceeds in three steps consisting of H_2S scrubbing, solids separation and copper sulfate regeneration [3]. Step I involves absorption of H_2S by three reaction pathways:

Pathway A:

$$H_2S_{(aq)} \rightarrow H^+ + HS^-$$

$$HS^- \rightarrow H^+ + S^{-2}$$

$$CuSO_{4(aq)} \rightarrow Cu^{+2} + SO_4^{-2}$$

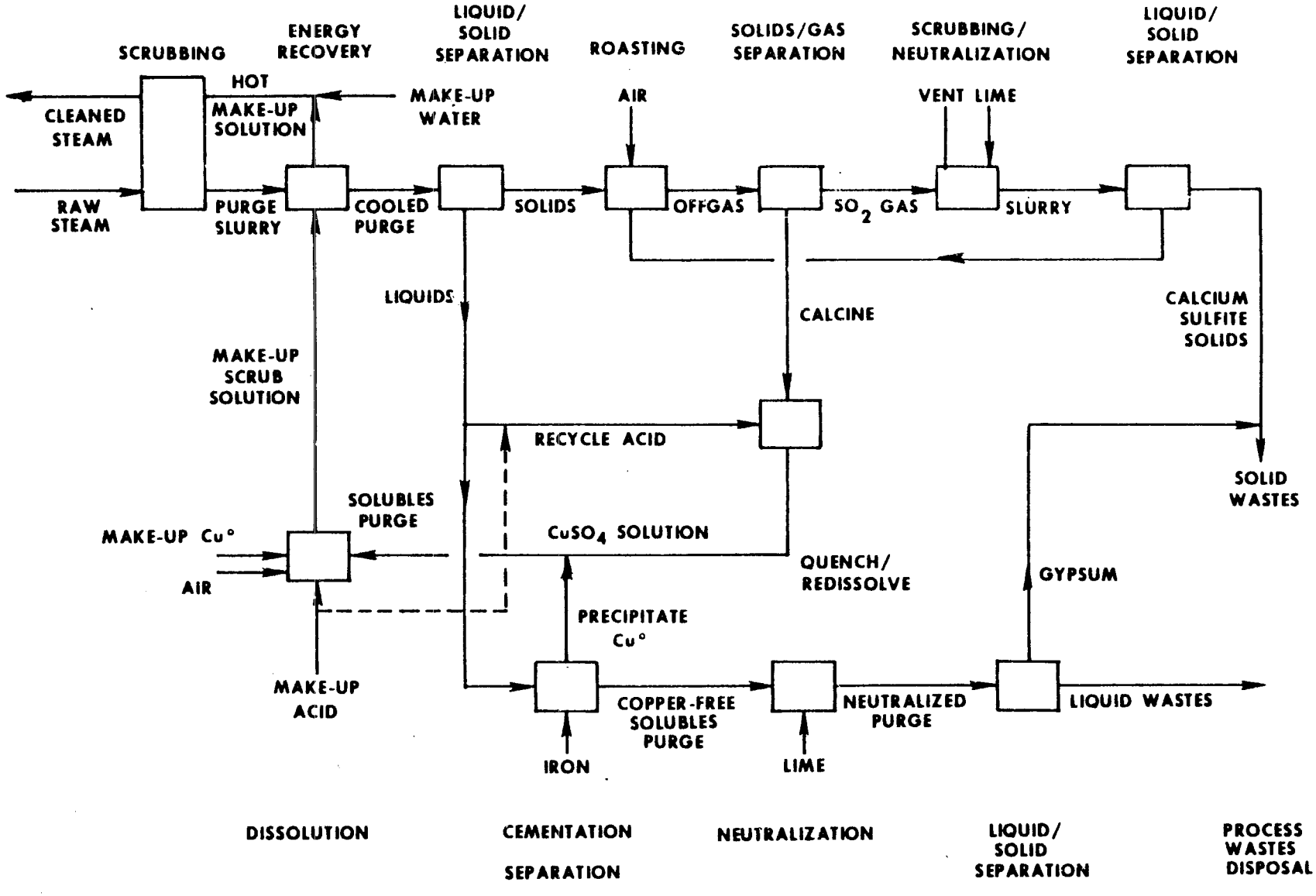

Figure V-5. A simplified flow diagram of the EIC process, with regeneration by roasting (from Ref. 3).

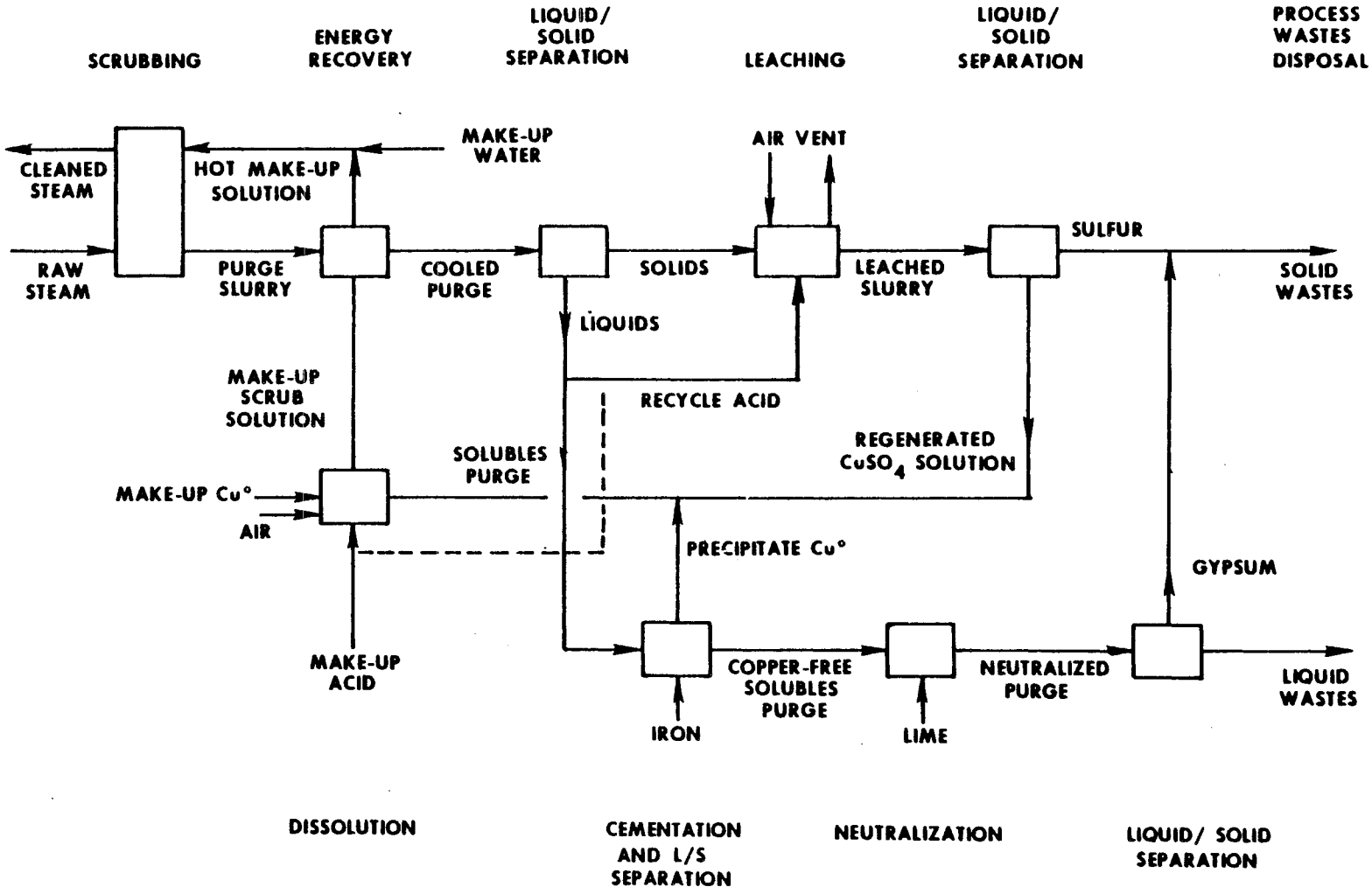

Figure V-6. A simplified flow diagram of the EIC process, with regeneration by leaching (From Ref. 3).

$$2H^+ + SO_4^{-2} \rightarrow H_2SO_4$$

$$Cu^{+2} + S^{-2} \rightarrow CuS$$

Overall: $CuSO_4 + H_2S \rightarrow CuS + H_2SO_4$ (V-1)

Pathway B: $H_2S_{(aq)} \rightarrow H^+ + HS^-$

$$HS^- \rightarrow H^+ + S^{-2}$$

$$CuO \rightarrow Cu^{+2} + O^{-2}$$

$$Cu^{+2} + S^{-2} \rightarrow CuS$$

$$2H^+ + O^{-2} \rightarrow H_2O$$

Overall: $CuO + H_2S \rightarrow CuS + H_2O$ (V-2)

Pathway C $Cu_2SO_4 + H_2S \rightarrow Cu_2S + H_2SO_4$ (V-3)

Step II involves recovery of precipitated solids:

Field trials at the Geysers have utilized an eight-inch diameter single sieve tray scrubbing column. The resulting copper sulfide slurry is passed through a centrifuge as the preliminary liquid separation step. Further upgrading of the liquid is required depending upon the scheme employed to regenerate copper sulfate.

Step III involves regeneration of copper sulfate. Two processes have been tested:

A. Regeneration by oxidative roasting proceeds as follows:

$$CuS + 2O_2 \rightarrow CuSO_4 \quad \text{(V-4)}$$

$$CuS + 3/2O_2 \rightarrow CuO + SO_2 \quad \text{(V-5)}$$

$$SO_2 + 1/2O_2 \rightarrow SO_3 \quad \text{(V-6)}$$

These reactions are exothermic and are, therefore, self-sustaining once initiated. Byproduct sulfur oxides are scrubbed in an ammonical solution and reinjected with cooling tower blowdown. The $CuSO_4$ - CuO slurry is recirculated to the hydrogen sulfide scrubber.

B. The alternative oxygen pressure leaching process operates as follows:

$$CuS + 2O_2 \rightarrow Cu^{+2} + SO_4^{-2} \qquad \text{(V-7)}$$

$$Cu_2S + 5/2O_2 \rightarrow 2H^+ \quad 2Cu^{+2} + SO_4^{-2} + H_2O \qquad \text{(V-8)}$$

Operating conditions can also be adjusted to promote elemental sulfur production:

$$CuS + 1/2O_2 + 2H^+ \rightarrow Cu^{+2} + S^\circ + H_2O \qquad \text{(V-9)}$$

$$Cu_2S + O_2 + 4H^+ \rightarrow 2Cu^{+2} + S^\circ + 2H_2O \qquad \text{(V-10)}$$

In general, reaction times ranging from 2 to 4 hours are needed for the conversion of sulfide solids by pressurized oxygen at about 100 psia. Carpenter 20Cb3 and stainless steels are claimed to provide adequate service as materials of construction for scrubbers and other components[3]. The pressure leaching process is attractive because 80 to 90 percent of the original boric acid and ammonia in the steam is eliminated.

Economics of the copper sulfate process have most recently been summarized by Stephens, et al.[4] using a method described by Hartley[2]. Capital costs are estimated using the known installed capital cost of $2,432,000 for a Stretford process on the unit 14, 117.5 MW power plant at the Geysers as the base case[26]. Capital costs for the Stretford process include a differential investment cost for installation of a surface condensor in lieu of a direct contact condenser. Griebe[34] derived the following equations for evaluating capital costs of Stretford units with H_2S levels or steam flow rates other than those defined in the base case:

$$IA = IB\ (SA/SB)^{0.4} \qquad \text{(V-11)}$$

for: $0.5 < SA < 5$ metric tons of sulfur per day

$$IA = IB\ (Sa/SB)^{0.5} \qquad \text{(V-12)}$$

for: $5 < SA < 250$ metric tons of sulfur per day

SA = metric tons of sulfur produced per day in the desired case

SB = metric tons of sulfur produced per day by the base case (unit 14)

I = capital investment for the desired or base (A or B) Stretford process

A summary of costs for the EIC process are provided in Figure V-7 and Refs. 3 and 4.

V-6-3b. Hydrothermal Studies - None.

V-6-3c. Hydrothermal Applications - The EIC process, as configured for use at the Geysers can be adapted for use at hydrothermal resources by direct integration with a flashed steam energy conversion process. The separated steam from one or more steam separators would be treated directly in analogous fashion to the treatment of dry steam at the Geysers. Potential difficulties involve interaction of dissolved brine constituents carried over during the steam separation process with the reagents used to precipitate copper sulfate. For example, the presence of calcium, barium or strontium as impurities in separated steam could lead to sulfate scaling of turbine components as well as increased consumption of reagent. The production of sulfuric acid as a by-product of the EIC process leads to the potential for significantly increased corrosivity of the scrubbing solution unless sufficient ammonia is present to neutralize the acid[1].

V-6-4. The Dow Oxygenation Process

V-6-4a. Description of the Process - Oxygenation of a hypersaline geothermal brine as a means of suppressing formation of heavy metal sulfide scale deposition was first described by Jackson and Hill[25]. The process was designed to eliminate only that part of the total sulfur in the system present as a dis-

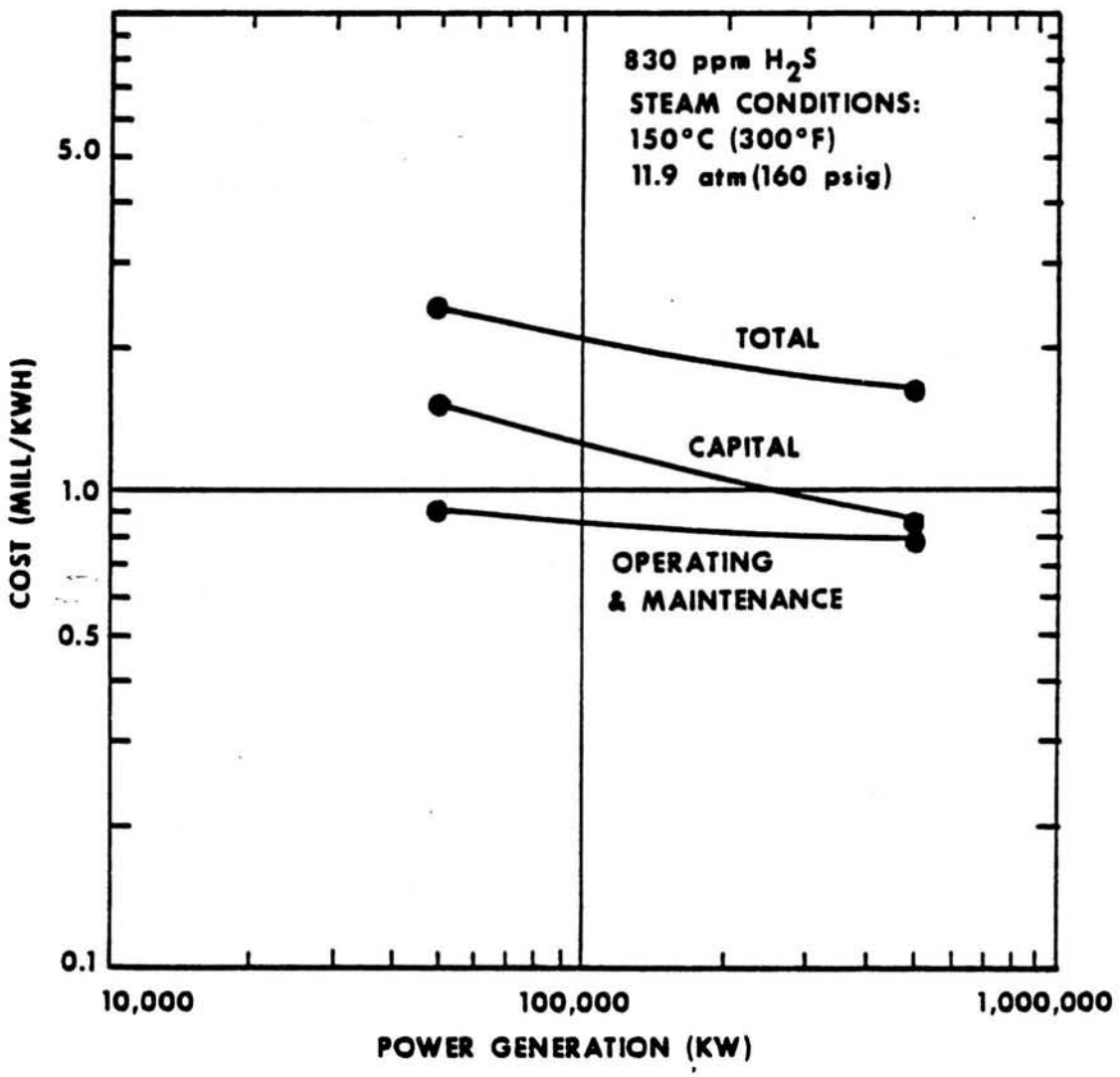

Figure V-7. Costs for application of the EIC Hydrogen Sulfide Abatement Process (From Ref. 3).

solved secies in the brine at high temperature/pressure, production wellhead conditions. The bulk of the total sulfur originally present in the reservoir was partitioned into the vapor phase as H_2S at wellhead conditions. The residual dissolved sulfur in the brine at wellhead conditions was 30 mg/l or less. The authors noted that utilization of the process for a typical hypersaline geothermal brine would result in a substantial reduction in brine pH thus increasing the corrosivity of the treated brine. They also noted that a significant potential for precipitation of sulfates existed if more than about 10 percent of the dissolved sulfur were converted to sulfate.

Subsequently, King and Wilson[26] suggested that pre-energy conversion oxidation of a geothermal brine, at production wellhead conditions, could be an effective H_2S control measure. The oxygenation process was subsequently reviewed[1,4] and it was noted that the process is not amenable to the treatment of vapor phase H_2S owing to insufficient residence time for reaction with vapor phase H_2S. It was also noted that operation of the process has a significant and detrimental effect on the corrosivity of treated brine. The governing reaction for the removal of H_2S is described by:

$$H_2S \text{ (aqueous)} + 2O_2 \text{ (gas)} \rightarrow H_2SO_4 \text{ (aqueous)} \qquad \text{(IV-13)}$$

The optimum removal of H_2S from brine was achieved at pH 7 (171°C) at a mole ratio oxygen:H_2S of 1.5. Application of the process at a typical hydrothermal resource would require the use of a downhole pump that could produce a single-phase liquid product at production wellhead conditions. A suitable downhole pump for use at elevated temperatures (200-270°C) is not available.

V-6-4b. Hydrothermal Studies - Results for the laboratory evaluation of the oxygenation process are described in Ref. 26.

V-6-4c. Hydrothermal Applications - The oxygenation process is of limited utility for the treatment of typical two-phase brine-steam mixtures produced at hydrothermal resources. The proess is not capable of removing H_2S in the vapor (steam) phase. Treatment of geothermal brine results in a substantial increase in the corrosivity of the brine. Treatment of hypersaline brines and other brines containing dissolved barium, calcium and strontium could result in the formation of sulfate scales. The process could be used to treat brine at production wellhead conditions if a downhole pump were used. However, reliable downhole pumps for high temperature geothermal service are not available.

V-6-5. UOP Catalytic Oxidation Process

V-6-5a. Description of the Process - The UOP or SULFOX process is described in Ref. 4. This process involves the use of a metal phthalocyanine-activated charcoal-supported catalyst designed to promote the oxidation of vapor phase H_2S to sulfur using air as the oxidant. The fundamental reaction which describes performance of this H_2S abatement system, initially developed for treatment of hydrocarbon gas streams, is:

$$2H_2S + O_2 \rightarrow 2S + 2H_2O \qquad \text{(V-14)}$$

The process was being evaluated under U.S. DOE sponsorship in 1980[4]. The process may also be useful in the treatment of condensate streams containing residual ammonia and H_2S as indicated by the following reactions:

$$2NH_4SH + O_2 \rightarrow 2S + 2NH_4OH, \qquad \text{(V-15)}$$

$$2NH_4SH + 2O_2 \rightarrow (NH_4)_2S_2O_3 + H_2O, \qquad \text{(V-16)}$$

$$2NH_4SH + 3O_2 + 2NH_4OH \rightarrow 2(NH_4)_2SO_3 + 2H_2O, \qquad \text{(V-17)}$$

$$NH_4SH + 2O_2 + NH_4OH \rightarrow (NH_4)_2SO_4 + H_2O \qquad \text{(V-18)}$$

V-6-5b. Hydrothermal Studies - None.

V-6-5c. Hydrothermal Applications - Utilization of the UOP process for the treatment of separated steam produced at a typical hydrothermal resource is possible but subject to some serious potential limitations. The stability of the supported catalyst is of concern in the presence of brine carryover that could lead to scale deposition on the catalyst and resulting loss of activity. Injection of air could exacerbate scale deposition in turbine components as well as enhance the corrosivity of separated steam. Utility of this process might require use of steam scrubbers to control brine carryover.

V-6-6. The SRI Electrolytic Oxidation Process

V-6-6a. Description of the Process - This process involves direct electrolytic oxidation of H_2S present as a dissolved species in aqueous solution[4]. The process is based on the following reaction:

$$HS^- \rightarrow H^+ + 2e \qquad \text{(V-19)}$$

Preliminary laboratory experimentation described in Ref. 4 indicated greater than 95 percent removal of H_2S from a solution at 200°C and 900-1000 psi.

V-6-6b. Hydrothermal Studies - No field studies have been completed to date.

V-6-6c. Hydrothermal Applications - Utilization of this process for the tretment of single phase high temperature/pressure production wellhead liquid is subject to similar limitations described for the DOW oxygenation process described in Section V-6-4. The SRI process could also be susceptible to accelerated scale formation on the carbon anode used in the preliminary laboratory experiments. Use of an electrolytic H_2S abatement system in conjunction with the production of hypersaline geothermal brine is most probably out of

the question owing to accelerated rates of scale formation and loss of electrode activity[27]. Successful development of this process might involve a simplified procedure for the treatment of off-gas emissions following the energy conversion process. For example, this process might be economically preferable to the Stretford process for the removal of H_2S in noncondensable gas streams. Integration of this process with the caustic scrubbing process described in Section V-8-2 could be highly beneficial especially in the presence of dissolved ammonia.

V-6-7. Solid Hydrogen Sulfide Sorbents

V-6-7a. Description of the Process - Ultra high efficiency removal of H_2S from a gas stream can be realized by the use of solid sorbents. A commercial product called IRONITE SPONGE is used as a drilling mud additive[28-29]. This product is manufactured by the IRONITE PRODUCTS CO., St. Louis, MO. The material is manufactured using powdered iron which is oxidized to yield a microporous iron oxide particle. The final product has a particle size distribution between 1.5 to 50 microns with 90 percent of the particles ranging in size between 2 to 20 microns. The material has low residual magnetism and is, therefore, not strongly attracted to steel surfaces. Removal of H_2S is accomplished via the following reactions:

$$Fe_3O_4 + 4H_2S \rightarrow 3FeS + 4H_2O + S \qquad (V\text{-}20)$$

$$FeS + S \rightarrow FeS_2 \qquad (V\text{-}21)$$

$$Fe_3O_4 + 6H_2S \rightarrow 3FeS_2 + 4H_2O + 2H_2 \qquad (V\text{-}22)$$

The product is not active at pH values above 10[30]. Optimum performance occurs at about neutral pH. The reaction product is pyrite, which is highly stable. The primary drawback to the use of this material for the continuous removal of H_2S from geothermal gas streams is the price. The material has an

activity of 1 pound of IRONITE per 2000 mg/l H_2S at a cost of $1.00 per pound [30]. Unfortunately, the material cannot be recharged.

Li, et al.[31], evaluated various solid sorbents. They found, for example, that ZnO was an excellent sorbent for H_2S gas. Unfortunately, attempts to regenerate this and other sorbent materials were not successful. Li, et al., also evaluated activated charcoal for use as an H_2S gas oxygenation catalyst. The oxidation process proceeds, using air or pure oxygen as the oxidant, as follows:

$$H_2S + \tfrac{1}{2}O_2 \rightarrow H_2O + S \qquad \text{(V-23)}$$

The process was found to have an H_2S removal efficiency of 90 percent or better at temperatures to 235°C provided the steam temperature was above its saturation temperature. Wet steam caused sulfur deposition on the catalyst and loss of activity. Treatment at temperatures in excess of 235°C resulted in entrainment of sulfur particulates by the treated steam. It was possible to reactivate spent catalyst by solvent extraction using carbon sulfide (CS_2). A conceptual design for a geothermal steam scrubbing process based on the oxygenation-catalyst process is shown in Figure V-8. The primary drawbacks to the proposed scheme are the need for minimizing pressure drops across the steam scrubber and the need to develop an environmentally acceptable method for disposal of spent CS_2 regeneration liquid.

V-6-7b. Hydrothermal Studies - Results of laboratory evaluations are reported in Ref. 31. No field studies have been reported.

V-6-7c. Hydrothermal Applications - Upstream oxygenation processes suffer from the potential for scale deposition on turbine components and elevated corrosivity of separated steam. Application of the catalyst-oxidation process

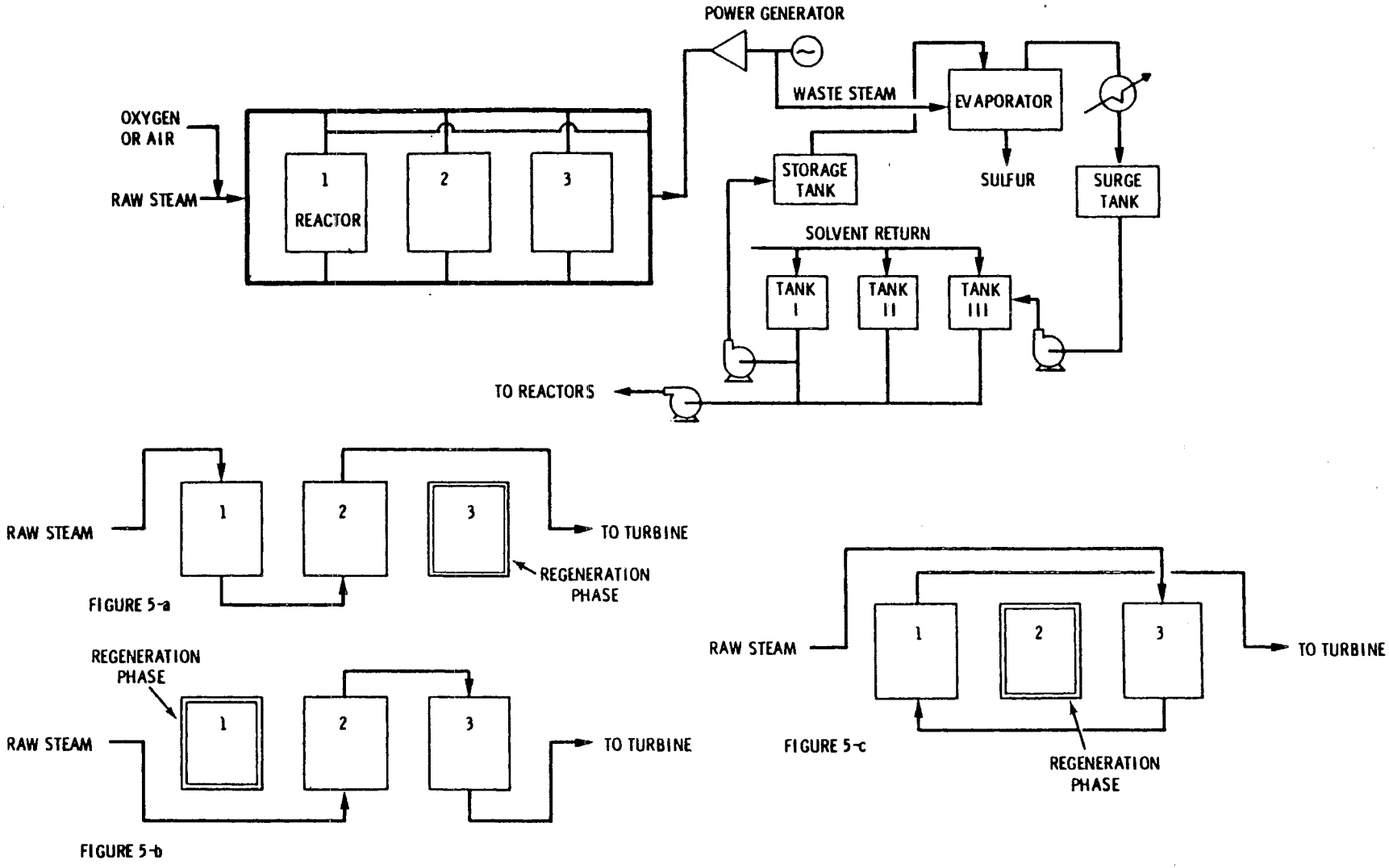

Figure V-8. Conceptual process design for the Battelle, PNL activated carbon catalyst-oxidation process. Figure A is the schematic illustration of the overall process. Figures B-D illustrate the sequential regeneration of spent catalyst (From Ref. 3).

for use on post-energy conversion noncondensable gas streams or on noncondensable gas streams produced by reboilers or steam converters are other possibilities. The solid sorbent process based on the use of IRONITE, ZnO or other sorbents does not seem practical for large scale, continuous geothermal applications owing to the high cost of the solid sorbents and the inability to regenerate activity of spent sorbent.

V-6-8. The Deuterium Process

V-6-8a. Description of the Process - A proprietary liquid absorption H_2S scrubber was successfully tested at the Geysers by the Deuterium Corporation of White Plains, New York[1,4]. Test results indicated better than 90 percent H_2S remoal efficiency. The most detailed description of this process is available in Ref. 1.

V-6-8b. Hydrothermal Studies - A successful field test of the process was carried out at the Geysers[1]. No field studies have been reported for hydrothermal resources.

V-6-8c. Hydrothermal Applications - Unknown at present.

V-7. Post-Energy Conversion (Downstream) Hydrogen Sulfide Abatement

Steam which passes through a turbine is condensed using either surface or direct contact units. The direct contact unit is more desirable because of its simplicity, lower cost and insensitivity to deposition of scales. The operating characteristics of both types of condensers are described in Ref. 39. Selection of a condenser for geothermal applications is strongly dependent upon the need for H_2S control and the particular H_2S control method selected. During the condensation process a significant fraction of the original H_2S may be partitioned into the condensed liquid (condensate) depending

upon its pH and temperature. Redistribution of H_2S could, therefore, complicate application of control measures.

The direct contact condenser is illustrated in Figure V-9. Steam vapor is condensed by interaction with a spray of water droplets. Direct contact condensers are desirable because they are simple in design, relatively inexpensive and practically immune to operational problems such as leakage and performance degradation due to scale formation. Since, in geothermal operations, steam condensate is the most likely source of cooling water, and maintenance of high chemical purity of the condensate is unnecessary, elaborate internals for the condensers are not needed.

The surface condenser operates most usually as a shell-and-tube heat exchanger which effectively isolates the coolant from the condensing steam. The steam most usually flows on the shell side of the heat exchanger as shown in Figure V-10. A surface contact condenser is more costly and more complicated to build in part because allowance must be made for the thermal expansion of the condenser tubes and deposition of scale on the inner and outer surfaces of the heat exchanger tubes must be controlled, most usually by treatment of the condensate. Deposition directly from the condensing steam can also be a problem that might require frequent downtime for removal of deposits.

Typical geothermal flashed steam plants with direct contact or surface contact condensers are shown in Figures V-11 and 12. The chemical interactions between noncondensable gases and condensate are important in determining the suitability of direct contact condensers for specific project if H_2S abatement is required. In the presence of ammonia, H_2S may have significant solubility in condensate and thus significant partitioning of H_2S between the vented noncondensable gases and the condensate is likely[1]. The problem may

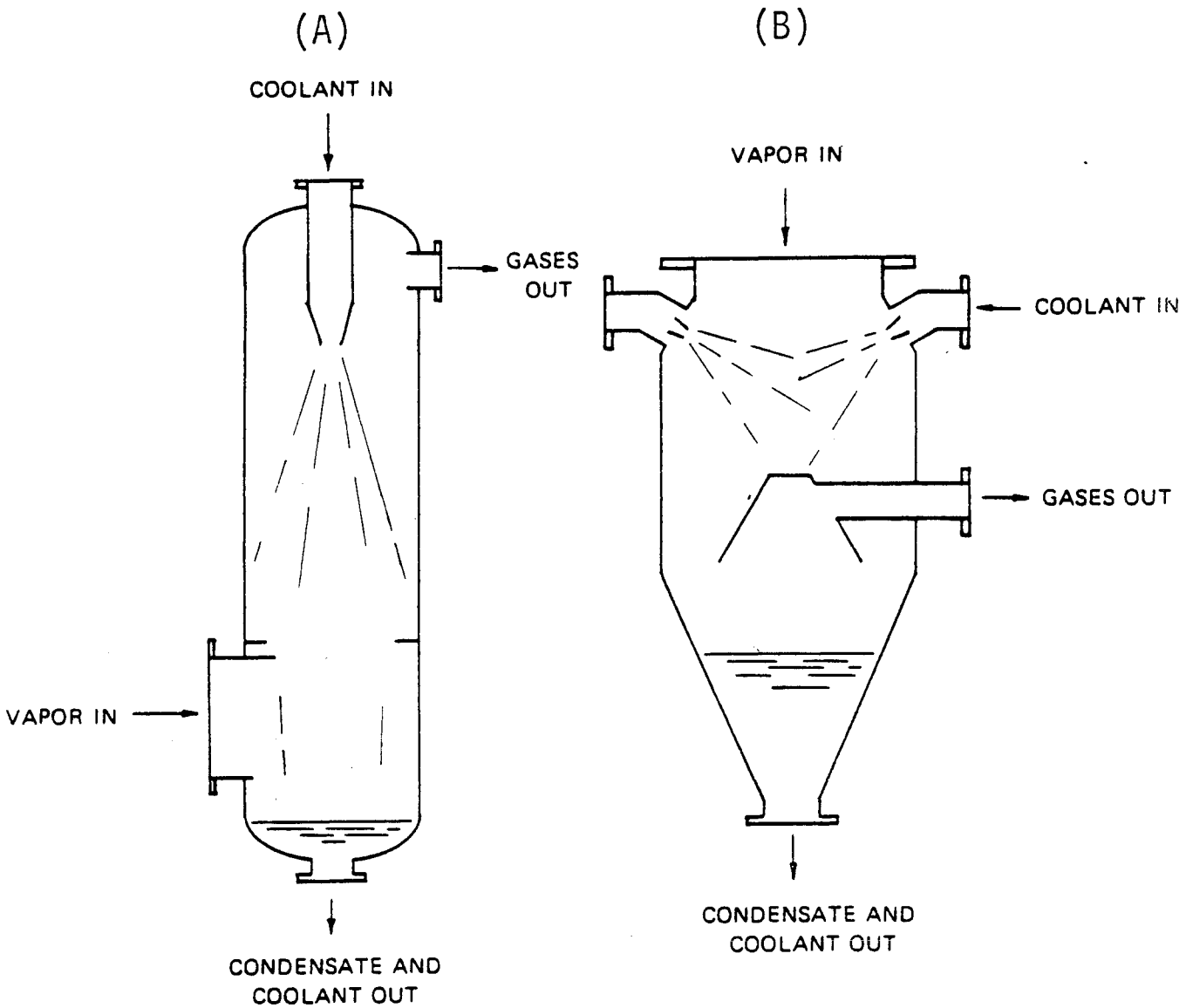

Figure V-9. Counter flow (a) and parallel flow direct contact condensers (From Ref. 39).

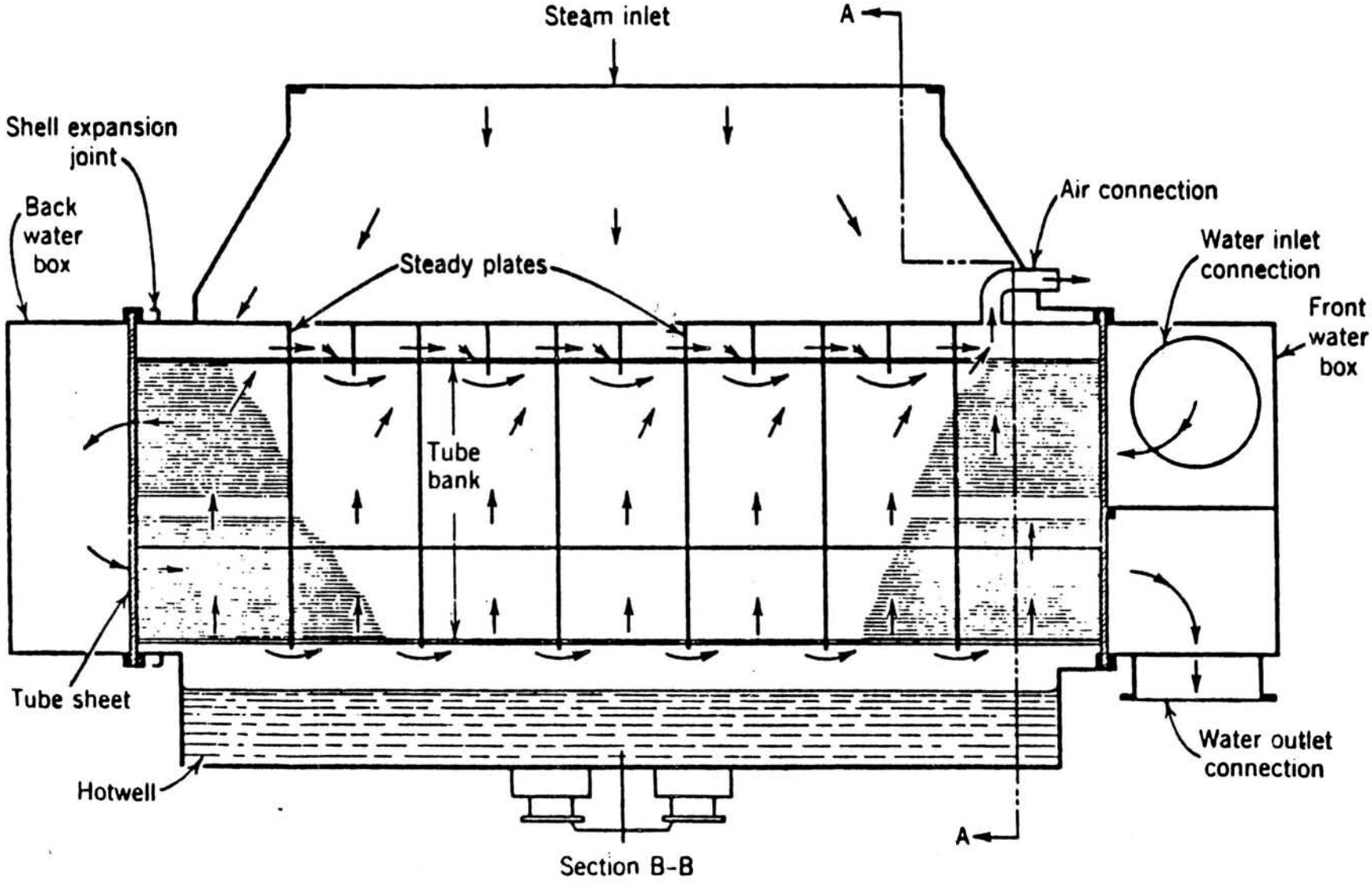

Figure V-10. Sections through a typical two-pass surface condenser (From Ref. 39)

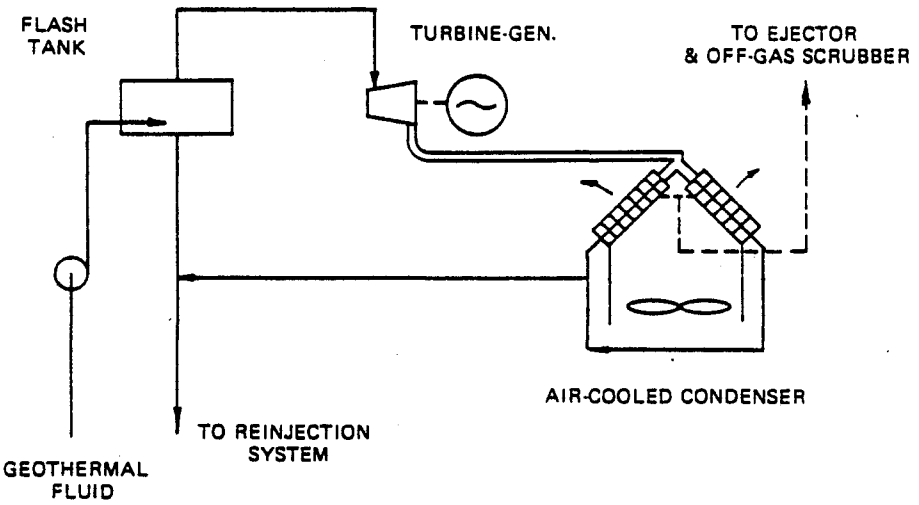

Figure V-11. Flashed steam cycle with direct condensation of steam in dry cooling tower (From Ref. 39).

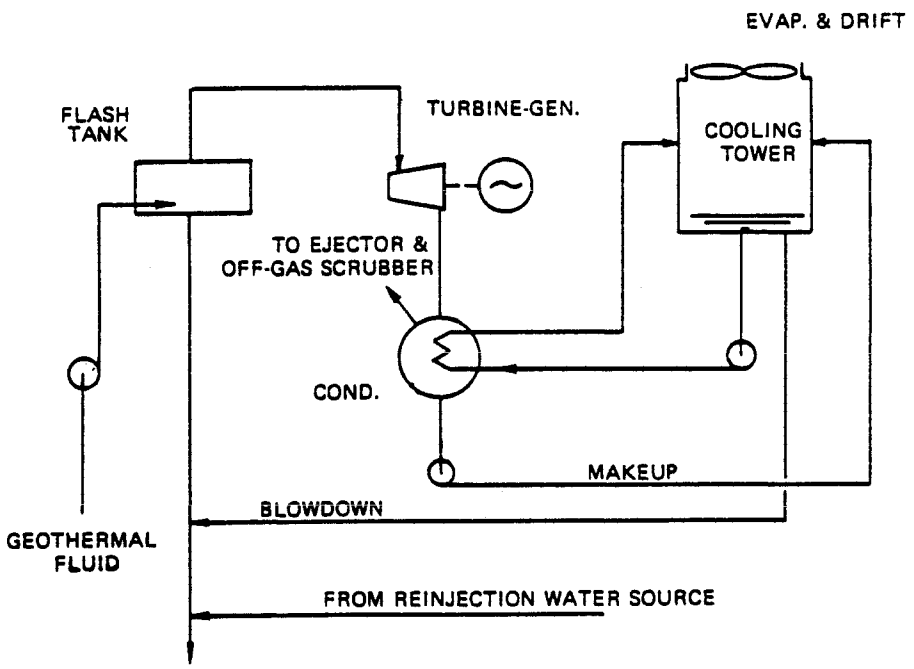

Figure V-12. Flashed-steam cycle using, surface condenser and wet mechanical-draft cooling tower (From Ref. 39).

be better understood by reference to Figure V-13 which illustrates the behavior of noncondensable gases in the Geysers unit number 3 where direct contact condensers are employed. In the surface contact condenser, noncondensable gases do not contact the coolant. They do, however, have the opportunity to interact with the liquid condensate formed during the condensation process. Since the volume of condensate is much lower with the surface contact condenser than with a direct contact condenser, partitioning of noncondensable gases is less of a problem given that in most cases the concentration of CO_2 is much greater than the corresponding concentrations of ammonia or H_2S. Thus, the CO_2 tends to control condensate pH and, thereby, limits the dissolution of H_2S. The chemistry of steam condensers is considered in some detail in Ref. 1.

To summarize, the selection of H_2S abatement technology is dependent in an important way on the method selected for the condensing of steam in a flashed steam cycle. The critical decision points are illustrated in Figure V-14. Simplified methods for calculation of the partitioning of H_2S, CO_2 and NH_3 between steam condensate and noncondensable gas streams produced by either surface or direct contact condensers are summarize in Ref. 4. Figure V-15, from Ref. 4, illustrates the partitioning of H_2S gas at a separation temperature of 120°F.

V-7-1. Post-Energy Conversion Hydrogen Sulfide Control Measures

It should be noted that some H_2S abatement techniques such as the EIC process could be utilized at either upstream or downstream H_2S release points. To avoid confusion, this section will describe only those processes that are intended for the treatment of steam condensate following the energy conversion process. In Section V-8, off-gas or vent gas H_2S emission control systems are

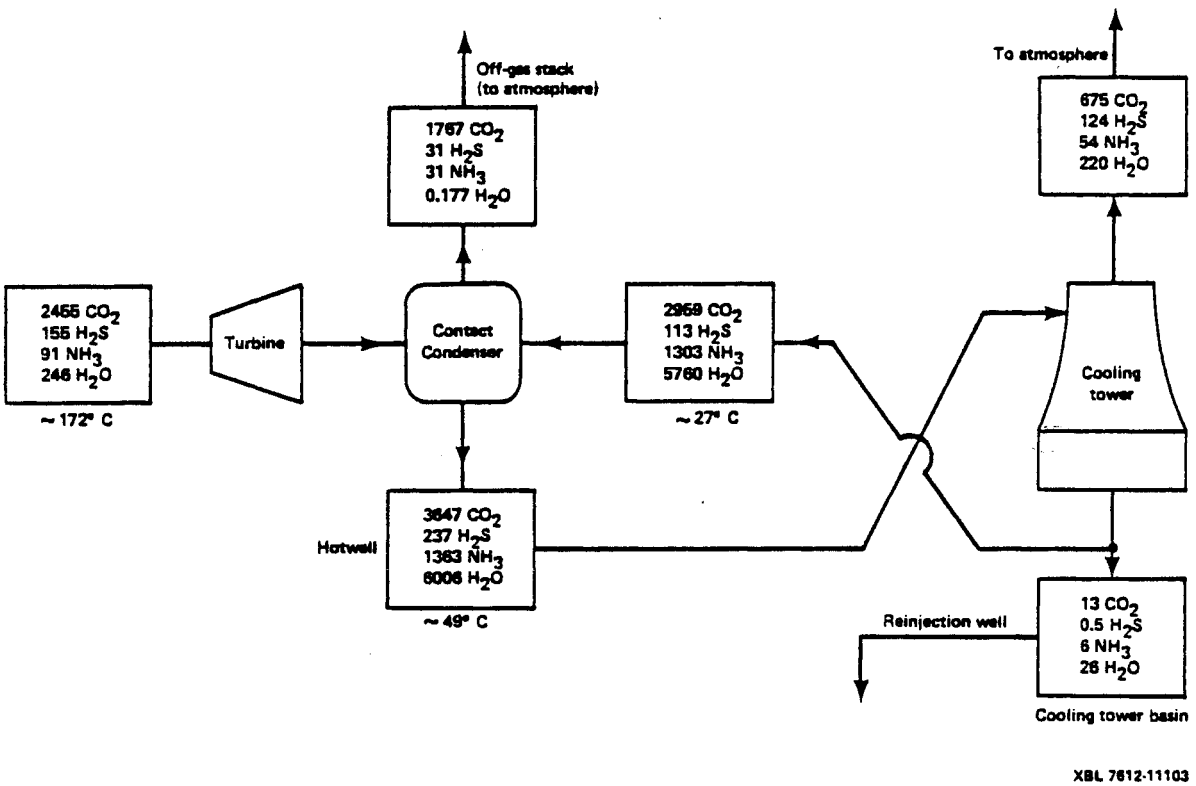

Figure V-13. Simplified mass balance for Geysers Unit 3 illustrating the fate of noncondensable gases when steam is passed through a direct contact condenser. Water flows are in metric tonnes/hour, other mass flows are in kg/hour. H_2, N_2, CH_4 and O_2 ignored (From Ref. 1).

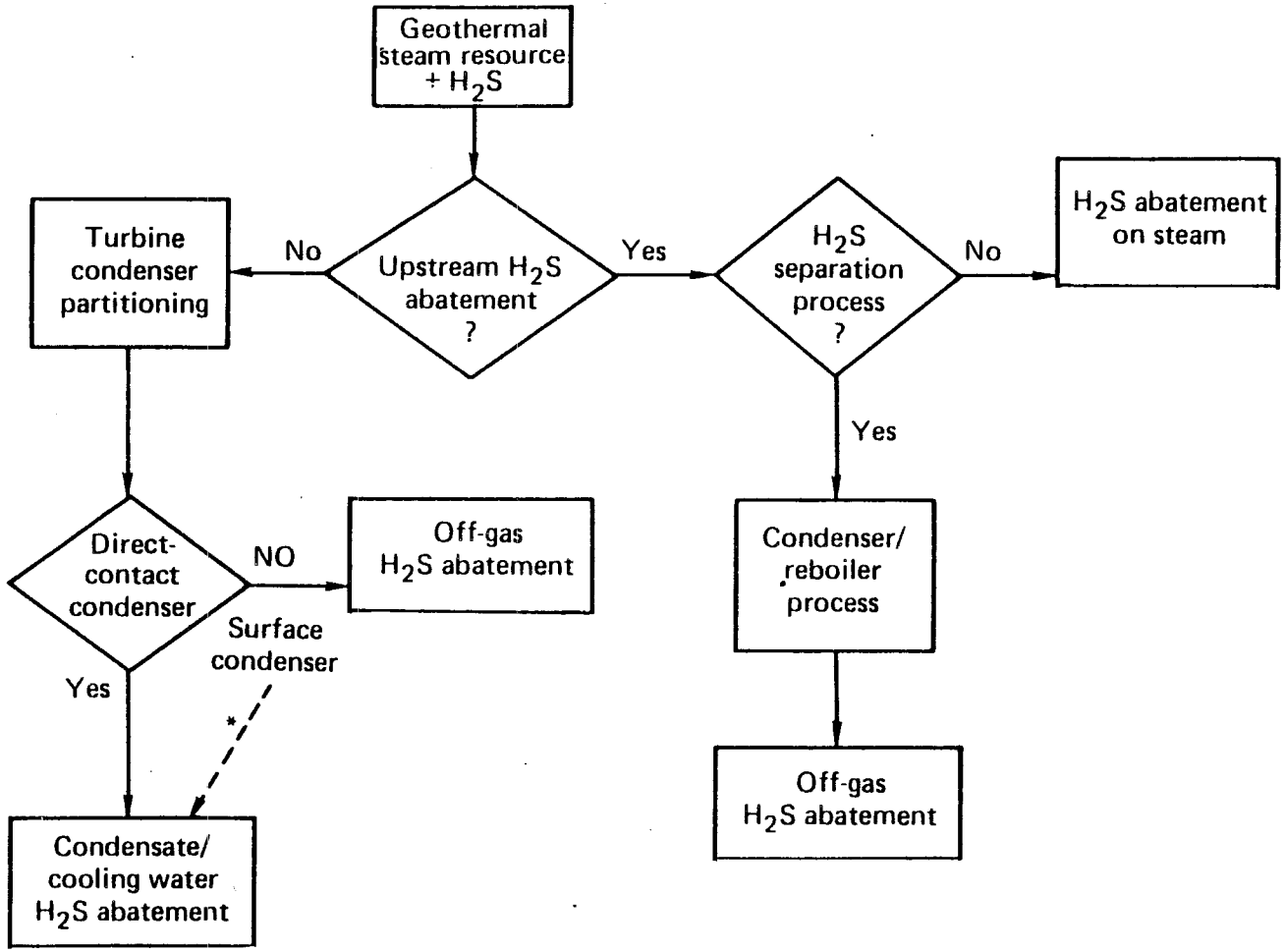

Figure V-14. Central points for the abatement of hydrogen sulfide emissons (From Ref. 4).

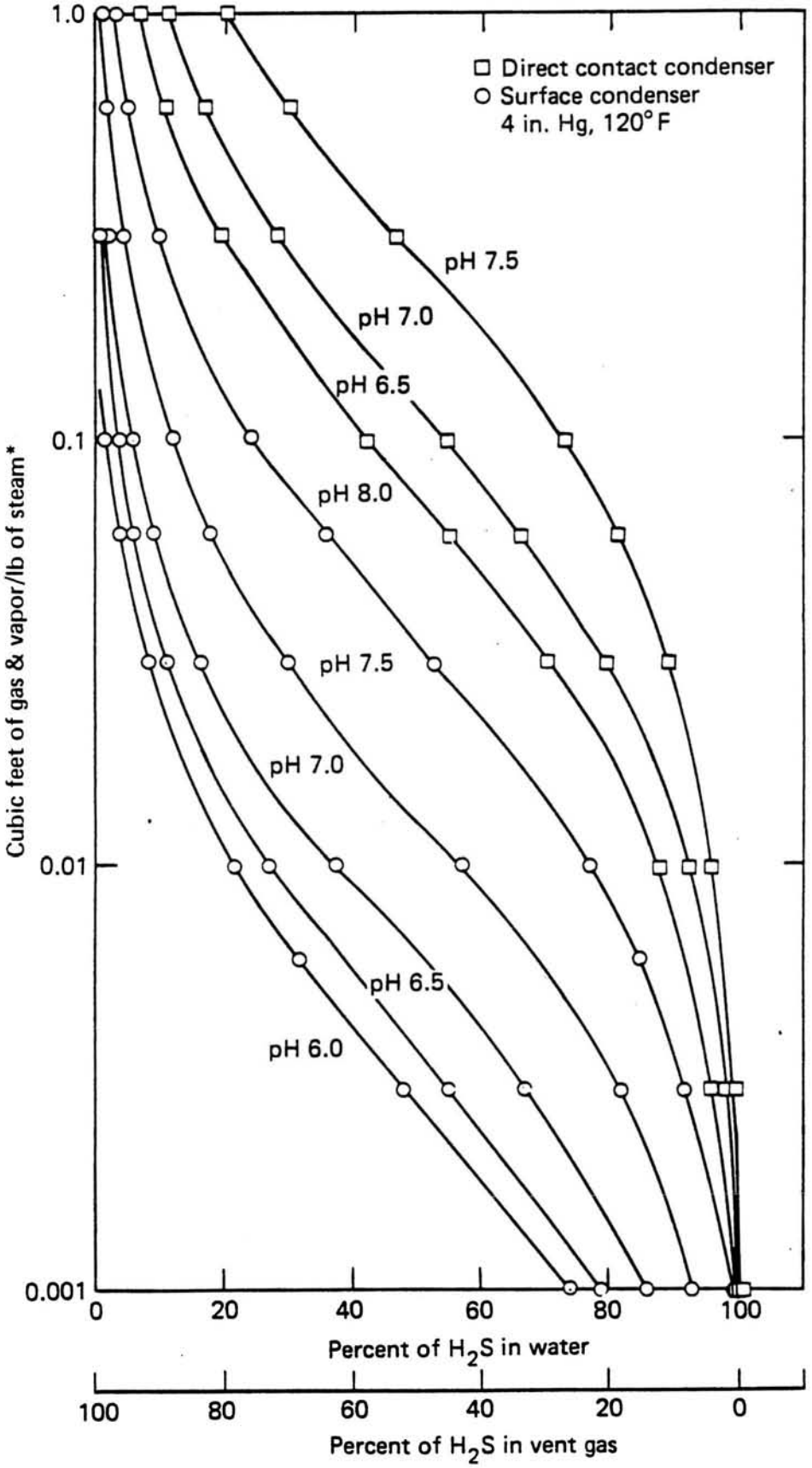

Figure V-15. Calculated H_2S distribution ratios in vent gas for direct contact and surface condensers. *Cu ft/lb = [(percent by weight noncondensible gas in steam)8] (From Ref. 4).

described. Several of these processes, such as the peroxide-caustic system, could also be used for the treatment of condensate.

V-7-2. The Iron Catalyst Process

V-7-2a. Description of the Process - This system was initially designed for the treatment of condensate at the Geysers, and with subsequent modifications, adapted for the treatment of cooling water also[1]. The basic scheme as employed at the Geysers is shown in Figure V-16. The iron catalyst system operation is based on the use of ferrous sulfate to convert H_2S to sulfur by the oxidation of ferrous iron to ferric iron:

$$Fe^{+2} + \tfrac{1}{2}O_2 + 2H^+ \rightarrow 2Fe^{+3} + H_2O \qquad \text{(V-24)}$$

$$H_2S \text{ (aqueous)} \rightarrow 2H^+ + S^{-2} \qquad \text{(V-25)}$$

$$2Fe^{+3} + S^{-2} \rightarrow 2Fe^{+2} + S \qquad \text{(V-26)}$$

The net reaction is:

$$H_2S + \tfrac{1}{2}O_2 \rightarrow H_2O + S \qquad \text{(V-27)}$$

The quantity of ferrous sulfate used for H_2S abatement must be carefully controlled to avoid precipitation of iron sulfide which causes fouling problems in the cooling tower and flowlines:

$$Fe^{+2} + S^{-2} \rightarrow FeS \qquad \text{(V-28)}$$

Subsequent modifications to the system have included the installation of a peroxide-caustic treatment system for the removal of H_2S from cooling water[4]. The optimized H_2S control system operates with a 90 percent H_2S removal efficiency. Difficulties with the system include accelerated corrosion of mild steel components and carryover of iron-enriched cooling tower spray that discolors areas immediately adjacent to the towers.

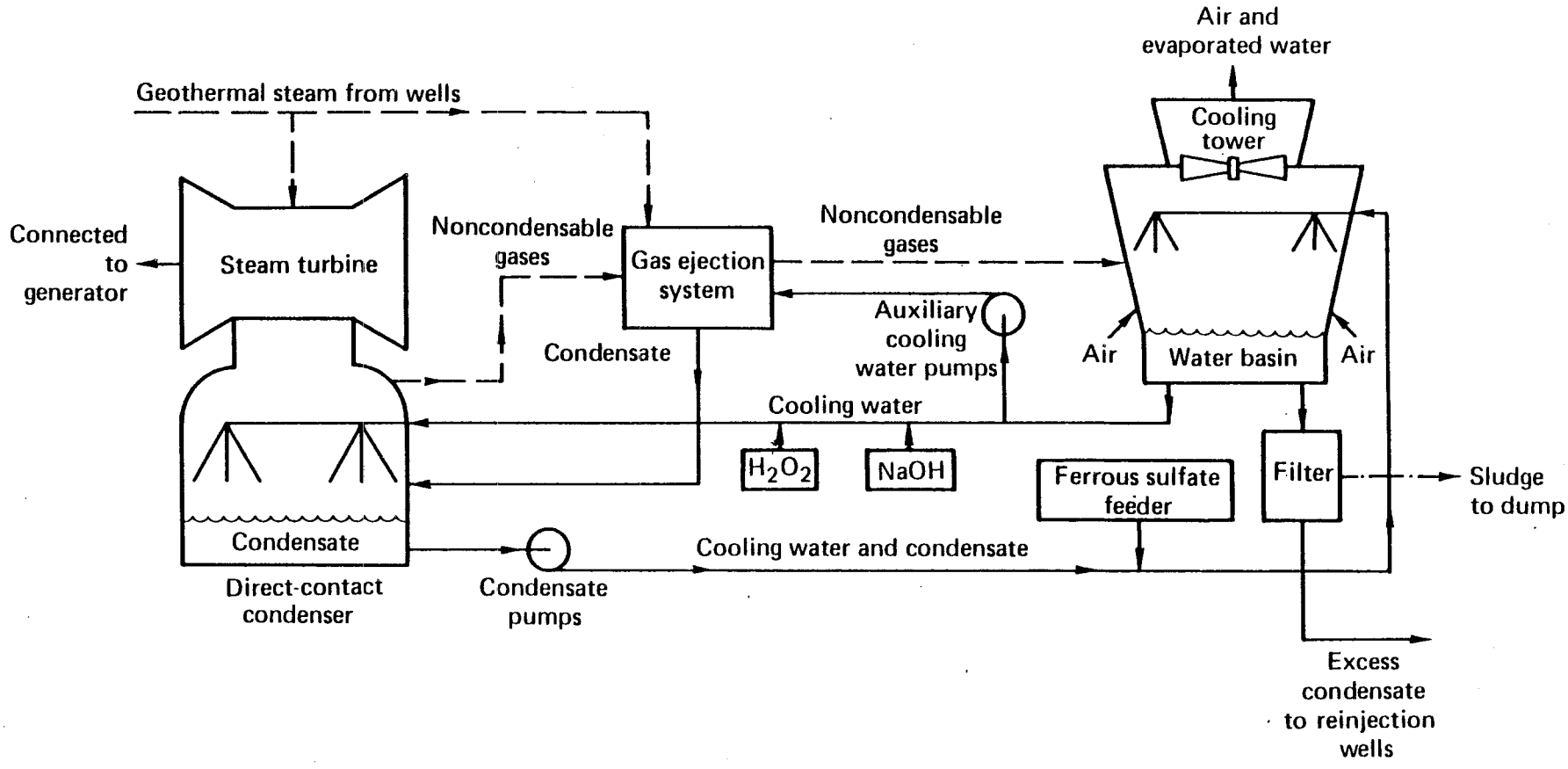

Figure V-16. The optimized iron catalyst - Peroxide - Causite H_2S Abatement System. This system is in use at the Geysers with direct contact condensers (From Ref. 4).

V-7-2b. Hydrothermal Studies - None reported.

V-7-2c. Hydrothermal Applications - The iron catalyst system will most probably be of limited utility in typical hydrothermal applictions. The disadvantages of the process include relatively high costs for chemical supplies as compared to equally effective or superior alternative abatement processes. The corrosion difficulties coupled with cooling tower carryover iron pollution can be eliminated by the selection of alternative abatement processes.

V-7-3. The Ozone Oxidation Process

V-7-3a. Description of the Process - The oxidation of aqueous H_2S in condensate by ozone is theoretically possible[4]:

$$3H_2S + O_3 \rightarrow 3S + 3H_2O \qquad \text{(V-29)}$$

$$3H_2S + 4O_3 \rightarrow 3H_2SO_4 \qquad \text{(V-30)}$$

If reaction V-30 predominates, ozone requirements will be increased four times relative to reaction V-29.

V-7-3b. Hydrothermal Studies - None.

V-7-3c. Hydrothermal Applications - Insufficient information is available to assess the potential utility of this process.

V-7-4. The Wackenroder Process

V-7-4a. Description of the Process - According to Ref. 4, this process is the liquid phase equivalent of the classical Claus process (see Section V-8). The process converts aqueous H_2S to free sulfur using sulfur dioxide as the oxidant:

$$2H_2S + SO_2 \rightarrow 3S + 2H_2O \qquad \text{(V-31)}$$

Preliminary laboratory experiments without the use of catalysts indicated some conversion of H_2S, but at a slow rate.

V-7-4b. Hydrothermal Studies - None.

V-7-4c. Hydrothermal Applications - Insufficient information is available to assess potential applicability of the process.

V-8. Off-Gas Hydrogen Sulfide Abatement Systems

The industrial processing of acid noncondensable gas for the removal of H_2S is well known and in common practice. The difficulties in applying these standard technologies to the abatement of geothermal emission stems more from process economics than from technical difficulties. Table V-4 lists the H_2S off-gas or vent gas control systems that have been evaluated for geothermal service or considered on the basis of technical merits. These systems are similar in that they treat gas streams directly without the requirement of preconcentration of H_2S into a large volume of liquid. The processes, either alone or in combination, reduce H_2S to a stable end-product which is suitable for either sale as a mineral commodity (sulfur) or for disposal in an appropriate landfill.

V-8-1. Hydrogen Peroxide-Sodium Hydroxide Process

V-8-1a. Description of the Process - This method was originally developed as a means of controlling H_2S emissions during well drilling operations at the Geysers[2,4,10-11]. Selective absorption of H_2S from sour gas in oil field operations by caustic gas/liquid scrubbing with sodium hydroxide has been shown to be effective[19]. Application of the peroxide-alkali technique is shown schematicaly in Figure V-17. Sodium hydroxide and hydrogen perioxide are injected into geothermal steam in a Blooie line while the well is being

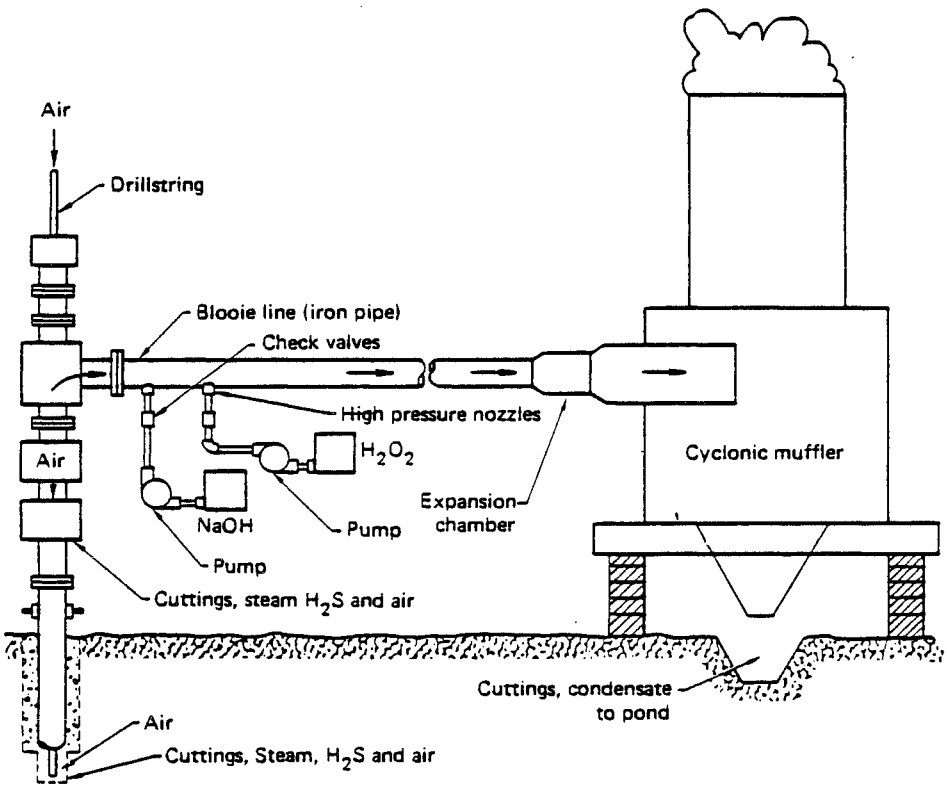

Figure V-17. Typical application for Caustic-Peroxide H_2S abatement during air drilling.

drilled with air. Normally, treatment is continued for 16 days, the nominal time required for completion of the well. The produced steam which contains H_2S is treated at a temperature of 100°C. Typical gas composition for Geyser geothermal steam where the process was first tested is:

Constituent	Mg/kg
CO_2	900 to 19,000
NH_3	60 to 1,100
C_2H_6	3 to 20
N_2 + Ar	20 to 640
H_2	20 to 290
H_2S	5 to 1,600

H_2S abatement in steam occurs by absorption of H_2S into NaOH to form hydrosulfide and sulfide ions followed by oxidation of these intermediates to sulfates by H_2O_2:

$$H_2S + NaOH \rightarrow NaHS + H_2O \quad (1)$$

$$H_2S + 2NaOH \rightarrow Na_2S + 2H_2O \quad (2)$$

$$NaHS + 4H_2O_2 \rightarrow NaHSO_4 + 4H_2O \quad (3)$$

$$Na_2S + 4H_2O_2 \rightarrow Na_2SO_4 + 4H_2O \quad (4)$$

Oxidation of sulfide ion to sulfate by H_2O_2 is essential in preventing redistribution of sulfide ions if pH changes occur due to subsequent mixing with low pH waters or by absorption of geothermal or atmospheric CO_2. Use of caustic to increase pH is also essential in promoting more complete dissociation of H_2S and hence more complete absorption of the gas. For a typical well drilling operation at the Geysers, treatment of H_2S emissions achieves 83 to 98% abatement at a cost of $8,600 to $11,400 per well or 1 to 1.6% of the total well cost.

The hydrogen peroxide process has been successfully used to eliminate H_2S emissions from Geysers condensate. Typical Geysers condensate has the following composition:

Constituent	Mg/kg
Ammonia	69 to 235
Sulfate	80 to 186
Calcium	1 to 10
Silica	1 to 8
Boron	1 to 27

Laboratory experiments, using Geysers condensate, demonstrated that 90 percent or more of the original H_2S could be eliminated at temperatures of 40 to 52°C in 15 seconds or less provided that small quantities of $FeSO_4$ catalyst (1 to 2 Mg/kg) were added to the condensate steam. Alternatively, higher concentrations of H_2O_2 also promoted more rapid reaction in the absence of catalyst. A peroxide/sulfide mole ratio of 400:1 was necessary in the absence of catalyst. Subsequent work at the Geysers demonstrated that H_2S could be scrubbed from steam condensate in both direct contact and surface contact condensing systems. Treatment cost in one case where a 1:1 mole ratio of peroxide to sulfide was maintained was $0.572 per pound of H_2S treated.

V-8-1b. Hydrothermal Studies - The caustic peroxide H_2S abatement system has been successfully demonstrated in conjunction with hydrothermal well tests at the HGP-A facility on the island of Hawaii[18]. The production well characteristics are summarized in Table V-5. Successful abatement of H_2S in separated steam (774 ppmv H_2S) was accomplished using caustic treatment (NaOH) only. The percent abatement reached 99 percent of the original H_2S in the steam (Table V-6). Spent steam condensate was percolated into the porous volcanic strata. Treatment with peroxide, which prevents re-release of H_2S if condensate pH drops by reaction with rocks or ground water, was deemed unnecessary. Temperature of the separated steam at the point of caustic injection was not specified.

V-8-1c. Hydrothermal Applications - The caustic-peroxide abatement technique has been demonstrated to be effective for the treatment of steam and low sa-

Table V-5

Throttled Flow Data
Well HGP-A

Separator Pressure (psig)	Total Mass Flow Rate (Klb/hr)	Steam Flow Rate (Klb/hr)	Water Flow Rate (Klb/hr)	Steam Quality (%)
56	111.5	70.9	40.6	63.6
110	110.3	64.7	45.6	58.7
132	108.0	61.0	47.0	56.5
161	105.9	56.6	49.3	53.4
54	99.0	65.0	34.0	66.0
100	93.0	57.0	36.0	64.0
165	89.0	54.0	35.0	60.0

(From Ref. 18)

Table V-6

H_2S Caustic Abatement Data
Well HGP-A

Caustic/H_2S Mole Ratio	H_2S in Discharged Steam	% Abatement in Steam Phase	% Abatement in Total Flow	pH
1.5	91	88	86	7
2.0	20	97	95	11
3.2	6	99	97	>11
8.0	1	99	98	>11

(From Ref. 18)

linity condensate. General utility of the method for hydrothermal resources will most probably be limited to post-energy conversion treatment of vent gas streams produced by reboilers or steam jet ejectors and steam condensate streams. In some cases, it may be necessary to reinject residual steam condensate. Some attention would have to be directed to the potential for incompatability between caustic sulfate bearing condensate and in-situ formation fluids. Precipitate formation could lead to premature failure of injection wells. Routine abatement of H_2S emissions during steam stacking operations may not be practical if caustic is rapidly consumed by reaction with produced CO_2. In most cases, geothermal steam from hydrothermal resources contains noncondensable gases which are highly enriched in CO_2 relative to H_2S. Thus, economics could be severely affected by partial absorption of CO_2 and resulting increased alkali consumption (see next section).

V-8-2. Selective Caustic Absorption of Hydrogen Sulfide Gas

V-8-2a. Description of the Process - According to Ref. 32, H_2S can be selectively absorbed from a gas mixture of H_2S and CO_2 by maintaining a proper residence contact time between the gas and an alkaline scrubbing solution. The absorption and reaction of H_2S in a strongly alkaline solution (pH 9 to 12) is essentially instantaneous while the absorption of CO_2 occurs at a much slower rate. Thus, proper application of this process results in high efficiency separation of H_2S from CO_2 and thereby significantly reduces caustic consumption. The governing chemical rections for the process are:

$$H_2S + 2NaOH \rightarrow Na_2S + 2H_2O \quad \text{(V-36)}$$

$$H_2S + Na_2S \rightarrow 2NaHS \quad \text{(V-37)}$$

$$CO_2 + 2NaOH \rightarrow Na_2CO_3 + H_2O \quad \text{(V-38)}$$

Reaction V-37 is most desirable and it is promoted at pH values between 9 and 12. Reaction V-38 is least desirable because it consumes caustic by absorption of CO_2. Proper operation of the process limits CO_2 absorption to values of less than 5 percent of the initial CO_2 concentration.

Figure V-18 illustrates the process. A gas stream, containing CO_2 and H_2S is flowed through a contactor and a separator. The off-gas is enriched in CO_2 while the liquid effluent is enriched in H_2S in the form of sodium bisulfide (NaHS). Sodium bisulfide has commercial value and is commonly used as an oxygen inhibitor. Common oilfield practice, however, is to dispose of the NaHS process stream via subsurface injection wells. Surface disposal of the liquid effluent is not feasible owing to the re-evolution of H_2S if the effluent pH is lowered. The sulfide in the waste stream could also be stabilized by conversion to sulfur and sulfates using the peroxide treatment described in Section V-8-1 or by application of the Stretford process.

Capital costs for installation of the caustic treatment system were estimated at $10,000 to $30,000 (1980). Operating costs were estimated to be $0.10/lb of H_2S removed assuming a caustic cost of $180/ton. The efficiency of the process was estimated to be 90 percent. Higher efficiencies can be achieved by use of dual stage contactors. The process has been successfully tested under field conditions where an initial H_2S concentration of 0.8 weight percent was reduced to 0.000 weight percent in the presence of 65 weight percent CO_2 at a total mass flowrate of 1300 MSCF.

V-8-2b. Hydrothermal Studies - see Section V-8-1.

V-8-2c. Hydrothermal Applications - This process has been used successfully to remove H_2S from steam. Large scale application of the process will be strongly controlled by cost of application, reagent costs being of dominant

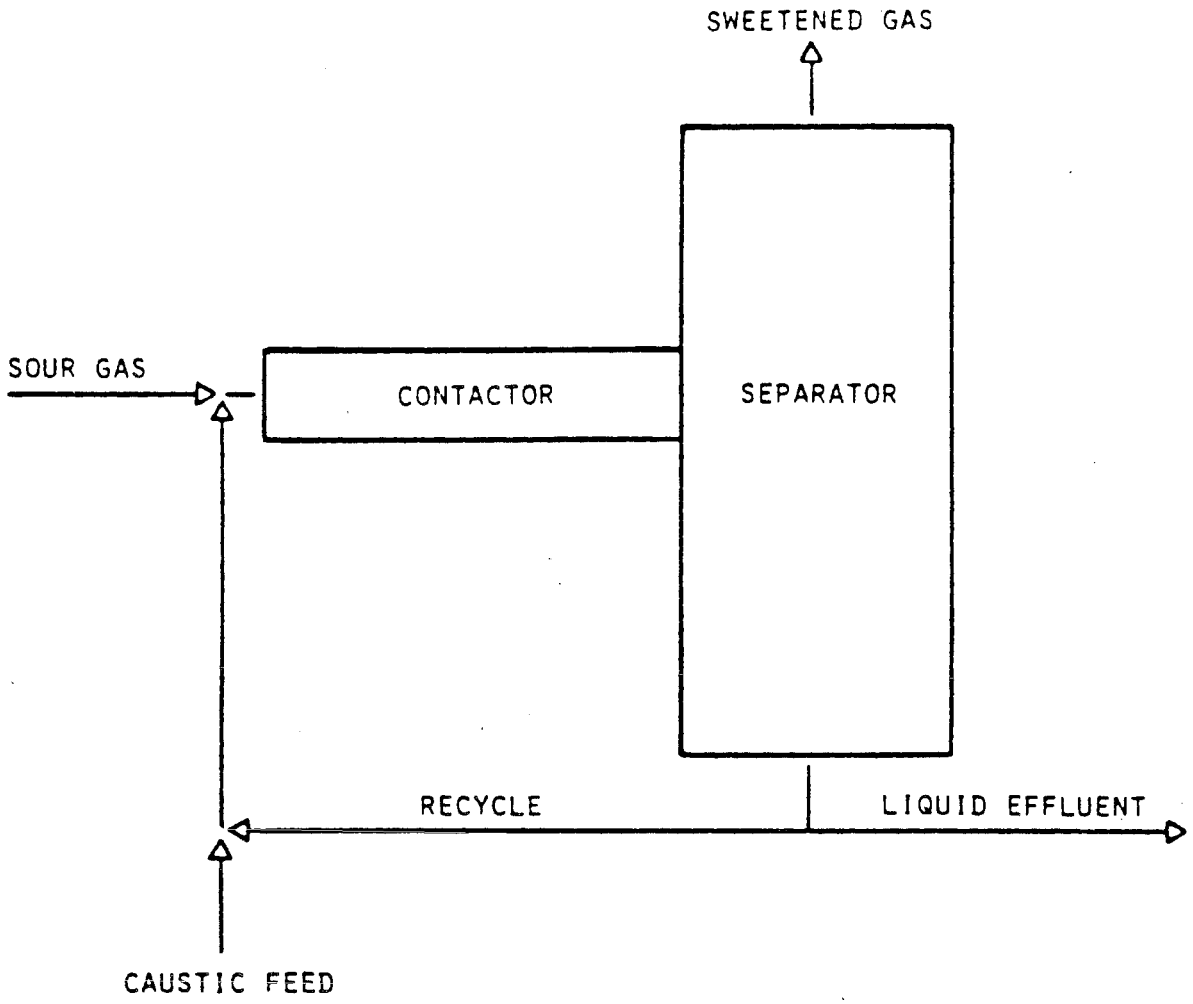

Figure V-18. Hydrogen Sulfide Caustic Scrubber (From Ref. 32).

importance. Since the process does not completely stabilize recovered H_2S, ultimate disposal of treated effluents must be considered. If peroxide treatment is used to destroy H_2S, the added reagent costs could prevent widespread application of the process. The caustic process or the caustic-peroxide processes could, however, be used as secondary control measures to recover the 10 to 20 percent of residual H_2S lost to condensate in a surface condenser in conjunction with the utilization of the Stretford process as the primary H_2S control measure.

V-8-3. The LLNL Brine Scrubbing Process

V-8-3a. Description of the Process - The hypersaline geothermal brines found in the Salton Trough of Southern California are characterized by extremely high concentrations of dissolved transition metals. For example, dissolved iron concentrations in brines from the Salton Sea Geothermal Field and the South Brawley Geothermal Field range from several hundred to several thousand mg/l. The total dissolved heavy metal content of these brines is significantly greater than the stoichiometric requirement for the quantitative precipitation of heavy metal sulfide minerals given the characteristic H_2S concentrations in the reservoir brines. In 1978, Owen, et al.[8] filed a patent disclosure describing a process for H_2S abatement specifically designed for a hypersaline geothermal brine containing a high dissolved content of transition metals. The disclosure suggested that flashed brine could be used as a highly efficient scrubbing agent for H_2S vent gas due to the precipitation of metal sulfides as shown by the following reactions:

Absorbtion

$$H_2S\ (g) = H_2S\ (aq) \qquad \text{(V-39)}$$

$$H_2S\ (aq) = H^+ + HS^- \qquad \text{(V-40)}$$

$$HS^- = H^+ + S^{=} \qquad \text{(V-41)}$$

Precipitation

$$\frac{2}{Z} = M^{Z+} + S^{=} \quad M_{2/Z}S(s) \qquad \text{(V-42)}$$

where: Z is the oxidation number of the heavy metal ion (M)

The overall reaction is

$$\frac{2}{Z} M^{Z+} + H_2S\ (g) \rightarrow M_{2/Z}S(s) + 2H^{+} \qquad \text{(V-43)}$$

It was subsequently demonstrated by means of a small-scale field experiment that the brine scrubbing process had an H_2S removal efficiency of greater than 96 percent at a 0.3 weight percent noncondensable gas to brine ratio[9]. The proces was eventually evaluated on a pilot scale by Magma Power Company and the San Diego Gas and Electric Co. at the Geothermal Loop Experimental Facility (GLEF). Noncondensable vent gas was injected into the reaction well of a 30 gpm EIMCO reactor-clarifer and H_2S scrubbing efficiencies of 97 percent were obtained[4]. The process is particularly attractive for application in the hypersaline brine resource areas because the chemical requirements for H_2S abatement are satisfied at no cost, the precipitation of additional heavy metal sulfides within a reactor-clarifier can actually improve performance of the unit, and the potential exists for economic recovery of mineral values represented by the recovered heavy metal precipitates.

V-8-3b. Hydrothermal Studies - The process has been successfully tested on a bench and pilot scale at the Salton Sea Geothermal Field[4,8,9]. The process is presently being used successfully by the Union Oil Company in conjunction with the operation of a 10 MWe demonstration plant, for Southern California Edison, located at the Salton Sea Geothermal Field.

V-8-3c. Hydrothermal Applications - The LLNL brine scrubbing process is the preferred method for achieving adequate abatement of H_2S emissions in conjunc-

tion with the exploitation of hypersaline brine resources. Application of the process requires use of surface contact condensers to preclude partitioning of H_2S into condensate. Satisfactory application of the process will also require use of a two-stage flash process to insure that the bulk of the H_2S in the reservoir brine is effectively separated from the brine. It has been found as a result of operational experience at the GLEF that the pH of second stage steam condensate is 8.5-9.5 as compared to the pH of first-stage condensate of about 6.2. At the higher pH, H_2S in contact with the condensate would tend to dissolve into the condensate.

V-8-4. The Stretford Process

V-8-4a. Description of the Process - A schematic illustration of the Stretford process is shown in Figure V-19. The process was originally developed for the treatment of Synthetic fuel gases in the United Kingdom[1-2,4]. The process converts H_2S to free sulfur by catalytic air oxidation. The scrubbing medium is an aqueous solution of sodium carbonate, sodium metavanadate and anthraquinone disulfonic acid (ADA). A counter-current scrubber is used to contact H_2S gas with the scrubbing solution. The reactor tower is operated at an optimum pH of about 8.8. H_2S reduction to free sulfur occurs as follows:

Absorption Reaction

$$H_2S + Na_2CO_3 \rightarrow NaHS + NaHCO_3 \qquad \text{(V-44)}$$

$$NaHS(aq) \rightarrow Na^+ + HS^- \qquad \text{(V-45)}$$

Conversion Reaction

$$HS^- + V^{+5} \rightarrow S + V^{+4} \qquad \text{(V-46)}$$

The process is catalytically promoted by ADA which acts to replenish quinquivalent vanadium:

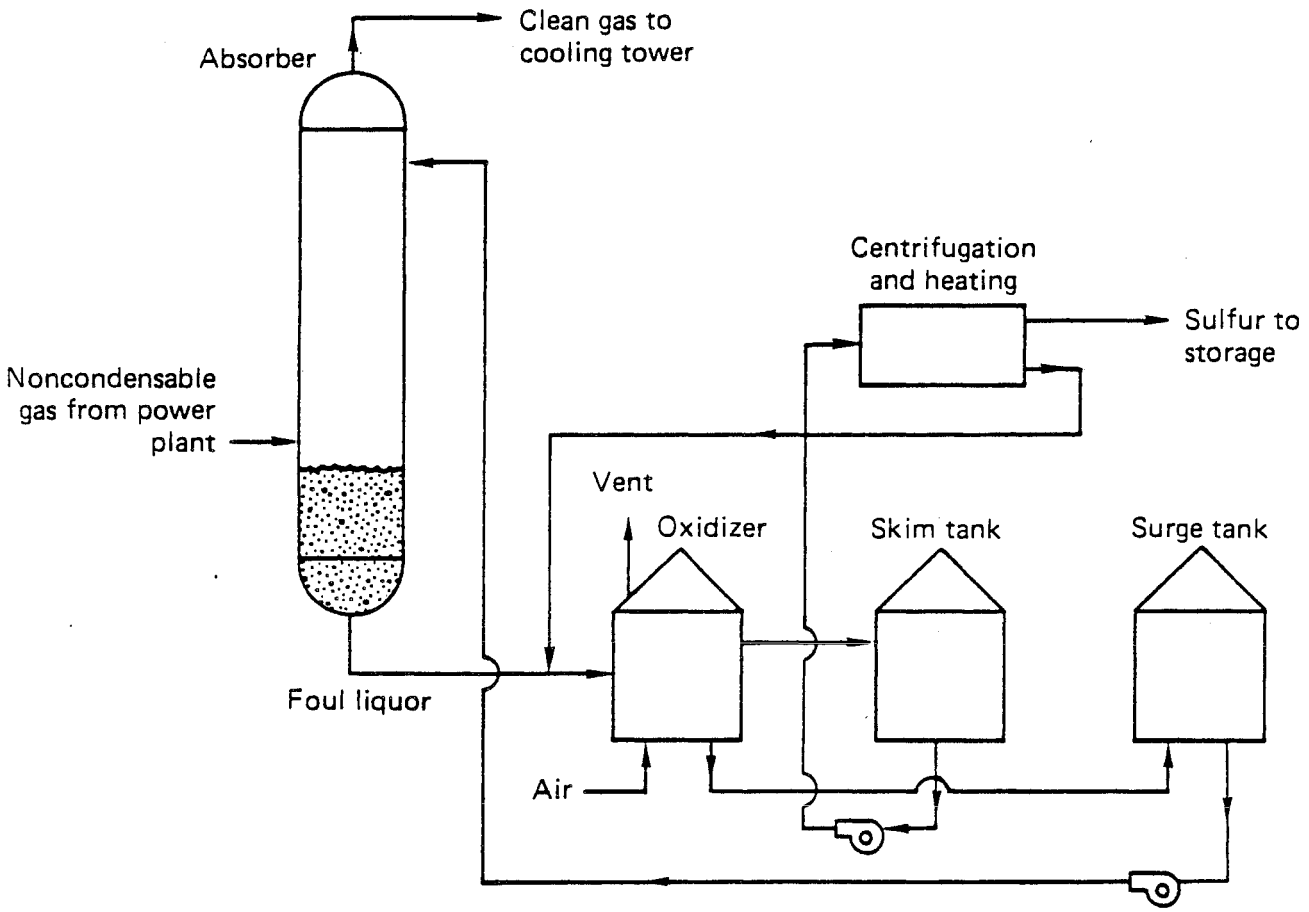

Figure V-19. The Stretford process (From Ref. 2).

$$V^{+4} + ADA \rightarrow V^{+5} + \text{reduced ADA} \quad \text{(V-47)}$$

$$\text{reduced ADA} + O_2 \rightarrow ADA + H_2O \quad \text{(V-48)}$$

Air serves the dual purpose of causing the oxidation of H_2S to free sulfur and floating produced sulfur to the top of a skimming tank where it is recovered as a saleable by-product. Process economics are strongly dependent upon the commodity value of the recovered sulfur. The overall scrubbing process is defined by the following reaction:

$$2H_2S + O_2 \rightarrow 2H_2O + 2S \quad \text{(V-49)}$$

A Stretford process will eliminate better than 99 percent of the H_2S in vent gas admitted to the scrubber tower. A surface contact condenser must be used with the process to preclude partitioning of H_2S into condensate. The small quantity of condensate produced in the surface contact condenser will scavenge from 10 to 20 percent of the total H_2S depending upon the pH of the condensate. This residual H_2S gas will be vented to the atmosphere via the cooling tower unless a secondary process such as the caustic-peroxide process is used to control the residual H_2S. Capital and annual O&M costs for the Stretfrd process are summarized in Figure V-20. The estimates were based on the following assumptions[2]:

- Amortization period: 15 years
- Maintenance materials: 2 percent of the installed capital cost
- Maintenance labor: 10 percent downtime, requiring a two man maintenance crew, earning approximately $30 per hour.
- Electrical power usage: 66 operating BHP per metric ton of sulfur produced per day
- Chemical cost: $35 per metric ton of sulfur produced per day
- Sulfur credit: $20 per metric ton

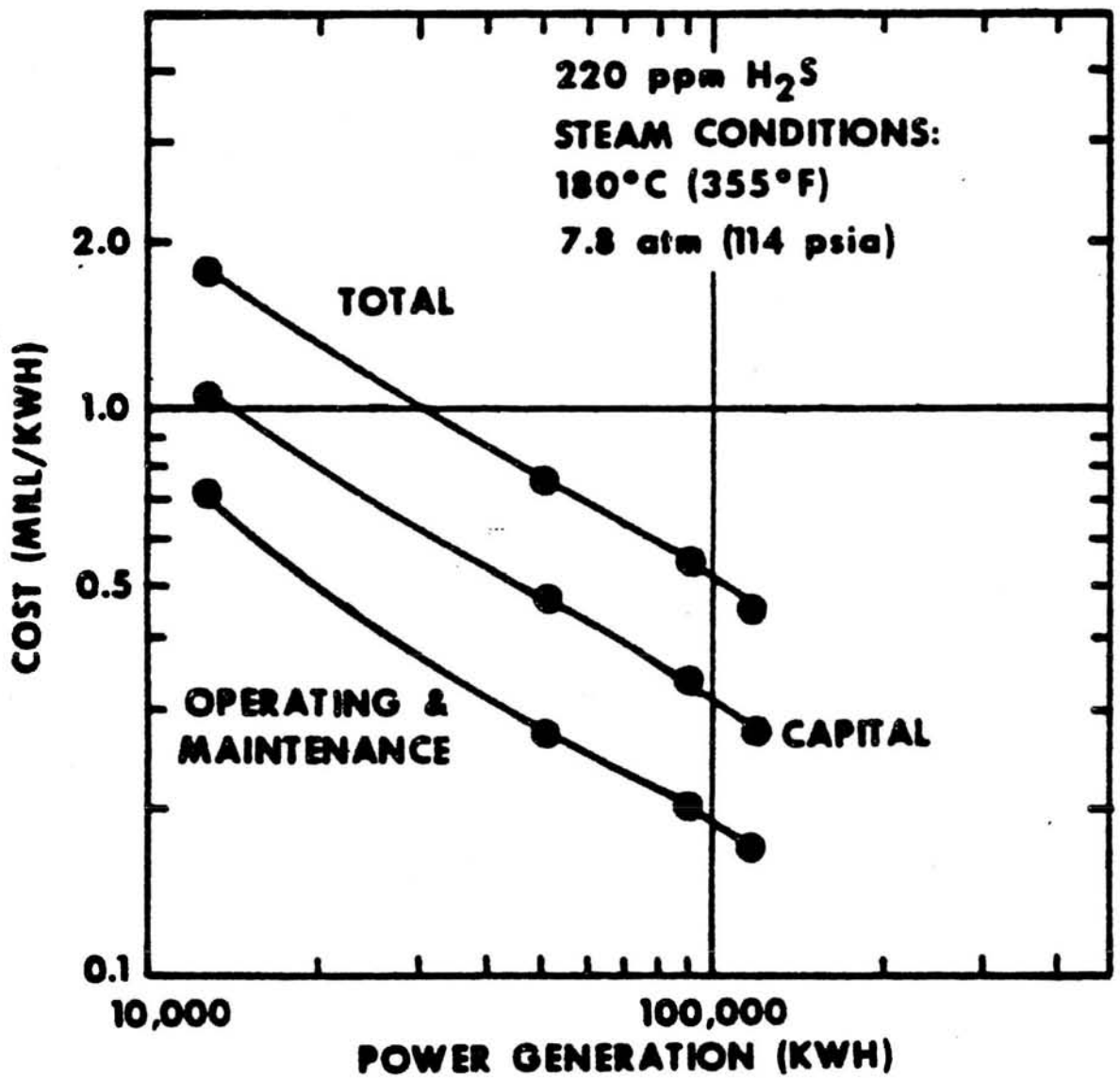

Figure V-20. Costs for hydrogen sulfide removal by the Stretford process (From Ref. 2).

- Construction site: The Geysers

and,

$IA = IB\ (SA/SB)^{0.4}$ for: $0.5 < SA < 5$ metric tons of sulfur per day

$IA = IB\ (SA/SB)^{0.5}$ for: $5 < SA < 250$ metric tons of sulfur per day

SA = metric tons of sulfur produced per day in the desired case

SB = metric tons of sulfur produced per day by the base case (The Geysers unit 14) Stretford process.

I = Capital investment for the desired or base (A or B) Stretford Process.

V-8-4b. Hydrothermal Studies - None.

V-8-4c. Hydrothermal Applications - With the installation of the appropriate surface contact condensers there are no compelling reasons other than cost factors which would argue against installation of Stretford abatement systems. Competing process would include the caustic-peroxide process and the EIC and LLNL processes which both affect removal of H_2S in the form of heavy metal sulfide precipitates. At conventional hydrothermal resources where produced brines do not include high concentrations of transition metals, reagent costs for precipitation of sulfides will become important. Regeneration of reagent as described in the EIC process will be of obvious importance. If clarifiers are not needed, application of the sulfide precipitation processes will require additional capitol expenditures for scrubbing towers.

V-8-5. The Claus Process

V-8-5a. Description of the Process - The Claus process was originally developed for the recovery of sulfur from a gas stream consisting of H_2S and sulfur dioxide (SO_2). A typical Claus plant is shown in Figure V-21. According to Refs. 2 and 15, the Claus process involves the splitting of vent gas into two streams. One-third of the H_2S is oxidized by a combustion process as follows:

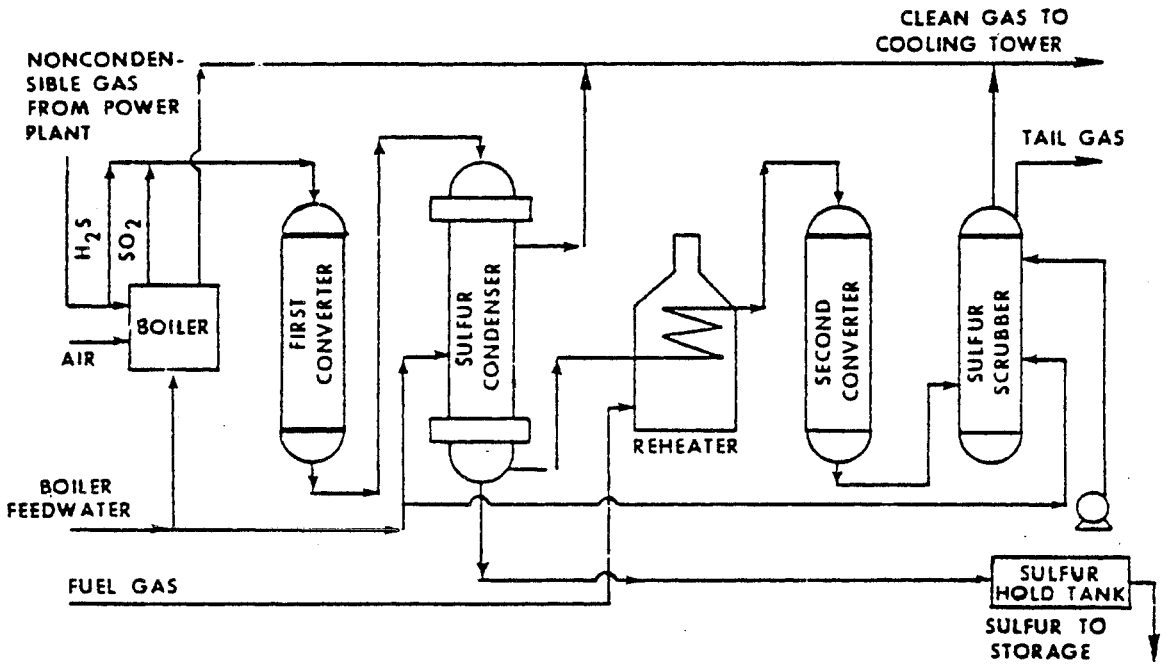

Figure V-21. Claus sulfur recovery process (From Ref. 2).

$$H_2S + 3/2\ O_2 \rightarrow SO_2 + H_2O \qquad \text{(V-50)}$$

Recovered SO_2 is recombined with the virgin gas stream and passed through two or more catalytic reactors where H_2S is converted to free sulfur as follows:

$$2H_2S + SO_2 \overset{CAT}{\rightarrow} 3S\downarrow + 2H_2O \qquad \text{(V-51)}$$

Reactions V-50 and V-51 are exothermic and recovered excess heat can be used to generate moderate pressure (150 psi) and low pressure (35 psi) steam for supplemental use. Recent modifications to the Claus process are described in Refs. 43-44.

V-8-5b. Hydrothermal Studies - None.

V-8-5c. Hydrothermal Applications - The principle difficulty with the Claus process is its sensitivity to CO_2 gas. The process cannot be sustained if CO_2 concentrations in the gas exceed 60 percent. Pre-processing for the removal of CO_2 would drastically impact process economics. The detrimental behavior of CO_2 is described by the following chemical reactions[2]:

$$CO_2 + H_2S \rightarrow COS + H_2O \qquad \text{(V-52)}$$

$$CO_2 + H_2S \rightarrow CS_2 + 2H_2O \qquad \text{(V-53)}$$

The presence of water in the raw gas stream also tends to poison catalyst activity. The Jefferson Lake process is a modification of the Claus process which moderates the CO_2 contamination problem (Section V-8-6).

V-8-6. Jefferson Lake Process

V-8-6a. Description of the Process - The inherent limitations of the classical Claus process in the presence of high CO_2 concentrations is overcome by the use of free sulfur in sulfur burner to generate SO_2 gas for use in reaction V-51[15]:

$$S + O_2 \rightarrow SO_2 \qquad \text{(V-54)}$$

A process flow-sheet for the Jefferson Lake process is shown in Figure V-22. The process is now used routinely for the processing of hydrocarbon gases.

V-8-6b. Hydrothermal Studies - The process has been evaluated for use at the Cerro Prieto Geothermal Field in northern Mexico[4].

V-8-6c. Hydrothermal Applications - Suitability of the proess for hydrothermal applications is controlled to a significant degree by process economics. A cost analysis for the process[15] indicates that the value of recovered sulfur by-product is extremely important. Plant cost (in 1975 dollars) are summarized in Table V-7. Plant size is in terms of the sulfur recovery rate. The impact of sulfur resale value on overall plant economics is summarized in Figure V-23. A 150 MWe generating capability at Cerro Prieto, Mexico would produce about 60 long tons of sulfur per day. According to Ref. 15, a plant that produces 80 tons per day or more of sulfur would be profitable at any Frash process, U.S. Gulf Coast sulfur price that had been obtained between 1958 to 1978. The Jefferson Lake process is of potential interest, but more evaluation work will be needed before implementation of the process could be undertaken.

V-8-7. Burner-Scrubber Process

V-8-7a. Description of the Process - Vent gases are incinerated and the residual gases are scrubbed using an aqueous solution[4]. The unit produces SO_2 as a by-product. Preliminary work was carried out at the Geysers. A direct contact condenser was employed. It was hoped that the SO_2 would reduce condensate pH and thereby partition more H_2S into the vapor phase, but insufficient SO_2 was produced to significantly alter condensate pH. The system is not under serious consideration for development at the Geysers.

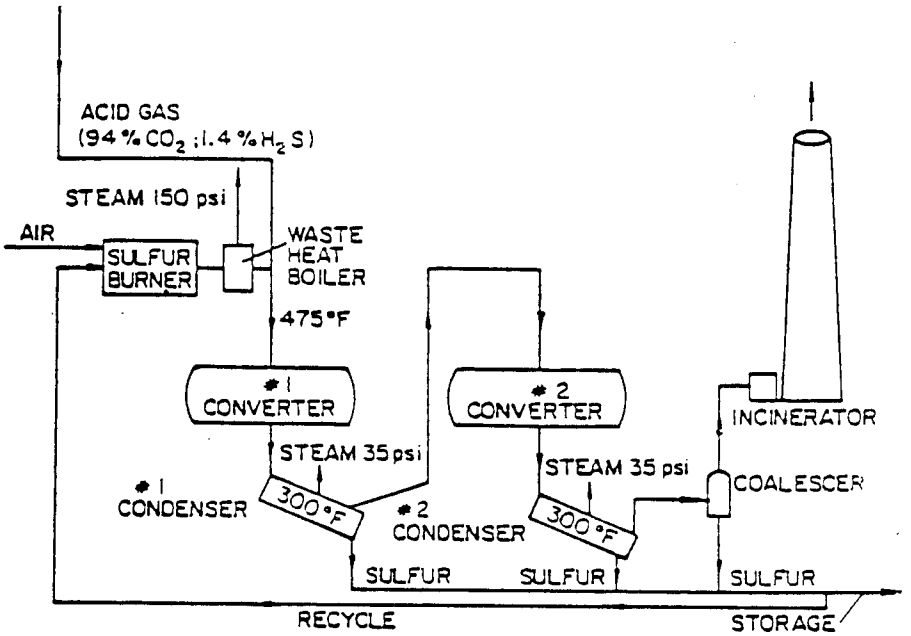

Figure V-22. Jefferson Lake Process Flow-Sheet (From Ref. 15).

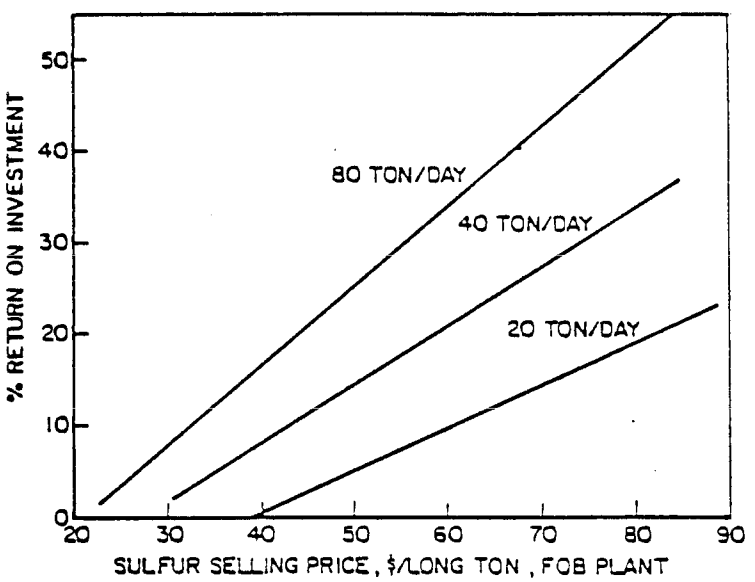

Figure V-23. Profitability, before income taxes, for the Jefferson Lake Process (From Ref. 15).

Table V-7

Plant Costs for the Jefferson Lake Process*

Plant Size (Long Tons Sulfur/day)	20	40	80
yearly capacity in long tons (90% load factor)	6,570	13,140	26,280
plant cost	1,222,000	1,775,000	2,625,000
working cap. (15% of plant cost)	183,000	266,000	394,000
capital investment	$1,405,000	$2,041,000	$3,019,000
Fixed Costs/Long Ton			
depreciation (straight-line; 15 yr. plant life)	$12.40	$9.01	$6.66
taxes, insurance	4.65	3.38	2.50
Operating Costs/Long Ton			
labor	3.50	2.00	2.00
supervision & clerical	4.75	2.37	1.19
maintenance	9.30	6.75	4.99
payroll overhead	1.20	0.64	0.50
elec.: 3-1/2 kwh/ton	0.12	0.12	0.12
fuel gas: 200,000 BTU/ton	0.40	0.40	0.40
instrument air	0.12	0.06	0.03
loading, sales	4.00	4.00	4.00
steam credit	(1.25)	(1.25)	(1.25)
Total Cost/Long Ton	$39.19	$27.48	$21.14

*July 1975 dollars. (From Ref. 15)

The catalyst-scrubber process is a catalytically-assisted incineration process, but H_2S removal efficiency is only on the order of 50 percent[4].

V-8-7b. Hydrothermal Studies - None.

V-8-7c. Hydrothermal Applications - Insufficient information is available to appraise potential applicability of the process.

V-8-8. The Benfield Process

V-8-8a. Description of the Process - The Benfield or hot carbonate process [4,13,14] involves gas-liquid absorption using an aqueous solution of potassium carbonate. Vent gas is injected into a counter-curent tower where H_2S is scavenged as follows:

$$K_2CO_3 + H_2S \rightarrow KHCO_3 + KHS \qquad (V\text{-}55)$$

The scrubbing solution is regenerated with low pressure steam. The process is widely used in industrial applications. Recovered H_2S must be further processed using, for example, a Stretford process, to stabilize the H_2S. For this reason, application of the process at hydrothermal resources is doubtful.

V-8-8b. Hydrothermal Studies - None.

V-8-8c. Hydrothermal Applications - None.

V-8-9. Miscellaneous Processes

V-8-9a. Description of the Process - The Ferrox and Sodium Hypochlorite processes are described in Ref. 4. These processes involve removal of H_2S by formation of iron sulfides and native sulfur and sulfites, respectively. The processes operate by contacting vent gas with the appropriate scrubbing solution in a tower. Neither process has been investigated in sufficient detail to evaluate suitability for hydrothermal applications.

V-9. Summary of Vent Gas H_2S Abatement Methods

Removal of H_2S upstream of the energy conversion process offers the best potential benefits in terms of reduced corrosivity of steam and significant reduction in scale deposition on turbine components. Of the methods considered for hydrothermal service, the use of optimized steam reboiler systems seems to offer the best potential benefits with the least amount of potential difficulties. The major unknown in the application of reboilers is the potential for scale deposition within the heat exchanger and the effects of such deposition. Cost evaluations need to be performed to establish impacts of various modes of operation.

Downstream or post-energy conversion removal of H_2S involves abatement techniques which treat steam condensate. The processes are of interest primarily for short term flow testing of geothermal wells and during drilling operations rather than for installation as primary H_2S abatement systems. Secondary application of these processes may be needed in conjunction with the operation of off gas abatement systems.

Vent gas abatement systems will most likely be employed at hydrothermal resources. These systems would be needed as secondary processes for the treatment of gas produced by steam reboilers. At the hypersaline geothermal resources where the brines are enriched in dissolved transition metals, the LLNL brine scrubbing process will undoubtedly be utilized. An integration of the brine scrubber with the reboiler system is most likely at these resources. While the LLN brine scrubbing process could be used at conventional hydrothermal resources, nonreplenishable supplies of heavy metals would be needed to scrub H_2S. These reagent costs may be excessive. The EIC process, which includes regeneration of sulfide precipitant, could also be considered provided that secondary precipitation of sulfates and scale deposition problems do not become serious.

One of the technical problems that needs to be addressed in more detail concerns the partitioning of H_2S between vapor and condensate. Although the Stretford process is highly efficient, for example, only that gas which is partitioned into the vapor phase can be treated. This problem needs additional evaluation including field studies at operating hydrothermal resources.

V-10. Ambient Air Monitoring

H_2S gas can accumulate about geothermal facilities in toxic and even lethal amounts. For example, large tanks used to store liquid condensate could accumulate high H_2S levels if the tanks are covered. Ambient air monitoring capabilities are a useful on-site analytical capability that can be easily provided[2]. A useful battery-powered H_2S monitoring device is described in Ref. 40.

V-11. References

1. Weres, O., Tsao, K., and Wood., B., 1977, Resource, Technology and Environment at the Geysers: Univ. of Calif., Lawrence Berkeley Laboratory Report, LBL-5231.

2. Hartley, R.P., 1978, Pollution Control Guidance for Geothermal Energy Development: Industrial Environmental Laboratory, U.S. EPA, EPA-60017-78-101, NTIS, Virginia.

3. Hartley, R.P., 1980, Environmental Considerations: In Sourcebook on the Production of Electricity from Geothermal Energy, J. Kestin Editor, Chap. 9, U.S. DOE EY-76-S-4051.A002, 786-866.

4. Stephens, F.B., Hill, J.H. and Phelps, P.L., Jr., 1979, State-of-the-Art Hydrogen Sulfide Control for Geothermal Energy Systems: Univ. of Calif. URRL 83959, 148 p.

5. Pasqualetti, M.J., 1980, Geothermal Energy and the Environment: The Global Experience: Energy, V. 5, N. 2, 111-165.

6. Layton, D.W., Anspaugh, L.R., O'Banion, K.D., 1981, Health and Environmental Effects Document on Geothermal Energy - 1981: Univ. of Calif., Lawrence Livermore National Laboratory Report UCRL-53232, 61 p.

7. James, R., 1980, Disposal of Hydrogen Sulfide Gas: Geothermal Energy, V. 8, No. 10-11, p. 26-27.

8. Owen, L.B., Tardiff, G.E., Quong, R., Stout, N.D. and Robinette, R., 1978, Method for Removing H_2S from Geothermal Vent Gas: Invention Case No. IL-6488, Univ. of Calif., Lawrence Livermore National Laboratory.

9. Quong, R., Knauss, K.G., Stout, N.D. and Owen, L.B., 1979, An Effective H_2S Abatement Process Using Geothermal Brine: Transactions Geothermal Resources Council, V. 3, p. 557-560.

10. Castrantas, H.M., Hampshire, L.R. and Woertz, B.B., 1978, H_2S Abatement During Geothermal Drilling: Petroleum Engineer International, p. 82-88.

11. Castrantas, H.M., 1981, Use of Hydrogen Peroxide to Abate Hydrogen Sulfide in Geothermal Operations: Jour. Pet. Tech., p. 914-919.

12. Chen, B.H., Lopez, L.P., Kuwada, J.T. and Farrington, R.J., 1980, Progress Report on HGP-A Wellhead Generator Feasibility Project: Geothermal Resources Council, Transactions, V. 4, p. 491-494.

13. Field, J.H., Benson, H.E., Johnson, G.E., Tosh, J.S. and Forney, A.J., 1962, Pilot-Plant Studies of the Hot-Carbonate Process for Removing Carbon Dioxide and Hydrogen Sulfide: U.S. Bureau of Mines, Bulletin 597.

14. Field, J.H. and McCrea, D.H., 1981, Selective Removal of H_2S from Gas Mixtures Containing CO_2 and H_2S: United States Patent No. 4,293,531.

15. Velker, J.A. and Axtmann, R.C., 1978, Sulfur Emission Control for Geothermal Power Plants: Journal of Environmental Science and Health, A13(8), p. 603-613.

16. Kawada, T. and Uchida, H., 1980, Gas Purification Process: U.S. Patent No. 4,199,553.

17. Sivalls, Develops New Chemical Gas Sweetener: Drill Bit, V. 30, N. 9, p. 51-53, Sept. 1981.

18. Coury, G., 1981, Upstream Reboiling for Noncondensable Gas Removal: EPRI Rept. AP-2098, 5B-5 to 5B-20.

19. Coury, G.E. and Vorum, M., 1977, Removing H_2S from Geothermal Steam: Chemical Engienering Progress, V. 68, N. 7, p. 83-86.

20. Coury, G.E., 1981, Upstream H_2S Removal from Geothermal Steam: EPRI Rept. AP-2100.

21. Harvey, W.W., Brown, F.C., and Turchan, M.J., 976, Control of Hydrogen Sulfide Emission from Geothermal Power Plants: EIC Corporation, Newton, MA, Rept. No. COO-2730-2.

22. Control of Hydrogen Sulfide Emission from Geothermal Power Plants: Final Report on Task C.6, Optimization and Economic Studies, EIC Corp. Newton, MA, 1978.

23. Brown, F.C., Harvey, W.W. And Warren, R.B., 19__, Hydrogen Sulfide Removal from Geothermal Steam:

24. Brown, F.C., 1980, Preliminary Evaluation of the Copper Sulfate Process for Removal of Hydrogen Sulfide Over a Range of Geothermal Steam Conditions: Proceedings, Fourth Annual Geothermal Conference and Workshop, EPRI, p. 3-29 - 3-37.

25. Jackson, D.D. and Hill, J.H., 1976, Possibilities for Controlling Heavy Metal Sulfides in Scale from Geothermal Brines: Univ. of Calif., Lawrence Livermore National Laboratory Rept. UCRL-51977.

26. King, J.E. and Wilson, J.S., 1977, Removal of Hydrogen Sulfide from Simulated Geothermal Brines by Reaction with Oxygen: ANS-ERDA Topical Meeting, Energy and Mineral Recovery Research, Colorado School of Mines, Golden, CO, Apr. 12-14, 221-232.

27. Schock, R.N. and Duba, A., 1975, The Effect of Electrical Potential on Scale Formation in Salton Sea Brine: Univ. of Calif., Lawrence Livermore National Laboratory Rept. UCRL-51944.

28. Shaw, K. and Willis, C., 1981, Drill-In Procedures for High Pressure Sour Reefs in the West Pembina Area, Alberta: Drilling Technology Conf., International Assoc. of Drilling Contractors, March 10-12, 21-40.

29. Samuels, A. and Wendt, R.P., 1981, Proper Fluid Pre-Treatment to Minimize Hydrogen Sulfide Dangers: JCPT, V. 20, N. 2, 1-9.

30. Samuels, A., 1983, Private Communication.

31. Li, C.T., Alzheimer, D.P. and Wilcox, W.A., 1978, Removal of Hydrogen Sulfide from Geothermal Steam: Geothermal Resources Council, Trans., V. 2, 403-406.

32. Hotilfeld, R.W., 1980, Selective Absorption of H_2S from Sour Gas: Jour. of Pet. Tech., p. 1083-1089.

33. Lazslo, J., 1976, Application of the Stretford Process for H_2S Abatement at the Geysers Geothermal Power Plant: Proceedings, AIChE Intersociety Energy Conversion Conference.

34. Griebe, M., 1977, Comparative Process Study for Pacific Gas & Electric Company, San Francisco, California, Hydrogen Sulfide Abatement for Geothermal Power Production Facilities, The Geysers, California: Ralph M. Parsons Company, Pasadena, California.

35. Wells, K.D. and Currie, J.W., 1979, Impact of H_2S Emission Abatement on Geothermal Power Costs: Proceedings, Institute of Environmental Studies.

36. Kohl, A.L. and Riesenfeld, F.C., 1960, Gas Purification: McGraw-Hill, New York.

37. Field, J.H., Benson, H.E., Johnson, G.E., Tosh, J.S. and Forney, A.J., 1962, Pilot-Plant Studies of the Hot-Carbonate Process for Removing Carbon Dioxide and Hydrogen Sulfide: U.S. Bureau of Mines, Bulletin 597.

38. Field, J.H. and McCrea, D.H., 1981, Selective Removal of H_2S Gas Mixtures Containing CO_2 and H_2S: U.S. Patent 4,293,531.

39. Robertson, R.C., 1980, Waste Heat Rejection From Geothermal Power Stations: In Sourcebook on the Production of Electricity from Geothermal Energy, J. Kestin, R. DiPippo, H.E. Khalifa and D.J. Ryley Editors, DOE/RA/4051-1, 541-600.

40. Sedlak, J.M., Blurten, K.F. and Cromer, R.B., Jr., 1976, Performance Characteristics of an Electrochemical Hydrogen Sulfide Analyzer: ISA Transactions, V. 15, 1-7.

41. H_2S Detection an Protection Handbook, 1983, Petroleum Engineer International, Publisher, Box 1589, Dallas, Texas.

42. Sulfur Removal and Recovery from Industrial Processes, 1983, American Chemical Society, Washington, D.C.

43. Amoco's Ultra Process is Successfully Pilot Tested, 1983, Technology, Oct. 31, Oil and Gas Journal, 123-124.

44. Madgavkar, A.M., and Swift, H.E., 1983, Selective Combusting of Hydrogen Sulfide in Carbon Dioxide Injection Gas: U.S. Patent 4,382,912.

Chapter VI

GEOTHERMAL MINERAL RECOVERY

VI. GEOTHERMAL MINERAL RECOVERY

VI-1. Chapter Summary

Compared to cool surface waters, geothermal waters collectively have an enormous range of composition. This is due to the varied geologic terrains they are found in and the large dissolving power of hot water. Additionally, the dissolved substances themselves further increase the dissolving power of water. Bicarbonate ion helps to leach rock components and chloride ions form strong complexes with some elements, stabilizing them in solution, especially at higher temperatures. Rare or unusual elements sometimes occur in thermal fluids, often inviting imaginative speculation about recovering mineral wealth.

Several projects have aimed at minerals recovery and a few have been successful. Criteria for success are many. Assessing the mineral potential for a geothermal resource requires a broad-ranging description of circumstances and requirements of technology, geology, economics, and institutions, features emphasized in this section.

VI-2. Introduction

This description begins with mention of some requirements for recovering mineral wealth, followed by a review of several attempts at minerals recovery from geothermal sites around the world. Evaluation of a specific resource is addressed by using the hypersaline brines of the Imperial Valley of California as an example. In the case of the Imperial Valley brines some useful technical reports are available because of the large number of studies carried out by the federal government. Elsewhere, recovering minerals from brines requires technical approaches tailored specifically for individual sites. Development of such processes is often proprietary.

Beyond the laboratory and pilot plant stage, industrial efforts require detailed designs of full-scale equipment so that cost estimates can be prepared for construction and operation. These lead to economic models for producing commodities that are followed by financial models that forecast the several aspects of capital flow.

All those factors have circumstances that are uniquely geothermal. It is hoped that by presenting them here as a set, aimed at interrelated examples, readers may apply and extend the interplay of factors toward a fuller assessment of their own specific interest.

VI-3. General Concepts

The recovery of minerals from geothermal fluids, as from other media, generally requires simultaneously favorable circumstances for all the several aspects of exploitation, namely:

1. The physical existence of the materials in contexts which can lead to (usually geological) means of forecasting the locations, amounts, and grades of the ore;
2. Accessibility in terms of technology, ownership, and institutional constraints;
3. The existence of technology for recovering and refining a product that can be sold at a profit via;
4. A market; and
5. Access to the market in terms of transportation costs, the existence of a distribution system, and the actions of cartels or free-market competitors.

A serious disadvantage for any single item above can deny the viability of a commercial operation, except that some institutional forces can override modest diseconomies.

Items 1 and 3 above provide a general assessment of a resource base.

Exploitation of a specific resource may be enhanced or made uncompetitive by new technologic developments depending on how Items 2, 3 and 5, are affected with regard to alternative resources. On the other hand, with regard to Items 2, 3 and 5, the geothermal resource provides several novel circumstances which challenge traditional minerals recovery. For example, the presence of thermal energy in the same medium as the mineral resource, invites economies in production by avoiding costs of externally derived energy to run the separation methods. Alternatively, cogeneration of electricity with other products can have economic advantages as well as involving novel approaches to pricing the various outputs.

The latter aspect divides minerals recovery methods into two general categories; those with cogeneration versus those without cogeneration of salable electricity; i.e., multiple use versus single purpose exploitation. The concept of multiple use also has two branches; geothermal energy could be used to obtain minerals from a geothermal or a nongeothermal source.

Examples of quasi-geothermal endeavors include evaporation of seawater to obtain salt[3]. Production of heavy water (deuterium) has been proposed using multiple effect evaporation[3] and using an H_2S/H_2O ion exchange method[4], all merely driven by geothermal heat. Those kinds of developments will not be pursued further. Instead, this review will focus on circumstances wherein the mineral component derives from the geothermal fluid, irrespective of whether or not the thermal energy component is used.

VI-3-1. Early Experience

Recovery of minerals from geothermal resources historically involved local circumstances. For example, the steam fields of Italy were also ex-

ploited for boron compounds, ammonium salts, sulfur, and CO_2[5-6]. The minerals recovery was single purpose. Energy in the steam which contained the minerals was used only to evaporate condensate as a means of concentrating and drying the product. Electricity production from the same fields involved different wells. Since 1971 no borax has been extracted from the Italian geothermal resource as it became more economical to use the steam to refine imported borax[7].

In Iceland, a pilot plant has been built and operated continuously for more than two years with a throughput of two tons of geothermal water per hour (0.5 kg/sec) that has a seawater-like composition[8]. A semi-commercial plant was constructed in 1982 to yield 8,000 to 12,000 tons of salt per year divided among several products. A 40,000 ton per year plant is planned for 1985. Major use of the NaCl will be for curing fish but some production will aim at industrial chemicals, food additives, and household uses. Production of KCl will yield fertilizer and industrial chemicals; calcium chloride for road deicing, drilling, dust prevention, and other industrial and domestic purposes; bromine for industry[9].

In New Zealand, useful calcium silicates were generated as a by-product of environmental control methods aimed at silica and arsenic[10]. A derivative of a general process known as "hot process water softening" was used in which lime is added to precipitate compounds of silica and heavy metals under conditions of controlled pH.

Water is itself a mineral resource of commercial value and several desalination schemes have been proposed[11-12]. Actual tests have occurred in some cases. Results from a pilot plant at Cerro Prieto[13] show that fresh water produced from geothermal water cost about one-tenth as much as water of similar quality produced from alternate sources. However, it appeared that

the electricity which could be produced from the same steam would be even more valuable than the water.

A most ambitious plan was tested by the U.S. Bureau of Reclamation[14-15] to solve water distribution problems that had become politically sensitive. Legal agreements among seven western states had resulted in an over-subscription of the water in the Colorado River[16] such that the remaining flow into Mexico was, in some years less than required by treaty and heavily salt-laden as well. By using self-heat and multiple effect evaporators, desalination of geothermal water was considered for augmenting the river flow. The ultimate use was for crop irrigation, but the driving motive was to provide legally allotted water intra- and internationally. In contrast, desalination schemes mentioned earlier aimed at industrial and domestic uses. In this case, institutional factors promoted the geothermal development of a substantial, but low-value, use of fresh water. The project has been abandoned as technically feasible, but lacking sufficient water reserves to be useful for the purposes of the Bureau of Reclamation.

Most geothermal resources have more economic value for their energy content than for the minerals. Hence, exploitation will tend to forego minerals recovery unless special circumstances enable it to be done without a penalty to the electrical generating capacity. Such circumstances exist at Cerro Prieto, Mexico. Solar evaporation is used there to concentrate residual geothermal liquids, ultimately recovering potash (KCl) for fertilizer[17]. The pilo-scale operation was very successful and ultimate development there is expected to convert Mexico into a net exporter of KCl, whereas before, it imported all of its domestic requirements. In addition, lithium can be recovered from Cerro Prieto brines and arrangements for production and marketing are in advanced stages of development. Similar proposals have been made for New Zealand[18].

Sulfur was recovered from geothermal steam at the Kokonoeyama Sulfur Mining Plant in Japan by channeling natural geothermal gases through long flues[19]. Upon cooling, sulfur of +99% purity would crystallize. The operation produced 2,412 tons in 1904, 2.4 in 1918, 1,540 in 1964, and became uneconomic in 1968. This variability mainly reflects the oscillations of Item 4; the geothermal gases were a stable resource, as was the technology.

In the Hubei Province of China, thermal waters associated with the Jiannan Gas Field have yielded minerals for many years[20]. Recent productions (tons per year) were: NaCl 10,000, boron, 40; ammonia, 29; bromine, 19; aluminum carbonate, 6.

Institutional constraints, Item 2 above, can inadvertently affect the minerals recovery aspect. In The Geysers of California, emission allowances for H_2S are limited by local and state ordinances. Consequently, the H_2S is chemically converted, at a net cost, to a nonvolatile form. The (patented) Stretford process[21], applied there to three of the 22 electric power plants, yields elemental sulfur of high quality and in industrially important amounts [22] but, unfortnuately, to a weak market. Although the sulfur is placed into the industrial sector, its value only partly covers hauling costs, and, in principle at least, depresses the market still further.

The Stretford-equipped plants have an electrical capacity of about 300 megawatts and yield 400 to 500 pounds of sulfur per hour when at full capacity. In this case, minerals recovery (sulfur) partly reduces a diseconomy of operation (H_2S removal) which is implemented solely to make the generating of electricity possible within institutional (environmental) constraints. An alternative method of H_2S control used on most other plants there, and known as the iron catalyst system[23] yields a waste sludge counterpart of the sulfur which contains about 90% water[24]. The sludge has no offsetting

economic value and incurs additional charges when delivered to waste disposal sites. Moreover, the sludge invites other concerns due to the corrosive aspects of the (ferric) iron and the very fact that it is "disposed" of in a land fill.

A similar response to institutional requirements may develop in the Imperial Valley of California where hypersaline brines[25] are being developed for electricity production. Sludges develop from the brine. Mainly they contain silica and must be removed before the brine is disposed of into injection wells. Trace elements zinc, boron, barium and lead cause the sludge to be classified as hazardous and costly requirements are imposed on their disposal.

Removal or even reduction of the toxic elements would yield economies from institutional access to a less costly disposal means. The amount of waste is formidable, a single plant of 50 megawatts would generate about 16 cubic meters of moist sludge per day. Current disposal charges of $\$27.74/m^3$ [26] are applied to the hazardous form. Alternatively, disposal charges of only $\$2.52/m^3$ would apply to toxic-free sludges[27]. The difference, \$400/day, is roughly equivalent to energy revenues from 2.5 megawatts of power, approximately one-half the energy output of a geothermal well.

Only a small fraction of the toxic elements in the brine are tranferred to the sludge. Thus, a minerals recovery program applied to the total brine flow would not only yield substantial tonnages of metals beyond those contained in the sludges but also would accrue any reduced costs for sludge disposal. However, placing the minerals recovery step ahead of sludge removal may be technologically difficult or noneconomic. Perhaps some method could be found either to treat the sludge separately or cause it to form without including the toxic elements.

VI-4. Estimations of Mineral Reserves in Geothermal Brines

Attempts to use geothermal fluids as mineral resources commonly fails because the concentrations of dissolved components are too low to invite serious development. For example, minerals availability calculated for The Geysers, Casa Diablo, and the Bureau of Reclamation wells at East Mesa in the Imperial Valley showed them to be of negligible interest[8]. None of those examples have particularly salty brines. Geopressured brines in Louisiana and Texas are saltier but a review of their mineral potential, presented later, suggests little. However, a remarkable brine occurs in California.

Some of the most spectacular hypersaline brines in the world occur in California's Imperial Valley. From them more than a dozen minerals are potentially recoverable in amounts such that the gross values of the minerals may exceed the energy value of the same fluid. The brines are currently being developed for electrical energy, with only small programs aimed at the mineral components. These brines are so extensive and so concentrated that they dominate the topic of minerals recovery from geothermal fluids in the U.S.

VI-4-1. Reserves Estimate for the Imperial Valley

The brines are best known from about twenty deep wells near the Salton Sea, around which are drawn the formal boundaries of the Salton Sea KGRA, and additional drilling has encountered similar brines many miles away. The "possible" reserves underlie several hundred square miles, and, though deep, they can be reached by conventional geothermal drilling. An additional favorable circumstance involves the applicability of solar evaporation of brine residues as an intermediate step in minerals recovery following the example at Cerro Prieto[28].

Two methods are available for estimating the magnitude of the minerals resource of a geothermal setting. The classical geological method aims at

identifying a volume of rock which contains the resource; finding some way to establish the average grade (mineral content) of that rock; and forecasting a fraction of the volume that could be trapped or removed by current, or anticipated, technology. Each step in that method yields numerical values (or ranges) so that the overall estimate of recoverability is simply a multiplication product of the several numerical values.

The second method derives from estimates or forecasts of electrical energy production, using the implied fluids as an "ore volume" component. These estimates involve some nongeological factors[29]. Hydrologic factors, politics and energy-company forecasts of energy demands are involved, placing qualitatively different kinds of uncertainties into the estimates of mineral resources.

In a similar way as before, the overall availability of the mineal component is given by the multiplication product of several terms. The two methods are not wholly independent since some rock-volume considerations are commonly invoked when forecasting the electrical capacity of a field.

The second method yields a rate at which reserves can be made available whereas the first method identifies the total amount available. In estimating the mineral reserves of the Imperial Valley, the electrical approach will be applied first.

VI-4-2. Rate of Production

The rate that mineral reserves can be delivered can be based on the electrical generating rate and the brine composition according to Equation VI-1:

$$q = (P)(h)(s)(1/f)(e)(k) \qquad \text{(VI-1)}$$

In equation VI-1, the quantity (q) of a mineral that is recoverable per megawatt year of power generation is given as the continuous product of the power output (P) in megawatts, the hours (h) of operation per year, the rate of steam supply(s) required in a flash system per megawatt of power output, the amount of brine (1/f) associated with a unit amount of steam where f = the weight fraction of the produced fluid that flashes to steam, the extractable concentration increment (e) of the element of interest, and a factor (k) to adjust dimensional units and/or convert mass of the dissolved form (indicated by chemical analysis of brine) to the equivalent mass of an industrial chemical form.

The results of working out (a) are that each ppm of mineral (element) recovered from a brine would amount to a recovery of 400 kg per megawatt-year [30].

For example, manganese is present in hypersaline brines at concentrations that average near 1,200 ppm before steam flashing. A 50-megawatt electrical plant that could recover 80 percent of that manganese would generate about 31 million kg of MnO_2 per year. That amount would be worth between $6.0 and $16 million, depending on where the quality of the actual product fitted into existing patterns of use. That dollar value represents an amount equal to 30 percent or more of the electrical values from the same plant. The tonnage amount represents about 1.8 percent of the 1971-1975 average annual U.S. consumption of manganese[31]. Full development of the Imperial Valley's hypersaline brines is forecast to exceed 1,400 megawatts[32]. At that time, the associated manganese could potentially satisfy about half of U.S. needs.

The potential outputs for several elements contained in the hypersaline brines are listed in Table VI-1 on the basis of a 50 megawatt electrical plant and a mid-range composition of the several brine analyses available[33-34] and

TABLE VI-1.

Potential Recovery Rates of Minerals from Hypersaline Brine
Based of Fluid Through-put of a 50 Mwe Power Plant

Element	Conc. ppm/wt	Industrial Form	Recovery Efficiency	Tons/Year Recoverable	$/Ton	Gross Value $ Millions/yr	
Sodium	57100	NaCl	0.9	2880000	50	144	(e)
Calcium	25700	$CaCl_2$(a)	0.8	3300000	32	106	(e)
Potassium	14700	KCl (b)	0.8	494000	60	30	(e)
Iron	1770	$Fe(OH)_3.2H_2O$	0.9	79000	120	9.5	(e)
Manganese	1230	MnO_2	0.8	34300	175	6	(f)
Zinc	715	Zn	0.8	12600	450	5.7	
Strontium	620	$SrSO_4$ (c)	0.4	11600	640	7.4	(e)
Barium	550	$BaSO_4$	0.9	10900	100	1.1	
Boron	365	H_3BO_3	0.05	2300	550	1.3	(e)
Lithium	283	Li_2CO_3	0.6	400	2800	1.12	
Lead	114	Pb	0.95	2400	300	0.72	
Bromine	29	Br_2	0.1	64	600	0.038	
Copper	2.4	Cu	0.5	26	1300	0.034	
Silver	0.09	Ag	0.5	9.9	250000(d)	2.5	
Electricity			0.8		(g)	21	

(a) 38% liquid

(b) fertilizer grade

(c) Requires conversion to $SrCO_3$

(d) $9 per Troy ounce

(e) inadequate market

(f) unknown marketabilily

(g) $.060 per kwh

other proprietary data[35]. Unfortunately, the technologies for recovering most of the listed components have not been demonstrated, nor even well developed, yet[34].

Mineral reserves associated with the full 1,400 megawatt development of the Salton Sea geothermal brines might be estimated in a crude way by simply multiplying the table values by 28, the equivalent number of 50-megawatt plants implied by the full 1,400 megawatt development. However, the markets for commodities like $CaCl_2$ and NaCl and lithium could not be sustained with full exploitation. Furthermore, it would be unlikely that land requirements for evaporation ponds could be met in full if they conflicted strongly with traditional agricultural uses.

VI-4-3. Ultimate Reserves

The volume of reserves can be estimated if the boundaries of the in-place resource can be defined along with the overall porosity[35].

The gross reserves can be calculated by equations similar to VI-2:

$$Q = (A)(t)(p)(e)(k) \qquad \text{(VI-2)}$$

Where the quantity (Q) of a material present in the resource is given as a continuous product of the gorund surface area (A) which overlies the resource, the average or integrated thickness (t) of the rock zone which contains the resource, the porosity fraction (p) of the rock, the extractable concentration increment (e) of the element of interest and a factor (k) to make adjustments among conventional units of measure.

Compared to equation VI-1, (e) and (k) are the same whereas q is the annual rate that Q can be tapped. Q represents a depletable resource that has a definite initial size. However, estimates for the magnitude of Q are uncertain due to uncertainties in determining values for the first four terms. The

first three terms, A, t, and p are subject to geologic interpretation and the limits of drilling results. The fourth, (e) depends on the technology of treating brines, including future improvements thereof.

For the Salton Sea field, as originally defined, volumetric estimates of total recoverable brine ($9x10^{12}$ kg) have been made[38]. This estimate was based on several presumptions, some of them guided by data from ten drilled wells. Specifically, it was inferred that a 1,000-ft (307 m) thick production zone no deeper than 5,000 ft (1,520 m) extended throughout 307 km^2 (118 sq. miles) of area. The boundaries were based jointly on temperature gradients [39] and on aeromagnetic data[40]. The derived area is larger than the 18 square miles contained within the formal boundaries of the KGRA, but smaller than more recent data would indicate. Additional assumptions included: a matrix porosity of 20 percent in the sands of the rocks; 59 percent sand, per producing section; and 80 percent efficiency for drainage of fluid into wells. Some additional useful data are now available[41].

Younker and Kasameyer[42] used a novel correlation between temperature gradients and the magnetic anomaly to obtain an area of 124 square km for the Salton Sea KGRA. The thickness chosen was 1-2 km and their estimate of gross rock volumes was 182 cubic km. No assignment of porosity was made which is required to obtain an estimate of liquid volume. However, if a porosity of 10 percent is used, the Younker and Kasameyer estimate is about twice as large as Towse's[38].

Subsequent data require modifying these estimates to account for deeper production, fracture permeability, and the greater geographic extent of the hypersaline brines that was perceived earlier.

The geographic distribution of hypersaline brines goes far beyond the original boundaries of the Salton Sea KGRA (Figure VI-1). Several wells

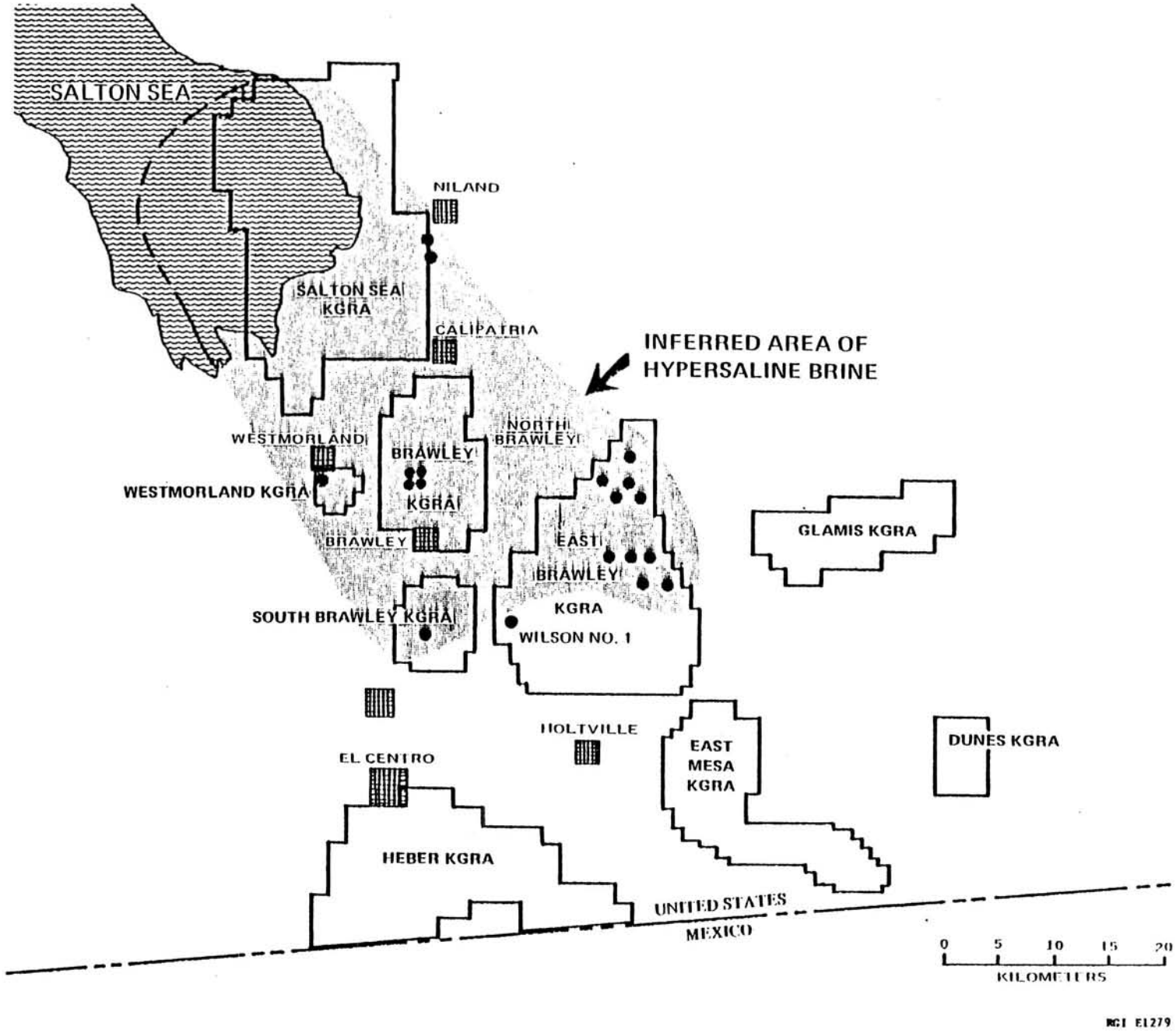

Figure VI-1. Hypersaline wells outside the Salton Sea KGRA and the extent of the Hypersaline Resource.

drilled since 1979 have encountered hypersaline brines at depths between 8,000 and 14,000 ft (2,500 to 4,500 meters). These include some newer fields locally designated as Brawley, East Brawley, South Brawley, Westmorland, and Niland. These occurrences describe an approximately rectangular area about 16 miles (25 km) wide and 25 miles (40 km) long, extending southeastward from the edge of the Salton Sea. The 400 square miles (1,000 km^2) contained therein does not include areas to the northwest of the southeast shore of the Salton Sea. An equally large zone is indicated to lie there mainly beneath the Salton Sea, and is indicated by the anomalies of temperature gradients and geophysical data[42].

The brine is contained within the pore structure of some of the rocks in that area. Some data are available to limit speculation about which rocks are involved and what the pore structure is like. Rock porosity is an uncertain factor. Sedimentary rocks in the Imperial Valley, as elsewhere, lose most of their matrix porosity during early stages of metamorphism[43], specifically at temperatures above 150°C[44]. Porosity is partly regained in the form of fractures as the metamorphic grade increases, making the rock more brittle, and as geologic forces operate, in episodic ways related to faulting and crustal spreading.

The average porosity of rocks in the hypersaline zone is problematic because the zone includes the transition between dominance of matrix porosity in shallower regions and fracture porosity at depth. The matrix porosity in producible sands may be on the order of 20 percent in unmetamorphosed places, but metamorphism reduces the matrix porosity toward values of 5± percent of the rock volume[45]. Fracturing increases the gross porosity in addition to making drainage possible from some of the matrix porosity. For the deep hypersaline brines the fractures are important for both volumetric storage and as conduits for fluid movement.

Perhaps the most definitive summary about the gradation of porosity with depth besides data in Ref. 43 appears in testimony regarding environmental impact of geothermal development[47].

In reference to a leasehold near the community of Niland, "All production is from fracture zones or individual fractures. Schlumberger logs (neutron, sonic, density) show a steady decrease in porosity and permeability from 15%± at 4,500 ft to about 10% at 8,000 ft and 6-8% from 8,000-10,000 ft in these wells."

Testimony continued, noting that hypersaline production was obtained from (similar) fractures at the following fields and depths: Brawley, 5,500 to 8,000 ft deep; East Brawley, 10,000 to 13,000; South Brawley, 10,000 to 14,000; and south of Westmorland, 8,000 to 10,000.

The profile of depth versus porosity applies best to the areas of thermal anomalies. For the cooler spaces in between, the metamorphic grade of the rock will be less (at similar depths) and the residual porosity will be greater. Thus, the overall porosity of rocks in the hypersaline zone will not be the minimum described in the hearings, but rather larger. Accordingly, a value of 12% is chosen for the overall total porosity (matrix plus fracture).

To complete this volumetric calculation, an estimate of the thickness of the hypersaline zone is required. Currently, there is little evidence to identify how thick the zone of hypersaline liquid may be, no parties appear to claim having drilled completely through it. However, it is clear that the upper boundary of the zone is significantly deeper beyond the formal boundaries of the Salton Sea KGRA. The position of the upper boundary may provide a basis to estimate the thickness.

Although a linear increase in salinity with increasing depth in the Salton Sea KGRA has been inferred[48], other data[49] suggest that a definite

interface exists. Such an interface would become an isopotential surface if the geologic circumstances permitted free lateral movement of the fluids and if the basin were stable enough for the liquids to find their isopotential positions in the gravity field. The topography of the interface would then reflect the joint effects due to thickness of and temperature gradients and salinity gradients within the hypersaline zone. This approach toward deducing the probable thickness has not been developed, apparently.

Preliminary attempts to apply it for this report suggest that depth may be tens of times greater than the topographic relief of the interface. The amount of relief appears to exceed 1,000 meters, hence the thickness would appear to be tens of thousands of meters. These great depths match estimates about how plate tectonics concepts apply to the Imperial Valley[50].

For the present, a thickness estimate of the brine zone will involve an arbitrarily defined bottom rather than one based on direct observation or on geologic inference. A thickness of 1,000 meters is selected. This value has several attributes including numerical roundness, implications for drilling and well completion that can be achieved with current technology, and temperature/pressure implications for the rocks which make plausible the presumptions of open, brine-filled fractures, in conformance with the estimate of overall porosity, described earlier.

The completed estimate for the volume of hypersaline brines in place involves 1,000 km^2 of area, 1 km of thickness and 0.12 porosity fraction; in all, 120 cubic kilometers of hypersaline brine appear to be present southeast of the Salton Sea. Density of the fluids, in place, is close to 1 kg per liter, or slightly greater[51]. Thus, the estimate of mass for brine in place is 1.2×10^{11} metric tons.

This is more than twelve times the Towse estimate[38] of brine hot enough to be used for generating electricity, 260±°C. All of the larger volume of

brine will be at least moderately hot, because it lies at substantial depth in a region of relatively high heat flow. For example, a thermal gradient of only 40°C/km will yield temperatures of 185°C at 4 km (13,000 ft). Thus, in all cases, the hypersaline brines will be thermally interesting, if not of electrical quality.

The tonnages of minerals in place can be estimated by introducing brine composition. The overall averages and other statistical data are shown in Table VI-2. The values in Table VI-2 are obtained by combining the analytical results from wells in the several subfields mentioned earlier. Some of the data are from published results for the main Salton Sea KGRA[33], the remainder are partly proprietary data[35]. The range of data values for individual components is fairly large such that the overall average concentrations may be given more accurately by the geometric average of the subfields rather than the arithmetic. However, the patterns of relative abundancies in the several subfields are quite similar. It is this latter aspect that suggests the resource is a single continuous unit. Not all available data was used in constructing Table VI-2. Instead, representative wells were selected from each subfield. Not all elements have been analyzed for in all subfields, a feature noted in the table.

VI-4-4. Quality of the Estimates

The technical quality of this estimate deserves scrutiny. The mineral industries have formalized several categories of "quality" that are commonly presented as a McKelvey Diagram[52].

The geologic assurity of the Imperial Valley resource, as described above, is divided among the categories "Demonstrated-Indicated" and "Identified-Inferred" (Figure VI-2). A higher ranking cannot be supported due to too few data on porosity and thickness in the vicinity of actual wells. Further-

TABLE VI-2.

NOMINAL CONCENTRATIONS IN HYPERSALINE BRINES
FROM THE IMPERIAL VALLEY [32], [33]

Key

n	Number of wells in average
$\bar{x}$	Arithmetic average
s	Standard deviation
$\bar{x}_g$	Geometric average
s_g	Geometric standard deviation

The gross resource contains 1.2 x 10" metric tons of brine

H																	He
7 Li 304 125 283 1.49	Be											6 B 379 121 364 1.37	C	2 NH_4 N 426 23 425 1.06	O	1 F 18	Ne
7 Na 57929 11316 57069 1.20	7 Mg 742 870 275 7.1											Al	Si	P	S	7 Cl 160000 32200 157200 1.22	Ar
7 K 15400 5280 14680 1.39	7 Ca 27460 9820 25690 1.52	Sc	2 Ti .15 .16 .10 3.8	1 V 6	1 Cr 1.4	6 Mn 1280 339 1230 1.40	7 Fe 2054 1416 1770 1.74	1 Co 1.5	Ni	4 Cu 3.8 3.2 2.4 4.0	6 Zn 765 345 715 1.47	Ga	Ge	As	Se	3 Br 51 60 29 3.9	Kr
2 Rb 104 47 98 1.61	5 Sr 752 619 619 1.88	Y	Zr	Nb	Mo	Tc	Ru	Rh	Pd	2 Ag .90 .14 .89 1.17	2 Cd .8 1.13 .09 59	In	Sn	Sb	Te	2 I 15.5 3.5 15.3 1.26	Xe
2 Cs 18 2.83 18 1.17	6 Ba 814 861 546 2.56	*	Hf	Ta	W	Re	Os	Ir	Pt	Au	1 Hg .006	1 Tl 1.5	6 Pb 131 84 114 1.71	Bi	Po	At	Rn
Fr	Ra	Ac	Th	Pa	U	Np	Pu										
		*	1 La 4.4	Ce	Pr	Nd	Pm	Sm	Eu	Gd	Tb	Dy	Ho	Er	Tm	Yb	Lu

La - Lu

RGI E1237

Form set for 12 pitch.

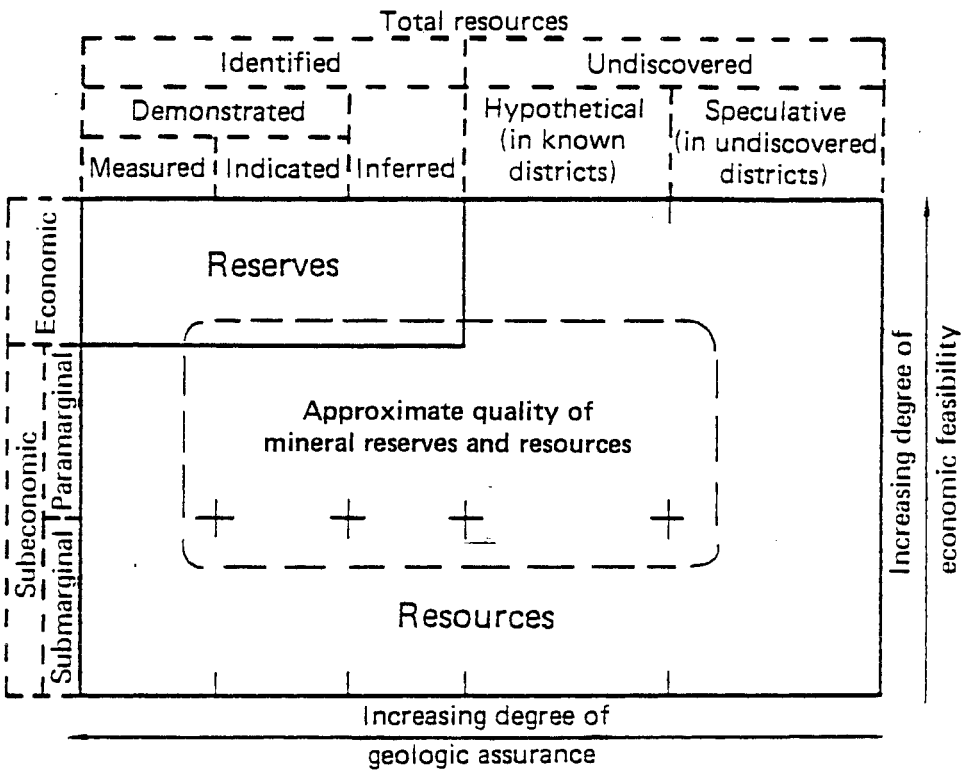

Figure VI-2. McKelvey Diagram for Imperial Valley Hypersalines (From Ref. 52).

more, no data exist to support the inference of metal-rich brines between demonstrated hot places. Significantly, one deep well (the Wilson No. 1; see Refs. 47 and 53) located approximately midway between the East Brawley and South Brawley fields was not hypersaline, suggesting a southern limit to the hypersaline resource. This limit is considered in the estimate above.

The economic quality is poorly defined because demonstrated recovery processes do not currently exist. Furthermore, there is uncertainty about how a minerals recovery operation fits into the economic circumstances of a multi-purpose plant which generates electricity. Thus, the economic feasibility cannot now be ranked as "economic" in the McKelvey diagram. However, the mineral values are substantial and some research on recovery processes, described in the next section, show considerable promise. Thus "paramarginal", appears to be an appropriate ranking for economic feasibility.

VI-5. Minerals in Geopressure Brines -- A Nonresource

Another category of geothermal resources that can be considered as a class are the geopressured zones in Louisiana and East Texas. Bottomhole depths range from 9,700 to 16,000 ft. Wellhead pressures range from 2,500 to 6,700 psi; temperatures are generally below 300°F, bottomhole. Dissolved minerals range from 13,000 to 160,000 ppm. These resources are most significant for their natural gas content. Plans for exploitation generally aim at recovering the methane and related gases without recovering the sensible heat from the associated brines. Despite that, geopressure resources have been lumped with the typically geothermal for purposes of national planning.

Evaluations of their minerals resources potential is presented here as an instructive exercise. The geopressure brines appear to exist in several unconnected fields, thus estimating their collective volumes has serious uncertainties. The approach used here is based on published estimates of

methane reserves, measurements of gas-to-brine ratios, and analyses of available brines.

The geopressure reserves of recoverable methane are estimated to be from 7 trillion cubic feet (TCF) to 5,000 TCF with some intermediate estimates [54-55]. Compositions for seven geopressured wells in different fields have gas/brine ratios that average 35 ± 13 standard cubic feet per barrel. The average gas composition is 84 ± 6 mole percent methane[56]. Applying those compositions to the estimates of methane imply that recoverable geopressure brine is from $4x10^{10}$ to $2.8x10^{13}$ metric tons. In relative magnitude this range is from something slightly smaller than the Imperial Valley brine volume to something considerably larger.

In terms of minerals, the geopressured brines appear to offer very little. Table VI-3 lists brine compositions for seven wells[56]. The great variability among them makes impossible the assignment of reasonable average concentrations for dissolved salt components, as was done for the methane. This variability conforms to the discontinuous nature of the geopressure occurrences, and stands in important contrast to the inferred continuity of the Imperial Valley hypersaline resource.

Importantly, the geopressure brines appear universally low in base metals (lead, zinc, manganese, copper, iron) compared to the hypersaline brines of the Imperial Valley. The elements sodium, potassium, and calcium, commonly removed as chlorides would appear unrecoverable from geopressure brines because the local climate makes evaporation ponds inoperable, unless freeze-crystallization methods could be applied[57].

Perhaps strontium, an element already in surplus supply, could be the only candidate for minerals recovery among the listed components[58]. The strontium market currently is small. Beyond their energy content due to flammable gas, geopressure resources have no significant mineral values.

Table VI-3. Composition of Geopressured-Geothermal Brine (From Ref. 56).

Well Code*	FFS-2	PB-2	BS-2	PC-1	WG-1	LK-1	RS-2
Dissolved Salts(ppm)							
Total	156200	129000	90300	42000	23740	14700	12900
Cl	96100	76800	53200	24100	12600	7280	6390
HCO_3		300		890	1910	2440	1835
SO_4	5	5	676	173	650	42	30
F	0.69	1.1	.85	1.5	2.7	3	2.2
Na	49300	37900	30400	14400	8740	5330	4860
Ca	7560	8990	29500	850	86	40	51
Mg	660	640	264	80	15	5.3	6.8
K	816	595	530	112	48	74	31
Fe	50	60	68	72	.54	2.4	19
Mn	16	22	4	1	.07	.11	.36
Zn	1	.8	.2	.1	.3	.12	.22
Sr	602	1010	262	80	16	7.4	6.4
Ba	165	730	10	15	.1	20	15
B	49	31	75	100+	74	43	88
Pb	.05	.2	.2	.2	.2	.2	.2
Cu	.3	.2	.2	.03	.02	.1	.04
Cd	.2	.2	.3		.03	.2	.1
NH_4		85	30	27	7.5	7.8	20
SiO_2	89	124	102	136	122	121	142
Dissolved Gases (Mole%)							
CH_4	88.7	83	89	84.7	91.4	79.5	73.6
C_2H_6	1.9	3.2	2	2.7	1.8	4.9	2.5
H_2	.15	.02	.4	.3	.5	.1	
CO_2	8.4	11.3	7	11.7	5.8	7.2	22.9
N_2	.4	.4	.4	nil	nil	nil	.2
H_2S				13ppm			60ppm
Gas/Water Ratio, ft^3/bbl	22.3	27.2	20.3	48	40	30-318	47-54
Bottomhole Temp. °F	270	306	266	294	274	260	300
Perf Zone, ft	15800	14700	14700	14800	14800	11700	9800

*Code: FFS-2 Fairfax-Foster-Sutter No. 2, Louisiana
PB-2 Pleasant Bayou No. 2, Texas
BS-2 Beulah-Simon No. 2, Louisiana
PC-1 Prarie Canal No. 1, Louisiana
WG-1 Wainoco-Girouard No. 1, Louisiana
LK-1 Lear-Koelemay No. 1, Texas
RS-2 Riddle-Saldana No. 2, Texas

VI-6. Minerals Recovery Processes for Imperial Valley Brines

The minerals potential of the Imperial Valley brines was recognized early and attempts for recovery were made by Union Oil Co., Shell Oil Co., Chevron Oil Co., and Morton International Research Co.[8]. Some of the efforts advanced to pilot plant stage[59]. Commercial production was never attempted, but not entirely for reasons of chemical problems. For example, start-up of large potash operations in Saskatchewan in the early 1960's, appeared to make Imperial Valley KCl uncompetitive on world markets. The local fertilizer market could not be captured because it uses K_2SO_4. The chloride form is mildly detrimental to the foliage of citrus trees. The heavy metal potential of the resource is described in Refs. 60-62. Commercial CO_2 production from fields along the southeastern shore of the Salton Sea is described in Refs. 63 and 64.

Details of the attempts at mineral recovery by commercial interests are not reported in detail. However, the U.S. Bureau of Mines supported several studies in the 1960's and 1970's which identify some possible approaches to recovery[65-71]. Unfortunately, the work has slowed to a report writing stage and the reports are not widely known.

The first chemical work on brines was done in laboratories, using spent brine, from several wells, that was cool and stale, and therefore different from what a field operation would encounter. Enough preliminary information was obtained to design a pilot plant and make preliminary technical and economic assessments. One Bureau of Mines pilot plant was built and operated at the Salton Sea GLEF, utilizing fluid from Magmamax No. 1 for three months in 1979. A short report of results is now available[72].

The Office of Saline Water also sponsored some research on minerals recovery, some of which appears to have relevance to the geothermal resource.

However, it will not be reviewed here because most of it applies to waters that are rich in sulfate and low in economically valuable constituents.

VI-6-1. Preliminary Considerations

Because the hypersaline brines are so complex chemically, and because they are so reactive when fresh, minerals recovery processes will have to cope with many problems that are generally absent in other circumstances that might appear superficially similar.

The chemical instability of the freshly produced brines is mainly due to the severe temperature change which occurs as the fluid rises, with continuous flashing of new steam, up the wellbore and through process equipment. Technology for pumping these brines, 200-260°C, without flashing does not exist and formation productivities are not high enough to justify pumping. Flashing flow on the other hand, yields very large pressure drawdowns and commercially attractive well flow rates. With the flashing there is a concommitant increase in concentration of (residual) dissolved salts. That effect on solubility, about 20 to 25 percent, is small compared to the effect of the 100 to 170°C temperature change which occurs in 5 to 40 minutes depending on well depth and discharge rate.

Industrially, the uncontrolled formation of scale in the wellhead and nearby equipment presents an intolerable situation. Methods of scale prevention are therefore obligatory (for example, see Chapters 3 and 4). These may involve injection of chemicals that cause the scale-forming materials to yield a sludge that passes on with the brine rather than hard scales that build up on pipes and valves[73]. Eventually, the sludge must be separated from the liquid before it is passed on to a minerals recovery process and/or disposed of by injection.

If the minerals recovery process begins after the silica-rich sludge has been removed, then it must be adapted to temperatures near 90°C and be immune to the presence of residual silica and other materials that tend to deposit spontaneously. The sludge should not carry away significant amounts of components aimed for in the minerals recovery scheme applied to the brine, nor can the recovery process be sensitive to residual additives used to control scale upstream.

These brines are so complex that they may never be processed for a single commodity. There would always be a temptation to convert a stream of waste into a salable product. The likelihood seems good for finding a modified process that takes advantage of the marginal economics involved with converting an earlier-planned waste stream to a product stream. Such comprehensive recovery operations are difficult to set up and are complicated to maintain since perturbations can propagate both up and downstream. They have been considered, however, and some details are reviewed below.

Minerals recovery processes will complement, but not substitute for scale and sludge control methods. Controls for sludge and scale, per se, have been attempted and reported broadly. Comprehensive reviews are available in Chapter 3 of this report and in Ref. 74. Minerals recovery methods are less common than scale-control efforts and more highly specialized, in comparison.

VI-6-2. Chemical Process Studies

The following review will emphasize results from studies funded by the U.S. Bureau of Mines and aimed at the Imperial Valley hypersaline brines. The work was done by Hazen Research, Inc., of Golden, Colorado[68]; SRI International, Stanford, California[65]; and DSS Engineers, Ft. Lauderdale, Florida [57]. These earlier studies provided sufficient background for the development of an integrated approach to mineral recovery from hypersaline brines

involving the process of cementation[75]. A tabulation of the potential mineral values recoverable from a typical hypersaline geothermal brine from the Salton Sea Geothermal Field are summarized in Table IV-4. These estimates are based on a 1000 MWe power production facility assuming 90% recovery of mineral values and a plant downtime of 25%.

VI-6-2a. Sulfidation Process - Preliminary studies aimed solely at recovering heavy metals (mainly lead and zinc), by precipitation with sulfide were made by SRI[65]. Coprecipitation includes silver, which is desirable, and iron and manganese, which are not. A single electrolysis experiment was reported.

The SRI work involved computer modeling and experimental runs on 250 ml batches of brine from Magmamax No. 1 and Woolsey No. 1, two of the less salty of the hypersaline wells. Additionally, they made experimental runs on 12 liter batches of brine from IID No. 2, one of the more salty of the hypersaline wells. However, the SRI analyses for Pb, Zn, Fe, and Mn showed similar concentrations in each of the three lots of brine used by them and these were generally different from the data in other literature. Thus, questions arise about what the experimental brine represents, beyond the laboratory results. SRI also made some continuous mixing and discharge experiments with brine from IID No. 2, using brine-filled 50 gallon drums as sources of material, mixing with regents, and settling and thickening the sludges (Figure VI-3).

The brines used by SRI had been stored. That from IID No. 2 was at least four years old at the time experiments were run. All the brines had apparently aged since the pH's (reported by SRI) were 2 to 4 units more acid than are reported for fresh brine from the respective wells. The as-received brines had pH's of 2.3 to 3.5.

Preliminary thermodynamic modeling suggested that separation of Pb, Zn, and Ag from Fe and Mn by sulfidation would occur best at a moderately acid pH.

Table VI-4.

Potential minerals recovery from a 1000-MWe geothermal power-minerals recovery plant in the Salton Sea (From Ref. 75).

Element	Potential minerals recovery (thousand metric tons/yr) Magmamax 1	Sinclair 4	U.S. consumption 1980 estimates (thousand metric tons[3])	Possible plant product and market value[26,27] (10/30/81)	Market value of possible plant product ($million/yr) Magmamax 1	Sinclair 4
SiO_2	53	135	–	Amorphous drying grade 93%, $31/ton	1.8	4.6
NH_3	12	117	15 800	Aqueous 29.4% anhydrous basis, $210/ton	2.7	27.1
Li	31	65	4.7[d]	Li_2CO_3, $1.41/lb	(511)[a]	(1 075)[a]
Mn	150	335	1 061	Ferromanganese 78%, 0.1% C, $0.685/lb	290	648
Fe	112 (79)[b]	346 (272)[b]	69 400	Black, magnetic iron oxide, $0.25/lb	28	97
Cu	0.2	0.8	3 902	Metal, $0.745/lb	–	–
Zn	60	133	920	Metal, $0.462/lb	61	135
Sn	6	–	53	Metal, $6.86/lb	90	–
Pb	18.6	24	1 100	Metal, $0.36/lb	14.8	19
Se	1.6	0.7	0.4	Metal, $3.80/lb	13.4	6
Subtotal					502	938
Ag[c]	4.2	4.2	99	Metal, $9.08/troy oz	38	38
Au[c]	0.8	0.8	3.0	Metal, $426/troy oz	341	341
Pt[c]	0.5	0.5	2.2[d]	Metal, $412/troy oz	206	206
Total					1 087	1 523

[a]Elasticity of lithium market not known.

[b]Iron in excess of that needed for 78% ferromanganese production.

[c]Precious metals production in million troy ounces (31.104 g).

[d]Total consumption, platinum-group metals.

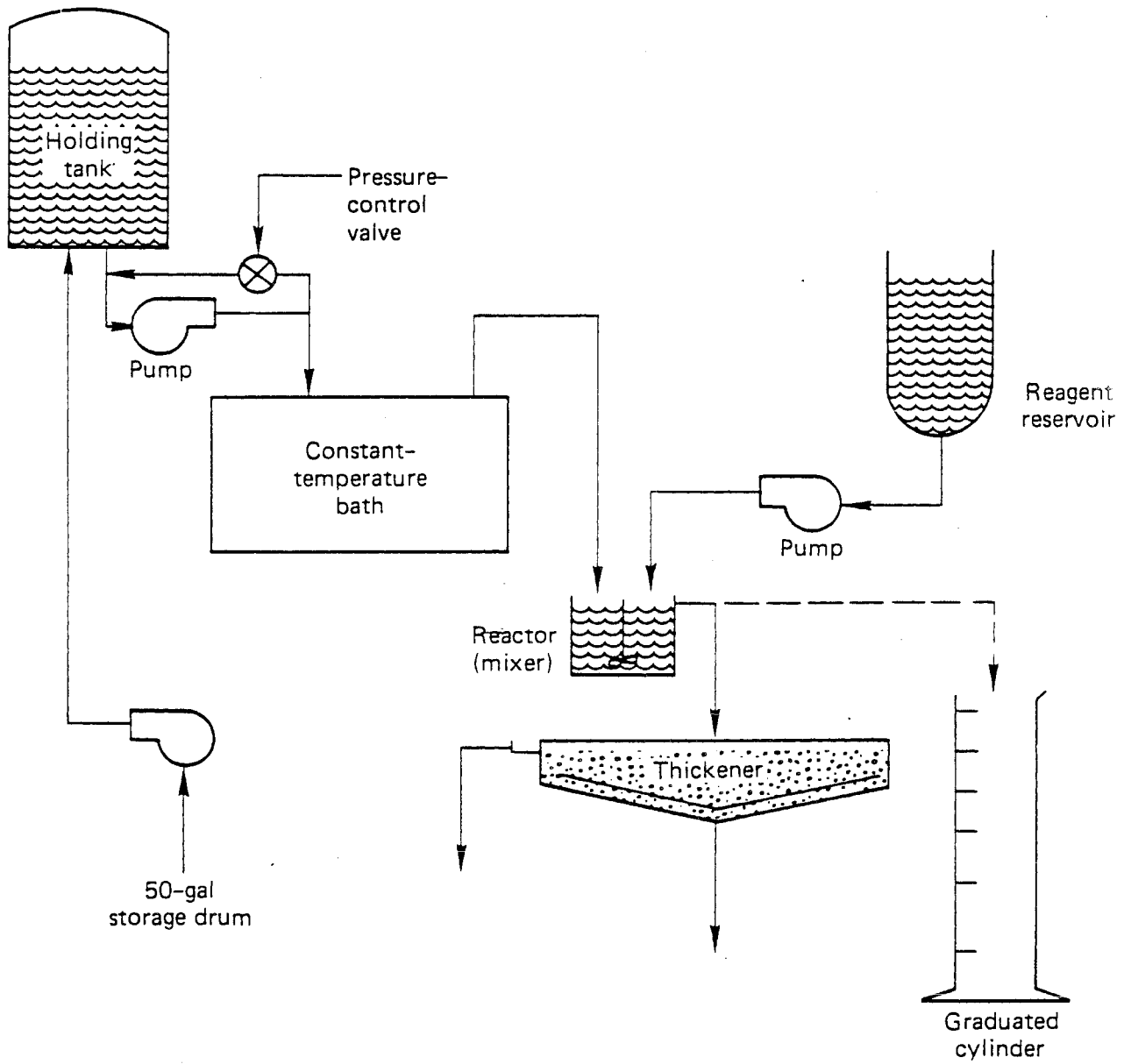

Figure VI-3. SRI International Field continuous sulfidation apparatus (From Ref. 65).

Accordingly, 250 ml batch-type experimental runs were begun at pH 3 and 1 atm. of H_2S pressure. Efficiencies for precipitation were low for Zn at room temperature, lower still (~50%) at 100°C. However, very little Fe and Mn were precipitated. Poor efficiency was partly due to increased acidity (to pH~2) resulting from reaction VI-3.

$$H_2S + M^{++} \rightarrow MS + 2H^+ \qquad \text{(VI-3)}$$

Experiments at higher pH were made by using an excess of Na_2S instead of H_2S compared to Pb + Zn. The pH rises significantly due to reaction VI-4.

$$Na_2S + H_2O \rightarrow 2Na^+ + OH^- + HS^- \qquad \text{(VI-4)}$$

At pH 6, the coprecipitations of Fe and Mn are small compared to their availability in brine, but are significant in regard to the composition of the final bulk precipitate.

The continuous sulfidation experiments involved brine temperatures of 80-90°C, without pH control:

> Mixing was done by injecting Na_2S through a needle into a Y-tubing of 4 mm inside diameter and a liquid speed of 30 cm/sec. Mixing appeared to be complete in about 1.5 cm (50 milliseconds), as indicated by the uniformity of density and dispersion of the newly-formed black solids.

Progressive plugging of the Y-tubing occurred as a cone of black material developed at the needle orifice. Subsequently, small in-line reactors of various volumes were used. Residence times in these ranged from 3.2 to 32 seconds without any variations in recovery efficiency, even compared to the Y-tubing reactor.

The precipitation produced flocs of 1 to 2 mm size that settled rapidly without appreciable effects by either cationic or anionic flocculants. Floc

size was not affected by residence time in the reactors. Recycling part of the sludge through the reactor apparatus yielded flocs that settled fster, but ultimate settled densities of the pulp (2.3 percent solids) were unaffected.

Settling speeds were measured and used[76] to obtain an estimate of the area of a thickener required to function with industrial-scale quantities. The result was 145 sq. ft. per ton of solids per day. Since the amount of precipitate was about 900 ppm, one can calculate that a liquid rate of 100,000 lb/hr, approximately enough to generate one megawatt of electrical power, would require 157 sq. ft. of thickener. A 50 MW plant would require a thickener 100 feet in diameter if all the brine were to be processed. Such a thickener would need to covered and insulated to prevent convection currents from disrupting the settling process.

X-ray studies of the sludge indicated that PbS and ZnS were crystalline, but the FeS and MnS were amorphous. Acid-insoluble silica precipitated in increasingly larger amounts at higher doses of sulfide, and comprised 40 to 50 percent of the solids. Overall, this sulfidation approach shows some promise, but requires much more development to improve specificity and setting rates. It should also be preceded with a silica removal step.

An inverse application of the sulfidation reactions are potentially useful as methods for abating H_2S emissions[66].

VI-6-2b. Hydroxide Precipitation Process and Follow-On Steps - Hazen Research, Inc. worked with brines from Sinclair No. 4 and Magammax No. 1 wells, both of which are among the more salty of the hypersaline brines. They attempted a comprehensive recovery scheme using Sinclair No. 4 brine[68]. It began with the removal of iron by air-sparge oxidation and precipitation as a hydroxide with pH values below neutral. Subsequently the pH was raised to 8.7 with a lime slurry in order to precipitate manganese, zinc and lead.

Thereafter, lithium was precipitated as a hydrated lithium aluminate by adding aluminum hydroxide. Removal of barium and strontium, as sulfates, was attempted next followed by evaporation to obtain sodium and potassium chlorides. The residual liquor contains calcium chloride in approximately a marketable form.

Those results were extended into a preliminary strategy for recovering minerals[69]. Additional suggestions involve the recovery of ammonia (at the step of lime addition) and recovery of bromine after recovery of potash. This report is augmented with useful summaries about mineral commodities as well as additional experimental data and interpretations. It is an excellent primer on the minerals potential of hypersaline brines.

A more advanced version of the Hazen flow scheme was developed later for Magmamax No. 1[70]. A flow sheet from that report is reproduced as Figure 6-3. Importantly, it begins with the sequential removal of silica and iron, which are the primary interferences in the recovery of desirable materials, and ends without recovery of sodium, potassium or calcium. That work formed the basis for engineering designs of two pilot plants. One[71] uses the process of Figure VI-4. The other[77] uses a simpler process in which all the heavy metals are taken in a bulk precipitation step following silica removal, and no other materials are recovered before disposal of the residual liquid by subsurface injection. The process flow sheets keyed to numbered call-outs in Figure VI-4 are summarized in Table VI-5.

Complete details of this series of reports cannot all be reviewed here, but some of the more interesting results are reviewed here.

Removal of iron from Sinclair No. 4 brine was helped by the formation of a magnetic precipitate which coagulates quickly into a relatively dense matt. However, the Magmamax brine yielded only a nonmagnetic counterpart. Develop-

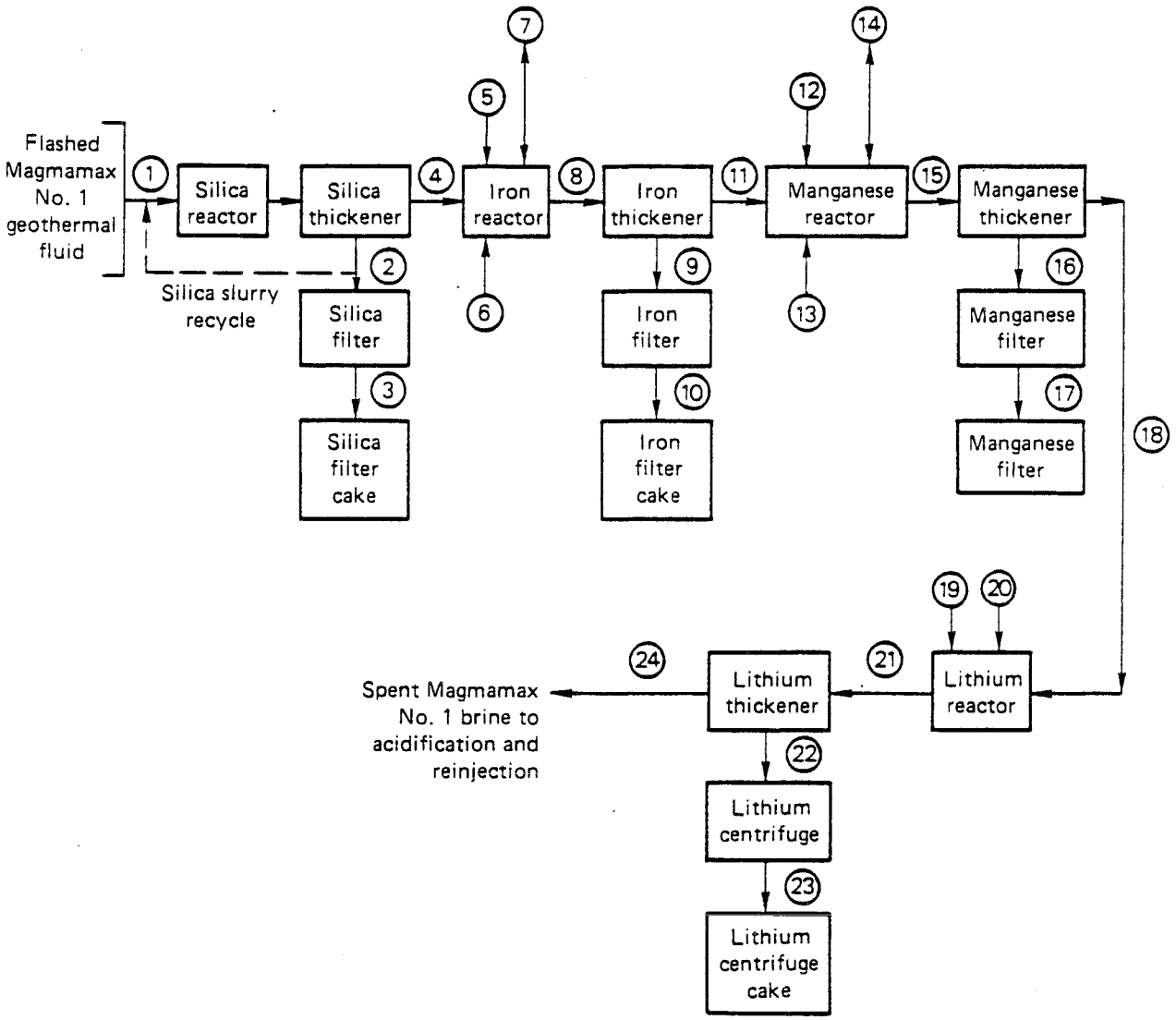

Figure VI-4. Hazen Research process materials balance for Magmamax No. 1 brine (From Ref. 77).

Table VI-5. Hazen Research process flow sheet for Magmamax No. 1 brine (From Ref. 77).

	Stream No.											
	1	2	3	4	5	6	7	8	9	10	11	12
SiO_2	230 ppm total 187 ppm solid	1.6 lb/h 10.2 wt%	1.6 lb/h 60 wt%	43 ppm				43 ppm	0.16 lb/h solids		22 ppm	
Fe	255 ppm			255 ppm				255 ppm total	375 lb/h solids		26 ppm	
Zn	333 ppm			333 ppm				333 ppm			333 ppm	
Mn	775 ppm			775 ppm				775 ppm			775 ppm	
Pb	70 ppm			70 ppm				70 ppm	0.13 lb/h solids		56 ppm	
Li	182 ppm			182 ppm				182 ppm			182 ppm	
Inertia	22.1%			22.1%				22.1%			22.1%	
H_2O	77.7%			77.7%			7 lb/h	77.7%			77.1%	
Specific grey	1.135	1.20		1.135	1.22			1.14	1.32	1.9	1.13	1.22
Temp. °C	93	93	93	93	25	29	92	92	92	92	92	25
Temp. °F	200	200	200	200	77	85	198	198	198	198	198	77
Flow, gpm	15	0.025		15	0.025			15	0.03		15	0.088
Flow, gph	900	1.5		900	1.50			901	1.8		901	5.25
Flow, cfm	–	–				5.0	6.2					
Flow, lb/h	8523	15.0	2.67	8520	15.3			8528	20	6.8	8508	54
Specific heat Btu/lb °F	0.85	0.78	0.46	0.85	0.77			0.85		0.48	0.85	0.77
Heat Btu/h	1.45×10^6	2340	2.46	1.45×10^6	2471			144×10^6		646	144×10^6	10,656
Density	9.47 lb/gal	9.99 lb/gal	≈50 lb/ft^3	9.47 lb/gal	10.2 lb/gal			951 lb/gal	11.0 lb/gal	15.8 lb/gal	944 lb/gal	10.2 lb/gal
NH_3	352 ppm			352 ppm				352 ppm			352 ppm	
	Post-flash Magmamax No. 1 brine input	SiO_2 thickener underflow at 11 wt% solids	SiO_2 filter cake	Brine feed to iron reactor	40% w/y $Ca(OH)_2$ slurry	Air sparge to iron reactor	Vent gases from iron reactor	Iron slurry to thickener	Iron thickener underflow at 20 wt% solids	Iron filter cake	Iron thickener overflow	40% w/y $CA(OH)_2$ slurry

Table VI-5. (Continued)

	Stream No.											
	13	14	15	16	17	18	19	20	21	22	23	24
SiO_2												
Fe			26 ppm	0.21 lb/h		13 ppm			13 ppm			13 ppm
Zn			333 ppm	4.11 lb/h		17 ppm			17 ppm			17 ppm
Mn			775 ppm	10.06 lb/h		39 ppm			39 ppm			39 ppm
Pb			56 ppm	0.48 lb/h		6 ppm			6 ppm			6 ppm
Li			182 ppm			182 ppm			182 ppm	43 lb/h solids		18 ppm
Inertia			22.1%			22.1%			22.1%			22.1%
H_2O		20 lb/h	777%			77.8%			77.0%			77.0%
Specific grey			1.132	1.303	1.86	1.13	1.109	1.315	1.13	1.434	1.86	1.13
Temp. °C	29	90	90	90	90	90	25	25	90	90	90	90
Temp. °F	85	195	195	195	195	195	77	77	195	195	195	195
Flow, gpm			15	0.11		15	0.22	0.05	15.3	0.15	0.1	15
Flow, gph			904	6.8	1.6	902	13.6	2.8	918	9.2	5.8	912
Flow, cfm	12.4	16.0										
Flow, lb/h			8540	74	24.8	8515	126	31	8672	110	78	8594
Specific heat Btu/lb °F			0.85			0.85	0.78	0.67	0.85		0.48	0.85
Heat Btu/h			1.41×10^6		2176	1.41×10^6	7568	16,000	1.44×10^6		7301	1.43×10^6
Density			9.45 lb/gal	10.9 lb/gal	15.5 lb/gal	9.44 lb/gal	9.24 lb/gal	10.9 lb/gal	9.45 lb/gal	12.0 lb/gal	15.5 lb/gal	9.43 lb/gal
NH_3		3.0 lb/h	352 ppm			35 ppm			35 ppm			35 ppm
	Air sparge to manganese reactor	Vent gases from manganese reactor incl. ammonia	Manganese slurry to thickener	Manganese thickener underflow at 20 wt% solids	Manganese filter cake	Manganese thickener overflow	$NaAlO_2$ solution 30 wt% $NaAlO_2$	$AlCl_3$ solution 40 wt% $AlCl_3$	Lithium aluminate slurry to thickener	Lithium aluminate thickener underflow at 39 wt% solids	Lithium aluminate centrifuge cake	Lithium aluminate thickener overflow

ment of the magnetic form requires careful control of pH and oxidation. It is favored by high temperatures and pressures and complexable anions, like chloride[78]. Its development is reported elsewhere at pH's above 7[79]. Interestingly, it formed in the Sinclair No. 4 brine at pH 5.5, but not in Magmamax brine at pH of 5.7. The chloride content of Sinclair No. 4 brine is about 15 percent lower than the Magmamax No. 1, the iron content is about 4-fold greater. The nonmagnetic form of iron precipitate carries higher levels of impurities, especially lead, a feature which depresses their recoverable amounts in subsequent steps of the process.

Iron removal is done by adding a lime slurry at a rate of 3,300 lb of $Ca(OH)_2$ per million lb of brine. Ammonia is given off at this point and would be available to a conventional wet scrubbing process. The lime addition yields a pH of 5.7 and precipitates 93 percent of the iron. Lead is the major heavy metal impurity, comprising somewhat more than 3 percent of the precipitate, but this involves more than 10 percent of the initially available lead. Precipitating iron at a lower pH reduces the lead content, but at the cost of having more iron impurity in the subsequent steps of precipitating manganese, zinc and lead at pH 8.7.

The iron and manganese are each susceptible to oxidation by oxygen of the air. Tests were made to determine what associated effects might occur with (1) minimal oxidation by holding the slurry-reacted brine under nitrogen, (2) moderate oxidation by being open to the atmosphere, and (3) maximal oxidation achieved by an air sparge. The lead was found to totally redissolve in (2), to partially redissolve in (3), and to subsequently precipitate after either. Fe, Mn, and Zn contents in residual liquid were unaffected, being near zero.

Those results were interpreted[68] to mean that Pb was initially coprecipitated with the Fe (II) hydroxide and released as oxidation converted Fe

(II) to FE (III). Subsequent to the oxidation of Fe (II), one expects Mn (II) to be oxidized to Mn (III), the hydroxide of which would appear to be a collector for Pb. The degree of oxidation also affects the settling rate (particle size) of the precipitate and the final settle volume[80].

Lithium recovery was based on three patents[81-83] that yield a hydrated lithium aluminate upon addition of $AlCl_3$ and/or $Al(OH)_3$. Control of pH is critical and is somewhat easier when using $AlCl_3$ with $NaAlO_2$. Recovery of lithium exceeded 99 percent with Sinclair No. 4 brine but was only 88 percent with Magmamax No. 1. The precipitate is fine-grained and requires extra effort to densify and avoid peptization.

Although strontium is more abundant in the brines than barium (mole ratios are near 5:1), a strontium-free barium was obtained by adding sodium sulfate. At a 3:1 mole ratio of SO_4:Ba, recovery was 75 percent. Use of gypsum as a source of sulfate yielded only a 60 percent recovery of barium and that with 2 percent strontium content.

Evaporation studies were made for the recovery of sodium and potassium chlorides. Useful data on the quaternary system $NaCl-KCl-CaCl_2-H_2O$ is available[84]. Both raw and purified brine (by hydroxide precipitation) were used. Not only were the concentrations of typical metals[85] reduced in resultant salts, due to the hydroxide pretreatment, but also, the contents of most other materials were sharply reduced including toxic materials As, B, Cr, and W. Results are shown in Table VI-6[68].

Upon evaporation NaCl precipitates first. About 60 percent is removed, free of potassium, in the first stage. Second stage evaporation yields approximately equal amounts of solid NaCl and KCl. The KCl is separable by a hot-leach, cool recrystallizer cycle which yields an industrially pure KCl. The resulting bittern contains 40 percent $CaCl_2$, which is adequate to market as a liquid, the more common industrial form, or dehydrate to a flake product.

Table VI-6

Recovery of Heavy Metals from Hypersaline Brine by Precipitation of Hydroxides

Element	Concentration		
	Feed Brine (g/l)	Product Brine (g/l)	Washed and Dried Product Solid (Wt. %)
Ba	0.233	0.207	0.002
Ca	34.6	36.6	12.4
Pb	0.139	<0.001	1.52
Li	0.255	0.261	0.06
Mg	0.150	0.0014	2.09
Mn	1.63	0.002	17.3
Fe	0.88	0.0053	11.0
Na	69.0	86.0	0.0088
Sr	0.710	0.719	0.009
K	19.1	18.7	0.007
Zn	0.497	0.004	6.03
SO_4	0.042	<0.001	--
NH_4	0.797	0.007	--

VI-6-3. Assessment of a Geothermal Mineral Extraction Complex

DSS Engineers prepared a Phase I-quality technical and economic assessment for a geothermal mineral extraction complex (GMEC)[57]. Their basic design required 26 million tons of geothermal fluid per year and 39 million tons of Salton Sea (nongeothermal) waters. It involved consumption of 226 megawatts of electricity while generating only 189 megawatts plus 4.5 million tons of clean process steam. An alternative, however would enable the plant to reallocate a large excess of electricity for direct sales. They forecast a net annual profit of $90 to $100 million on net sales of $175 million and an overall return on investment of 38 percent. Eight such complexes were deemed developable by the year 2000 without exceeding the limits of the resource or the markets.

VI-6-3a. Technologic Approach - Although some of their design was based on the laboratory work by Hazen Research, DSS included several items and approaches that are not discussed elsewhere in regard to the Imperial Valley resource. Many of these "novel" items do have technologic experience elsewhere. However, their economic suitability to the Imperial Valley resources is not always clear.

To make maximum use of the resource, DSS Engineers allocated production of electricity and removal of process steam prior to implementing the steps aimed at minerals recovery. They proposed that silica and all heavy metals be precipitated by lime addition. Subsequent recovery of heavy metals would then deal with the sludge. Lithium recovery from brine would follow according to the process described earlier[70].

A freeze-crystallization technique was proposed for recovering NaCl and KCl. It has the advantage of a slightly higher yield of KCl and noncompetition with agriculture for land that otherwise would be occupied by evaporation ponds.

Some of the KCl would be converted to K_2SO_4 for local agricultural use. Also, low-value NaCl would be converted to high-value caustic and chlorine. The production of caustic/chlorine would require 180 megawatts of electric power, thus, a decision to not convert the NaCl would free about 140 megawatts of salable electricity. The excess NaCl could be disposed of by dissolution and injection. Since both caustic and chloride are in surplus supply, it appears that the highest use of the geothermal energy is for electricity generation.

Soda ash (Na_2CO_3) can be produced from NaCl by a process which uses Salton Sea (nongeothermal) water, yielding $MgCl_2$ as an additional product. The processed Salton Sea water would then be available for injection to stabilize pressures in the geothermal reservoir as well as slowing both the rise of the Salton Sea level and its increasing salinity. Currently, however, the soda ash market is amply supplied by trona from the Green River formation of Colorado and Wyoming.

VI-6-3b. Economic Modeling - The DSS report contains several flow sheets that include material balances. Equipment lists have been prepared for each module of the complex, including material selections and sizing. These lists are followed by cost estimates for separate modules.

These estimates of direct capital costs involve process equipment, field materials and field labor. Costs for production and injection wells (in the ratio of 2:1) are estimated separately, but may be judged disproportionately low on the average since their presumed depths of 1,500 meters is appropriate only for a small portion of the resource.

Indirect costs included insurance, freight, taxes, and labor indirects. The total capital estimate includes the basic module cost plus engineering, fees and contingency.

Production costs were estimated by including raw material feedstocks, utilities, miscellaneous process materials and supplies, operating and maintenance labor including payroll burdens and plant overhead, maintenance parts and supplies, taxes, royalties, insurance, interest and depreciation. Not included were workover costs for wells or replacement wells.

Several economic variables were related according to Equation VI-5 wherein:

$$NUS = \frac{(ROI)(TCI)}{100} + \frac{PC}{TP} \qquad \text{(VI-5)}$$

where NUS = net unit sales price

ROI = percent return on investment

TCI = total capital investment

PC = total production cost of the product

TP = annual total production

The net unit sales price was taken as mid-1977 for selling prices for the respective products, less an allowance of 10% for general, administrative and sales expenses.

The sensitivity of the ROI to inaccurate presumptions about, or fluctuations in, the other factors in Equation VI-5, was partly explored by considering one-at-a-time variations of power cost and selling prices of power or mineral product.

That level of economic analysis is barely adequate for a Phase I quality review wherein the capital costs and production costs are very uncertain. The proposed chemical processes have not been actually demonstrated, for example.

The next level of evaluation should divide the so-called return-on-investments, as computed above, into two parts, a return of capital and an

interest component. Forecasts for escalation of unit sales prices and production costs need to be incorporated as well.

A separate market analysis would be required to estimate the balance between unit sales price and annual production. Transportation costs for some bulk commodities, like KCl and $CaCl_2$, are significant fractions of the selling prices and relative distances between markets and alternative producers can be especially critical. They may deserve to be estimated for each competitor.

VI-6-3c. Financial Modeling - No financial model was provided in the DSS study, perhaps because details would differ among alternate ventures. Descriptions of financial plans and how to model them comprise a large segment of the literature on economics. It is impractical, here, to describe details because of the large number of plausible combinations of factors that would affect the financial scheme. Many of these are fairly common factors, but geothermal ventures currently enjoy some institutionalized advantages that are less commonly understood.

These advantages include an alternative energy tax credit of 15 percent for capitalized expenditures in addition to the regular 10 percent investment tax credit. The drilling phase of a geothermal development receives a tax deduction for intangible drilling costs, a feature based on the same rationale used in the petroleum industry.

An electricity selling price advantage exists under Sections 201 and 210 of the PURPA Act of 1978. This yields the possibility for the small (less than 80 megawatt) power producer to sell electricity at a price corresponding to the highest incremental generation cost in the system, and buy power at the average system cost.

Financing can be aided by seeking cities as development partners that can use tax-free funds by issuing revenue bonds to help secure their future energy

requirements. Also, some counties provide special load arrangements for geothermal developers that have favorable terms compared to conventional money sources[86]. Tax, sales, and finance opportunities affect both parts of an economic model about feasibility. The first part considers financing requirements in regard to amount and timing of capital expenditures. This includes a detailed capital expenditure budget, by operations, which is fitted to a desired mix of debt and equity contributions. The second part forecasts revenue and operating costs based on output and escalation factors in sales and costs and debt service requirements. It compares cash flows before taxes and depreciation with tax liability and cash flows after taxes. It leads to calculations for internal rate of return on equity, net present value, and paybacks. Various scenarios need to be explored based on variations of some parameters, perhaps selected or adjusted for their statistical probabilities.

VI-6-4. The Cementation Process

The metal cementaton process is described in Ref. 75. The basic cementation process is described by equation VI-6:

$$M_1^n + M_2^o \rightarrow M_1^o + n/2\ M_2^{2+} \qquad \text{(VI-6)}$$

where: M_1^n = a dissolved metal of valence n

M_2^o = a metal substrate

The process involves electrochemical reduction of the dissolved ion by a metal substrate such as iron. The estimated recovery of dissolved metal ions or metal sulfide complexes by cementation using iron as the reducing agent are summarized in Table VI-7. The recoveries are based on average compositions of brine produced by the Magmamax No. 1 and Sinclair No. 4 wells as described in Ref. 75.

Table VI-7

Estimated Cement Composition (%)

Precious Metal	Magmamax No. 1 Brine		Sinclair No. 4 Brine	
	Precious Metal Included	No Precious Metal	Precious Metal Included	No Precious Metal
Copper	0.7	0.7	2.9	2.9
Lead	64.7	65.0	87.1	87.7
Tin	19.7	19.8	--	--
Arsenic	0.2	0.2	6.8	6.9
Antimony	3.7	3.8	--	--
Bismuth	4.7	4.7	--	--
Selenium	5.6	5.7	2.4	2.5
Silver	0.5	--	0.5	--
Gold	0.1	--	0.1	--
Platinum	0.06	--	0.06	--
	100.00	99.9	99.90	100.0

The cementation process is implemented as shown in Figure VI-5. The process involves use of a wellhead mixer in which two-phase brine-steam mixtures are contacted by recycled finely dispersed iron fillings. The wellhead brine must be acidified to a pH of about 3, by injection of hydrochloric acid, to prevent silica deposition in the iron fillings. The fillings act as nucleation centers for metal sulfide complexes and dissolved metal ions. The cement product and the iron fillings are recovered in a fluidized bed reactor. Iron fillings are recovered by magnetic separation and recycled. The cement, which has been abraded from their iron substrates in the fluidized bed are recovered by thickeners and filters or centrifuges. The downstream portion of the mineral recovery process is basically the scheme developed by Hazen Research for the recovery of metals as hydrated oxides and lithium.

In considering the details of the cementation process, it should be noted that the use of hydrochloric acid at production wellhead conditions implies

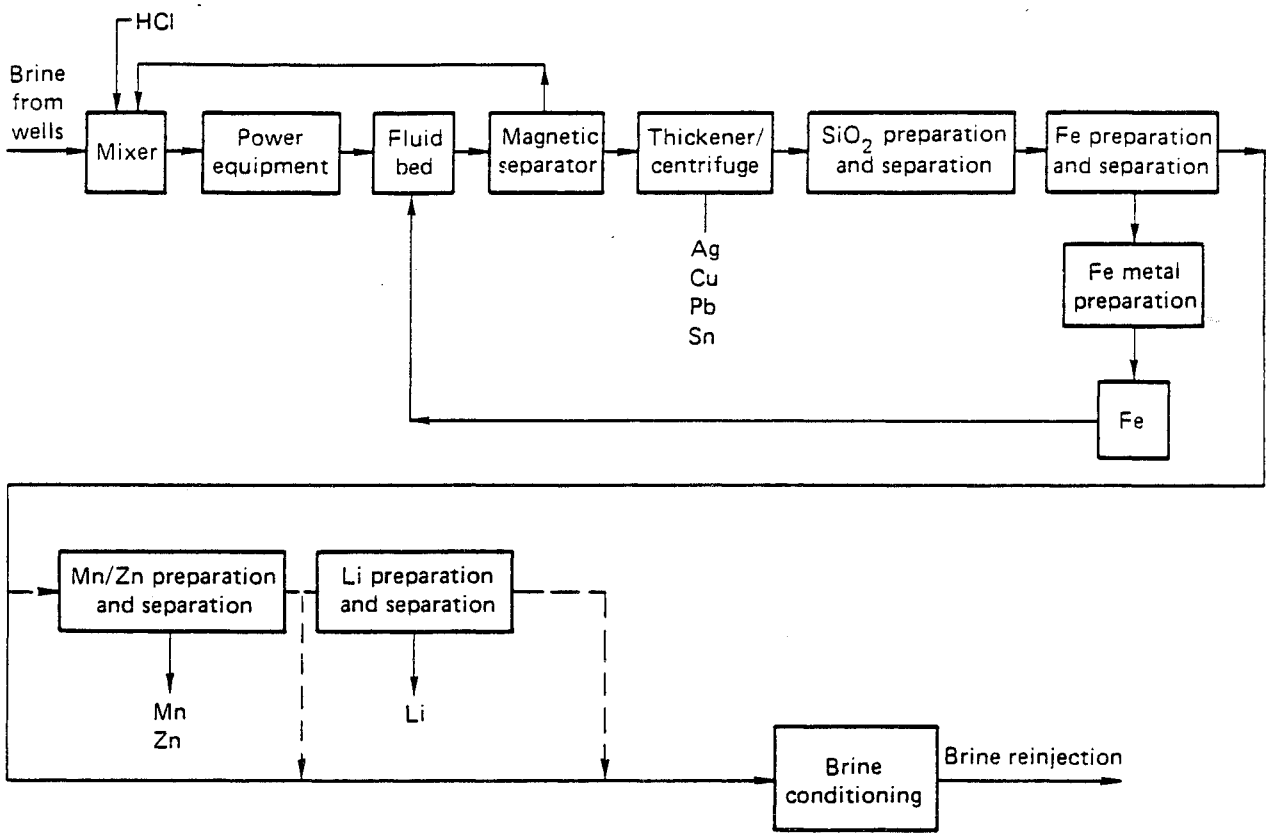

Figure VI-5. The Cementation process for recovery of metal values (From Ref. 75).

a serious potential for turbine corrosion due to the volatility of hydrochloric acid. The separated steam would have to be neutralized to reduce its corrosivity to acceptable levels. It is not clear that acidification would, in fact be necessary to control silica deposition. At production wellhead conditions, silica scaling rates are quite low. The observation of massive silica deposition by Schock and Duba[87] during the course of electro deposition experiments is not necessarily indicative of silica behavior in the absence of an electric potential. The cementation process probably merits additional research. A proposed research plan is provided in Ref. 75.

Estimates of recoverable mineral values from hypersaline geothermal brines such as the data presented in Table VI-4 clearly shows that lithium is the major commodity that should be targeted for recovery. If estimates of lithium demand[31] materialize, then recovery processes for the brine saline components will dominate any discussion of minerals recovery potential. The technology for recovery of salines is well developed. If market demands permit, the necessary modifications to proven extraction procedures will be forthcoming.

VI-7. References

1. Scherbakov, A.V. and Dvorov, V.I., 1970, Thermal waters as a source for extraction of chemicals: U.N. Symp. PISA, Geothermics v. 2, p. 2, p. 1636-39.

2. Balashov, L.S., 1975, Rare elements in thermal ground water: Proceedings, Second U.N. Symp. on the Development and Use of Geothermal Resources, San Francisco, p. 2187-2195.

3. Lindal B., 1961, The extraction of salt from seawater by multiple-effect evaporators using natural steam: U.N. Conf., New Sources of Energy, Rome, G/27.

4. Valfells, A., 1970, Heavy water production with geothermal steam: U.N. Symp. PISA, Geothermics v. 2, p. 896-900.

5. Lenzi, D., 1961, Utilization de l'energie geothermique pour la production de l'acide borique et des sous - produit contenue dans les "Soffloni" de Larderello: U.N. Conf., New Sources of Energy, Rome, G/39.

6. Garbato, C., 1961, Problèmes techniques et èconomiques souelevès par la prèsence d'impuretès chimiques dans les fluides d'orgine gèothermique: U.N. Conf., New Sources of Energy, Rome, G/63.

7. Blake, R.L., 1974, Extracting minerals from geothermal brines; A literature study: U.S. Bureau of Mines, NTIS BP-240 861, 25 pp.

8. Lindal, Baldur, Gudmundsson, S.R. and Hallsson, S.V., 1982, Pilot plant for extraction of salt from geothermal brine at Reykjanes Iceland during 1979-1981: Int'l. Conf. on Geothermal Energy, Florence, Italy, May 1982 G/13.

9. Lindal, Baldur, 1982, Personal communication.

10. Rothbaum, H.P. and Anderton, B.H., 1975, Removal of silica and arsenic from geothermal discharge waters by precipitation of useful calcium silicates: Proceedings, Second U.N. Symp. on Geothermal Development, San Francisco, p. 1417-1425.

11. Bodvarsson, G., 1961, Utilization of geothermal energy for heating purposes and combined schemes involving power generation, heating and/or by-products: U.N. Conf., New Sources of Energy, Rome, GR/5.

12. Bodvarsson, Ibid (5), Armstead, H.C.H., 1967, Fresh water from geothermal fluids: International Water for Peace Conference, Paper P/673, Washington, D.C.

13. De Anda, L.F., et al., 1970, Production of fresh water from the endogenous steam of Cerro Prieto geothermal field: U.N. Symp. PISA, Geothermics v. 2, p. 1632-1635.

14. U.S. Bureau of Reclamation, Geothermal resource investigations East Mesa site: Status Report 1974, 64 pp., also Status Report, 1977, 99 pp.

15. Fernelius, W.M., 1975, Production of fresh water by desalting geothermal brines - A pilot desalting program at the East Mesa Geothermal Field, Imperial Valley, California: Second U.N. Symp. on Geothermal Energy, San Francisco, Proceedings, p. 2801-2208.

16. Water and choice in the Colorado Basin; An example of alternatives in water management: Report by Committee on Water, Natl. Acad. of Sci., Washington, D.C., Pub. 1698, 107 pp.

17. Mercado, S., Lopez, J.A. and Angulo, R., 1979, Chemical recovery as alternative of environmental solution by geothermal brines in Cerro Prieto: Geothermal Resources Council, v. 3, p. 449-452.

18. Kennedy, A.M., 1961, The recovery of lithium and other minerals from geothermal water at Wairakei: U.N. Conf., New Sources of Energy, Rome, G/56, p. 502.

19. Komagata, S., et al., 1970, The status of geothermal utilization in Japan: U.N. Symp. PISA, Geothermics, v. 2, p. 185-196.

20. Yihan, Cai, 1982, Present status of the utilization of geothermal energy in the People's Republic of China: Geo. Heat Center, Quarterly, v. 7, n. 1, Oregon Inst. Tech., Klamath Falls, p. 15.

21. Riesenfeld, F.C. and Kohl, A.L., 1974, Gas purification: Gulf Publishing Co., Houston, 2nd ed.

22. Laszlo, J., 1976, Application of the Stretford process for H_2S abatement at The Geysers Geothermal Power Plant: AIChE HT&EC Division, Intersociety Energy Conference.

23. Allen, G.W., McCluer, H.K. and Semprini, L., 1975, Measurement of hydrogen sulfide emissions abatement at Unit 11, The Geysers, using iron catalyst: Pacific Gas and Electric Co., Dept. of Eng. Res., Rpt. 7485, Dec. 3, 1975, p. 29-75.

24. Weres, D., Tsao, K. and Wood, B., 1977, Resource, technology and environment at The Geysers: Lawrence Berkeley Laboratory Rpt. LBL-5231.

25. Total dissolved solids are in the range of 15 to 25 percent by weight of produced fluids.

26. IT Corporation, P.O. Box 158, Westmorland, CA. Disposal rate schedule: Nov. 1, 1981.

27. Solid waste fee schedule: Pursuant to section 57202 of the Imperial County Codified Ordinance, as amended, July 1, 1981.

28. "Pan" evaporation rates in the Imperial Valley are the highest in the U.S., about 100 inches per year (25,000 metric tons of evaporated water per hectare per year).

    Nominally, 15 to 20 acres of ponds are sufficient to evaporate enough water, from the brine used to generate one megawatt-year of electricity, to recovery the NaCl, KCl, and $CaCl_2$ contained in the same brine. This evaporation rate corresponds to electrical output of about 32 megawatts per square mile, a rate close to the electrical energy recovery rate anticipated for the Salton Sea field. Minerals recovery and electrical generation are approximately in balance, regarding gross space demands for combined operations. Evaporation ponds could occupy the spaces between wells so that simultaneous operations would be possible.

29. Ermak, D.L., 1977, Potential growth of electric power production from Imperial Valley geothermal resources: Lawrence Livermore Laboratory, UCRL-52252, 29 p.

30. Nominally, one megawatt of electrical power capacity requires about 220,000 kg of steam per day. Such steam would be derived from flashing liquid. At a nominal 20 percent flash (effective resource temperature near 210°C) one megawatt of electrical capacity is associated with about 1.1 million kg of (pre-flash) liquid per megawatt-day or 400 million kg of liquid per megawatt-year.

31. Maimoni, A. and Borg, I.Y., 1981, Strategic materials shortages: Institutional and Technical Issues: Lawrence Livermore Laboratory, UCRL-53203, 49 pp.

32. Final Salton Sea Anomaly Master Environmental Impact Report, Vol. 1, County of Imperial, El Centro, CA.

33. Cosner, S.R. and Apps, J.A., 1978, A compilation of dataon fluids from geothermal resources in the United States: Lawrence Berkeley Laboratory, LBL-5936, 107 pp.

34. Shannon, D.W., et al., 1978, Brine chemistry and combined heat/mass transfer: Electric Power Research Institute, EPRI ER-635.

35. Analyses for fluids from wells of the Westmorland, Niland, Main Salton Sea, East Brawley, and South Brawley subfield, have been included. The South Brawley subfield composition is given in Nesewich, J.P., and Gracey, C.M., 1982, Hydrodynamic/Kinetic reactions in liquid-dominated geothermal systems: Final Report by Aerojet Energy Conversion Co., Submitted to Los Alamos National Laboratory, DOE Contract No. 4-X29-9916F-1.

36. Full-spectrum recovery effort implies substantial space requirements for a surface facility. Recovery of NaCl, KCl, and $CaCl_2$ probably would require solar evaporation ponds although a freeze-crystallization method has been proposed (see Ref. 57). A collective pond area of 750 acres or more, plus space for access roads and stationary equipment would be required to handle all the flash-spent brine from a 50 megawatt power plant.

37. For the purposes of minerals recovery, the hypersaline brines in the Imperial Valley are inferred to be a continuous liquid mass which occupies the spaces between the known occurrences. Those brines need not be hot in order to be valuable for their mineral content, although the field data suggest they are not everywhere. Perhaps, exploitation of the mineral components would be easier if the brines were cool because their tendency to deposit scales and sludges might be much less. However, cool brines might have to be pumped at considerable cost hence an uncertainty looms about the value of any cool brines.

38. Towse, D.F. and Palmer, T.D., 1976, Summary of geology at the ERDA-MAGMA-SDG&E geothermal test site: Lawrence Livermore Laboratory, UCID-17008, 6 pp.

39. Combs, J. 1971, Heat flow and geothermal resource estimates for the Imperial Valley: in Cooperative Geophysical-Geochemical Investigations of Geothermal Resources in the Imperial Valley of California, Univ. Calif. Riverside, Rex, R.W., Ed., Rpt. to U.S. Bureau Reclamation.

40. Griscom A. and Muffler, L.J.P., 1971, Salton Sea Aeromagnetic Map: U.S. Geo. Surv. Map GP-754.

41. Chan, M.A. and Tewhey, J.D., 1977, Subsurface structure of the southern portion of the Salton Sea goethermal field: Lawrence Livermore Laboratory, UCRL-52354, 13 pp.

42. Younker, L. and Kasameyer, P., 1978, A revised estimate of recoverable thermal energy in the Salton Sea geothermal resource area: Lawrence Livermore Laboratory, UCRL-52450, 13 pp.

43. Tewhey, J.D., 1977, Geologic characteristics of a portion of the Salton Sea geothermal field: Lawrence Livermore Laboratory, UCRL-52267, 51 pp.

44. Elders, W.A., 1981, Applications of petrology and geochemistry to the study of active geothermal systems in the Salton Trough of California and Baja California: AIME Symposium Volume, Process Mineralogy in Extractive Metallurgy.

45. Aguilera, R., 1980, Naturally fractured reservoirs: PennWell Pub. Co., Tulsa, 702 pp.

46. Pirson, S.J., 1967, How to map fracture development from well logs: World Oil, March, p. 106-114.

The relationships among total porosity, matrix porosity, and fracture porosity are described as a sophisticated model for reservoir engineering by Pirson (1967). Charts provided by Aguilera (1980) follow that approach and show how electrical resistivity logs and a formation factor (for matrix resistivity) can be used to deduce separate values for porosities of the matrix and the fractures. Data to use the charts is scarce because not all wells are logged with appropriate tools and because the logging tools often fail, due to very high temperatures in the wells and for mechanical reasons. Data that are recovered tend to be held as proprietary. The point to be made is that data on this matter can be obtained and do exist, albeit in incomplete forms among a few commercial interests.

47. Final Salton Sea anomaly master envronmental impact report, comments and responses: County of Imperial, El Centro, CA.

48. Helgesen, H.C., 1968, Geologic and thermodynamic characteristics of the Salton Sea geothermal system: Amer. Jour. Sci., v. 266, p. 129-166.

49. Republic Geothermal, Inc. reports its well Britz No. 3 produces a mixed brine for which the separate component brines are respectively similar to the brines obtained from Sinclair No. 3 which was completed twice at different depths. The latter is described in Rex, R.W., et al, 1971, Cooperative geological-geophysical-geochemical investigations of geothermal resources in the Imperial Valley area of California: Univ. Cal., Riverside, IGPP-UCR-71-Rpt. to U.S. Bureau of Reclamation.

50. Rex, R.W., 1981, Keynote speech to Geothermal Resources Council Annual Meeting, Houston.

51. Helgesen (Ibid, 45) noted that the effect of temperature on the volume of a unit mass largely cancels the effect of salt content on the mass of a unit volume.

52. U.S. Bureau of Mines, 1975, Mineral facts and problems: Bur. Mines Bul. 667, p. 16.

53. Muffler, L.J. and White, D.E., 1969, Active metamorphism of upper cenozoic sediments in the Salton Sea Geothermal Field and the Salton Trough, Southeastern California: Geol. Soc. Amer. Bull., V. 80, 157-182..

54. Swanson, R.K., 1980, Geopressured Energy Availability: EPRI Report AP-1457.

55. House, P.A., Johnson, P.M. and Towse, D.F., 1975, Potential power generation and gas production from Gulf Coast geopressure reservoirs: Univ. Calif. Livermore, UCRL-51813, 40 pp.

56. Karkalits, O.C. and Hankins, B.E., 1981, Standardization of sampling and analysis of geopressured fluids Part II: Monitoring of geopressured wells: Gas Research Institute, GRI-80/0061, Contract No. 5080-321-0301, 77 pp.

57. Urbanek, M.W., et al, 1978, Research on a geothermal mineral extraction complex Phase I; Preliminary technical and economic assessment: Final Rpt. by DSS Engineers, Inc., Fort Lauderdale, Florida, for U.S. Bureau of Mines, Reno, Contract No. J0275019.

58. Chemical Reporter, 3 May 1982, Notes a 1982 estimated market for 19,000 tons of $SrCO_3$. The U.S. Market is reliably served by Mexican sources refined in Georgia and California.

59. Werner, H.H., 1970, Contribution to the mineral extraction from supersaturated geothermal brines, Salton Sea Area, California: U.N. Symp. PISA, Geothermics v. 2, p. 1651-1655.

60. Skinner, B.J., White, D.E., Rose, H.J. and Mays, R.E., 1967, Sulfides associated with the Salton Sea Geothermal Brine: Economic Geology, V. 62, 316-330.

61. White, D.E., Anderson, E.T. and Grubbs, D.K., 1963, Geothermal brine well: Mile-deep hole may tap ore-bearing magmatic water and rock undergoing metamorphism: Science, V. 139, 919-922.

62. White, D.E., 1968, Environments of generation of some base-metal ore deposits: Economic Geology, V. 63, No. 4, 301-335.

63. Muffler, L.J.P. and White, D.E., 1968, Origin of CO_2 in the Salton Sea Geothermal Systm, southeastern California, U.S.A.: XXIII International Geological Congress, V. 17, 185-194.

64. Hook, S.H. and Williams, G.C., 1942, Imperial carbon dioxide gas field: Summary of Operations, California Oil Fields, California Div. Oil and Gas, V. 28, No. 2, 12-33.

65. Farley, E.P., et al, 1980, Recovery of heavy metals from high salinity geothermal brine: Final Report by SRI International to U.S. Bureau of Mines, Contract No. J0188076, 129 pp.

66. Quong, R., Knauss, K.G., Stout, N.D. and Owen, L.B., 1979, An effective H_2S abatement process using geothermal brine effluents: Lawrence Livermore Laboratory, PREPRINT UCRL-83010, 3 pp.

67. Brown, F.C., Harvey, W.W. and Warren, R.B., 1977, Hydrogen sulfide removal from geothermal steam: EIC Corporation, Newton, Mass.

68. Christopher, D.H., Stewart, M. and Rice, J. 1975, The recovery and separation of mineral values from geothermal brines: Hazen Research, Inc., Supported by USBM Rpt. OFR 81-75, NTIS PB-245 686, 39 pp.

69. Berthold, C.E., Hadzeriga, P., Christopher, D.H., Applegate, T.A. and Gillespie, D.M., 1975, Process technology for recovering geothermal brine minerals: Hazen Research Rpt. to U.S. Bureau of Mines, Rpt. No. Bu. Mines OFR35-75, also NTIS PB 241867, 255 pp.

70. Berthold, C.E. and Stevens, F.M., 1977, The recovery of mineral values from Magmamax No. 1 post-flash geothermal brine: Hazen Research, Golden, Colo., HRI Project 4049G, submitted to U.S. Bureau of Mines, Reno.

71. Berthold, C.E. and Stevens, F.M., 1978, Magmamax No. 1 Geothermal minerals recovery pilot plant engineering design: Hazen Research, Golden, Colo., HRI Project 4049G-02, submitted to U.S. Bureau of Mines, Reno.

72. Schultze, L.E. and Bauer, D.J., 1982, Operation of a mineral recovery unit on brine from the Salton Sea known geothermal resource area: U.S. Bur. Mines RI-8680 Supt. of Docs. no.: I 28.23:8680, 12 pp.

73. Michels, D.E., 1982, Chemical experiments with fresh, hot, partly-flashed hypersaline brine: Geothermal Resources Council Trans. v. 6, p.

74. Phillips, S.L., et al, 1977, A study of brine treatment: Electric Power Res. Inst. Pub. EPRI ER-476, prepared by Lawrence Berkeley Laboratory, Report LBL-6371.

75. Maimoni, Arturo, 1982, A cementation process for minerals recovery from Salton Sea Geothermal brines: Lawrence Livermore Laboratory, UCRL-53252, 21 p.

76. Talmadge, W.F. and Fitch, E.B., 1955, Ind. Eng. Chem., v. 47, n. 1, p. 38.

77. Berthold, CE., and Stevens, F.M., 1978, Magmamax No. 1 Geothermal brine bulk solids precipitation pilot plant engineering design: Hazen Research, Golden, Colo., HRI Project 4049G-03, submitted to U.S. Bureau of Mines, Reno.

78. Mellor, J.W., 1964, A comprehensive treatise on inorganic and theoretical chemistry: Longmans-Green & Co.

79. Bituminous Coal Research, Inc., 1971, Studies on the densification of coalmine drainage sludge: Env. Prot. Agency Project 14010 EJT.

80. Svanks, K. and Shumate, K.S., 1973, Factors controlling sludge density during acid mine drainage neutralization: State of Ohio Water Resources Center, Ohio State Univ.

81. Rathmell, R.K., 1967, U.S. patent 3,261,665 assigned to E.I. duPont.

82. Goodenaugh, R.D., U.S. patent 2,964,381, assigned to Dow Chemical Co.

83. Neipert, M.P. and Bon, C.D., U.S. patent 3,306,700, assigned to Dow Chemical Co.

84. Assavson, G.O., 1950, Equilibria in aqueous systems containing K^+, Na^+, Ca^{+2}, Mg^{+2}, and Cl^-, Part II. The Quaternary system $CaCl_2$-KCl-NaCl-H_2O: Swedish Jour. Sci., v. 72, p. 1437-1444.

85. Seidell, A., 1958, Solubilities of inorganic and metal-organic compounds: Amer. Chem. Soc., Vol. II.

86. Director of Community Economic Development, Industrial Development Authority of Imperial County, County Administrative Office, 939 Main Street, El Centro, CA 92243.

87. Schock, R.N. and Duba, A., 1975, The effect of electrical potential on scale formation in Salton Sea Brine: Univ. of Calif., Lawrence Livermore National Labortory Rept. UCRL-51944.